Addendum for - Phase II Groundwater Flow Model of Corrective Action Unit 98: Frenchman Flat, NevadaTest Site, Nye County, Nevada

Addendum - May 2007

Appendix C

C.3.1
C.3.2
C.3.3
C.3.4
C.3.5
C.3.6
C.3.7

Preface

An Addendum to the *Phase II Groundwater Flow Model of Corrective Action Unit 98: Frenchman Flat, Nevada Test Site, Nye County, Nevada*, S-N/99205--074, Revision 0 (May 2006) was prepared to address review comments on this final document provided by the Nevada Division of Environmental Protection (NDEP) in a letter dated June 20, 2006. The Addendum includes revised pages that address NDEP review comments and comments from other document users. Change bars are included on these pages to identify where the text was revised.

In addition to the revised pages incorporated in the Addendum, the following clarifications are made:

- Section 6.0 Conceptual Model Uncertainty Analyses. Please note that in this section figures showing the observed versus simulated well head (Figures 6-1, 6-5, 6-7, 6-16, 6-28, 6-30, 6-32, 6-34, 6-37, 6-42, 6-47, 6-52, 6-57, 6-62, 6-71, and 6-86) have a vertical break in scale on the y axis.

- Section 7.0 Parameter Sensitivity Analysis. In Section 7.2, the parameter perturbation analysis defines two components of the objective function PHI. These two components include the WELL component that represents the head portion of the objective function as measured in wells and the FLUX component that represents the lateral boundary flux portion of the objective function. In the text and figures in Section 7.2, the phrases “well portion of the objective function” and “head portion of the objective function” are used interchangeably in discussions of the WELL component of the objective function.

fits to the calibration data recognizing the non-unique nature of the multiple conceptual models and parameter sets. The conceptual model uncertainty includes alternative HFMs, boundary condition uncertainty, and model results that have a constant permeability with depth below ground surface. These analyses are referred to as analyses of conceptual model uncertainty and the results are presented separate from parameter sensitivity analysis.

The primary goal of the assessment of the conceptual model uncertainty is to define the uncertainty of the flow model responses associated with alternative HFM uncertainty, boundary condition uncertainty, and HSU fault parameter uncertainty, and to provide guidance on how to include or represent that uncertainty in the transport simulation.

HFM Uncertainty Analysis

Steady-state groundwater flow models used to assess conceptual model uncertainty were calibrated using different HFMs that interpreted aspects of the Frenchman Flat hydrostratigraphy somewhat differently. Each of the HFMs included 17 HSUs, of which 8 were considered as aquifers and 9 as confining units, and more than 70 faults that were included based on their potential hydrologic significance. Each of these HFMs was used in conjunction with a map of recharge for the Frenchman Flat area that was taken from a water-balance model of infiltration and recharge (designated the USGSD model) originally developed for the regional model area.

Independently calibrated models for the BASE and CPBA HFMs provide generally similar fits for boundary fluxes and simulated heads, with the exception of measured heads at Wells WW-C, WW-C1, WW-4, and WW-4A, where the heads are better simulated by the BASE-USGSD model. Calibration fits are generally superior for the BASE-USGSD model compared to the CPBA-USGSD alternative for multiple statistical parameters that characterize goodness of fit. Particle tracks are generally similar for the northern testing area for both models with the exception of particle tracks starting in the vicinity of the PIN STRIPE test location. The DISP-USGSD model calibration indicated that a completely open connection between the alluvium and the LCA is unrealistic, but that modest adjustments to fault parameters allow for a good simulation of water-level observations. The BLFA-USGSD and DETA-USGSD alternatives were calibrated using the unchanged parameters estimated during calibration of the BASE-USGSD model. Both models show similar patterns of particle tracks for the central testing area compared to the BASE-USGSD model and show some

variability in particle tracks compared to the BASE model for the northern testing area. The primary differences are in the direction of the particle trajectories and in HSUs traversed along the pathways. The significance of model differences will be further evaluated during transport modeling studies.

Discrete Uncertainty Analysis

Discrete uncertainty analyses were conducted to evaluate likely scenarios that would lead to longer-range contaminant transport for particles starting at the northern or central testing areas. Discrete uncertainty analyses were used to examine the effects of several model parameters on the model calibration and groundwater flow paths calculated by the BASE-USGSD and BLFA-USGSD models in the northern or central testing areas of the Frenchman Flat basin. The permeability of two faults (35 and 38) in the alluvial and volcanic sections and one HSU (BLFA) were increased to the point where the model calibration was significantly impacted. These parameters were selected because of their great uncertainty and conceptual possibility to affect flow from underground nuclear tests. Changes to parameters in the northern testing area suggest that flow trajectories may be modified through adjustment to the selected model parameters, but the ability of other model parameters to compensate for the model misfit was not determined. In this sense, the effects of these changes may be exaggerated. Changes to tested model parameters in the central testing area have little influence on the resulting flow field. The impact of these flow fields to contaminant transport for the time frame of interest will be investigated during the contaminant migration analysis that will be documented in a later report.

Boundary Conditions Uncertainty Analysis

Results from seven flow models investigating boundary condition uncertainty were evaluated. The two alternative HFMs that are most distinctly different based on calibration with the USGSD boundary conditions (BASE and CPBA HFM alternatives) were combined with the DRIA-, MME-, and DVRFS-boundary conditions. These models were used to bound the uncertainty in the CAU flow system resulting from variations in boundary conditions that were determined through the use of several regional groundwater flow models. Because areal recharge provides limited water flux into the top of the Frenchman Flat CAU flow model domain, differences among the boundary heads and boundary fluxes dominated this component in the flow field of the uncertainty analyses. An

Relative groundwater ages and geochemical evolutionary trends were used to identify pairs of groundwaters that are likely to lie along a common flow path. Inverse geochemical models were created with the geochemical modeling code PHREEQC to confirm that plausible water/rock interactions could be found that would explain the observed chemical differences and thus, that the groundwaters could indeed lie on a specific flow path. These models confirmed that groundwater at Well UE-5 PW-1 could originate by the southerly flow of groundwater from Well UE-5 PW-2, coupled with plausible water/rock interactions. Similar models developed for Well ER-5-4 in the central part of the basin indicate this groundwater could originate from either the southerly flow of groundwater from Well UE-5 PW-1 or the southeastward flow of groundwater from UE-5c WW. Geochemical inverse models for Well ER-5-4 #2 could only explain the composition of this groundwater using both mixing and water/rock interactions. This groundwater appears to originate from a mixture of groundwater from the CP basin and groundwater from northwestern Frenchman Flat, suggesting that this groundwater may have been recharged in the low hills separating these two basins. This result agrees with evidence from hydraulic heads that the groundwater near Well ER-5-4 #2 has a strong hydraulic connection with groundwater in the vicinity of the CP basin.

Groundwater velocities were calculated at pairs of wells in the alluvium that were likely to lie along a flow path based on their relative chemical evolution. Groundwater velocities in the alluvium between well pairs with ^{14}C-based ages ranged between 0.12 meters per year (m/yr) and 0.85 m/yr. A higher groundwater velocity of 1.1 m/yr was estimated for a UE-5 PW-1 to WW-1 flow path, but this velocity is subject to greater uncertainty because it is based on an age for WW-1 groundwater estimated indirectly from its dissolved cation concentrations. An analysis of groundwater travel time for a mixture of groundwaters involving components from the CP basin (Well WW-4) and from Well UE-5c WW indicated a groundwater velocity in the volcanic rocks along the flow path of 0.60 m/yr.

The low rates of groundwater movement estimated for Frenchman Flat basin are consistent with the near absence of recharge to the basin over the last 8,500 years and with the nearly flat water table within the alluvial deposits of the basin. The estimated groundwater velocities in the alluvium calculated from the ^{14}C ages indicate that lateral transport distance of between about 120 to 1,100 m can be expected near the testing areas over the next 1,000 years.

ES-9 SUMMARY AND CONCLUSIONS

The steady-state groundwater flow model described in this report was undertaken to satisfy the groundwater flow model requirement of the *Addendum to Revision 1 of the Corrective Action Investigation Plan for Corrective Action Unit 98: Frenchman Flat, Nevada Test Site, Nevada* (NNSA/NV, 2001).

A 3-D finite-element steady-state groundwater flow model was constructed for the Frenchman Flat CAU. The emphasis of this flow model analysis is not on identification of a unique model and associated parameters. Instead, the approach was to consider conceptual model uncertainties by using different combinations of the hydrostratigraphic framework models, recharge models, hydrologic boundary conditions, and the application of depth decay to propagate the high-level uncertainty associated with each of these model elements into the resulting flow fields. This suite of flow fields provides a spectrum of flow paths from individual underground nuclear tests that will be examined through transport modeling analyses.

The FFACO requires that the contaminant transport model predict the contaminant boundary at 1,000 years and "at a 95% level of confidence" (FFACO, 1996). The Frenchman Flat Phase II flow model described in this report provides, through the flow fields derived from alternative HFMs and boundary conditions, one of the tools required to compute the contaminant boundary. Other components include the simplified source model, which incorporates uncertainty and variability in the factors that control radionuclide release from an underground nuclear test, and the transport model with the associated parameter uncertainty. The synthesis of all this information contributes to the calculation of the final contaminant boundary.

The salient points of the Frenchman Flat setting and hydrostratigraphic framework model are as follows:

- Frenchman Flat is a closed-drainage intermontane basin. The valley floor of the basin slopes gently from the surrounding highlands to a playa at the lowest point in the basin.
- Frenchman Flat was filled with sedimentary and volcaniclastic rocks, followed by ash-fall and ash-flow tuffs and finally alluvial and playa deposits, as it developed. More than 1,400 m of alluvium exists in the center of the basin. The alluvium thins towards and beyond the structural margin of the basin where it directly overlies the LCA. Along the northern, eastern,

During the regional evaluation (DOE/NV, 1997), the HFM of the UGTA regional groundwater flow system was subdivided into nine HSUs in the Frenchman Flat area. Table 2-2 summarizes the HSUs in the UGTA regional model that occur in the Frenchman Flat model area (IT, 1996d).

2.1.1.2 Groundwater Occurrence and Movement

Within the NTS region, groundwater occurs in alluvial, volcanic, and carbonate materials. Saturated alluvial materials are present in central and southern Yucca Flat, Frenchman Flat, and Jackass Flats on the NTS and in the basins located throughout the flow system. Saturated Tertiary volcanics are present in the western section of the region. The distribution and thickness of alluvial and volcanic aquifers are highly variable throughout the region and are not interpreted to be continuous. In most instances, an AA is confined to a basin by surrounding mountain ranges. In some basins, AAs are discontinuous aquifers due to structural controls elevating the bottom of the alluvium above the water table. In general, alluvial and volcanic aquifers are considered to be depositional elements overlying the regional flow system and only influence regional flow in localized areas. The underlying LCA is the principal aquifer of the Death Valley regional flow system. The LCA forms a nearly continuous aquifer across the region except where interrupted by calderas, truncated by structural controls, or penetrated by intrusive rocks.

An interesting feature of the hydraulic conductivity data compiled for the region was that a linear trend was found showing a decrease in hydraulic conductivity (on a log scale) with increased depth below land surface (DOE/NV, 1997, Section 5.5.1.5). The data, however, displayed a significant level of scatter.

Based on the water-level dataset compiled during the regional evaluation (IT, 1996c; DOE/NV, 1997), depths to groundwater beneath the NTS and surrounding region vary greatly. Groundwater depths in the southern NTS range from about 23 m beneath upper Fortymile Wash to more than 213 m beneath Frenchman Flat, compared to more than 610 m beneath Pahute Mesa in the northern NTS (IT, 1996c; DOE/NV, 1997). Perched groundwater is found locally throughout the NTS and occurs within the TCUs and, to some extent, overlying units. In the highlands, springs emerge from perched groundwater lenses. Spring discharge rates are low, and this water is used only by wildlife.

Table 2-2
Hydrostratigraphic Units of the Frenchman Flat Area Included in the UGTA Regional Hydrostratigraphic Framework Model

Hydrostratigraphic Unit (Symbol)	Dominant Hydrogeologic Unit(s)[a]	General Description
Alluvial Aquifer (AA) (this term is also used to designate a hydrogeologic unit)	AA	Consists mainly of alluvium that fills extensional basins such as Gold Flat, Crater Flat, Kawich Valley, and Sarcobatus Flat. Also includes generally older Tertiary gravels, tuffaceous sediments, and nonwelded tuffs (where thin) that partially fill other basins such as Oasis Valley and the moat of the Timber Mountain caldera complex.
Timber Mountain Aquifer (TMA)	Mostly WTA, minor VTA; TCU within the Timber Mountain caldera complex	The uppermost welded tuffs in the Frenchman Flat model area consists mainly of extra-caldera welded ash-flow tuffs (aquifer-like lithologies). However, the altered intra-caldera equivalent rocks within the Timber Mountain caldera are modeled as confining units.
Tuff Confining Unit (TCU)	TCU	Mostly zeolitized nonwelded tuffs.
Volcanic Aquifer (VA)	WTA, VTA, LFA	Imprecisely known grouping of volcanic rocks; generally with aquifer-like qualities. Also used as a lumping unit away from the more data-rich NTS.
Volcaniclastic Confining Unit (VCU)	TCU, minor AA, lesser CA	Complex 3-D distribution of zeolitic nonwelded tuff, gravels, mudstones, and limestones. Present in the southern portion of the Frenchman Flat model area.
Volcanics undifferentiated (VU)	WTA,TCU, lesser LFA	All Quaternary and Tertiary volcanics outside the NTS proper and the proximal NTS caldera complex.
Upper Clastic Confining Unit (UCCU)	CCU	Late Devonian through Mississippian siliciclastic rocks. Present in the northeastern corner (CP basin) of the Frenchman Flat model area.
Lower Carbonate Aquifer (LCA)	CA	Cambrian through Devonian mostly limestone and dolomite. Widespread throughout the Frenchman Flat model area.
Lower Clastic Confining Unit (LCCU)	CCU	Late Proterozoic through Early Cambrian siliciclastic rocks. Widespread throughout the Frenchman Flat model area.

[a]See Table 2-1 for definitions of HGUs

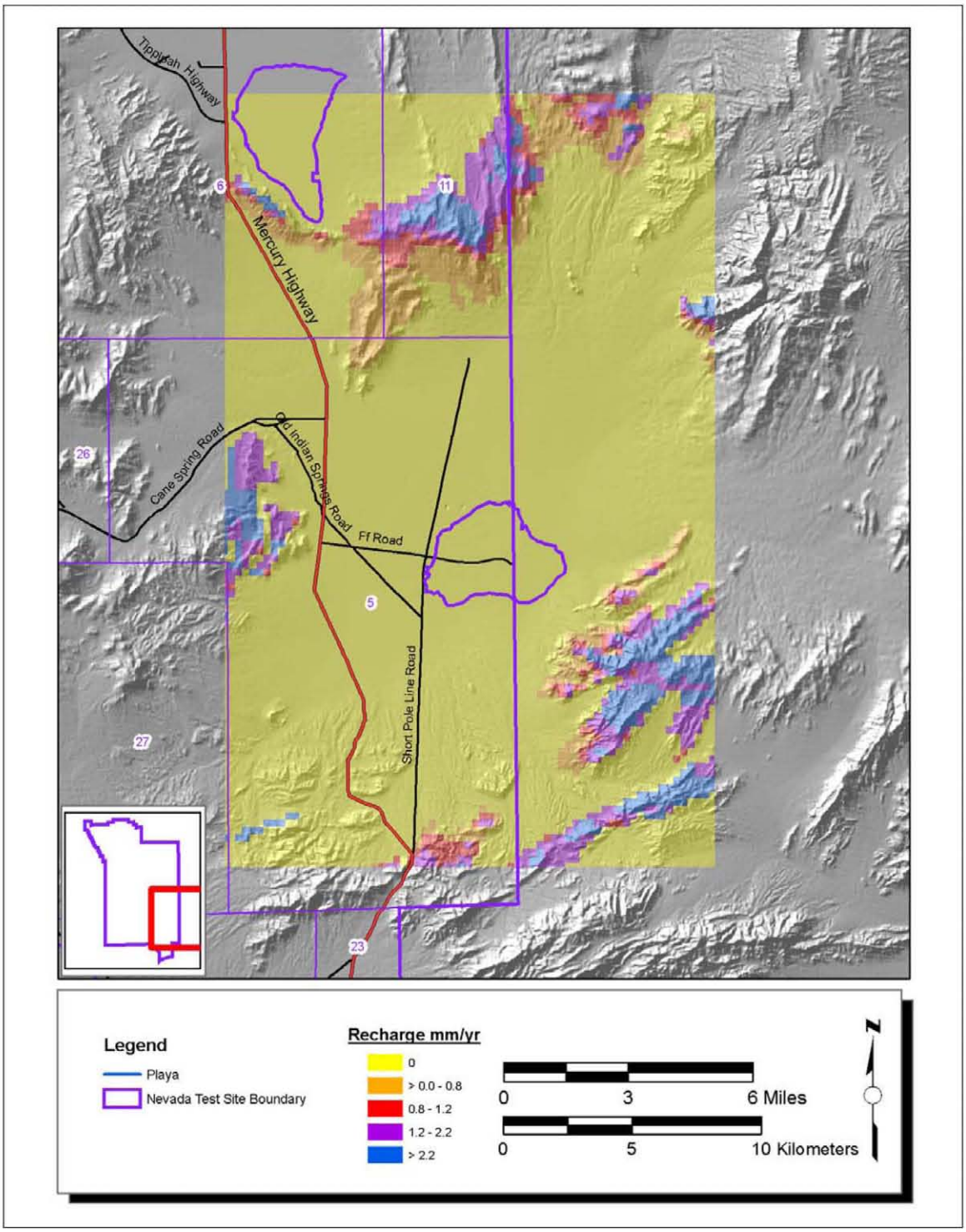

Figure 2-3
USGS Recharge Distribution without Overland Flow (USGSND)

Note: As part of this Addendum, Figure 2-3 replaces the original Figure 2-3 that appears in the *Phase II Groundwater Flow Model for Corrective Action Unit 98: Frenchman Flat, Nevada Test Site, Nye County, Nevada*, S-N/99205--074 (May 2006).

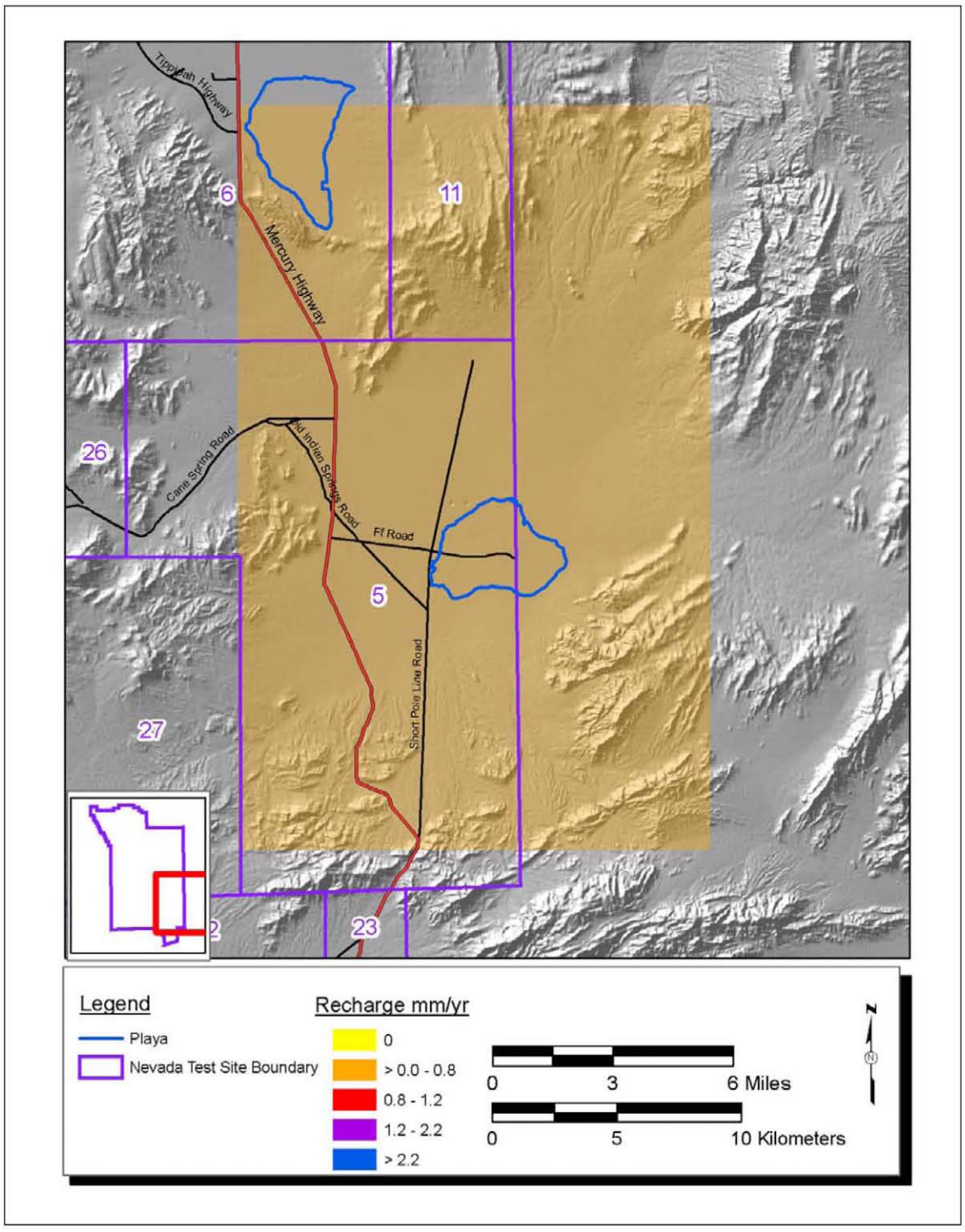

Figure 2-5
DRI Recharge Distribution with Alluvial Mask (DRIA)

Note: As part of this Addendum, Figure 2-5 replaces the original Figure 2-5 that appears in the *Phase II Groundwater Flow Model for Corrective Action Unit 98: Frenchman Flat, Nevada Test Site, Nye County, Nevada*, S-N/99205--074 (May 2006).

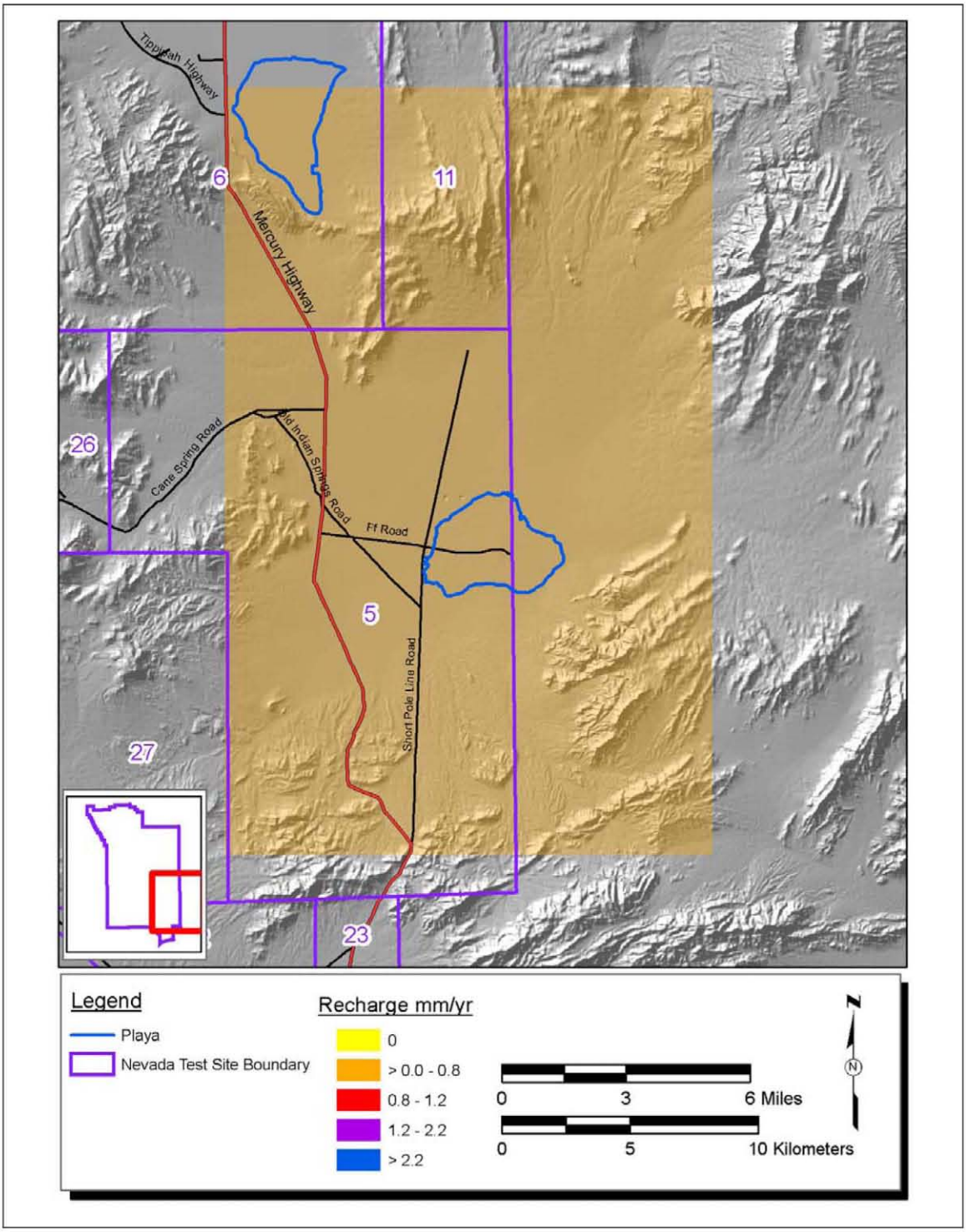

Figure 2-6
DRI Recharge Distribution with Alluvial and Elevation Mask (DRIAE)

Note: As part of this Addendum, Figure 2-6 replaces the original Figure 2-6 that appears in the *Phase II Groundwater Flow Model for Corrective Action Unit 98: Frenchman Flat, Nevada Test Site, Nye County, Nevada*, S-N/99205--074 (May 2006).

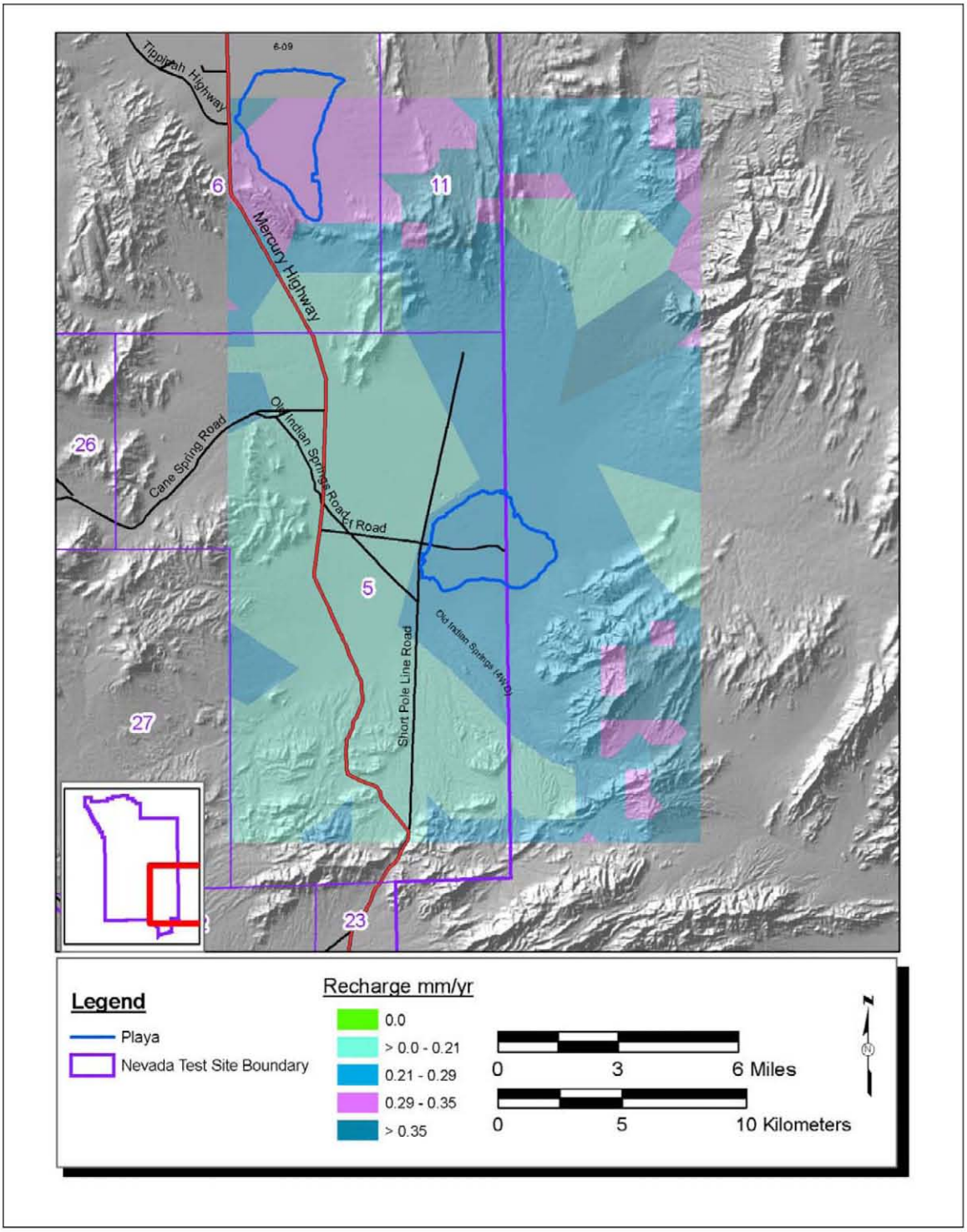

Figure 2-7
DRI Recharge Distribution with Alluvial Mask (DRIA) - Revised Scale

Note: As part of this Addendum, Figure 2-7 replaces the original Figure 2-7 that appears in the *Phase II Groundwater Flow Model for Corrective Action Unit 98: Frenchman Flat, Nevada Test Site, Nye County, Nevada*, S-N/99205--074 (May 2006).

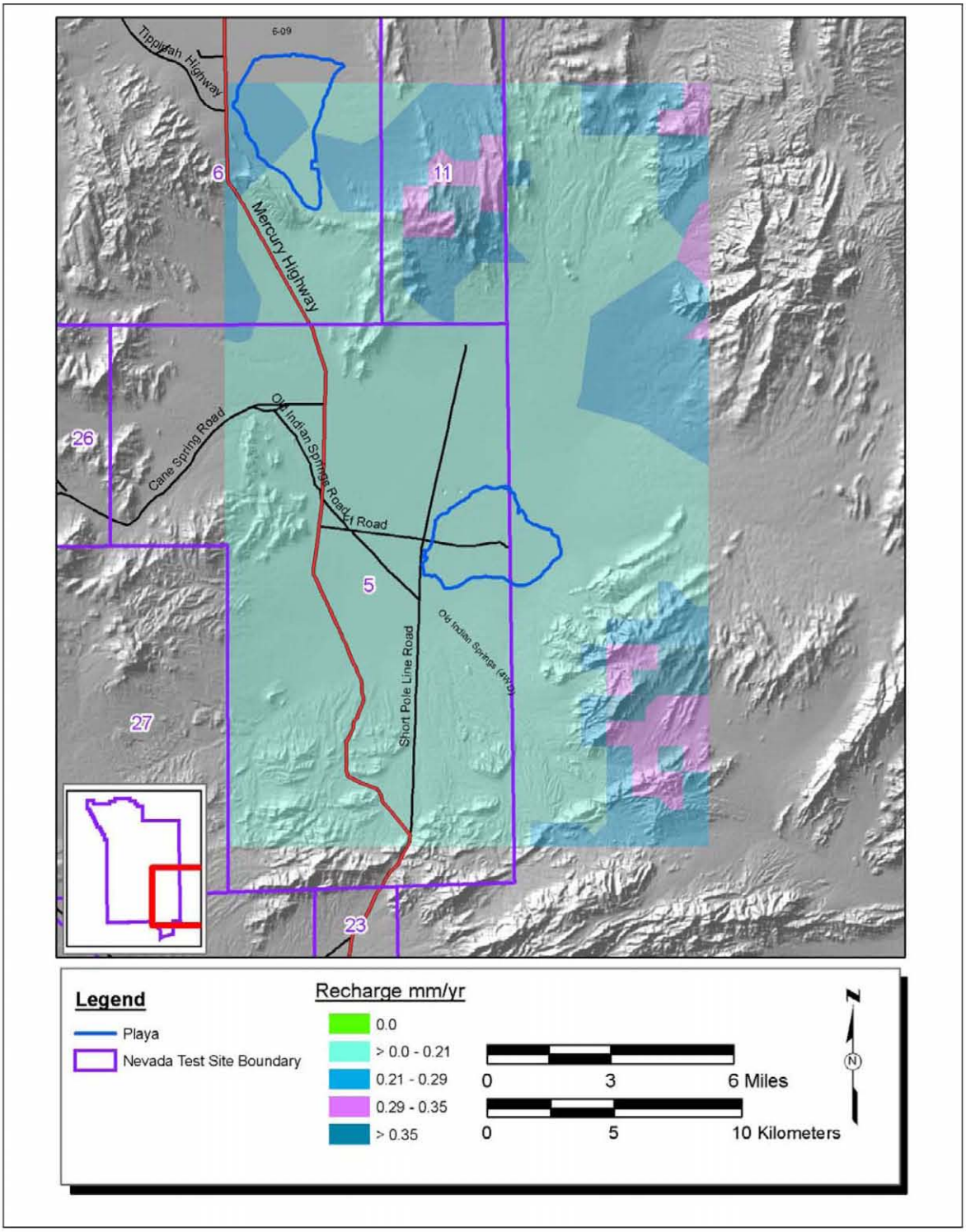

Figure 2-8
DRI Recharge Distribution with Alluvial and Elevation Mask (DRIAE) - Revised Scale

Note: As part of this Addendum, Figure 2-8 replaces the original Figure 2-8 that appears in the *Phase II Groundwater Flow Model for Corrective Action Unit 98: Frenchman Flat, Nevada Test Site, Nye County, Nevada*, S-N/99205--074 (May 2006).

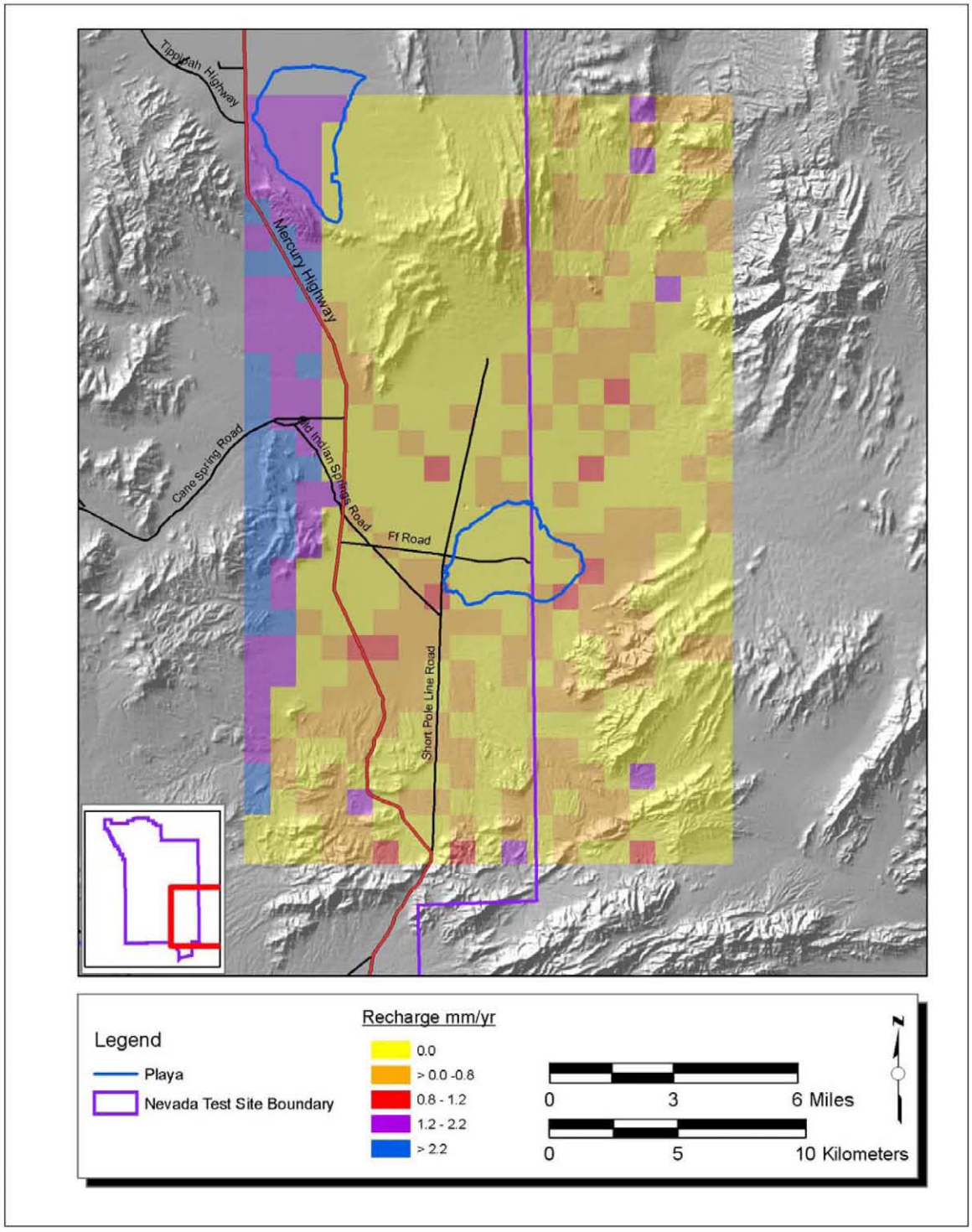

Figure 2-10
Revised UGTA Modified Maxey-Eakin (MME-revised) Recharge Model

Note: As part of this Addendum, Figure 2-10 replaces the original Figure 2-10 that appears in the *Phase II Groundwater Flow Model for Corrective Action Unit 98: Frenchman Flat, Nevada Test Site, Nye County, Nevada*, S-N/99205--074 (May 2006).

2.3.3 Phase II Hydrostratigraphic Framework Model

Following the Frenchman Flat CAIP Addendum (NNSA/NV, 2001) additional characterization work was undertaken. Relevant to the HFM, these activities included the drilling and completion of five new wells in the vicinity of the two testing areas in Frenchman Flat, and geophysical investigations including gravity, ground and aeromagnetic, seismic, and magnetotelluric data. The integrated use of geophysics was suggested by the peer review (IT, 1999a). The well drilling and geophysical investigations contributed new data and information for use in the development of the Phase II HFMs.

The Phase II Frenchman Flat CAU-specific HFM was constructed using EarthVision® (Dynamic Graphics, 2002), a 3-D geologic model building and visualization software package. Input data included drill-hole data, DEM data, and outcrop and fault data from surface geologic maps. Where deemed necessary, the data were supplemented with interpretations in the form of cross sections and structure-contour maps.

The Phase II Frenchman Flat BASE HFM was constructed based on drill-hole and geophysical data collected in the Frenchman Flat model area. The conceptual model is still broadly consistent with the NTS hydrologic system described by Winograd and Thordarson (1975) and Phase I HFM, and consists of a thick, fractured LCA overlain by volcanic rocks that have been depressed and buried by alluvium.

Data collected during the Phase II acquisition clearly show that the basin is deeper than originally depicted in the Phase I HFM. In the vicinity of the underground nuclear test locations in the central portion of Frenchman Flat, the LCA is 1,000 m deeper than estimated in Phase I. In northern Frenchman Flat, near Well Cluster ER-5-3, the LCA is about 380 m deeper in the Phase II HFM (BN, 2005a).

The greater depth to pre-Tertiary rocks (e.g., LCA, UCCU, LCCU) in the Phase II model results in greater thicknesses of the overlying alluvial and volcanic deposits. The alluvium is more than 100 m thicker in the northern portion of the basin, and more than 800 m thicker beneath the central testing area. Likewise, Tertiary-age volcanic rocks are 300 m thicker beneath northern Frenchman Flat and 600 m thicker beneath the central portion of the basin (BN, 2005a).

The Phase II Frenchman Flat HFM area encompasses more than 570 km^2 in the southeastern portion of the NTS. The model area has a north-south length of 30 km and an east-west length of 19 km, and includes geologic units as deep as -5 km amsl (BN, 2005a). Figure 2-11 is an HSU surface map of the Frenchman Flat CAU model domain showing the locations of Well Clusters ER-5-3 and ER-5-4. The wells at both of these locations penetrated Quaternary and Tertiary alluvium to depths of 622.4 m and 1,120.4 m, respectively.

A BASE HFM and four alternative HFMs (different geologic interpretations that are equally consistent with the available data) were developed. The BASE HFM represents the consensus view of the currently most viable model based on existing data. The inherent uncertainty in such a model is recognized and addressed via a suite of models that are equally permissive within the constraints of available data. The primary purpose for establishing a base model is to have a reference point for describing alternative HFMs. Details on the development of the BASE and alternative HFM development, and selection criteria for the alternative HFMs, are documented in A Hydrostratigraphic Framework Model and Alternatives for the Groundwater Flow and Contaminant Transport Model of Corrective Action Unit 98: Frenchman Flat, Clark, Lincoln and Nye Counties, Nevada (BN, 2005a).

2.3.3.1 BASE Hydrostratigraphic Framework Model

This section summarizes the structural features, HGUs, and HSUs of the BASE HFM (the HFM considered most likely based on geologist expert judgement) developed for the Frenchman Flat area and vicinity. Figure 2-11 shows the HSUs at the surface for the Frenchman Flat BASE HFM. A 3-D view of this model is shown in Figure 2-12. Plate 1 shows cross sections through the BASE HFM.

The BASE HFM model includes a total of 71 faults and 17 HSUs (9 aquifers and 8 confining units). The structural elements are typically normal faults (basin and range-style faults) but also includes several strike-slip and older thrust faults. Only faults that were considered to be hydrologically significant were included in the model, which includes the larger faults (those with offsets typically greater than 61 m) and the faults that seem to form significant structural boundaries (Figure 2-13) (BN, 2005a).

value of approximately 755 m (SNJV, 2004d). Well ER-5-4 #2 did not penetrate the LCA, but LCA head measurements within the flow model area suggest heads in the LCA near the ER-5-4 well complex would not exceed 730 m (see Figure 3-6). Therefore, the heads in the LTCU at ER-5-4 #2 are higher than the heads in both the AA and the LCA by at least 20 m.

Because the only known areas near Frenchman Flat with heads of 755 m or higher are to the west in CP basin or the Wahmonie Hills, the high heads in the LTCU at ER-5-4 #2 must be maintained by a strong hydraulic connection between ER-5-4 #2 and one of these areas. This conceptual model is supported by hydrogeologic cross sections through the ER-5-4 well cluster that show the LTCU rising up along the western flanks of the basin in the Wahmonie Hills area (Plate 1). Moreover, to prevent the heads in the LTCU from being dissipated by leakage to the overlying AA or the underlying LCA, groundwater must be moving through the LTCU under relatively confined conditions. This suggests the presence of a fractured welded interval or lava flow within the thick LTCU that is bounded by less permeable zeolitic rock. It also implies the absence of transmissive faults cross-cutting the LTCU over a several kilometer distance between the Wahmonie Hills and ER-5-4 #2. In conclusion, it appears that the LTCU is overpressurized in the central testing area and that high heads in this HSU effectively prevent groundwater movement from the alluvium downward to the LCA.

3.6 Hydraulic Properties

The rate and direction of groundwater flow depends on both the vertical and lateral hydraulic gradients, and on the magnitude, spatial variability, and directional dependence of permeability within the basin. To help develop the conceptual model of how permeability varies within the Frenchman Flat basin, an initial compilation of permeability data from analogous HGUs in the NTS investigation area was completed and compared to more limited data from comparable HGUs in the Frenchman Flat area (SNJV, 2004d). Data were grouped by HGUs — such as the AA, VA, TCU, CCU, and CA — so that data from similar rock types could be considered collectively and compared to the permeability of individual HSUs in the model. Subsequent to that analysis, additional screening, binning, and analysis of hydraulic test data from the NTS area were done for the purpose of estimating likely ranges of permeability for the different rock types present in Frenchman Flat (Appendix E). These data, along with the more limited data from Frenchman Flat, are used to provide

initial guidance on the permeability values assumed in the Frenchman Flat flow model and, later, to help evaluate alternative flow models by comparing the measured and calibrated permeabilities.

Although permeabilities are initially assigned in the model by HSU, other factors influence and modify these permeabilities, including the anisotropy assigned to the HSU, the rate of decrease in the permeability of the HSU with depth, and the permeability modifications induced by faulting. When horizontal permeabilities (k_h) are higher than the vertical permeabilities (k_v), HSUs with higher anisotropy ratios (k_h/k_v) tend to promote lateral flow at the expense of vertical flow under a given hydraulic gradient. Where permeability decreases with depth because of compaction under increasing lithologic loads, there is also an effective anisotropy introduced by this phenomenon that can exert a similar effect on flow directions (Haneberg et al., 1998). Faults provide potential conduits for flow, or can compartmentalize portions of the flow system depending on whether they channelize or block flow, or some combination of the two, depending on the relative anisotropy associated with fault zone structures like gouge zones.

In summary, the permeability distribution in Frenchman Flat is conceptualized as resulting from the superposition of effects controlled by the HGU type, anisotropy, the decay of permeability with depth, and faulting. Therefore, in addition to summarizing HSU permeability data, the following sections provide site-specific data from Frenchman Flat on anisotropy, depth decay in permeability, and fault hydraulic properties. These data are supplemented with discussions of field data or model results from other sites that might serve as appropriate analogs when sufficient site-specific data from Frenchman Flat are not available, or the site-specific data are ambiguous or contradictory.

3.6.1 HSU Permeability Data

Analysis of hydraulic conductivity data considered three distinct datasets based on the scale of the tests. Evaluations consisted of measurement scale (laboratory-scale, slug- and packer-test-scale, and pumping-test-scale), scaling and spatial distribution, vertical anisotropy, and variation due to temperature. Hydraulic conductivity parameters for each HSU are presented at the end of this section. Figure 3-9 shows the locations where the hydraulic property data were obtained in the Frenchman Flat area and vicinity. For the purposes of the Frenchman Flat CAU flow model, the pumping-scale data are the most appropriate (SNJV, 2004d). Slug tests involve the movement of smaller volumes of water through the formation than would be typical for a pumping test. Therefore,

This input is used to modify the reference intrinsic permeability, k_0, initially input and assigned to each node of the HSU.

Depth decay via *fperm* adjustment was computed in a modification of the depth integration described in the UGTA regional model (DOE/NV, 1997) using the following formula, which gives the permeability reduction over a vertical interval defined by $z1$ and $z2$ with depth-decay coefficient λ:

$$fperm = \frac{1}{2.303(-\lambda)} 10^{-\lambda z}\Big|_{z1}^{z2} \qquad (4\text{-}2)$$

Because FEHM determines its control volumes from node locations (unlike the block-centered code used in the UGTA regional model), which also may not necessarily be rectangles or squares, the bounding control volume coordinates were used in the depth-decay calculation. In the case of non-rectangular control volumes, the computed depth decay is approximate because the height of the control volume may not be constant. This was deemed a reasonable approximation in light of the overall uncertainty surrounding the depth-decay process.

4.4.2 Fault Permeability

Faults are also specified by material zones and are specified after the HSUs are defined. However, the material properties associated with the HSU nodes remain assigned to the fault nodes pending another property assignment. The approach to parameterizing the faults is to multiply existing fault node properties (still derived from an HSU) by a permeability factor. Thus, the difficulty that could be encountered by directly assigning a fault permeability that is reconciled with each HSU that it crosses is avoided. For instance, if a fault crosses both aquifers and confining units (which most do) and a fault permeability of 10^{-16} m^2 is assigned to a node with a permeability of 10^{-12} m^2, the aquifer would see the fault as a barrier, but a confining unit with a permeability of 10^{-16} m^2 would see the fault as neutral. This approach tacitly assumes that a fault acts the same in each HSU that it encounters. Some faults (mainly within the Rock Valley fault system) are defined differently within the LCA. In the displacement fault HFM, fault zones are defined separately for the AA than for the rest of the HSUs.

4.5 Boundary Conditions

The solution of the groundwater flow equations requires specification of head and/or flow at the edges and at internal discharge points of the numerical model. This is particularly important for the Frenchman Flat CAU model because the model boundaries do not coincide with natural hydrologic boundaries. The Frenchman Flat CAU model must account for regional inflow and outflow across all four lateral edges and internal flow from precipitation recharge. There are no internal discharge locations within the Frenchman Flat CAU flow model domain. The following sections describe the implementation of these conditions in the Frenchman Flat CAU flow model.

4.5.1 Recharge

Recharge is implemented in the CAU model as a specified flux condition, where a given volume (mass) of water is applied based on the above recharge models. Recharge flux is considered to be constant over time, but it varies over the domain as a function of altitude and soil and vegetation types. To obtain the required model input in mass per time for each top node, recharge flows were calculated as the total mass for each node. Total mass was calculated at each Thiessen polygon defining the contributing area of each node at the top of the FEHM model via geographic information system operations. When two or more nodes are located exactly above each other (a staircase formation), the recharge flux was allocated between these nodes according to their physical location. Figure 2-2 through Figure 2-10 show the resulting recharge distributions for the USGSD, MME, DRIA, and DVRFS datasets, respectively, as implemented for FEHM input. Table 4-5 summarizes the total mass flows over the Frenchman Flat model domain area for each recharge model considered. It must be noted that the amount of recharge over the Frenchman Flat model domain is very small. Differences among the recharge distributions are primarily manifested in the boundary heads and lateral boundary fluxes that are derived from the corresponding calibrated regional model.

Table 5-1
Calibration Components and Implementation

Calibration Component[a]	Implementation in the Frenchman Flat CAU Flow Model
Apply the principle of parsimony.	Hydrostratigraphic units or other geologic properties are not subdivided. Faults are only divided when geologic rationale justified the division.
Include many kinds of data as observations.	Well head and regional model estimated fluxes at the model edges are considered.
Assign weights that reflect measurement errors.	Weights are developed from uncertainty estimates published in the Frenchman Flat hydrologic data document (SNJV, 2004d).
Evaluate model fit.	Model fit is continually evaluated with residual post plots and other tools and statistics.
Evaluate optimized parameter values.	The reasonableness of calibrated model parameters is compared to available measured values.
Evaluate the potential for additional estimated parameters.	Sensitivity analysis and post plots are used to identify locations where additional parameter adjustments are necessary.

[a] Hill, 1998

The PEST code also includes a variety of statistical analyses that help develop understanding of the model. These features include sensitivity and correlation coefficients, parameter confidence limits, and eigenvalue and eigenvector analysis. The sensitivity and correlation coefficients describe how much the model calibration changes relative to a parameter's change, and how parameters may influence one another. This is useful in testing the conceptual model as to what parameters are believed to control model behavior, and what parameters may act similarly on model results. In addition, parameters that may be important to model calibration can be quantitatively identified and considered in more detail. The confidence limits and eigenvalue and eigenvector analysis are useful in understanding how well the measured data support the model parameters, and how many parameters should be considered for calibration.

The ASTM Standard Guide D 5490-93 (ASTM, 1993b) describes several approaches for evaluating the agreement between a flow model and modeled system. These procedures were used in calibrating the Frenchman Flat flow model, and include qualitative and quantitative comparisons between model results and the following:

- Measured heads at wells
- Boundary fluxes from regional models reflecting different recharge models
- Estimated ranges of HSU hydraulic parameters from pumping-scale hydraulic test data

A variety of numerical and graphical tools are used to investigate flow model calibration. These include summary statistical measures such as the mean error *(ME)*, largest and smallest errors, standard deviation (*SD*) of error, and sum of weighted squared error. Error, or residual head $(r_{h,i})$, is defined as follows:

$$r_{h,i} = H_i - h_i \qquad (5\text{-}1)$$

where h_i is the computed head at the location where observed head H_i is measured. A similar definition is used for boundary flux residuals $(r_{f,i})$:

$$r_{f,i} = F_i - f_i \qquad (5\text{-}2)$$

where f_i is the computed flux at a location where the flux from the regional model (F_i) is determined.

Mean error is defined as follows for head residuals (Watermark Numerical Computing, 2004):

$$ME = \Sigma\, w_{h,i}\, r_{h,i} / n \qquad (5\text{-}3)$$

where $w_{h,i}$ is the weight assigned to the head measurement H_i. Standard deviation of error is defined as follows (ASTM, 1993b):

$$SD = [\Sigma\, w_{h,i}\, (r_{h,i} - ME)^2 / \ (n\text{-}1)]^{1/2} \qquad (5\text{-}4)$$

where n is the number of computed and measured heads being compared.

The sum of the weighted errors squared (also called phi, after the Greek alphabet symbol used to denote it, as well as "goodness of fit" or the "objective function") is defined as (Watermark Numerical Computing, 2004):

$$\Phi = \Sigma\, (w_{h,i}\, r_{h,i})^2 \ + \Sigma\, (w_{f,i}\, r_{f,i})^2 \qquad (5\text{-}5)$$

where w_h and w_f are the observation weights assigned to head and flux targets, respectively; and r_h and r_f are defined in equations (5-1) and (5-2).

If the weights assigned to calibration data change, all these measures will change even if the model results are the same. Thus, as discussed in Section 7.2, it is important to compare results using a consistent weighting scheme.

Table 5-3
Initial Intrinsic Permeability (m^2) Reference Values at Land Surface Used in CAU Flow Model Calibration

Frenchman Flat Phase II HSU	Symbol	Number of Observations	Data Analysis Results	
			Mean	Standard Deviation
			Log k_0 (m^2)	
Alluvial Aquifer	AA	17	-8.76	1.67
Older Altered Alluvial Aquifer	OAA	AA (17) [a]	-8.76	1.67
Timber Mountain Welded Tuff Aquifer	TM-WTA	5	-6.86	0.52
Timber Mountain Lower Vitric Tuff Aquifer	TM-LVTA	TM-WTA (5) [a]	-6.86	0.52
Topopah Spring Aquifer	TSA	(VA, 38) [b]	-7.99	1.23
Lower Vitric Tuff Aquifer	LVTA	(VA, 38) [b]	-7.99	1.23
Upper Tuff Confining Unit	UTCU	LTCU (1) [a]	-11.49	N/A
Lower Tuff Confining Unit	LTCU	1	-11.49	N/A
Playa Confining Unit	PCU	(VCU, 110) [b]	-10.63	2.12
Wahmonie Confining Unit	WCU	(VCU, 110) [b]	-10.63	2.12
Volcaniclastic Confining Unit	VCU	(VCU, 110) [b]	-10.63	2.12
Lower Carbonate Aquifer	LCA	5	-8.45	1.28
Upper Clastic Confining Unit	UCCU	(UCCU, 2) [b]	-10.02	1.07

[a] Data mean and range from similar Frenchman Flat HSU listed here.
[b] Data mean and range from NTS-wide pumping-scale conductivity data for the HSU listed here.

Faunt et al. (2004) observed that using conductivity depth decay in the DVRFS model produced some hydraulic conductivity values outside the range of expected values and suggested that this may indicate that hydraulic conductivity does not decrease below a certain threshold. To mitigate this potential problem, the implementation of depth decay in the Frenchman Flat model included setting a minimum possible intrinsic permeability of 10^{-25} m^2 in each HSU.

5.5.1 Initial Parameter Adjustments

Different sets of parameters were considered as adjustable or fixed during the early and late phases of the calibration. In general, most of the calibration effort focused on optimizing HSU permeabilities. In addition, fault permeability factors were also adjusted, as necessary, to match the target boundary fluxes or hydraulic heads. Other types of parameters were adjusted only during the initial

phase of the calibration, after which they remained fixed. Parameters included in this latter category were:

- Permeability depth-decay coefficients for model HSUs (Table 3-6)
- Vertical-to-horizontal anisotropy of HSU permeabilities
- Boundary impedance for aquitard HSUs along the model boundaries.

The depth-decay coefficients for the model were set to the values listed in Table 3-6 in recognition that simultaneously estimating both the reference permeabilities and the depth-decay coefficients would induce correlations that would leave the problem of calibrating the flow model intractable. This is because (1) there is not enough range in the depths of the head measurements in any HSU to constrain the estimate of depth decay the Frenchman Flat basin, and the (2) the permeability at a given depth could be adjusted by mutual changes to either depth decay coefficient or the reference permeability, thus giving rise to an unavoidable correlation in the model parameters.

The vertical-to-horizontal anisotropy ratios were set to unity in the BLFA and LCA, to 0.015 in the LTCU, and 0.5 to all other HSUs. The relatively small value of 0.5 ($k_h/k_v = 2.0$) for most of the HSUs was driven by a recognition that depth decay in permeability also contributed an effective anisotropy to the system, and that stipulating larger values for k_h/k_v would unduly restrict the potential of the model to explore the possibility of vertical leakage between the AA and underlying HSUs. The value of 0.015 (corresponding to a $k_h/k_v = 6.667$) was chosen based on the bedded nature of the tuffs that comprise the LTCU and the need to match the simulated heads in the AA to their measured values.

The last of these parameter types, boundary impedance, is assigned to model boundary nodes in order to maintain heads interpolated from the regional model onto the BASE-USGSD flow model boundary (Zyvoloski et al., 1997a and b). Normally, a large value (10^6 or 10^7) is recommended to achieve this goal. However, in early phases of calibration, anomalously large groundwater fluxes were observed to enter the model along the four lateral boundaries adjacent to various confining units that had been assigned low permeability values. This behavior was in conflict with the expectation that confining units would transmit only small fluxes, and indicated that adjustments to the assigned boundary impedance were necessary. The problem was resolved by assigning a low value of impedance to nodes in confining HSUs when these were present along the lateral boundaries of the model. After initial testing with other values, a value of 10^{-5} was ultimately applied at boundary nodes in the confining units, but several other values were investigated during early phases of the

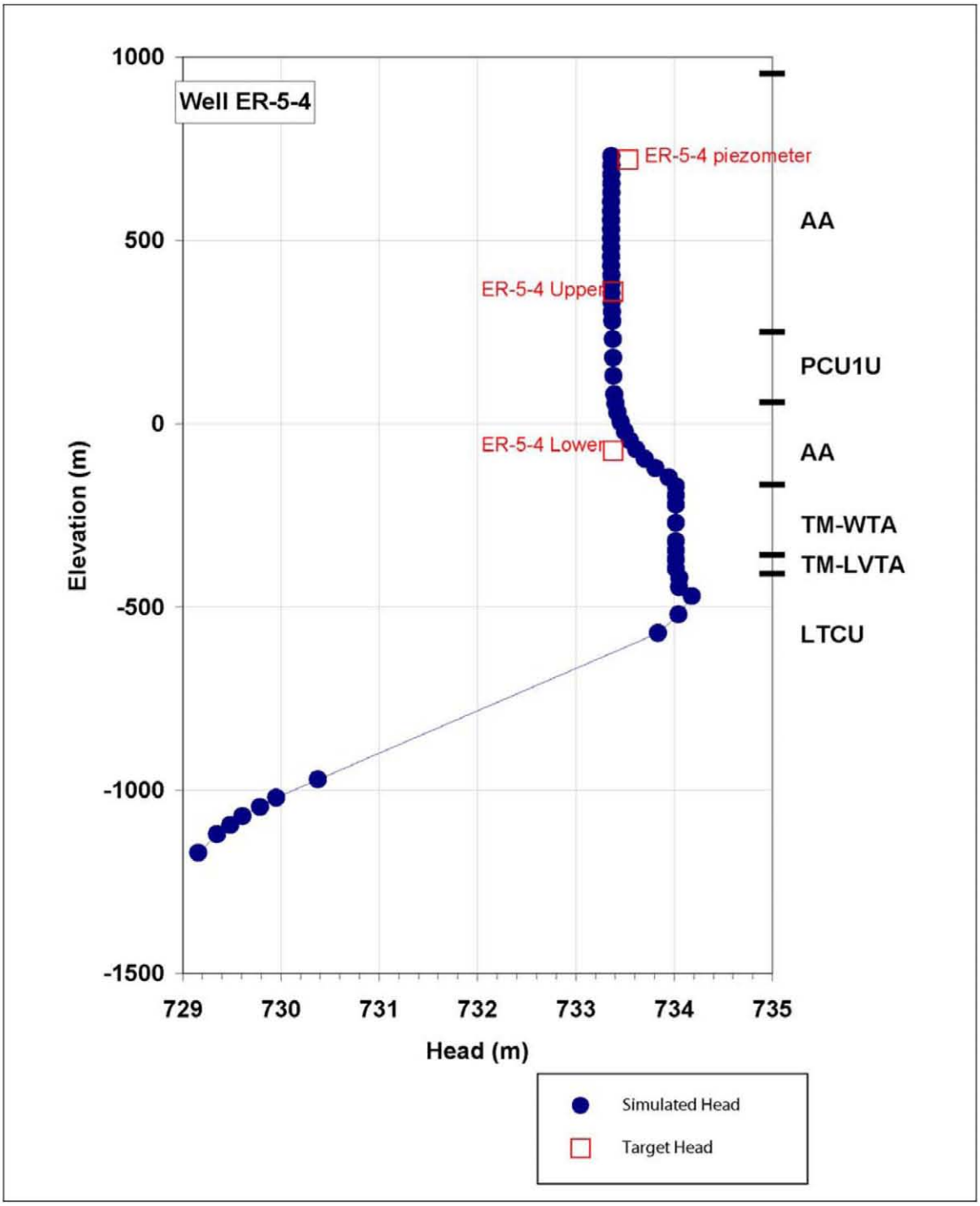

Figure 5-8
Comparison Between Hydraulic Heads Simulated with BASE-USGSD Flow Model and the Calibration Target Heads at the ER-5-4 Well Complex

Note: As part of this Addendum, Figure 5-8 replaces the original Figure 5-8 that appears in the *Phase II Groundwater Flow Model for Corrective Action Unit 98: Frenchman Flat, Nevada Test Site, Nye County, Nevada*, S-N/99205--074 (May 2006).

5.5.3 Hydraulic Head and Flux Residuals

The groundwater fluxes calculated along the perimeter of the Frenchman Flat model domain with the UGTA regional model are compared to the fluxes calculated with the BASE-USGSD flow model in Figure 5-9. The net fluxes calculated by the Frenchman Flat model are in good agreement with the net fluxes calculated with the UGTA model along each of the boundaries (Figure 5-9).

Simulated hydraulic heads are compared to the measured hydraulic heads that were used as calibration targets in Figure 5-10 and plots of posted weighted residuals are shown in Figure 5-11.

Figure 5-10 shows that the simulated heads within Frenchman Flat generally agree with the measured heads to within the estimated uncertainties, but somewhat larger residuals exist at Wells ER-5-3 #2, RNM-1, WW-1, WW-5B and WW-5C, and WW-C and WW-C1.

- The simulated head at Well ER-5-3 #2, completed in the LCA, is higher than the heads measured in the LCA at this well, but lower than heads measured at nearby Wells ER-5-3 (alluvium and tuff) and ER-5-3 #3 (alluvium). This signifies that the observed downward head gradient between the alluvium and LCA in northern Frenchman Flat is captured in the model, but that its magnitude is only one-third to one-half that of the observed vertical gradient.

- The simulated heads at Well RNM-1, completed in the alluvium, are about 2.2 m higher than the heads reported for this well (731.31+/- 1.60) (SNJV, 2004d, Table 8-3); however, because the reported heads at Well RNM-1 are approximately 2.2 m lower than the measured heads at nearby Wells RNM-2, RNM-2s and ER-5-4, it is possible that difficulties in estimating depths in Well RNM-1, which was drilled at an angle into the CAMBRIC test cavity, are primarily responsible for the head residuals at this well. Although the simulated head at RNM-1 is higher than the observed head, the simulated head falls within the error bounds associated with the measurement that reflect the difficulties in obtaining an accurate measurement at RNM-1.

- The simulated head at Well WW-1, completed in the alluvium, is about 1.2 m higher than the head reported for this well (725.25 +/- 4.4 m), but within the error bounds that result from uncertainty in nearby land surface elevation.

- The simulated hydraulic heads at Wells WW-5B and WW-5C, completed in the alluvium, are about 2 m too low and too high, respectively, compared to the measured heads (734.68 +/- 1.15 m and 729.68 +/- 1.29 m) at these wells. The low hydraulic head reported for Well WW-5C compared to heads measured at Well WW-5B to the north and Well WW-5A to the south (730.91 +/- 1.14 m) suggests that there may be a stronger hydraulic connection or

hydraulic barrier between the tuffs and the LCA in the vicinity of Well WW-5C, as originally proposed by Winograd and Thordarson (1975).

- Simulated heads in the LCA at Well WW-C and WW-C1 (both completed in the LCA) in the northwest corner of the Frenchman Flat model (southern Yucca Flat) exceed the measured heads at these wells by about 15 m. These residuals are the result of inaccuracies in the heads taken from the UGTA regional model that were used to assigned heads along the northern boundary of the Frenchman Flat CAU model (Section 5.3). These comparatively large residuals are not expected to significantly impact simulated groundwater movement through the alluvium and tuffs in the Frenchman Flat basin given the small residuals at Wells UE-5 PW-3, UE-5c WW, UE-5f, and UE-11b located on the perimeter of Frenchman Flat basin.

The plot of the weighted residuals associated with the calibrated BASE-USGSD flow model is shown in Figure 5-11. The plot is useful because it provides an indication of how errors in the simulated water levels are distributed throughout the flow model when the weights are also considered. The use of weighted residuals (rather than unweighted residuals) in the figures is appropriate because the weights are calculated from the inverse of the measurement error and therefore reflect the importance that should be place on calculated differences between the measured and simulated heads. Ideally, the distribution of weighted residuals should be randomly distributed and free of trends that would indicate a systematic spatial bias in the model results. Figure 5-11 shows that positive and negative weighted residuals are contained in each region of the flow model, indicating that there is no spatial biases in the simulated heads relative to the measured heads.

Histograms of weighted residuals are sometimes used to determine whether there is a systematic bias in the calibration. Ideally, if the calibration lacks bias towards either overestimating or underestimating the heads, the weighted residuals will be normally distributed around zero. The histogram of weighted residuals from the tuffs and alluvium in Frenchman Flat shows that these residuals are approximately normally distributed around zero (Figure 5-12). The inclusion of residuals from the LCA introduces a negative bias in the residuals because of the relatively large negative residuals at Wells WW-C and WW-C1.

Table 5-4 shows the metrics that characterize the goodness of fit associated with the calibration of the BASE-USGSD flow model. The table lists the mean-weighted error, maximum and minimum weighted residuals, the error variances and standard deviations, and the contributions to the objective function associated with water-level and flux target data in each of the models. The negative

movement into the LCA. Although data do not exist to evaluate the presence of a pressure barrier in the TM-WTA, measured hydraulic heads of more than 754 m in the LTCU at Well ER-5-4 #2 indicate that the concept of a pressure barrier in the central part of Frenchman Flat is feasible. The results of the BASE-USGSD flow model indicate this pressure barrier could arise when high-permeability units like the TM-WTA (or similar lithologies embedded within the thick LTCU) act as confined aquifers and connect the deep parts of the Frenchman Flat basin with areas of higher head to the west.

The permeabilities estimated during calibration of the BASE-USGSD flow model were compared to the data from the general NTS area and from Frenchman Flat. The match between the estimated and measured permeabilities is good in most cases. For some HSUs, such as the AA and the LTCU, the estimated permeabilities were toward the lower end of the observed data range. The effects of increasing the permeability in the AA to bring it into better agreement with the data would be to increase the rate of groundwater movement in the model if the horizontal head gradient were to remain the same. Alternative calibrations with improved matches to AA data are presented in the conceptual model uncertainty analysis (see Section 6.0).

The final permeability field associated with the calibrated models reflects differences among the permeabilities estimated for the different HSUs, the effect of the decay in permeability with increasing depth, and the effects of permeability changes associated with faults. The permeability fields that result from the superposition of these effects can be very complex in some areas, particularly in the northern testing area, where groundwater flow bifurcates, with flow north of a detachment fault flowing east or northeast, and groundwater to the south of the detachment fault flowing predominantly southward. In the central testing area, particle trajectories are toward the southeast. Eventually, all particles initially located beneath the testing areas eventually exit the model through the Rock Valley fault system in the southwest corner of the model.

Table 6-1
List of Priority C Alternative Scenarios for the Frenchman Flat 3-D Hydrostratigraphic Model

Alternative (as described by BN, 2005a)	Comment/Discussion
Subdivide the volcaniclastic confining unit (VCU) in the southern portion of the model	The VCU is dominated by fine-grained clastic rocks and zeolitic tuff. However, lenses of gravel and freshwater carbonate beds have been observed in southern Frenchman Flat where the VCU outcrops. Observation of the outcrop exposures of the VCU and assessments of basin-fill carbonate and gravel deposits show that these deposits are generally of limited thickness and lateral extent, and probably are not a significant component of the VCU. Little is known about the VCU beneath the Frenchman Flat basin, where the VCU is overlain by a thick LTCU. Because the VCU in overlain by a thick LTCU, it is not likely that even large variations of the VCU properties under the Frenchman Flat basin will be of any significance to the resulting flow fields. However, the southern part of the VCU could be examined in further detail by varying model parameters to approximate the occurrence of aquifer-like rocks within the VCU. This was not necessary for calibration of the flow model, suggesting that changes to the VCU flow parameters are unnecessary for representing the flow field within the data constraints.
Add width to faults	The faults are represented in the model using the set of nodes around them. The node spacing depends on the level of discretization and the fault location. In general, these fault nodes are discretized using a finer mesh near the top, and the node spacing increases towards the bottom of the model. This fault representation is conceptual and does not reflect any attempt to model the fault widths. This representation is not likely to have any effect on the flow model results but could have significant effects on the transport model results in terms of travel times required to go through (or across) some of the faults. This could be dealt with during the transport model evaluation by assigning appropriate effective porosity values to the fault nodes that will reflect different fault width values. For example, if a narrow fault width is evaluated, a small effective porosity value can be assigned to the fault nodes.
Represent faults in model as multiple planes	This is similar to the previous alternative.
Vary fault dips for basin and range faults (from the 75 degrees used)	This alternative cannot be reasonably handled by the flow model because the fault locations have a significant effect on the node locations and spacing in the model mesh. However, it can be evaluated in a simplified total system model-context where the flow velocities and directions are obtained from the flow model, and different fault dip angle can be investigated using different fault lengths or distance to fault interception within different HSUs.

As a consequence, these two alternative HFMs did not require further calibration. The similar heads and fluxes produced with the BLFA-USGSD and DETA-USGSD alternatives and the BASE-USGSD models at the target locations do not necessarily mean that the models are identical, but rather that there were no data from locations that could reveal the differences in hydrologic behavior among the models. Pertinent results from the BLFA-USGSD and DETA-USGSD alternatives, and a description of the calibration process and results for the DISP-USGSD and CPBA-USGSD alternatives, are

provided in the following four sections. Table 6-2 summarizes the model parameters used for the final calibration of each alternative HFM.

Table 6-2
Summary of Calibrated Reference Permeability Values and Fault Permeability Multipliers
(Page 1 of 3)

	Hydrostratigraphic Framework Model				
	BASE	**BLFA**	**DETA**	**CPBA**	**DISP**
HSU Permeability at Ground Surface - log (k_0 in m^2)[a]					
AA	-11.30	-11.30	-11.30	-11.15	-10.90
PCU	-14.50	-14.50	-14.50	-14.04	-14.50
BLFA	-12.00	-12.00	-12.00	-12.20	-12.00
OAA	-12.00	-12.00	-12.00	-12.16	-11.40
PCU1L	-11.00	-11.00	-11.00	-14.19	-10.00
PCU1U	-11.00	-11.00	-11.00	-14.19	-11.00
TM-WTA	-9.15	-9.15	-9.15	-10.10	-9.79
TM-LVTA	-9.20	-9.20	-9.20	-9.29	-9.30
UTCU	-14.00	-14.00	-14.00	-14.04	-14.00
TSA	-11.00	-11.00	-11.00	-9.00	-9.75
LVTA	-10.50	-10.50	-10.50	-9.29	-10.50
LTCU	-13.50	-13.50	-13.50	-15.50	-13.20
WCU	-11.88	-11.88	-11.88	-11.50	-11.88
VCU	-13.60	-13.60	-13.60	-13.25	-13.80
LCA3	-11.00	-11.00	-11.00	-11.12	-11.00
UCCU	-13.50	-13.50	-13.50	-14.26	-13.50
LCA	-10.40	-10.40	-10.40	-10.15	-10.35
Fault Permeability Multiplier					
1	0.3	0.3	0.3	1.0	0.2
2	0.5	0.5	0.5	5.0	0.5
3	1.8E-04	1.8E-04	1.8E-04	1.0E-05	4.0E-02
4	1.0	1.0	1.0	0.2	1.0
5	0.5	0.5	0.5	0.2	0.5
6	1.0	1.0	1.0	0.2	1.0
7	1.0	1.0	1.0	5.0	1.0
8	1.1	1.1	1.1	0.2	1.06
9	1.0	1.0	1.0	0.2	1.0
10	0.3	0.3	0.3	0.2	0.29
11	1.0E-05	1.0E-05	1.0E-05	1.0	1.0E-05
12	1.0E-05	1.0E-05	1.0E-05	2.0E-05	1.0E-05
13	1.0	1.0	1.0	0.2	1.0
14	1.0E-05	1.0E-05	1.0E-05	2.0E-05	1.0E-05
15	1.0E-05	1.0E-05	1.0E-05	2.0E-05	1.0E-05
16	5.0E-04	5.0E-04	5.0E-04	1.0	5.0E-04
17	18.0	18.0	18.0	75.0	21.0

Note: As part of this Addendum, Table 6-2 replaces the original Table 6-2 that appears in the *Phase II Groundwater Flow Model for Corrective Action Unit 98: Frenchman Flat, Nevada Test Site, Nye County, Nevada*, S-N/99205--074 (May 2006).

Table 6-2
Summary of Calibrated Reference Permeability Values and Fault Permeability Multipliers
(Page 2 of 3)

	Hydrostratigraphic Framework Model				
	BASE	**BLFA**	**DETA**	**CPBA**	**DISP**
18	15.0	15.0	15.0	1.0	15.0
19	1.0	1.0	1.0	1.0	1.0
20	1.0	1.0	1.0	1.0	1.0
Fault Permeability Multiplier					
21[b]	67.8	67.8	67.8	75.0	67.833
22	1.0	1.0	1.0	5.0	1.0
23	1.0	1.0	1.0	5.0	1.0
24	1.0	1.0	1.0	5.0	1.0
25	1.0	1.0	1.0	5.0	1.0
26	1.0	1.0	1.0	1.0	1.0
27	1.0	1.0	1.0	5.0	1.0
28	1.0	1.0	1.0	5.0	1.01
29	1.0	1.0	1.0	5.0	1.0
30	1.0	1.0	1.0	1.0	1.0
31	1.0	1.0	1.0	1.0	1.0
32	1.0	1.0	1.0	1.0	1.0
33[b]	150.9	150.9	150.9	75.0	150.9
34[b]	155.2	155.2	155.2	75.0	1.96E-03
35	1.0	1.0	1.0	0.1	1.0
36	1.0	1.0	1.0	0.1	1.0
37	1.0	1.0	1.0	0.1	0.99
38	5.0	5.0	5.0	0.1	5.0
39	34.0	34.0	34.0	75.0	94.11
40	1.0	1.0	1.0	0.1	0.1
41	1.0	1.0	1.0	0.1	0.1
42	1.0	1.0	1.0	0.1	0.1
43	1.0	1.0	1.0	0.1	0.1
44	1.0	1.0	1.0	0.1	0.1
45	1.0	1.0	1.0	0.1	0.1
46	10.0	10.0	10.0	1.0	70.0
47	10.0	10.0	10.0	1.0	50.0
48	1.0	1.0	1.0	0.1	0.1
49	1.0	1.0	1.0	0.1	0.1
50	1.0	1.0	1.0	0.1	0.1
51	1.0	1.0	1.0	0.1	0.1
52	1.0	1.0	1.0	0.1	0.1
53	1.0	1.0	1.0	0.1	0.1
54	1.0	1.0	1.0	0.1	0.1
55	1.0	1.0	1.0	0.1	0.1
56	1.0	1.0	1.0	0.1	0.1

Note: As part of this Addendum, Table 6-2 replaces the original Table 6-2 that appears in the *Phase II Groundwater Flow Model for Corrective Action Unit 98: Frenchman Flat, Nevada Test Site, Nye County, Nevada*, S-N/99205--074 (May 2006).

Table 6-2
Summary of Calibrated Reference Permeability Values and Fault Permeability Multipliers
(Page 3 of 3)

	Hydrostratigraphic Framework Model				
	BASE	**BLFA**	**DETA**	**CPBA**	**DISP**
57[b]	31.05	31.05	31.05	75.00	15.50
58[b]	108.39	108.39	108.39	75.00	108.39
59	1.0	1.0	1.0	0.9	1.5
Fault Permeability Multiplier					
60	1.45	1.45	1.45	0.90	1.5
61	0.45	0.45	0.45	0.90	0.45
62	0.82	0.82	0.82	0.90	1.5
63	0.84	0.84	0.84	0.90	0.84
64	0.74	0.74	0.74	0.90	0.74
65	0.93	0.93	0.93	0.90	0.93
66	0.88	0.88	0.88	0.90	1.5
67	0.92	0.92	0.92	0.90	0.92
68	0.98	1.0	1.0	0.9	1.5
69	0.35	0.35	0.35	0.90	0.35
70	1.0	1.0	1.0	0.9	1.0
71	1.0	1.0	1.0	0.9	1.0
72	1.39	1.39	1.39	0.90	1.39
73	1.0	1.0	1.0	0.9	1.5
74	1.0	1.0	1.0	1.0	1.0
75[c]	1.8E+04	1.8E+04	1.8E+04	0.32	1.8E+04
76	1.0	1.0	1.0	1.0	1.0
78	1.0	1.0	1.0	1.0	1.0
79[d]	--	--	--	--	114.11
80[e]	--	--	--	--	6.47E-2

Notes: All listed models used the USGSD recharge data and the associated boundary heads and flows from the UGTA regional model.

[a]The depth decay coefficients were fixed at the mean values reported in Table 3-6 (page 3-38).
[b]The Rock Valley fault system (faults 21, 33, 34, 57, and 58) have different properties only through the LCA. These faults are neutral throughout all other HSUs.
[c]Fault 75 is the northern part of the Cane Spring fault (fault 3).
[d]Fault 79 is only defined for the DISP HFM. It is the part of fault 34 that crosses volcanic HSUs.
[e]Fault 80 is also defined only for the DISP HFM. It is the part of fault 34 within the AA HSU.

Note: As part of this Addendum, Table 6-2 replaces the original Table 6-2 that appears in the *Phase II Groundwater Flow Model for Corrective Action Unit 98: Frenchman Flat, Nevada Test Site, Nye County, Nevada*, S-N/99205--074 (May 2006).

6.3.6 Summary of Hydrostratigraphic Framework Model Conceptual Model Uncertainty Analysis

Steady-state groundwater flow models used to assess conceptual model uncertainty use different HFMs that interpreted aspects of the Frenchman Flat hydrostratigraphy somewhat differently. Each of the HFMs included 17 HSUs, of which 8 were considered as aquifers and 9 as confining units, and more than 70 faults that were included based on their potential hydrologic significance. Each of these HFMs was used in conjunction with a map of recharge for the Frenchman Flat area that was taken from a water-balance model of infiltration and recharge model (designated the USGSD model) originally developed for the regional model area. Each alternative HFM model calibration above documents the final fit along with comparison plots for calibrated and measured permeability. Particle tracks from test locations are also shown.

Independently calibrated models for the BASE-USGSD and CPBA-USGSD models provide generally similar fits for boundary fluxes and simulated heads, with the exception of measured heads at WW-C, WW-C1, WW-4, and WW-4A, where the heads are better simulated by the BASE-USGSD model. Calibration fits are generally superior for the BASE-USGSD model compared to the CPBA-USGSD alternative for multiple statistical parameters that characterize goodness of fit. Particle tracks are generally similar for the northern test area for both models with the exception of particle tracks starting in the vicinity of PIN STRIPE. The DISP-USGSD model calibration indicated that a completely open connection between the alluvium and the LCA is unrealistic, but that modest adjustments to fault parameters allow for a good simulation of water-level observations. The BLFA-USGSD and DETA-USGSD model alternatives were calibrated using the parameters estimated during calibration of the BASE-USGSD model. Both models show similar patterns of particle tracks for the southern testing area compared to the BASE-USGSD model and show some variability in particles tracks compared to the BASE-USGSD model for the northern testing area. The primary differences are in the direction of the particle trajectories and in HSUs traversed along the pathways.

6.4 Discrete Uncertainty Analysis

As with most models covering large areas, considerable parameter uncertainty exists that may have significant effects on the resulting calculations made by the model, but cannot be identified based on model calibration data alone. In the context of the Frenchman Flat CAU flow model, the most relevant results involve the direction and velocity of travel for particles starting near the northern and central underground nuclear tests.

Discrete uncertainty analyses are used to evaluate the effect of these uncertainties on the likely travel paths for particles starting at the northern or central testing areas. As with all particle tracking calculations presented in this report, the calculations are completed assuming that particles do not diffuse and that the medium porosity is uniformly 0.01. This value is arbitrary and does not reflect the effective porosity that will be used to evaluate radionuclide transport. To map the groundwater flow paths, particle tracking is run for 100,000 years, until all reasonably mobile particles have left the flow model domain.

The approach is to define a possible pathway of enhanced or adjusted particle movement resulting from a change in the model parameters. Model parameters are adjusted until the calibration is significantly affected. For example, if a tested scenario involves vertical migration down a specific fault, the vertical permeability multiplier of the fault is increased to the point where the model is unable to simulate water levels around this fault reasonably. Ideally, parameters are adjusted up to the limit of either available data or until plausible limits for the value of the parameter are violated. However, available data for most of the calibrated parameters do not provide reliable upper or lower bounds for most of the parameter values. Therefore, parameter adjustments were made without imposing any bounds until the model-calculated water levels changed by about 1 m or, based on the analysts' judgment that the parameter adjustment was outside the range of observed values for other similar features in the Frenchman Flat flow model. At this point, vertical migration down the selected fault is evaluated.

This approach also addresses other questions related to calibrated model parameter uncertainty. For example, it is not clear whether local vertical or horizontal anisotropy of hydraulic conductivity exists at a critical location that would result in particles (starting near underground nuclear test locations)

Table 6-5
Summary of Calibrated Reference Permeability Values and Permeability Multiplier for Non-Neutral Faults for Calibrated Models with Varying Boundary Conditions
(Page 1 of 4)

Hydrostratigraphic Framework Model and Boundary Conditions								
	BASE-USGSD	**BASE-MME**	**BASE-DRIA**	**BASE-DVRFS**	**CPBA-USGSD**	**CPBA-MME**	**CPBA-DRIA**	**CPBA-DVRFS**
HSU Permeability at Ground Surface - (log k_0 in m^2)[a]								
AA	-11.30	-11.30	-11.20	-11.00	-11.15	-11.15	-10.55	-10.60
PCU	-14.50	-14.50	-14.50	-14.50	-14.04	-14.50	-14.00	-13.50
BLFA	-12.00	-12.00	-12.00	-12.00	-12.20	-12.70	-10.00	-12.00
OAA	-12.00	-11.80	-12.00	-11.80	-12.16	-12.50	-10.98	-11.50
PCU1L	-11.00	-11.00	-14.00	-11.00	-14.19	-11.00	-14.00	-11.00
PCU1U	-11.00	-11.00	-14.00	-11.00	-14.19	-11.00	-14.00	-11.00
TM-WTA	-9.15	-9.15	-9.15	-9.00	-10.10	-7.90	-10.85	-9.00
TM-LVTA	-9.20	-9.25	-9.30	-9.00	-9.29	-7.90	-10.80	-9.00
UTCU	-14.00	-14.00	-14.00	-14.00	-14.04	-14.00	-11.00	-13.00
TSA	-11.00	-11.00	-12.00	-11.00	-9.00	-10.20	-10.20	-11.00
LVTA	-10.50	-10.50	-12.50	-10.50	-9.29	-10.50	-12.50	-10.50
LTCU	-13.50	-13.17	-13.50	-13.50	-15.50	-13.17	-13.00	-13.50
WCU	-11.88	-11.88	-11.88	-11.88	-11.50	-12.66	-11.88	-11.88
VCU	-13.60	-13.10	-13.10	-13.30	-13.25	-13.33	-12.45	-13.06
LCA3	-11.00	-11.00	-11.00	-10.50	-11.12	-11.00	-11.00	-10.50
UCCU	-13.50	-13.50	-14.50	-13.50	-14.26	-13.50	-13.50	-13.50
LCA	-10.40	-9.70	-9.99	-10.74	-10.15	-9.76	-10.00	-10.60
Permeability Multiplier for Faults[b]								
1	0.30	0.30	0.25	0.30	1.03	0.30	0.25	150.00
2	0.50	0.506	0.50	0.52	5.00	0.51	6.00	10.18
3	1.8E-04	1.8E-04	1.8E-04	1.4E-04	1.0E-05	1.8E-04	1.8E-04	1.4E-04
5	0.50	0.50	0.50	0.50	0.20	0.50	0.50	0.50
6	1.00	1.00	1.00	1.00	0.20	1.00	1.00	1.00
7	1.00	1.00	1.00	1.00	5.00	1.00	1.00	1.00
8	1.10	1.06	1.06	1.06	0.20	1.06	1.06	1.06
9	1.00	1.00	1.00	1.00	0.20	1.00	1.00	1.00

Note: As part of this Addendum, Table 6-5 replaces the original Table 6-5 that appears in the *Phase II Groundwater Flow Model for Corrective Action Unit 98: Frenchman Flat, Nevada Test Site, Nye County, Nevada*, S-N/99205--074 (May 2006).

Table 6-5
Summary of Calibrated Reference Permeability Values and Permeability Multiplier for Non-Neutral Faults for Calibrated Models with Varying Boundary Conditions
(Page 2 of 4)

Hydrostratigraphic Framework Model and Boundary Conditions								
	BASE-USGSD	**BASE-MME**	**BASE-DRIA**	**BASE-DVRFS**	**CPBA-USGSD**	**CPBA-MME**	**CPBA-DRIA**	**CPBA-DVRFS**
Permeability Multiplier for Faults								
10	0.29	0.29	0.29	0.29	0.20	0.29	0.29	0.29
11	1.0E-05	1.0E-05	1.0E-05	1.0E-05	1.00	1.0E-05	1.00	1.00
12	1.0E-05	1.0E-05	1.0E-05	1.0E-05	2.0E-05	1.0E-05	1.0E-05	1.0E-05
14	1.0E-05	1.0E-05	1.0E-05	1.0E-05	2.0E-05	1.0E-05	1.0E-05	1.0E-05
15	1.0E-05	1.0E-05	1.0E-05	1.0E-05	2.0E-05	1.0E-05	1.0E-05	1.0E-05
16	5.0E-04	5.0E-04	5.0E-04	5.0E-04	1.00	5.0E-04	1.00	1.00
17	18.00	18.00	18.00	2.00	75.00	40.00	52.00	15.00
18	15.00	15.00	100.00	2.00	1.00	50.00	500.00	50.00
19	1.00	1.00	1.00	1.00	1.00	10.00	1.00	1.00
20	1.00	1.00	1.00	1.00	1.00	10.00	1.00	1.00
21	67.80	27.80	17.70	100.18	75.00	26.80	75.70	180.18
26	1.00	1.00	10.00	1.00	1.00	1.00	100.00	1.00
27	1.00	0.85	1.00	10.00	5.00	0.85	1.00	10.00
28	1.01	1.01	1.01	10.01	5.00	1.01	1.01	10.01
29	1.00	0.42	1.00	1.00	5.00	0.42	1.00	1.00
30	1.00	1.00	10.00	10.00	1.00	1.00	10.00	10.00
31	1.00	1.00	1.00	1.00	1.00	1.00	150.00	50.00
33	150.85	262.07	242.99	150.85	75.00	280.07	242.99	150.85
34	155.25	523.97	191.23	100.99	75.00	523.97	191.23	100.99
35	1.00	1.00	1.00	1.00	0.10	0.10	1.00	100.00
36	1.00	1.00	1.00	1.00	0.10	1.00	1.00	1.00
37	1.00	0.99	0.99	0.99	0.10	0.99	0.99	0.99
38	5.00	1.00	5.00	1.00	0.10	1.00	5.00	1.00
39	34.00	17.29	36.00	2.00	75.00	40.29	52.00	18.00
40	1.00	1.00	1.00	1.00	0.10	1.00	1.00	1.00
41	1.00	1.00	1.00	1.00	0.10	1.00	1.00	1.00
42	1.00	1.00	1.00	1.00	0.10	1.00	1.00	1.00

Table 6-5
Summary of Calibrated Reference Permeability Values and Permeability Multiplier for Non-Neutral Faults for Calibrated Models with Varying Boundary Conditions
(Page 3 of 4)

	Hydrostratigraphic Framework Model and Boundary Conditions						
	BASE-USGSD	**BASE-MME**	**BASE-DRIA**	**BASE-DVRFS**	**CPBA-USGSD**	**CPBA-MME**	**CPBA-DRIA**	**CPBA-DVRFS**
	Permeability Multiplier for Faults							
43	1.00	1.00	1.00	1.00	0.10	1.00	1.00	1.00
44	1.00	1.00	1.00	1.00	0.10	1.00	1.00	1.00
45	1.00	1.00	1.00	1.00	0.10	1.00	1.00	10.00
46	10.00	10.00	12.00	4.35	1.03	50.00	24.00	14.35
47	10.00	10.00	12.00	10.00	1.03	1.00	24.00	10.00
48	1.00	1.00	1.00	1.00	0.10	1.00	1.00	1.00
49	1.00	1.00	1.00	1.00	0.10	1.00	1.00	1.00
50	1.00	1.00	1.00	1.00	0.10	0.10	1.00	10.00
51	1.00	1.00	1.00	0.50	0.10	0.05	1.00	0.25
52	1.00	1.00	1.00	1.00	0.10	1.00	1.00	1.00
53	1.00	1.00	1.00	1.00	0.10	1.00	1.00	1.00
54	1.00	1.00	1.00	1.00	0.10	1.00	1.00	1.00
55	1.01	1.01	1.01	1.01	0.10	0.05	1.01	10.01
56	1.00	1.00	1.00	1.00	0.10	1.00	1.00	1.00
57	31.05	31.05	31.05	31.05	75.00	25.05	31.05	31.05
58	108.39	108.39	112.79	108.39	75.00	50.39	112.79	108.39
59	1.00	2.09	1.00	1.00	0.90	0.19	1.00	1.00
60	1.45	1.45	1.45	1.45	0.90	0.11	1.45	1.45
61	0.45	0.65	0.45	25.00	0.90	1.00	0.45	25.00
62	0.82	0.82	0.82	0.82	0.90	1.00	0.82	0.82
63	0.84	2.00	0.84	100.84	0.90	1.00	0.84	100.84
64	0.74	0.74	0.74	0.74	0.90	1.01	0.74	0.74
65	0.93	0.93	0.93	0.93	0.90	1.01	0.93	0.93
66	0.88	0.88	0.88	0.88	0.90	1.00	0.88	0.88
67	0.92	0.92	0.92	0.92	0.90	1.01	0.92	0.92
68	0.98	0.98	0.98	0.98	0.90	1.01	0.98	0.98

Table 6-5
Summary of Calibrated Reference Permeability Values and Permeability Multiplier for Non-Neutral Faults for Calibrated Models with Varying Boundary Conditions
(Page 4 of 4)

Hydrostratigraphic Framework Model and Boundary Conditions								
	BASE-USGSD	**BASE-MME**	**BASE-DRIA**	**BASE-DVRFS**	**CPBA-USGSD**	**CPBA-MME**	**CPBA-DRIA**	**CPBA-DVRFS**
Permeability Multiplier for Faults								
69	0.35	0.39	0.35	25.00	0.90	1.00	0.35	25.00
71	1.00	1.00	1.00	25.00	0.90	1.00	1.00	25.00
72	1.39	1.40	1.39	1.39	0.90	1.40	1.39	1.39
73	1.00	0.66	1.00	1.00	0.90	1.06	1.00	1.00
75	1.8E+04	1.8E+04	1.8E+04	1.4E+04	3.2E-01	1.8E+04	1.8E+04	1.4E+04
76	1.00	10.00	1.00	1.00	1.00	10.00	1.00	1.00

[a]The depth decay coefficients were fixed at the mean values reported in Table 3-6 (page 3-38).
[b]Faults not shown have a permeability multiplier close to 1 (0.90 to 1.05).

Note: As part of this Addendum, Table 6-5 replaces the original Table 6-5 that appears in the *Phase II Groundwater Flow Model for Corrective Action Unit 98: Frenchman Flat, Nevada Test Site, Nye County, Nevada*, S-N/99205--074 (May 2006).

6.5.7.5 Estimated Groundwater Flow Paths

Figure 6-81 shows the trajectory of particles initially located near test locations in the northern and central testing areas. The particle tracks are colored based on HSU and reflect the advective water movement through the CAU model.

Near the northern test area, particle movement reflected the complex distribution of permeabilities in northern Frenchman Flat. Particles starting beneath the NEW POINT, DERRINGER, DIANA MOON, and MINUTE STEAK test locations indicate movement to the northeast through the OAA and tuffs and to the southeast through the OAA into the AA (Figure 6-81). The flow conditions in the vicinity of these tests are not enhanced due to the properties of nearby faults (see faults 35, 36, 45, 50, 51, 54 and 55), all of which have *fperm* factors of 1 or 0.1 (Table 6-8). The groundwater flow paths seem to be dominated by the influx of water along the northwestern edge of the Frenchman Flat basin-fill units from water moving from CP basin across the Cane Spring fault in the volcanic HSUs.

The trajectory of particles starting near the PIN STRIPE test is eastward within the TSA and LVTA (Figure 6-81). As shown in Figure 6-78, the TSA and LVTA create an arcuate band of higher permeability where they intersect the water table along the northern flank of the Frenchman Flat basin. This band of higher permeability creates a strong hydraulic connection in the model between the higher hydraulic heads in the CP basin to the west and locations beneath the PIN STRIPE test in the northern testing area. The higher hydraulic heads adjacent to the western part of the CP basin (Figures 6-67 and 6-68) cause groundwater to flow eastward through the LTCU toward a major fault in the Rock Valley fault system (fault 33) and enter the LCA.

In the central testing area of Frenchman Flat, groundwater flow is substantially less complex than in the northern testing area. The movement of particles initially located near the water table near the CAMBRIC test cavity and beneath the DILUTED WATERS and WISHBONE test locations indicate that groundwater flow out of the central testing area will be through the alluvium toward the southeast. Eventually, these particles will encounter the Rock Valley fault system and exit the flow system along the southern part of the western boundary of the model.

7.2.4 DETA Hydrostratigraphic Framework Model and USGS with Redistribution Recharge (DETA-USGSD) Model

Similar to the BLFA alternative HFM, the DETA alternative HFM required no changes to the calibrated reference permeability values or fault multipliers from the BASE-USGSD, as discussed in Section 5.6. Changes to the HFM included more continuous and thicker Timber Mountain aquifers (TM-WTA and TM-LVTA), removal of the detachment fault (fault 36), and greater continuity of the TSA. Unlike the enhanced sensitivity seen of the BLFA HSU in the BLFA-USGSD perturbation analysis, no comparable changes in model sensitivity occurred in the DETA analysis for the changed HSUs.

7.2.5 CPBA Hydrostratigraphic Framework Model and USGS with Redistribution Recharge (CPBA-USGSD) Model

Although differences between the BASE and CPBA HFMs were isolated to the CP basin area, the calibration approach for the CPBA flow model was different and produced a different set of reference permeability and anisotropy values and fault multipliers (see Section 6.3.5 for more information). As a result, the flow field is slightly different and the sensitivity analysis reveals a somewhat different model response to parameter adjustments.

Sensitivity to HSU Reference Permeability (k_0)

The objective function is most sensitive within two standard deviations of calibration to the LCA k_0 (see Appendix C, which contains perturbation plots for all model metrics). The sensitivity is dominated by the effect of the LCA on boundary flux (or overall flow direction) (Figure 7-17). The flow model domain is dominated on all edges by the LCA, and the perturbation analysis of the CPBA-USGSD HFM indicates that this flow model is more sensitive to the LCA than for the BASE-USGSD model (Figure 7-3). The boundary flux portion of the objective function, however, is noticeably less sensitive to the TSA k_0 while exhibiting enhanced sensitivity to the AA k_0 (Figures 7-17 and 7-3).

The well portion of the objective function is most sensitive to the LCA k_0 as observed in the BASE-USGSD perturbation analysis (Figure 7-4), but increases to the LCA k_0 in the CPBA-USGSD model result in greater model sensitivity than is observed for the BASE-USGSD model (Figure 7-18). Among the aquitard units, there are three units to which the well portion of the objective function is

sensitive: the VCU, LTCU, and WCU (Figure 7-18). The model sensitivity to the AA is dominated by many of the target wells being in the AA. The model demonstrates no sensitivity to the calibrated OAA k_0 within the four orders of magnitude tested (Figure 7-18). The largest change in model response to HSU k_0 is observed in the volcanic aquifer group (Figure 7-18). In the BASE-USGSD model, changes to the TM-LVTA k_0 have the largest impact to the well portion of the objective function (Figure 7-4); however, in the CPBA-USGSD calibration, the model is most sensitive to the TM-WTA k_0 (Figure 7-18). Additionally, decreasing the reference permeability of the TSA or TM-WTA would have resulted in reducing the well portion of the objective function in the CPBA-USGSD calibration (Figure 7-18). Whereas the BASE-USGSD model is most sensitive to the TM-LVTA, the CPBA-USGSD model exhibited very little sensitivity. The BASE-USGSD model also indicates that increasing the TM-LVTA k_0 results in a larger objective function, but in the CPBA-USGSD model, increasing the TM-LVTA k_0 results in decreasing the objective function.

In general, the sensitivity of the water-table elevation of the AA in the CPBA-USGSD model (Figure 7-19) has similar trends as those observed in the BASE-USGSD model analysis (Figure 7-7). Increasing the AA k_0 results in a decrease in the elevation of the water table (Figure 7-19). Conversely, increasing the Timber Mountain aquifers (TM-LVTA and TM-WTA) and TSA k_0s results in an increase in the AA water-table elevation (Figure 7-19). The water-table elevation of the AA is insensitive to all HSUs interfingered with the AA, including the BLFA, PCU1U, PCU1L, and PCU. Unlike the other volcanic aquitard units, which increase the AA water-table elevation as their reference permeability decreases, decreasing the permeability of the WCU results in a lower water-table elevation. This result is consistent with the observed parameter sensitivity in the BASE-USGSD model.

UE-5 PW-1 can be calculated from the groundwater velocity (v) and the average porosity ($\varphi = 0.36$) using the relationship ($q = v\varphi$) to obtain $q = 0.16$ m/yr.

The second pair of wells to be considered is WW-5b and WW-5c in southern Frenchman Flat (Figure 8-19). These wells were selected for analysis because (1) they are both in the AA, (2) they are separated by only 1,458 m along a southeasterly trajectory in an area where groundwater flow is likely to be southeastward because of an increasing component of flow from the Wahmonie Hills or CP basin, and (3) their relative ages and chemical evolution suggest that groundwater flow from WW-5b to WW-5c is possible (Figure 8-7). Based on the difference in the corrected DI14C ages of groundwater at WW-5c and WW-5b (23,147 years – 15,677 years = 7,470 years) and their distance between the wells, the average groundwater velocity is 0.20 m/yr (Table 8-4). Thus, groundwater in the alluvium near the central testing area would travel approximately 210 m in the next 1,000 years. By a similar calculation as outlined in the previous paragraph, the groundwater flux in the alluvium is estimated to be 0.072 m/yr. The PHREEQC models described in Section 8.7.2 indicated that groundwater at Well ER-5-4 could evolve either by the evolution of groundwater flowing south from Well PW-1, or by the evolution of groundwater flowing southeast from UE-5c WW. The distances and age differences between these combinations of wells lead to estimates of groundwater velocity between Well PW-1 and ER-5-4 of 0.19 to 0.25 m/yr and a groundwater velocity between Wells UE-5c WW and ER-5-4 of 0.12 to 0.85 m/yr.

Groundwater velocities were calculated between Wells UE-5 PW-1 and WW-1. These wells were selected because of the southeastward trajectory of particles leaving the central testing area in many of the flow models described in Section 4.0 and this combination of wells best approximated that trajectory. An average age of 17,200 years was used for the groundwater at WW-1 based on the ages estimated from the Ca and Na concentrations in Section 8.5.3. The groundwater velocity of 1.06 m/yr estimated for this combination of wells (Figure 8-19 and Table 8-4) is higher than the velocities estimated for the other well combinations. This velocity estimate is subject to greater uncertainty than velocities estimated for other flow paths because the age of groundwater at WW-1 was estimated indirectly.

The PHREEQC models presented in Section 8.7.3 interpreted the composition of groundwater at Well ER-5-4 #2 to result through the evolution of a groundwater mixture that included groundwater

from Wells WW-4 and UE-5c WW. Using the mixing fractions estimated in the inverse model for Well ER-5-4 #2 (Figure 8-16) and the DIC and ^{14}C activities at each well in the mixture, a ^{14}C activity for the mixture was calculated (11.1 pmc). Using the decay equation (8-5) with these values (adjusted using a qDIC factor to account for dolomite dissolved in the inverse models) yielded travel times of 8,340 to 8,380 years. When combined with average upgradient location of the mixture calculated from the coordinates of the mixing end-members and their fractions of the mixture, these travel time estimates yielded a groundwater velocitiy of 0.60 m/yr. The groundwater velocity estimated from this analysis is shown in Figure 8-20.

Table 8-4
Estimated Groundwater Travel Times and Velocities

Well #1	Well #2	Distance (m)	Travel time (years)	Velocity (m/yr)
UE-5 PW-2	UE-5 PW-1	1,430	3,304	0.43
WW-5b	WW-5c	1,458	7,470	0.20
UE-5c WW	ER-5-4	1,909	2,321 to 15,712	0.12 to 0.85
UE-5 PW-1	ER-5-4	3,250	13,109 to 17,207	0.19 to 0.25
UE-5 PW-1	WW-1	5,972	5,631	1.1
WW-4 and UE-5c WW	ER-5-4 #2	5,010[a]	8,340 to 8,380	0.60

[a]The distance between ER-5-4 #2 and the upgradient wells in the mixture was estimated using mixing-fraction-weighted coordinates of the upgradient wells.

m = Meter
m/yr = Meters per year

An interesting result associated with this analysis is that when the travel times of 8,340 to 8,380 years to Well ER-5-4 #2 are added to the age calculated for the upgradient mixture using the average $DI^{14}C$ ages listed in Table 8-1, an average age of 26,000 years is obtained for the ER-5-4 #2 groundwater. This age is similar to the age of 33,000 years calculated from the cation concentrations in the groundwater at Well ER-5-4 #2, and supports the concept that groundwater at ER-5-4 #2 is quite old.

8.9 Summary and Conclusions

Groundwater ^{14}C data from the tuffs and alluvium in Frenchman Flat were used to calculate ages (residence times) for these groundwaters. The analysis of ^{14}C associated with the DIC ($DI^{14}C$) considered the effects of calcite dissolution and isotope exchange on the groundwater $DI^{14}C$ through two simple correction methods that estimated the dilution of 14C originally in the groundwater recharge. The two correction methods yielded estimates of groundwater ages that were in good

between the alluvial aquifers and the carbonate aquifer occurs across the thick confining units like the VCU and LTCU that line the bottom and flanks of Frenchman Flat basin.

The permeabilities estimated during calibration of the BASE-USGSD flow model were compared to the data from the general NTS area and Frenchman Flat. The match between the estimated and measured permeabilities was satisfactory in most cases. For AA, the estimated permeability was toward the lower end of the observed data range. The effects of increasing the estimated permeability in the AA to bring it into better agreement with the data would be to increase the lateral rate of groundwater movement in the model if the horizontal head gradient were to remain the same. However, with these increases in horizontal permeability of the AA, it is likely that either greater anisotropy or depth decay would be required, thus limiting vertical migration even further.

The simulated heads in the AA matched the head data with a high degree of accuracy and correctly simulated the near-absence of both vertical and lateral gradients within the AA indicated in the data. A comparison of measured heads at the ER-5-3 well complex with a vertical profile of simulated heads produced with the BASE-USGSD flow model indicated that both measured and modeled vertical head gradients are virtually non-existent between the alluvium and the underlying volcanic aquifers near the ER-5-3 well complex. Therefore, there seems to be very little potential for downward flow in the alluvium in the northern testing area, despite the overall drop in heads between the alluvium and the LCA. The data and the model results indicated that most of the head loss between the alluvium and the carbonate aquifer occurs across the thick confining units, like the LTCU, that are present beneath the northern testing area. A similar comparison between measured and simulated heads at the ER-5-4 well complex indicates that simulated heads in the BASE-USGSD model again accurately depict the near-constant heads in the alluvium. Again, this would suggest that there is very little downward gradient through the alluvium that would create downward flow in the central testing area. Simulated heads show an almost 1-m increase between the lower alluvium and the TM-WTA, creating a pressure barrier that would also prevent groundwater movement into the LCA. Although data do not exist to evaluate the presence of a pressure barrier in the TM-WTA, measured hydraulic heads of more than 754 m in the LTCU at Well ER-5-4 #2 indicate that the concept of a pressure barrier in the central part of Frenchman Flat is feasible. The results of the BASE-USGSD flow model indicate the this pressure barrier could arise when high-permeability units

like the TM-WTA (or similar lithologies embedded within the thick LTCU) act as confined aquifers and connect the deep parts of the Frenchman Flat basin with areas of higher head to the west.

The distribution of HSUs, combined with the superimposed effects of faults and depth decay of HSU permeability serves to create an extremely complex distribution of permeability within the model that results in a correspondingly complex flow field. Flow patterns in the northern testing area, identified from particle tracks, show that large contrasts in the permeability among the HSUs results in groundwater flow focused into certain units and around other HSUs. The geometry of the HSUs and their estimated permeability cause groundwater flow to bifurcate in the northern testing area, with flow north of a detachment fault flowing east or northeast, and groundwater to the south of the detachment fault flowing predominantly southward. In the central testing area, where the shallow hydrostratigraphy is considerably simpler, groundwater flow is toward the southeast. From particle tracking, it appears that most of the shallow groundwater flowing beneath the testing areas eventually exits the model through the Rock Valley fault system in the southwest corner of the model.

A sensitivity analyses using local techniques where all parameters are adjusted slightly over their range of uncertainty and perturbation analysis where parameters are changed significantly by multiple standard deviations or orders of magnitude were used to evaluate the influence of the model parameters on the model response. The perturbation analysis varied properties of HSUs and faults over their range of uncertainty, providing a comprehensive picture of model behavior (although this analysis does not evaluate changes to other model parameters that may be required to maintain model calibration when a selected parameter is perturbed). From these detailed sensitivity studies, considerable insight has been gained about the factors that influence the flow model's ability to match the target water levels and boundary fluxes, and, in the process, insight about the factors that influence the overall behavior of the groundwater flow system.

Faults in the Rock Valley fault system are the dominant features in the LCA underlying Frenchman Flat and exert significant control on the direction of regional groundwater movement. The faults in the Rock Valley fault system are assumed not to propagate upward into the alluvial or volcanic units in the BASE-USGSD flow model. The effect of the Rock Valley fault system on the water levels at target well locations was modest. Faults located in the central portion of the basin appear to decrease

Calibration of an alternative BASE-USGSD flow model with permeability depth decay applied to volcanic and carbonate units, but not to the alluvium, was generally successful in matching the available head data within the constraints of the field-scale permeability data. However, model calibration did require higher values of anisotropy (than the BASE-USGSD with permeability depth decay) in the OAA and AA and similar values for horizontal permeability, nearly eliminating any vertical flow in the most shallow portion of the AA and OAA. The BASE-USGSD model with constant permeability in the AA and OAA has similar flow paths to other models used to bound conceptual model uncertainty of the Frenchman Flat flow system. Thus, while there is uncertainty in the applicability of depth decay in the AA and OAA (the HSUs into which most of the underground nuclear test radionuclide source will be applied) as well as the value of the depth decay coefficients, the parameters required to calibrate the flow model in the absence of such effects do not greatly change the direction of groundwater movement. In the areas near the underground nuclear testing, the model tends to overpredict heads in the tuff confining units and the LCA while underpredicting heads at the edges of the basin-fill units. Assessment of radionuclide transport using realistic transport parameters will consider variability in the conceptual model of the flow system provided by this model calibration.

The steady-state groundwater flow models that were used to assess conceptual model uncertainty of the Frenchman Flat groundwater flow system demonstrated that shallow groundwater flow near the testing areas is similar in these models despite considerably different hydrostratigraphy, approaches to defining boundary conditions, discrete HSU and fault permeability changes, and methods of model parameterization. All of the models evaluated demonstrated that the shallow flow system had lateral migration with only modest vertical flow until particles reached the edges of the basin. Upon reaching the edge of the basin, particles moved from the VCU or LTCU into the LCA and exited the flow system through the regional, Rock Valley fault system. To maintain higher heads in the basin-fill HSUs, compared to the lower heads present in the LCA, the calibrated head fields showed regions of higher head occurring in the volcanic HSUs. The presence of these high head zones in the volcanic HSUs effectively separates the shallow flow system from the regional flow system. Attempts to increase the vertical flow through the center of the basin by both decreasing and eliminating depth decay of permeability demonstrated that vertical flow was unlikely based on the need to increase anisotropy and decrease HSU permeability. Additionally, attempts to create a connection between the alluvial and volcanic aquifers and the LCA across a basin-bounding fault in the DISP alternative

indicated that this hydrologic connection could not be maintained without a reduction in fault permeability. In this alternative a good match to heads in the area adjacent to Frenchman Lake playa was achieved through a reduction in fault permeability in the basin-fill materials.

The flow models demonstrated that the AA and OAA of Frenchman Flat basin are fed by water originating in CP basin and the Wahmonie Hills. The proportion of flow from either of these areas is highly uncertain, but through the application of two regional models and several sets of boundary conditions the relative magnitude of water entering the basin from these two areas was varied.

Overall, conceptual model uncertainty analyses indicate that groundwater flow in Frenchman Flat basin near the northern testing area tends to be north to south or northwest to southeast for flow paths near NEW POINT, DERRINGER, DIANA MOON, and MINUTE STEAK test locations. Water flows through the OAA and BLFA into the AA and TM-WTA and moves to the southeast until reaching the basin edge. The groundwater flow paths seem to be dominated by the influx of water moving across the Cane Spring fault in the volcanic HSUs and into the basin-fill units along the northwest edge of the Frenchman Flat basin.

Along the northern edge of the basin, water flows eastward within the TSA and LVTA. These units form an arcuate band of higher permeability where they intersect the water table along the northern flank of the Frenchman Flat basin. This band of higher permeability creates a strong hydraulic connection in the model between the higher hydraulic heads in the CP basin to the west and locations beneath the PIN STRIPE test.

In the central testing area of Frenchman Flat, groundwater flow is substantially less complex than in the northern testing area. The movement of particles initially located near the water table near the CAMBRIC test cavity and beneath the DILUTED WATERS and WISHBONE test locations indicate that groundwater flow out of the central testing area will be through the alluvium toward the southeast.

As a means to independently verify the flow paths generated by the Phase II Frenchman Flat CAU flow model, groundwater ^{14}C data from the tuffs and alluvium in Frenchman Flat were used to calculate ages (residence times) for these groundwaters. The calculated DI^{14}C ages of Frenchman Flat groundwater ranged from ~ 8,500 years to ~ 29,000 years. In general, younger groundwater is found

Beven, K., and J. Freer. 2001. "Equifinality, Data Assimilation, and Uncertainty Estimation in Mechanistic Modelling of Complex Environment Systems Using the GLUE Methodology." In *Journal of Hydrology, 249,* 11-29.

Blankennagel, R.K., and J.E. Weir, Jr. 1973. *Geohydrology of the Eastern Part of Pahute Mesa, Nevada Test Site, Nye County, Nevada*, Professional Paper 712-B. Denver, CO: U.S. Geological Survey.

Bright, D.J., S.A. Watkins, and B.A. Lisle. 2001. *Analysis of Water Levels in the Frenchman Flat Area, Nevada Test Site,* Water-Resources Investigations Report 00-4272. Denver, CO: U.S. Geological Survey.

Budd, D.A. 2001. "Permeability Loss with Depth in the Cenozoic Carbonate Platform of West-Central Florida." In *American Association of Petroleum Geologists*. Bulletin v. 85: (7): 1253-1272.

Burton, W.C., L.N. Plummer, E. Busenberg, B.D. Lindsey, and W.R. Gburek. 2002. "Influence of Fracture Anisotropy on Ground-Water Ages and Chemistry, Valley and Ridge Province, Pennsylvania." In *Ground Water* v. 40: 242-257.

Byers, F.M., Jr., and C.H. Miller. 1966. *Geologic and Geophysical Log of the Ue5k Exploratory Hole, Frenchman Flat, Nevada Test Site,* USGS Technical Letter NTS-164. U.S. Geological Survey.

Caine, J.S., J.P. Evans, and C.B. Forster. 1996. "Fault Zone Architecture and Permeability Structure." In *Geology*, v. 24(11): 1025-1028.

Carle, S. F., M. Zavarin, and G. Pawloski. 2002. *Geostatistical Analysis of Spatial Variability of Mineral Abundance and Kd in Frenchman Flat, NTS, Alluvium*. Livermore, CA: Lawrence Livermore National Laboratory.

Carr, W.J. 1974. *Summary of Tectonic and Structural Evidence for Stress Orientation at the Nevada Test Site*. Open File Report, 74-176, U.S. Geological Survey.

Cashman, S., and K. Cashman. 2000. "Cataclasis and Deformation-Band Formation in Unconsolidated Marine Terrace Sand, Humboldt County, California." In *Geology*, v. 28(2): 111-114.

Clark, I.D., and P. Fritz. 1997. *Environmental Isotopes in Hydrogeology.* Boca Raton, FL: Lewis Publishers.

Crowe, B.M. 1990. *Basaltic Volcanic Episodes of the Yucca Mountain Region*, Preceding of the International Meeting on High-Level Radioactive Waste Management, American Nuclear Society, 65-73. Las Vegas, NV.

Cullen, A.C., and H.C. Frey. 1999. *Probabilistic Techniques in Exposure Assessment*. New York, NY: Plenum Press.

DOE, see U.S. Department of Energy.

DOE/NV, see U.S. Department of Energy, Nevada Operations Office.

DOE/ORD, see U.S. Department of Energy, Office of Civilian Radioactive Waste Management, Office of Repository Development.

D'Agnese, F.A., C.C. Faunt, A.K. Turner, and M.C. Hill. 1997. *Hydrogeologic Evaluation and Numerical Simulation of the Death Valley Regional Ground-water Flow System, Nevada and California,* Water-Resources Investigations Report 96-4300. Denver, CO: U.S. Geological Survey.

Davis, S.N., S. Moysey, L.D. Cecil, and M. Zreda. 2003. "Chlorine-36 in Groundwater of the United States: Empirical Data." In *Hydrogeology Journal* v. 11: 217-227.

Davisson, M.L., D.K. Smith, J. Kenneally, and T.P. Rose. 1999. "Isotope Hydrology of Southern Nevada Groundwater: Stable Isotopes and Radiocarbon." In *Water Resources Research,* vol. 35 (1): 279-294.

Dynamic Graphics, Inc. 2002. *EarthVision® 7: Software for 3-D Modeling and Visualization*. Alameda, CA.

Edmunds, W.M., and P.L. Smedley. 2000. "Residence Time Indicators in Groundwater: The East Midlands Triassic Sandstone Aquifer." In *Applied Geochemistry*, v. 15: 737-752.

EPA, see U.S. Environmental Protection Agency.

FFACO, see *Federal Facility Agreement and Consent Order.*

Fabryka-Martin, J., S.J. Wightman, W.J. Murphy, M.P. Wickham, M.W. Caffee, G.J. Nimz, J.R Southon, and P. Sharma. 1993. *Distribution of Chlorine-36 in the Unsaturated Zone at Yucca Mountain: An Indicator of Fast Transport Path*s. Paper presented at FOCUS'93 Site Characterization and Model Validation. Las Vegas, NV.

Faunt, C.C., J.B. Blainey, M.C. Hill, F.A. D'Agnese, and G.M. O'Brien. 2004. "Transient Numerical Model," Chapter F, pp. 265-352. In *Death Valley Regional Ground-Water Flow System, Nevada and California*- Hydrogeologic Framework and Transient Ground-Water Flow Model, Belcher, W.R., ed., Scientific Investigations Report 2004-5205. As accessed at http://water.usgs.gov/pub/sir/2004/5205/on 28 October 2005.

Federal Facility Agreement and Consent Order. 1996, as amended. Agreed to by the State of Nevada, the U.S. Department of Energy, and the U.S. Department of Defense. Appendix VI,

permeability decreasing with increasing depth. The data showed a trend but also a large scatter. A straight-line approximation on the log-permeability/linear-depth plot (representative of an exponential relationship) showed up to about four to five orders of magnitude decrease in permeability to depths of about 17,000 ft.

A quasi 3-D groundwater model of the Denver basin and adjacent Mid-Continent region was developed by Belitz and Bredehoeft (1988) that found a regional trend of east-to-west decreasing permeability with east-to-west increasing depth for the Dakota and basal sandstones. In the first modeling phase, which included the Dakota and basal Cretaceous sandstone layer, three different permeability-depth relationships (log-permeability versus depth, log-permeability versus log-depth, and log-permeability versus depth) were used. The best model results were obtained using the log log-permeability versus depth relationship:

$$log\ log\text{-}k \sim depth \qquad (B\text{-}10)$$

Belitz and Bredehoeft (1988) originally proposed the log log-permeability versus depth relationship and noted that many researchers find a correlation between log-permeability and porosity and log-porosity and depth. Three functional relationships were illustrated graphically to depths of about 13,000 ft with permeability decreasing by about three orders of magnitude over the depth range. Also, depth-dependent hydraulic conductivity was incorporated into the groundwater model for the overlying Cretaceous shales using a log-permeability versus depth relationship. In the final modeling phase, which included the Dakota and basal sandstones overlying Cretaceous shales and underlying Paleozoic and Mesozoic sedimentary strata, the best match was obtained between observed and simulated potentiometric surfaces when the hydraulic conductivities of all lithologic units in the model were made dependent on depth. The same log log-permeability versus depth function was used for all lithologies, which resulted in a decrease in permeability of three orders of magnitude for depths up to about 10,000 ft.

Williams and Narasimhan (1989) developed a mathematical model to study the effects of hydrothermal circulation on heat flow along the San Andreas Fault and its effect on the state of stress on the fault for three cases (San Francisco peninsula, Cholame Hills, and San Gabriel Mountains/Mojave Desert) designed to investigate the effects of topography on the regional

groundwater flow system and heat flow. They chose an exponential relationship for permeability versus depth over 15 km of the form:

$$k = 10^{-(0.20\,Z + 15)} \qquad (B\text{-}11)$$

where:

k = Permeability (m^2)
Z = Depth (km)

Williams and Narasimhan (1989) included fault zone permeabilities of either 7.5 x 10^{-17} m^2 or 4 x 10^{-17} m^2 for the upper 5 km and decreasing exponentially with depth below 5 km. Simulation results for these cases that included the topographic effects on regional groundwater flow provided fair to reasonable matches to regional heat flow measurement profiles normal to the fault.

A calibrated regional-scale groundwater flow model for the Culebra dolomite at the Waste Isolation Pilot Plant site in southeastern New Mexico was developed by Lavenue et al. (1990). The depth of the Culebra dolomite, varying from about 8 to 420 m at well locations, exhibits an increasing trend from west to east across the modeled region. The initial kriged and the final calibrated transmissivity (or hydraulic conductivity) fields show a pronounced decrease in transmissivity (about seven orders of magnitude) from west to east. The reduction in transmissivity is the result of increased burial depth and reduction in fracturing that results when halite layers are removed by post-depositional dissolution from either above or below the Culebra dolomite layer. Regional dissolution is greatest in the west and decreases eastward as shown by an increase in the number and thickness of the halite beds.

Domenico and Schwartz (1990) discuss the physical and chemical changes that sediments undergo because of increases in overburden pressure and temperature, and chemical interaction between minerals and migrating porewater subsequent to the progressive burial of sediments in depositional environments. It was indicated that there is a reduction in porosity from compaction and pressure solution (grain dissolution at grain-to-grain contacts). There is also deformation from pressure solution accompanying basin loading and driven by the same stress that causes closer grain packing. A figure is presented that shows a relationship of porosity reduction as a function of increasing depth

for shales and sandstones, noting, "Whatever the mechanism, the reduction of porosity causes a rather large reduction in permeability."

An evaluation of hydraulic conductivities from 1,500 aquifer-test analyses and more than 5,000 specific-capacity data is presented by Prudic (1991) from wells in sediments of the Gulf Coast region in the south-central United States. Additionally, the hydraulic conductivity of an unconsolidated sediment should decrease with depth because of sediment compaction from increasing overburden pressure. The depths of the middle of the screened test intervals varied down to depths below 3,000 ft. Analyses were performed to evaluate correlation between geographic areas, geologic layer, and depth to screen midpoint, and functional relationships were developed exhibiting decreasing hydraulic conductivity with depth for 31 of 42 area-layer combinations. The functional relation was of the form:

$$K = C / 10^{\lambda D} \qquad (B\text{-}12)$$

where:

K = Hydraulic conductivity
C and λ = Constants
D = Depth

The sediments of the Gulf Coast region in the south-central United States were also studied by Kuiper (1994), who found that the hydraulic conductivity of the coarse-grained sediments decreased with depth due to decreasing porosity and increased due to decreased viscosity resulting from higher temperatures, with a net effect of decreasing hydraulic conductivity with depth. A functional relationship was provided that represented decreasing sand hydraulic conductivity with depth based on the data from Loucks et al. (1986) of the form:

$$K = C_1\, 10^{-0.8dd} \qquad (B\text{-}13)$$

where:

K = Hydraulic conductivity (L/T) with L = length and T = time
C_1 = Constant
dd = depth (km)

Kuiper (1994) stated that the hydraulic conductivity of the fine-grained sediments or clays tended to decrease with increasing depth as a consequence of compaction and provided a clay hydraulic conductivity-depth relationship:

$$K = C_2 10^{(-1.167dd + 0.0833dd^2)} \qquad (B\text{-}14)$$

where C_2 is a constant.

Kuiper provided plots of the data (which showed a large amount of scatter about the trend line) and the functional relationships for the coarse- and fine-grained sediments, with hydraulic conductivity variations of about five and three orders of magnitude, respectively, for depths up to about 17,000 ft. A multiple-regression methodology was used to calibrate several groundwater flow models of the regional Gulf Coast aquifer system.

A groundwater investigation of the Austin chalk of North-Central Texas was conducted by Mace and Dutton (1994), who found that groundwater flow is controlled by fractures that decline in intensity with depth. They presented a data plot of log-hydraulic conductivity versus linear-depth that showed a corresponding decline in hydraulic conductivity with depth (data to about 380 m depth). Mace (1998) presented additional data and evaluations from the same study area to a depth of about 150 m for weathered and unweathered chalk. A data plot provided a log hydraulic conductivity versus linear-depth fitted with the exponential functional relation:

$$K = 10^{-4.35 \log(d/3.28)} \qquad (B\text{-}15)$$

where:

K = Hydraulic conductivity (m/day)
d = Depth (m)

Hydraulic conductivity data varied over about eight orders of magnitude in both the Mace and Dutton (1994) and Mace (1998) investigations. The larger hydraulic conductivities at shallower depths were attributed to unloading and weathering, resulting in increased fracturing.

A calibrated regional groundwater flow model of the NTS and vicinity was developed by DOE/NV (1997), in which site-specific data were used to develop relationships between hydraulic conductivity and depth for each of the three rock types that form the major aquifers (alluvial, volcanic, and

carbonate). A linear trend in the logarithm of hydraulic conductivity, with increased depth, was expressed as:

$$K_{depth} = K_h \, 10^{-\lambda d} \qquad (B\text{-}16)$$

where:

K_{depth} = Horizontal hydraulic conductivity at a specified depth (L/T) with L = length and T = time
K_h = Horizontal hydraulic conductivity at land surface (L/T)
λ = Hydraulic conductivity decay coefficient (1/L)
d = Depth from land surface (L)

This hydraulic conductivity depth-decay functional relation is the same type as that previously adopted by Prudic (1991) and Kuiper (1994). The site-specific hydraulic conductivity versus depth data showed a large amount of scatter about the functional line used to describe the relationship. Depth-dependent conductivity relationships were used for the entire model.

Haneberg et al. (1998) conducted laboratory measurements on core samples from a site in Albuquerque, New Mexico, to investigate the impact of effective stress on hydraulic conductivity. The investigation found that "the hydraulic conductivities of consolidated, undisturbed, and typically fine-grained sediments, decreased two to three orders of magnitude between vertical effective stresses of about 50 and 1,000 kPa." A series of plots were shown with a linear relationship of log-hydraulic conductivity versus log-vertical effective stress for data from nine samples. Those data demonstrated the relationship of decreasing hydraulic conductivity that would be expected from increasing depth or effective stress.

A permeability-depth relationship for the continental crust based on geothermal and metamorphic data was evaluated by Manning and Ingebritsen (1999) and Ingebritsen and Manning (1999). Based on a variety of geologic settings in the United States and worldwide with depths to about 30 km, a relationship was developed of decaying permeability with depth of the form:

$$\log k = -3.2 \log z - 14 \qquad (B\text{-}17)$$

where:

k = Permeability (m^2)
z = Depth (km)

The constant in the equation provides *k* at a depth of 1 km. Fault zones were noted but not addressed in the analysis, which may locally yield higher permeability values. The above relationship was presented based on geothermal and metamorphic data and also data from direct hydraulic measurements from two investigations (sedimentary facies in the Uinta basin in Utah and the Pierre Shale) that showed decreasing permeability with increasing depth. The direct hydraulic measurement permeability data plotted, as log-permeability versus linear-depth, showed about seven orders of magnitude variation over 4.5 km depth for the Uinta basin and about 4.5 orders of magnitude variation over 3.2 km depth for the Pierre Shale. The direct hydraulic measurement permeability data were fairly scattered. It was found that "the crustal-scale k-z relation from geothermal and metamorphic data was at least as coherent as typical k-z data relations determined from direct hydraulic measurements of the upper crust."

Williamson and Grubb (2001) studied the sediments of the Gulf Coast region in the south-central United States, and used the equations of Kuiper (1994) for hydraulic conductivity as a function of depth for the coarse-grained sediments expressed as:

$$K = 30\ 10^{-0.000243D} \qquad \textit{(B-18)}$$

and for the clays expressed as:

$$K = C\ 10^{-0.000356D + 0.0000254D^{-2}} \qquad \textit{(B-19)}$$

where:

K = Hydraulic conductivity (ft/day)
D = Depth (ft)
C = Constant

For the coarse-grained sediments, Williamson and Grubb (2001) presented a plot of log hydraulic conductivity versus linear-depth with a straight-line approximation representing the hydraulic conductivity relation. The data showed a large amount of scatter about the best-fit line. Therefore, a regional groundwater flow model was developed consisting of 10 aquifers and 5 regional confining units.

An investigation of the relationship between permeability and depth (0 to 470 m) in the Cenozoic platform of west-central Florida was conducted by Budd (2001). Permeability-depth relationships were developed based on more than 12,000 minipermeameter measurements on 1,210 m of core from

where:

K = Hydraulic conductivity (m/day)
K_1 (m/day), K_2 (m/day), f (1/m), and g (1/m) = Parameters varied during model calibration
za = Depth in the colluvium measured from ground surface (m)
zb = Depth in the rock measured from the soil-rock interface (m)

Anderman and Hill (2003) published an update to the USGS groundwater flow model MODFLOW-2000, which included the addition of the capability to handle hydraulic-conductivity depth-dependence. The update discusses that hydraulic conductivity can decline systematically with depth and cites a field example in Whittemore et al. (1993). Whittemore et al. (1993) used a log-log vertical hydraulic-conductivity versus depth relationship to represent decreasing hydraulic conductivity, with depth for the aquitard in the regional-scale groundwater flow model of the Dakota aquifer system. Anderman and Hill (2003) include the hydraulic conductivity decrease with depth in MODFLOW-2000 using the function:

$$K_{Depth} = K_{Surface} 10^{-\lambda d} \qquad (B\text{-}29)$$

where:

K_{Depth} = Hydraulic conductivity at depth (L/T) with L = length and T = time
$K_{Surface}$ = Hydraulic conductivity projected to a reference surface (L/T)
λ = Depth-dependence coefficient (1/L)
d = Depth below the reference surface (L)

The depth-dependence coefficient can be defined separately for different HGUs or for different regions in each HGU. The hydraulic conductivity depth-decay functional relation is the same form as adopted by Prudic (1991), Kuiper (1994), and DOE/NV (1997).

An enhancement to MODFLOW-96 that includes a variation of hydraulic conductivity with depth option (code called MODFLOW-VKD) was published by the Environment Agency (2003). The agency noted that hydraulic conductivity is a function of depth for many aquifers. The revised code package introduced two new layer types to represent aquifers where hydraulic conductivity reduces with depth within the layer. The conceptualization for varying hydraulic conductivity with depth is based on Rushton et al. (1982 and 1989), where hydraulic conductivity decreases continuously until reaching a reference level and is then constant below the reference level. This hydraulic conductivity

variation with depth was developed from an investigation in a chalk aquifer in the United Kingdom and was incorporated into their mathematical model of the groundwater flow system.

The USGS has developed a transient groundwater flow model (with 16 layers) of the Death Valley region that includes the NTS and vicinity (Belcher et al., 2004). Belcher et al. (2004) discussed that hydraulic conductivity is expected to decrease with depth as "geostatic load increases, compressing favorably oriented fractures, faults, and sedimentary units." Depth decay of hydraulic conductivity is included in the model through use of the HUF package in MODFLOW-2000 (Anderman and Hill, 2003). The hydraulic conductivity depth-decay functional relation is the same form as adopted by Prudic (1991), Kuiper (1994), and DOE/NV (1997). Initial parameter estimates for hydraulic-conductivity decay with depth were based on the previous estimates in IT (1996) (these initial estimates were also used in the model in DOE/NV, 1997). Belcher et al. (2004) found that depth decay was important in all volcanic-rock and basin-fill units, and was of somewhat less importance in the carbonate-rock aquifer. It was also found that including depth decay in selected confining units improved the model. Belcher et al. (2004) provide comparison of the initial and calibrated depth-decay parameter for 10 HGUs, and a plot showing hydraulic conductivity relative to surface-hydraulic conductivity versus depth (to 3 km) for the calibrated depth-decay parameters for the 10 HGUs.

A regional-scale groundwater flow model was developed for the Pahute Mesa CAU. The area of interest for the Pahute Mesa CAU is defined by the potentially affected portion of the regional groundwater flow system, which includes a region stretching from the northern side of Pahute Mesa south and southwestward to Oasis Valley. The hydraulic conductivity data with plots of log hydraulic conductivity versus depth for selected HSUs are presented in SNJV (2004), which found that there is considerable scatter in the data at any particular depth. The model calibration approaches for parameterizing the HSUs for Pahute Mesa included no depth decay, no anisotropy; depth decay and anisotropy in selected units; and depth decay and anisotropy in all units. The no-depth-decay, no-anisotropy case was rejected as reasonable because of permeabilities and flow paths judged to be unrealistic. The calibration approaches with depth decay resulted in successful calibrations judged to be representative of the flow system based on matching head and flow calibration targets and examination of flow paths. The hydraulic conductivity depth-decay functional relation is the same form as that adopted by Prudic (1991), Kuiper (1994), DOE/NV (1997), and Belcher et al. (2004).

Appendix C

C.3.1

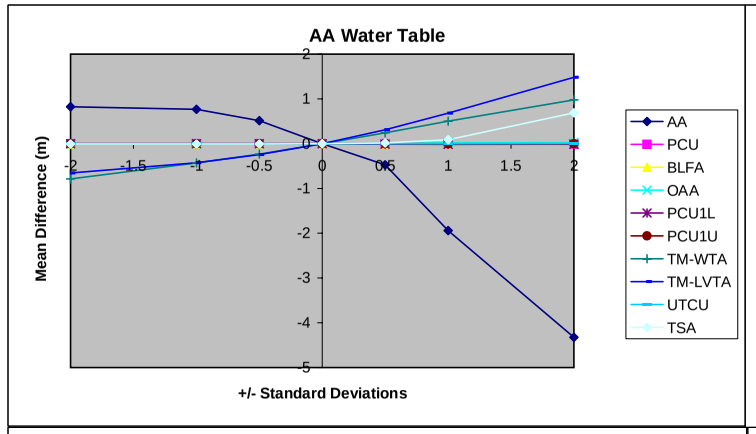
AA Water Table
Mean Difference (m)
+/- Standard Deviations
AA
PCU
BLFA
OAA
PCU1L
PCU1U
TM-WTA
TM-LVTA
UTCU
TSA

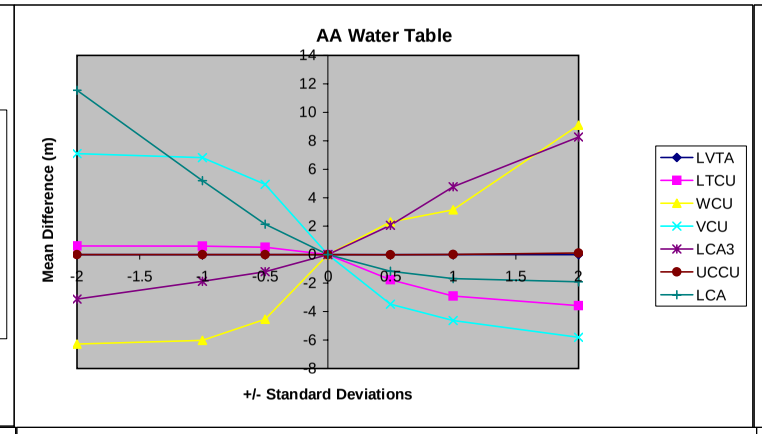
AA Water Table
Mean Difference (m)
+/- Standard Deviations
LVTA
LTCU
WCU
VCU
LCA3
UCCU
LCA

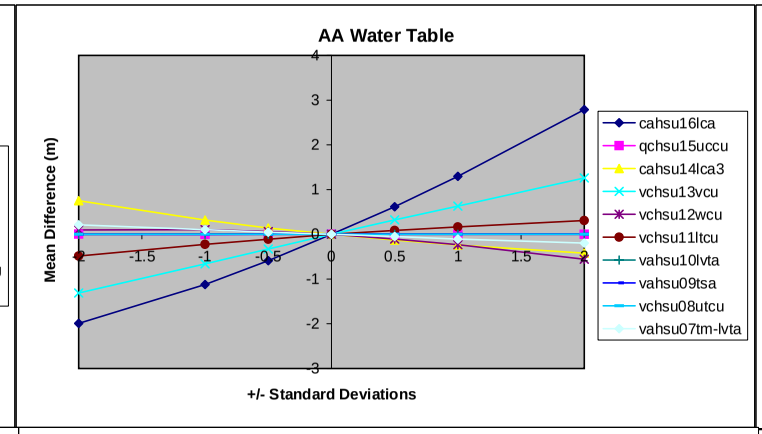
AA Water Table
Mean Difference (m)
+/- Standard Deviations
cahsu16lca
qchsu15uccu
cahsu14lca3
vchsu13vcu
vchsu12wcu
vchsu11ltcu
vahsu10lvta
vahsu09tsa
vchsu08utcu
vahsu07tm-lvta

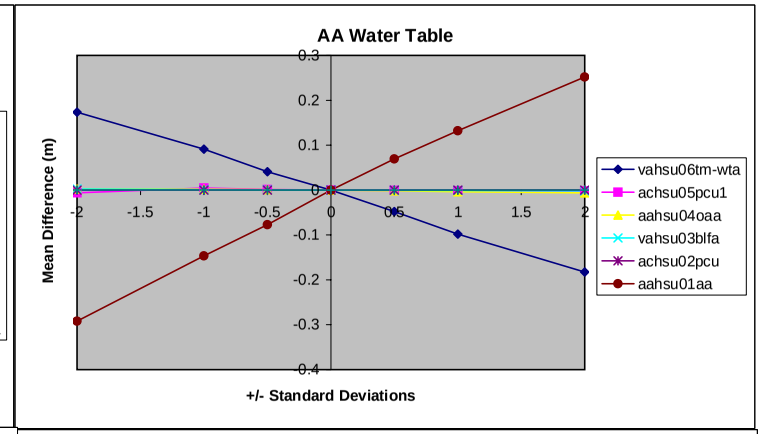
AA Water Table
Mean Difference (m)
+/- Standard Deviations
vahsu06tm-wta
achsu05pcu1
aahsu04oaa
vahsu03blfa
achsu02pcu
aahsu01aa

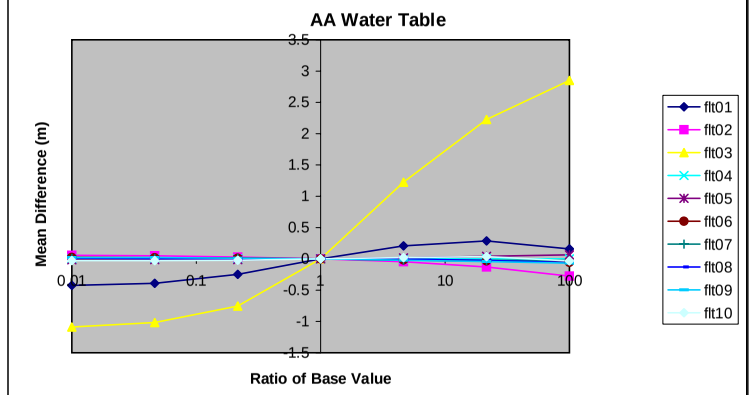
AA Water Table
Mean Difference (m)
Ratio of Base Value
flt01
flt02
flt03
flt04
flt05
flt06
flt07
flt08
flt09
flt10

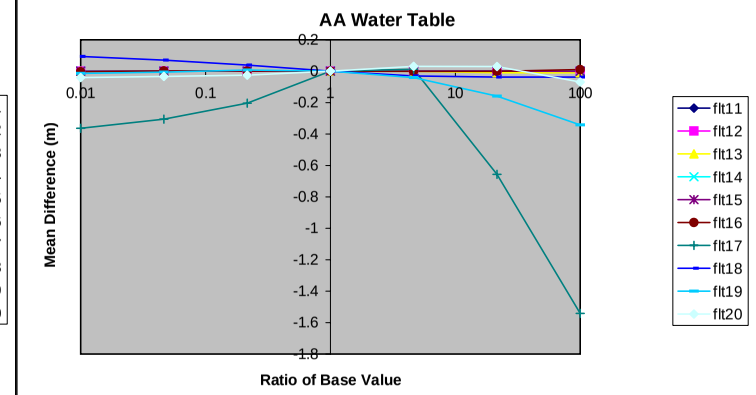
AA Water Table
Mean Difference (m)
Ratio of Base Value
flt11
flt12
flt13
flt14
flt15
flt16
flt17
flt18
flt19
flt20

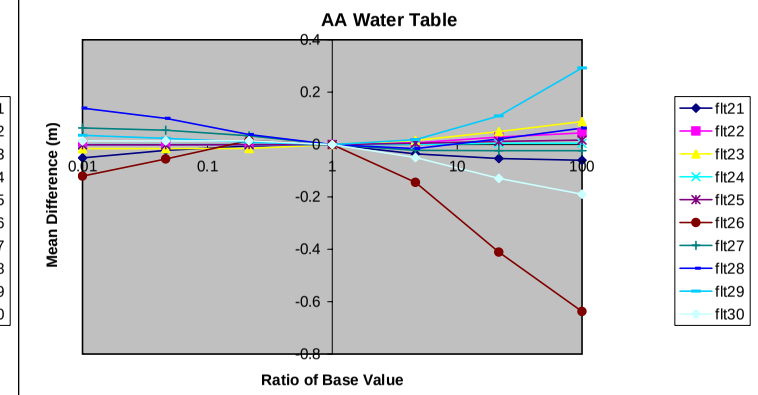
AA Water Table
Mean Difference (m)
Ratio of Base Value
flt21
flt22
flt23
flt24
flt25
flt26
flt27
flt28
flt29
flt30

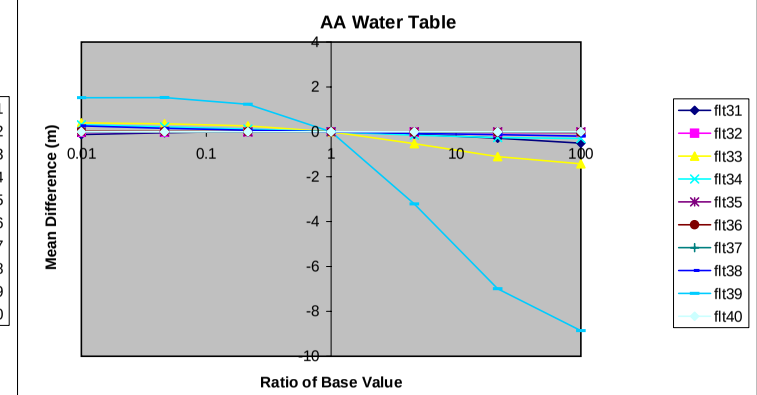
AA Water Table
Mean Difference (m)
Ratio of Base Value
flt31
flt32
flt33
flt34
flt35
flt36
flt37
flt38
flt39
flt40

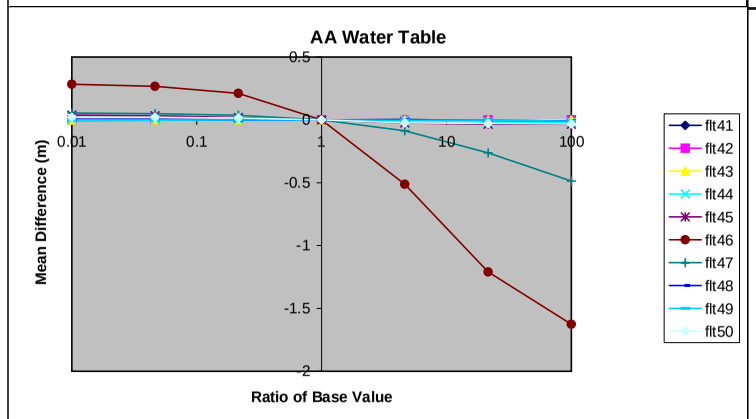
AA Water Table
Mean Difference (m)
Ratio of Base Value
flt41
flt42
flt43
flt44
flt45
flt46
flt47
flt48
flt49
flt50

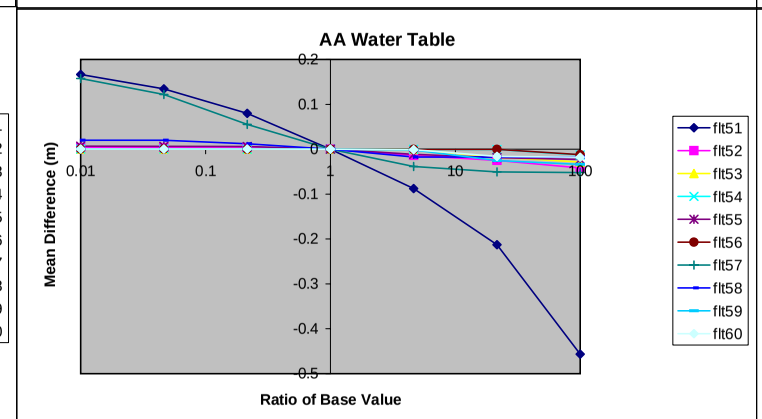
AA Water Table
Mean Difference (m)
Ratio of Base Value
flt51
flt52
flt53
flt54
flt55
flt56
flt57
flt58
flt59
flt60

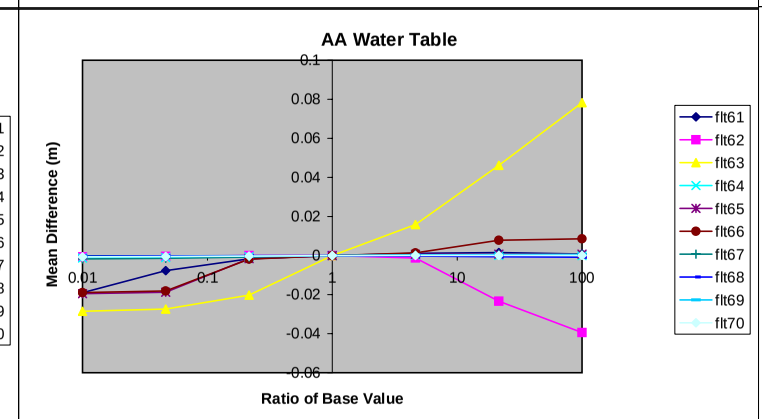
AA Water Table
Mean Difference (m)
Ratio of Base Value
flt61
flt62
flt63
flt64
flt65
flt66
flt67
flt68
flt69
flt70

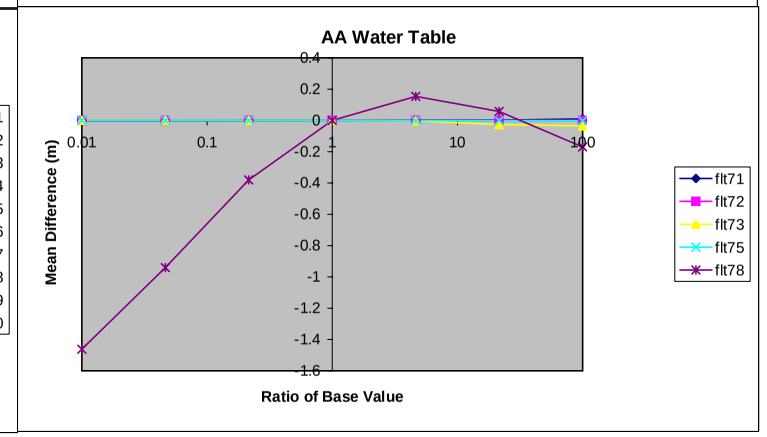
AA Water Table
Mean Difference (m)
Ratio of Base Value
flt71
flt72
flt73
flt75
flt78

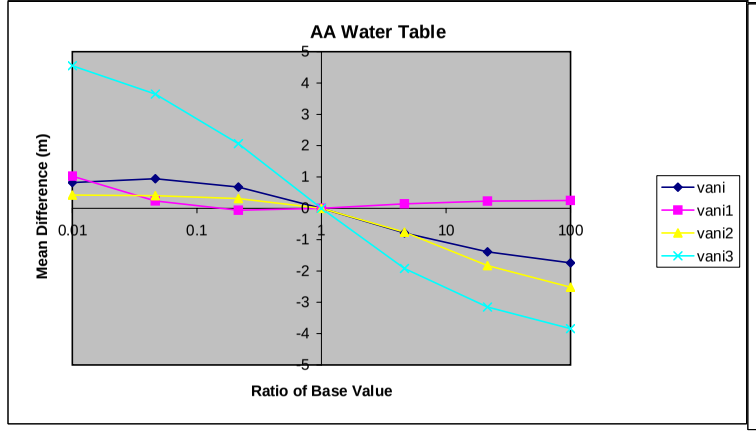
AA Water Table
Mean Difference (m)
Ratio of Base Value
vani
vani1
vani2
vani3

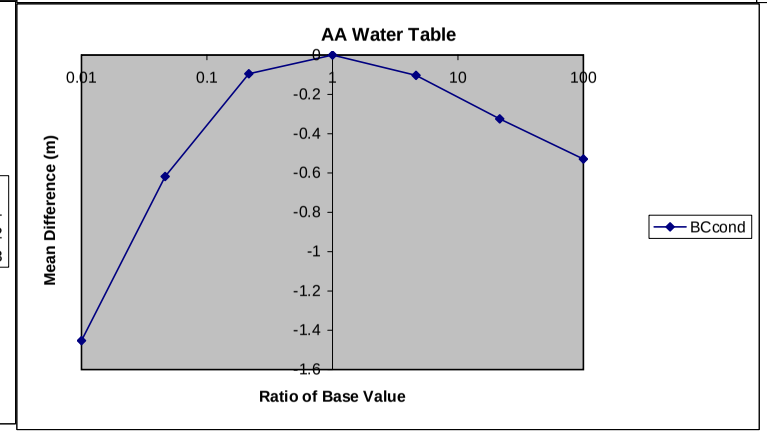
AA Water Table
Mean Difference (m)
Ratio of Base Value
BCcond

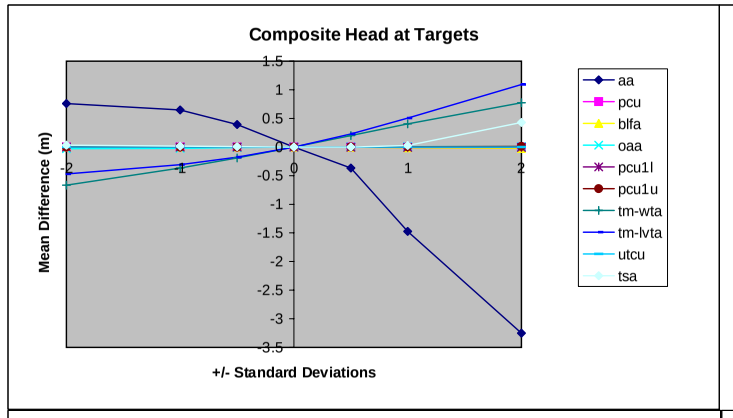
Composite Head at Targets
Mean Difference (m)
+/- Standard Deviations
aa
pcu
blfa
oaa
pcu1l
pcu1u
tm-wta
tm-lvta
utcu
tsa

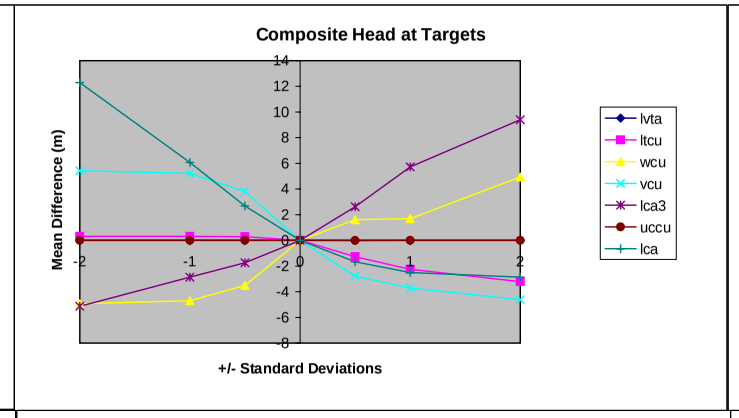
Composite Head at Targets
Mean Difference (m)
+/- Standard Deviations
lvta
ltcu
wcu
vcu
lca3
uccu
lca

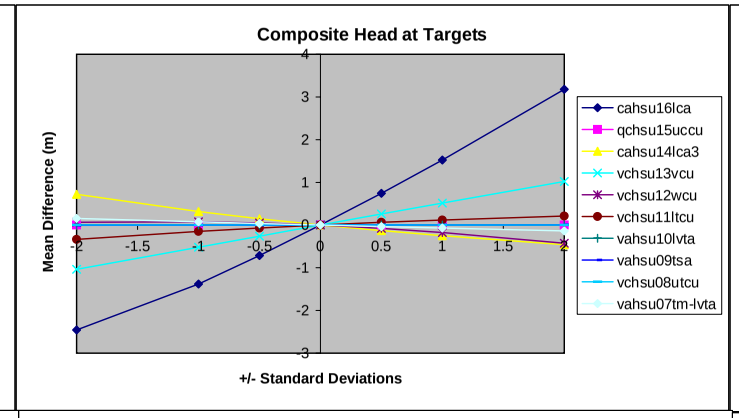
Composite Head at Targets
Mean Difference (m)
+/- Standard Deviations
cahsu16lca
qchsu15uccu
cahsu14lca3
vchsu13vcu
vchsu12wcu
vchsu11ltcu
vahsu10lvta
vahsu09tsa
vchsu08utcu
vahsu07tm-lvta

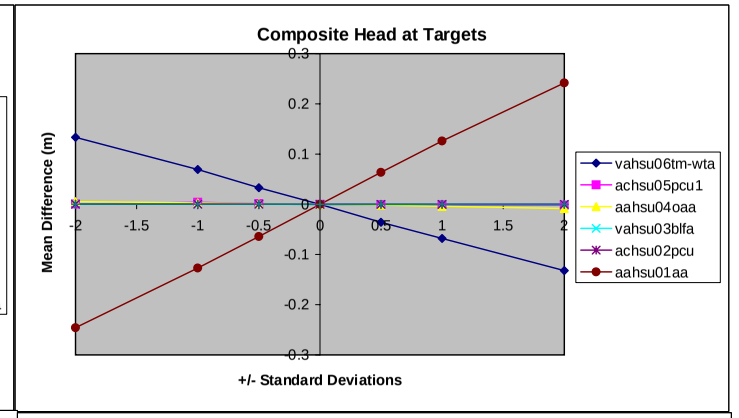
Composite Head at Targets
Mean Difference (m)
+/- Standard Deviations
vahsu06tm-wta
achsu05pcu1
aahsu04oaa
vahsu03blfa
achsu02pcu
aahsu01aa

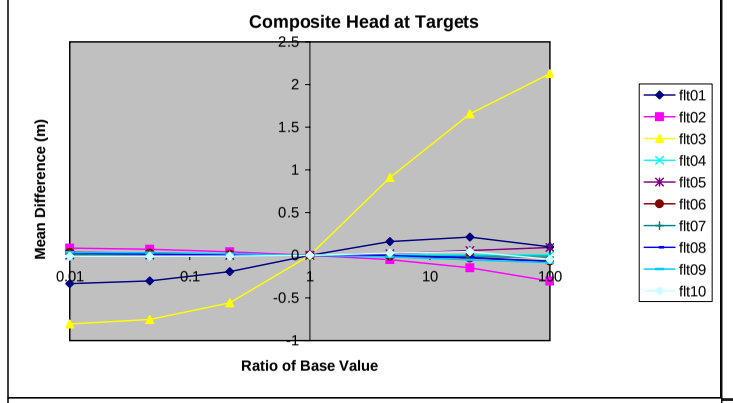
Composite Head at Targets
Mean Difference (m)
Ratio of Base Value
flt01
flt02
flt03
flt04
flt05
flt06
flt07
flt08
flt09
flt10

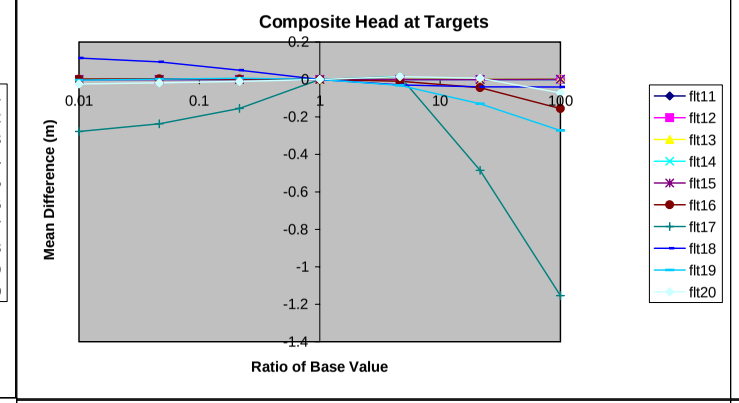
Composite Head at Targets
Mean Difference (m)
Ratio of Base Value
flt11
flt12
flt13
flt14
flt15
flt16
flt17
flt18
flt19
flt20

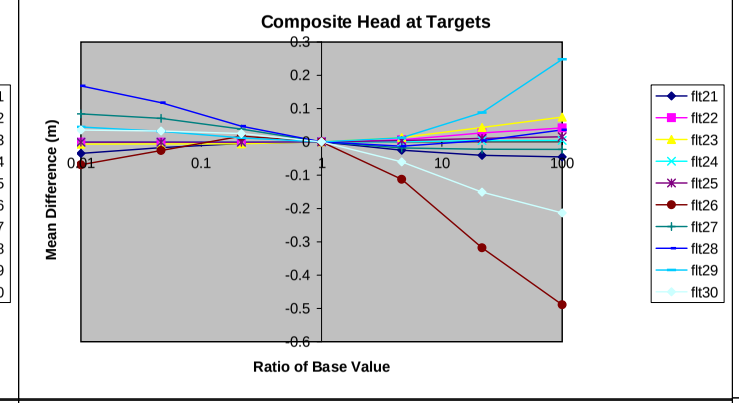
Composite Head at Targets
Mean Difference (m)
Ratio of Base Value
flt21
flt22
flt23
flt24
flt25
flt26
flt27
flt28
flt29
flt30

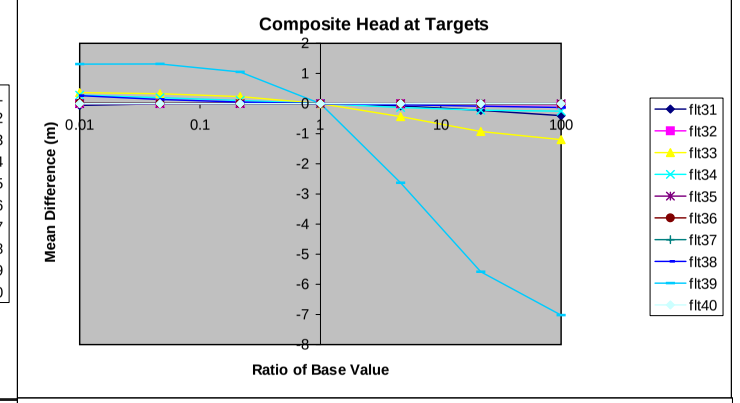
Composite Head at Targets
Mean Difference (m)
Ratio of Base Value
flt31
flt32
flt33
flt34
flt35
flt36
flt37
flt38
flt39
flt40

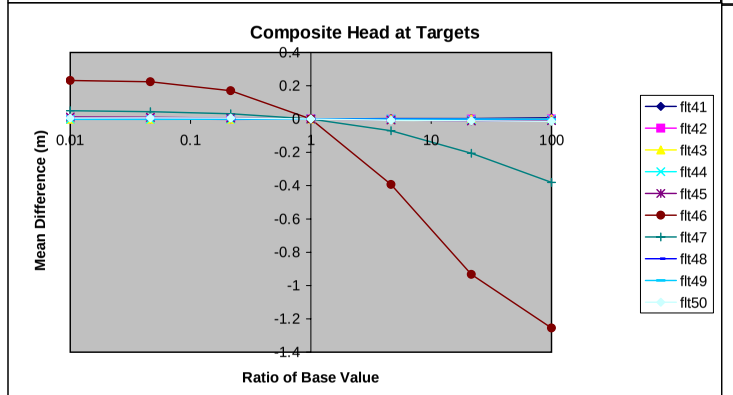
Composite Head at Targets
Mean Difference (m)
Ratio of Base Value
flt41
flt42
flt43
flt44
flt45
flt46
flt47
flt48
flt49
flt50

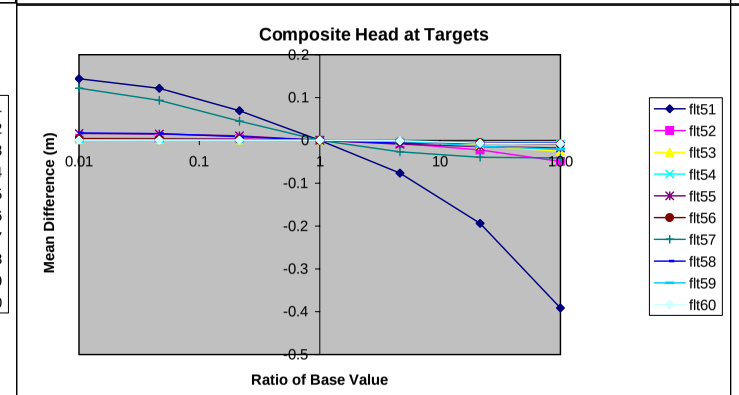
Composite Head at Targets
Mean Difference (m)
Ratio of Base Value
flt51
flt52
flt53
flt54
flt55
flt56
flt57
flt58
flt59
flt60

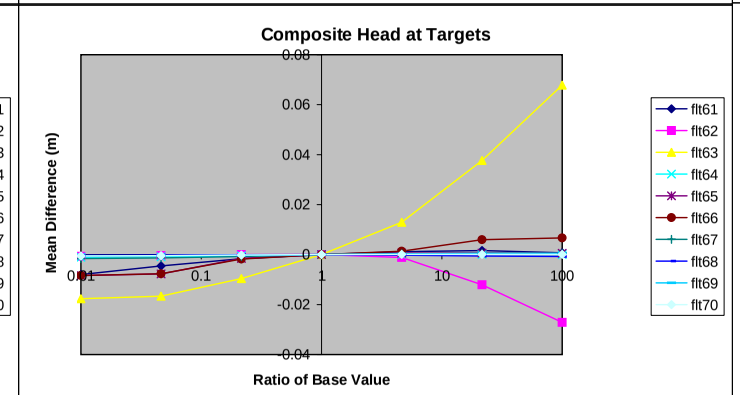
Composite Head at Targets
Mean Difference (m)
Ratio of Base Value
flt61
flt62
flt63
flt64
flt65
flt66
flt67
flt68
flt69
flt70

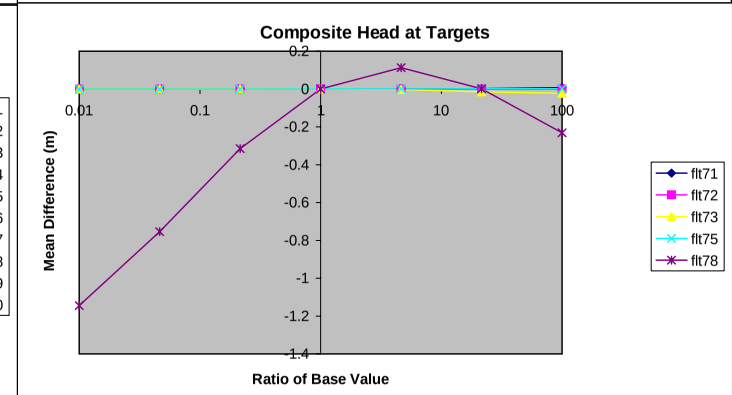
Composite Head at Targets
Mean Difference (m)
Ratio of Base Value
flt71
flt72
flt73
flt75
flt78

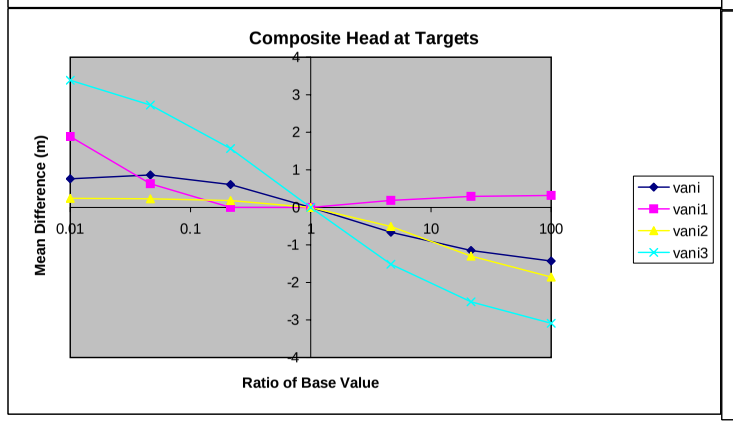
Composite Head at Targets
Mean Difference (m)
Ratio of Base Value
vani
vani1
vani2
vani3

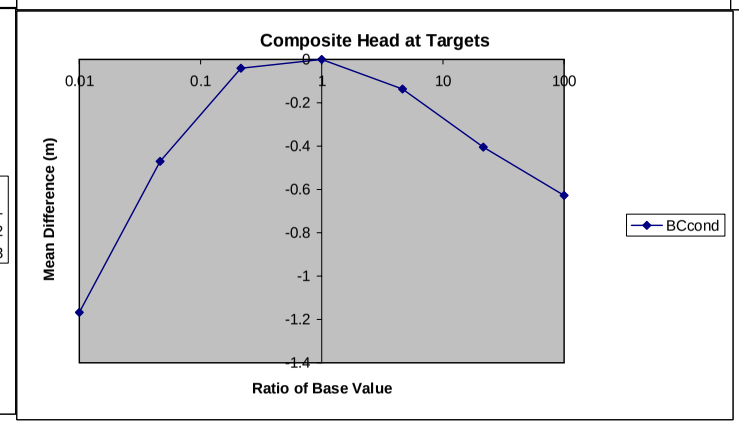
Composite Head at Targets
Mean Difference (m)
Ratio of Base Value
BCcond

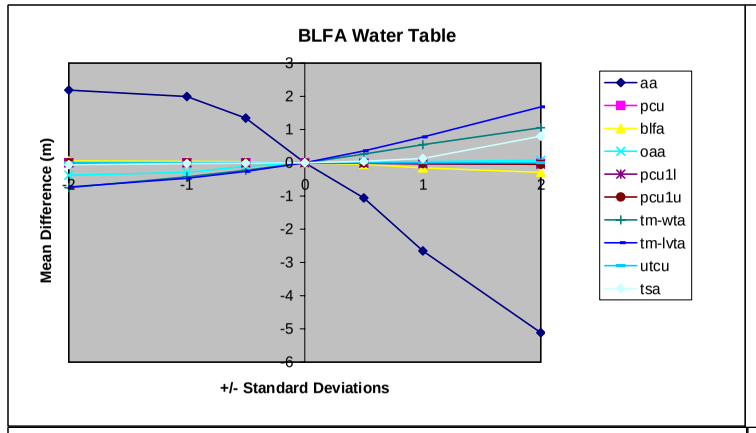
BLFA Water Table
Mean Difference (m)
+/- Standard Deviations
aa
pcu
blfa
oaa
pcu1l
pcu1u
tm-wta
tm-lvta
utcu
tsa

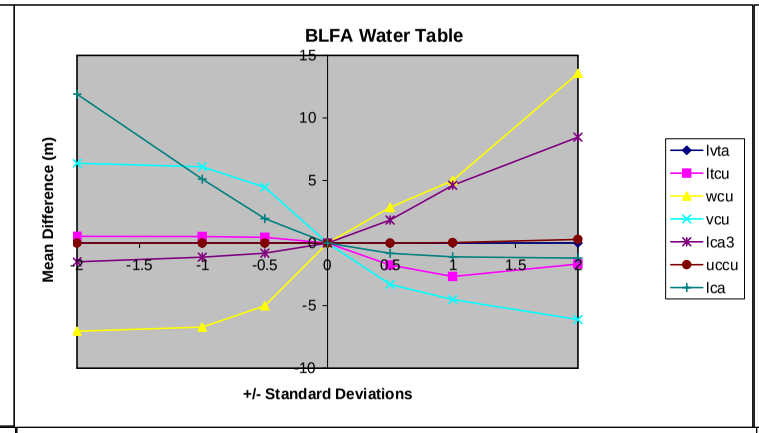
BLFA Water Table
Mean Difference (m)
+/- Standard Deviations
lvta
ltcu
wcu
vcu
lca3
uccu
lca

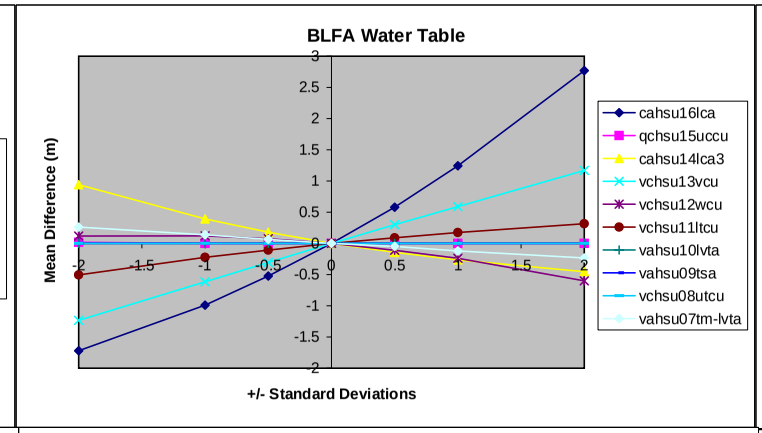
BLFA Water Table
Mean Difference (m)
+/- Standard Deviations
cahsu16lca
qchsu15uccu
cahsu14lca3
vchsu13vcu
vchsu12wcu
vchsu11ltcu
vahsu10lvta
vahsu09tsa
vchsu08utcu
vahsu07tm-lvta

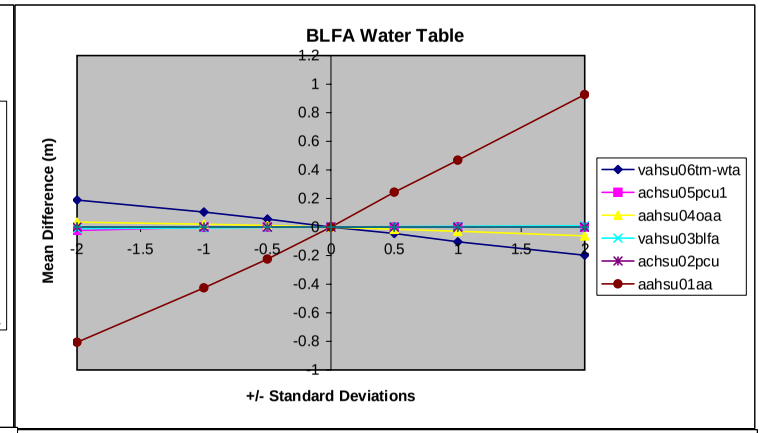
BLFA Water Table
Mean Difference (m)
+/- Standard Deviations
vahsu06tm-wta
achsu05pcu1
aahsu04oaa
vahsu03blfa
achsu02pcu
aahsu01aa

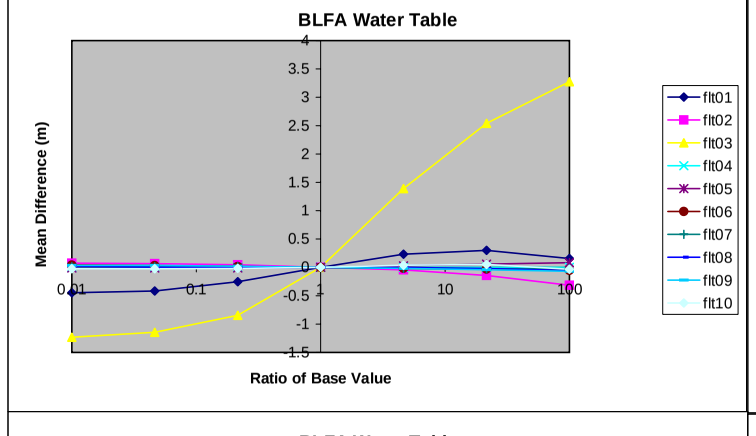
BLFA Water Table
Mean Difference (m)
Ratio of Base Value
flt01
flt02
flt03
flt04
flt05
flt06
flt07
flt08
flt09
flt10

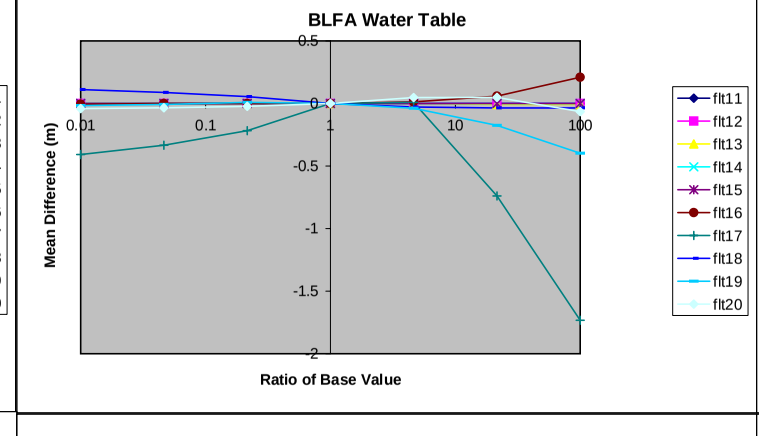
BLFA Water Table
Mean Difference (m)
Ratio of Base Value
flt11
flt12
flt13
flt14
flt15
flt16
flt17
flt18
flt19
flt20

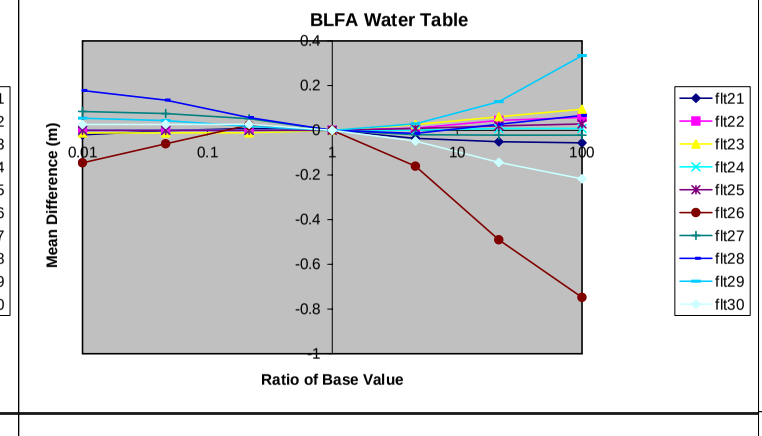
BLFA Water Table
Mean Difference (m)
Ratio of Base Value
flt21
flt22
flt23
flt24
flt25
flt26
flt27
flt28
flt29
flt30

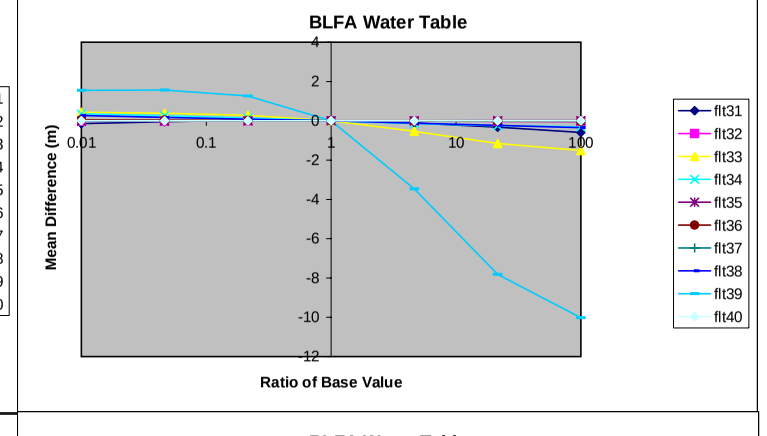
BLFA Water Table
Mean Difference (m)
Ratio of Base Value
flt31
flt32
flt33
flt34
flt35
flt36
flt37
flt38
flt39
flt40

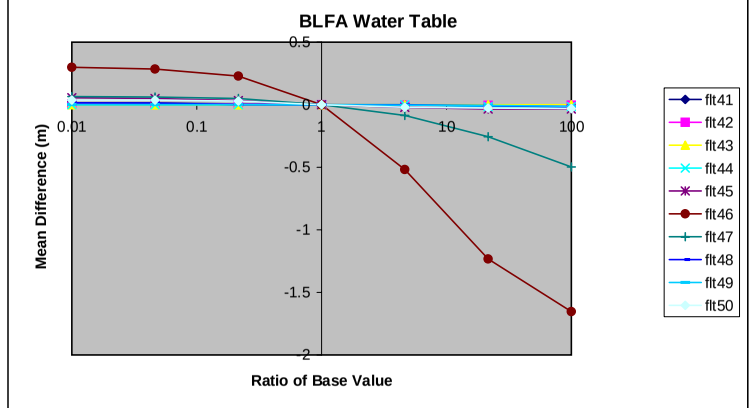
BLFA Water Table
Mean Difference (m)
Ratio of Base Value
flt41
flt42
flt43
flt44
flt45
flt46
flt47
flt48
flt49
flt50

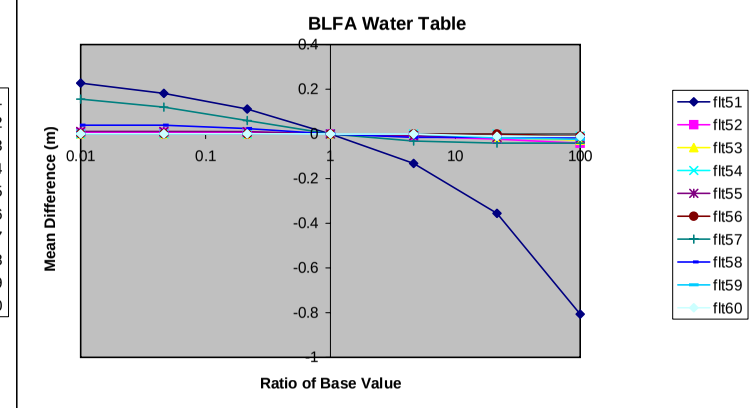
BLFA Water Table
Mean Difference (m)
Ratio of Base Value
flt51
flt52
flt53
flt54
flt55
flt56
flt57
flt58
flt59
flt60

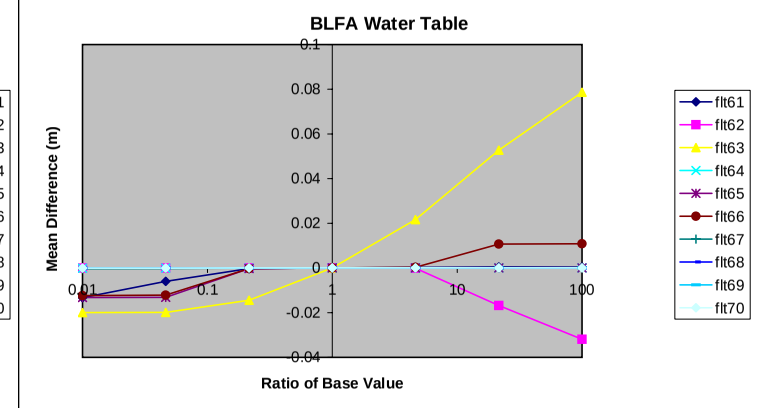
BLFA Water Table
Mean Difference (m)
Ratio of Base Value
flt61
flt62
flt63
flt64
flt65
flt66
flt67
flt68
flt69
flt70

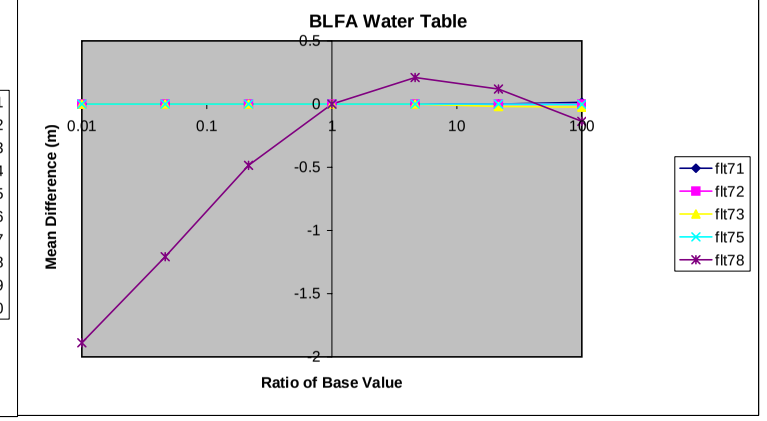
BLFA Water Table
Mean Difference (m)
Ratio of Base Value
flt71
flt72
flt73
flt75
flt78

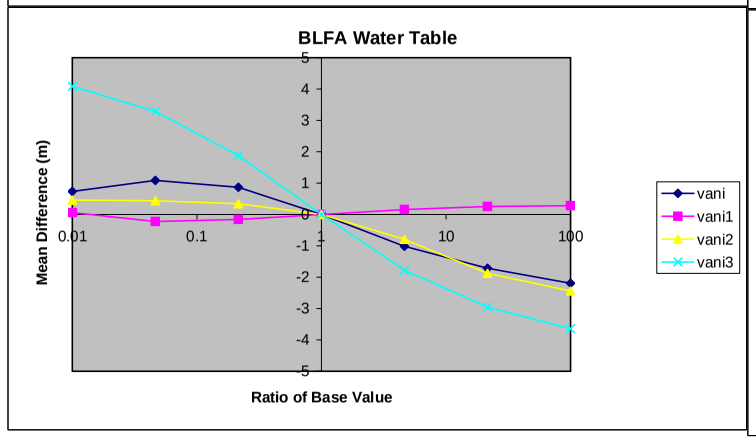
BLFA Water Table
Mean Difference (m)
Ratio of Base Value
vani
vani1
vani2
vani3

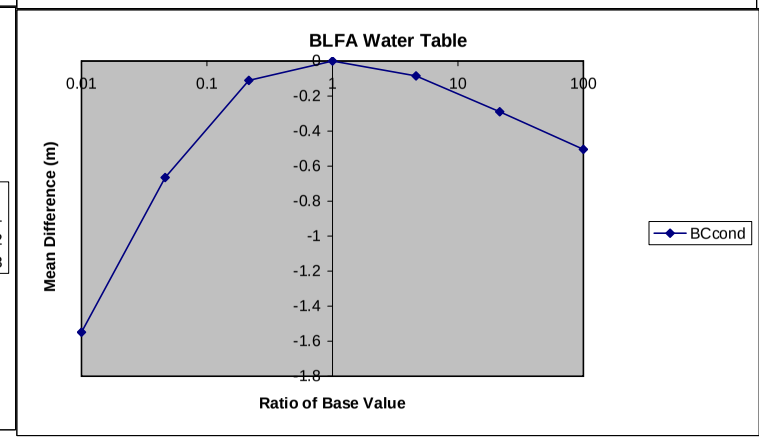
BLFA Water Table
Mean Difference (m)
Ratio of Base Value
BCcond

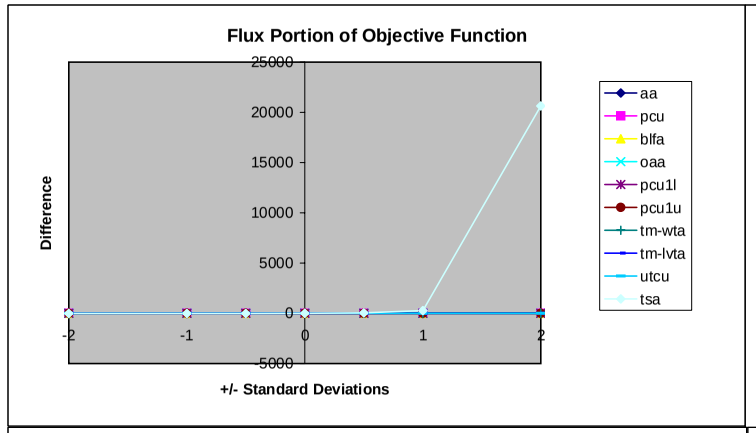
Flux Portion of Objective Function
Difference
+/- Standard Deviations
aa
pcu
blfa
oaa
pcu1l
pcu1u
tm-wta
tm-lvta
utcu
tsa

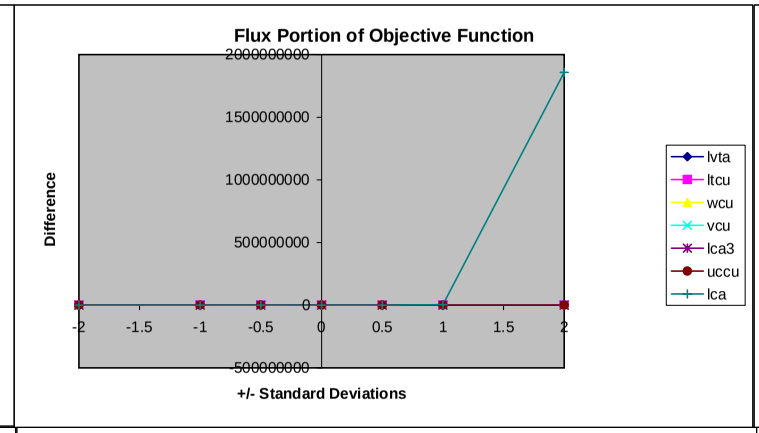
Flux Portion of Objective Function
Difference
+/- Standard Deviations
lvta
ltcu
wcu
vcu
lca3
uccu
lca

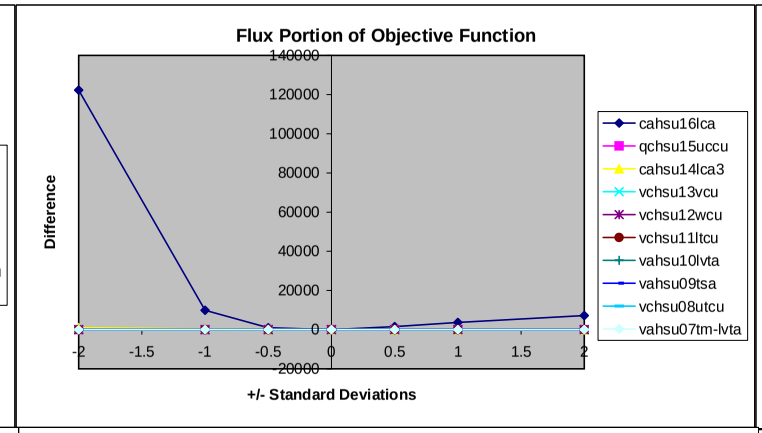
Flux Portion of Objective Function
Difference
+/- Standard Deviations
cahsu16lca
qchsu15uccu
cahsu14lca3
vchsu13vcu
vchsu12wcu
vchsu11ltcu
vahsu10lvta
vahsu09tsa
vchsu08utcu
vahsu07tm-lvta

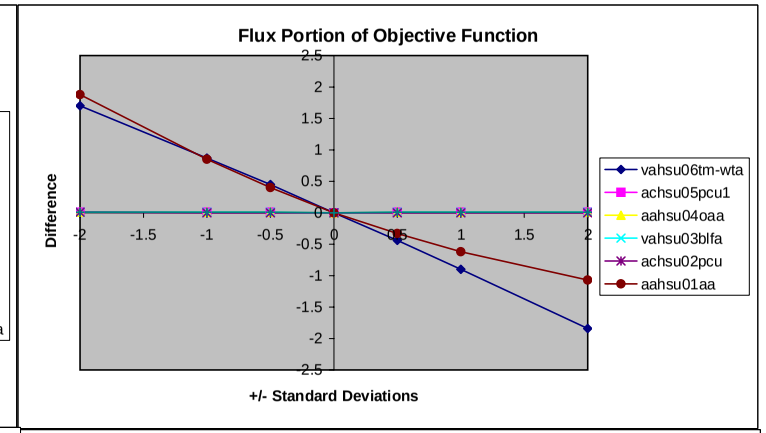
Flux Portion of Objective Function
Difference
+/- Standard Deviations
vahsu06tm-wta
achsu05pcu1
aahsu04oaa
vahsu03blfa
achsu02pcu
aahsu01aa

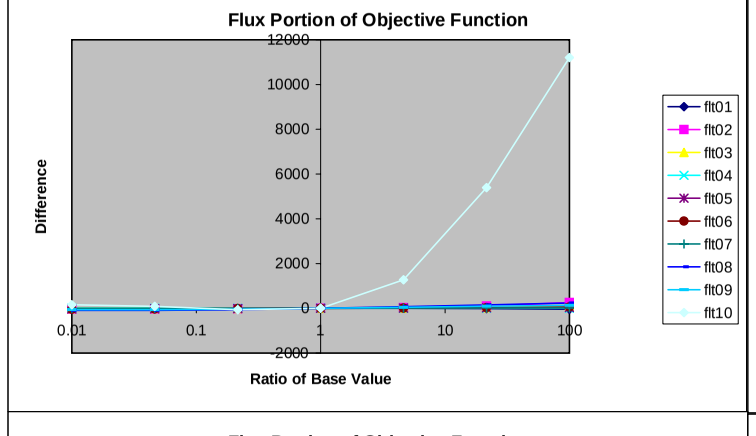
Flux Portion of Objective Function
Difference
Ratio of Base Value
flt01
flt02
flt03
flt04
flt05
flt06
flt07
flt08
flt09
flt10

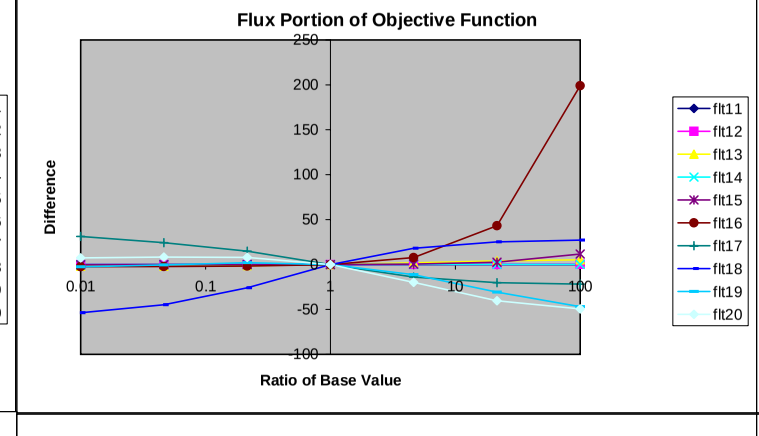
Flux Portion of Objective Function
Difference
Ratio of Base Value
flt11
flt12
flt13
flt14
flt15
flt16
flt17
flt18
flt19
flt20

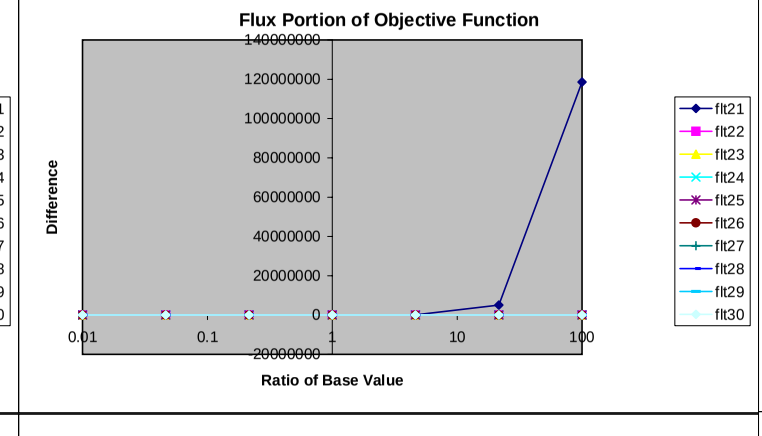
Flux Portion of Objective Function
Difference
Ratio of Base Value
flt21
flt22
flt23
flt24
flt25
flt26
flt27
flt28
flt29
flt30

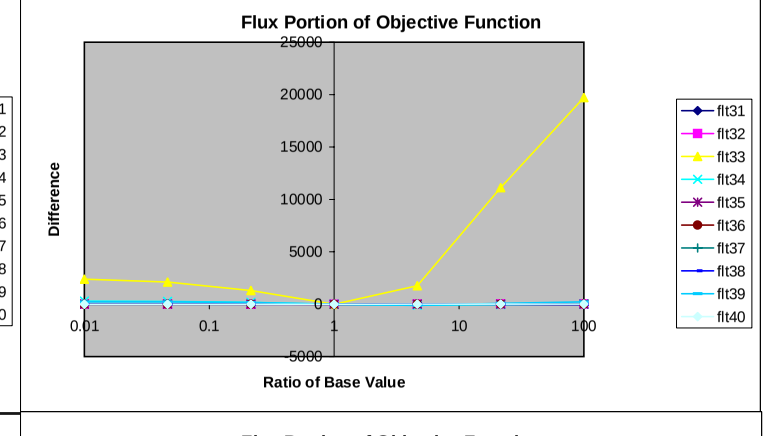
Flux Portion of Objective Function
Difference
Ratio of Base Value
flt31
flt32
flt33
flt34
flt35
flt36
flt37
flt38
flt39
flt40

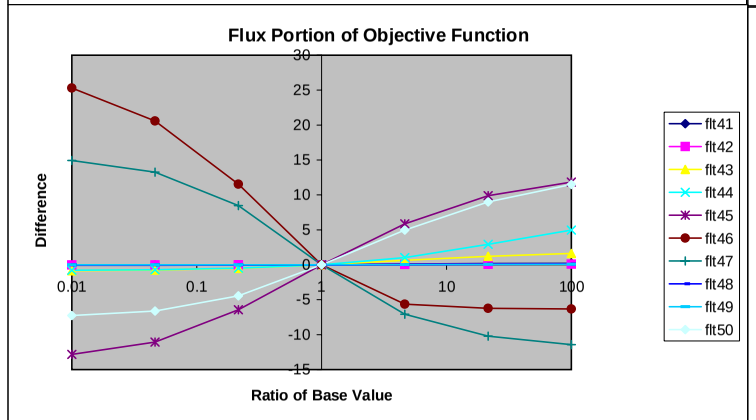
Flux Portion of Objective Function
Difference
Ratio of Base Value
flt41
flt42
flt43
flt44
flt45
flt46
flt47
flt48
flt49
flt50

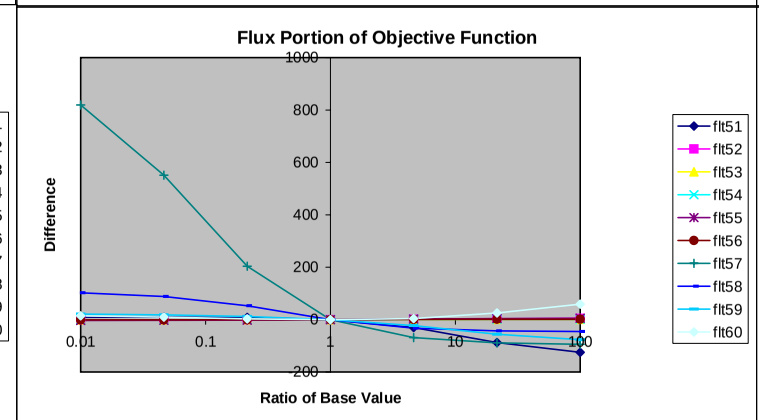
Flux Portion of Objective Function
Difference
Ratio of Base Value
flt51
flt52
flt53
flt54
flt55
flt56
flt57
flt58
flt59
flt60

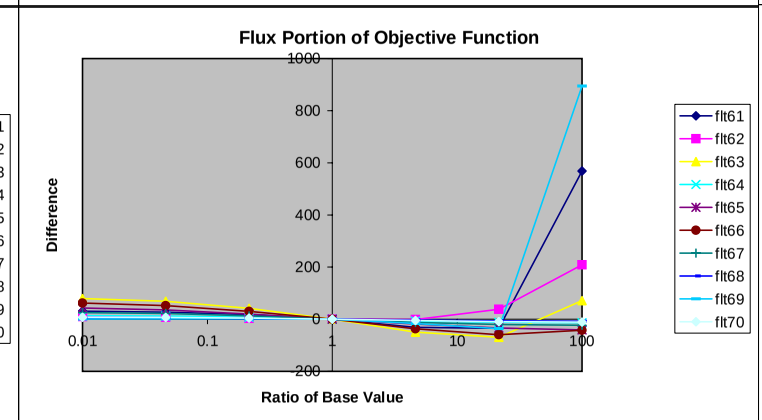
Flux Portion of Objective Function
Difference
Ratio of Base Value
flt61
flt62
flt63
flt64
flt65
flt66
flt67
flt68
flt69
flt70

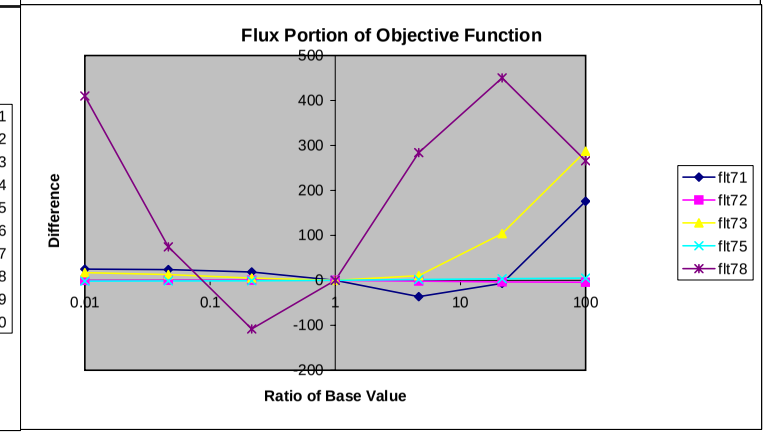
Flux Portion of Objective Function
Difference
Ratio of Base Value
flt71
flt72
flt73
flt75
flt78

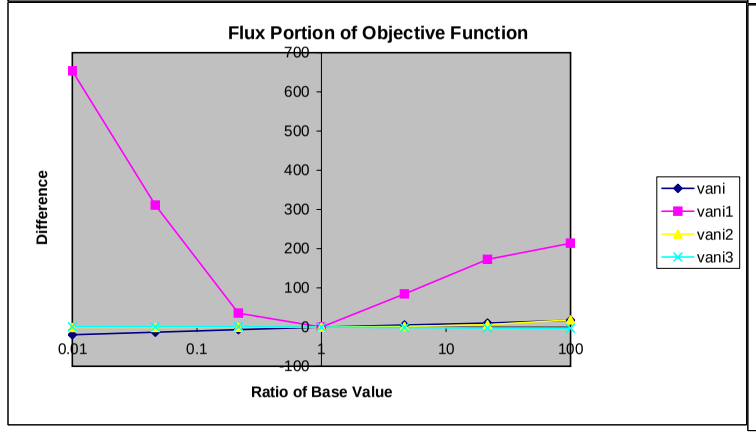
Flux Portion of Objective Function
Difference
Ratio of Base Value
vani
vani1
vani2
vani3

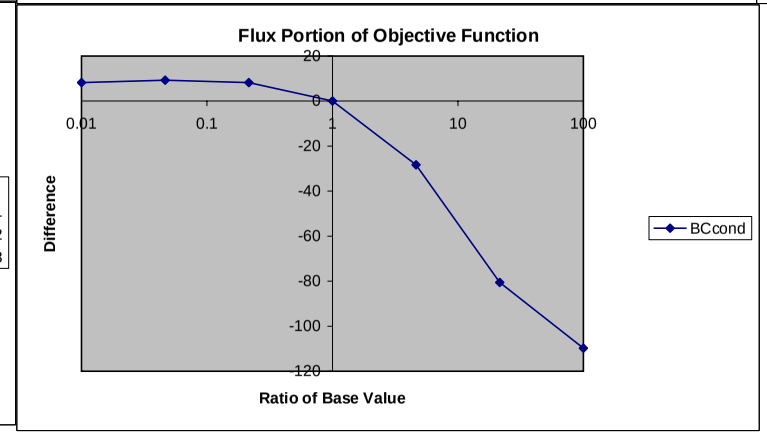
Flux Portion of Objective Function
Difference
Ratio of Base Value
BCcond

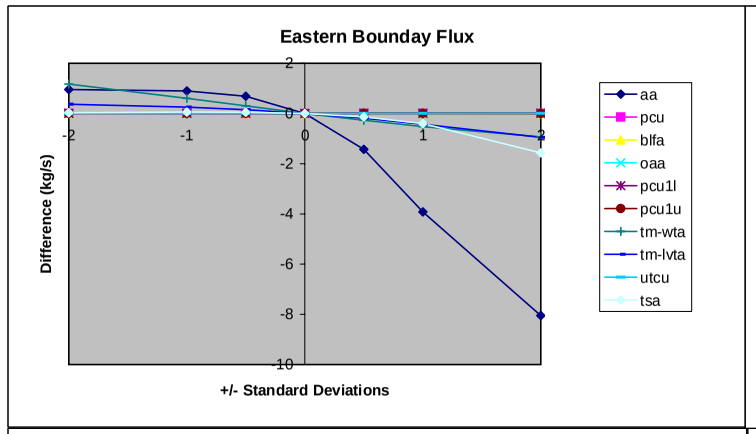
Eastern Bounday Flux
Difference (kg/s)
+/- Standard Deviations
aa
pcu
blfa
oaa
pcu1l
pcu1u
tm-wta
tm-lvta
utcu
tsa

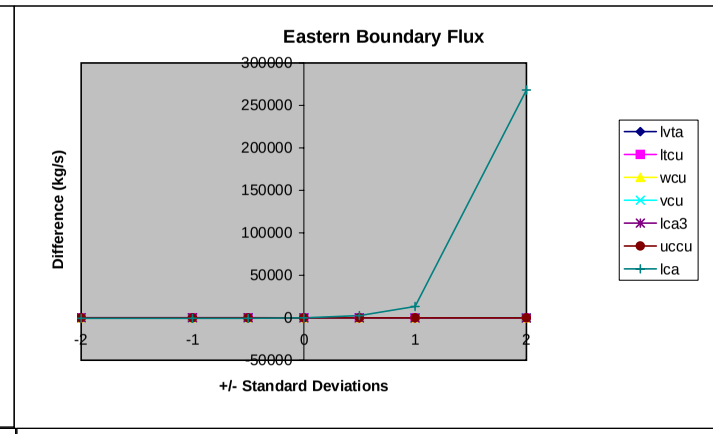
Eastern Boundary Flux
Difference (kg/s)
+/- Standard Deviations
lvta
ltcu
wcu
vcu
lca3
uccu
lca

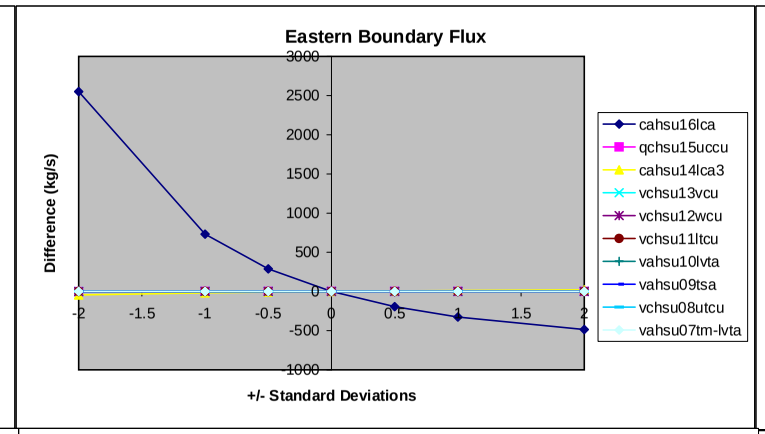
Eastern Boundary Flux
Difference (kg/s)
+/- Standard Deviations
cahsu16lca
qchsu15uccu
cahsu14lca3
vchsu13vcu
vchsu12wcu
vchsu11ltcu
vahsu10lvta
vahsu09tsa
vchsu08utcu
vahsu07tm-lvta

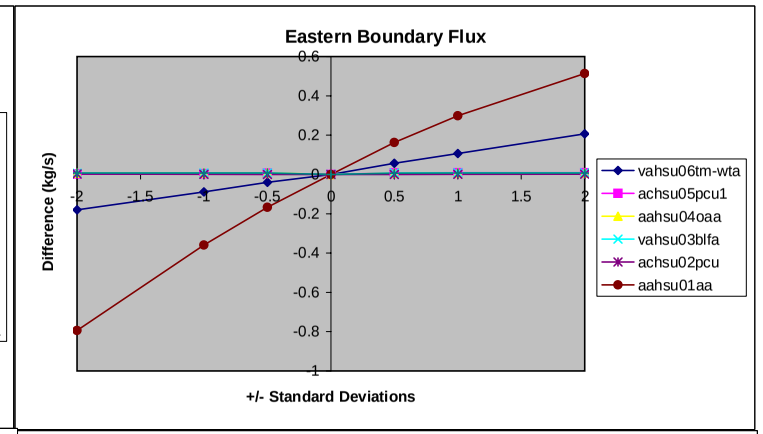
Eastern Boundary Flux
Difference (kg/s)
+/- Standard Deviations
vahsu06tm-wta
achsu05pcu1
aahsu04oaa
vahsu03blfa
achsu02pcu
aahsu01aa

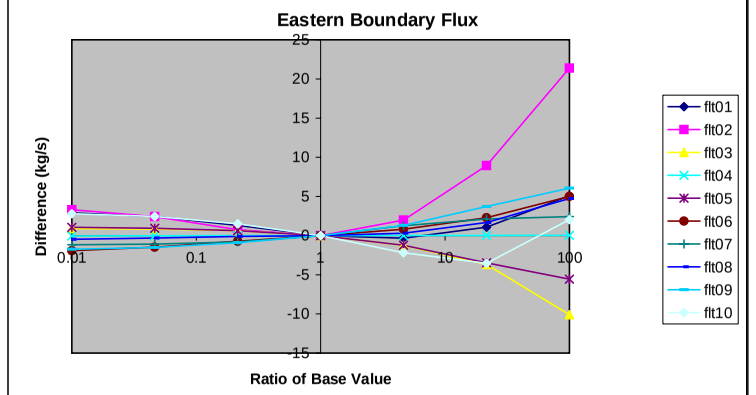
Eastern Boundary Flux
Difference (kg/s)
Ratio of Base Value
flt01
flt02
flt03
flt04
flt05
flt06
flt07
flt08
flt09
flt10

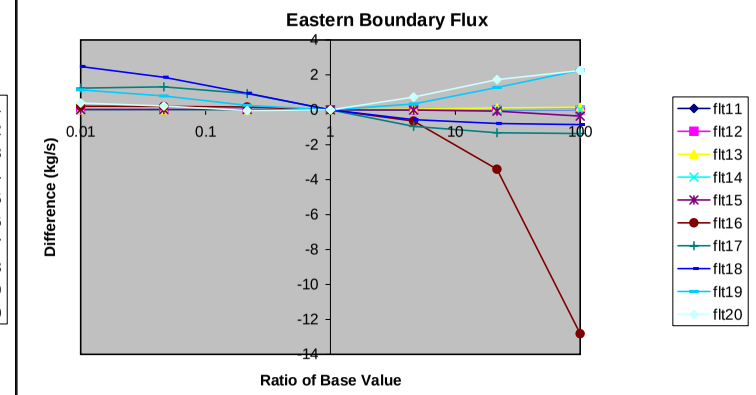
Eastern Boundary Flux
Difference (kg/s)
Ratio of Base Value
flt11
flt12
flt13
flt14
flt15
flt16
flt17
flt18
flt19
flt20

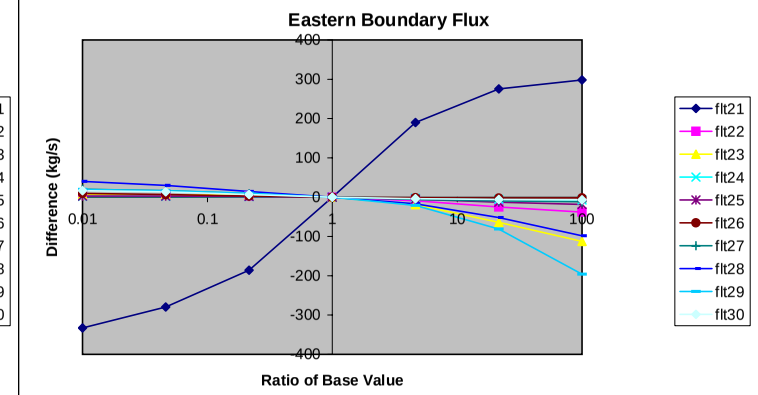
Eastern Boundary Flux
Difference (kg/s)
Ratio of Base Value
flt21
flt22
flt23
flt24
flt25
flt26
flt27
flt28
flt29
flt30

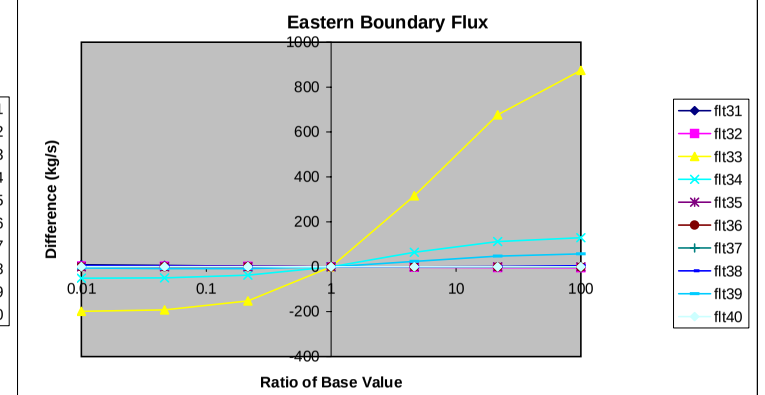
Eastern Boundary Flux
Difference (kg/s)
Ratio of Base Value
flt31
flt32
flt33
flt34
flt35
flt36
flt37
flt38
flt39
flt40

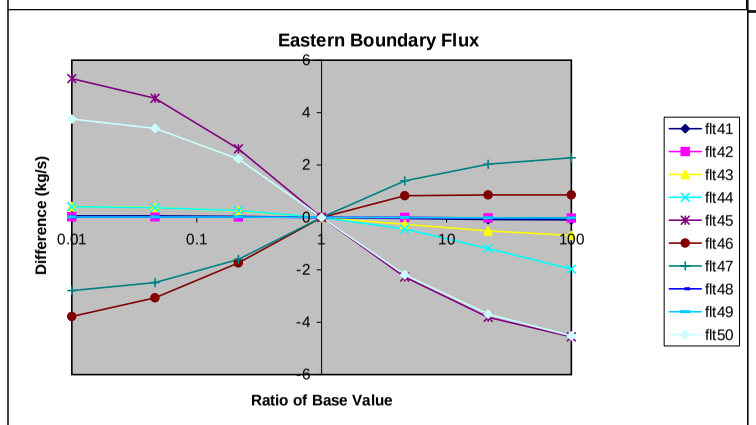
Eastern Boundary Flux
Difference (kg/s)
Ratio of Base Value
flt41
flt42
flt43
flt44
flt45
flt46
flt47
flt48
flt49
flt50

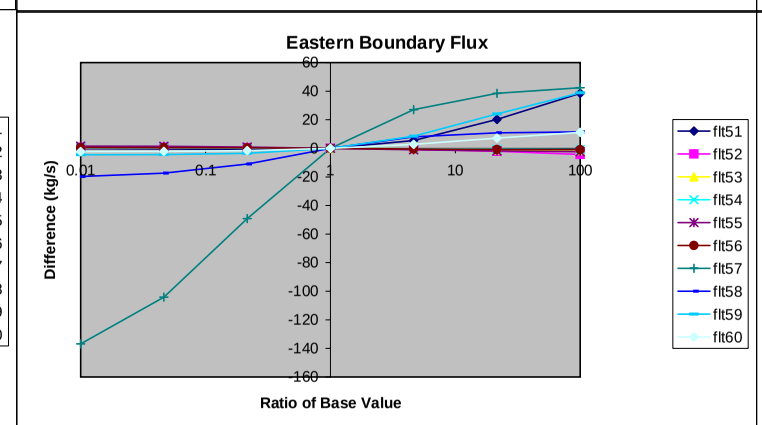
Eastern Boundary Flux
Difference (kg/s)
Ratio of Base Value
flt51
flt52
flt53
flt54
flt55
flt56
flt57
flt58
flt59
flt60

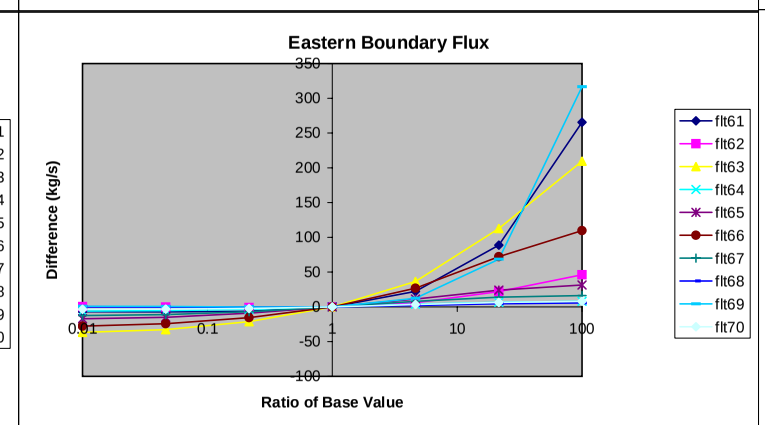
Eastern Boundary Flux
Difference (kg/s)
Ratio of Base Value
flt61
flt62
flt63
flt64
flt65
flt66
flt67
flt68
flt69
flt70

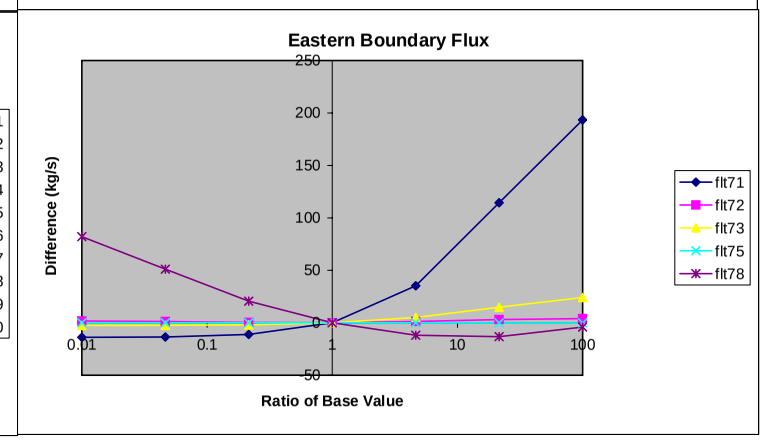
Eastern Boundary Flux
Difference (kg/s)
Ratio of Base Value
flt71
flt72
flt73
flt75
flt78

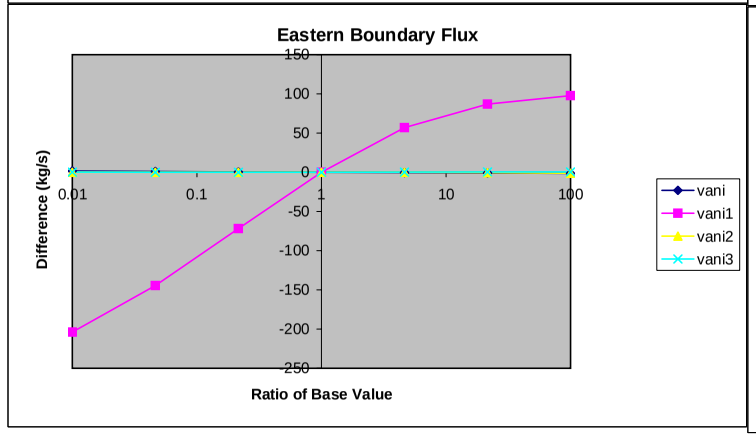
Eastern Boundary Flux
Difference (kg/s)
Ratio of Base Value
vani
vani1
vani2
vani3

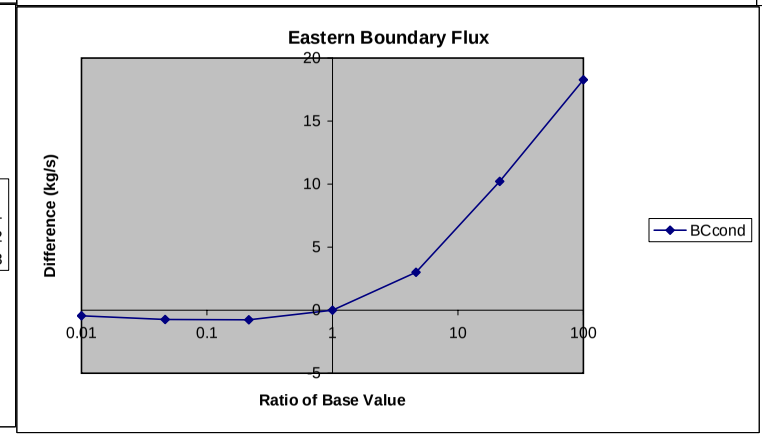
Eastern Boundary Flux
Difference (kg/s)
Ratio of Base Value
BCcond

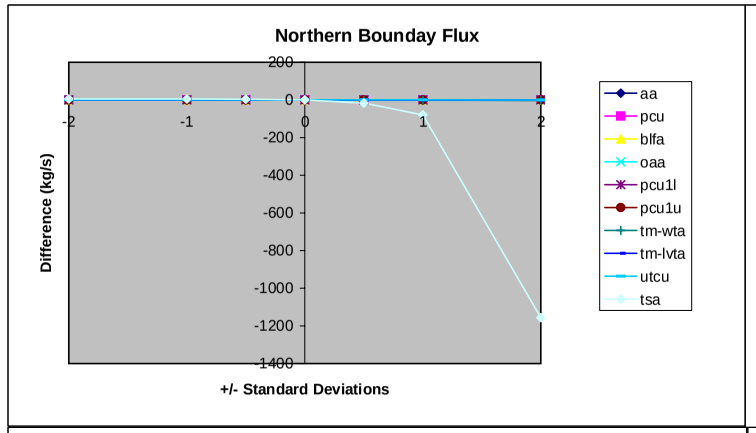
Northern Bounday Flux
Difference (kg/s)
+/- Standard Deviations
aa
pcu
blfa
oaa
pcu1l
pcu1u
tm-wta
tm-lvta
utcu
tsa

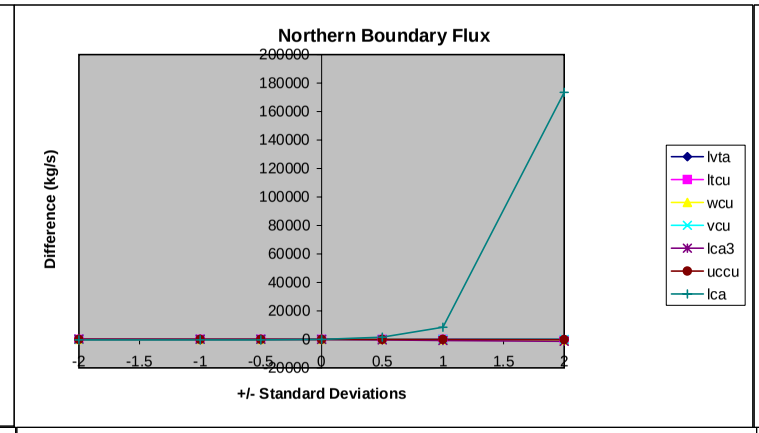
Northern Boundary Flux
Difference (kg/s)
+/- Standard Deviations
lvta
ltcu
wcu
vcu
lca3
uccu
lca

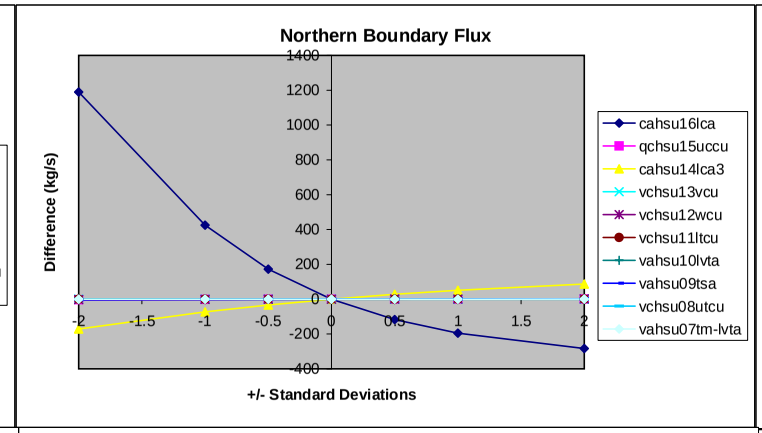
Northern Boundary Flux
Difference (kg/s)
+/- Standard Deviations
cahsu16lca
qchsu15uccu
cahsu14lca3
vchsu13vcu
vchsu12wcu
vchsu11ltcu
vahsu10lvta
vahsu09tsa
vchsu08utcu
vahsu07tm-lvta

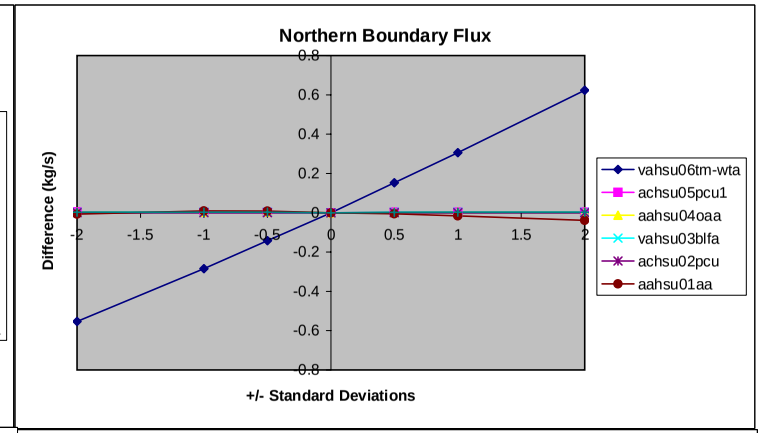
Northern Boundary Flux
Difference (kg/s)
+/- Standard Deviations
vahsu06tm-wta
achsu05pcu1
aahsu04oaa
vahsu03blfa
achsu02pcu
aahsu01aa

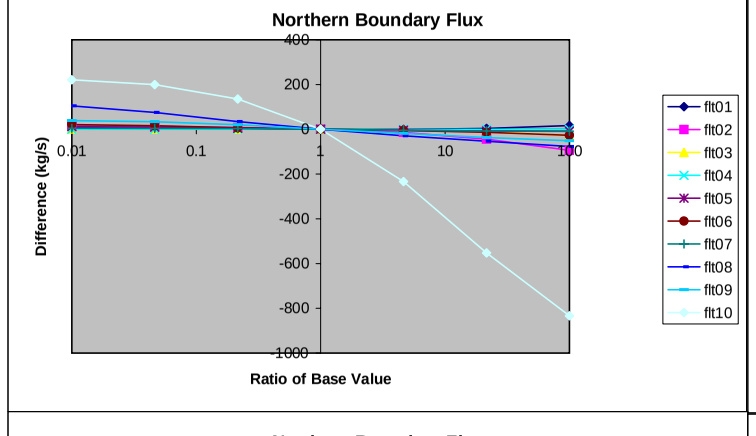
Northern Boundary Flux
Difference (kg/s)
Ratio of Base Value
flt01
flt02
flt03
flt04
flt05
flt06
flt07
flt08
flt09
flt10

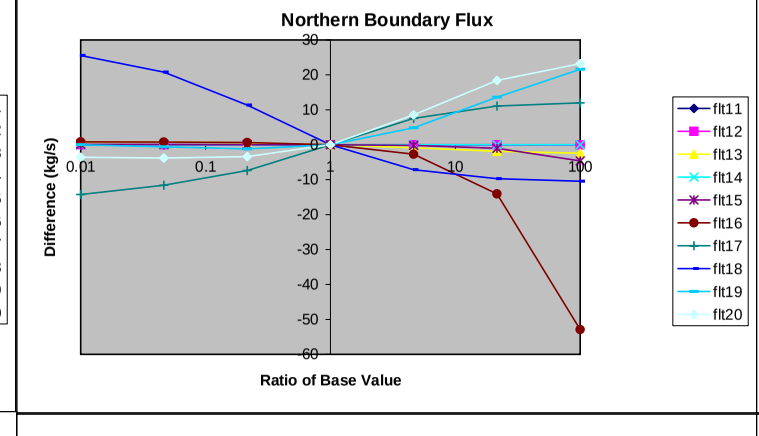
Northern Boundary Flux
Difference (kg/s)
Ratio of Base Value
flt11
flt12
flt13
flt14
flt15
flt16
flt17
flt18
flt19
flt20

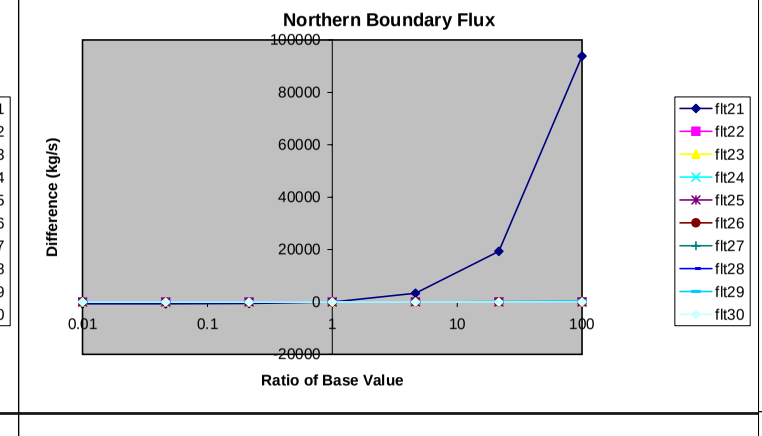
Northern Boundary Flux
Difference (kg/s)
Ratio of Base Value
flt21
flt22
flt23
flt24
flt25
flt26
flt27
flt28
flt29
flt30

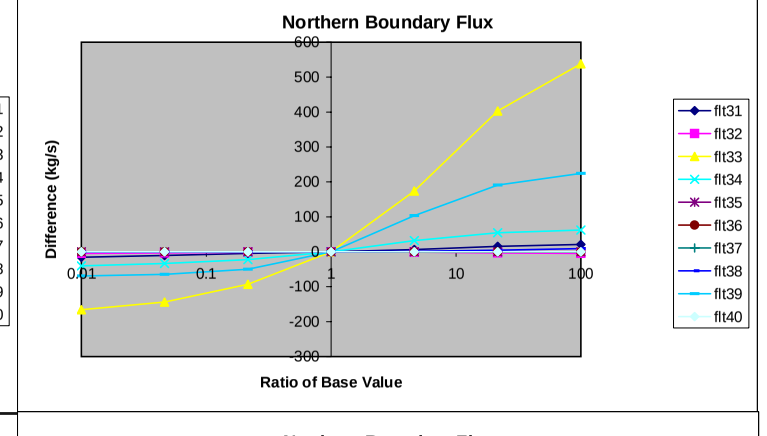
Northern Boundary Flux
Difference (kg/s)
Ratio of Base Value
flt31
flt32
flt33
flt34
flt35
flt36
flt37
flt38
flt39
flt40

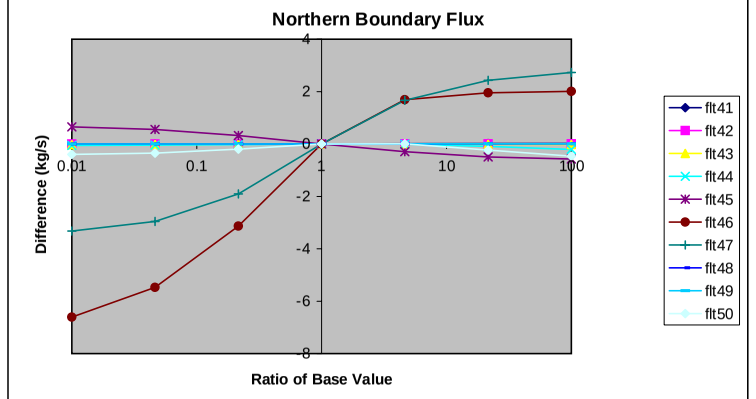
Northern Boundary Flux
Difference (kg/s)
Ratio of Base Value
flt41
flt42
flt43
flt44
flt45
flt46
flt47
flt48
flt49
flt50

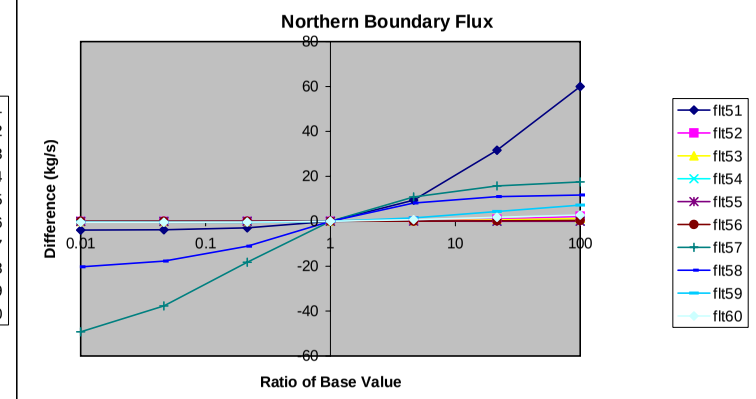
Northern Boundary Flux
Difference (kg/s)
Ratio of Base Value
flt51
flt52
flt53
flt54
flt55
flt56
flt57
flt58
flt59
flt60

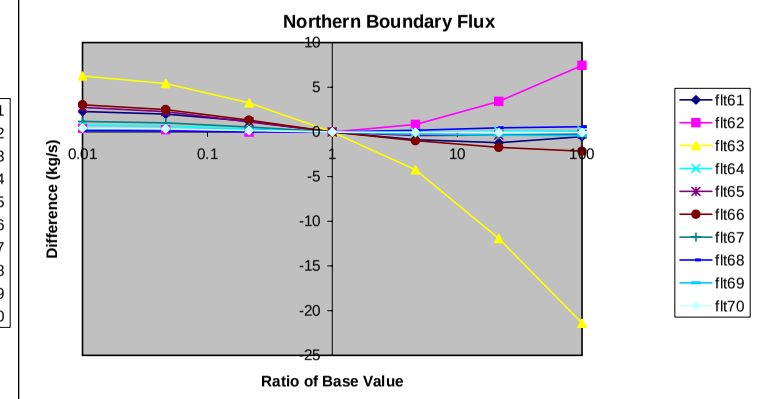
Northern Boundary Flux
Difference (kg/s)
Ratio of Base Value
flt61
flt62
flt63
flt64
flt65
flt66
flt67
flt68
flt69
flt70

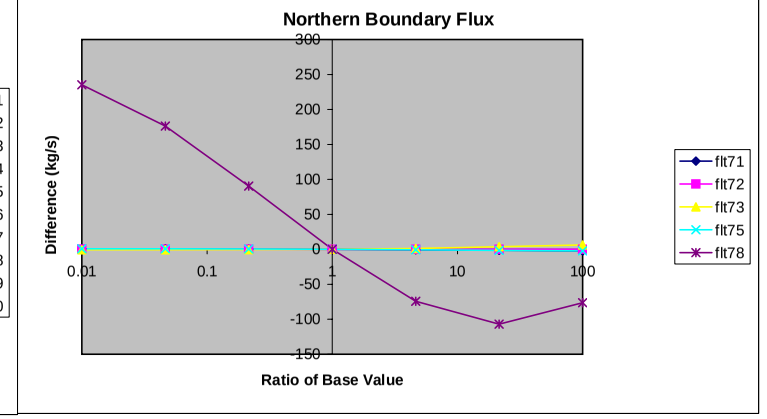
Northern Boundary Flux
Difference (kg/s)
Ratio of Base Value
flt71
flt72
flt73
flt75
flt78

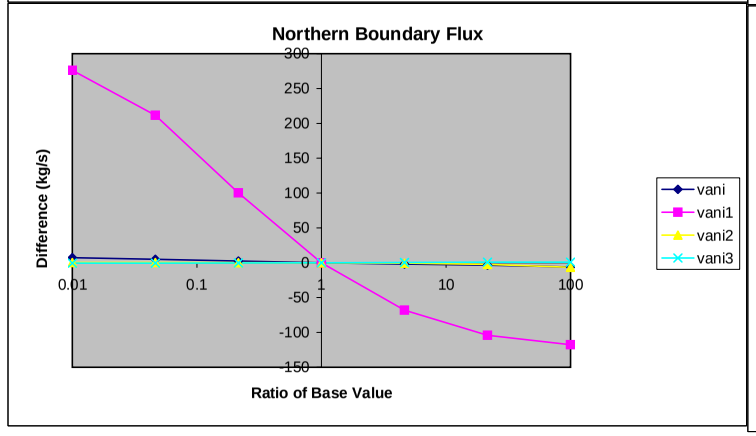
Northern Boundary Flux
Difference (kg/s)
Ratio of Base Value
vani
vani1
vani2
vani3

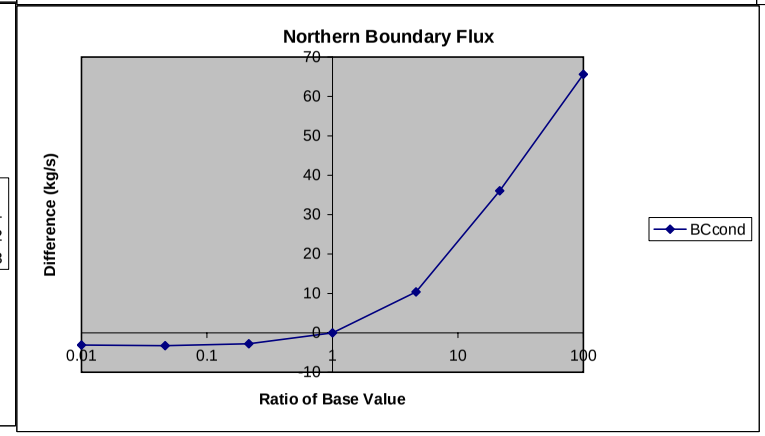
Northern Boundary Flux
Difference (kg/s)
Ratio of Base Value
BCcond

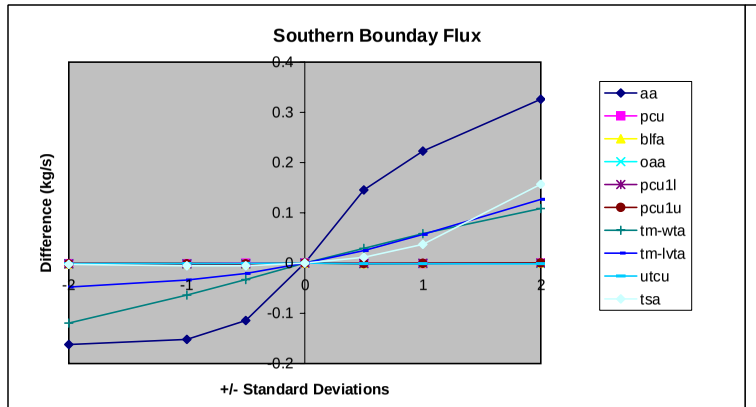
Southern Bounday Flux
Difference (kg/s)
+/- Standard Deviations
aa
pcu
blfa
oaa
pcu1l
pcu1u
tm-wta
tm-lvta
utcu
tsa

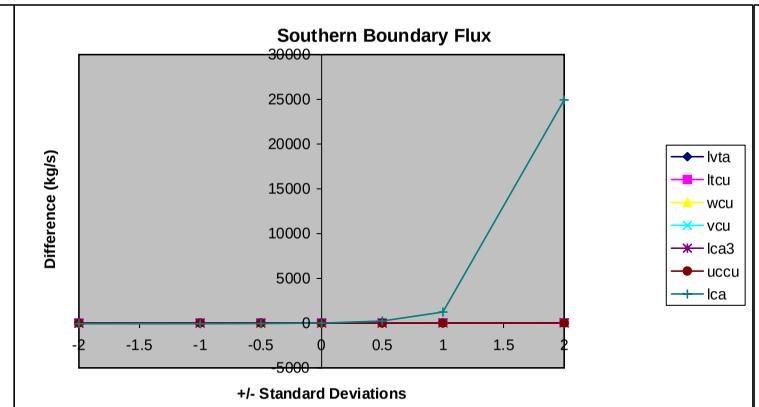
Southern Boundary Flux
Difference (kg/s)
+/- Standard Deviations
lvta
ltcu
wcu
vcu
lca3
uccu
lca

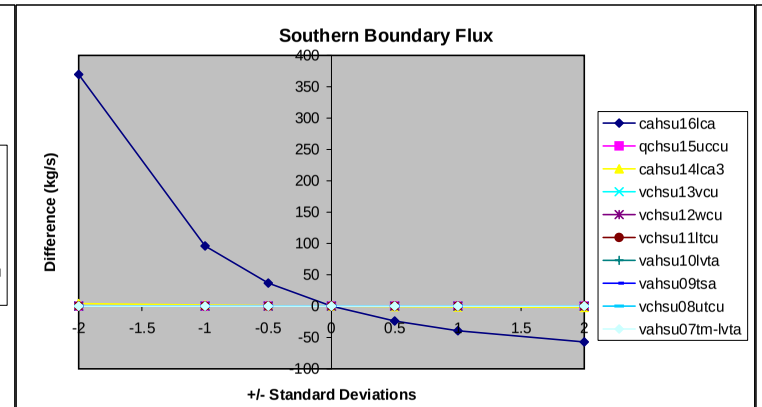
Southern Boundary Flux
Difference (kg/s)
+/- Standard Deviations
cahsu16lca
qchsu15uccu
cahsu14lca3
vchsu13vcu
vchsu12wcu
vchsu11ltcu
vahsu10lvta
vahsu09tsa
vchsu08utcu
vahsu07tm-lvta

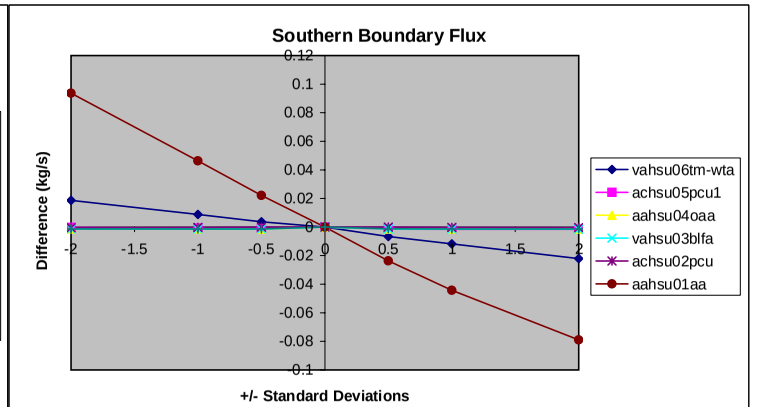
Southern Boundary Flux
Difference (kg/s)
+/- Standard Deviations
vahsu06tm-wta
achsu05pcu1
aahsu04oaa
vahsu03blfa
achsu02pcu
aahsu01aa

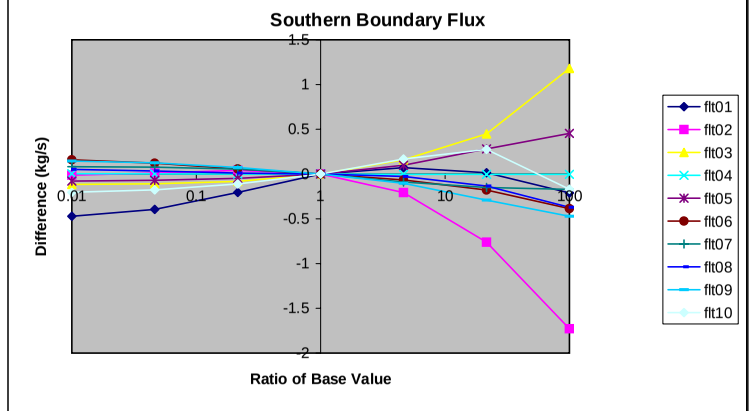
Southern Boundary Flux
Difference (kg/s)
Ratio of Base Value
flt01
flt02
flt03
flt04
flt05
flt06
flt07
flt08
flt09
flt10

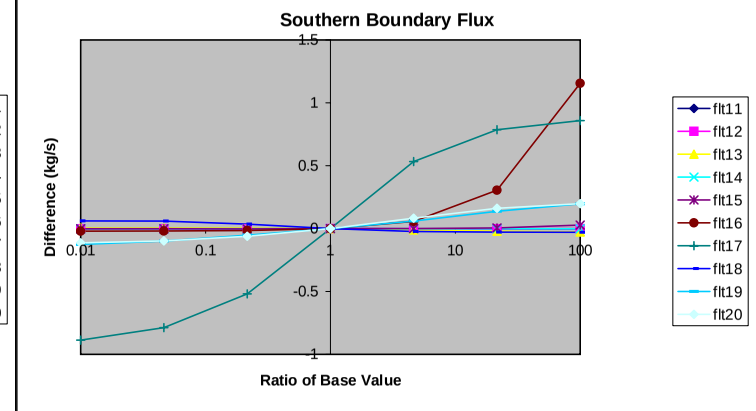
Southern Boundary Flux
Difference (kg/s)
Ratio of Base Value
flt11
flt12
flt13
flt14
flt15
flt16
flt17
flt18
flt19
flt20

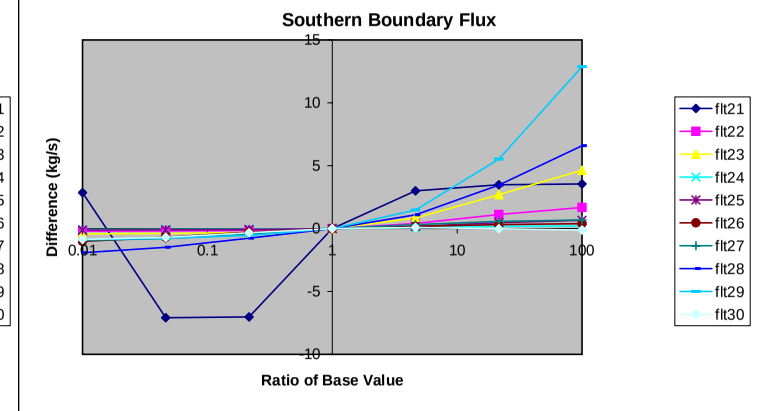
Southern Boundary Flux
Difference (kg/s)
Ratio of Base Value
flt21
flt22
flt23
flt24
flt25
flt26
flt27
flt28
flt29
flt30

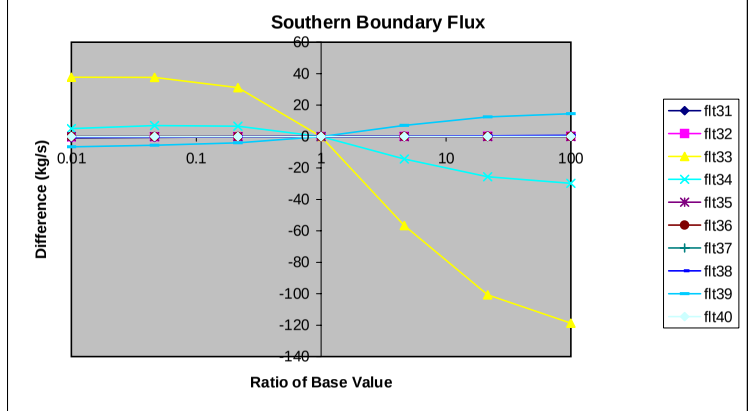
Southern Boundary Flux
Difference (kg/s)
Ratio of Base Value
flt31
flt32
flt33
flt34
flt35
flt36
flt37
flt38
flt39
flt40

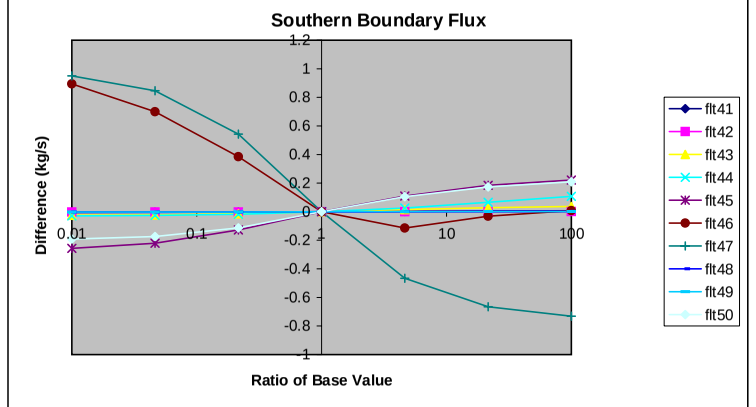
Southern Boundary Flux
Difference (kg/s)
Ratio of Base Value
flt41
flt42
flt43
flt44
flt45
flt46
flt47
flt48
flt49
flt50

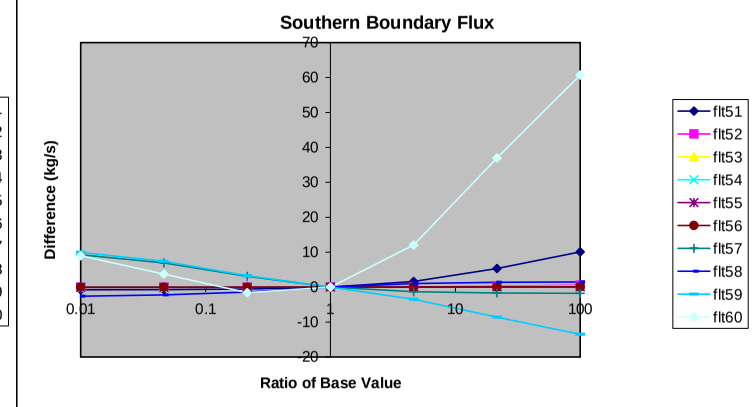
Southern Boundary Flux
Difference (kg/s)
Ratio of Base Value
flt51
flt52
flt53
flt54
flt55
flt56
flt57
flt58
flt59
flt60

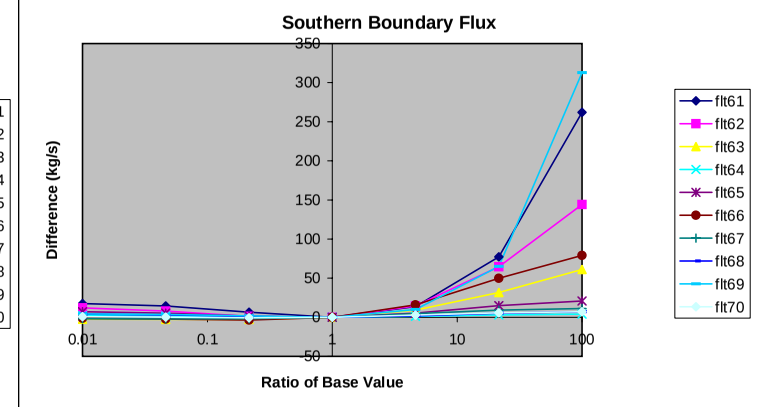
Southern Boundary Flux
Difference (kg/s)
Ratio of Base Value
flt61
flt62
flt63
flt64
flt65
flt66
flt67
flt68
flt69
flt70

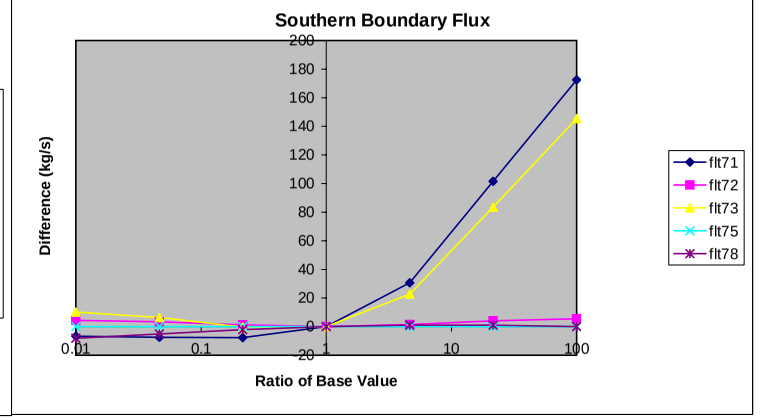
Southern Boundary Flux
Difference (kg/s)
Ratio of Base Value
flt71
flt72
flt73
flt75
flt78

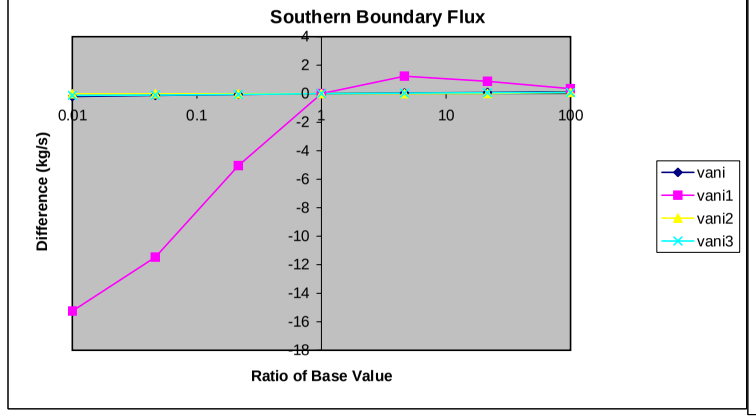
Southern Boundary Flux
Difference (kg/s)
Ratio of Base Value
vani
vani1
vani2
vani3

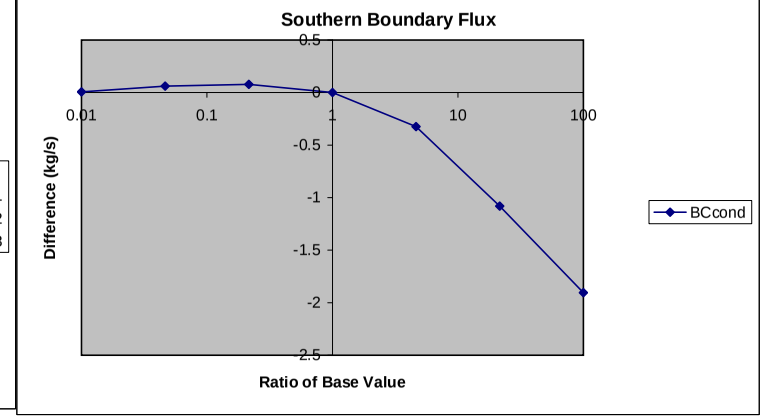
Southern Boundary Flux
Difference (kg/s)
Ratio of Base Value
BCcond

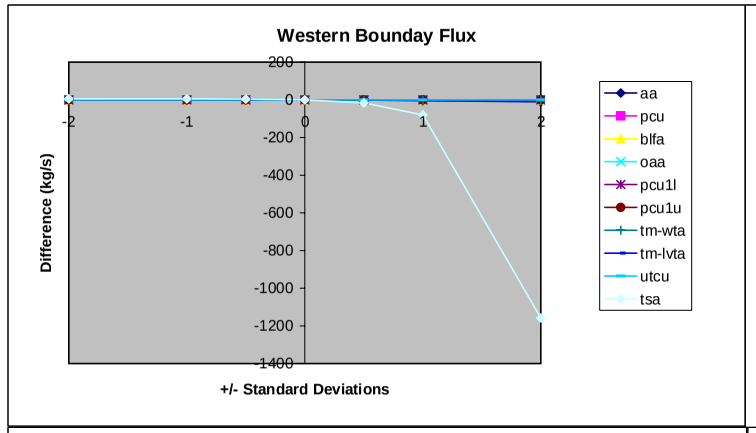
Western Bounday Flux
Difference (kg/s)
+/- Standard Deviations
aa
pcu
blfa
oaa
pcu1l
pcu1u
tm-wta
tm-lvta
utcu
tsa

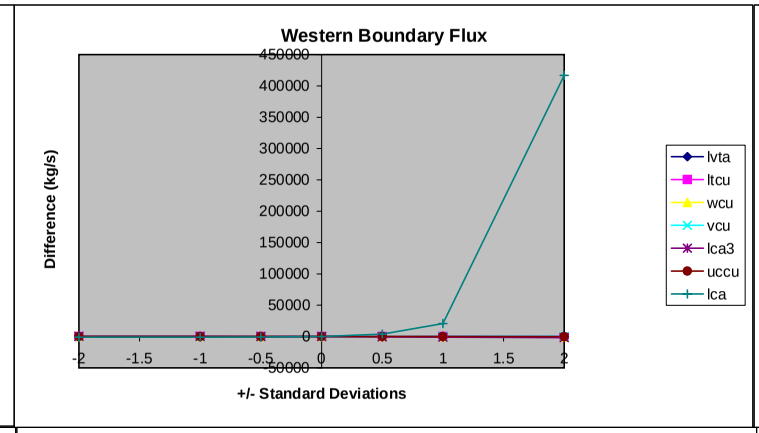
Western Boundary Flux
Difference (kg/s)
+/- Standard Deviations
lvta
ltcu
wcu
vcu
lca3
uccu
lca

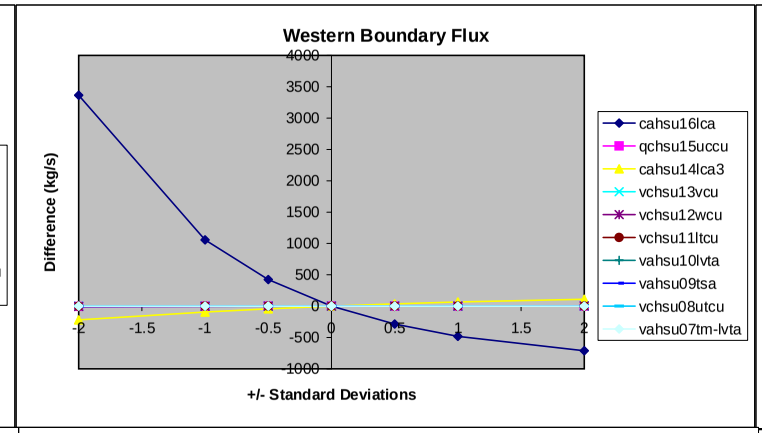
Western Boundary Flux
Difference (kg/s)
+/- Standard Deviations
cahsu16lca
qchsu15uccu
cahsu14lca3
vchsu13vcu
vchsu12wcu
vchsu11ltcu
vahsu10lvta
vahsu09tsa
vchsu08utcu
vahsu07tm-lvta

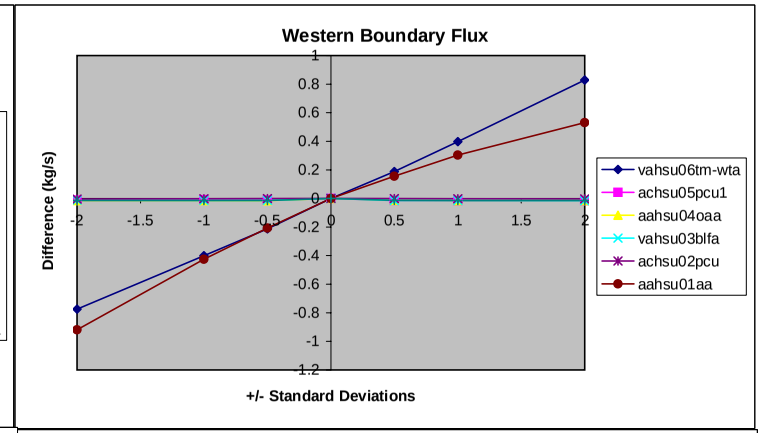
Western Boundary Flux
Difference (kg/s)
+/- Standard Deviations
vahsu06tm-wta
achsu05pcu1
aahsu04oaa
vahsu03blfa
achsu02pcu
aahsu01aa

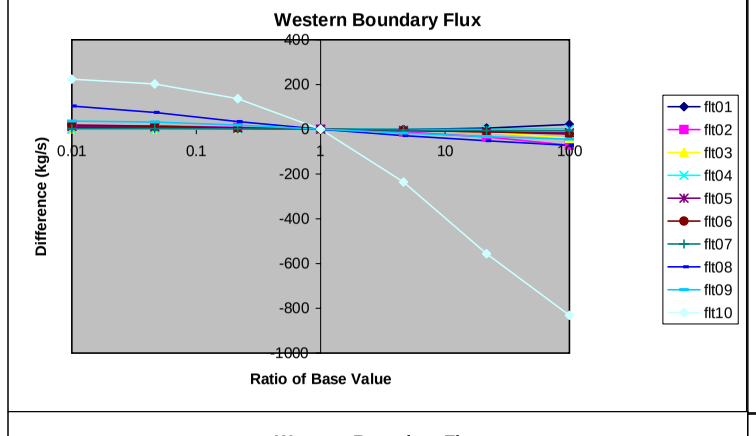
Western Boundary Flux
Difference (kg/s)
Ratio of Base Value
flt01
flt02
flt03
flt04
flt05
flt06
flt07
flt08
flt09
flt10

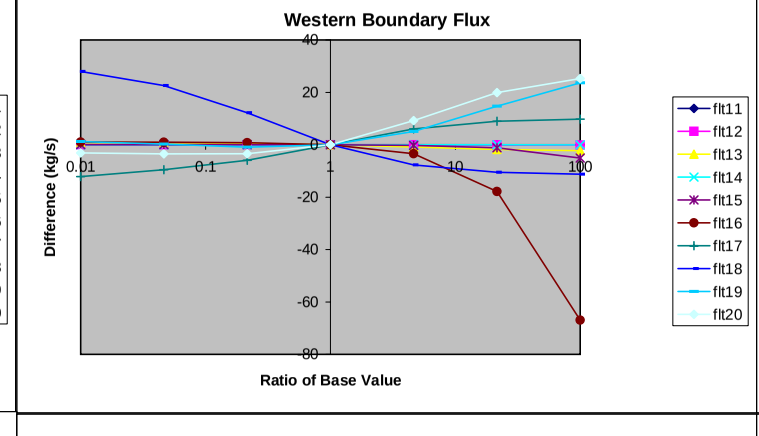
Western Boundary Flux
Difference (kg/s)
Ratio of Base Value
flt11
flt12
flt13
flt14
flt15
flt16
flt17
flt18
flt19
flt20

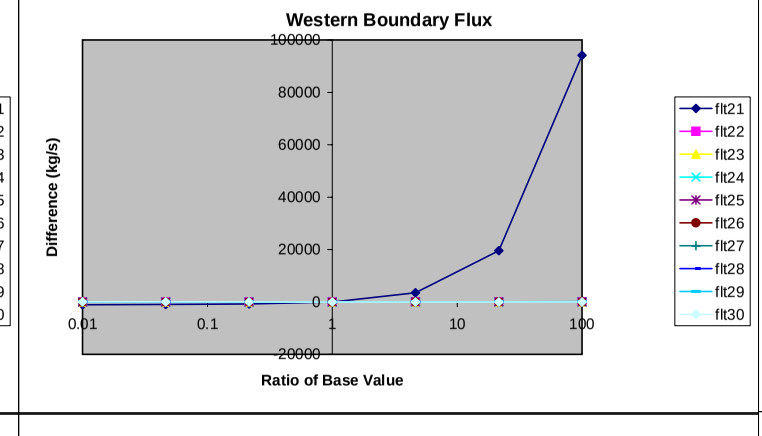
Western Boundary Flux
Difference (kg/s)
Ratio of Base Value
flt21
flt22
flt23
flt24
flt25
flt26
flt27
flt28
flt29
flt30

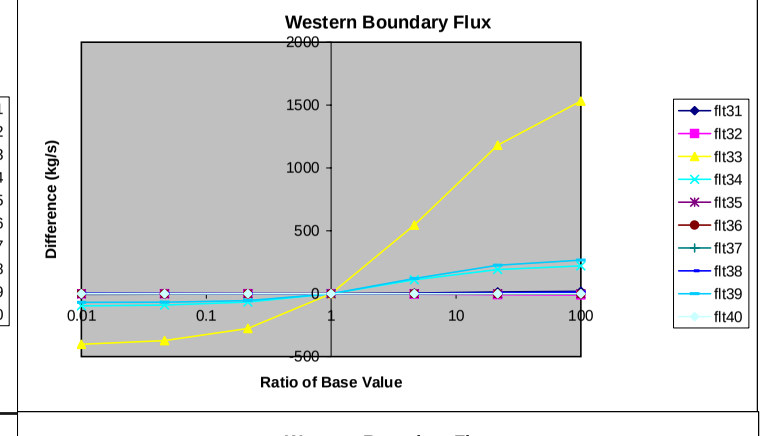
Western Boundary Flux
Difference (kg/s)
Ratio of Base Value
flt31
flt32
flt33
flt34
flt35
flt36
flt37
flt38
flt39
flt40

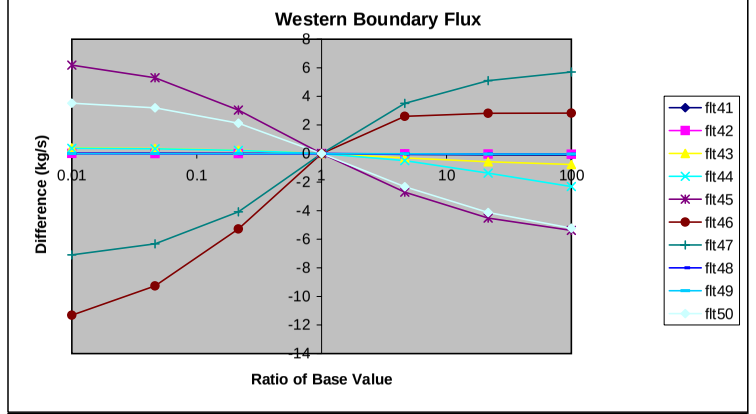
Western Boundary Flux
Difference (kg/s)
Ratio of Base Value
flt41
flt42
flt43
flt44
flt45
flt46
flt47
flt48
flt49
flt50

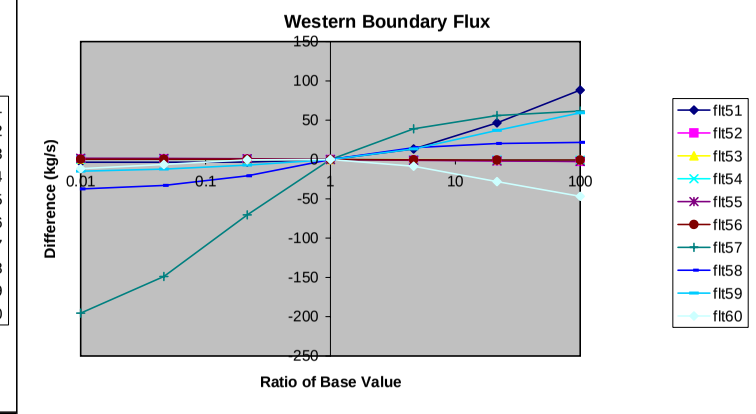
Western Boundary Flux
Difference (kg/s)
Ratio of Base Value
flt51
flt52
flt53
flt54
flt55
flt56
flt57
flt58
flt59
flt60

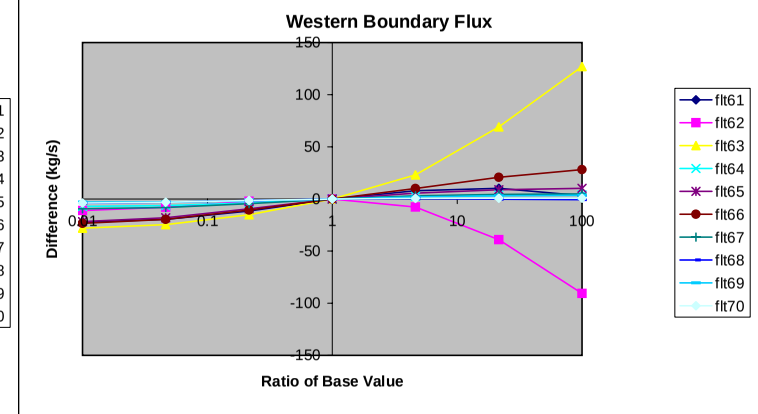
Western Boundary Flux
Difference (kg/s)
Ratio of Base Value
flt61
flt62
flt63
flt64
flt65
flt66
flt67
flt68
flt69
flt70

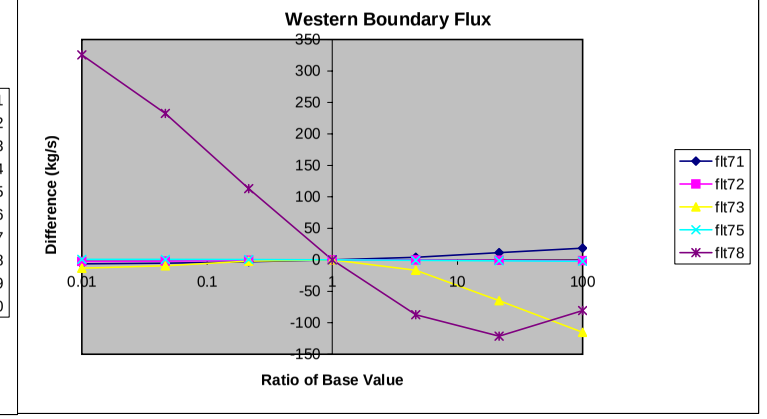
Western Boundary Flux
Difference (kg/s)
Ratio of Base Value
flt71
flt72
flt73
flt75
flt78

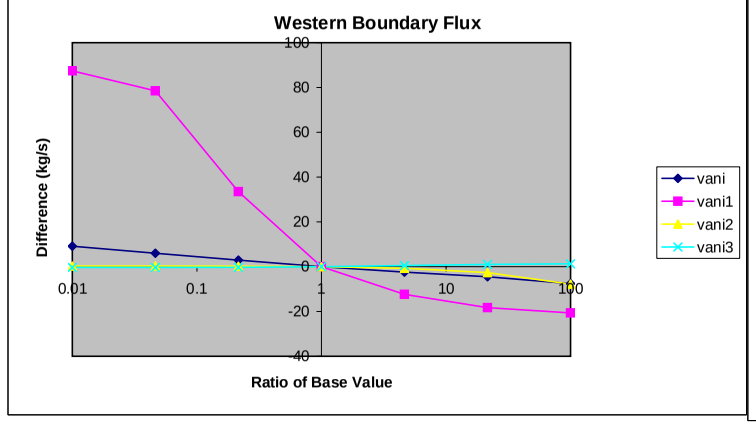
Western Boundary Flux
Difference (kg/s)
Ratio of Base Value
vani
vani1
vani2
vani3

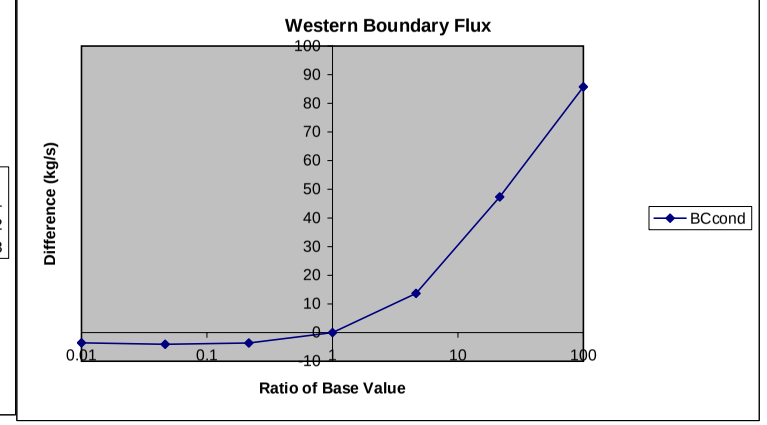
Western Boundary Flux
Difference (kg/s)
Ratio of Base Value
BCcond

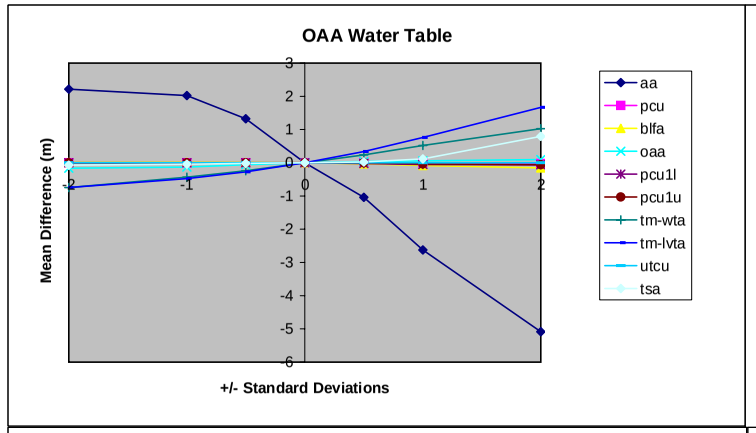
OAA Water Table
Mean Difference (m)
+/- Standard Deviations
aa
pcu
blfa
oaa
pcu1l
pcu1u
tm-wta
tm-lvta
utcu
tsa

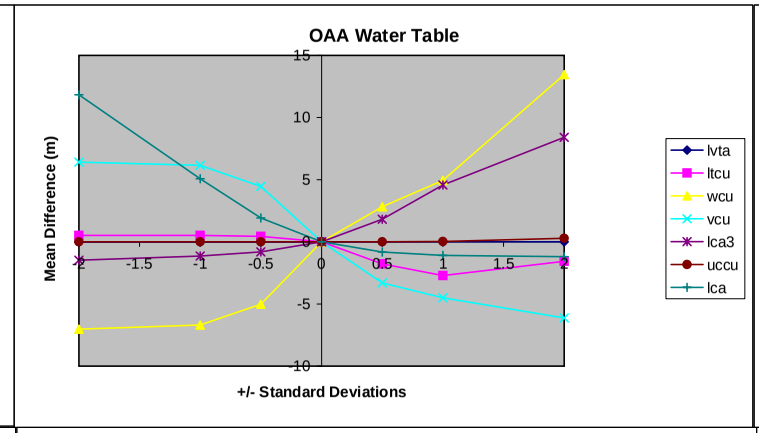
OAA Water Table
Mean Difference (m)
+/- Standard Deviations
lvta
ltcu
wcu
vcu
lca3
uccu
lca

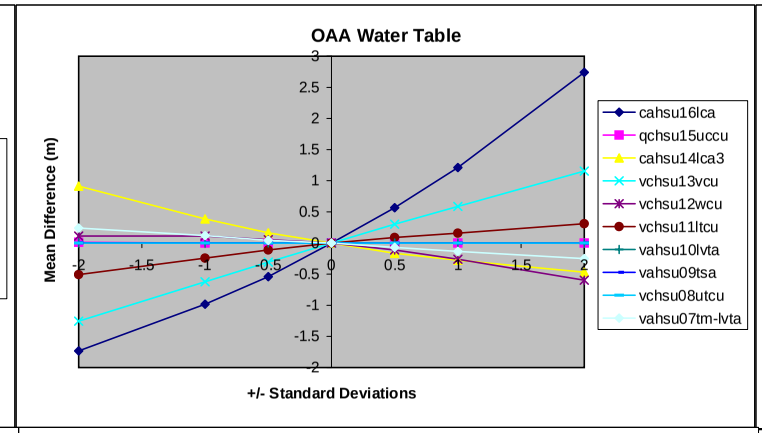
OAA Water Table
Mean Difference (m)
+/- Standard Deviations
cahsu16lca
qchsu15uccu
cahsu14lca3
vchsu13vcu
vchsu12wcu
vchsu11ltcu
vahsu10lvta
vahsu09tsa
vchsu08utcu
vahsu07tm-lvta

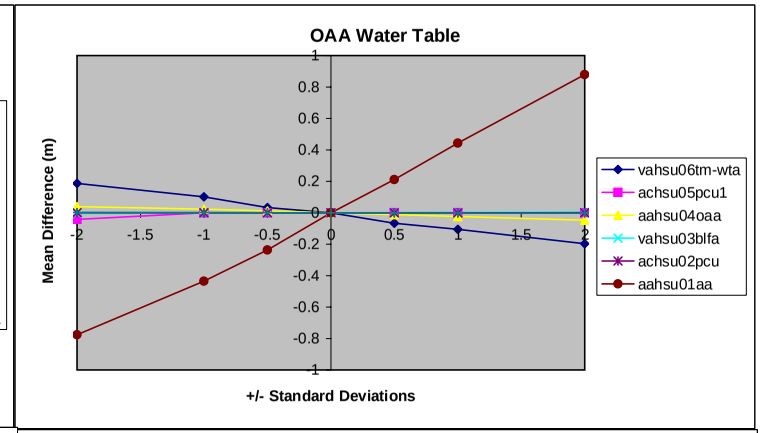
OAA Water Table
Mean Difference (m)
+/- Standard Deviations
vahsu06tm-wta
achsu05pcu1
aahsu04oaa
vahsu03blfa
achsu02pcu
aahsu01aa

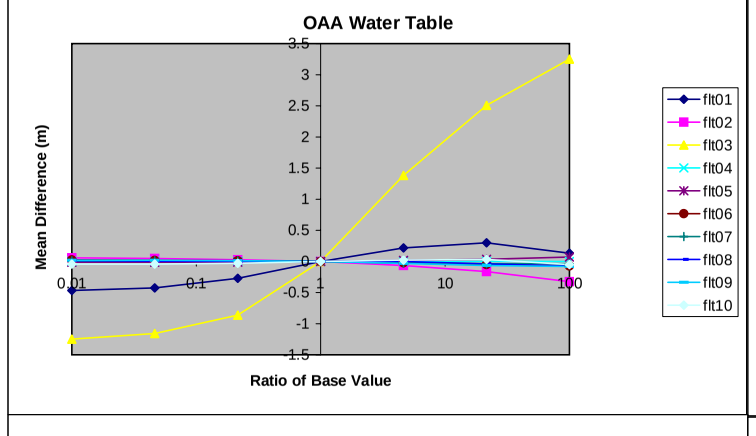
OAA Water Table
Mean Difference (m)
Ratio of Base Value
flt01
flt02
flt03
flt04
flt05
flt06
flt07
flt08
flt09
flt10

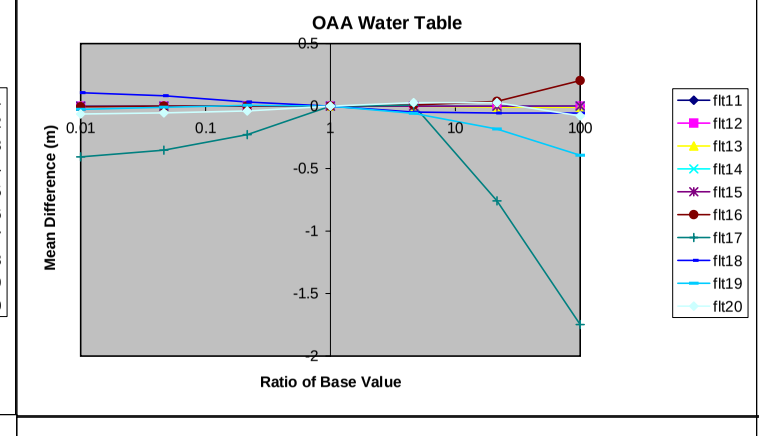
OAA Water Table
Mean Difference (m)
Ratio of Base Value
flt11
flt12
flt13
flt14
flt15
flt16
flt17
flt18
flt19
flt20

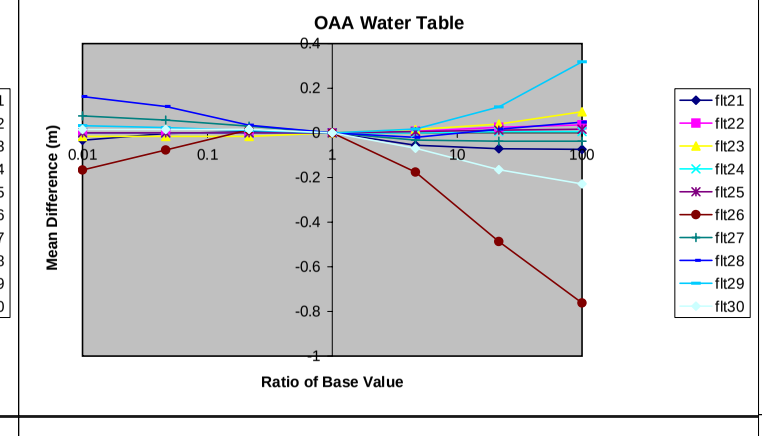
OAA Water Table
Mean Difference (m)
Ratio of Base Value
flt21
flt22
flt23
flt24
flt25
flt26
flt27
flt28
flt29
flt30

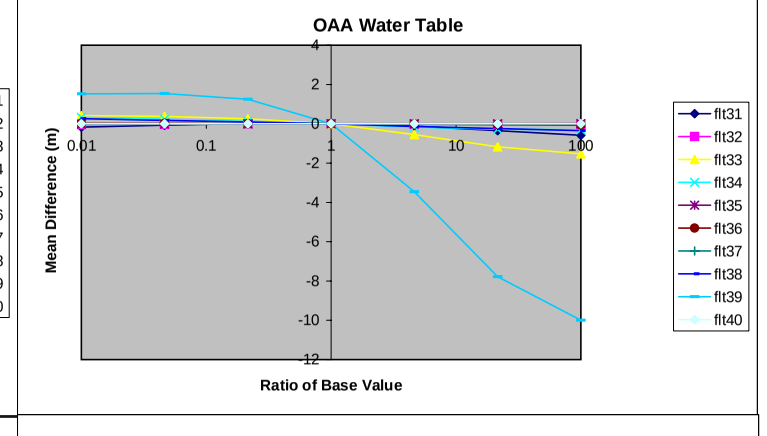
OAA Water Table
Mean Difference (m)
Ratio of Base Value
flt31
flt32
flt33
flt34
flt35
flt36
flt37
flt38
flt39
flt40

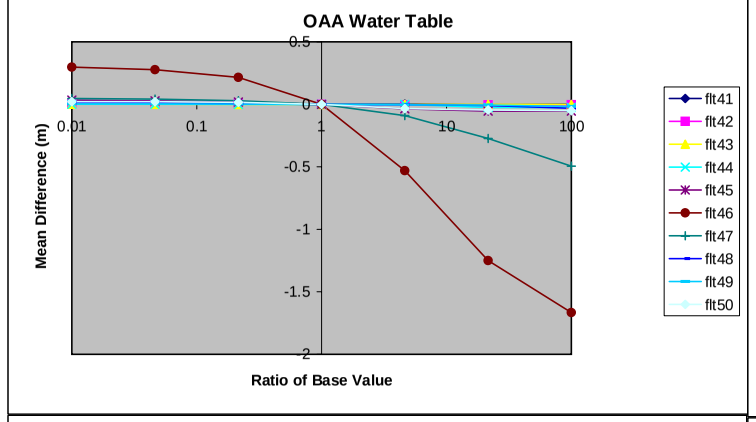
OAA Water Table
Mean Difference (m)
Ratio of Base Value
flt41
flt42
flt43
flt44
flt45
flt46
flt47
flt48
flt49
flt50

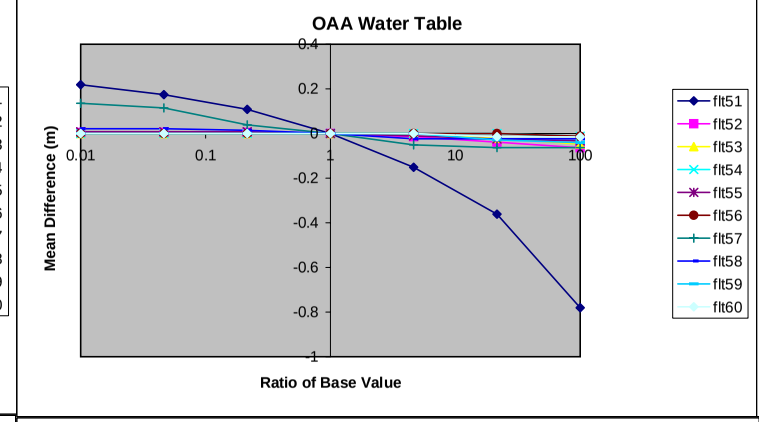
OAA Water Table
Mean Difference (m)
Ratio of Base Value
flt51
flt52
flt53
flt54
flt55
flt56
flt57
flt58
flt59
flt60

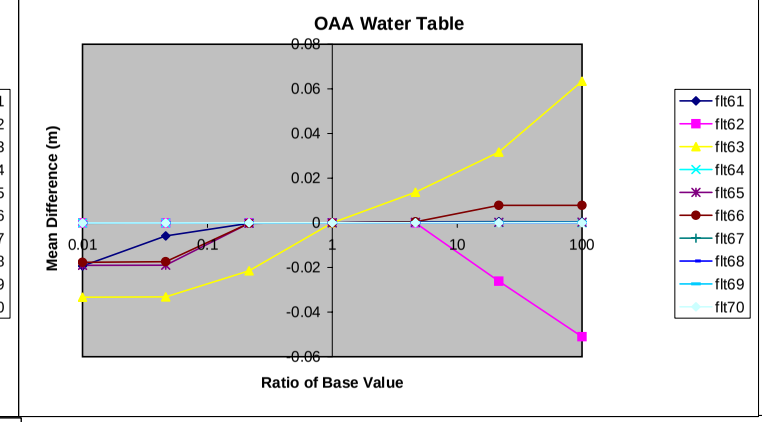
OAA Water Table
Mean Difference (m)
Ratio of Base Value
flt61
flt62
flt63
flt64
flt65
flt66
flt67
flt68
flt69
flt70

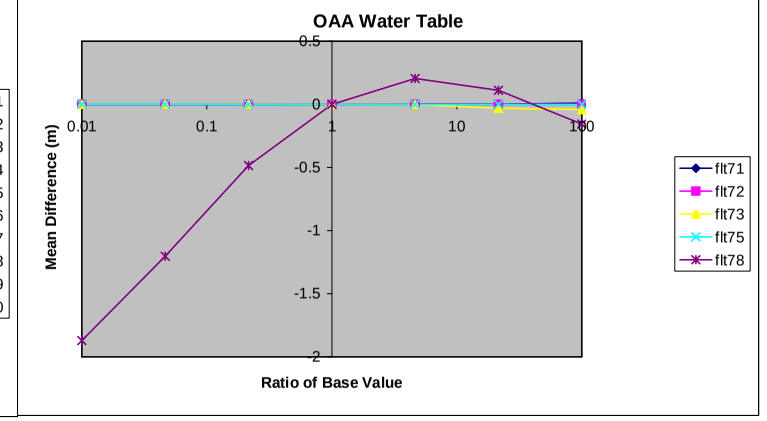
OAA Water Table
Mean Difference (m)
Ratio of Base Value
flt71
flt72
flt73
flt75
flt78

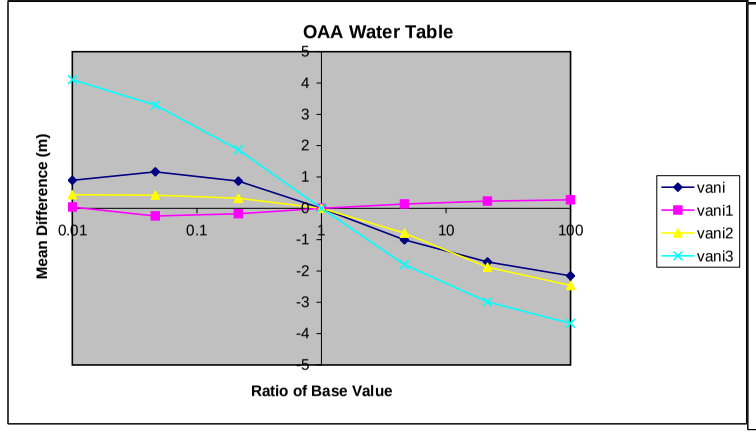
OAA Water Table
Mean Difference (m)
Ratio of Base Value
vani
vani1
vani2
vani3

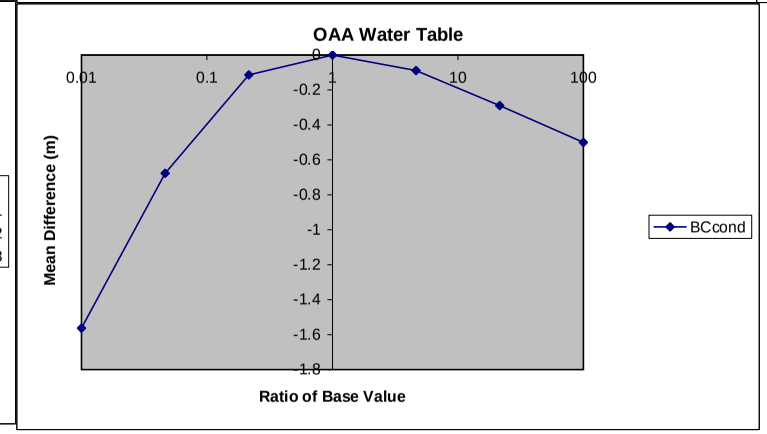
OAA Water Table
Mean Difference (m)
Ratio of Base Value
BCcond

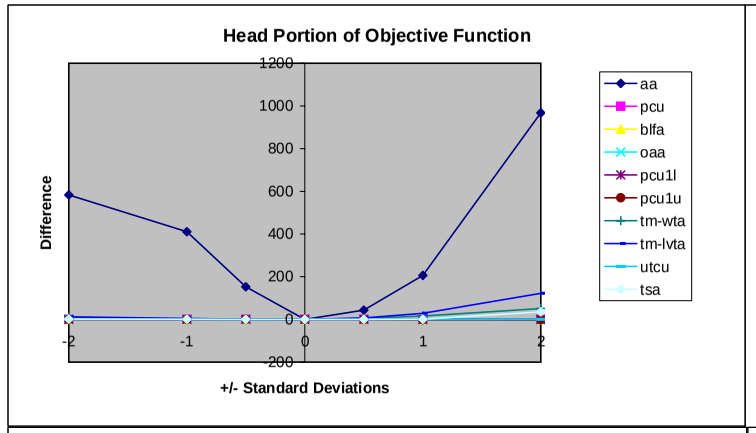
Head Portion of Objective Function
Difference
+/- Standard Deviations
aa
pcu
blfa
oaa
pcu1l
pcu1u
tm-wta
tm-lvta
utcu
tsa

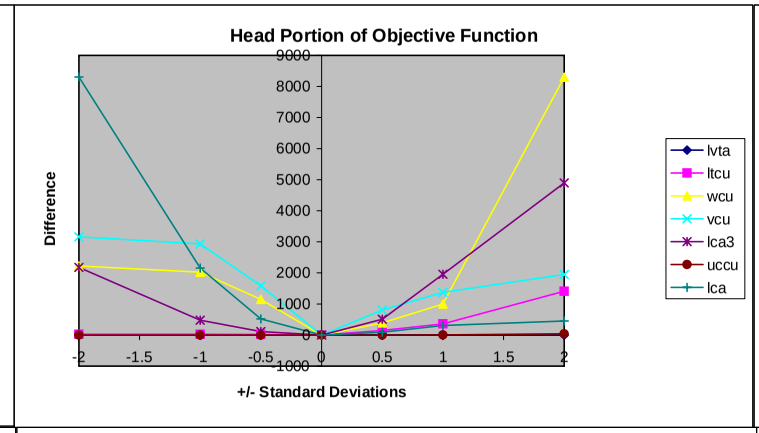
Head Portion of Objective Function
Difference
+/- Standard Deviations
lvta
ltcu
wcu
vcu
lca3
uccu
lca

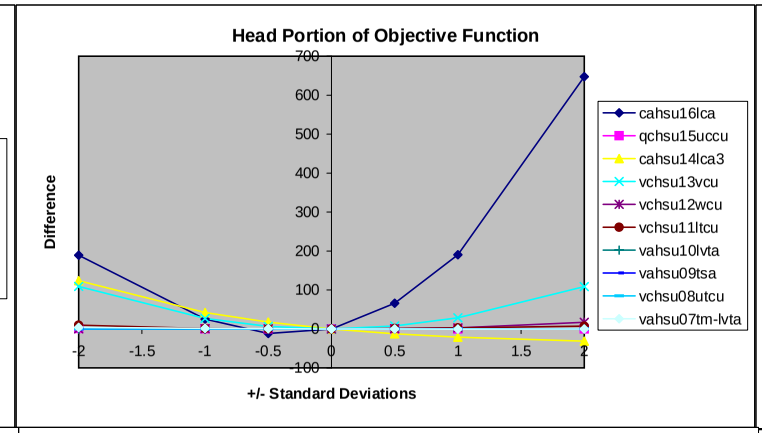
Head Portion of Objective Function
Difference
+/- Standard Deviations
cahsu16lca
qchsu15uccu
cahsu14lca3
vchsu13vcu
vchsu12wcu
vchsu11ltcu
vahsu10lvta
vahsu09tsa
vchsu08utcu
vahsu07tm-lvta

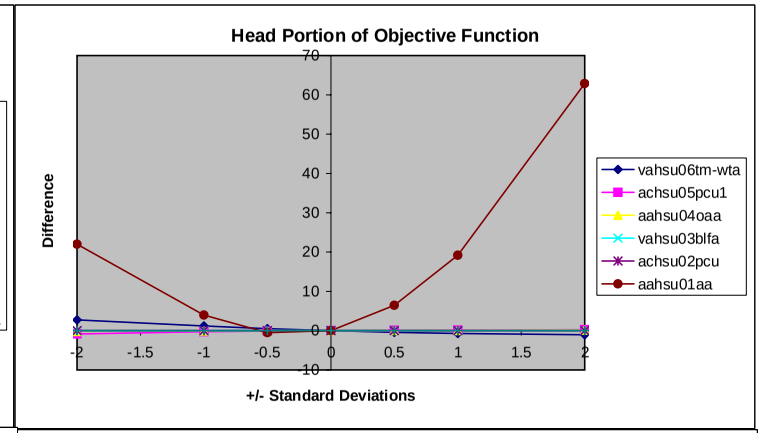
Head Portion of Objective Function
Difference
+/- Standard Deviations
vahsu06tm-wta
achsu05pcu1
aahsu04oaa
vahsu03blfa
achsu02pcu
aahsu01aa

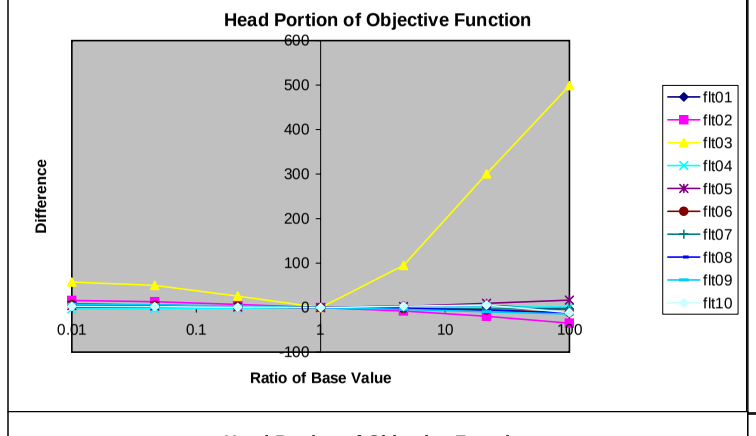
Head Portion of Objective Function
Difference
Ratio of Base Value
flt01
flt02
flt03
flt04
flt05
flt06
flt07
flt08
flt09
flt10

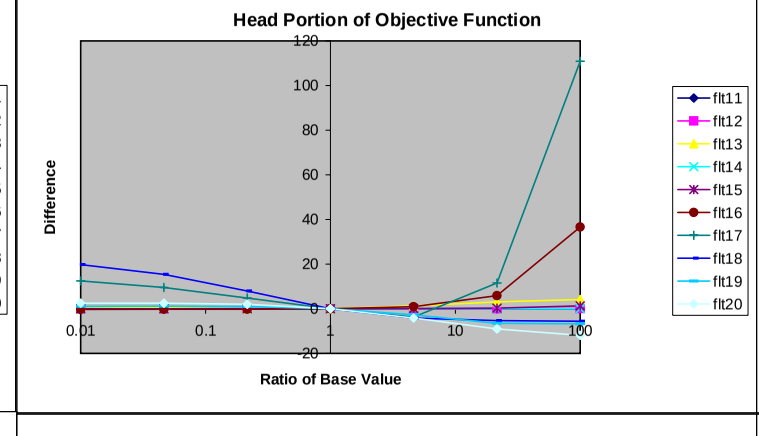
Head Portion of Objective Function
Difference
Ratio of Base Value
flt11
flt12
flt13
flt14
flt15
flt16
flt17
flt18
flt19
flt20

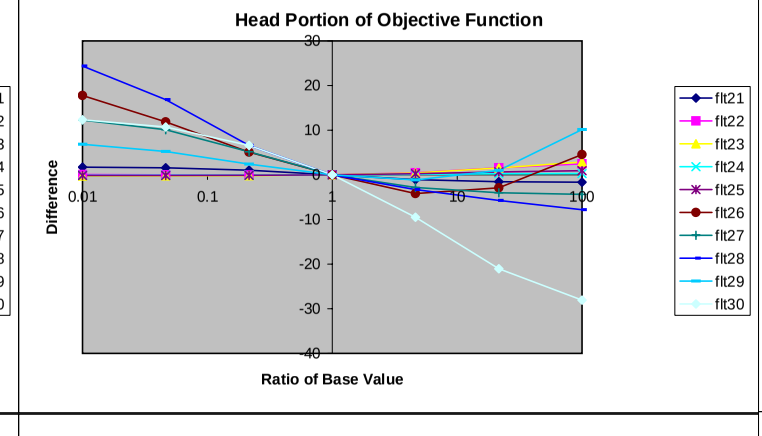
Head Portion of Objective Function
Difference
Ratio of Base Value
flt21
flt22
flt23
flt24
flt25
flt26
flt27
flt28
flt29
flt30

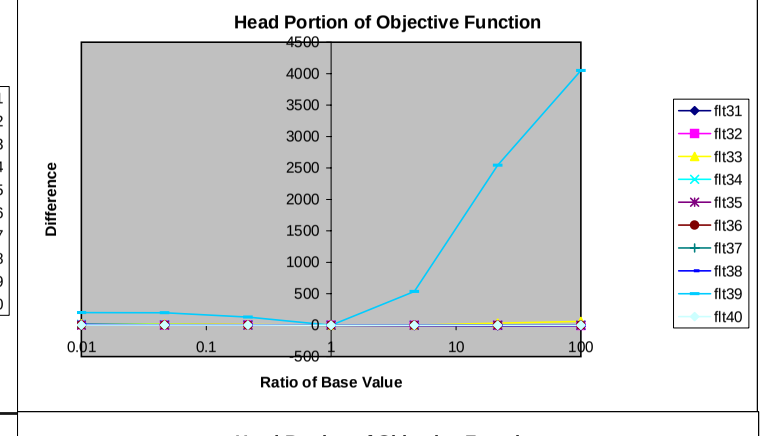
Head Portion of Objective Function
Difference
Ratio of Base Value
flt31
flt32
flt33
flt34
flt35
flt36
flt37
flt38
flt39
flt40

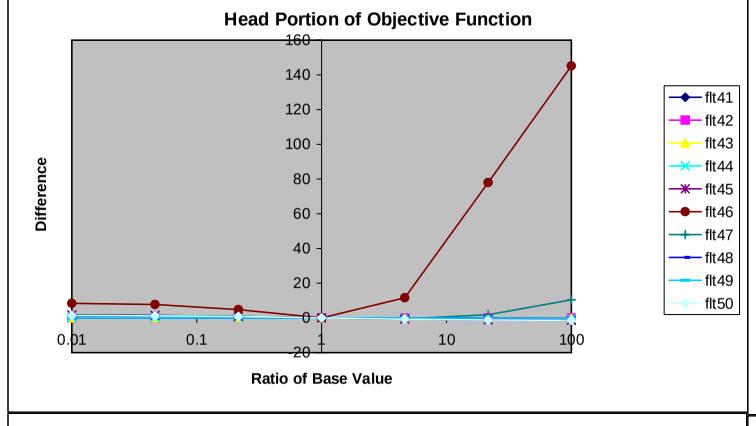
Head Portion of Objective Function
Difference
Ratio of Base Value
flt41
flt42
flt43
flt44
flt45
flt46
flt47
flt48
flt49
flt50

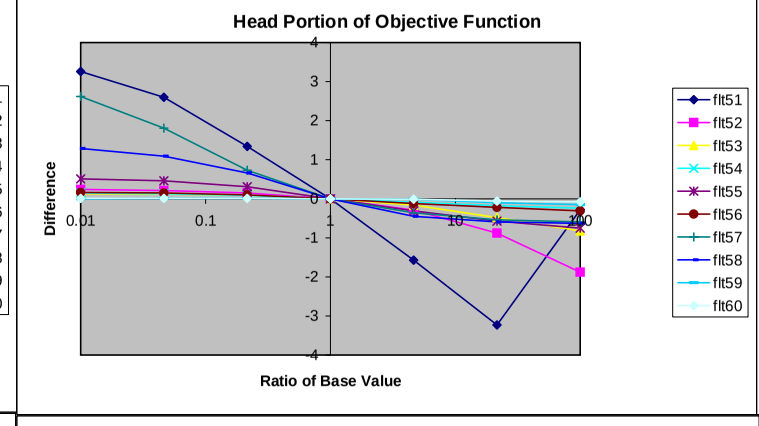
Head Portion of Objective Function
Difference
Ratio of Base Value
flt51
flt52
flt53
flt54
flt55
flt56
flt57
flt58
flt59
flt60

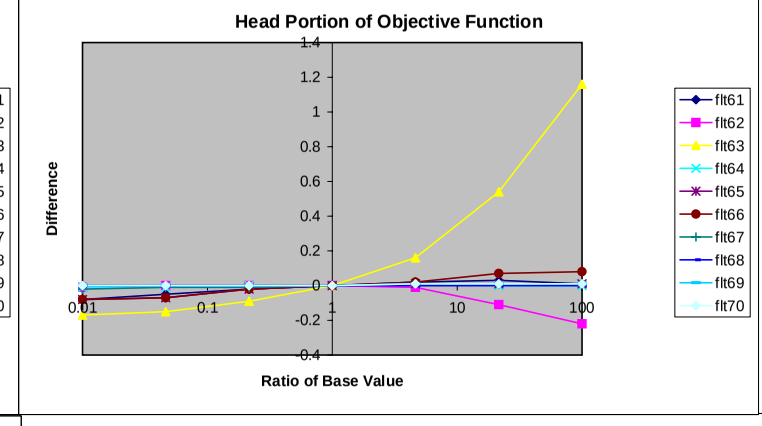
Head Portion of Objective Function
Difference
Ratio of Base Value
flt61
flt62
flt63
flt64
flt65
flt66
flt67
flt68
flt69
flt70

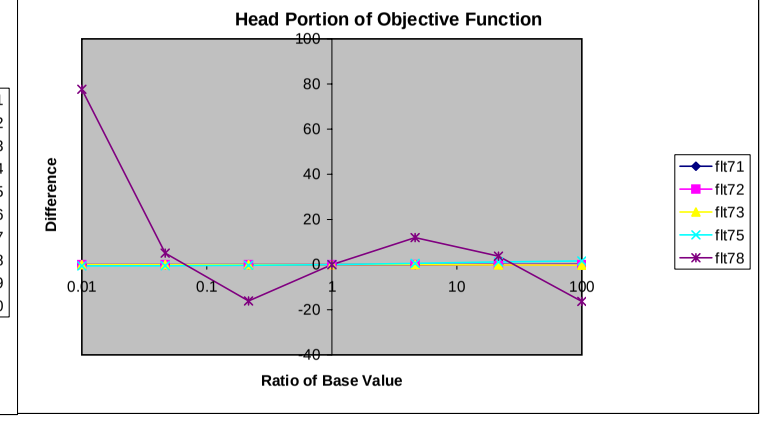
Head Portion of Objective Function
Difference
Ratio of Base Value
flt71
flt72
flt73
flt75
flt78

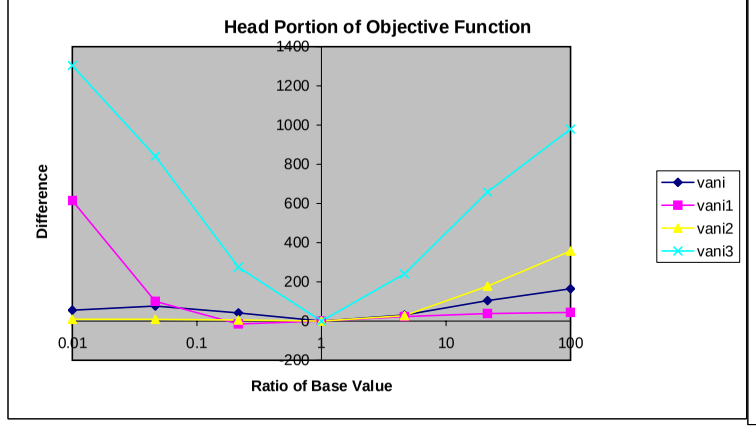
Head Portion of Objective Function
Difference
Ratio of Base Value
vani
vani1
vani2
vani3

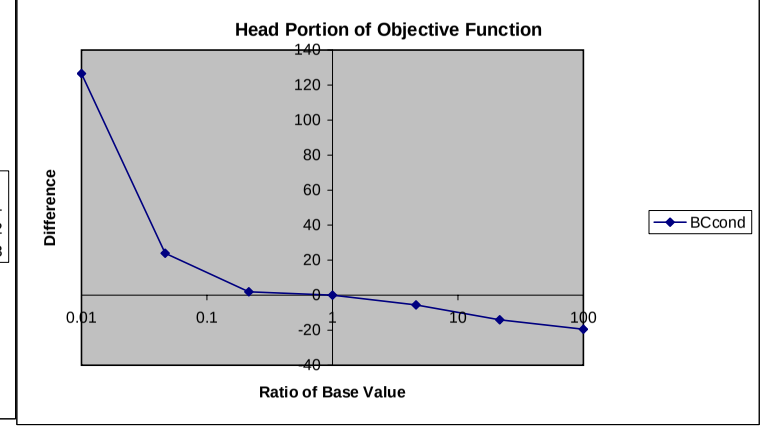
Head Portion of Objective Function
Difference
Ratio of Base Value
BCcond

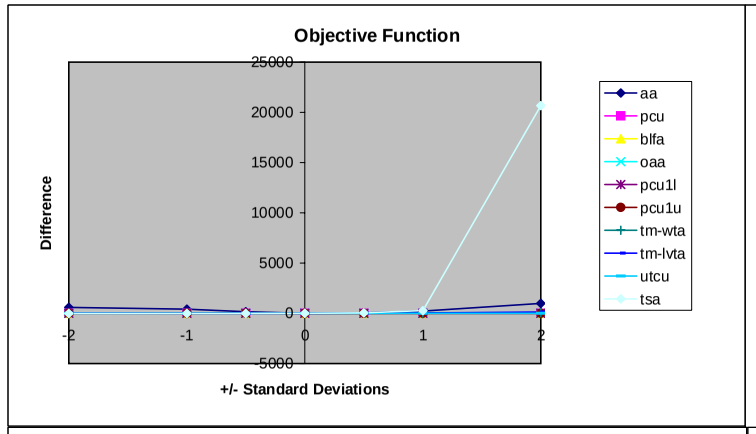
Objective Function
Difference
+/- Standard Deviations
aa
pcu
blfa
oaa
pcu1l
pcu1u
tm-wta
tm-lvta
utcu
tsa

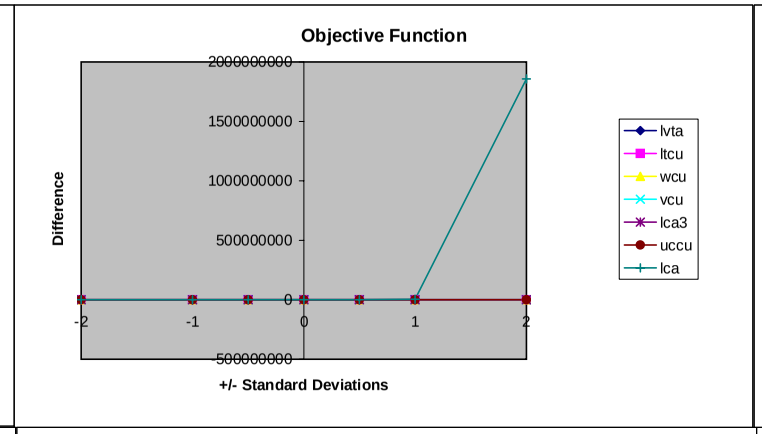
Objective Function
Difference
+/- Standard Deviations
lvta
ltcu
wcu
vcu
lca3
uccu
lca

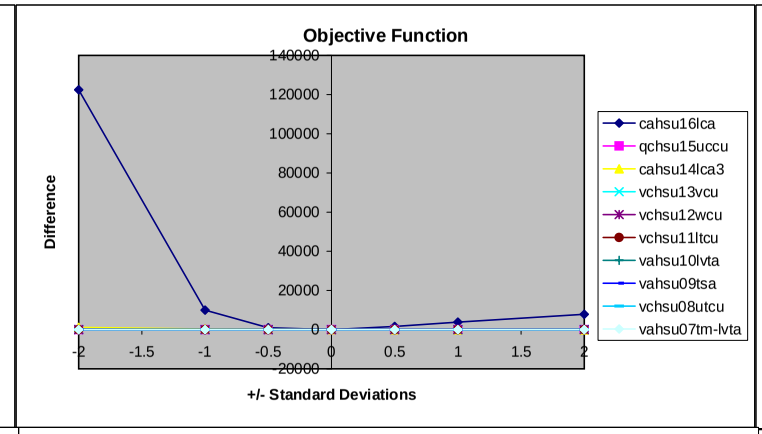
Objective Function
Difference
+/- Standard Deviations
cahsu16lca
qchsu15uccu
cahsu14lca3
vchsu13vcu
vchsu12wcu
vchsu11ltcu
vahsu10lvta
vahsu09tsa
vchsu08utcu
vahsu07tm-lvta

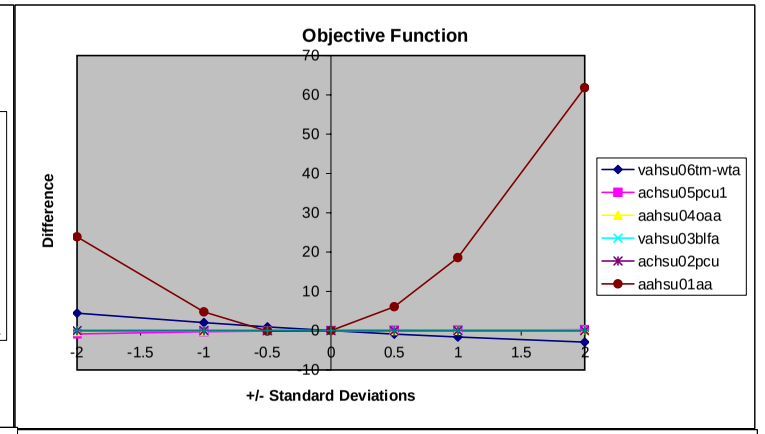
Objective Function
Difference
+/- Standard Deviations
vahsu06tm-wta
achsu05pcu1
aahsu04oaa
vahsu03blfa
achsu02pcu
aahsu01aa

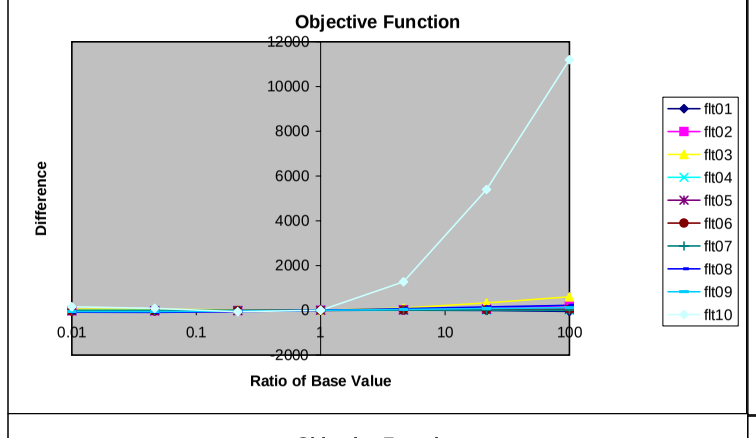
Objective Function
Difference
Ratio of Base Value
flt01
flt02
flt03
flt04
flt05
flt06
flt07
flt08
flt09
flt10

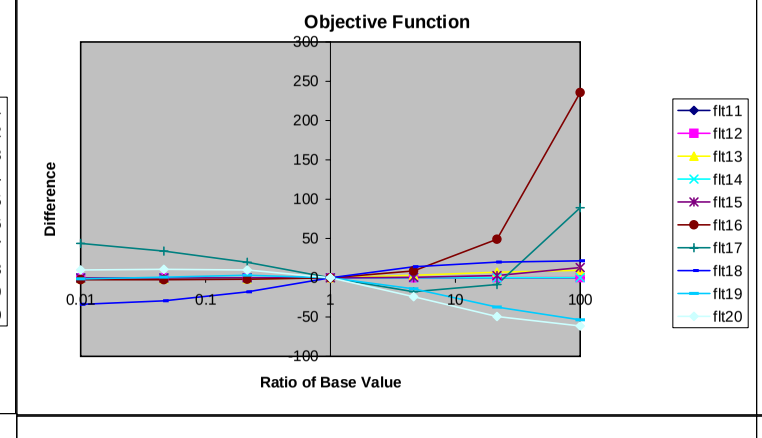
Objective Function
Difference
Ratio of Base Value
flt11
flt12
flt13
flt14
flt15
flt16
flt17
flt18
flt19
flt20

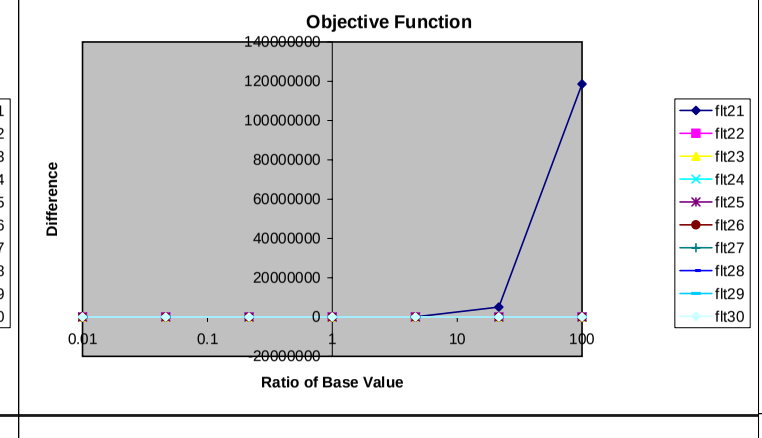
Objective Function
Difference
Ratio of Base Value
flt21
flt22
flt23
flt24
flt25
flt26
flt27
flt28
flt29
flt30

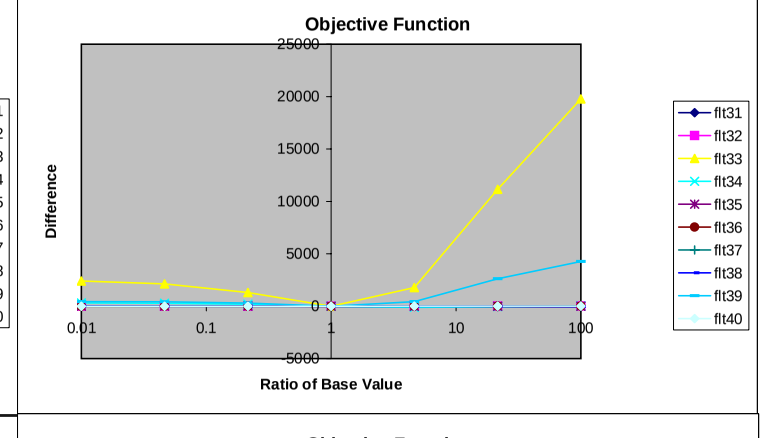
Objective Function
Difference
Ratio of Base Value
flt31
flt32
flt33
flt34
flt35
flt36
flt37
flt38
flt39
flt40

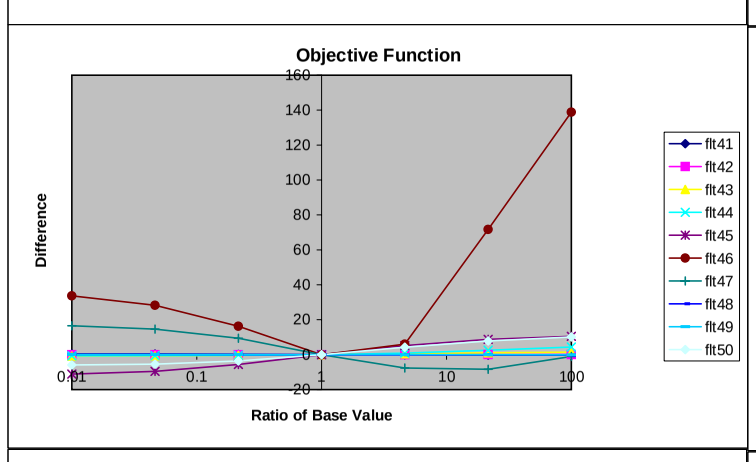
Objective Function
Difference
Ratio of Base Value
flt41
flt42
flt43
flt44
flt45
flt46
flt47
flt48
flt49
flt50

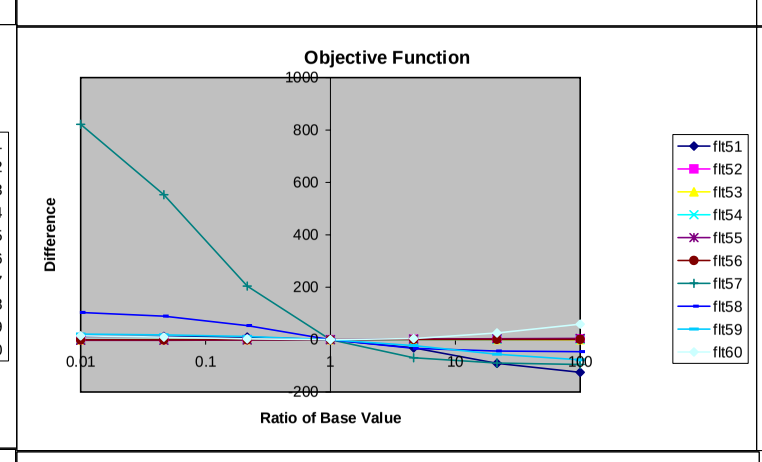
Objective Function
Difference
Ratio of Base Value
flt51
flt52
flt53
flt54
flt55
flt56
flt57
flt58
flt59
flt60

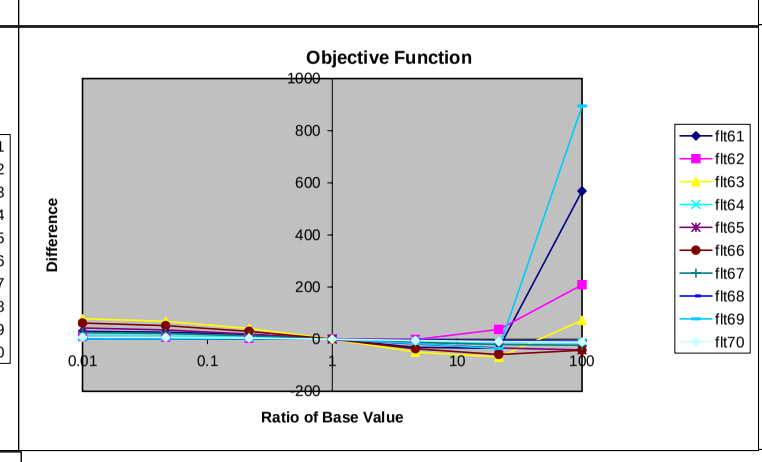
Objective Function
Difference
Ratio of Base Value
flt61
flt62
flt63
flt64
flt65
flt66
flt67
flt68
flt69
flt70

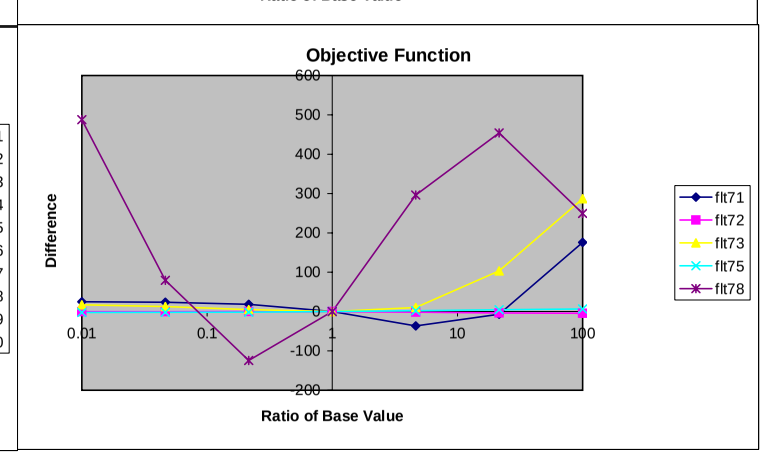
Objective Function
Difference
Ratio of Base Value
flt71
flt72
flt73
flt75
flt78

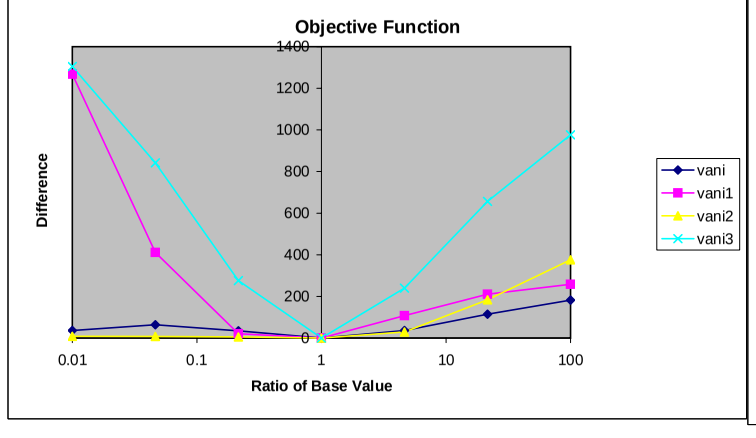
Objective Function
Difference
Ratio of Base Value
vani
vani1
vani2
vani3

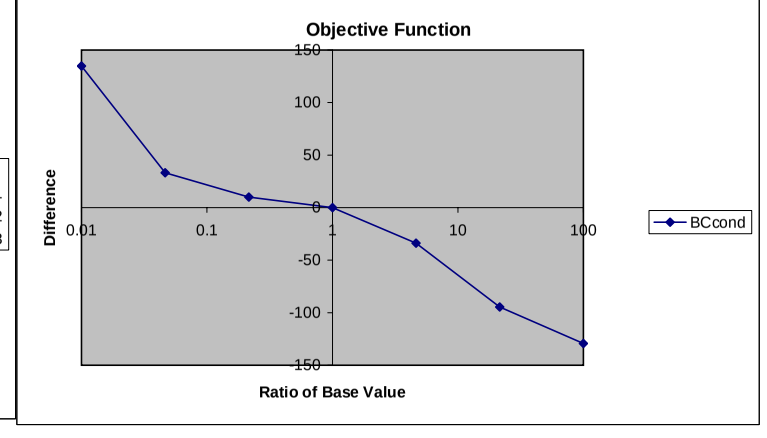
Objective Function
Difference
Ratio of Base Value
BCcond

C.3.2

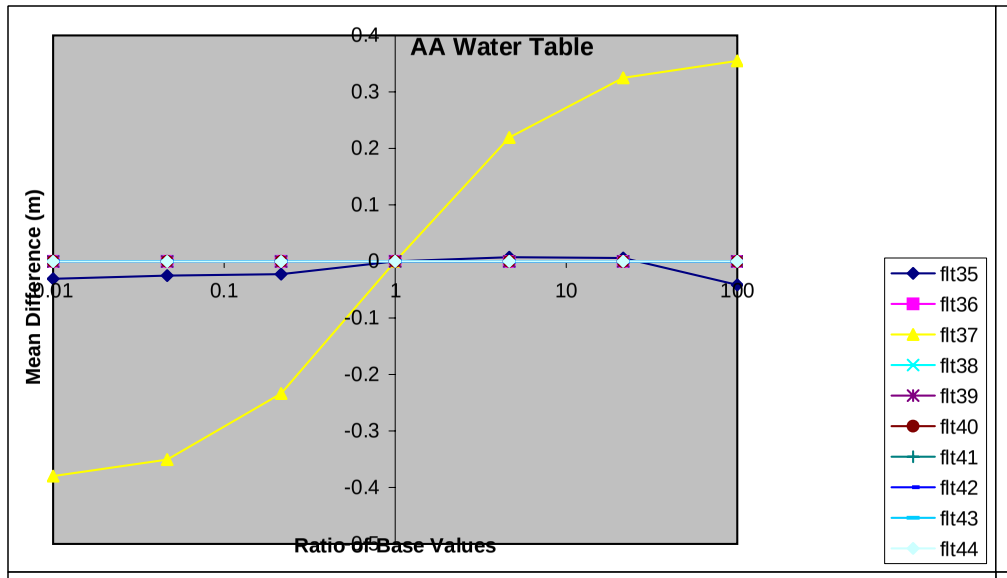
AA Water Table
Mean Difference (m)
Ratio of Base Values
flt35
flt36
flt37
flt38
flt39
flt40
flt41
flt42
flt43
flt44

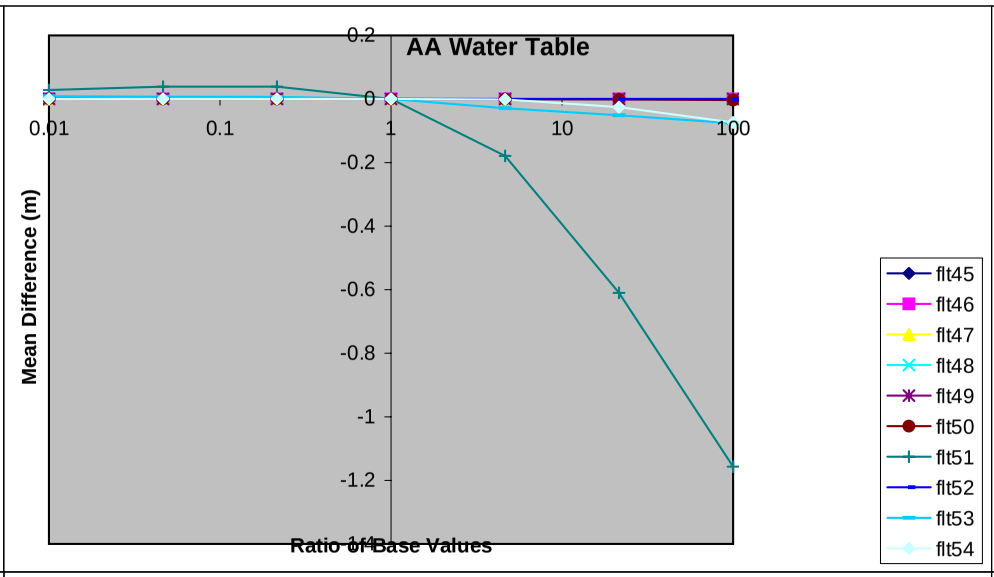
AA Water Table
Mean Difference (m)
Ratio of Base Values
flt45
flt46
flt47
flt48
flt49
flt50
flt51
flt52
flt53
flt54

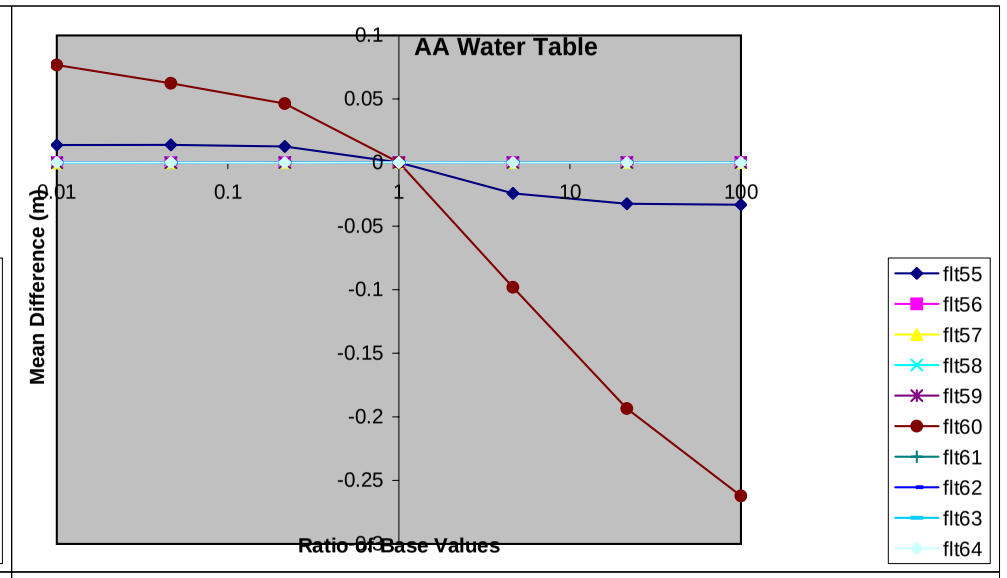
AA Water Table
Mean Difference (m)
Ratio of Base Values
flt55
flt56
flt57
flt58
flt59
flt60
flt61
flt62
flt63
flt64

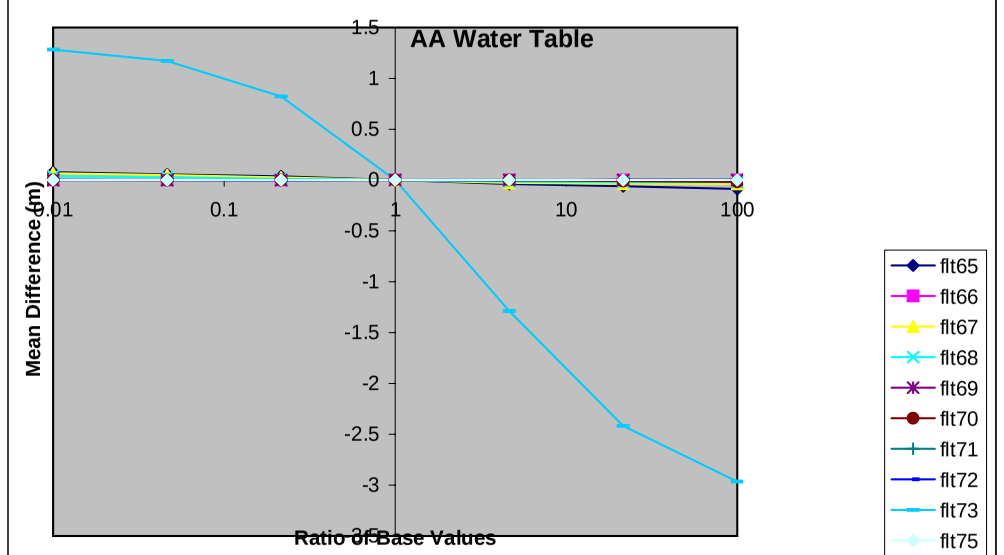
AA Water Table
Mean Difference (m)
Ratio of Base Values
flt65
flt66
flt67
flt68
flt69
flt70
flt71
flt72
flt73
flt75

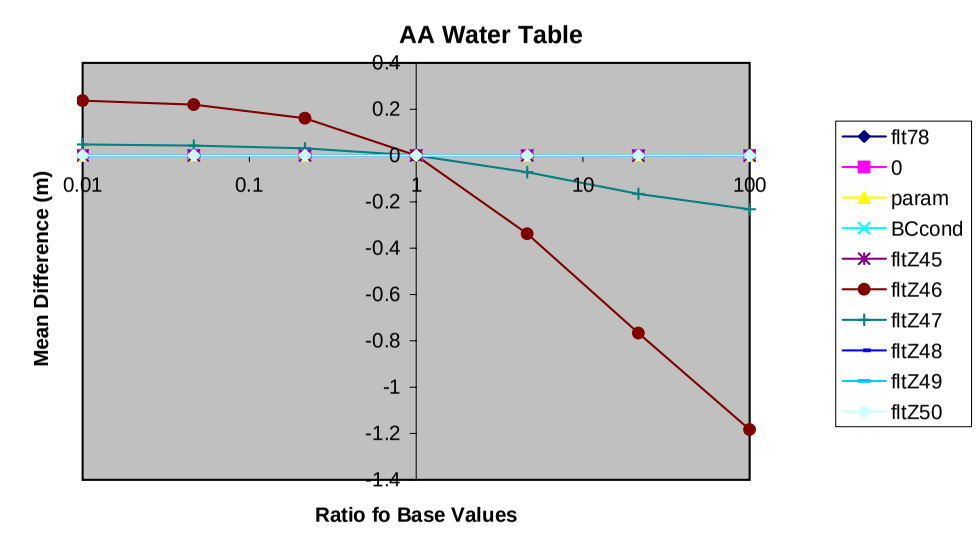
AA Water Table
Mean Difference (m)
Ratio fo Base Values
flt78
0
param
BCcond
fltZ45
fltZ46
fltZ47
fltZ48
fltZ49
fltZ50

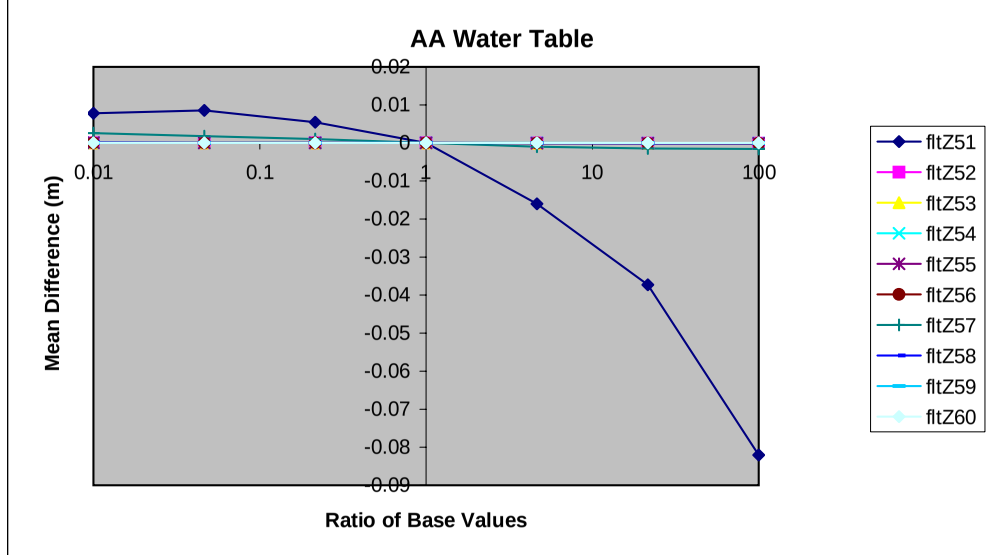
AA Water Table
Mean Difference (m)
Ratio of Base Values
fltZ51
fltZ52
fltZ53
fltZ54
fltZ55
fltZ56
fltZ57
fltZ58
fltZ59
fltZ60

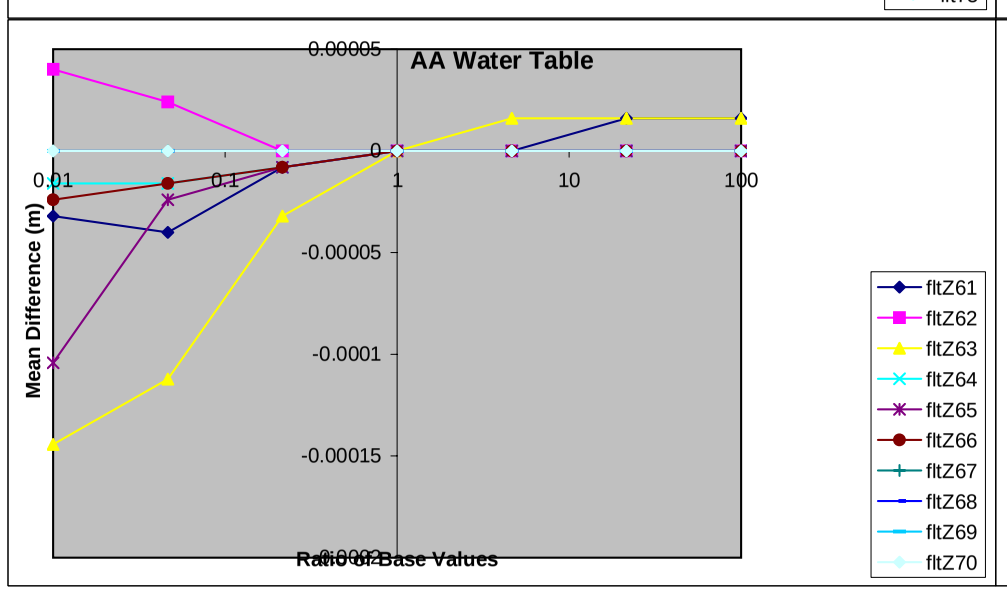
AA Water Table
Mean Difference (m)
Ratio of Base Values
fltZ61
fltZ62
fltZ63
fltZ64
fltZ65
fltZ66
fltZ67
fltZ68
fltZ69
fltZ70

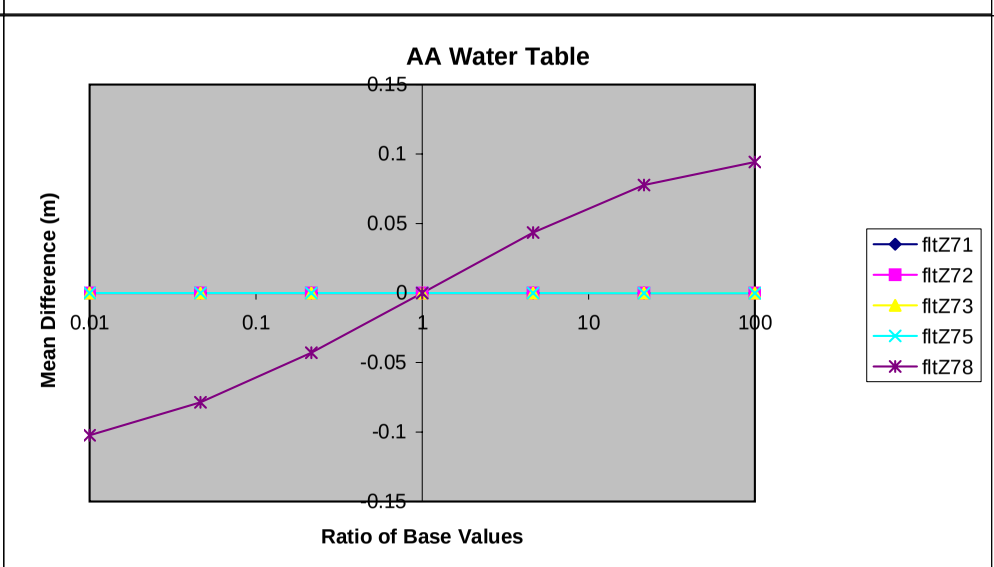
AA Water Table
Mean Difference (m)
Ratio of Base Values
fltZ71
fltZ72
fltZ73
fltZ75
fltZ78

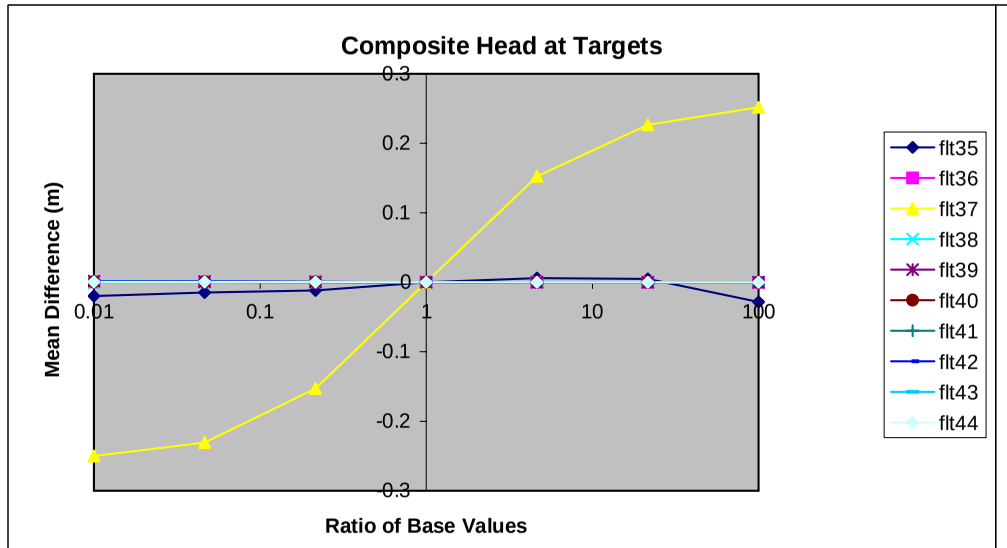
Composite Head at Targets
Mean Difference (m)
Ratio of Base Values
flt35
flt36
flt37
flt38
flt39
flt40
flt41
flt42
flt43
flt44

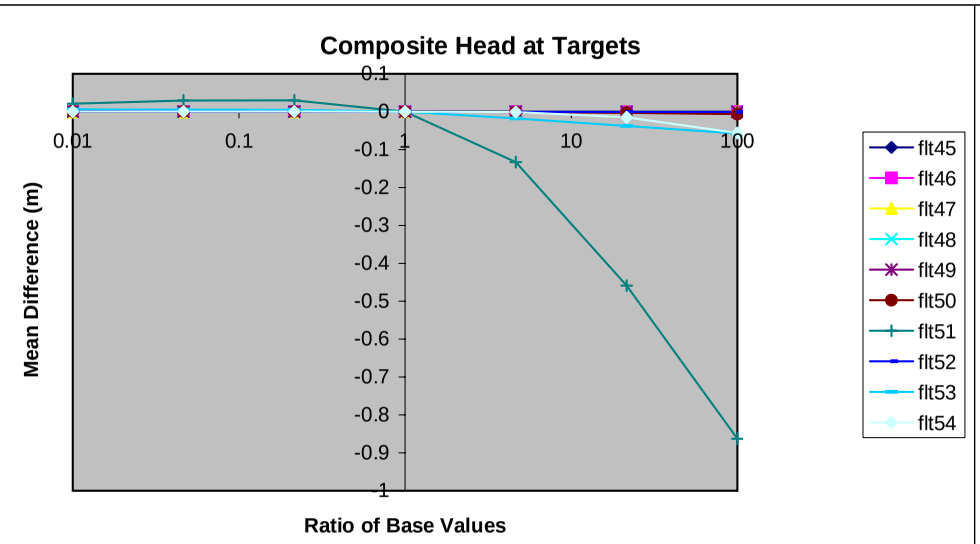
Composite Head at Targets
Mean Difference (m)
Ratio of Base Values
flt45
flt46
flt47
flt48
flt49
flt50
flt51
flt52
flt53
flt54

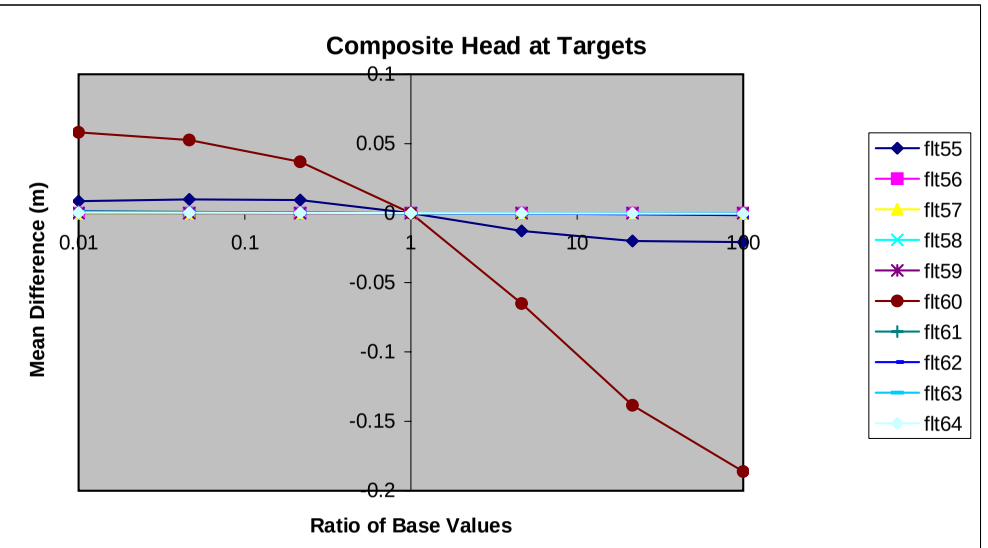
Composite Head at Targets
Mean Difference (m)
Ratio of Base Values
flt55
flt56
flt57
flt58
flt59
flt60
flt61
flt62
flt63
flt64

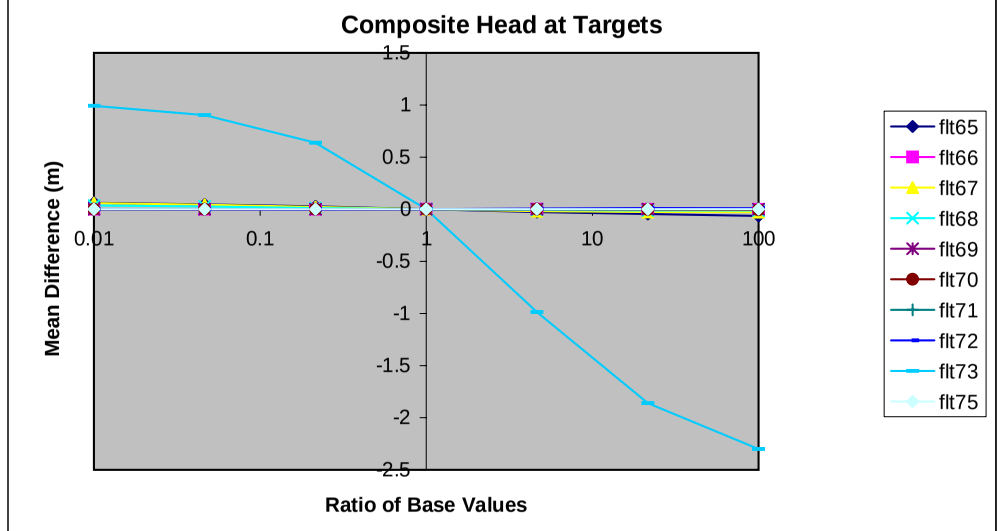
Composite Head at Targets
Mean Difference (m)
Ratio of Base Values
flt65
flt66
flt67
flt68
flt69
flt70
flt71
flt72
flt73
flt75

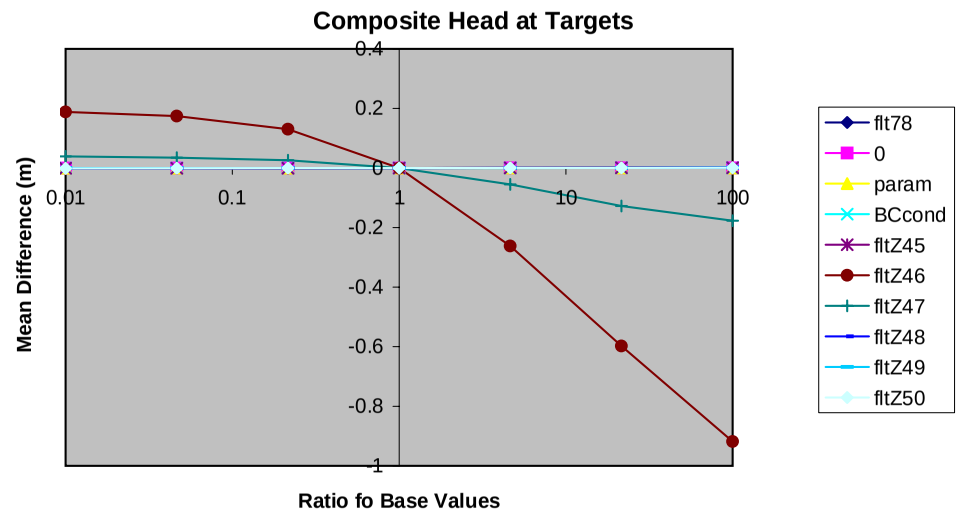
Composite Head at Targets
Mean Difference (m)
Ratio fo Base Values
flt78
0
param
BCcond
fltZ45
fltZ46
fltZ47
fltZ48
fltZ49
fltZ50

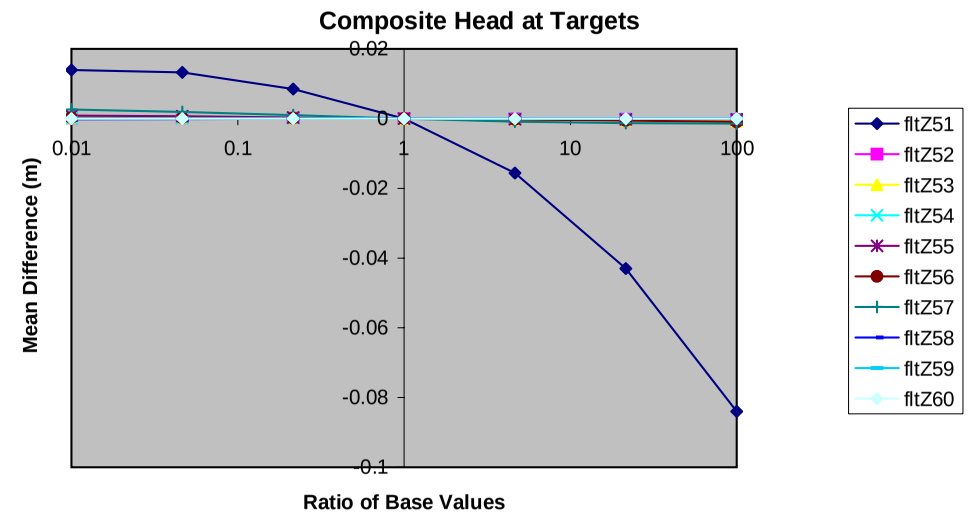
Composite Head at Targets
Mean Difference (m)
Ratio of Base Values
fltZ51
fltZ52
fltZ53
fltZ54
fltZ55
fltZ56
fltZ57
fltZ58
fltZ59
fltZ60

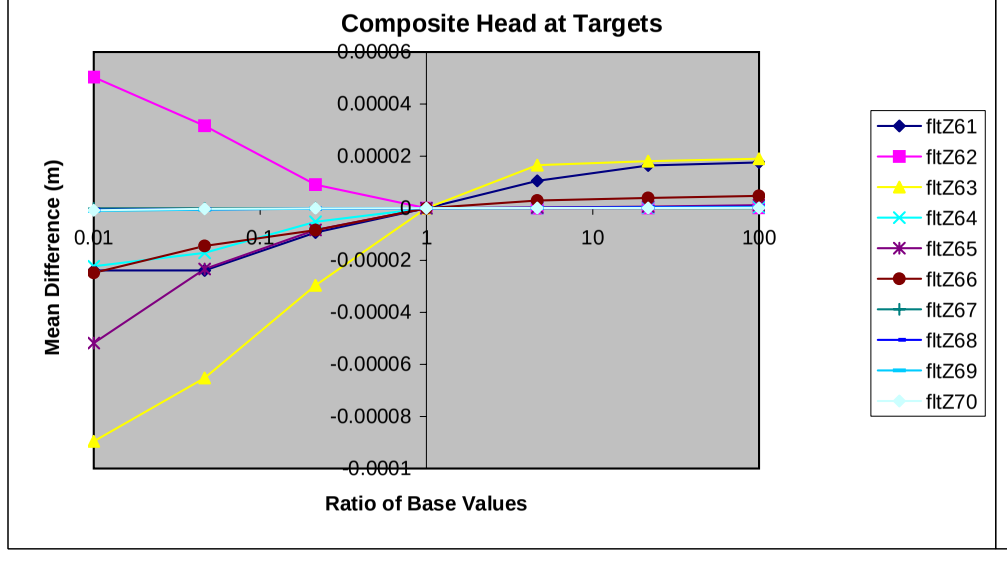
Composite Head at Targets
Mean Difference (m)
Ratio of Base Values
fltZ61
fltZ62
fltZ63
fltZ64
fltZ65
fltZ66
fltZ67
fltZ68
fltZ69
fltZ70

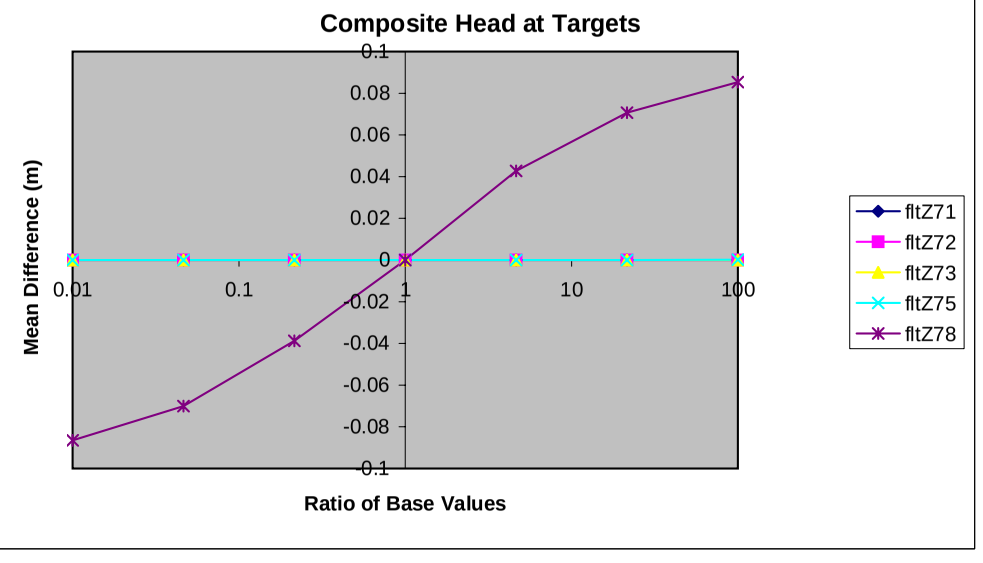
Composite Head at Targets
Mean Difference (m)
Ratio of Base Values
fltZ71
fltZ72
fltZ73
fltZ75
fltZ78

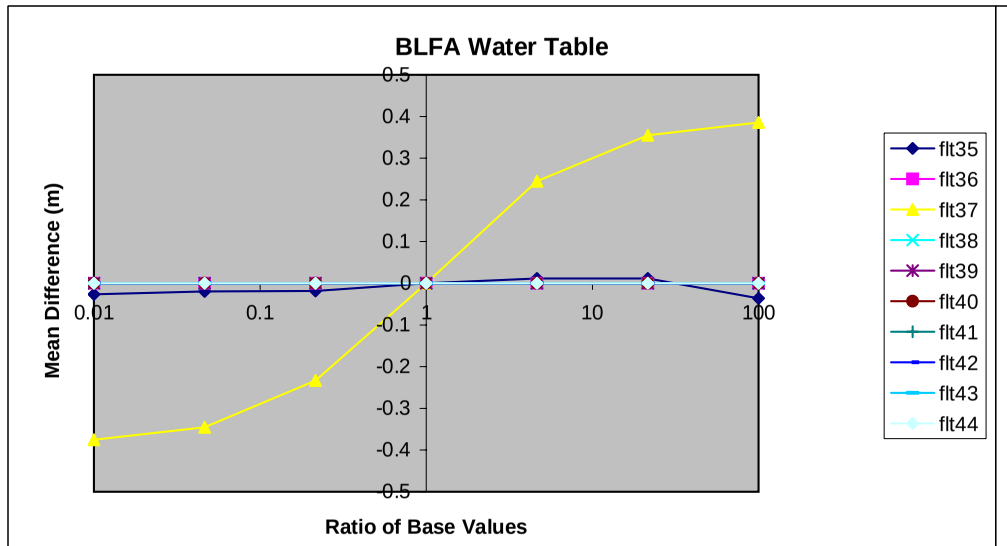
BLFA Water Table
Mean Difference (m)
Ratio of Base Values
flt35
flt36
flt37
flt38
flt39
flt40
flt41
flt42
flt43
flt44

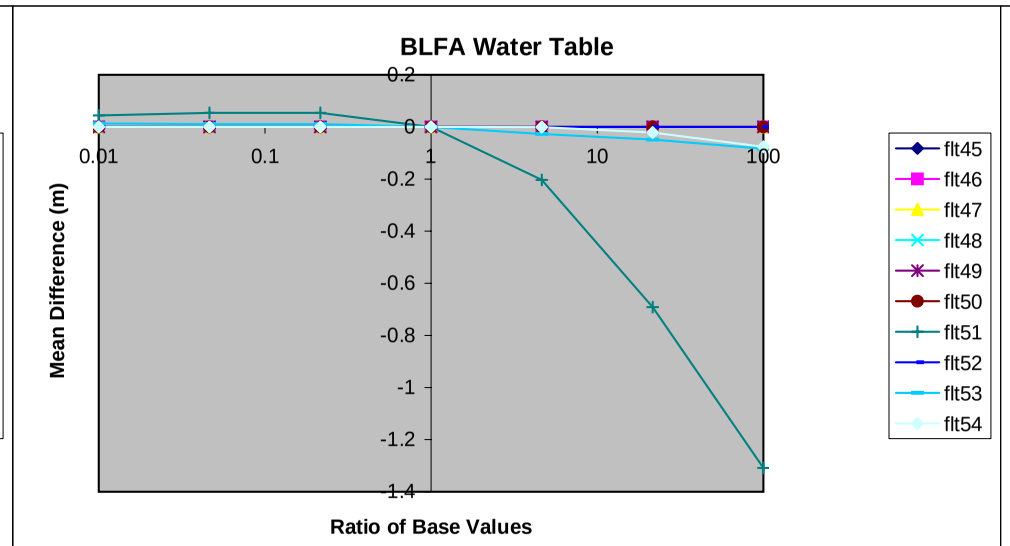
BLFA Water Table
Mean Difference (m)
Ratio of Base Values
flt45
flt46
flt47
flt48
flt49
flt50
flt51
flt52
flt53
flt54

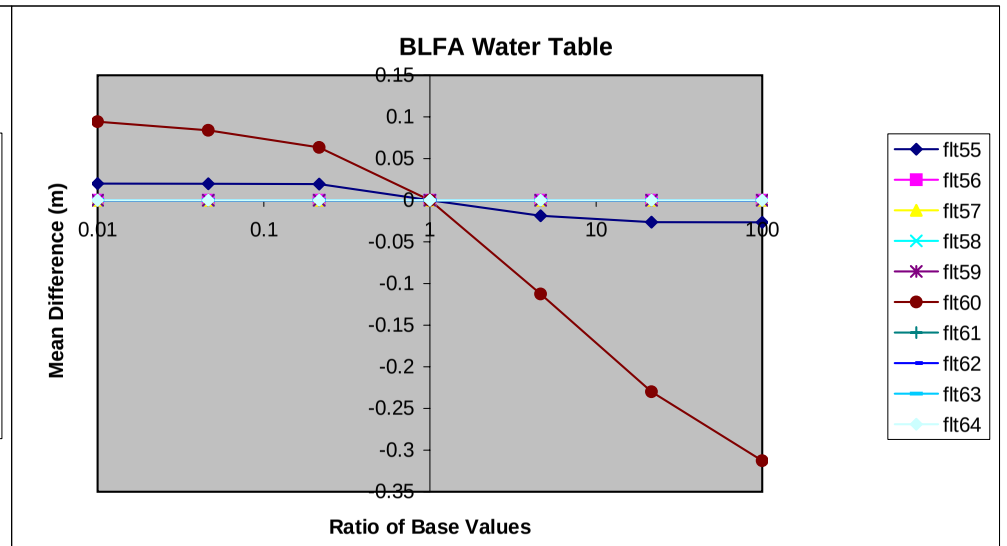
BLFA Water Table
Mean Difference (m)
Ratio of Base Values
flt55
flt56
flt57
flt58
flt59
flt60
flt61
flt62
flt63
flt64

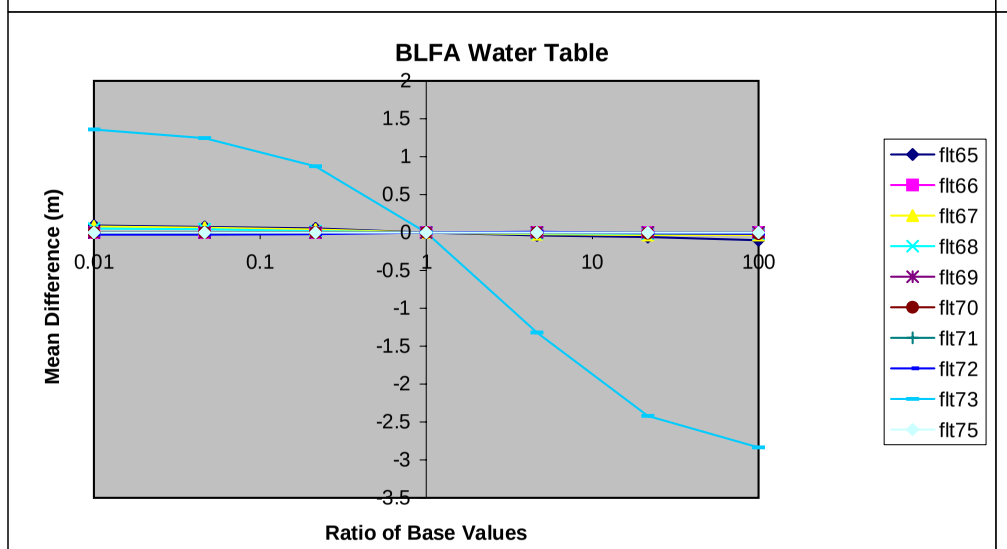
BLFA Water Table
Mean Difference (m)
Ratio of Base Values
flt65
flt66
flt67
flt68
flt69
flt70
flt71
flt72
flt73
flt75

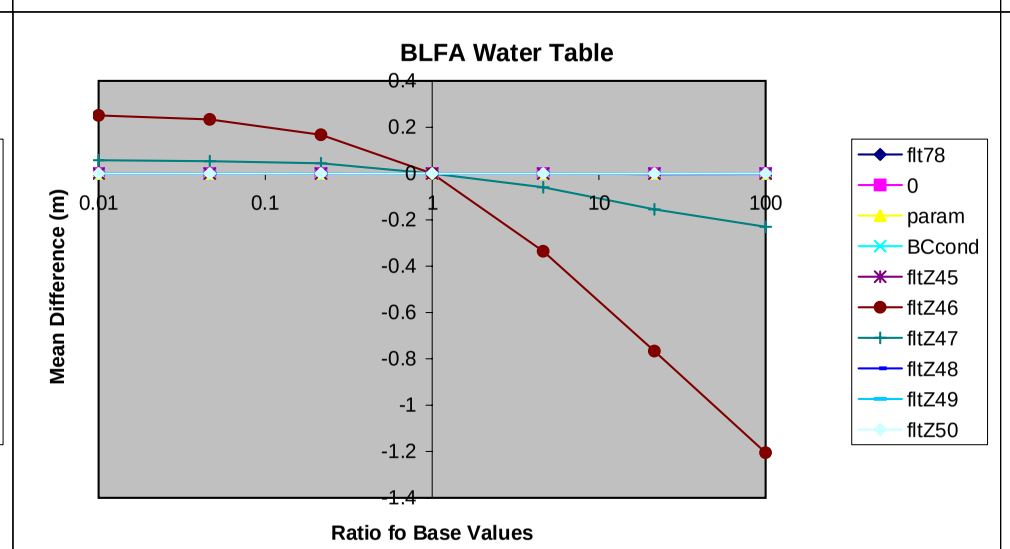
BLFA Water Table
Mean Difference (m)
Ratio fo Base Values
flt78
0
param
BCcond
fltZ45
fltZ46
fltZ47
fltZ48
fltZ49
fltZ50

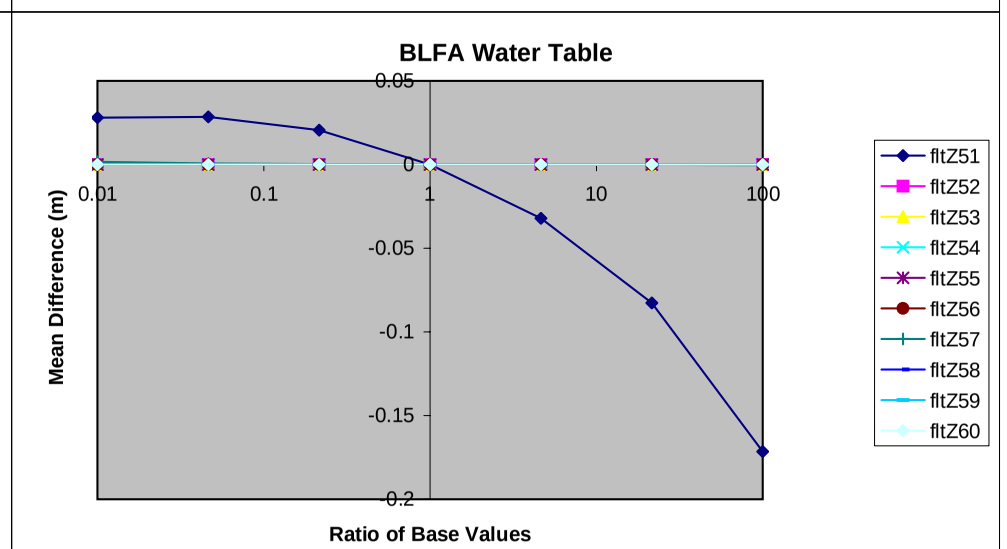
BLFA Water Table
Mean Difference (m)
Ratio of Base Values
fltZ51
fltZ52
fltZ53
fltZ54
fltZ55
fltZ56
fltZ57
fltZ58
fltZ59
fltZ60

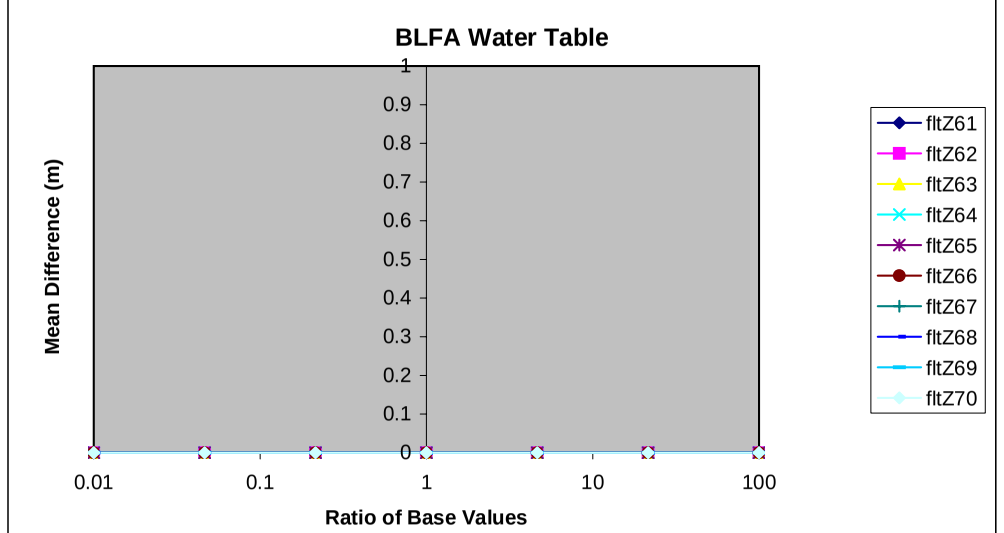
BLFA Water Table
Mean Difference (m)
Ratio of Base Values
fltZ61
fltZ62
fltZ63
fltZ64
fltZ65
fltZ66
fltZ67
fltZ68
fltZ69
fltZ70

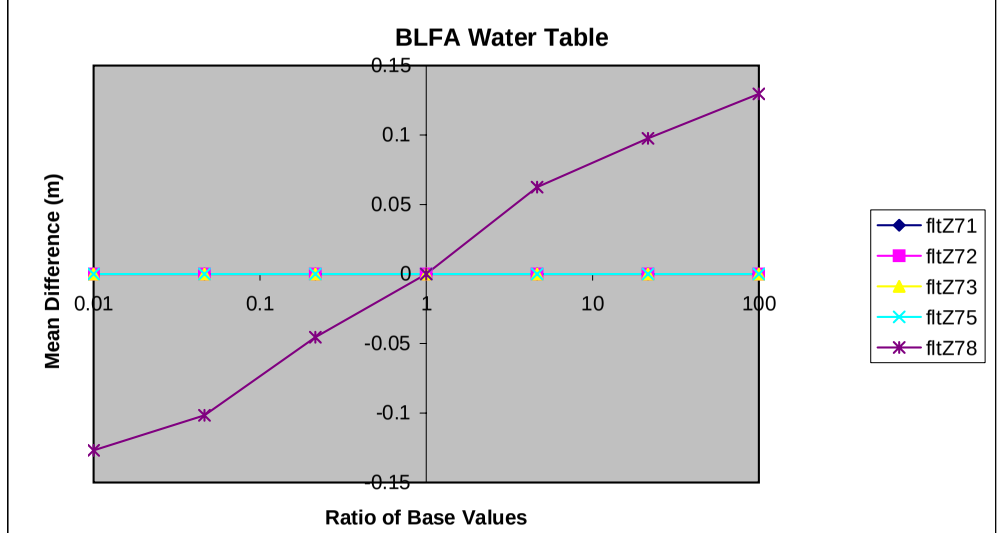
BLFA Water Table
Mean Difference (m)
Ratio of Base Values
fltZ71
fltZ72
fltZ73
fltZ75
fltZ78

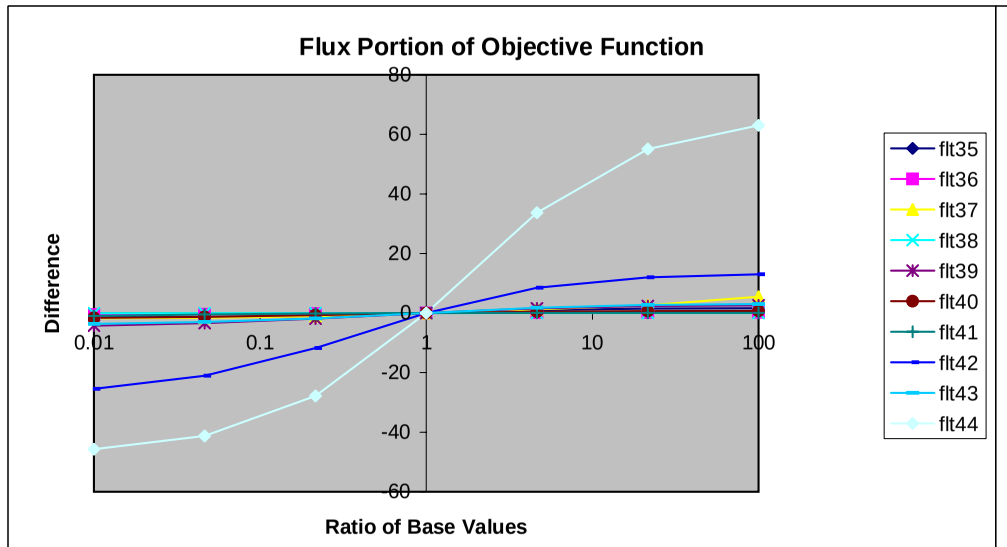
Flux Portion of Objective Function
Difference
Ratio of Base Values
flt35
flt36
flt37
flt38
flt39
flt40
flt41
flt42
flt43
flt44

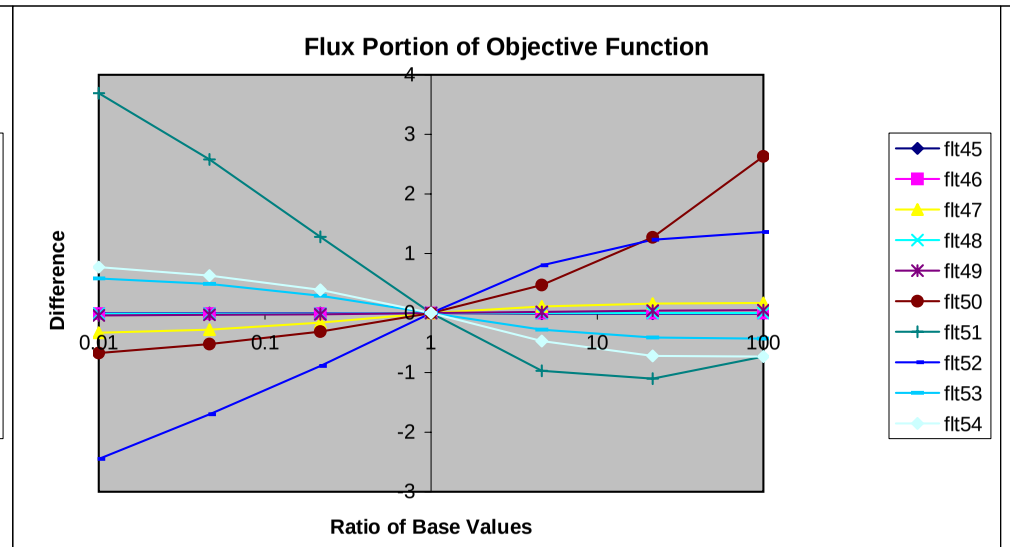
Flux Portion of Objective Function
Difference
Ratio of Base Values
flt45
flt46
flt47
flt48
flt49
flt50
flt51
flt52
flt53
flt54

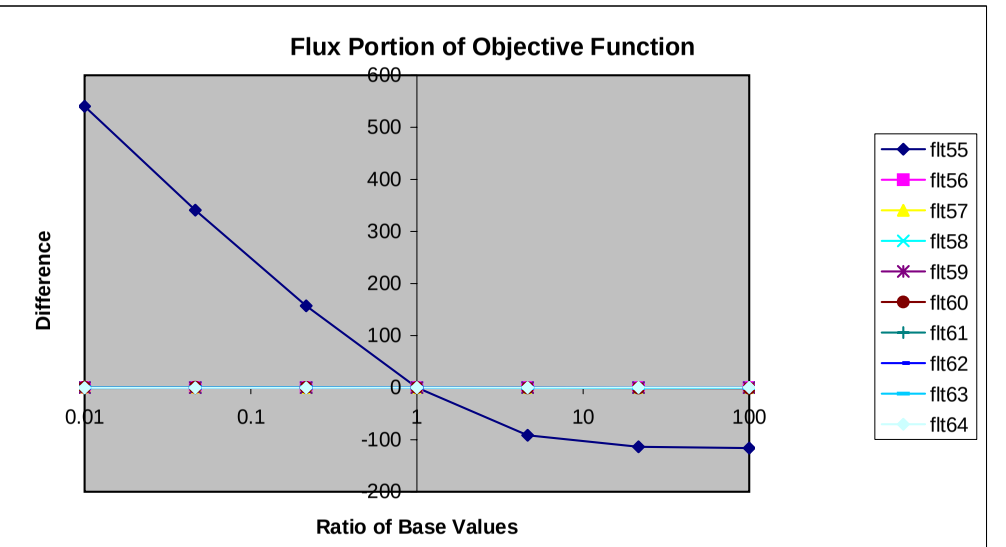
Flux Portion of Objective Function
Difference
Ratio of Base Values
flt55
flt56
flt57
flt58
flt59
flt60
flt61
flt62
flt63
flt64

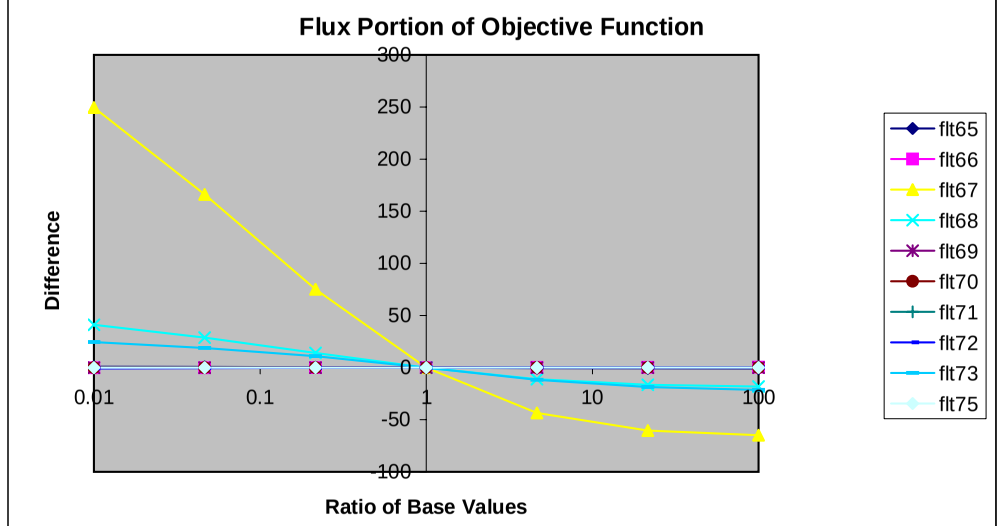
Flux Portion of Objective Function
Difference
Ratio of Base Values
flt65
flt66
flt67
flt68
flt69
flt70
flt71
flt72
flt73
flt75

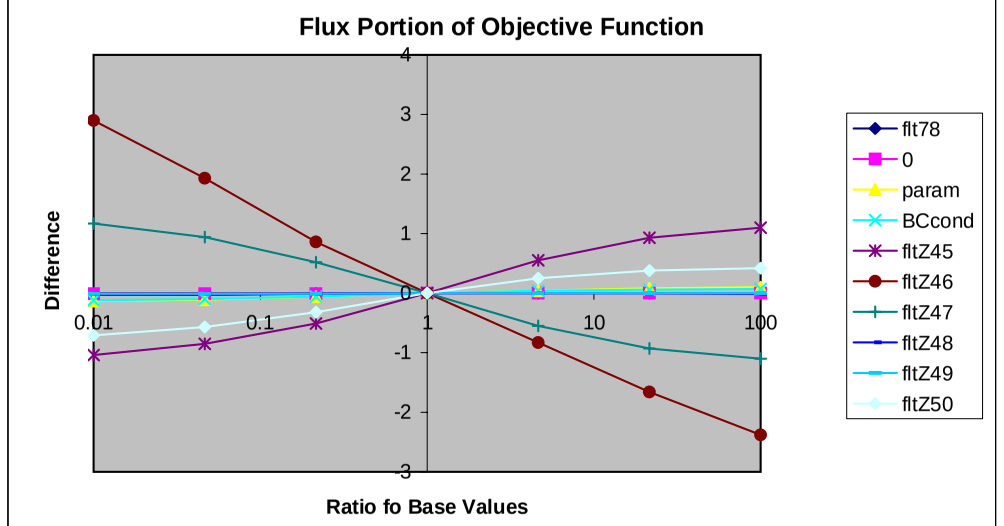
Flux Portion of Objective Function
Difference
Ratio fo Base Values
flt78
0
param
BCcond
fltZ45
fltZ46
fltZ47
fltZ48
fltZ49
fltZ50

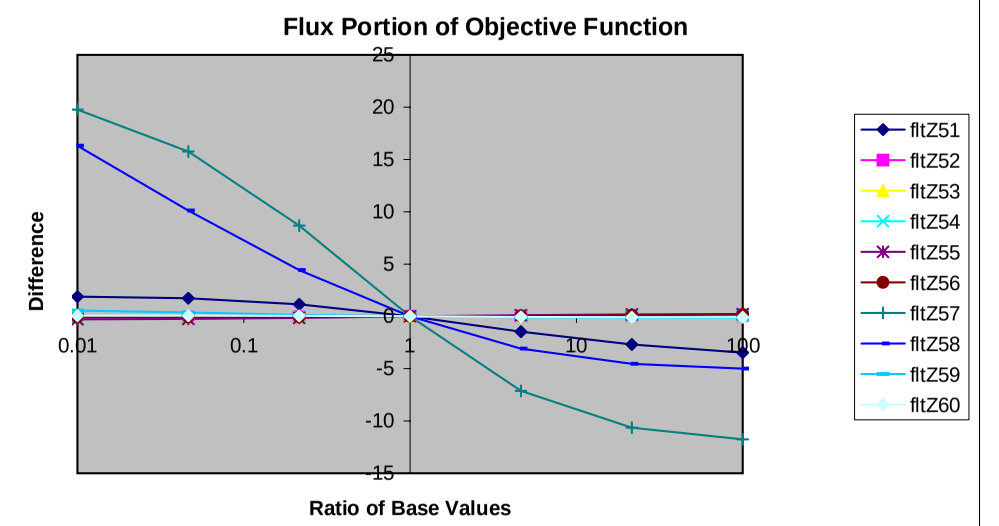
Flux Portion of Objective Function
Difference
Ratio of Base Values
fltZ51
fltZ52
fltZ53
fltZ54
fltZ55
fltZ56
fltZ57
fltZ58
fltZ59
fltZ60

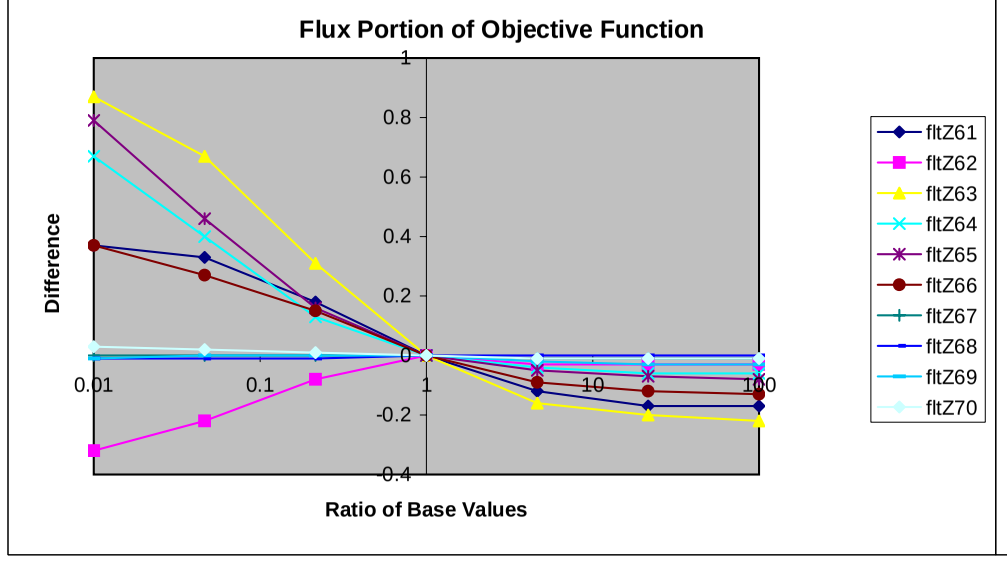
Flux Portion of Objective Function
Difference
Ratio of Base Values
fltZ61
fltZ62
fltZ63
fltZ64
fltZ65
fltZ66
fltZ67
fltZ68
fltZ69
fltZ70

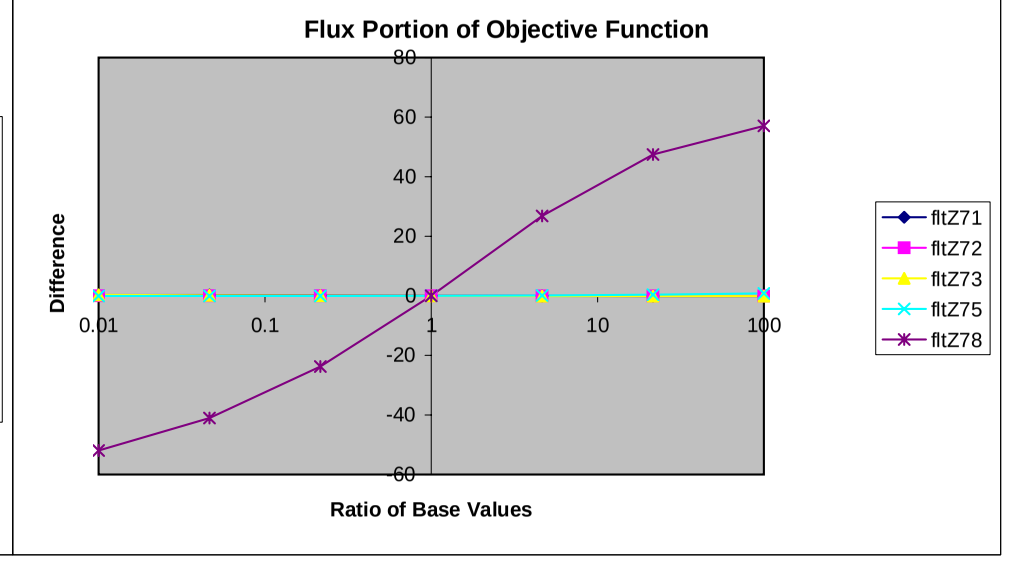
Flux Portion of Objective Function
Difference
Ratio of Base Values
fltZ71
fltZ72
fltZ73
fltZ75
fltZ78

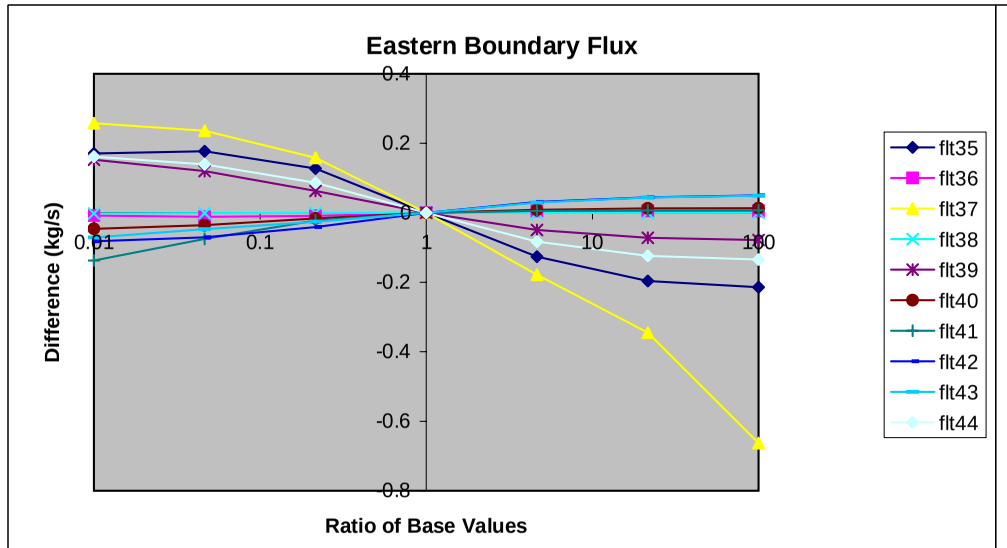
Eastern Boundary Flux
Difference (kg/s)
Ratio of Base Values
flt35
flt36
flt37
flt38
flt39
flt40
flt41
flt42
flt43
flt44

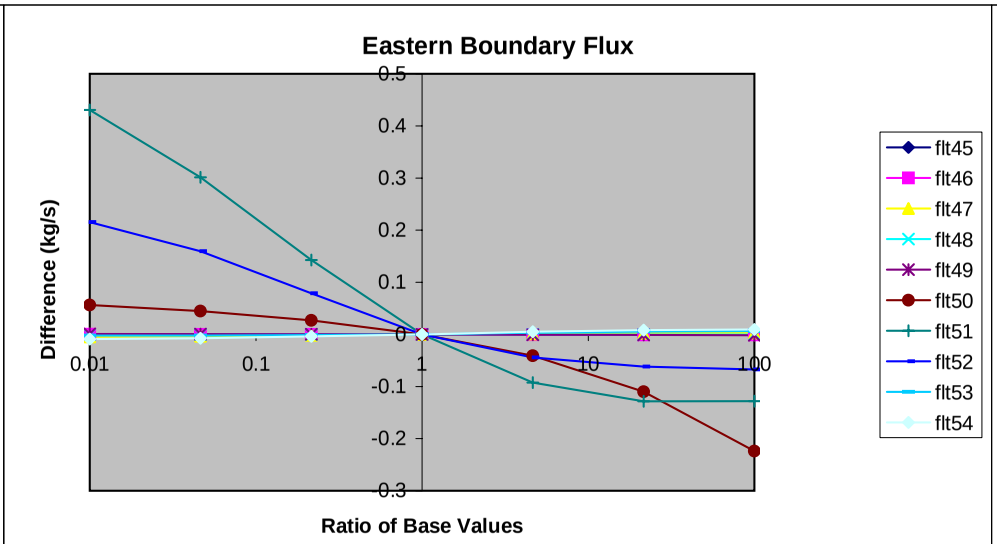
Eastern Boundary Flux
Difference (kg/s)
Ratio of Base Values
flt45
flt46
flt47
flt48
flt49
flt50
flt51
flt52
flt53
flt54

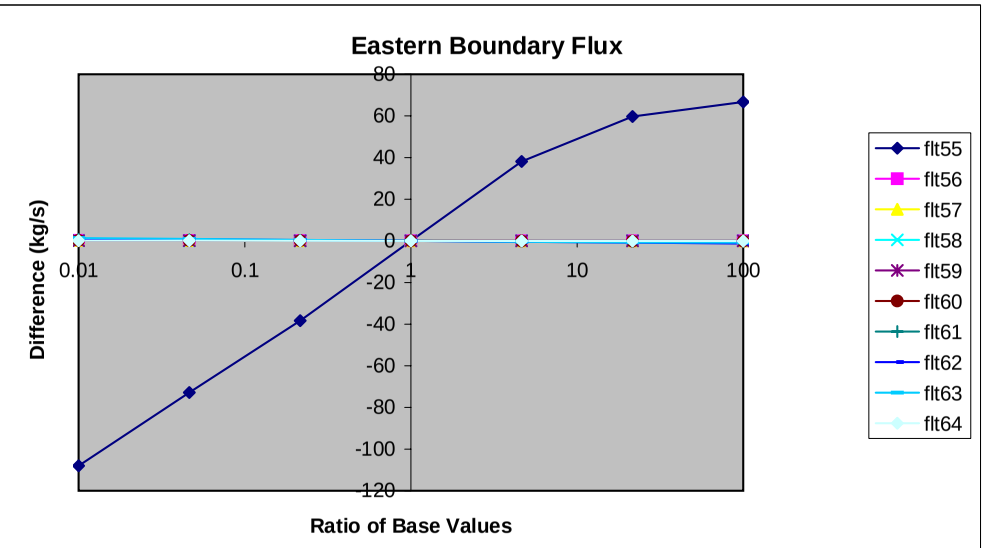
Eastern Boundary Flux
Difference (kg/s)
Ratio of Base Values
flt55
flt56
flt57
flt58
flt59
flt60
flt61
flt62
flt63
flt64

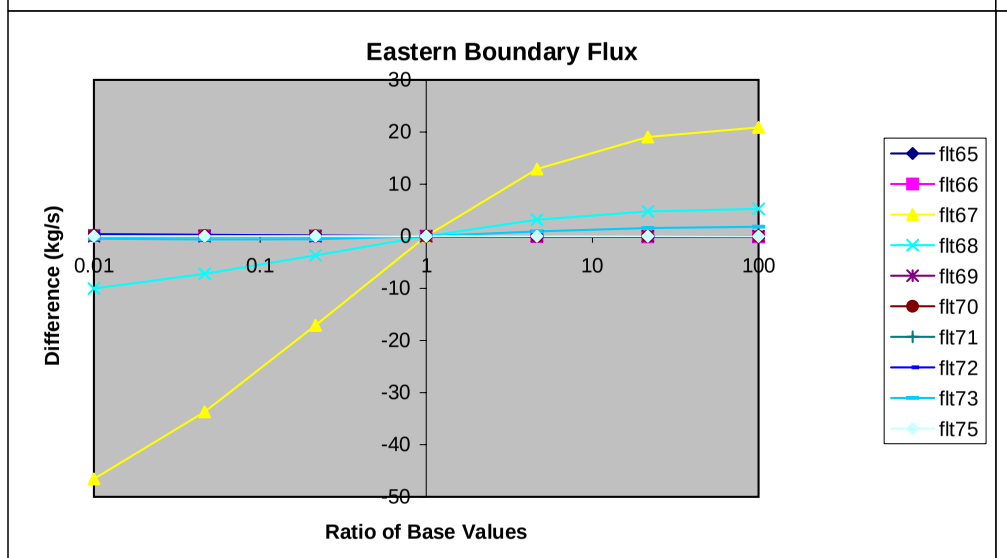
Eastern Boundary Flux
Difference (kg/s)
Ratio of Base Values
flt65
flt66
flt67
flt68
flt69
flt70
flt71
flt72
flt73
flt75

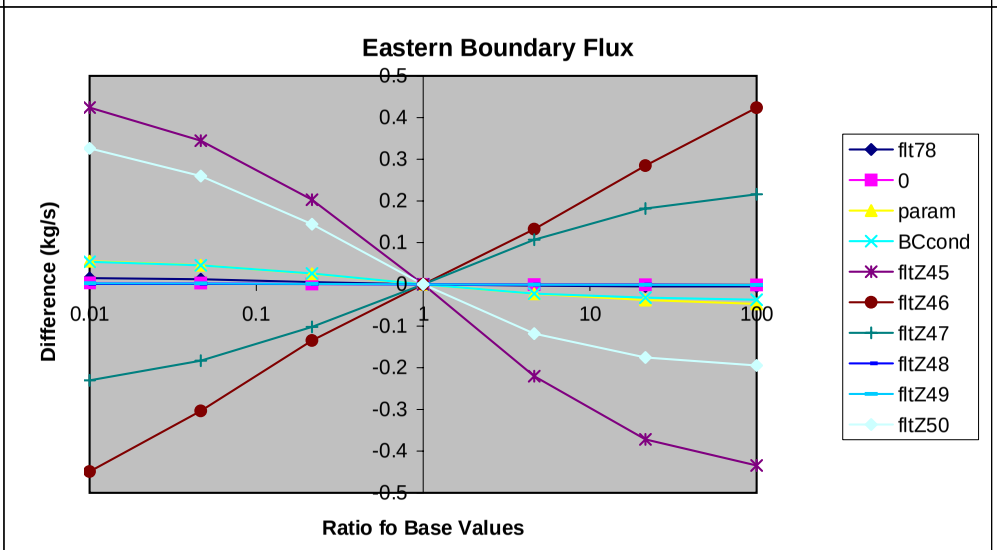
Eastern Boundary Flux
Difference (kg/s)
Ratio fo Base Values
flt78
0
param
BCcond
fltZ45
fltZ46
fltZ47
fltZ48
fltZ49
fltZ50

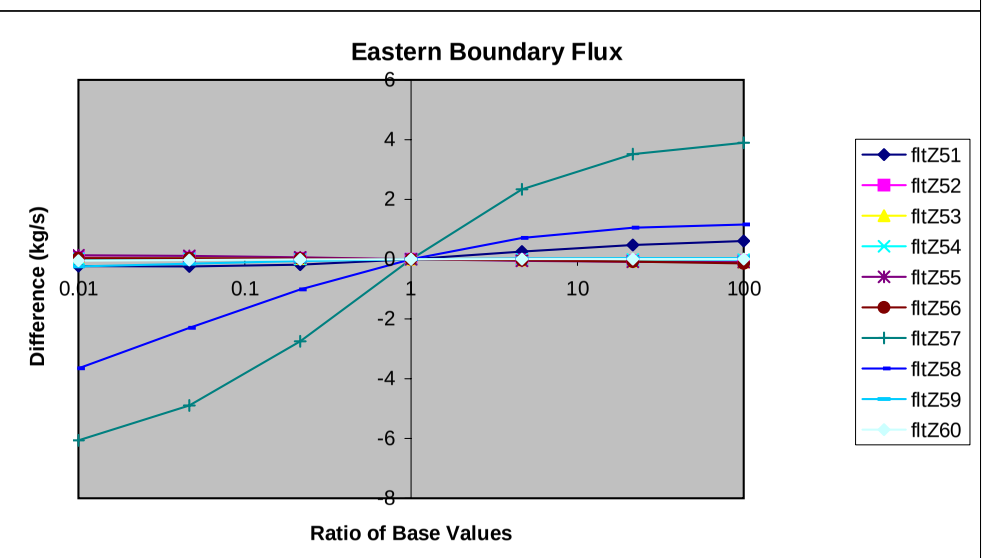
Eastern Boundary Flux
Difference (kg/s)
Ratio of Base Values
fltZ51
fltZ52
fltZ53
fltZ54
fltZ55
fltZ56
fltZ57
fltZ58
fltZ59
fltZ60

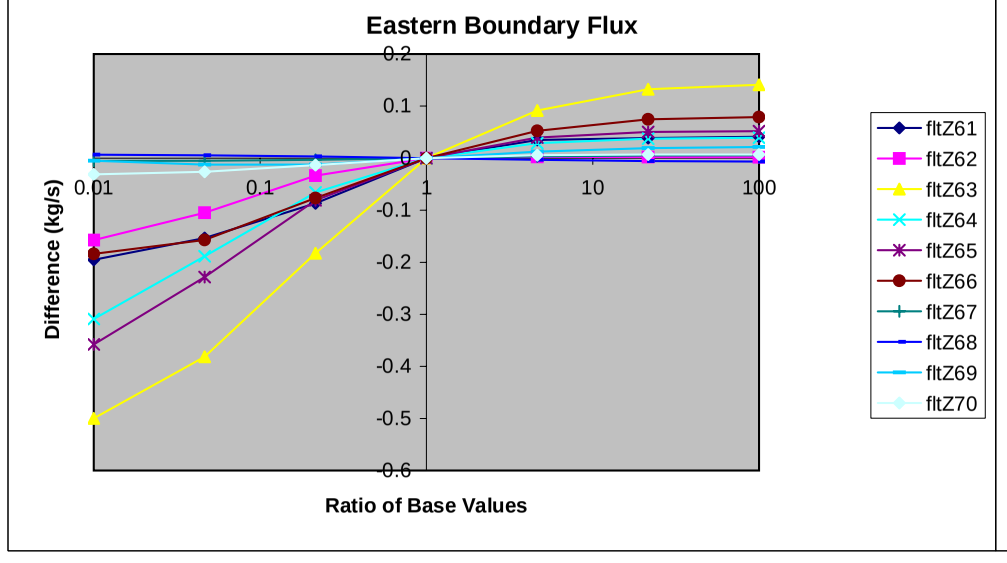
Eastern Boundary Flux
Difference (kg/s)
Ratio of Base Values
fltZ61
fltZ62
fltZ63
fltZ64
fltZ65
fltZ66
fltZ67
fltZ68
fltZ69
fltZ70

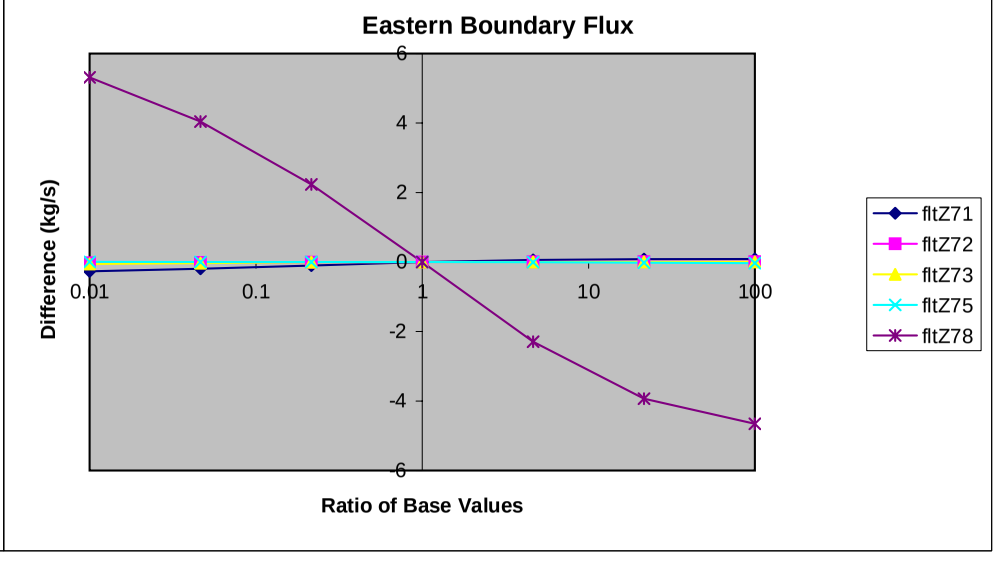
Eastern Boundary Flux
Difference (kg/s)
Ratio of Base Values
fltZ71
fltZ72
fltZ73
fltZ75
fltZ78

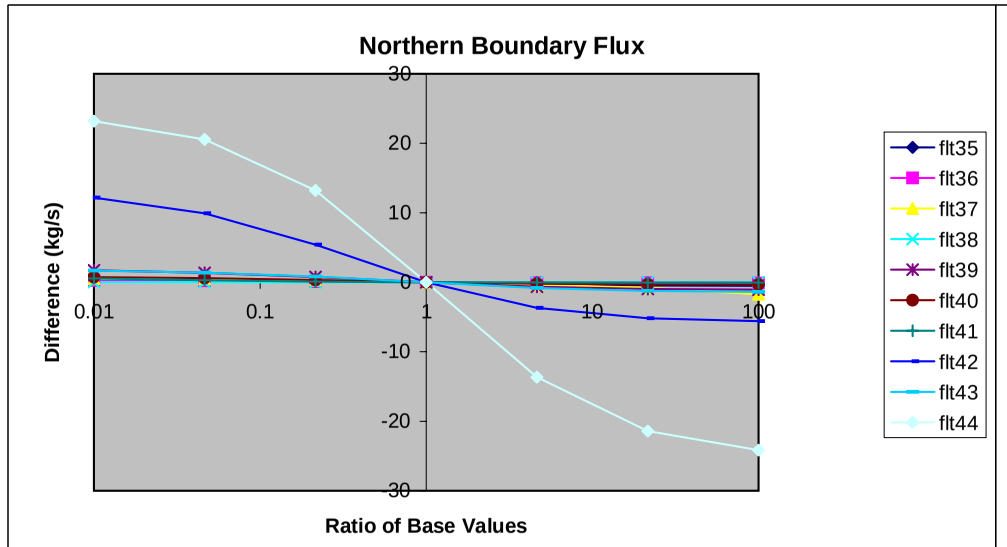
Northern Boundary Flux
Difference (kg/s)
Ratio of Base Values
flt35
flt36
flt37
flt38
flt39
flt40
flt41
flt42
flt43
flt44

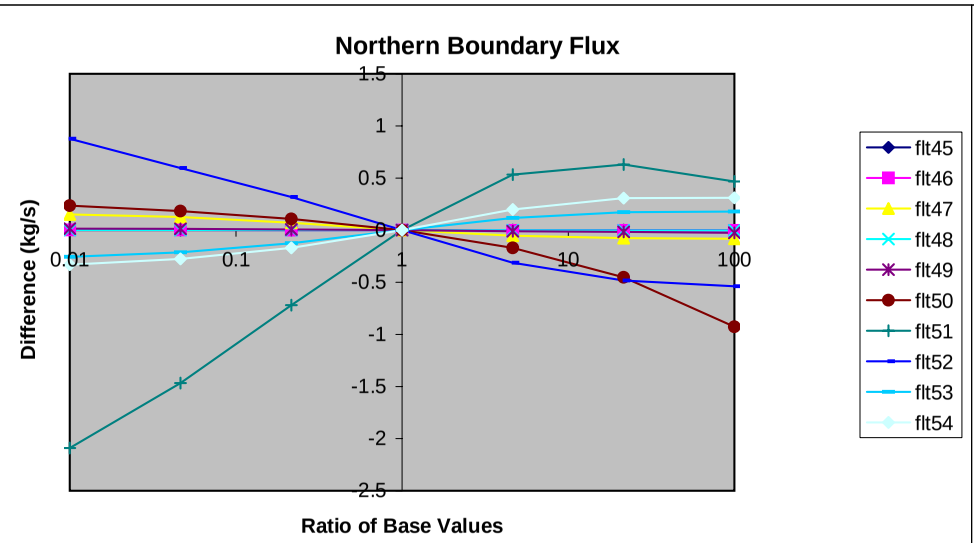
Northern Boundary Flux
Difference (kg/s)
Ratio of Base Values
flt45
flt46
flt47
flt48
flt49
flt50
flt51
flt52
flt53
flt54

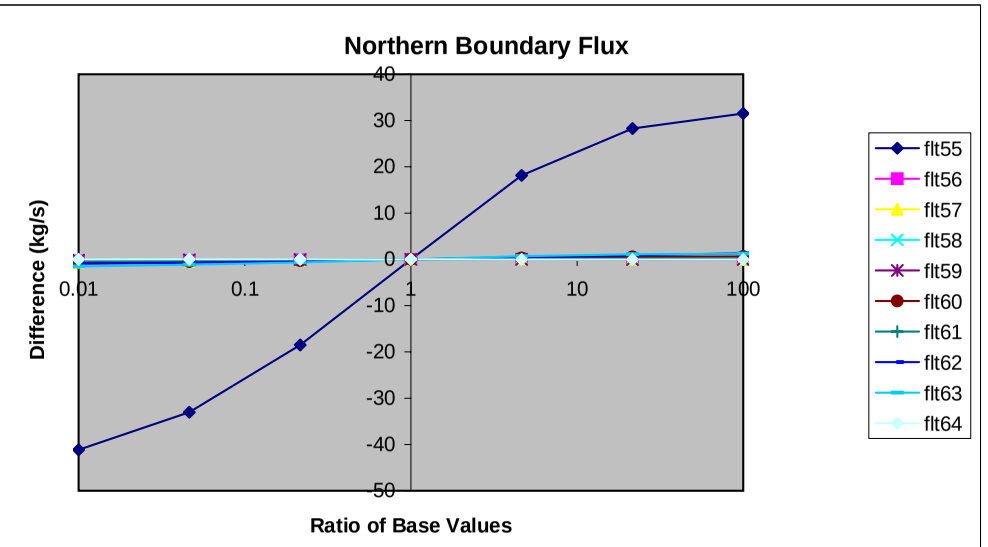
Northern Boundary Flux
Difference (kg/s)
Ratio of Base Values
flt55
flt56
flt57
flt58
flt59
flt60
flt61
flt62
flt63
flt64

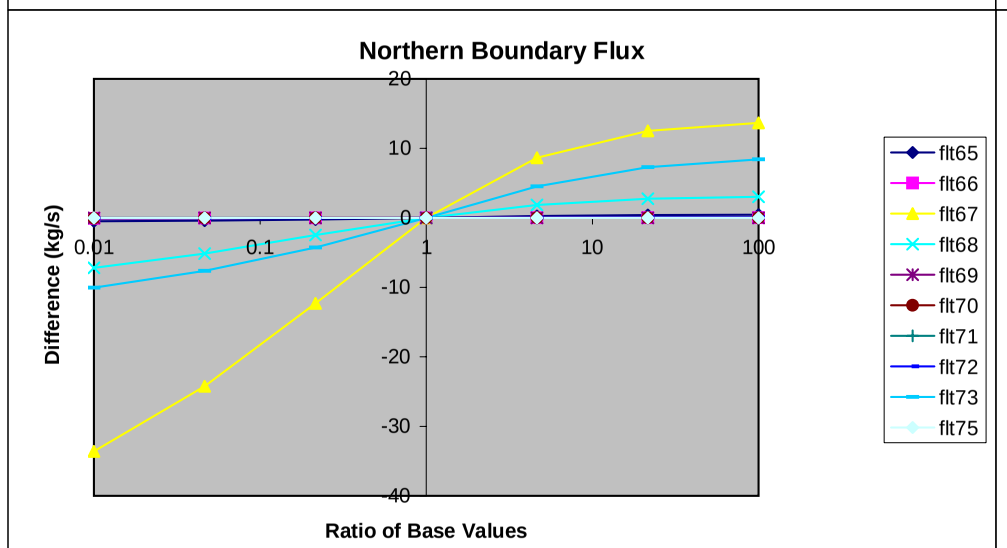
Northern Boundary Flux
Difference (kg/s)
Ratio of Base Values
flt65
flt66
flt67
flt68
flt69
flt70
flt71
flt72
flt73
flt75

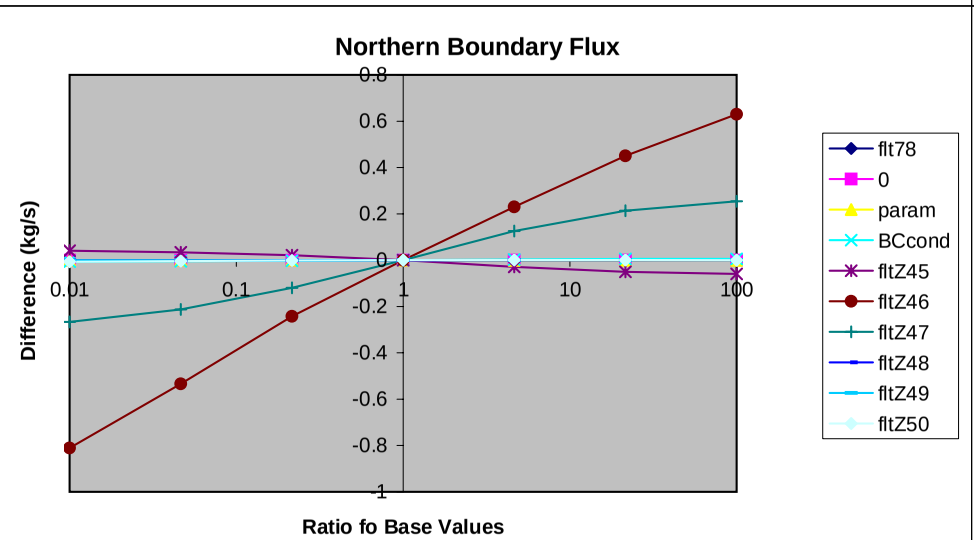
Northern Boundary Flux
Difference (kg/s)
Ratio fo Base Values
flt78
0
param
BCcond
fltZ45
fltZ46
fltZ47
fltZ48
fltZ49
fltZ50

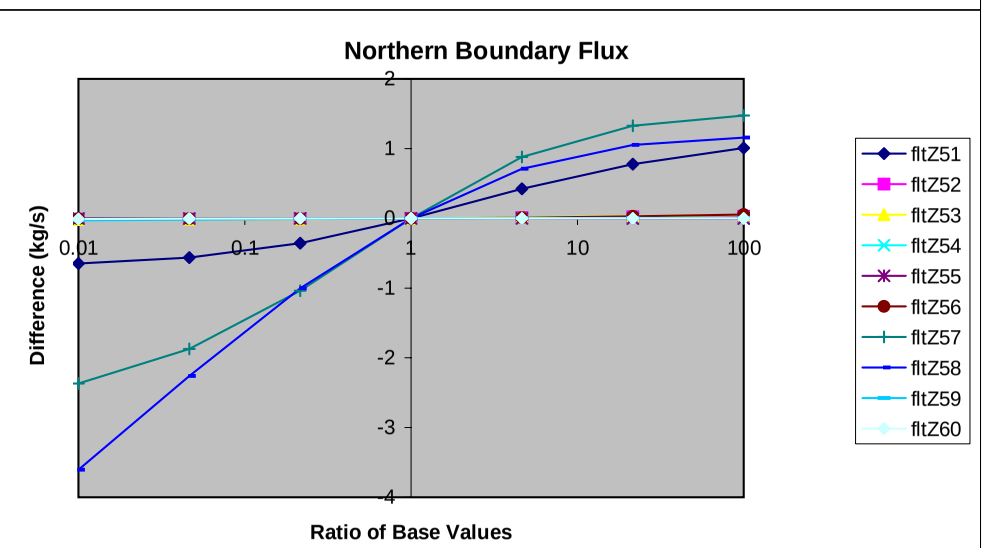
Northern Boundary Flux
Difference (kg/s)
Ratio of Base Values
fltZ51
fltZ52
fltZ53
fltZ54
fltZ55
fltZ56
fltZ57
fltZ58
fltZ59
fltZ60

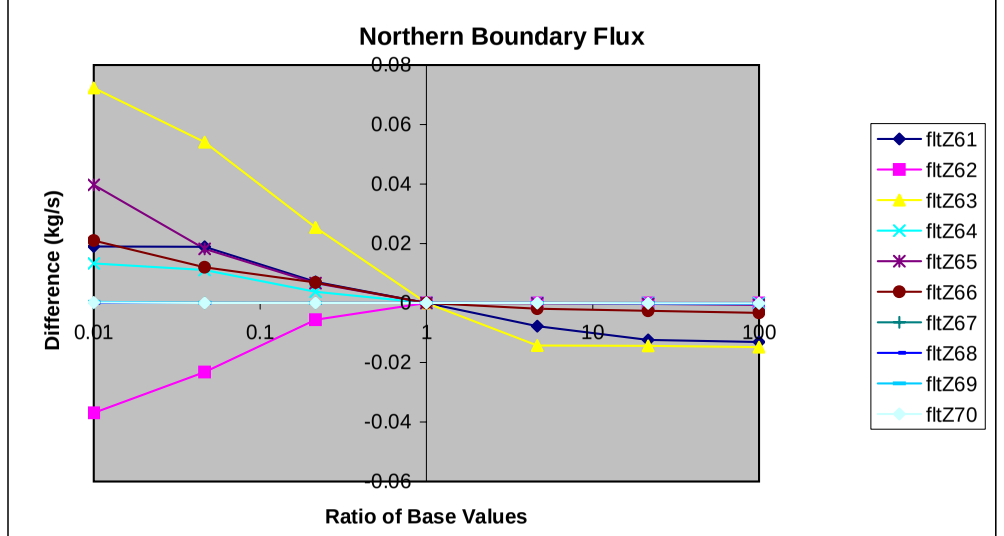
Northern Boundary Flux
Difference (kg/s)
Ratio of Base Values
fltZ61
fltZ62
fltZ63
fltZ64
fltZ65
fltZ66
fltZ67
fltZ68
fltZ69
fltZ70

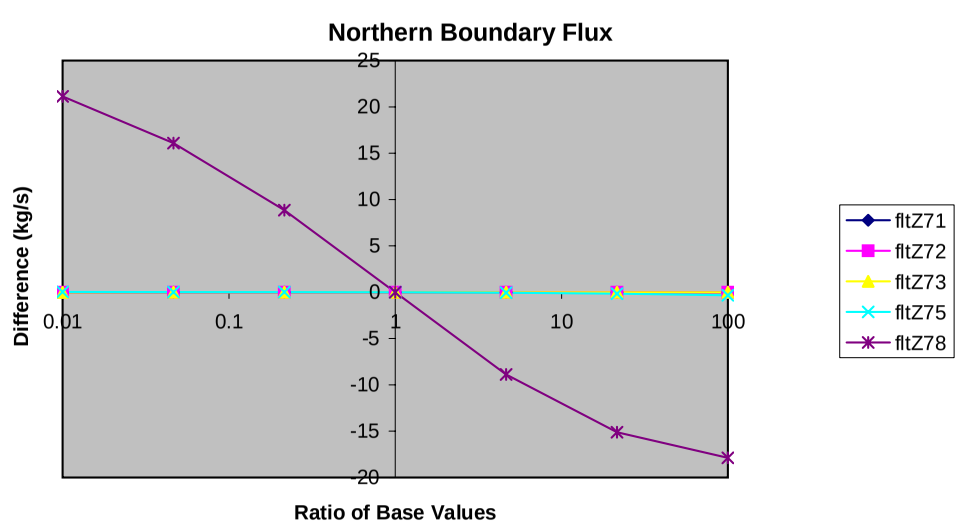
Northern Boundary Flux
Difference (kg/s)
Ratio of Base Values
fltZ71
fltZ72
fltZ73
fltZ75
fltZ78

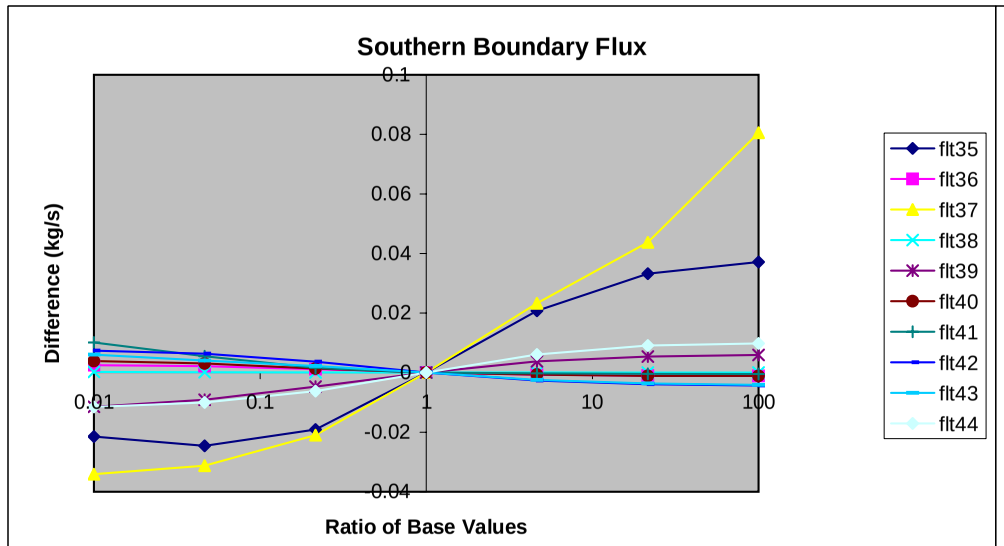
Southern Boundary Flux
Difference (kg/s)
Ratio of Base Values
flt35
flt36
flt37
flt38
flt39
flt40
flt41
flt42
flt43
flt44

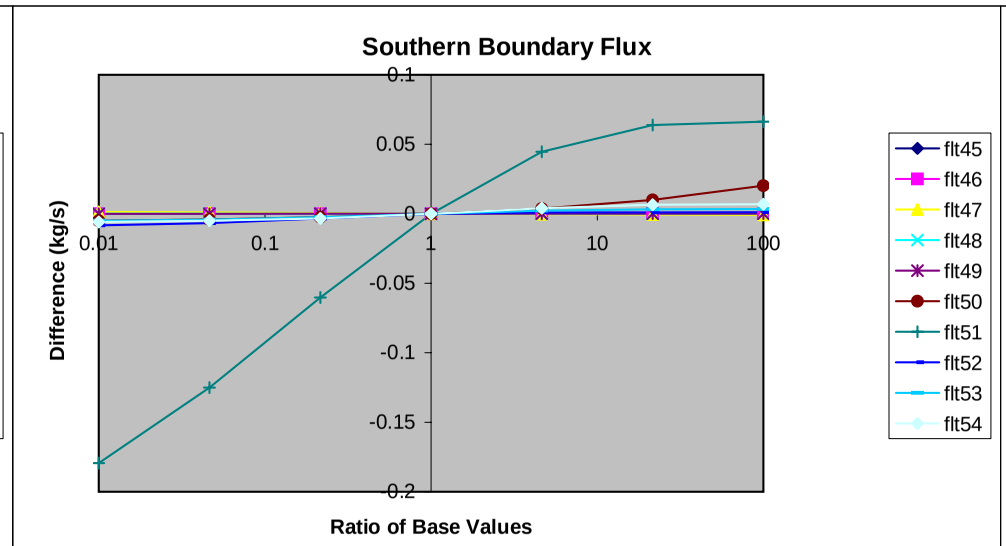
Southern Boundary Flux
Difference (kg/s)
Ratio of Base Values
flt45
flt46
flt47
flt48
flt49
flt50
flt51
flt52
flt53
flt54

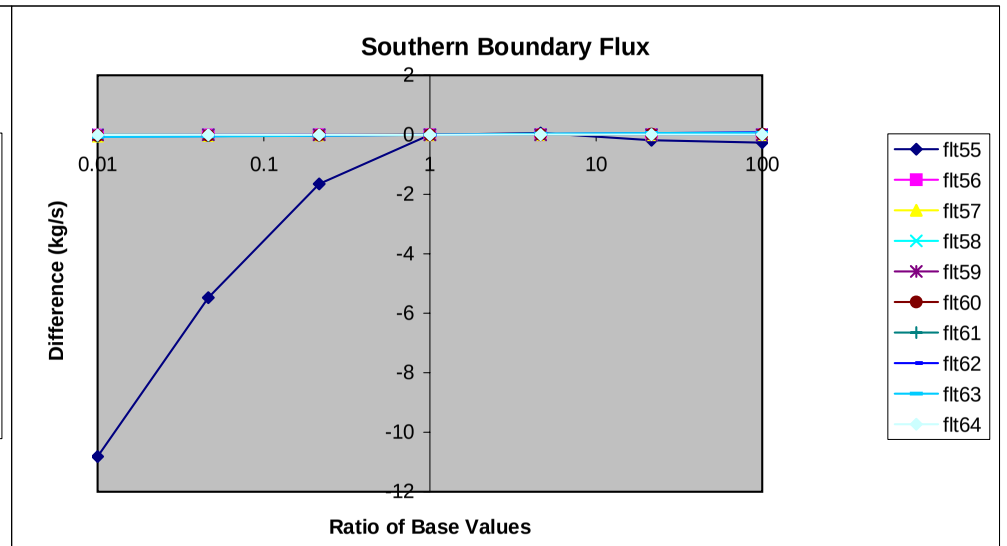
Southern Boundary Flux
Difference (kg/s)
Ratio of Base Values
flt55
flt56
flt57
flt58
flt59
flt60
flt61
flt62
flt63
flt64

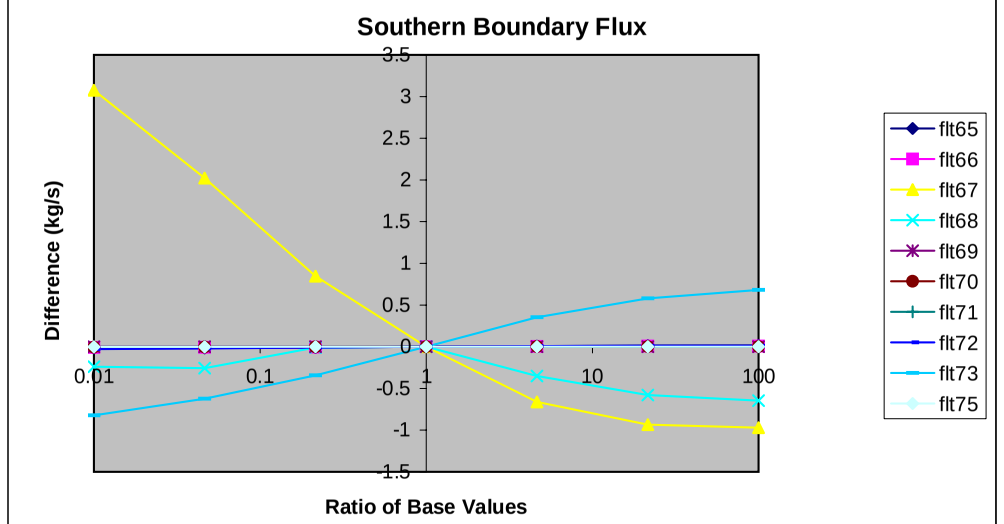
Southern Boundary Flux
Difference (kg/s)
Ratio of Base Values
flt65
flt66
flt67
flt68
flt69
flt70
flt71
flt72
flt73
flt75

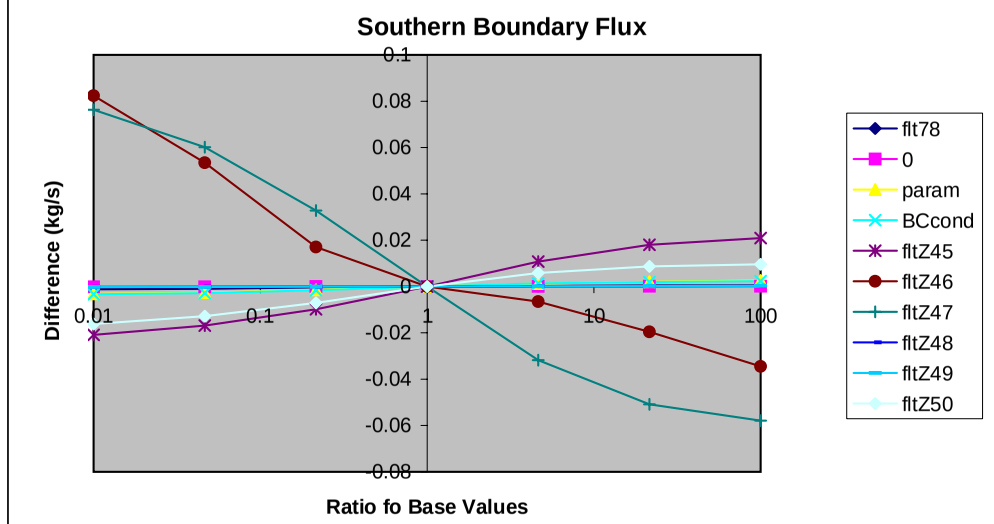
Southern Boundary Flux
Difference (kg/s)
Ratio fo Base Values
flt78
0
param
BCcond
fltZ45
fltZ46
fltZ47
fltZ48
fltZ49
fltZ50

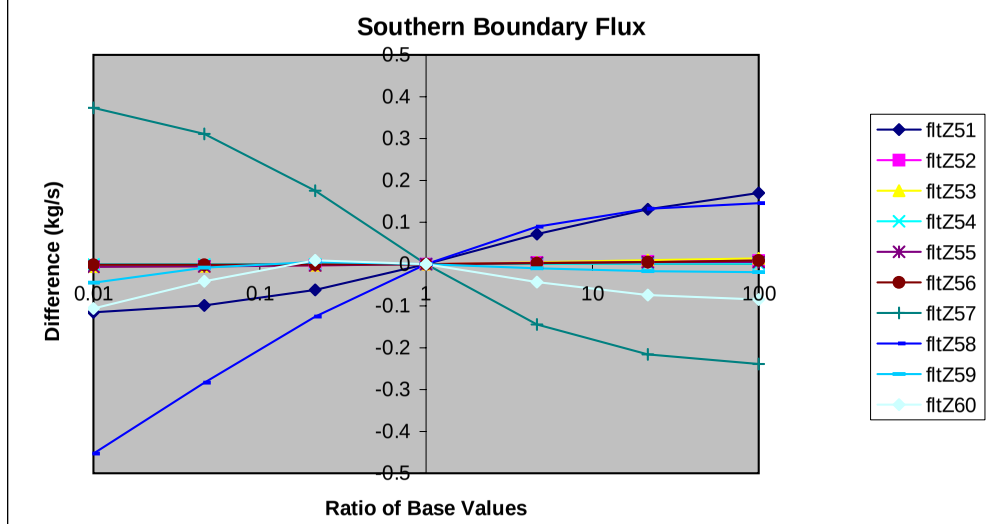
Southern Boundary Flux
Difference (kg/s)
Ratio of Base Values
fltZ51
fltZ52
fltZ53
fltZ54
fltZ55
fltZ56
fltZ57
fltZ58
fltZ59
fltZ60

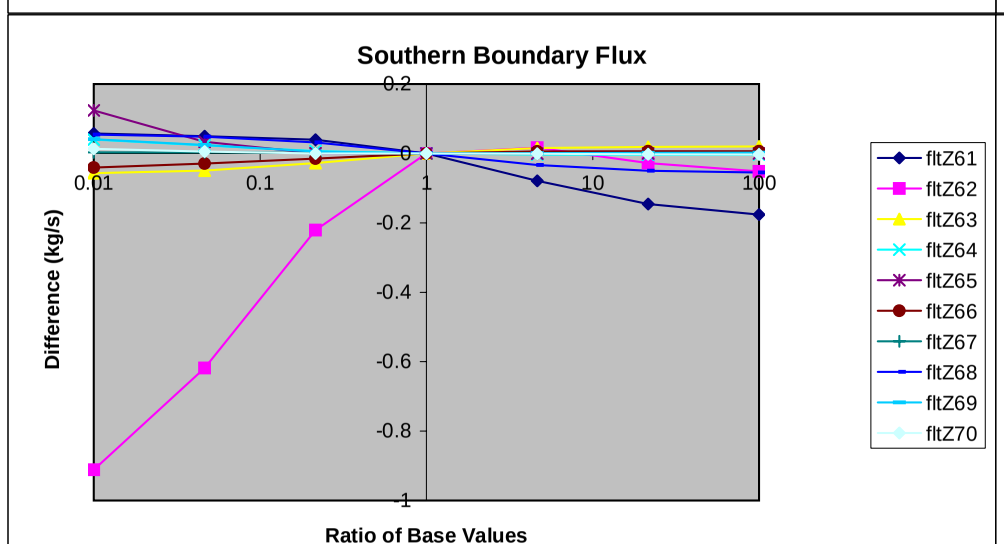
Southern Boundary Flux
Difference (kg/s)
Ratio of Base Values
fltZ61
fltZ62
fltZ63
fltZ64
fltZ65
fltZ66
fltZ67
fltZ68
fltZ69
fltZ70

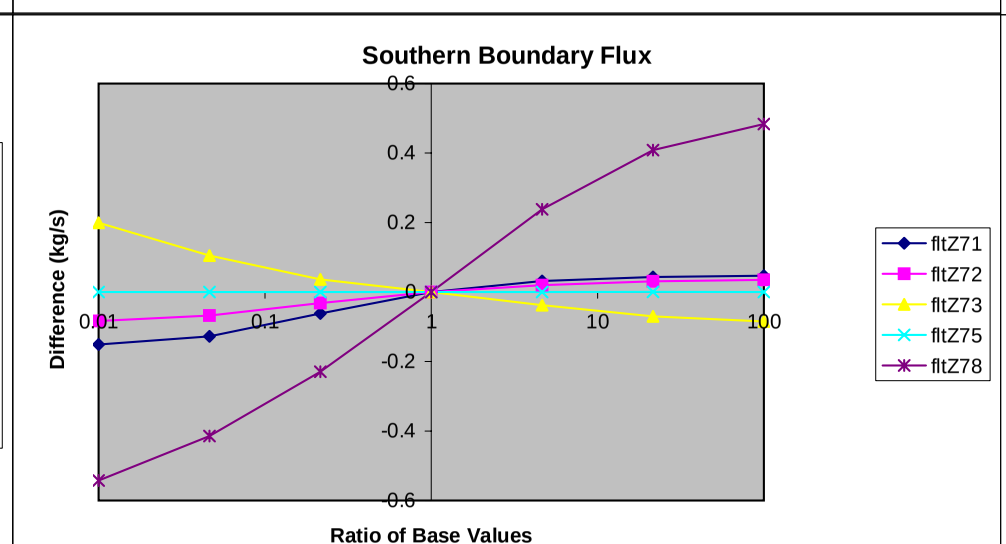
Southern Boundary Flux
Difference (kg/s)
Ratio of Base Values
fltZ71
fltZ72
fltZ73
fltZ75
fltZ78

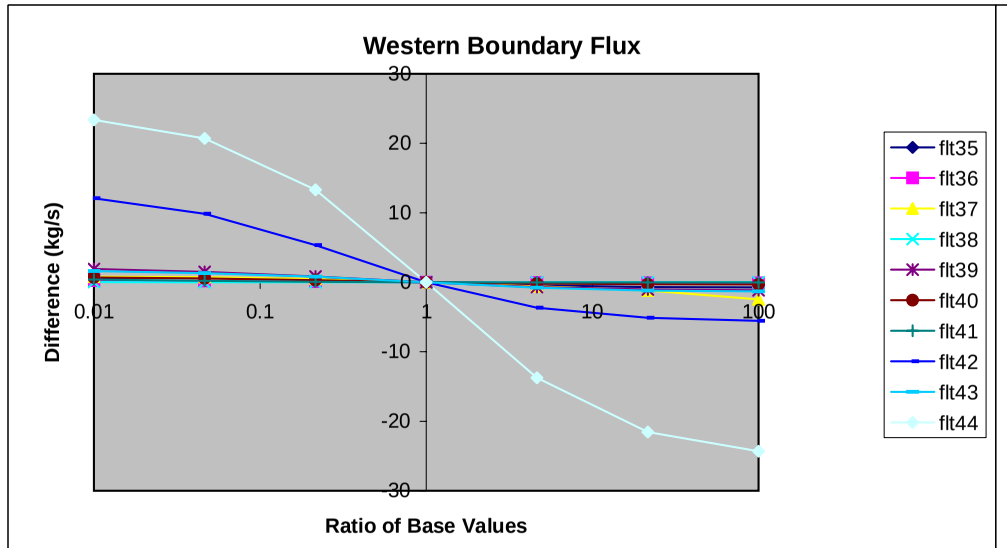
Western Boundary Flux
Difference (kg/s)
Ratio of Base Values
flt35
flt36
flt37
flt38
flt39
flt40
flt41
flt42
flt43
flt44

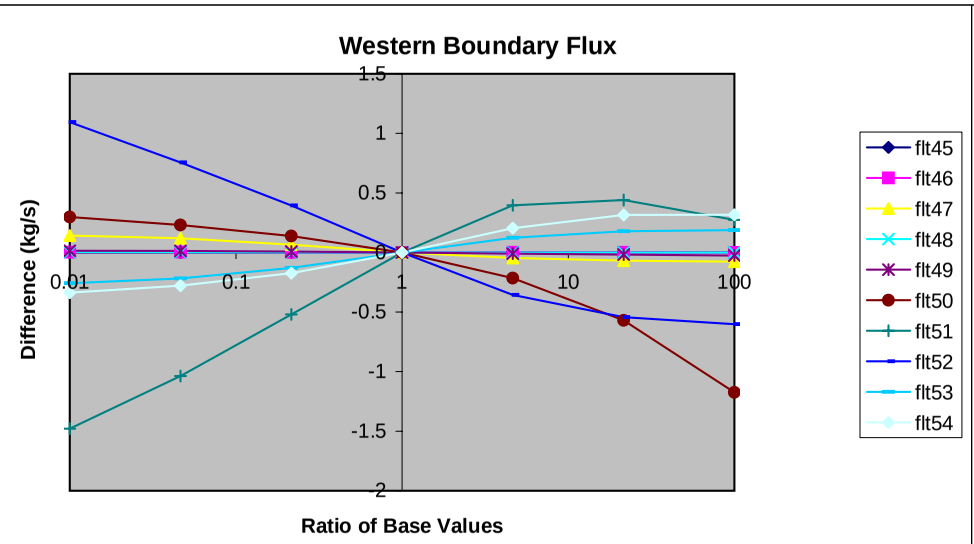
Western Boundary Flux
Difference (kg/s)
Ratio of Base Values
flt45
flt46
flt47
flt48
flt49
flt50
flt51
flt52
flt53
flt54

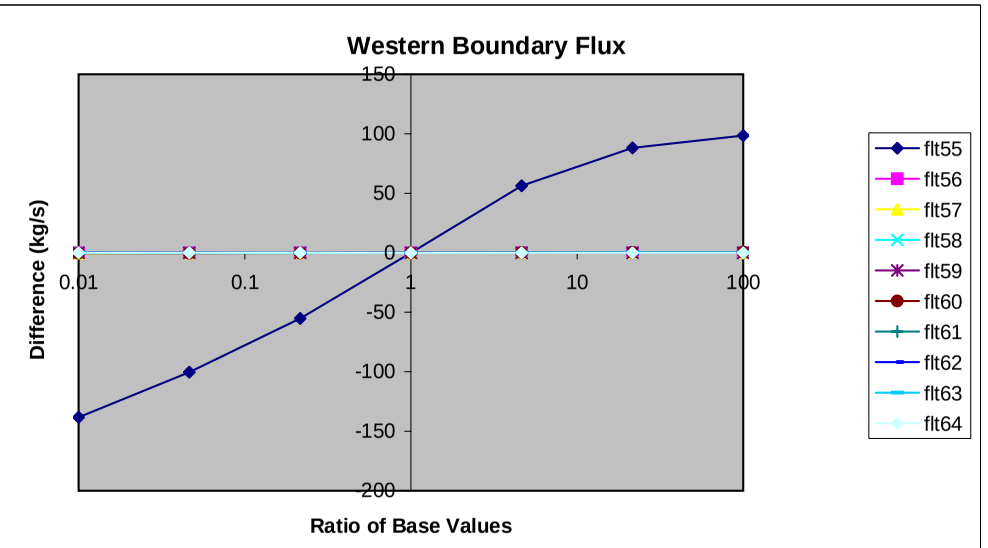
Western Boundary Flux
Difference (kg/s)
Ratio of Base Values
flt55
flt56
flt57
flt58
flt59
flt60
flt61
flt62
flt63
flt64

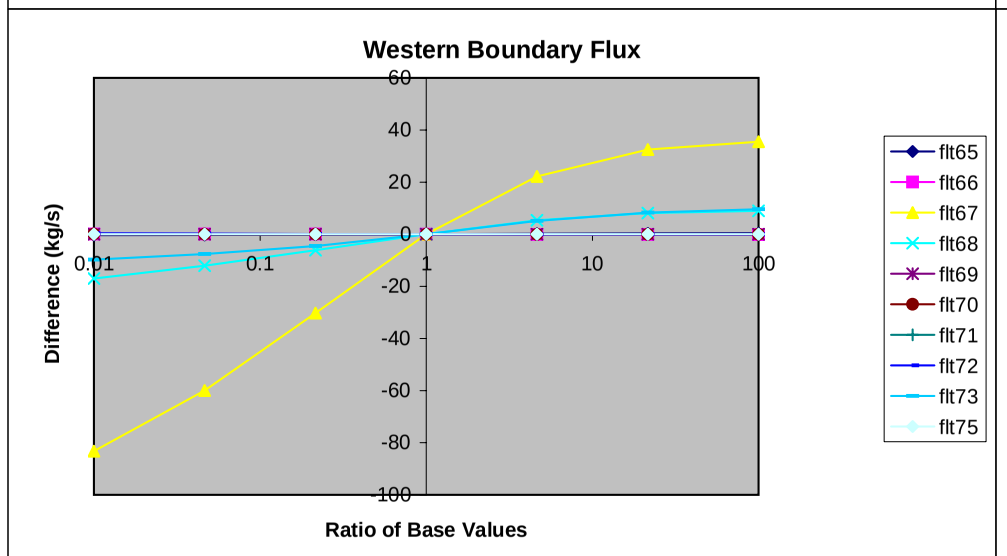
Western Boundary Flux
Difference (kg/s)
Ratio of Base Values
flt65
flt66
flt67
flt68
flt69
flt70
flt71
flt72
flt73
flt75

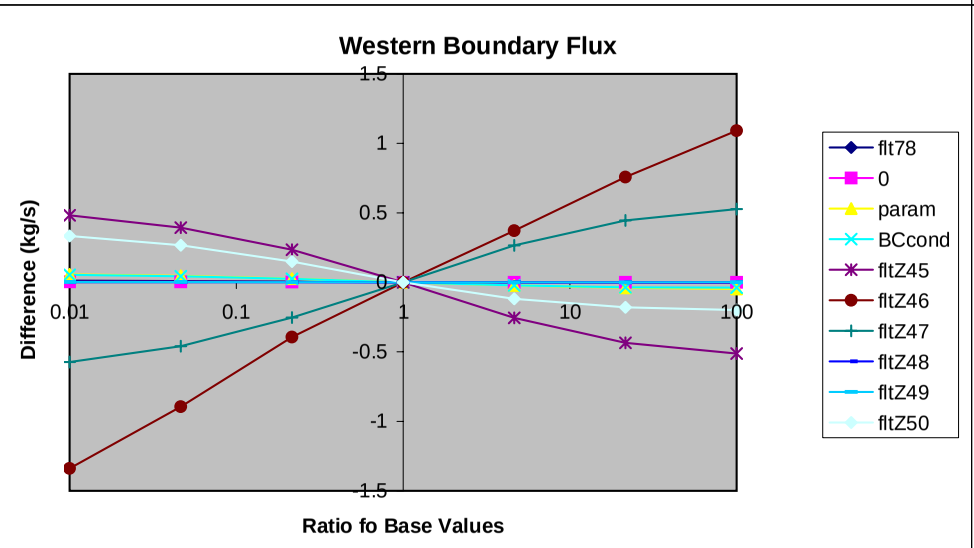
Western Boundary Flux
Difference (kg/s)
Ratio fo Base Values
flt78
0
param
BCcond
fltZ45
fltZ46
fltZ47
fltZ48
fltZ49
fltZ50

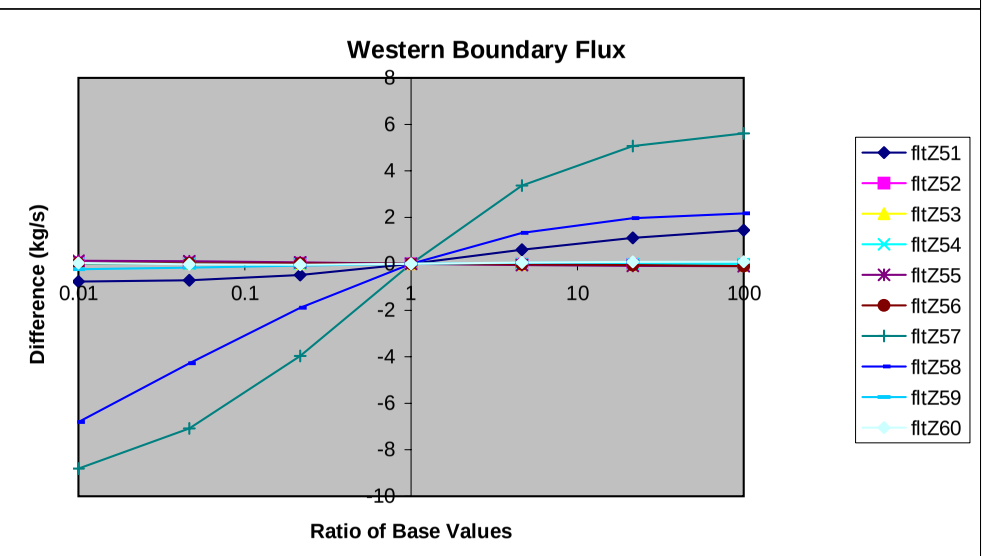
Western Boundary Flux
Difference (kg/s)
Ratio of Base Values
fltZ51
fltZ52
fltZ53
fltZ54
fltZ55
fltZ56
fltZ57
fltZ58
fltZ59
fltZ60

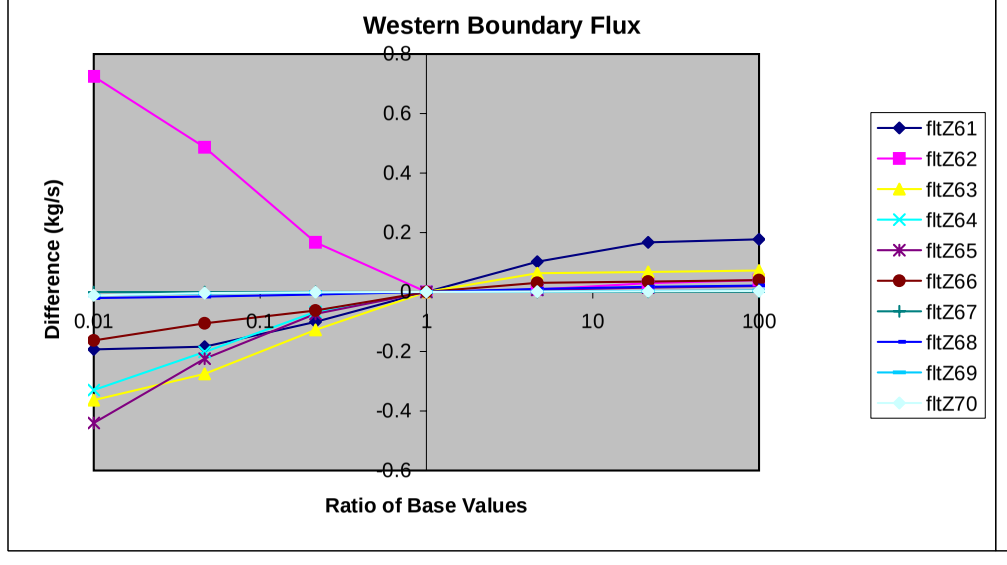
Western Boundary Flux
Difference (kg/s)
Ratio of Base Values
fltZ61
fltZ62
fltZ63
fltZ64
fltZ65
fltZ66
fltZ67
fltZ68
fltZ69
fltZ70

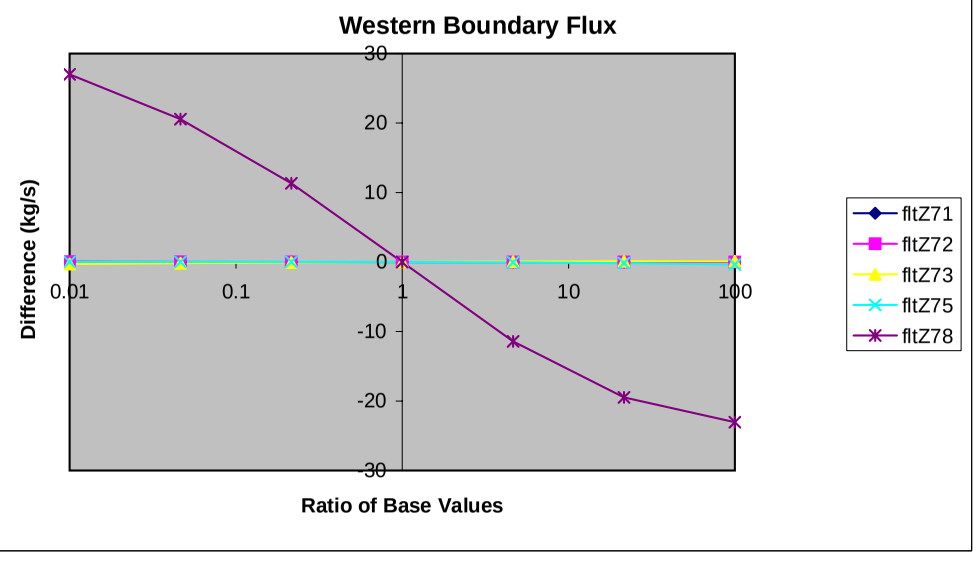
Western Boundary Flux
Difference (kg/s)
Ratio of Base Values
fltZ71
fltZ72
fltZ73
fltZ75
fltZ78

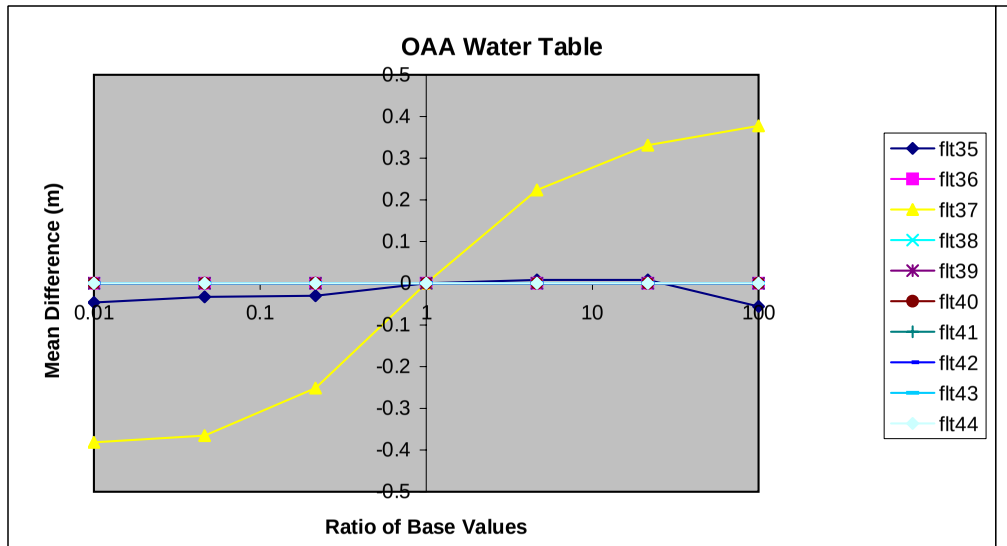
OAA Water Table
Mean Difference (m)
Ratio of Base Values
flt35
flt36
flt37
flt38
flt39
flt40
flt41
flt42
flt43
flt44

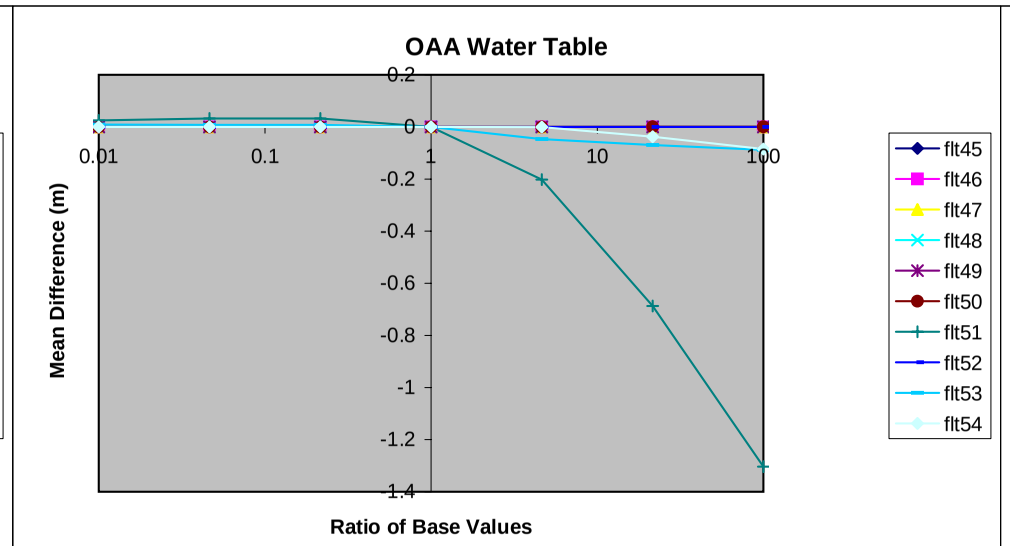
OAA Water Table
Mean Difference (m)
Ratio of Base Values
flt45
flt46
flt47
flt48
flt49
flt50
flt51
flt52
flt53
flt54

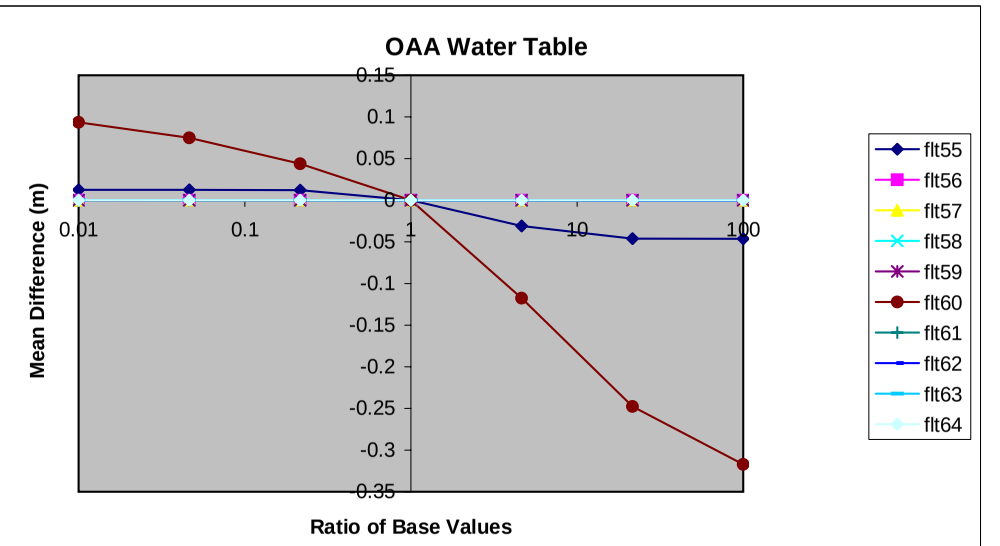
OAA Water Table
Mean Difference (m)
Ratio of Base Values
flt55
flt56
flt57
flt58
flt59
flt60
flt61
flt62
flt63
flt64

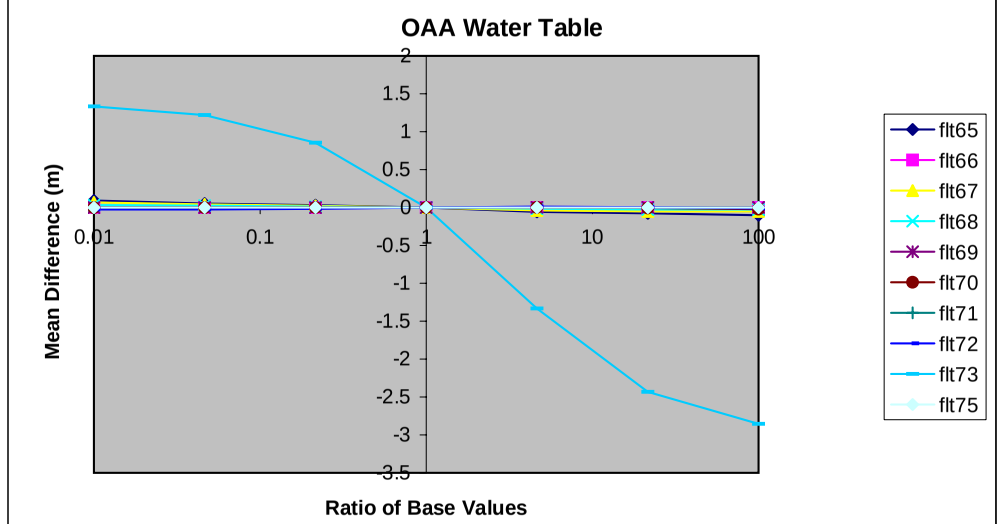
OAA Water Table
Mean Difference (m)
Ratio of Base Values
flt65
flt66
flt67
flt68
flt69
flt70
flt71
flt72
flt73
flt75

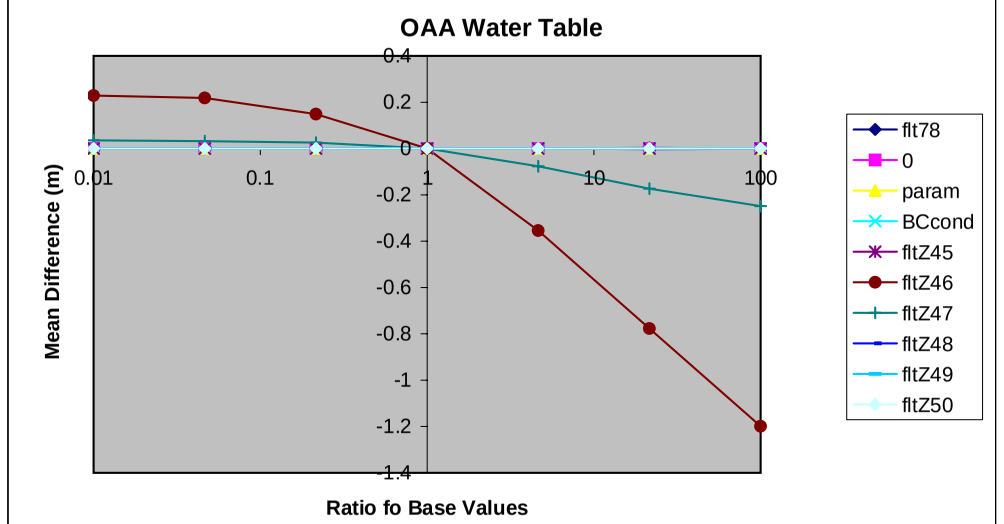
OAA Water Table
Mean Difference (m)
Ratio fo Base Values
flt78
0
param
BCcond
fltZ45
fltZ46
fltZ47
fltZ48
fltZ49
fltZ50

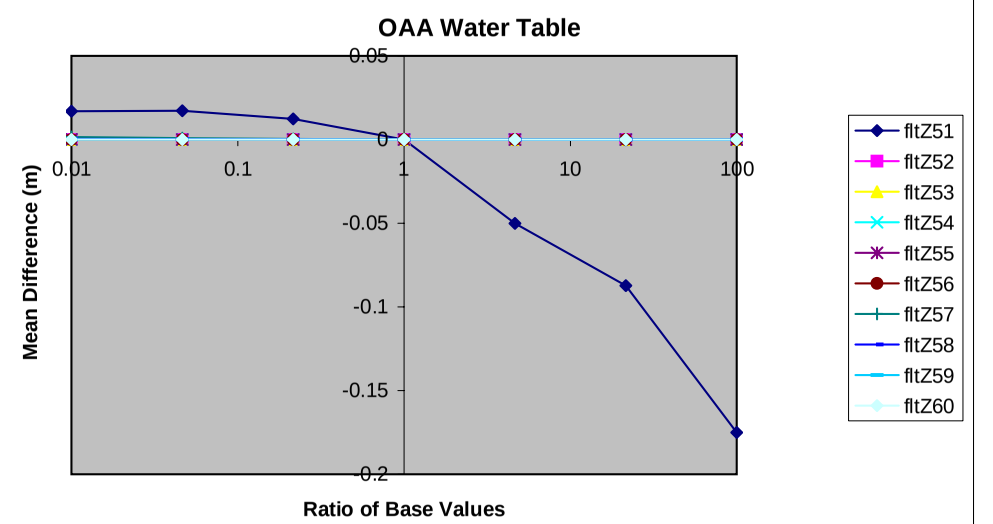
OAA Water Table
Mean Difference (m)
Ratio of Base Values
fltZ51
fltZ52
fltZ53
fltZ54
fltZ55
fltZ56
fltZ57
fltZ58
fltZ59
fltZ60

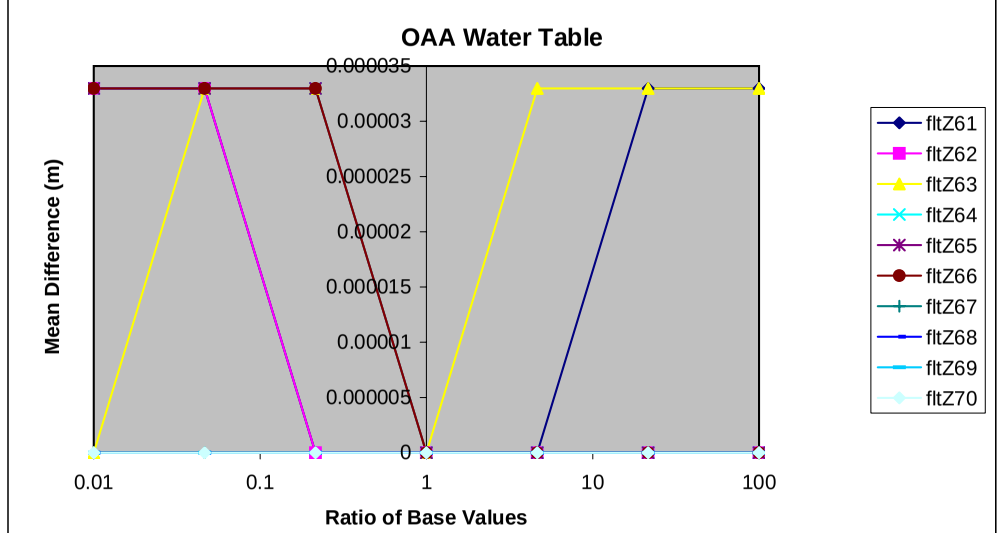
OAA Water Table
Mean Difference (m)
Ratio of Base Values
fltZ61
fltZ62
fltZ63
fltZ64
fltZ65
fltZ66
fltZ67
fltZ68
fltZ69
fltZ70

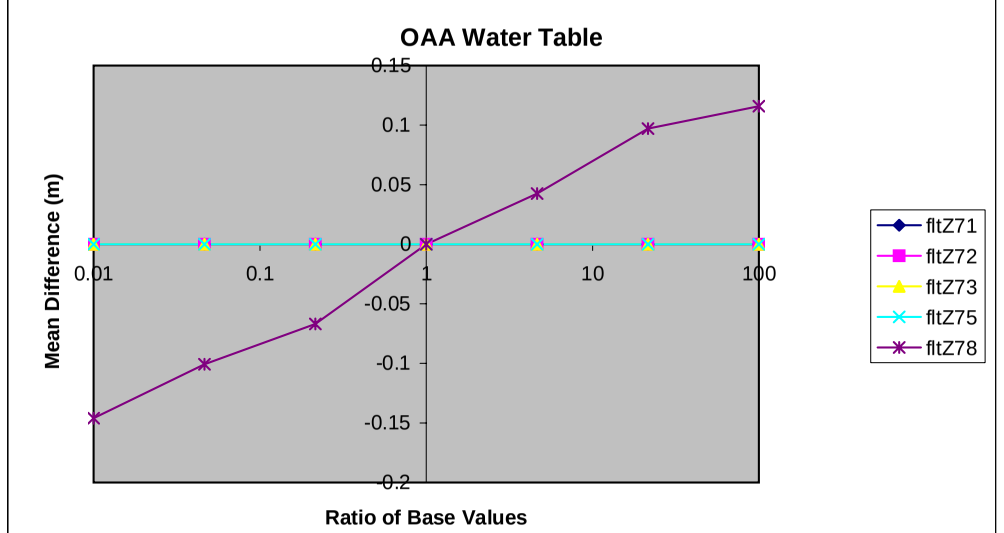
OAA Water Table
Mean Difference (m)
Ratio of Base Values
fltZ71
fltZ72
fltZ73
fltZ75
fltZ78

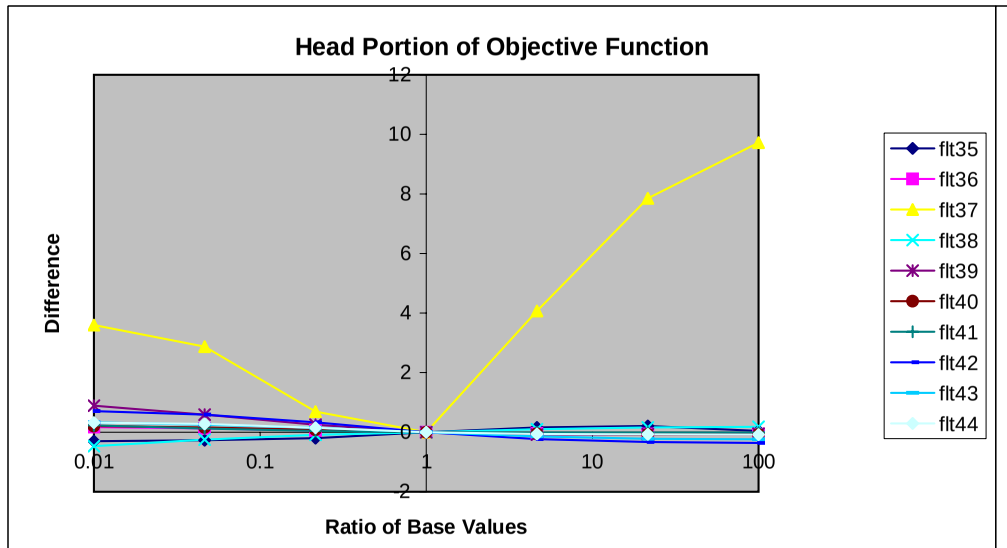
Head Portion of Objective Function
Difference
Ratio of Base Values
flt35
flt36
flt37
flt38
flt39
flt40
flt41
flt42
flt43
flt44

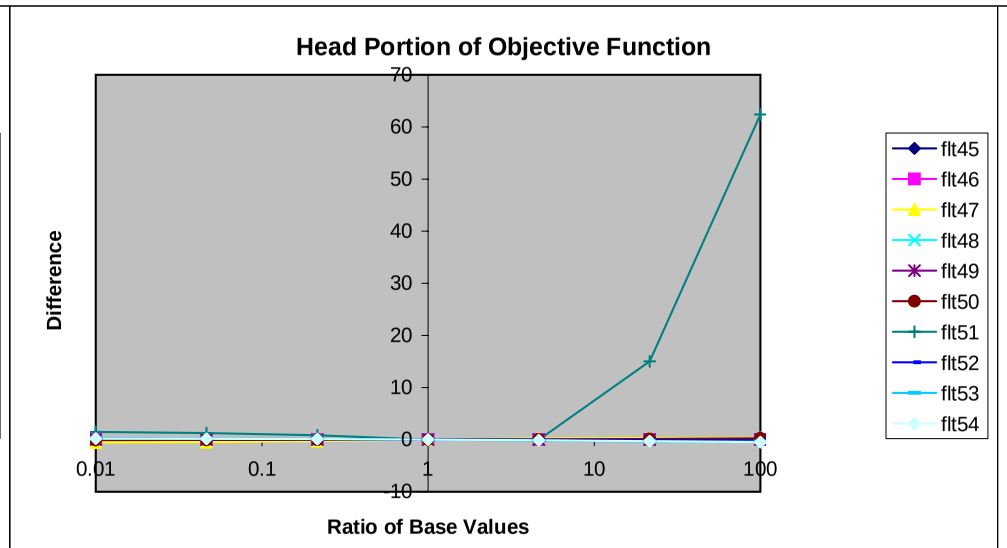
Head Portion of Objective Function
Difference
Ratio of Base Values
flt45
flt46
flt47
flt48
flt49
flt50
flt51
flt52
flt53
flt54

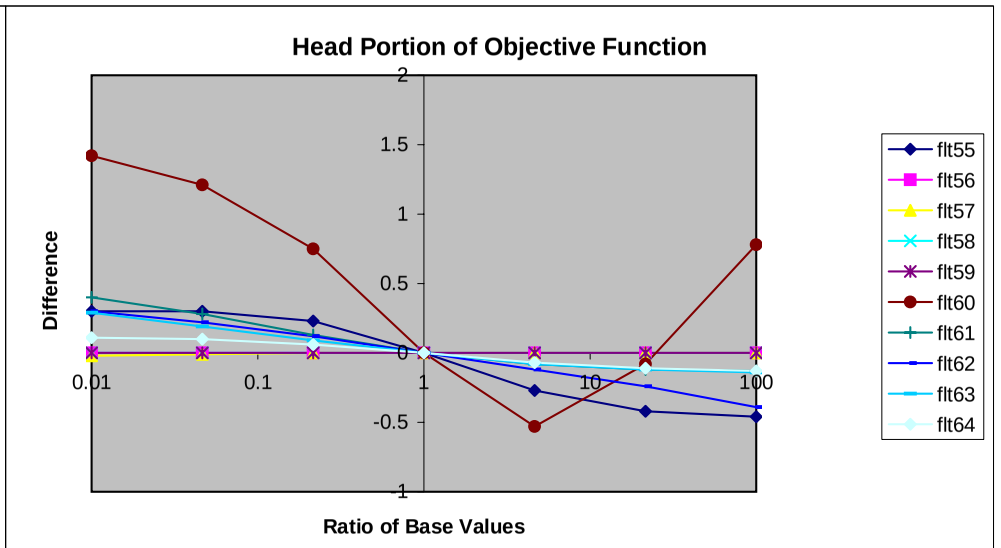
Head Portion of Objective Function
Difference
Ratio of Base Values
flt55
flt56
flt57
flt58
flt59
flt60
flt61
flt62
flt63
flt64

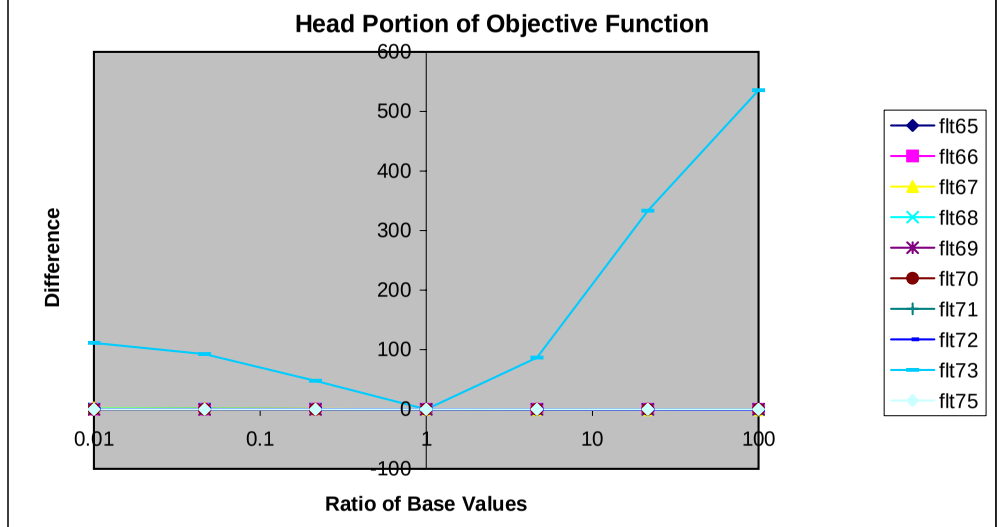
Head Portion of Objective Function
Difference
Ratio of Base Values
flt65
flt66
flt67
flt68
flt69
flt70
flt71
flt72
flt73
flt75

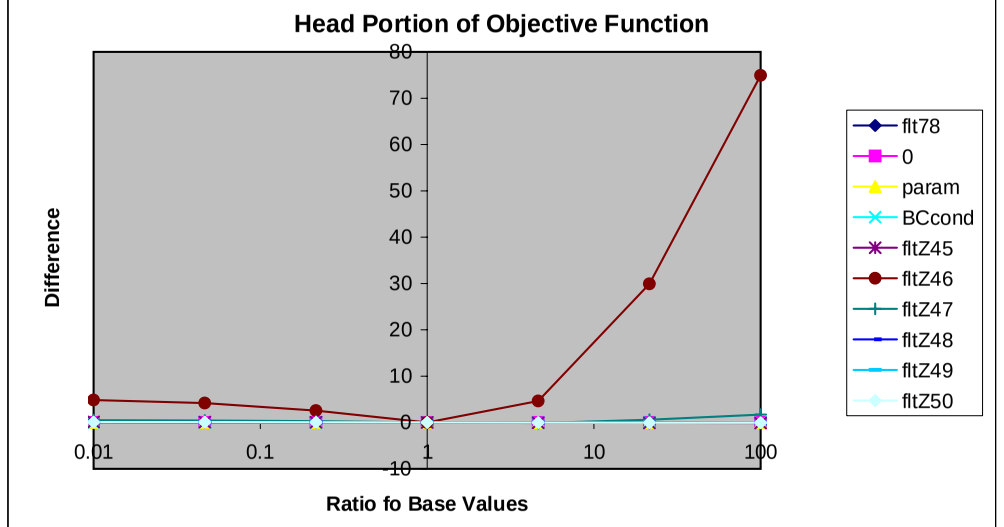
Head Portion of Objective Function
Difference
Ratio fo Base Values
flt78
0
param
BCcond
fltZ45
fltZ46
fltZ47
fltZ48
fltZ49
fltZ50

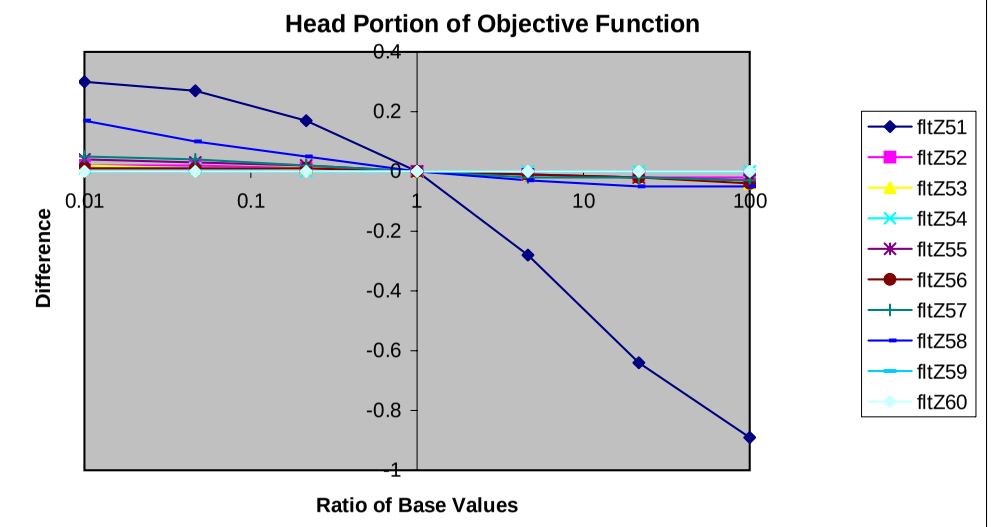
Head Portion of Objective Function
Difference
Ratio of Base Values
fltZ51
fltZ52
fltZ53
fltZ54
fltZ55
fltZ56
fltZ57
fltZ58
fltZ59
fltZ60

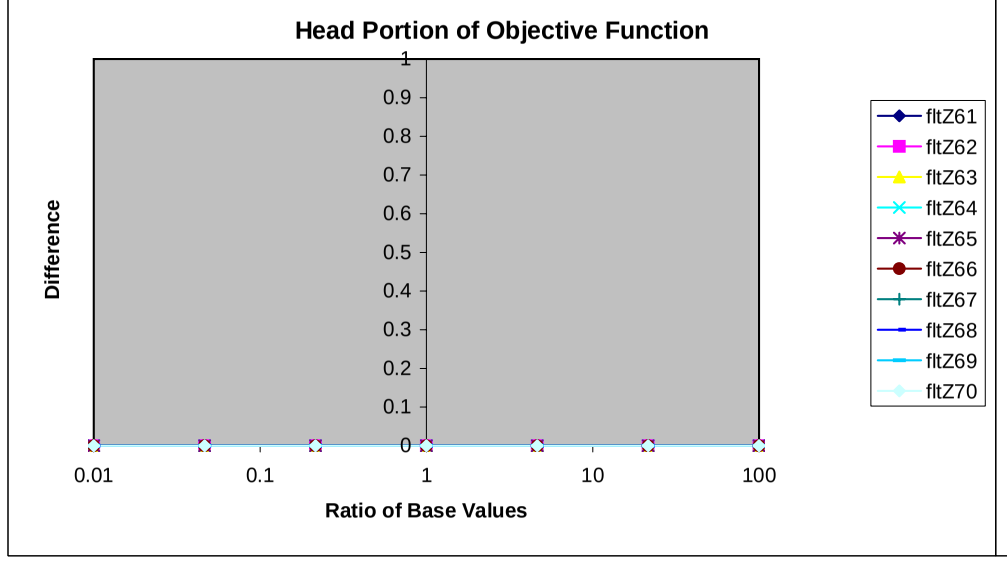
Head Portion of Objective Function
Difference
Ratio of Base Values
fltZ61
fltZ62
fltZ63
fltZ64
fltZ65
fltZ66
fltZ67
fltZ68
fltZ69
fltZ70

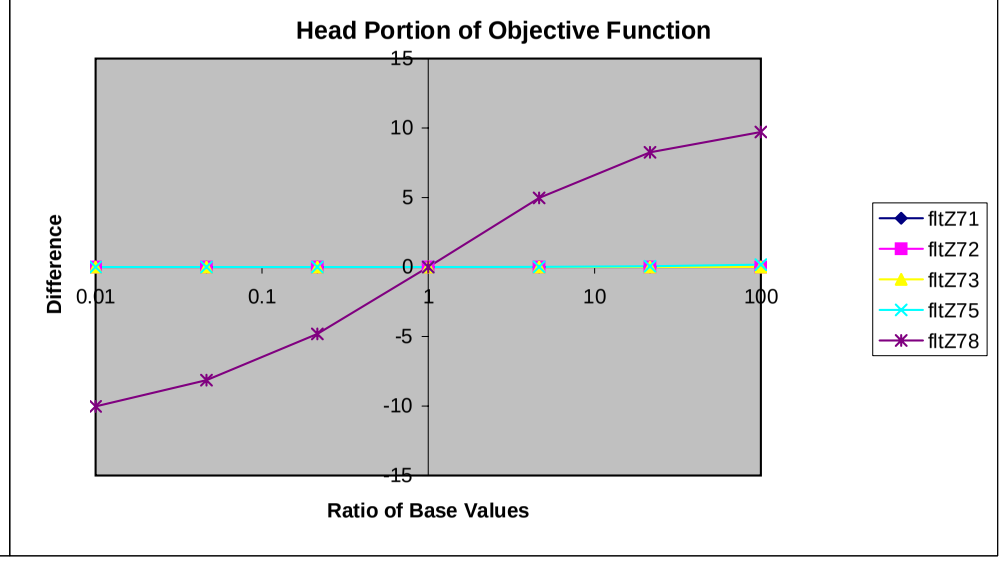
Head Portion of Objective Function
Difference
Ratio of Base Values
fltZ71
fltZ72
fltZ73
fltZ75
fltZ78

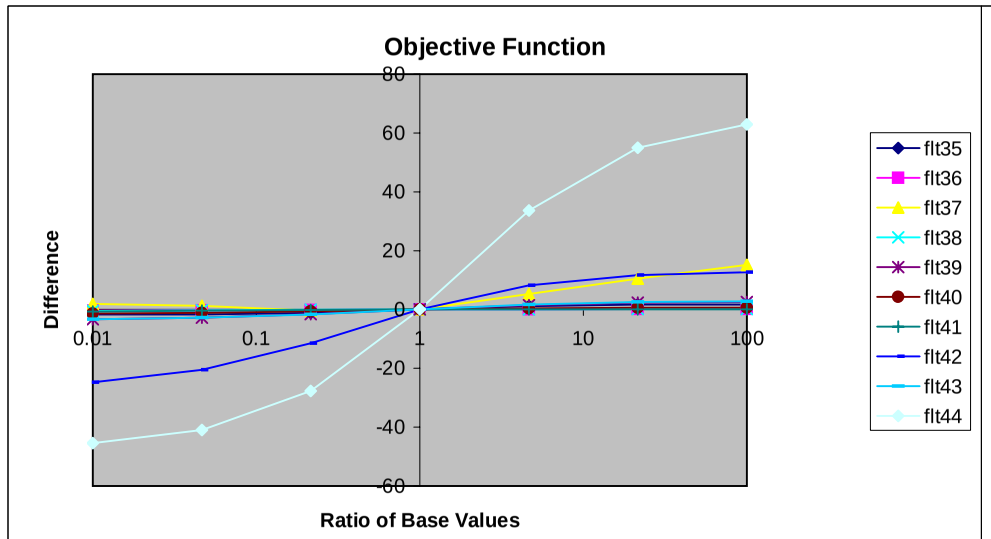
Objective Function
Difference
Ratio of Base Values
flt35
flt36
flt37
flt38
flt39
flt40
flt41
flt42
flt43
flt44

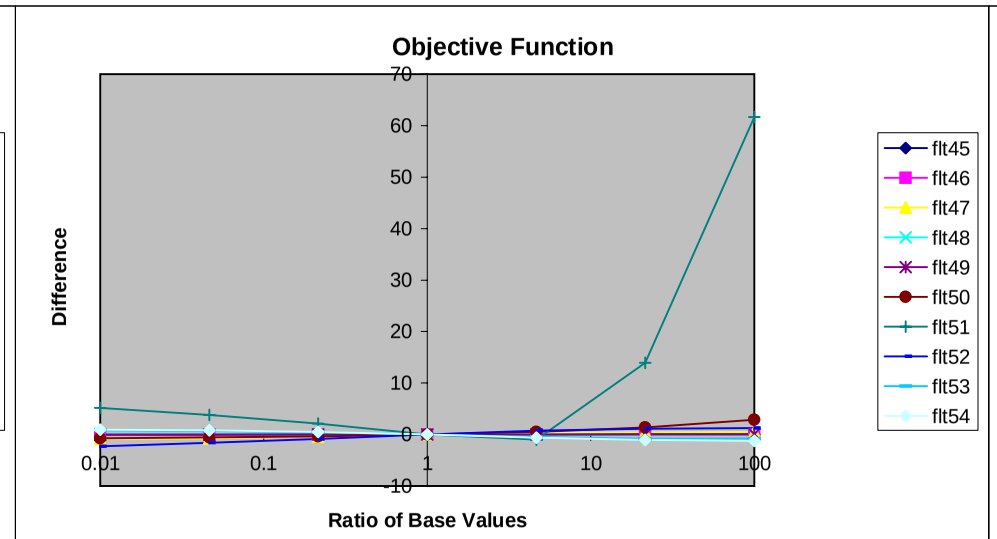
Objective Function
Difference
Ratio of Base Values
flt45
flt46
flt47
flt48
flt49
flt50
flt51
flt52
flt53
flt54

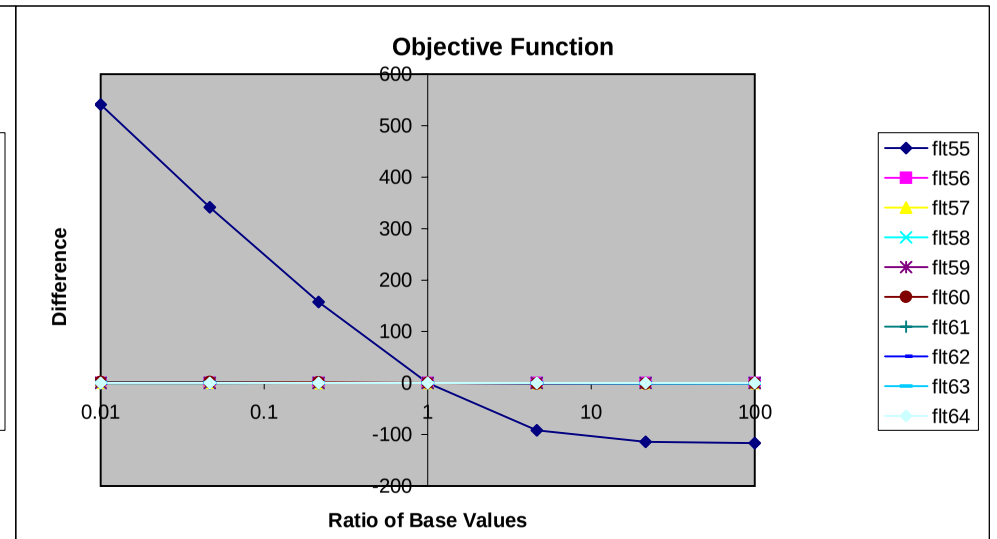
Objective Function
Difference
Ratio of Base Values
flt55
flt56
flt57
flt58
flt59
flt60
flt61
flt62
flt63
flt64

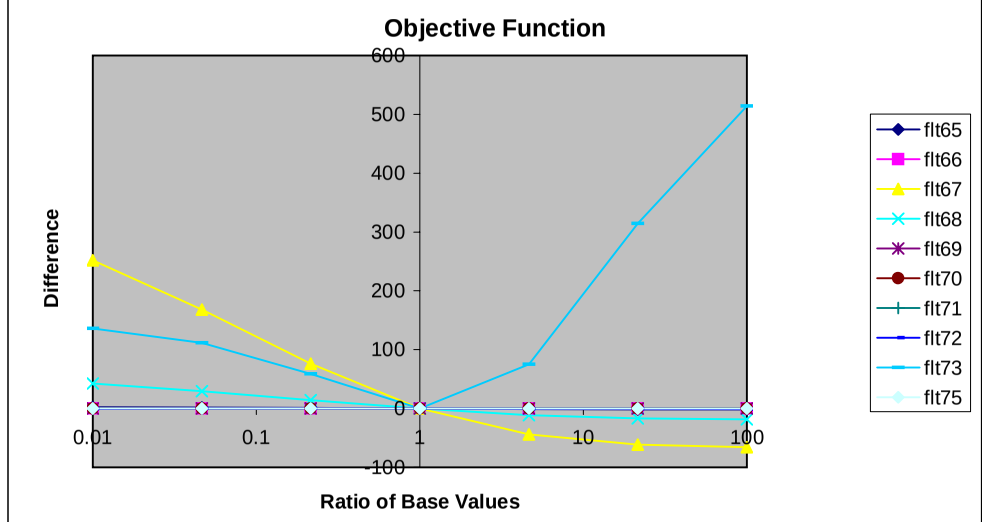
Objective Function
Difference
Ratio of Base Values
flt65
flt66
flt67
flt68
flt69
flt70
flt71
flt72
flt73
flt75

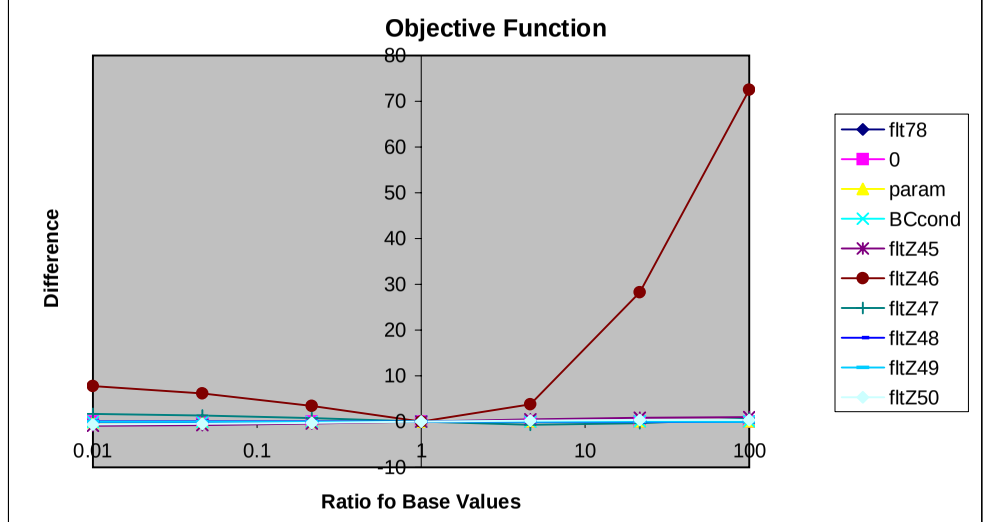
Objective Function
Difference
Ratio fo Base Values
flt78
0
param
BCcond
fltZ45
fltZ46
fltZ47
fltZ48
fltZ49
fltZ50

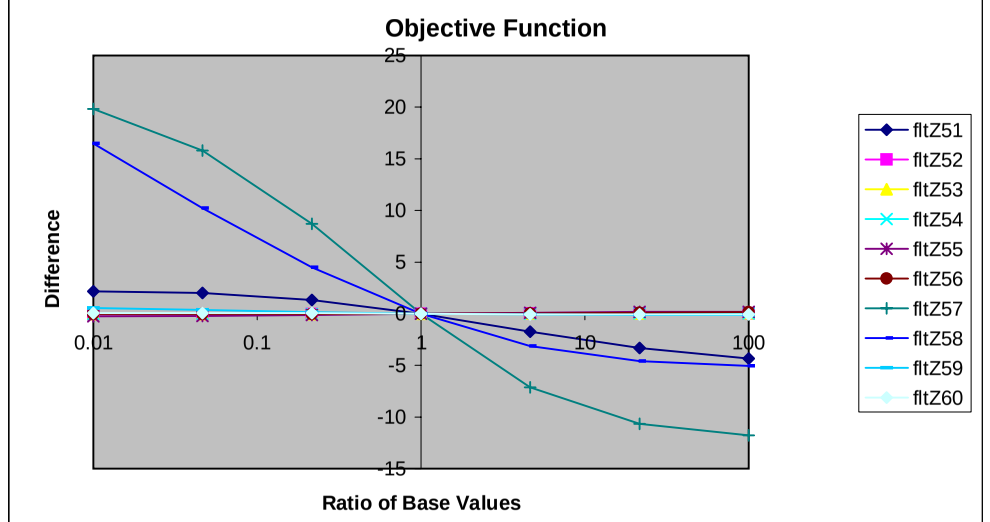
Objective Function
Difference
Ratio of Base Values
fltZ51
fltZ52
fltZ53
fltZ54
fltZ55
fltZ56
fltZ57
fltZ58
fltZ59
fltZ60

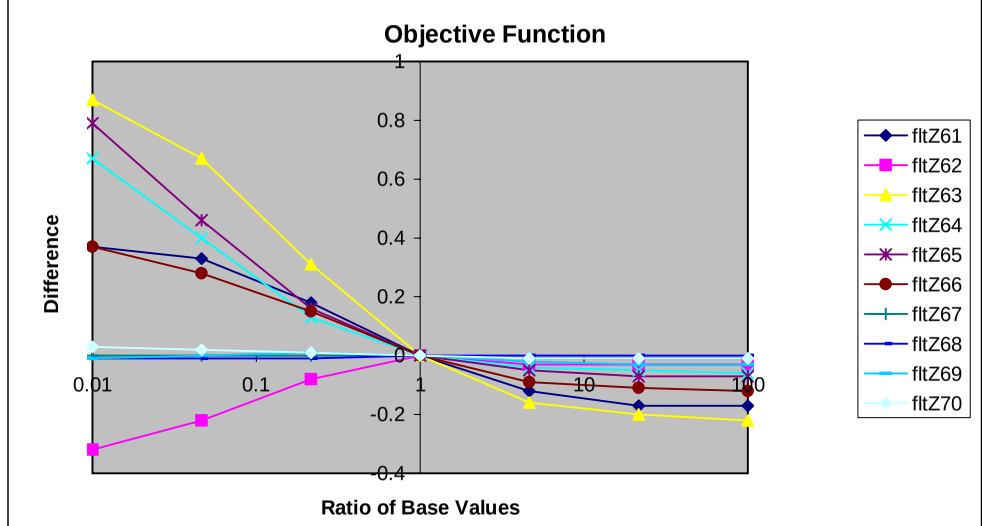
Objective Function
Difference
Ratio of Base Values
fltZ61
fltZ62
fltZ63
fltZ64
fltZ65
fltZ66
fltZ67
fltZ68
fltZ69
fltZ70

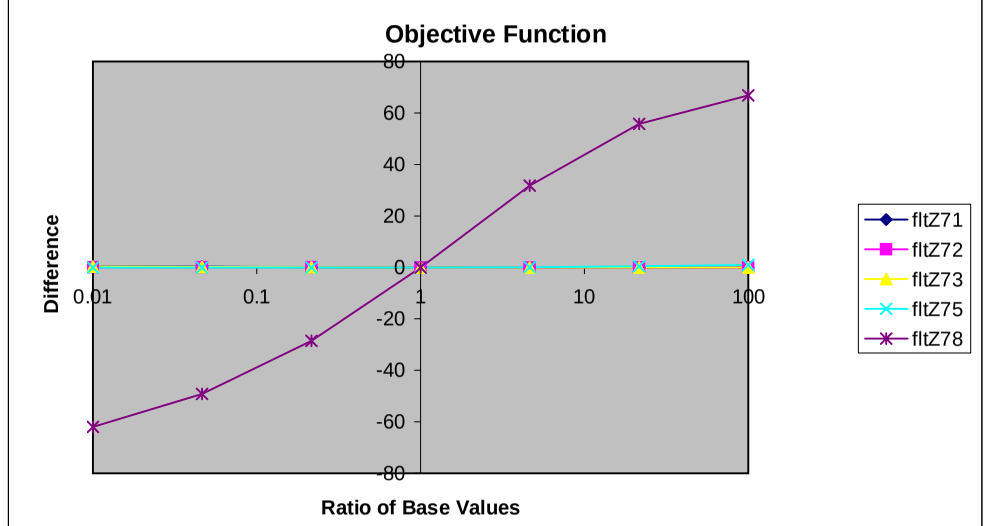
Objective Function
Difference
Ratio of Base Values
fltZ71
fltZ72
fltZ73
fltZ75
fltZ78

C.3.3

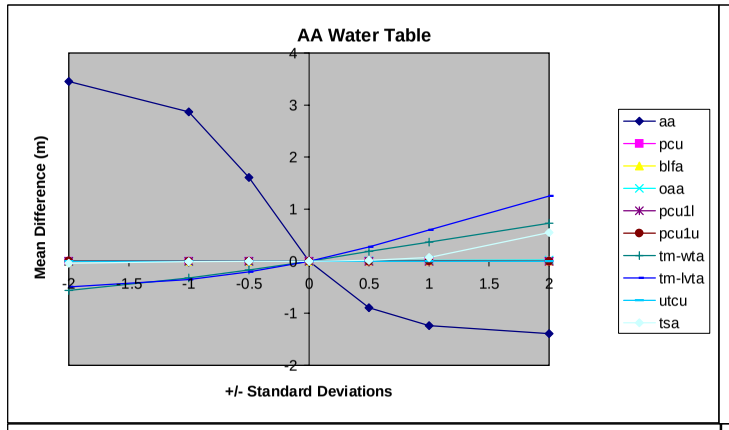
AA Water Table
Mean Difference (m)
+/- Standard Deviations
aa
pcu
blfa
oaa
pcu1l
pcu1u
tm-wta
tm-lvta
utcu
tsa

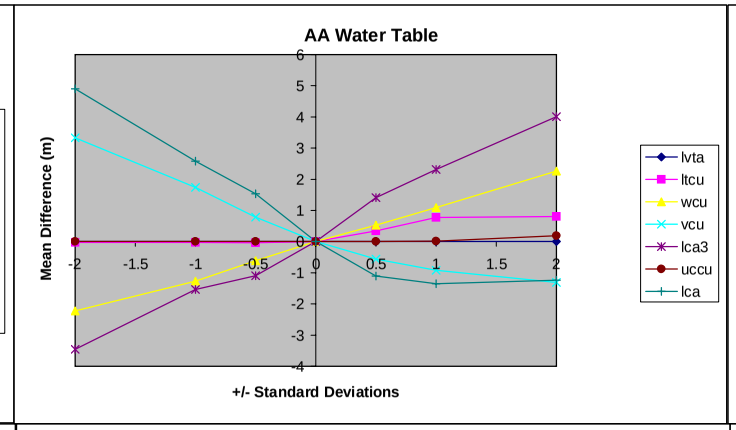
AA Water Table
Mean Difference (m)
+/- Standard Deviations
lvta
ltcu
wcu
vcu
lca3
uccu
lca

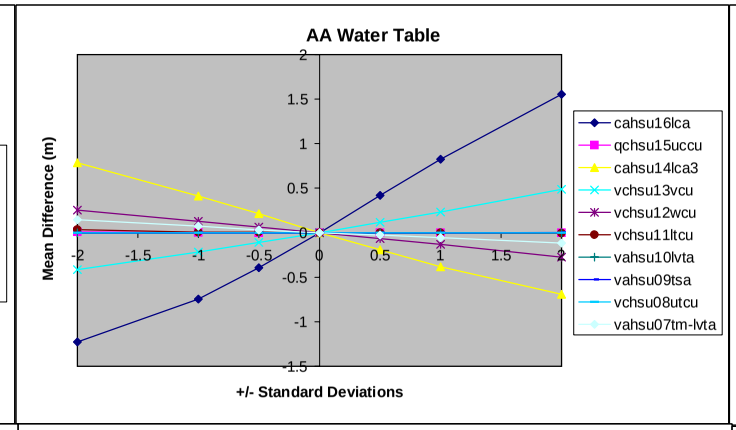
AA Water Table
Mean Difference (m)
+/- Standard Deviations
cahsu16lca
qchsu15uccu
cahsu14lca3
vchsu13vcu
vchsu12wcu
vchsu11ltcu
vahsu10lvta
vahsu09tsa
vchsu08utcu
vahsu07tm-lvta

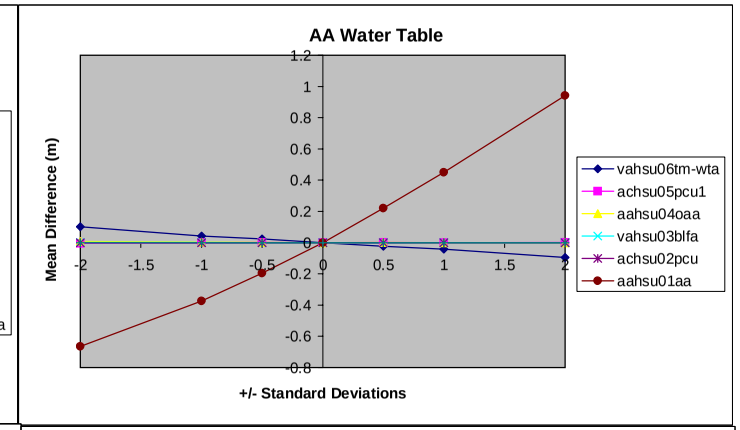
AA Water Table
Mean Difference (m)
+/- Standard Deviations
vahsu06tm-wta
achsu05pcu1
aahsu04oaa
vahsu03blfa
achsu02pcu
aahsu01aa

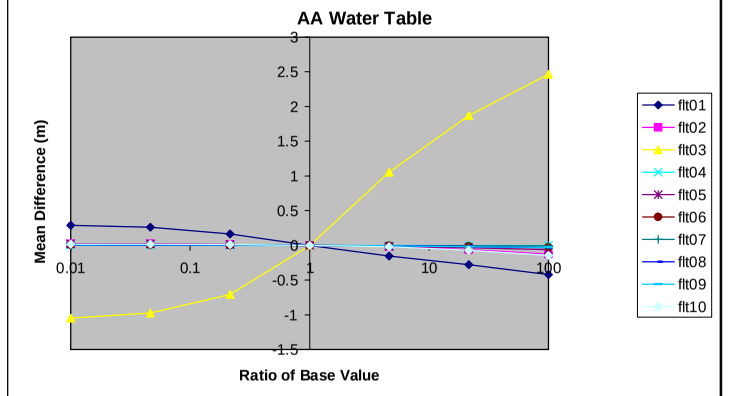
AA Water Table
Mean Difference (m)
Ratio of Base Value
flt01
flt02
flt03
flt04
flt05
flt06
flt07
flt08
flt09
flt10

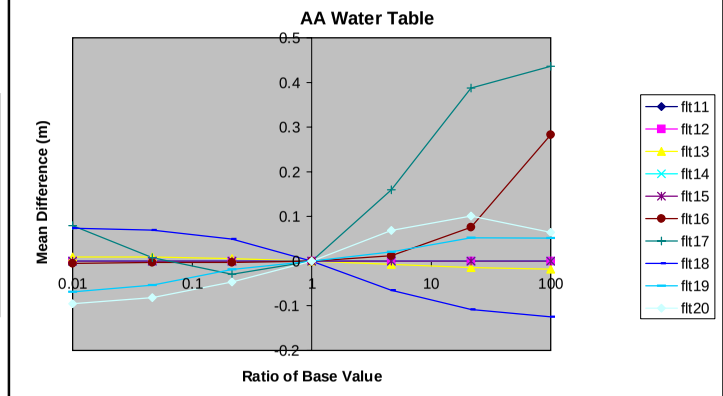
AA Water Table
Mean Difference (m)
Ratio of Base Value
flt11
flt12
flt13
flt14
flt15
flt16
flt17
flt18
flt19
flt20

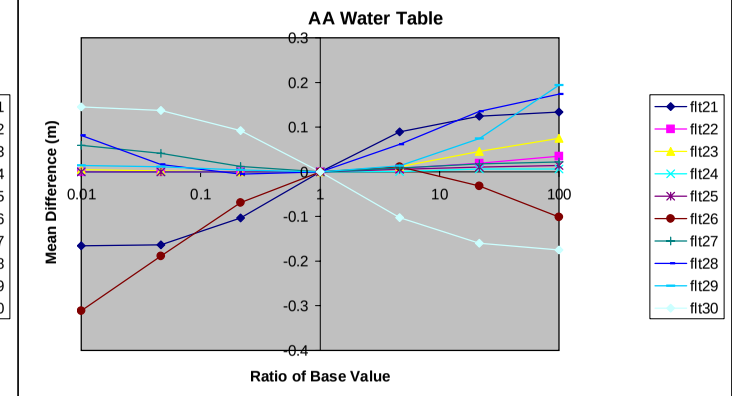
AA Water Table
Mean Difference (m)
Ratio of Base Value
flt21
flt22
flt23
flt24
flt25
flt26
flt27
flt28
flt29
flt30

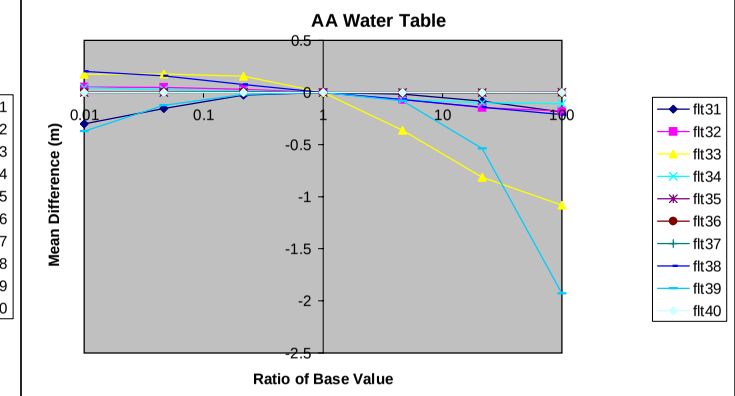
AA Water Table
Mean Difference (m)
Ratio of Base Value
flt31
flt32
flt33
flt34
flt35
flt36
flt37
flt38
flt39
flt40

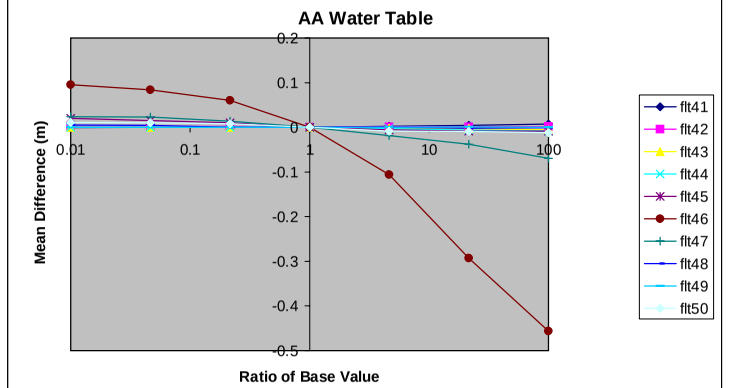
AA Water Table
Mean Difference (m)
Ratio of Base Value
flt41
flt42
flt43
flt44
flt45
flt46
flt47
flt48
flt49
flt50

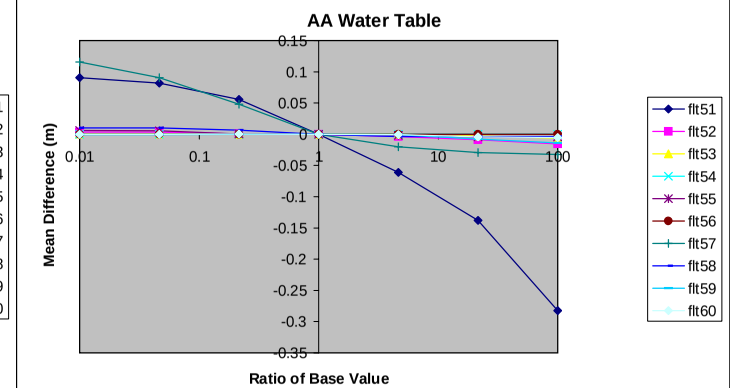
AA Water Table
Mean Difference (m)
Ratio of Base Value
flt51
flt52
flt53
flt54
flt55
flt56
flt57
flt58
flt59
flt60

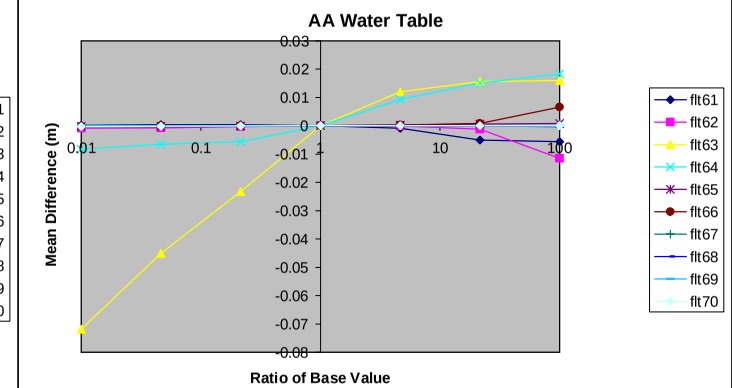
AA Water Table
Mean Difference (m)
Ratio of Base Value
flt61
flt62
flt63
flt64
flt65
flt66
flt67
flt68
flt69
flt70

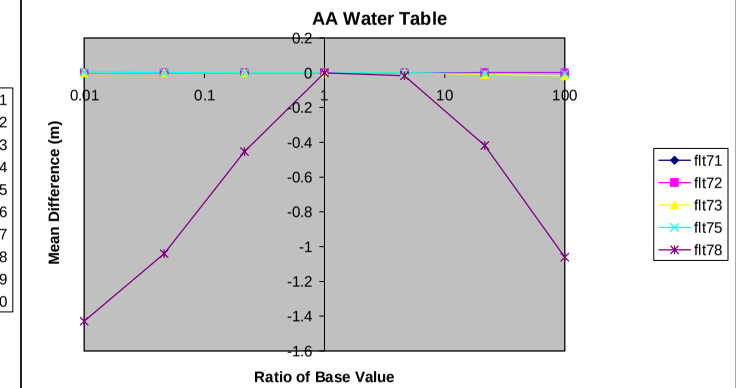
AA Water Table
Mean Difference (m)
Ratio of Base Value
flt71
flt72
flt73
flt75
flt78

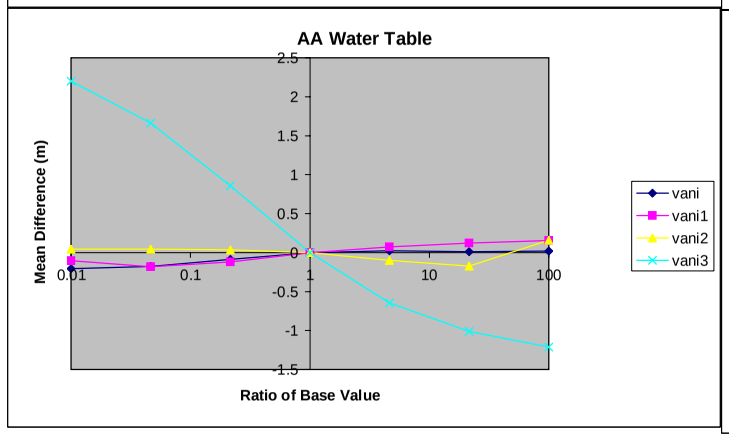
AA Water Table
Mean Difference (m)
Ratio of Base Value
vani
vani1
vani2
vani3

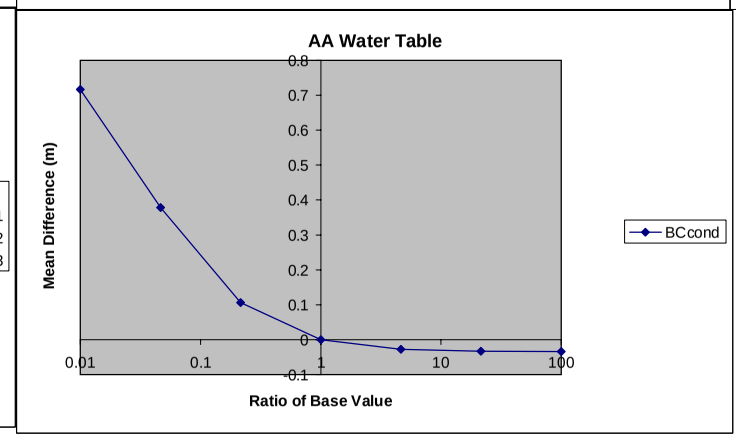
AA Water Table
Mean Difference (m)
Ratio of Base Value
BCcond

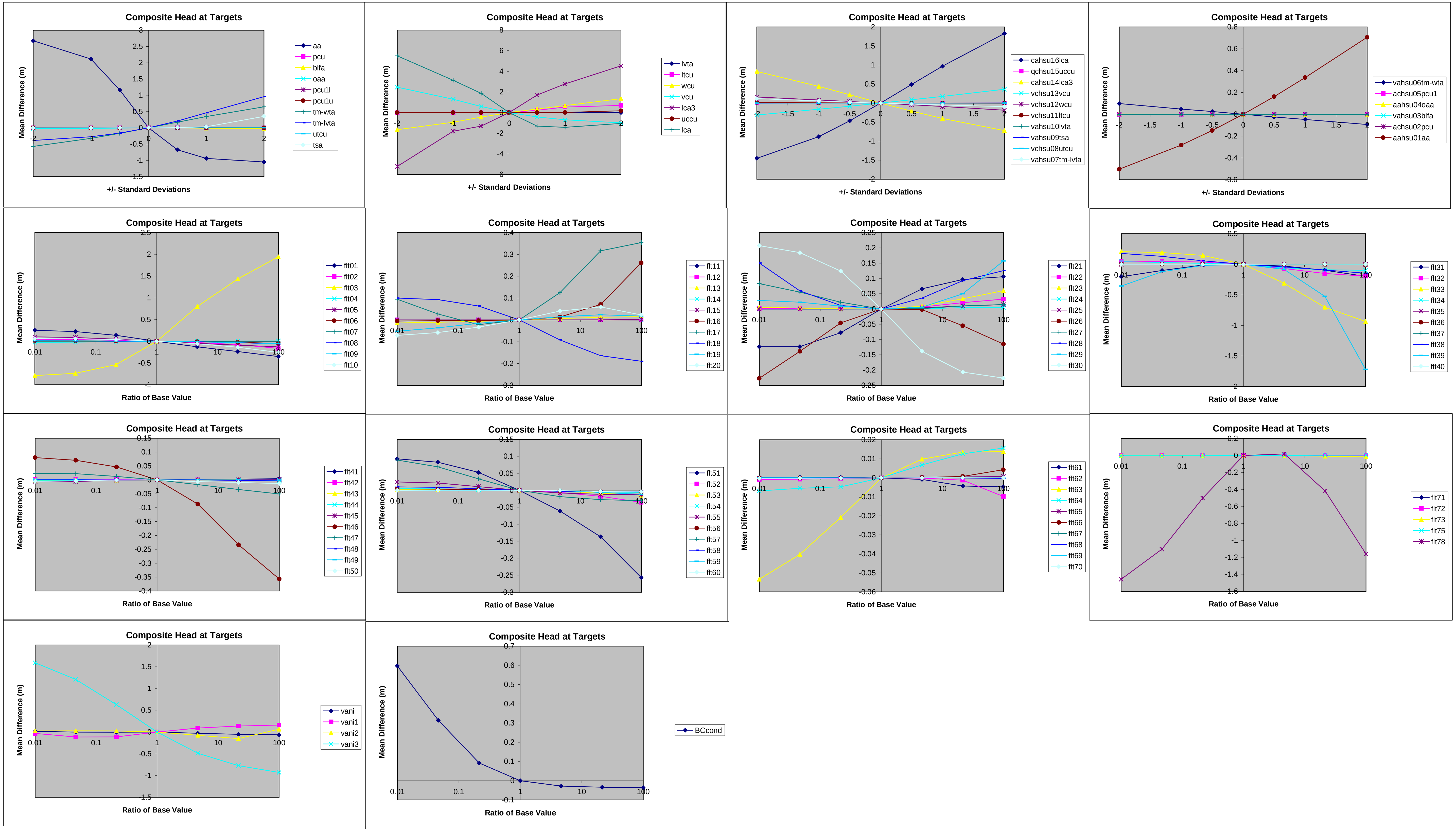
Composite Head at Targets
Mean Difference (m)
+/- Standard Deviations
aa
pcu
blfa
oaa
pcu1l
pcu1u
tm-wta
tm-lvta
utcu
tsa
Composite Head at Targets
Mean Difference (m)
+/- Standard Deviations
lvta
ltcu
wcu
vcu
lca3
uccu
lca
Composite Head at Targets
Mean Difference (m)
+/- Standard Deviations
cahsu16lca
qchsu15uccu
cahsu14lca3
vchsu13vcu
vchsu12wcu
vchsu11ltcu
vahsu10lvta
vahsu09tsa
vchsu08utcu
vahsu07tm-lvta
Composite Head at Targets
Mean Difference (m)
+/- Standard Deviations
vahsu06tm-wta
achsu05pcu1
aahsu04oaa
vahsu03blfa
achsu02pcu
aahsu01aa
Composite Head at Targets
Mean Difference (m)
Ratio of Base Value
flt01
flt02
flt03
flt04
flt05
flt06
flt07
flt08
flt09
flt10
Composite Head at Targets
Mean Difference (m)
Ratio of Base Value
flt11
flt12
flt13
flt14
flt15
flt16
flt17
flt18
flt19
flt20
Composite Head at Targets
Mean Difference (m)
Ratio of Base Value
flt21
flt22
flt23
flt24
flt25
flt26
flt27
flt28
flt29
flt30
Composite Head at Targets
Mean Difference (m)
Ratio of Base Value
flt31
flt32
flt33
flt34
flt35
flt36
flt37
flt38
flt39
flt40
Composite Head at Targets
Mean Difference (m)
Ratio of Base Value
flt41
flt42
flt43
flt44
flt45
flt46
flt47
flt48
flt49
flt50
Composite Head at Targets
Mean Difference (m)
Ratio of Base Value
flt51
flt52
flt53
flt54
flt55
flt56
flt57
flt58
flt59
flt60
Composite Head at Targets
Mean Difference (m)
Ratio of Base Value
flt61
flt62
flt63
flt64
flt65
flt66
flt67
flt68
flt69
flt70
Composite Head at Targets
Mean Difference (m)
Ratio of Base Value
flt71
flt72
flt73
flt75
flt78
Composite Head at Targets
Mean Difference (m)
Ratio of Base Value
vani
vani1
vani2
vani3
Composite Head at Targets
Mean Difference (m)
Ratio of Base Value
BCcond

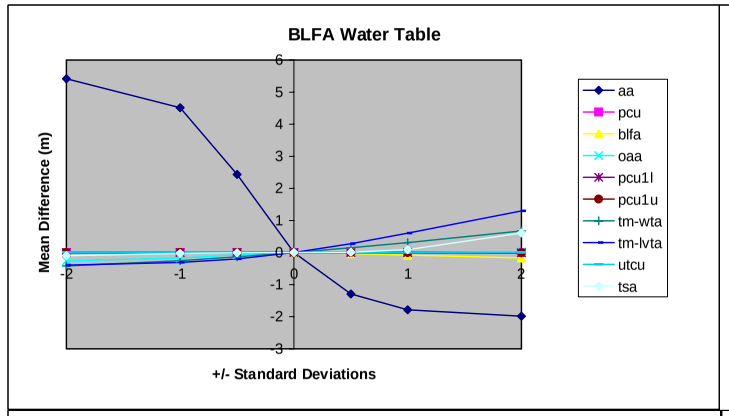
BLFA Water Table
Mean Difference (m)
+/- Standard Deviations
aa
pcu
blfa
oaa
pcu1l
pcu1u
tm-wta
tm-lvta
utcu
tsa

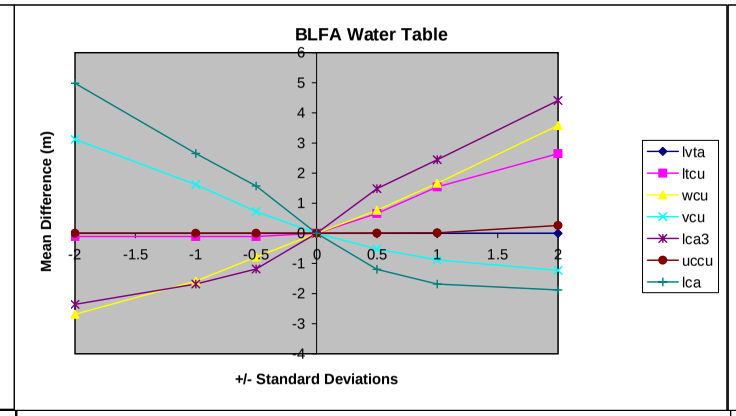
BLFA Water Table
Mean Difference (m)
+/- Standard Deviations
lvta
ltcu
wcu
vcu
lca3
uccu
lca

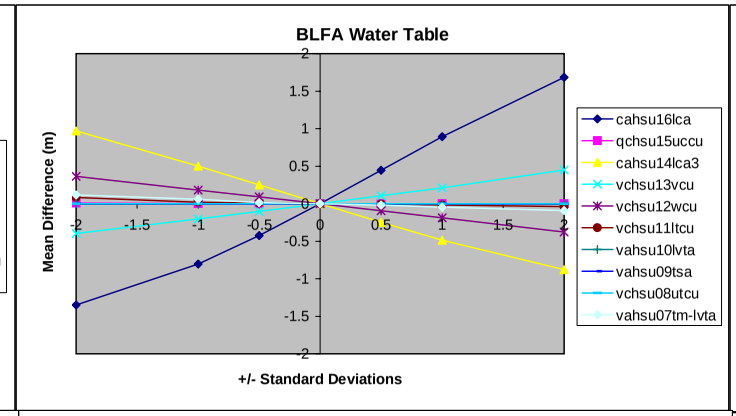
BLFA Water Table
Mean Difference (m)
+/- Standard Deviations
cahsu16lca
qchsu15uccu
cahsu14lca3
vchsu13vcu
vchsu12wcu
vchsu11ltcu
vahsu10lvta
vahsu09tsa
vchsu08utcu
vahsu07tm-lvta

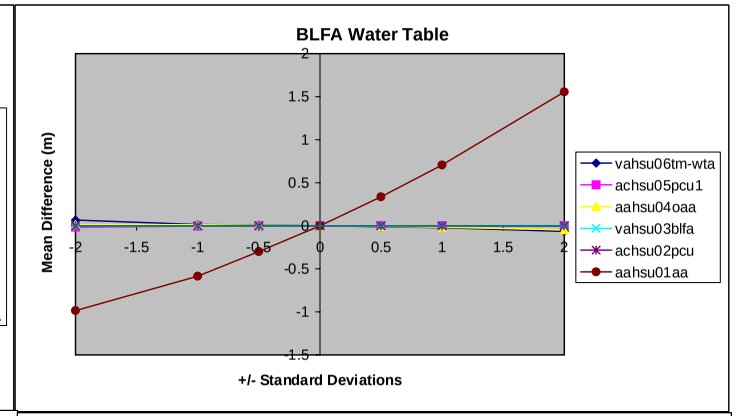
BLFA Water Table
Mean Difference (m)
+/- Standard Deviations
vahsu06tm-wta
achsu05pcu1
aahsu04oaa
vahsu03blfa
achsu02pcu
aahsu01aa

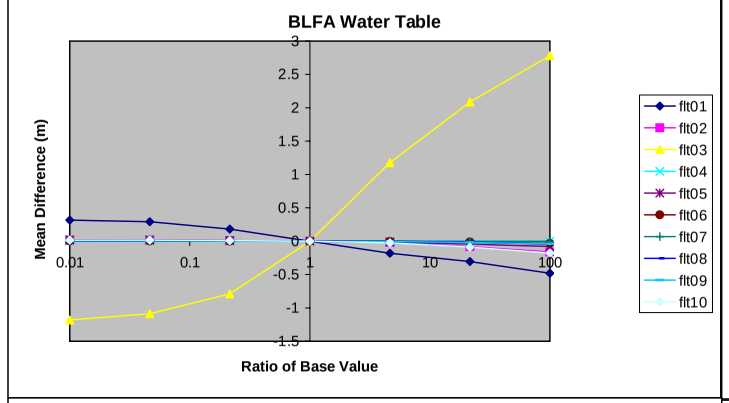
BLFA Water Table
Mean Difference (m)
Ratio of Base Value
flt01
flt02
flt03
flt04
flt05
flt06
flt07
flt08
flt09
flt10

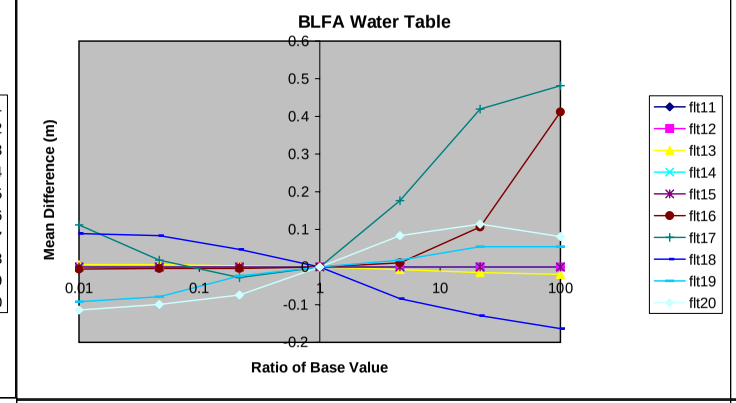
BLFA Water Table
Mean Difference (m)
Ratio of Base Value
flt11
flt12
flt13
flt14
flt15
flt16
flt17
flt18
flt19
flt20

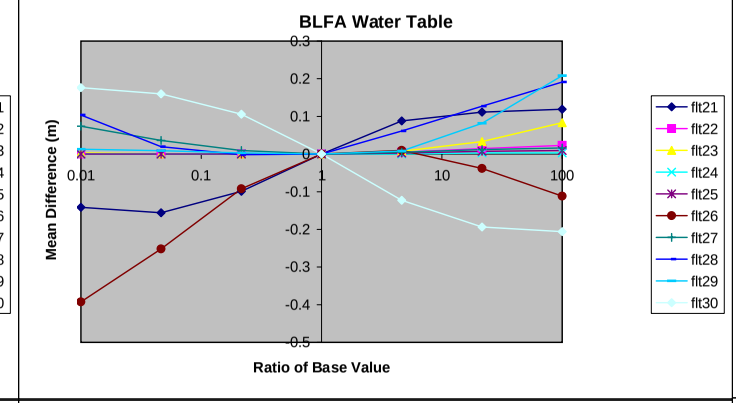
BLFA Water Table
Mean Difference (m)
Ratio of Base Value
flt21
flt22
flt23
flt24
flt25
flt26
flt27
flt28
flt29
flt30

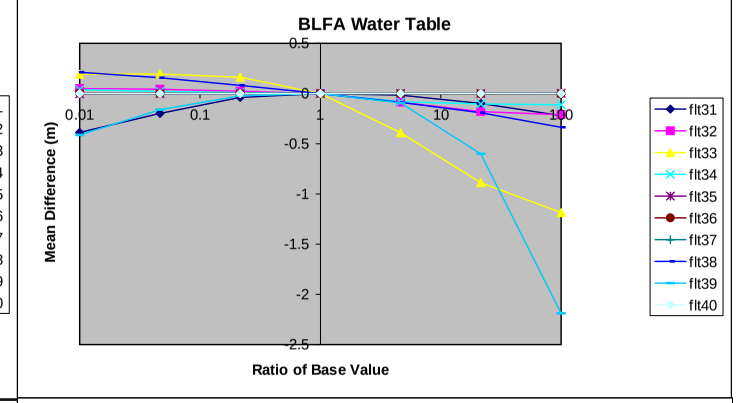
BLFA Water Table
Mean Difference (m)
Ratio of Base Value
flt31
flt32
flt33
flt34
flt35
flt36
flt37
flt38
flt39
flt40

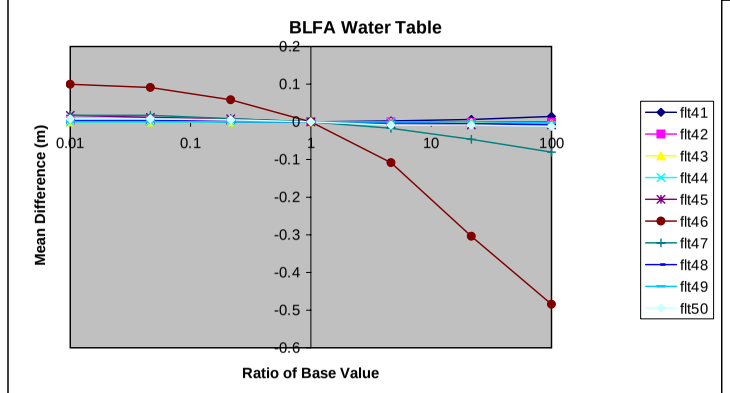
BLFA Water Table
Mean Difference (m)
Ratio of Base Value
flt41
flt42
flt43
flt44
flt45
flt46
flt47
flt48
flt49
flt50

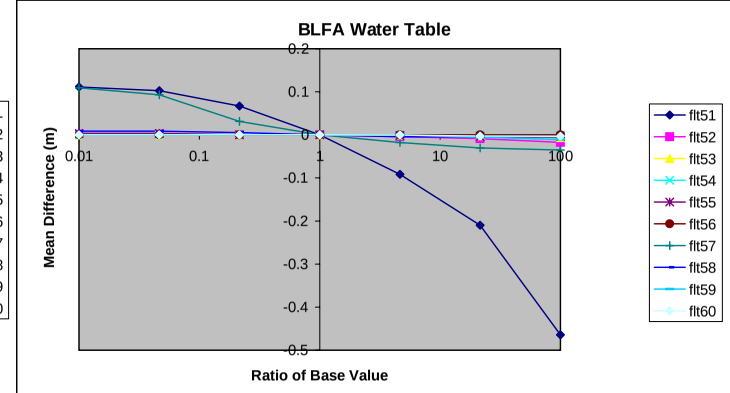
BLFA Water Table
Mean Difference (m)
Ratio of Base Value
flt51
flt52
flt53
flt54
flt55
flt56
flt57
flt58
flt59
flt60

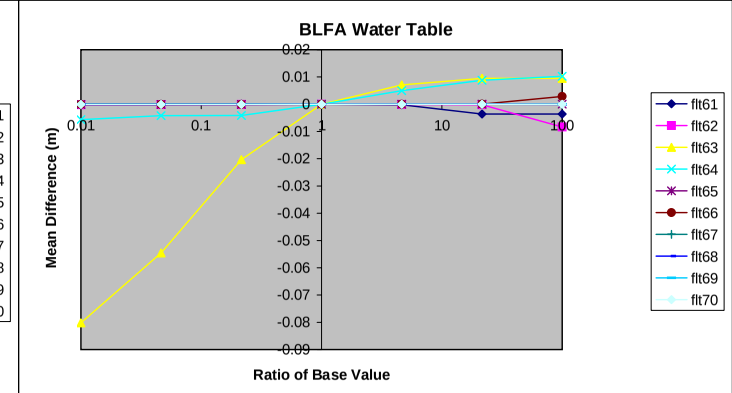
BLFA Water Table
Mean Difference (m)
Ratio of Base Value
flt61
flt62
flt63
flt64
flt65
flt66
flt67
flt68
flt69
flt70

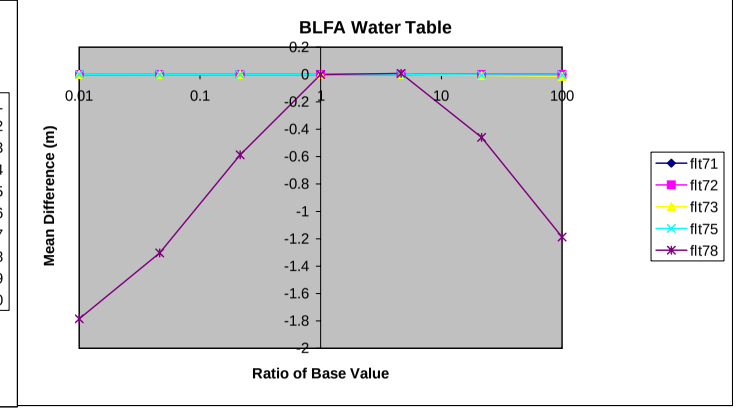
BLFA Water Table
Mean Difference (m)
Ratio of Base Value
flt71
flt72
flt73
flt75
flt78

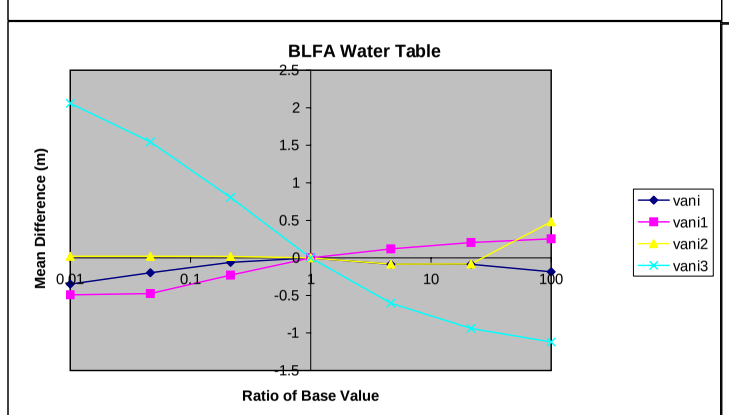
BLFA Water Table
Mean Difference (m)
Ratio of Base Value
vani
vani1
vani2
vani3

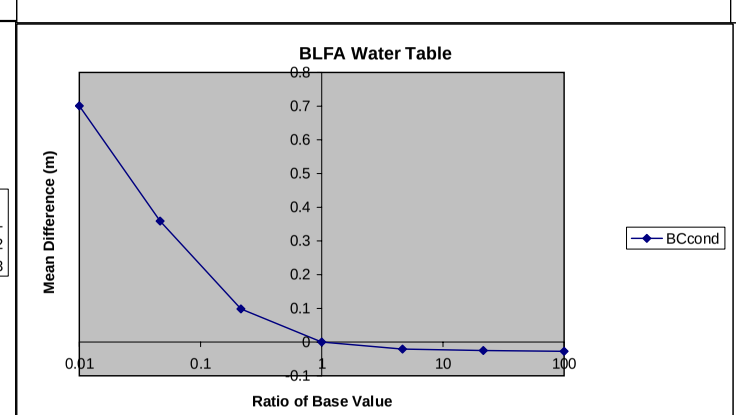
BLFA Water Table
Mean Difference (m)
Ratio of Base Value
BCcond

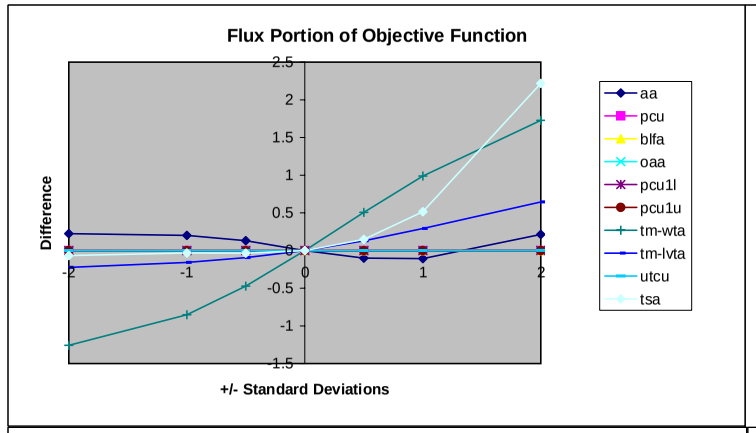
Flux Portion of Objective Function
Difference
+/- Standard Deviations
aa
pcu
blfa
oaa
pcu1l
pcu1u
tm-wta
tm-lvta
utcu
tsa

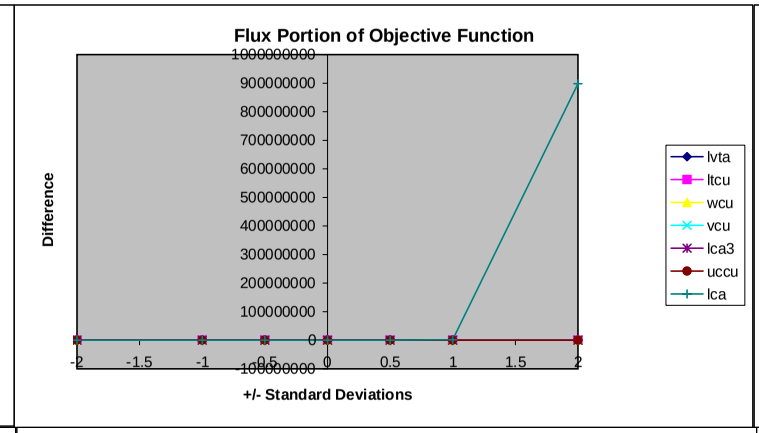
Flux Portion of Objective Function
Difference
+/- Standard Deviations
lvta
ltcu
wcu
vcu
lca3
uccu
lca

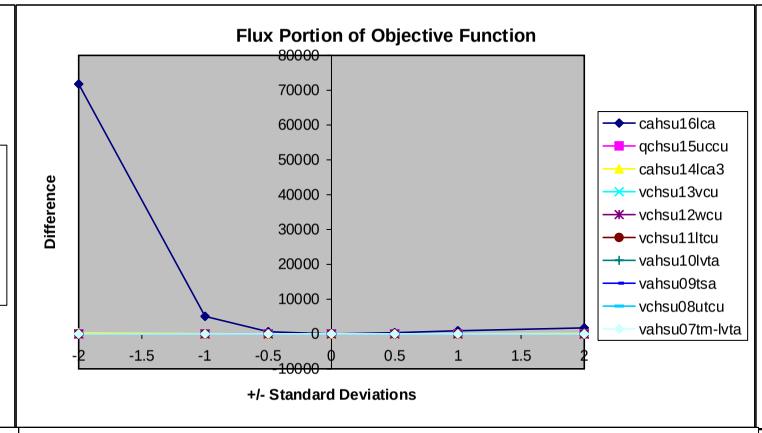
Flux Portion of Objective Function
Difference
+/- Standard Deviations
cahsu16lca
qchsu15uccu
cahsu14lca3
vchsu13vcu
vchsu12wcu
vchsu11ltcu
vahsu10lvta
vahsu09tsa
vchsu08utcu
vahsu07tm-lvta

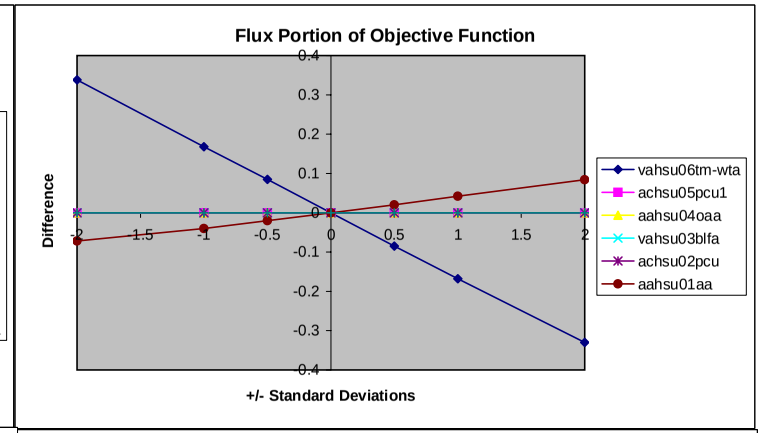
Flux Portion of Objective Function
Difference
+/- Standard Deviations
vahsu06tm-wta
achsu05pcu1
aahsu04oaa
vahsu03blfa
achsu02pcu
aahsu01aa

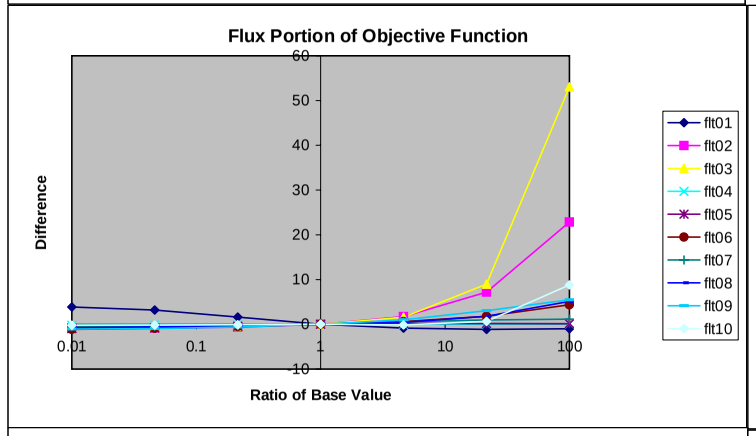
Flux Portion of Objective Function
Difference
Ratio of Base Value
flt01
flt02
flt03
flt04
flt05
flt06
flt07
flt08
flt09
flt10

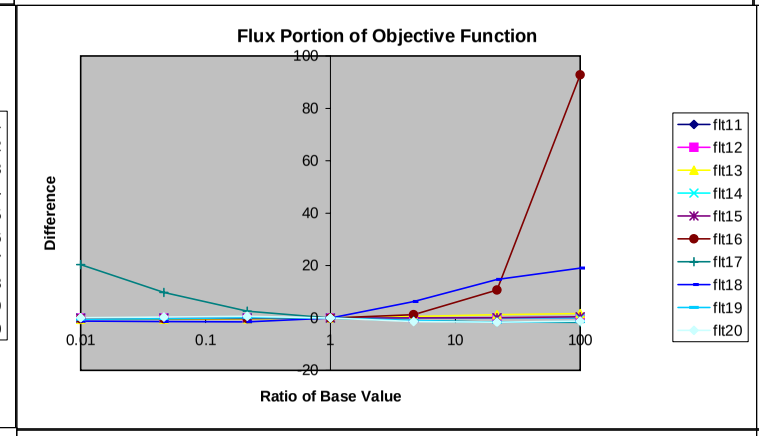
Flux Portion of Objective Function
Difference
Ratio of Base Value
flt11
flt12
flt13
flt14
flt15
flt16
flt17
flt18
flt19
flt20

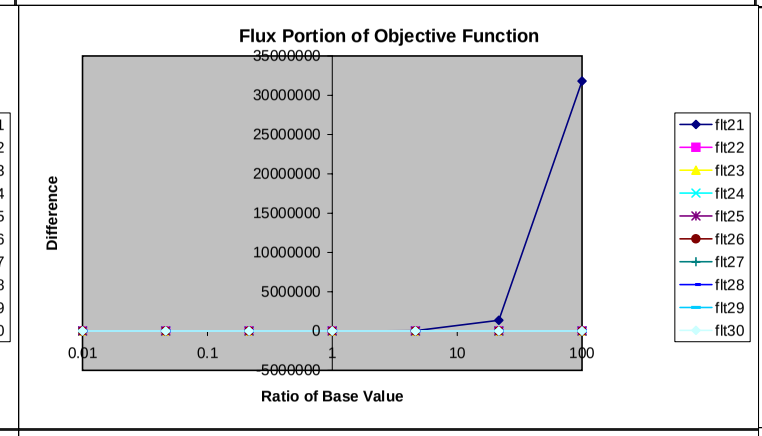
Flux Portion of Objective Function
Difference
Ratio of Base Value
flt21
flt22
flt23
flt24
flt25
flt26
flt27
flt28
flt29
flt30

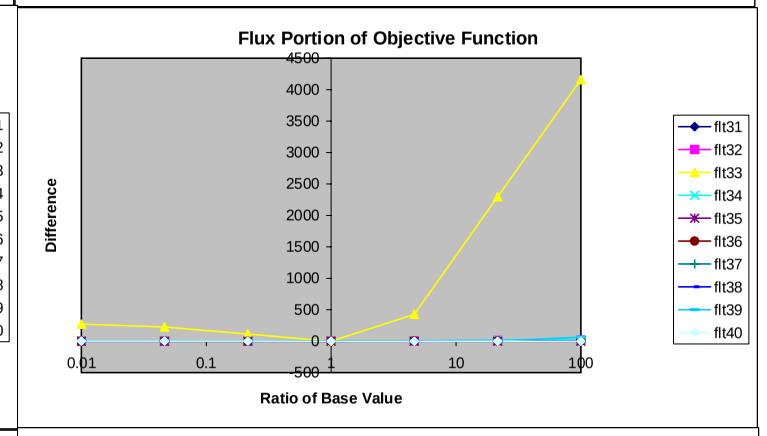
Flux Portion of Objective Function
Difference
Ratio of Base Value
flt31
flt32
flt33
flt34
flt35
flt36
flt37
flt38
flt39
flt40

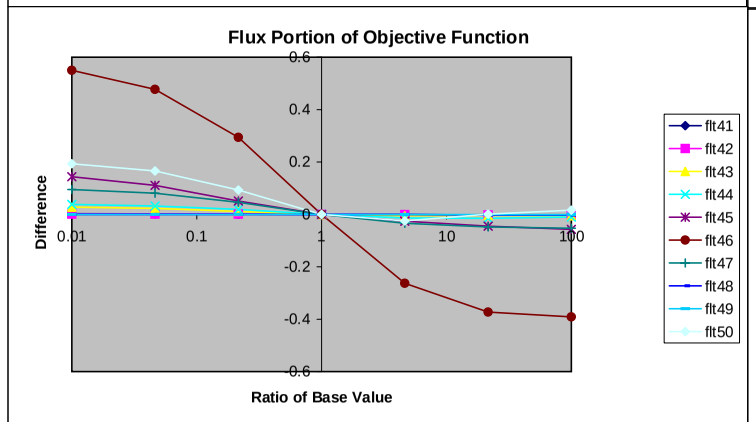
Flux Portion of Objective Function
Difference
Ratio of Base Value
flt41
flt42
flt43
flt44
flt45
flt46
flt47
flt48
flt49
flt50

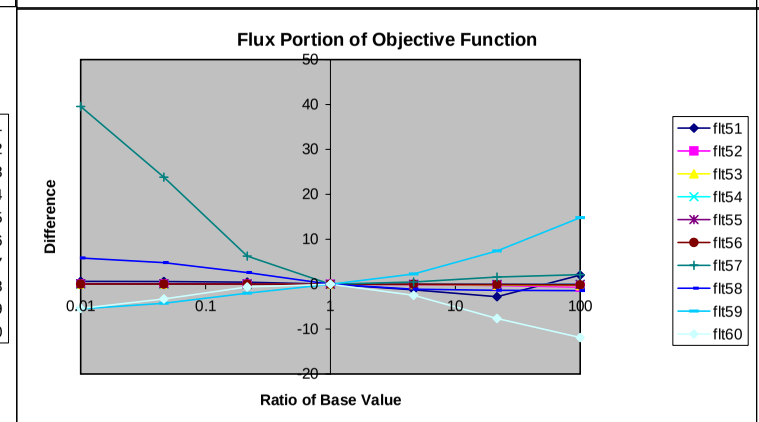
Flux Portion of Objective Function
Difference
Ratio of Base Value
flt51
flt52
flt53
flt54
flt55
flt56
flt57
flt58
flt59
flt60

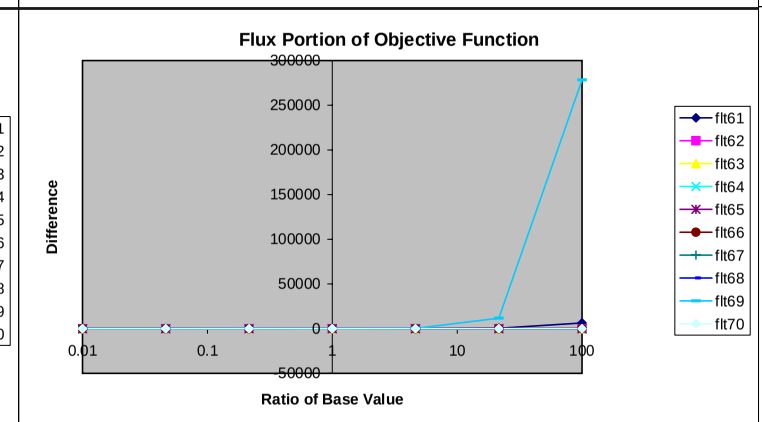
Flux Portion of Objective Function
Difference
Ratio of Base Value
flt61
flt62
flt63
flt64
flt65
flt66
flt67
flt68
flt69
flt70

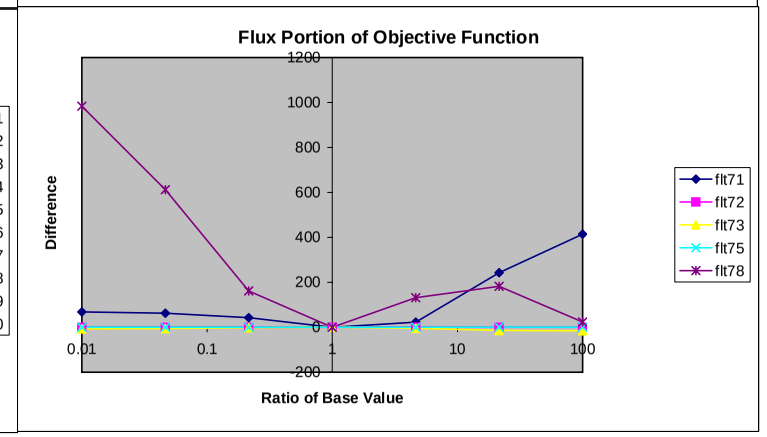
Flux Portion of Objective Function
Difference
Ratio of Base Value
flt71
flt72
flt73
flt75
flt78

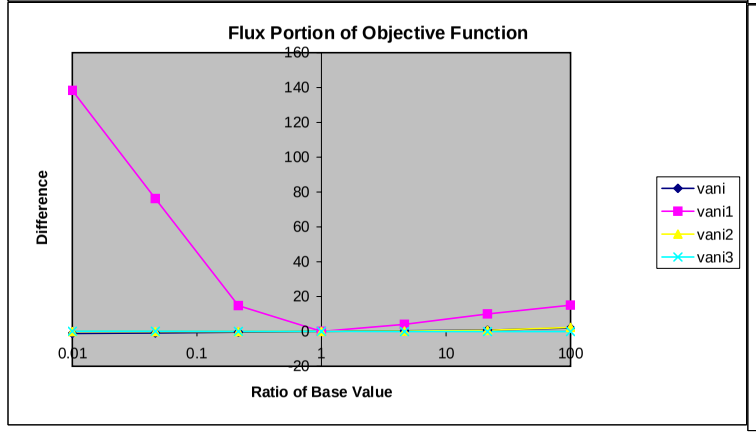
Flux Portion of Objective Function
Difference
Ratio of Base Value
vani
vani1
vani2
vani3

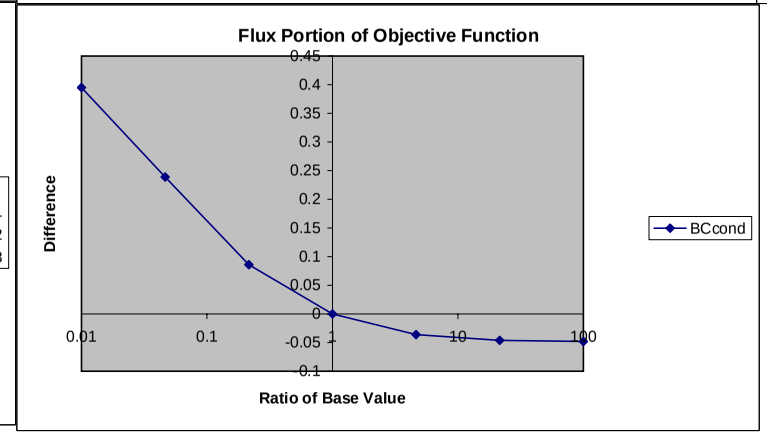
Flux Portion of Objective Function
Difference
Ratio of Base Value
BCcond

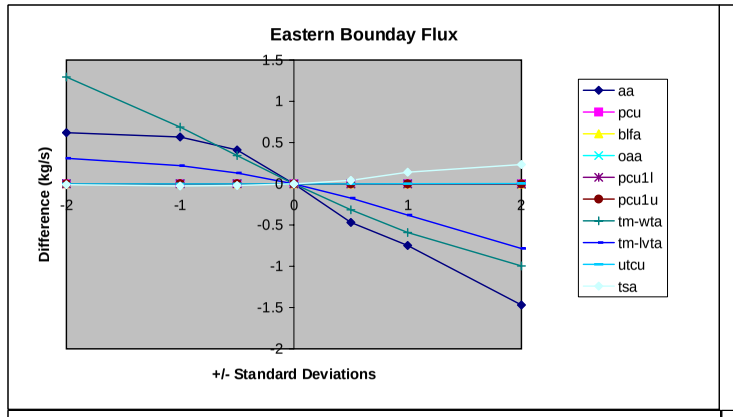
Eastern Bounday Flux
Difference (kg/s)
+/- Standard Deviations
aa
pcu
bfa
oaa
pcu1l
pcu1u
tm-wta
tm-lvta
utcu
tsa

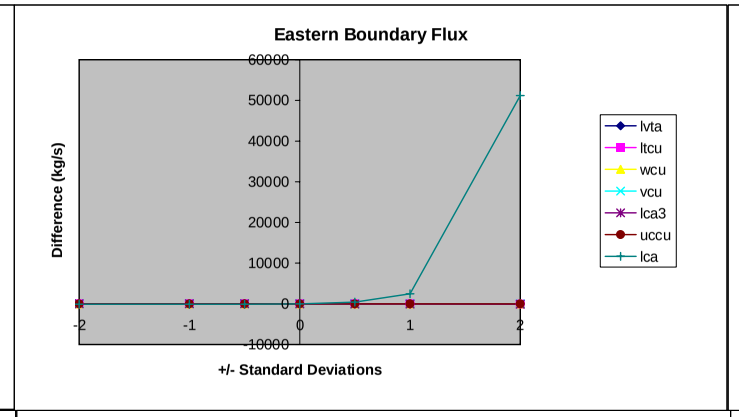
Eastern Boundary Flux
Difference (kg/s)
+/- Standard Deviations
lvta
ltcu
wcu
vcu
lca3
uccu
lca

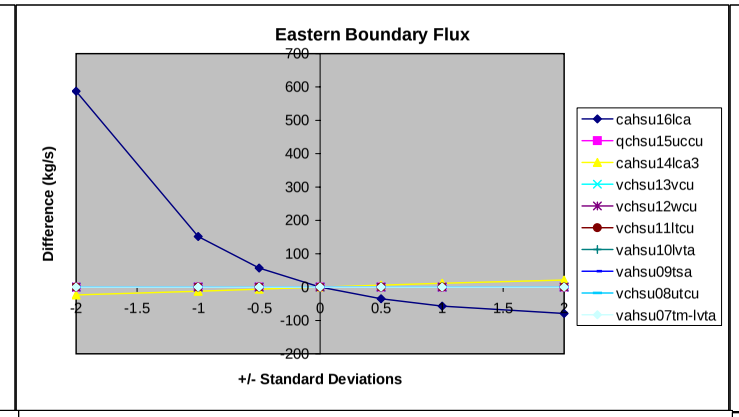
Eastern Boundary Flux
Difference (kg/s)
+/- Standard Deviations
cahsu16lca
qchsu15uccu
cahsu14lca3
vchsu13vcu
vchsu12wcu
vchsu11ltcu
vahsu10lvta
vahsu09tsa
vchsu08utcu
vahsu07tm-lvta

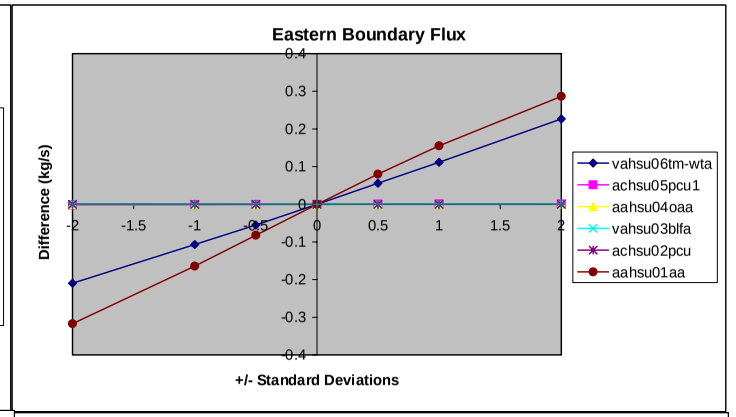
Eastern Boundary Flux
Difference (kg/s)
+/- Standard Deviations
vahsu06tm-wta
achsu05pcu1
aahsu04oaa
vahsu03blfa
achsu02pcu
aahsu01aa

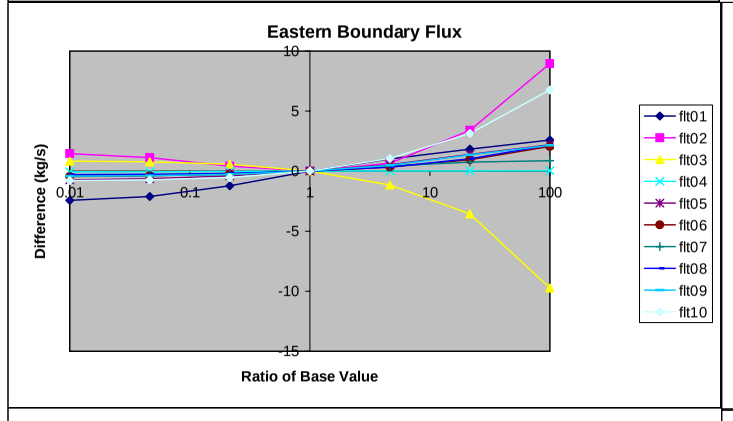
Eastern Boundary Flux
Difference (kg/s)
Ratio of Base Value
flt01
flt02
flt03
flt04
flt05
flt06
flt07
flt08
flt09
flt10

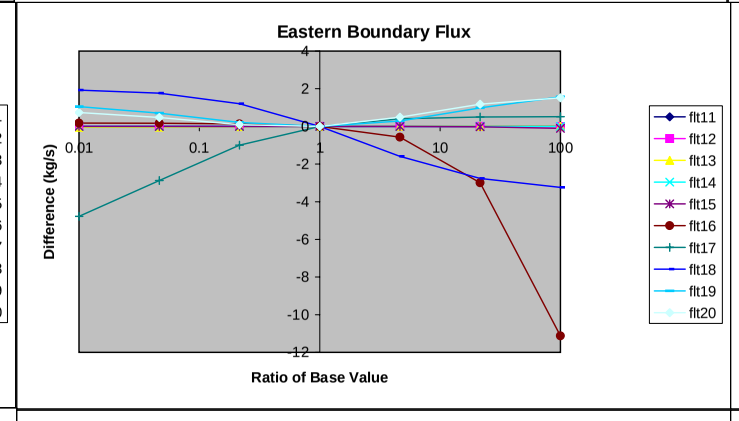
Eastern Boundary Flux
Difference (kg/s)
Ratio of Base Value
flt11
flt12
flt13
flt14
flt15
flt16
flt17
flt18
flt19
flt20

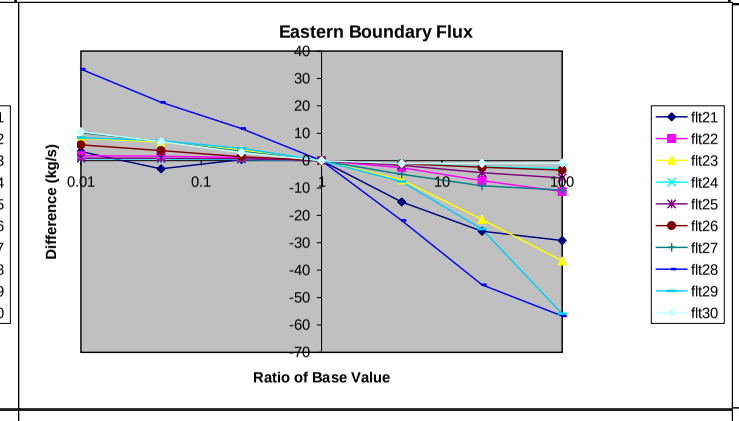
Eastern Boundary Flux
Difference (kg/s)
Ratio of Base Value
flt21
flt22
flt23
flt24
flt25
flt26
flt27
flt28
flt29
flt30

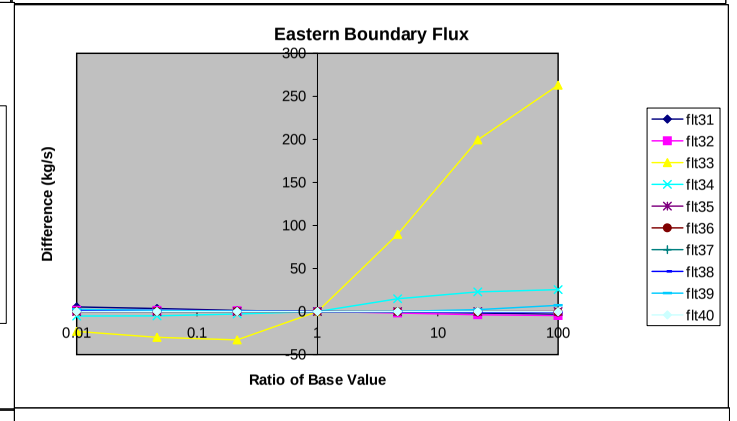
Eastern Boundary Flux
Difference (kg/s)
Ratio of Base Value
flt31
flt32
flt33
flt34
flt35
flt36
flt37
flt38
flt39
flt40

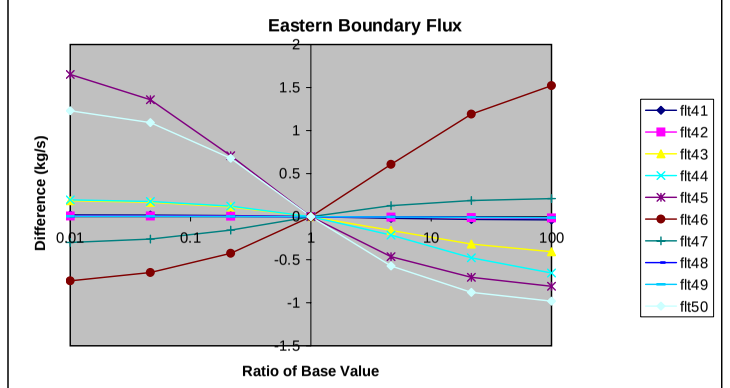
Eastern Boundary Flux
Difference (kg/s)
Ratio of Base Value
flt41
flt42
flt43
flt44
flt45
flt46
flt47
flt48
flt49
flt50

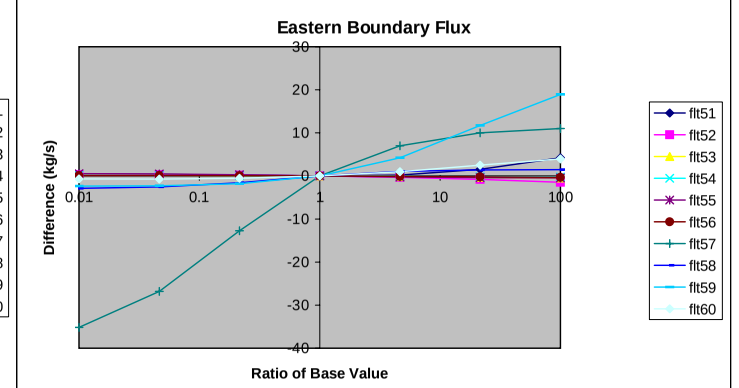
Eastern Boundary Flux
Difference (kg/s)
Ratio of Base Value
flt51
flt52
flt53
flt54
flt55
flt56
flt57
flt58
flt59
flt60

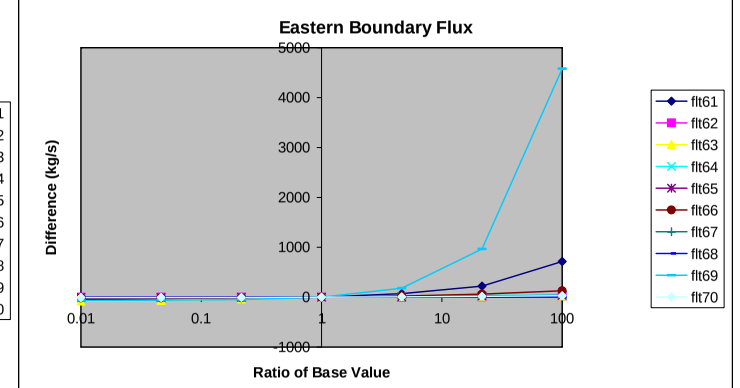
Eastern Boundary Flux
Difference (kg/s)
Ratio of Base Value
flt61
flt62
flt63
flt64
flt65
flt66
flt67
flt68
flt69
flt70

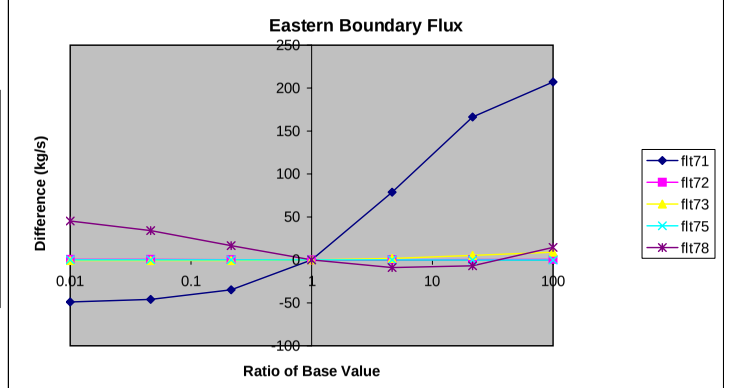
Eastern Boundary Flux
Difference (kg/s)
Ratio of Base Value
flt71
flt72
flt73
flt75
flt78

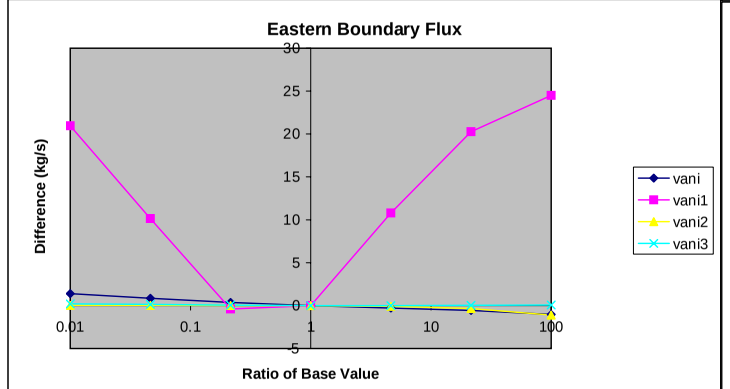
Eastern Boundary Flux
Difference (kg/s)
Ratio of Base Value
vani
vani1
vani2
vani3

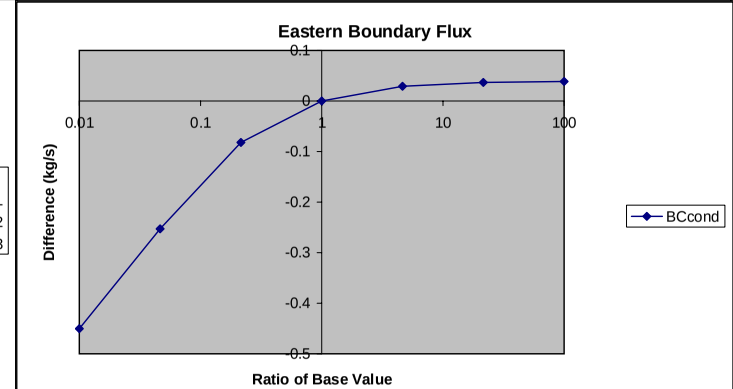
Eastern Boundary Flux
Difference (kg/s)
Ratio of Base Value
BCcond

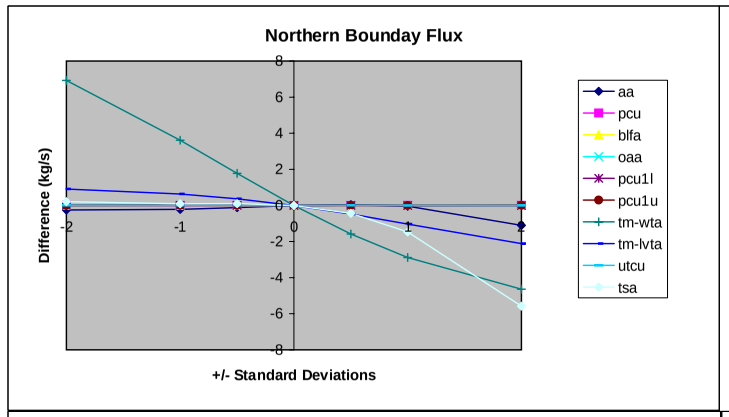
Northern Bounday Flux
Difference (kg/s)
+/- Standard Deviations
aa
pcu
blfa
oaa
pcu1l
pcu1u
tm-wta
tm-lvta
utcu
tsa

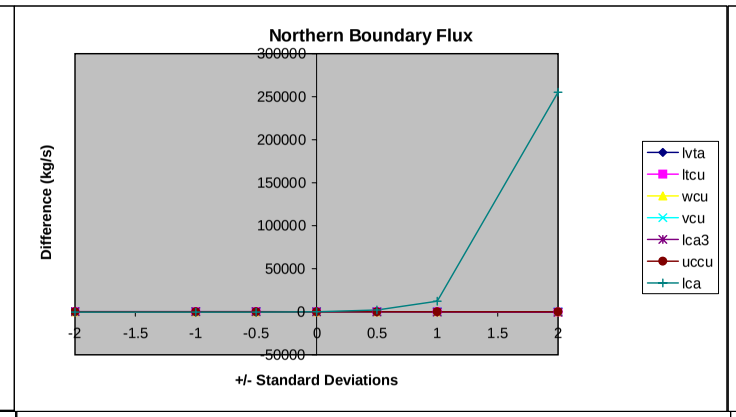
Northern Boundary Flux
Difference (kg/s)
+/- Standard Deviations
lvta
ltcu
wcu
vcu
lca3
uccu
lca

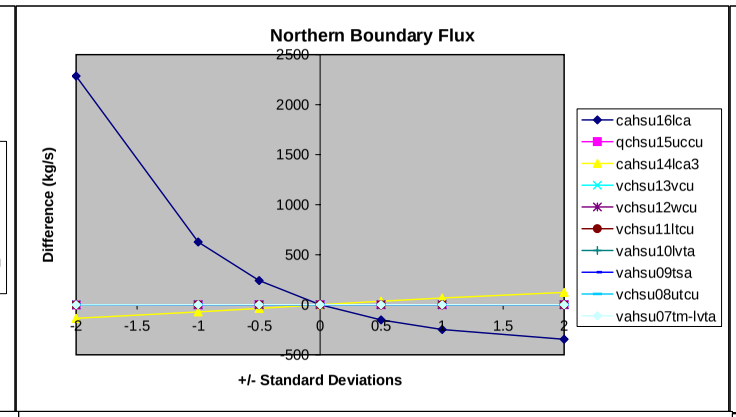
Northern Boundary Flux
Difference (kg/s)
+/- Standard Deviations
cahsu16lca
qchsu15uccu
cahsu14lca3
vchsu13vcu
vchsu12wcu
vchsu11ltcu
vahsu10lvta
vahsu09tsa
vchsu08utcu
vahsu07tm-lvta

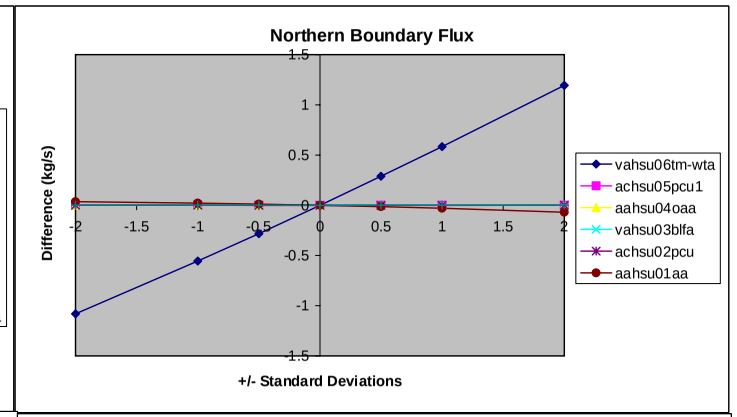
Northern Boundary Flux
Difference (kg/s)
+/- Standard Deviations
vahsu06tm-wta
achsu05pcu1
aahsu04oaa
vahsu03blfa
achsu02pcu
aahsu01aa

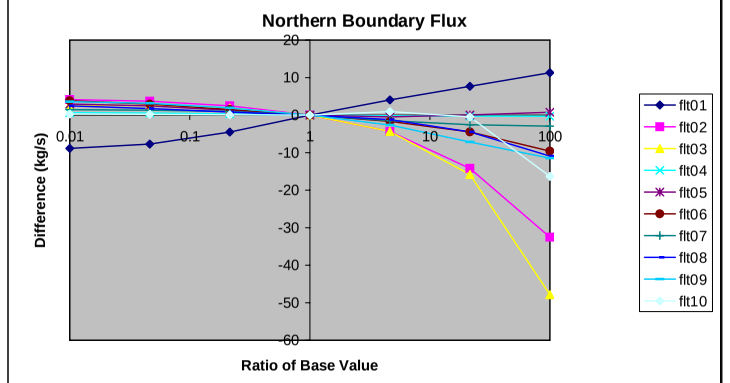
Northern Boundary Flux
Difference (kg/s)
Ratio of Base Value
flt01
flt02
flt03
flt04
flt05
flt06
flt07
flt08
flt09
flt10

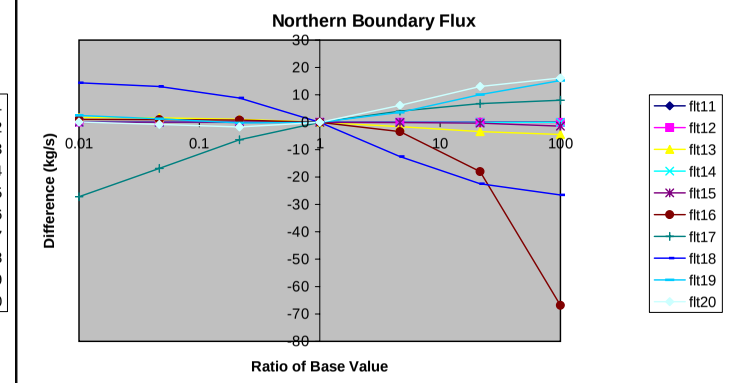
Northern Boundary Flux
Difference (kg/s)
Ratio of Base Value
flt11
flt12
flt13
flt14
flt15
flt16
flt17
flt18
flt19
flt20

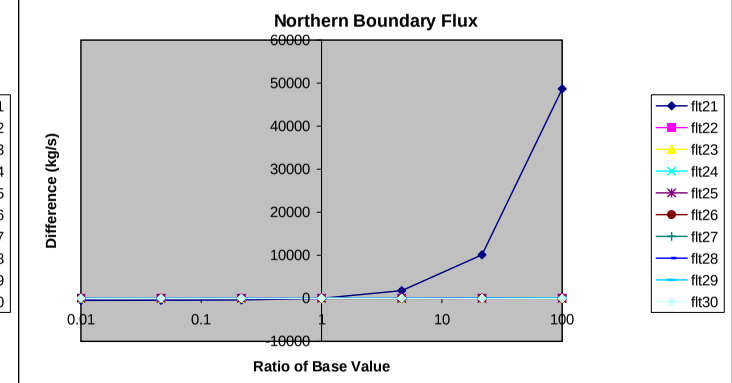
Northern Boundary Flux
Difference (kg/s)
Ratio of Base Value
flt21
flt22
flt23
flt24
flt25
flt26
flt27
flt28
flt29
flt30

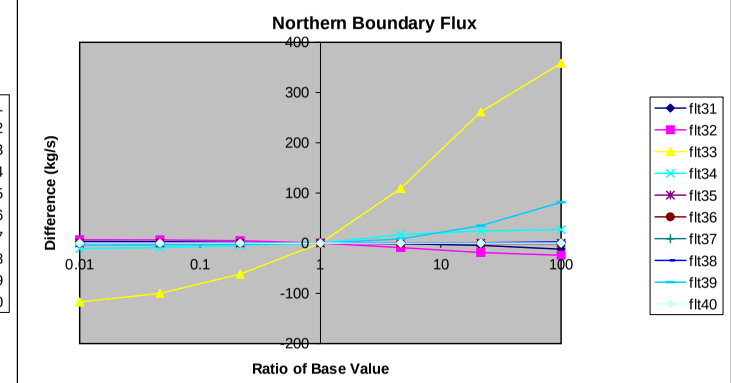
Northern Boundary Flux
Difference (kg/s)
Ratio of Base Value
flt31
flt32
flt33
flt34
flt35
flt36
flt37
flt38
flt39
flt40

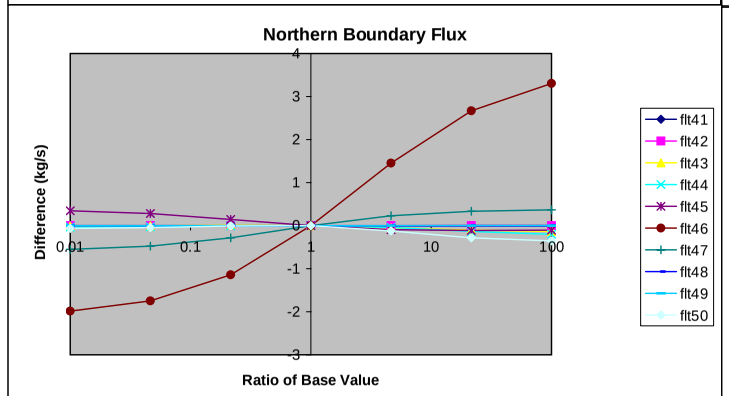
Northern Boundary Flux
Difference (kg/s)
Ratio of Base Value
flt41
flt42
flt43
flt44
flt45
flt46
flt47
flt48
flt49
flt50

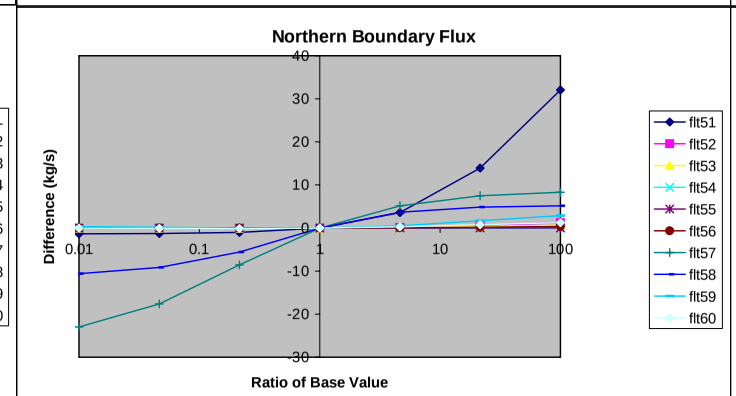
Northern Boundary Flux
Difference (kg/s)
Ratio of Base Value
flt51
flt52
flt53
flt54
flt55
flt56
flt57
flt58
flt59
flt60

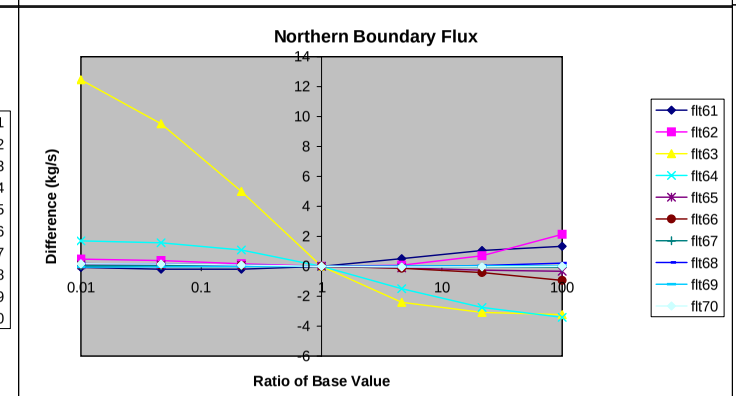
Northern Boundary Flux
Difference (kg/s)
Ratio of Base Value
flt61
flt62
flt63
flt64
flt65
flt66
flt67
flt68
flt69
flt70

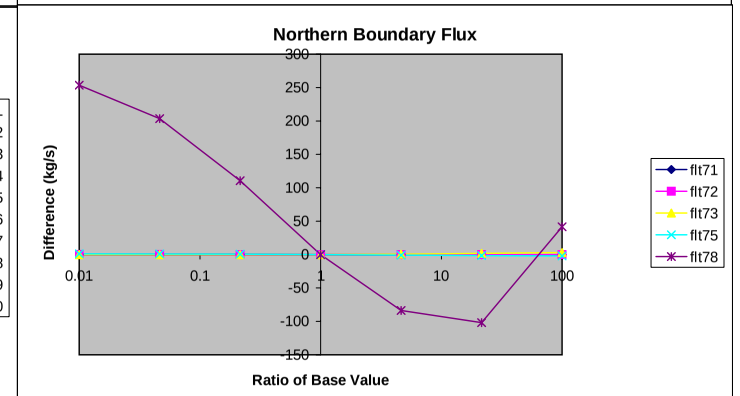
Northern Boundary Flux
Difference (kg/s)
Ratio of Base Value
flt71
flt72
flt73
flt75
flt78

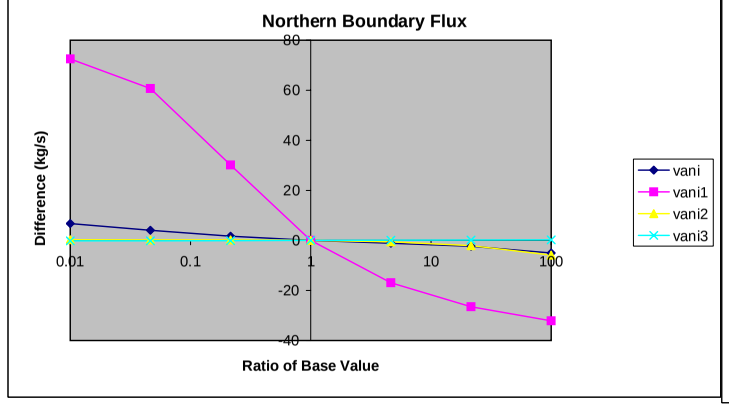
Northern Boundary Flux
Difference (kg/s)
Ratio of Base Value
vani
vani1
vani2
vani3

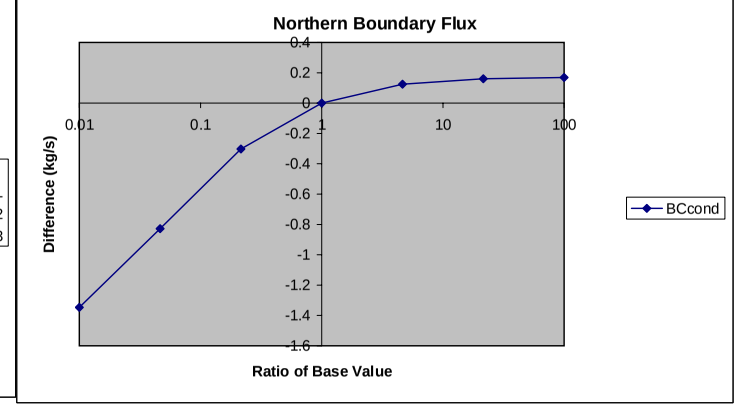
Northern Boundary Flux
Difference (kg/s)
Ratio of Base Value
BCcond

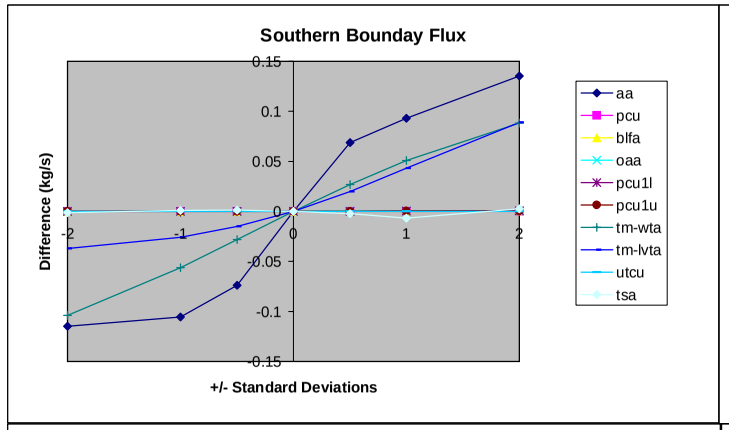
Southern Bounday Flux
Difference (kg/s)
+/- Standard Deviations
aa
pcu
blfa
oaa
pcu1l
pcu1u
tm-wta
tm-lvta
utcu
tsa

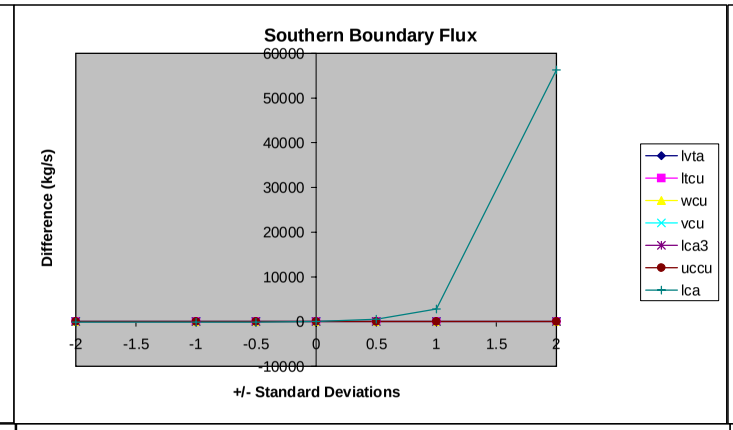
Southern Boundary Flux
Difference (kg/s)
+/- Standard Deviations
lvta
ltcu
wcu
vcu
lca3
uccu
lca

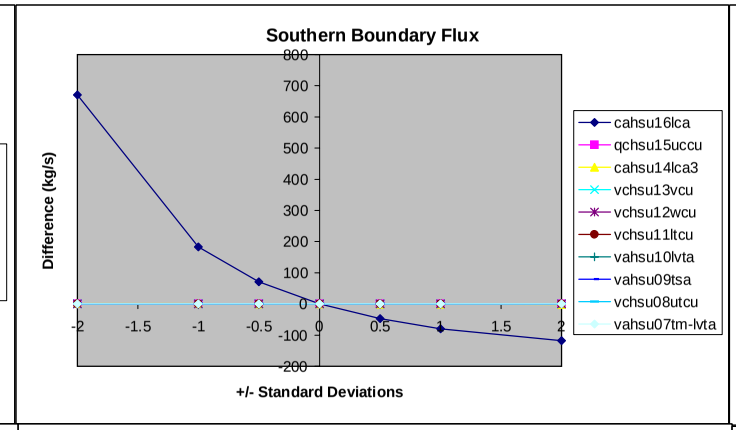
Southern Boundary Flux
Difference (kg/s)
+/- Standard Deviations
cahsu16lca
qchsu15uccu
cahsu14lca3
vchsu13vcu
vchsu12wcu
vchsu11ltcu
vahsu10lvta
vahsu09tsa
vchsu08utcu
vahsu07tm-lvta

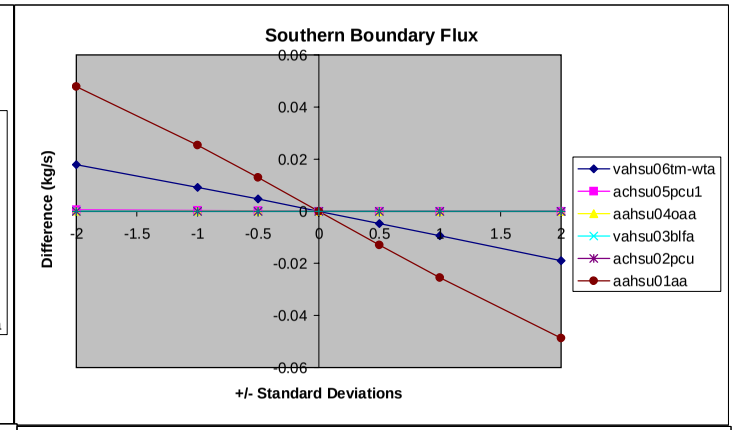
Southern Boundary Flux
Difference (kg/s)
+/- Standard Deviations
vahsu06tm-wta
achsu05pcu1
aahsu04oaa
vahsu03blfa
achsu02pcu
aahsu01aa

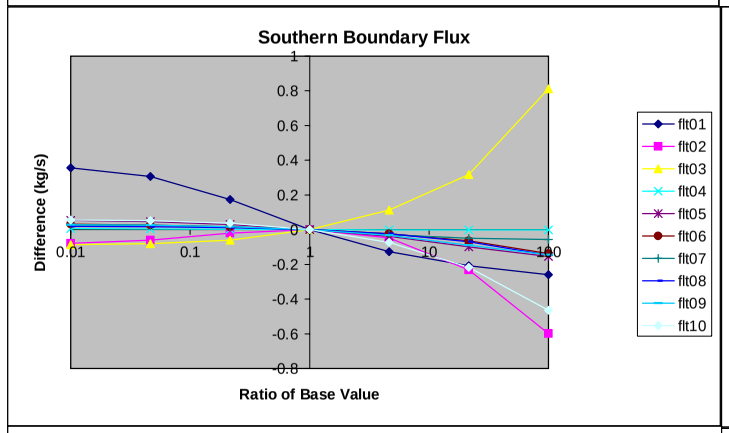
Southern Boundary Flux
Difference (kg/s)
Ratio of Base Value
flt01
flt02
flt03
flt04
flt05
flt06
flt07
flt08
flt09
flt10

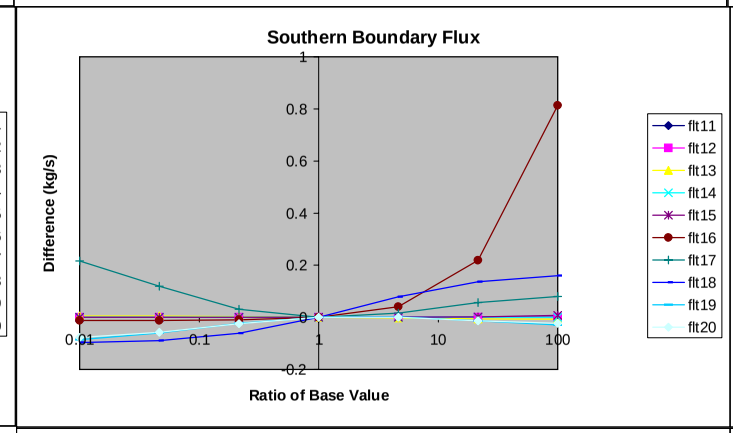
Southern Boundary Flux
Difference (kg/s)
Ratio of Base Value
flt11
flt12
flt13
flt14
flt15
flt16
flt17
flt18
flt19
flt20

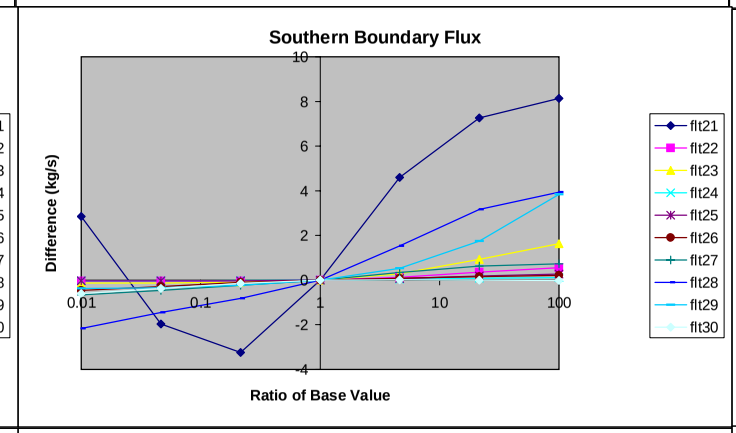
Southern Boundary Flux
Difference (kg/s)
Ratio of Base Value
flt21
flt22
flt23
flt24
flt25
flt26
flt27
flt28
flt29
flt30

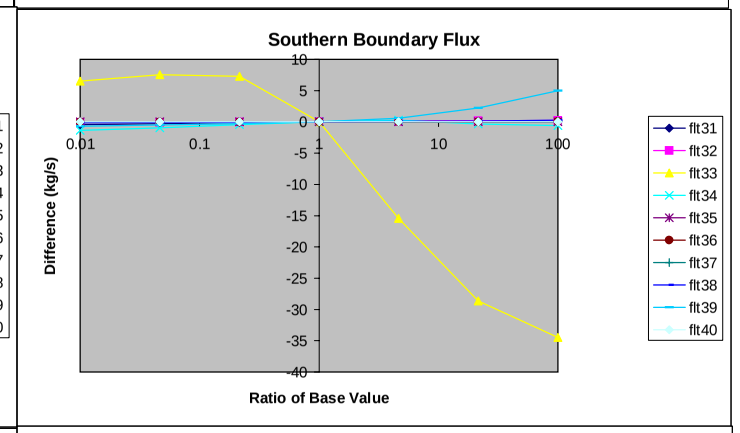
Southern Boundary Flux
Difference (kg/s)
Ratio of Base Value
flt31
flt32
flt33
flt34
flt35
flt36
flt37
flt38
flt39
flt40

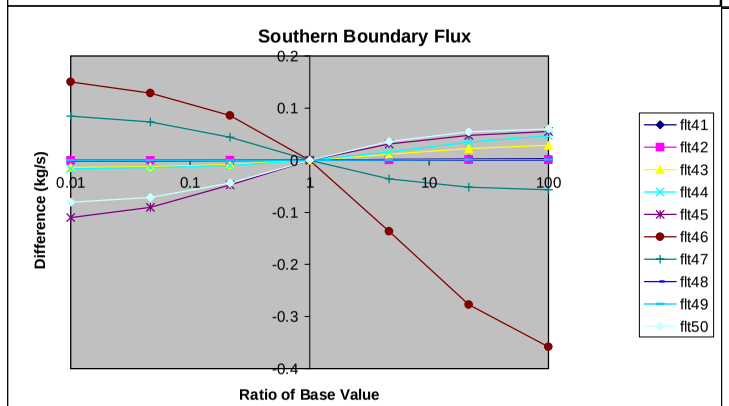
Southern Boundary Flux
Difference (kg/s)
Ratio of Base Value
flt41
flt42
flt43
flt44
flt45
flt46
flt47
flt48
flt49
flt50

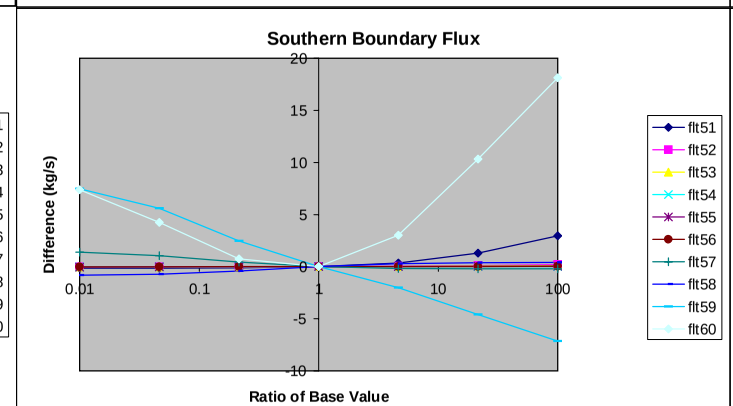
Southern Boundary Flux
Difference (kg/s)
Ratio of Base Value
flt51
flt52
flt53
flt54
flt55
flt56
flt57
flt58
flt59
flt60

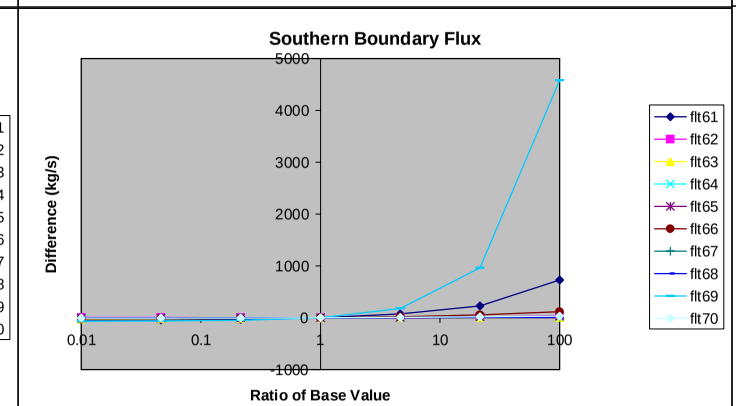
Southern Boundary Flux
Difference (kg/s)
Ratio of Base Value
flt61
flt62
flt63
flt64
flt65
flt66
flt67
flt68
flt69
flt70

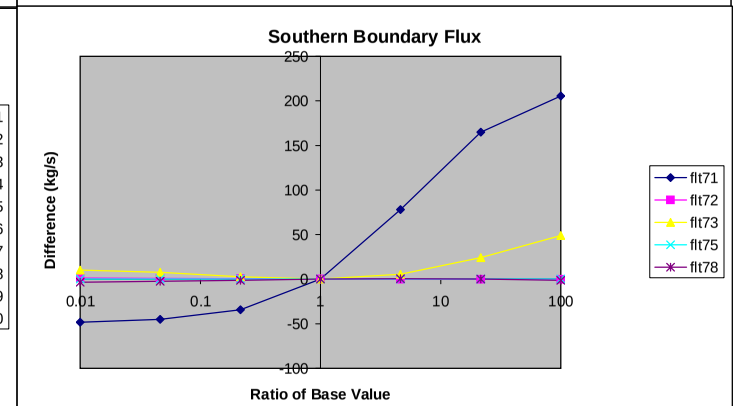
Southern Boundary Flux
Difference (kg/s)
Ratio of Base Value
flt71
flt72
flt73
flt75
flt78

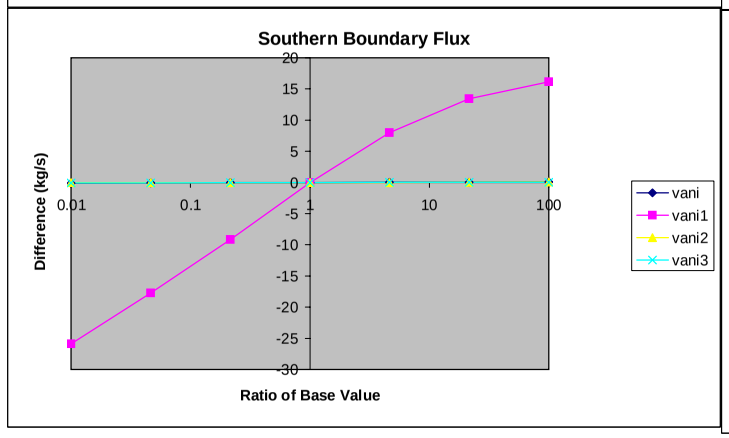
Southern Boundary Flux
Difference (kg/s)
Ratio of Base Value
vani
vani1
vani2
vani3

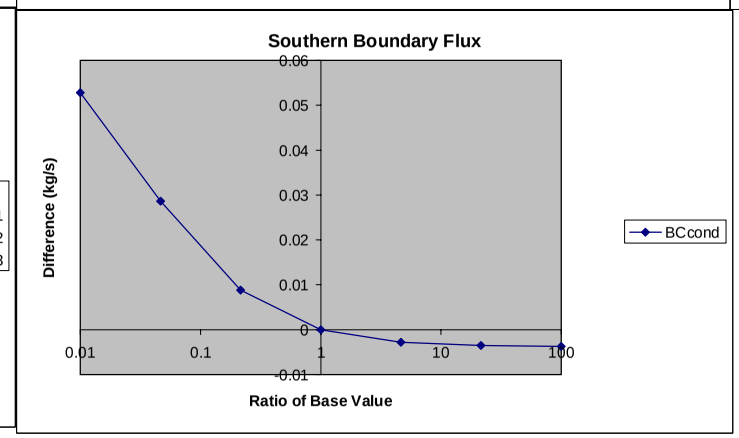
Southern Boundary Flux
Difference (kg/s)
Ratio of Base Value
BCcond

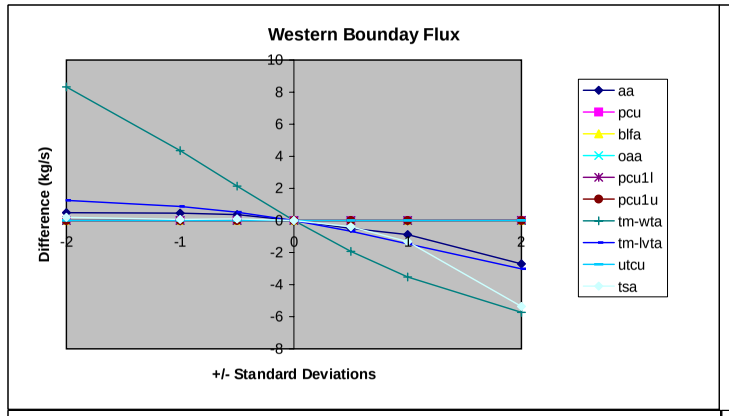
Western Bounday Flux
Difference (kg/s)
+/- Standard Deviations
aa
pcu
bfa
oaa
pcu1l
pcu1u
tm-wta
tm-lvta
utcu
tsa

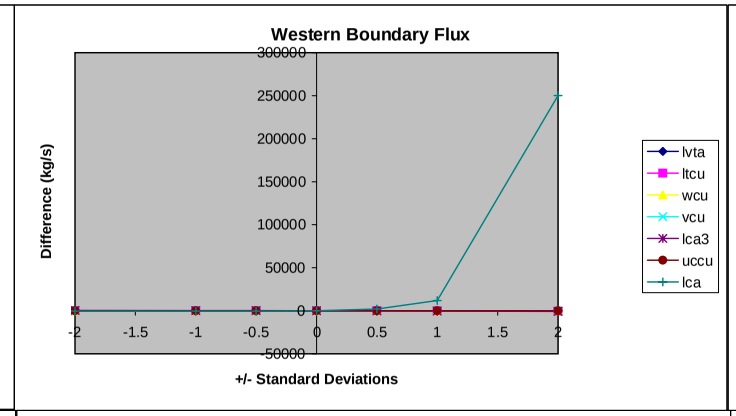
Western Boundary Flux
Difference (kg/s)
+/- Standard Deviations
lvta
ltcu
wcu
vcu
lca3
uccu
lca

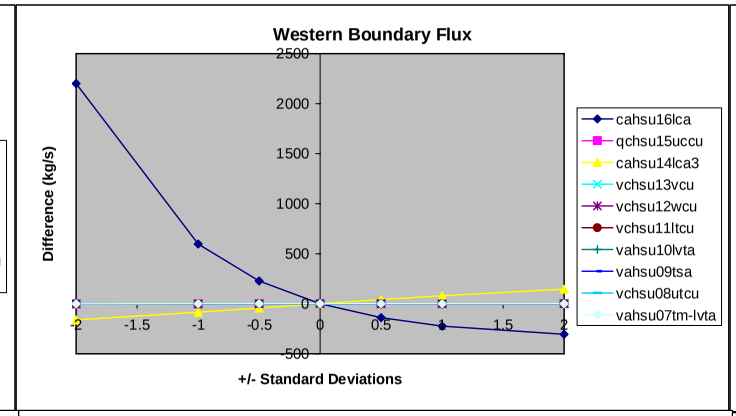
Western Boundary Flux
Difference (kg/s)
+/- Standard Deviations
cahsu16lca
qchsu15uccu
cahsu14lca3
vchsu13vcu
vchsu12wcu
vchsu11ltcu
vahsu10lvta
vahsu09tsa
vchsu08utcu
vahsu07tm-lvta

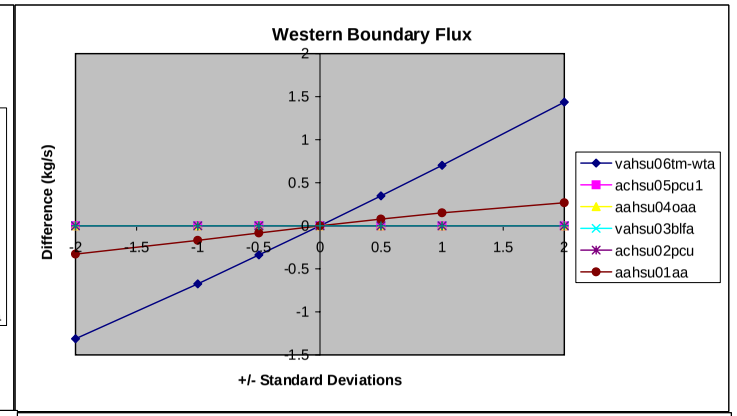
Western Boundary Flux
Difference (kg/s)
+/- Standard Deviations
vahsu06tm-wta
achsu05pcu1
aahsu04oaa
vahsu03blfa
achsu02pcu
aahsu01aa

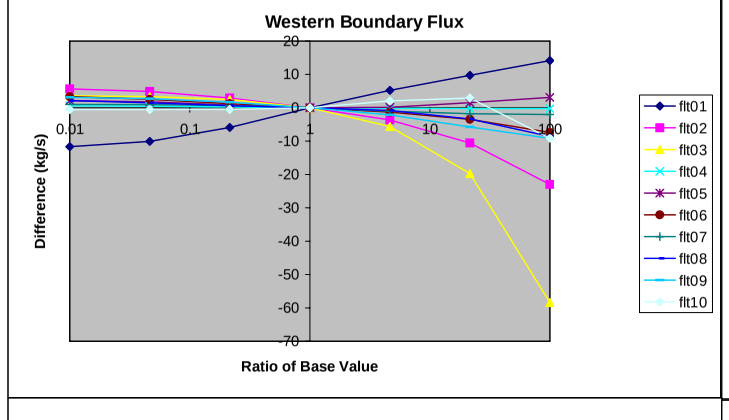
Western Boundary Flux
Difference (kg/s)
Ratio of Base Value
flt01
flt02
flt03
flt04
flt05
flt06
flt07
flt08
flt09
flt10

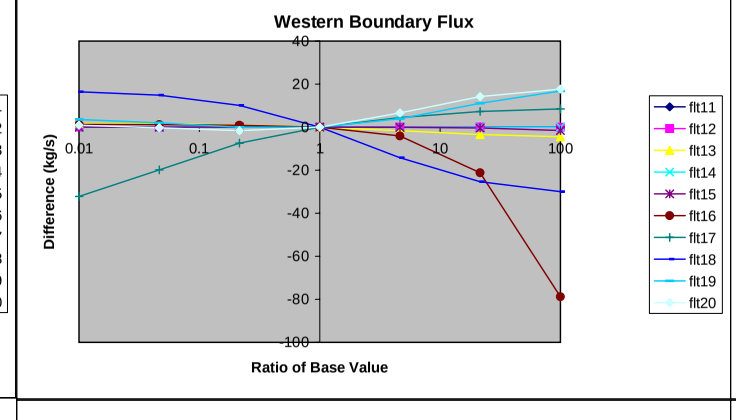
Western Boundary Flux
Difference (kg/s)
Ratio of Base Value
flt11
flt12
flt13
flt14
flt15
flt16
flt17
flt18
flt19
flt20

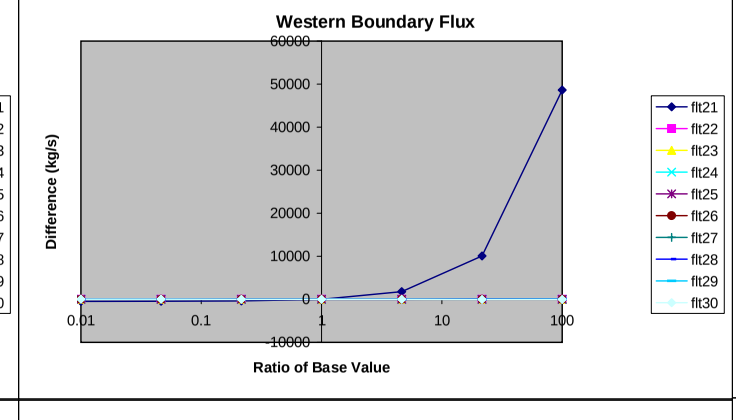
Western Boundary Flux
Difference (kg/s)
Ratio of Base Value
flt21
flt22
flt23
flt24
flt25
flt26
flt27
flt28
flt29
flt30

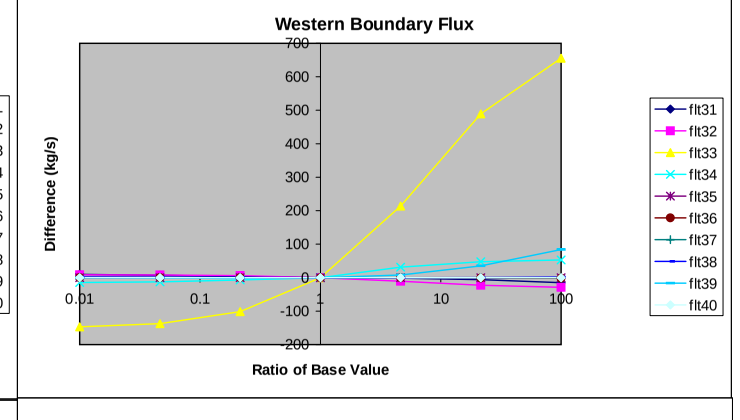
Western Boundary Flux
Difference (kg/s)
Ratio of Base Value
flt31
flt32
flt33
flt34
flt35
flt36
flt37
flt38
flt39
flt40

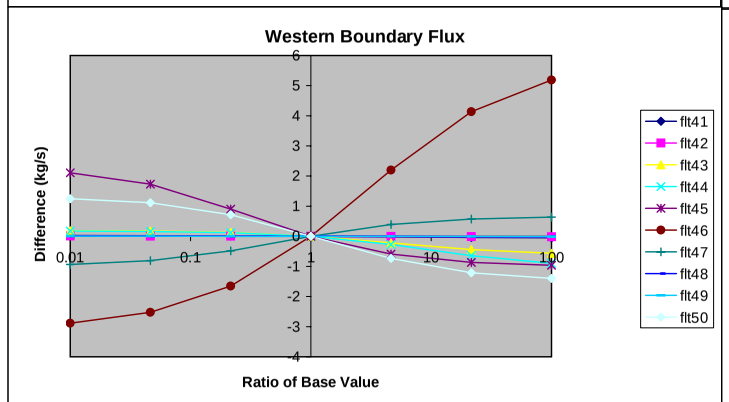
Western Boundary Flux
Difference (kg/s)
Ratio of Base Value
flt41
flt42
flt43
flt44
flt45
flt46
flt47
flt48
flt49
flt50

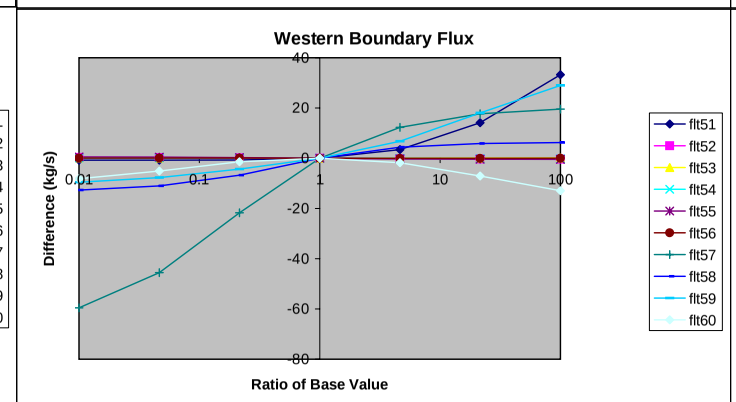
Western Boundary Flux
Difference (kg/s)
Ratio of Base Value
flt51
flt52
flt53
flt54
flt55
flt56
flt57
flt58
flt59
flt60

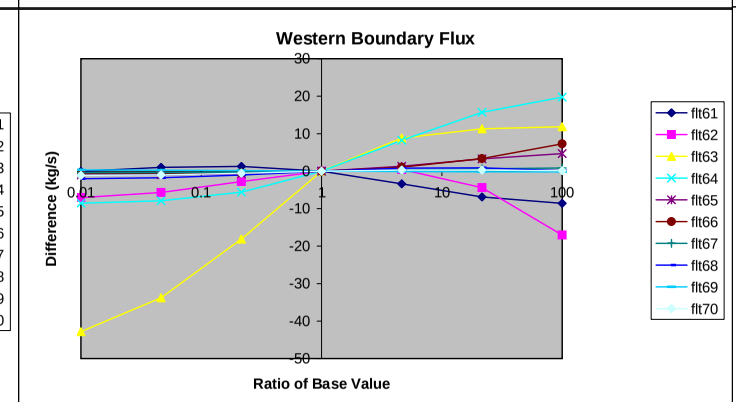
Western Boundary Flux
Difference (kg/s)
Ratio of Base Value
flt61
flt62
flt63
flt64
flt65
flt66
flt67
flt68
flt69
flt70

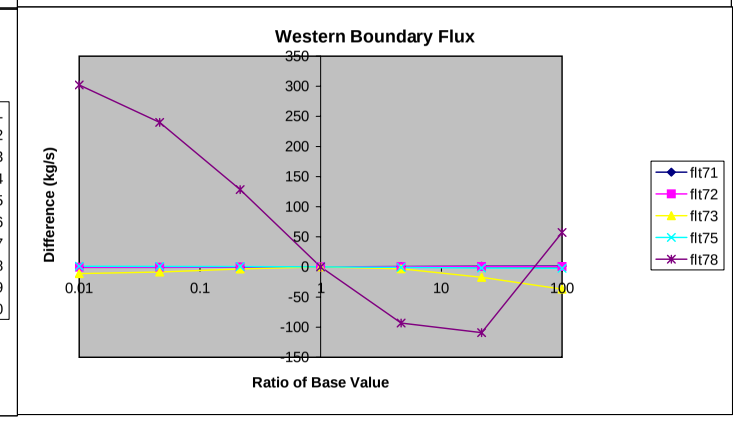
Western Boundary Flux
Difference (kg/s)
Ratio of Base Value
flt71
flt72
flt73
flt75
flt78

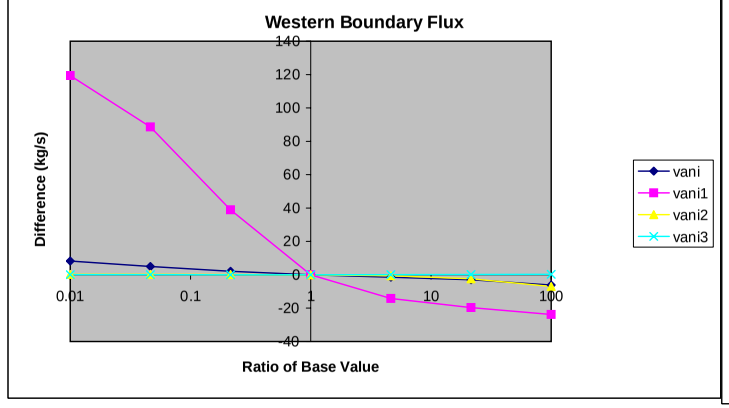
Western Boundary Flux
Difference (kg/s)
Ratio of Base Value
vani
vani1
vani2
vani3

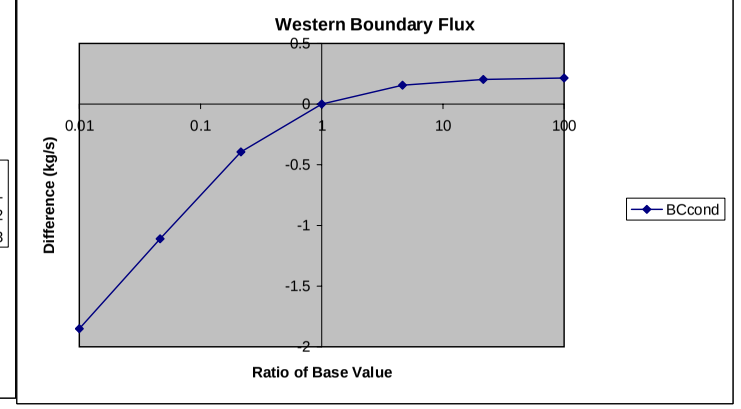
Western Boundary Flux
Difference (kg/s)
Ratio of Base Value
BCcond

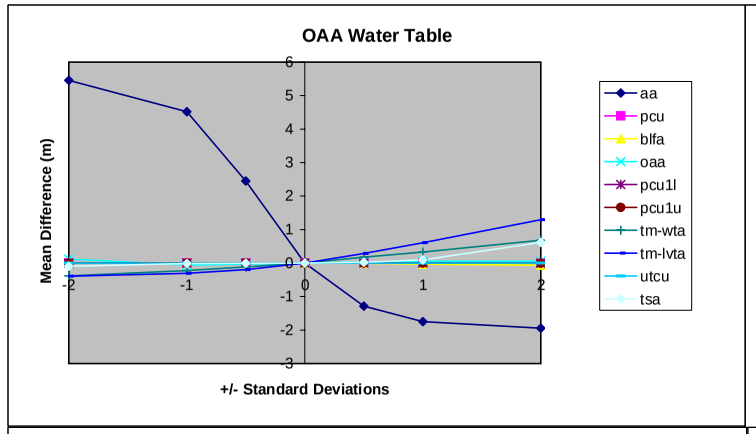
OAA Water Table
Mean Difference (m)
+/- Standard Deviations
aa
pcu
blfa
oaa
pcu1l
pcu1u
tm-wta
tm-lvta
utcu
tsa

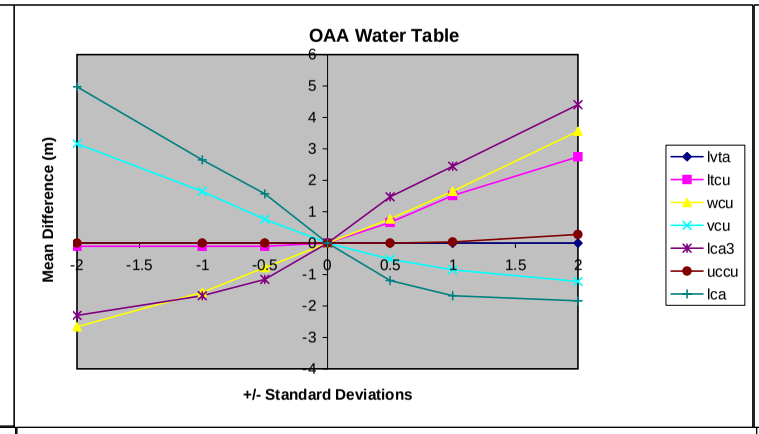
OAA Water Table
Mean Difference (m)
+/- Standard Deviations
lvta
ltcu
wcu
vcu
lca3
uccu
lca

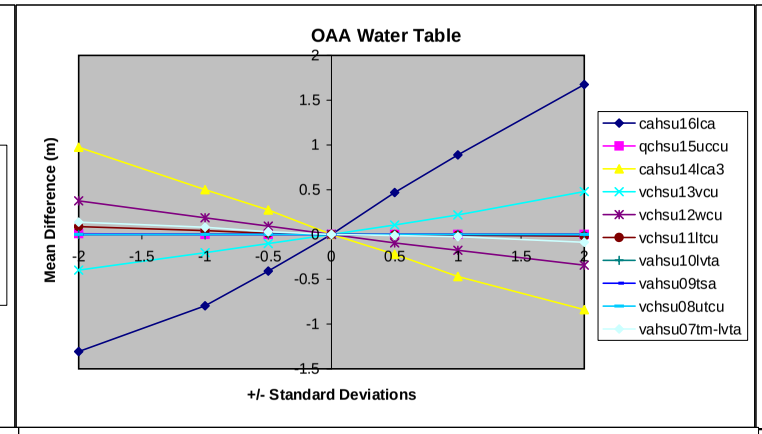
OAA Water Table
Mean Difference (m)
+/- Standard Deviations
cahsu16lca
qchsu15uccu
cahsu14lca3
vchsu13vcu
vchsu12wcu
vchsu11ltcu
vahsu10lvta
vahsu09tsa
vchsu08utcu
vahsu07tm-lvta

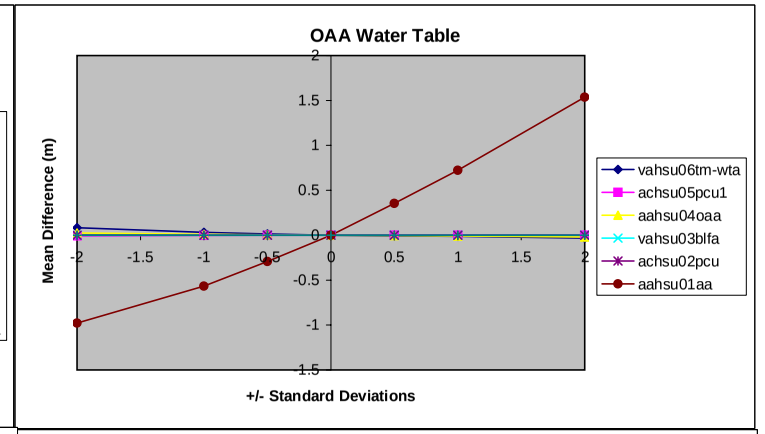
OAA Water Table
Mean Difference (m)
+/- Standard Deviations
vahsu06tm-wta
achsu05pcu1
aahsu04oaa
vahsu03blfa
achsu02pcu
aahsu01aa

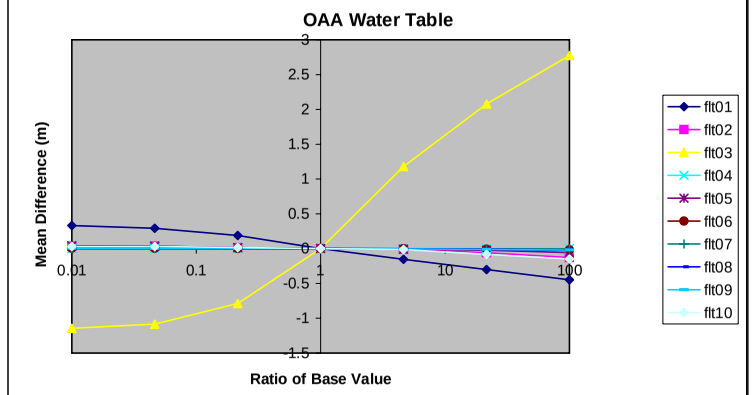
OAA Water Table
Mean Difference (m)
Ratio of Base Value
flt01
flt02
flt03
flt04
flt05
flt06
flt07
flt08
flt09
flt10

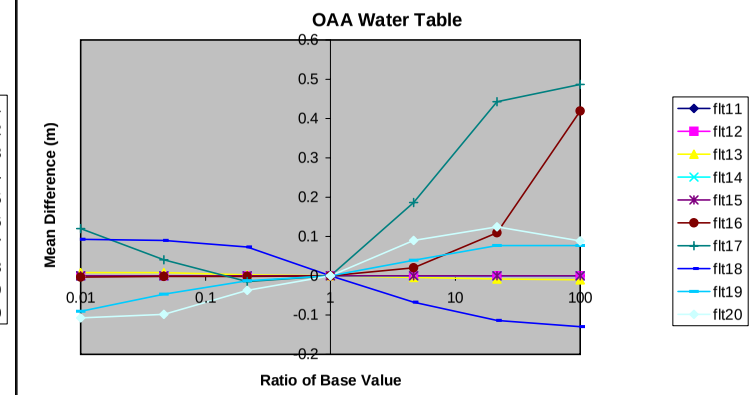
OAA Water Table
Mean Difference (m)
Ratio of Base Value
flt11
flt12
flt13
flt14
flt15
flt16
flt17
flt18
flt19
flt20

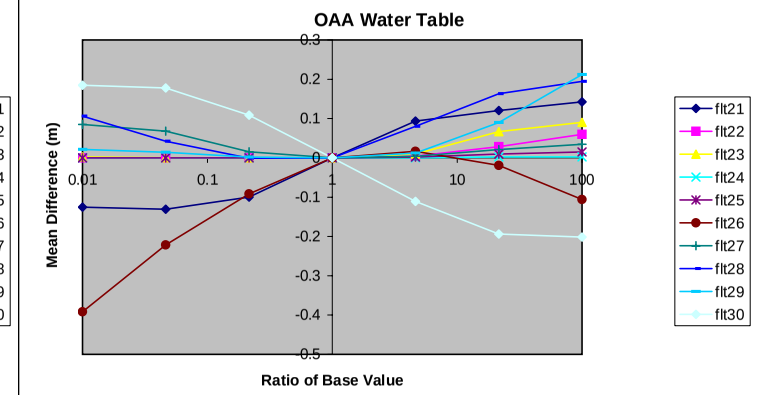
OAA Water Table
Mean Difference (m)
Ratio of Base Value
flt21
flt22
flt23
flt24
flt25
flt26
flt27
flt28
flt29
flt30

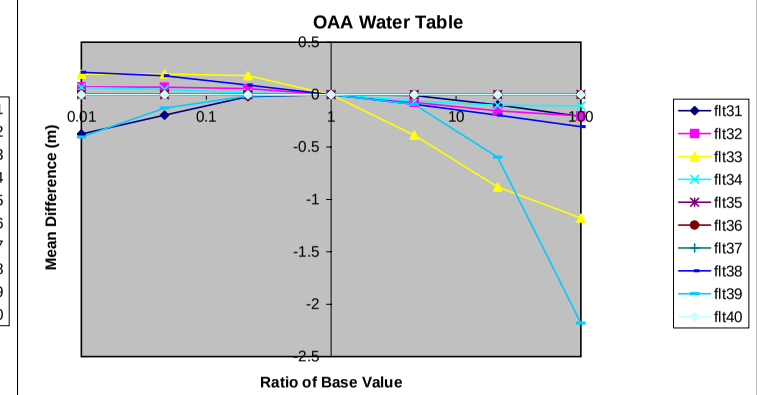
OAA Water Table
Mean Difference (m)
Ratio of Base Value
flt31
flt32
flt33
flt34
flt35
flt36
flt37
flt38
flt39
flt40

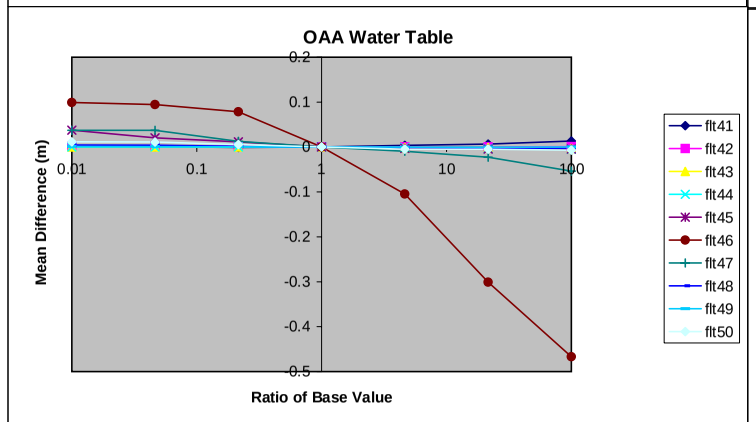
OAA Water Table
Mean Difference (m)
Ratio of Base Value
flt41
flt42
flt43
flt44
flt45
flt46
flt47
flt48
flt49
flt50

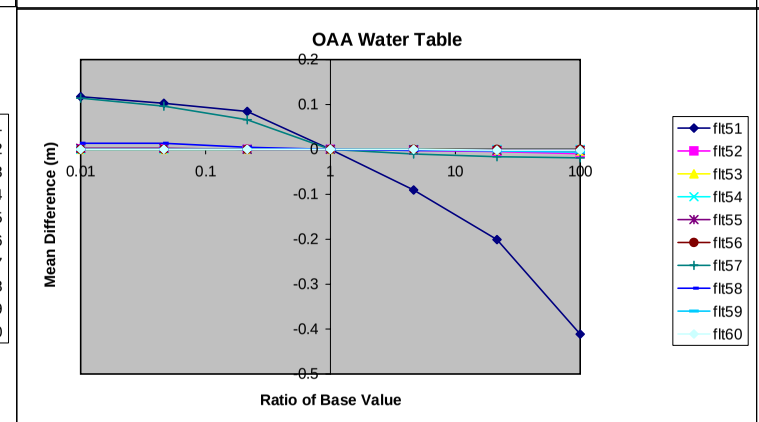
OAA Water Table
Mean Difference (m)
Ratio of Base Value
flt51
flt52
flt53
flt54
flt55
flt56
flt57
flt58
flt59
flt60

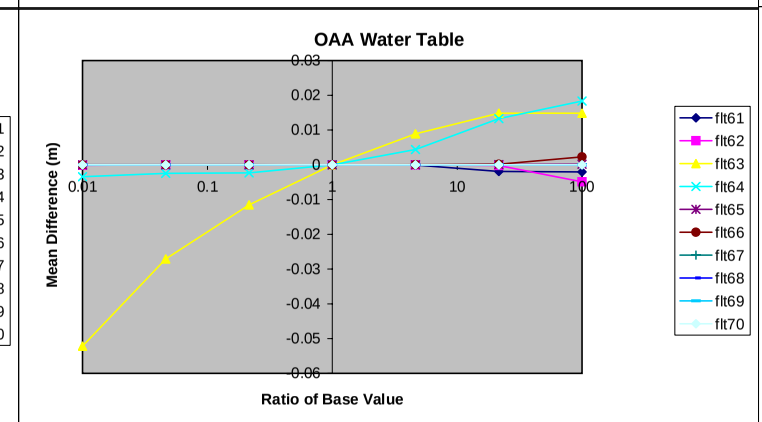
OAA Water Table
Mean Difference (m)
Ratio of Base Value
flt61
flt62
flt63
flt64
flt65
flt66
flt67
flt68
flt69
flt70

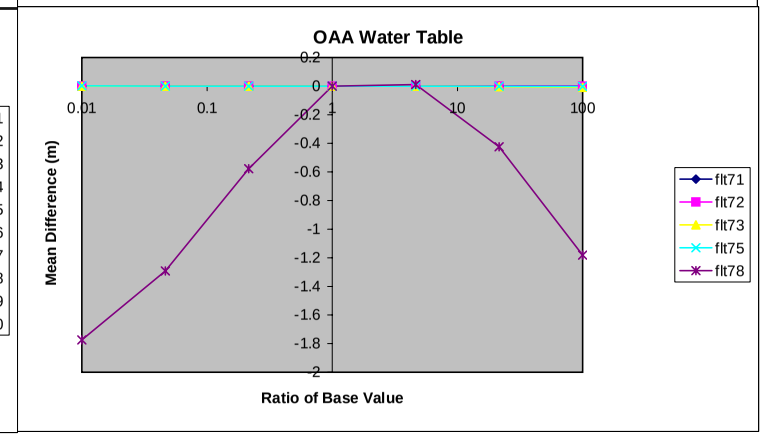
OAA Water Table
Mean Difference (m)
Ratio of Base Value
flt71
flt72
flt73
flt75
flt78

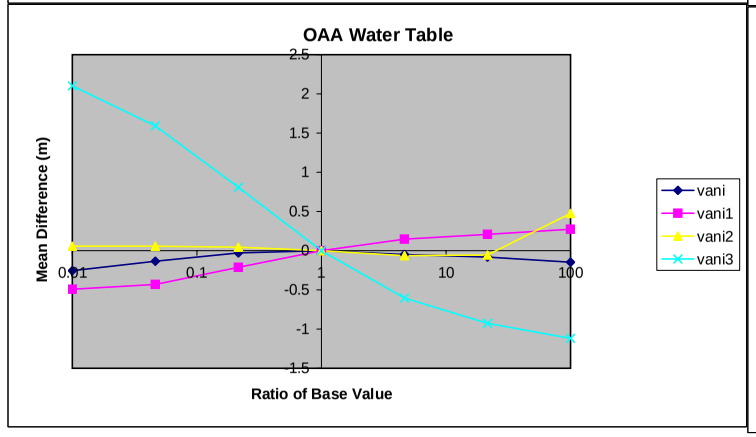
OAA Water Table
Mean Difference (m)
Ratio of Base Value
vani
vani1
vani2
vani3

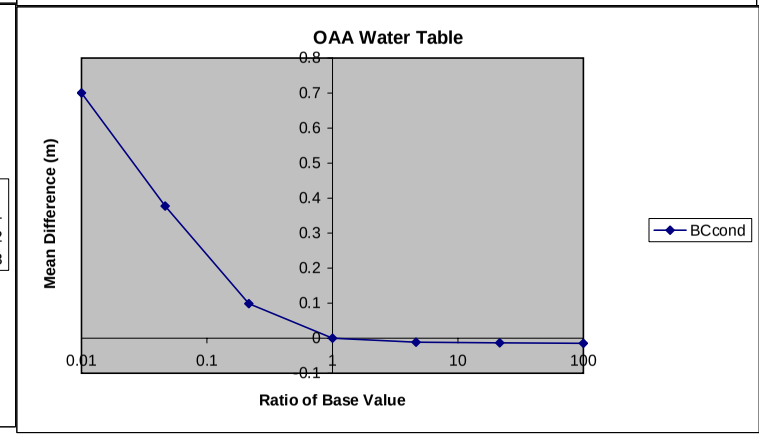
OAA Water Table
Mean Difference (m)
Ratio of Base Value
BCcond

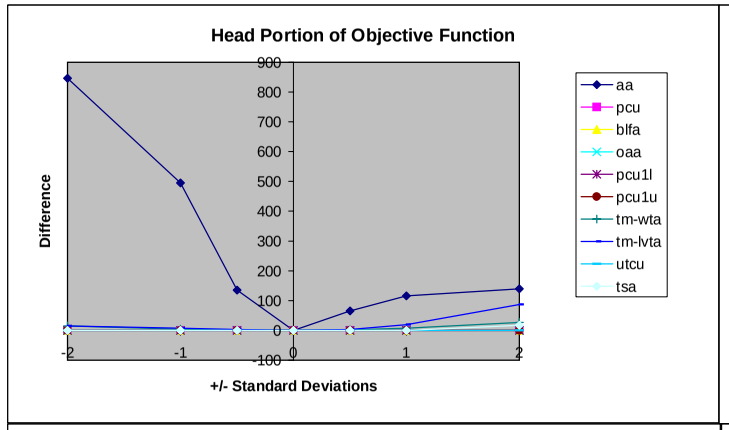
Head Portion of Objective Function
Difference
+/- Standard Deviations
aa
pcu
blfa
oaa
pcu1l
pcu1u
tm-wta
tm-lvta
utcu
tsa

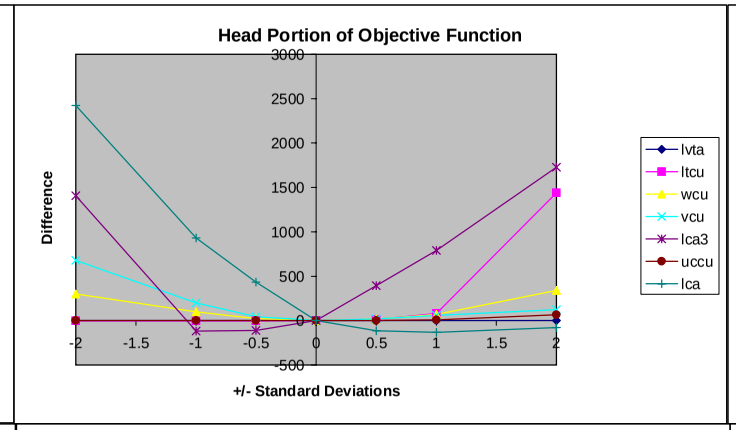
Head Portion of Objective Function
Difference
+/- Standard Deviations
lvta
ltcu
wcu
vcu
lca3
uccu
lca

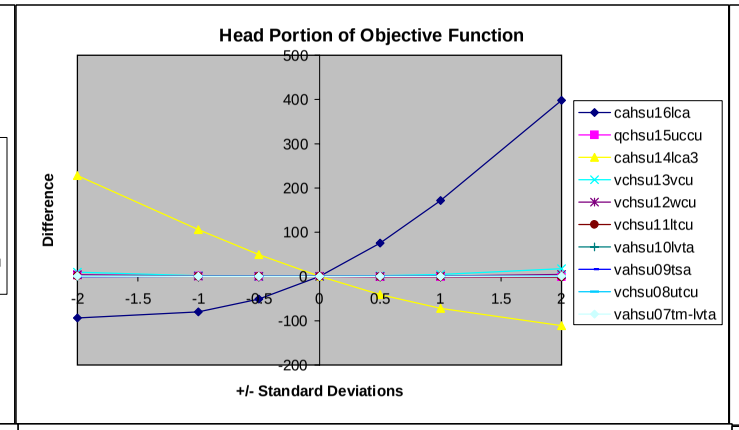
Head Portion of Objective Function
Difference
+/- Standard Deviations
cahsu16lca
qchsu15uccu
cahsu14lca3
vchsu13vcu
vchsu12wcu
vchsu11ltcu
vahsu10lvta
vahsu09tsa
vchsu08utcu
vahsu07tm-lvta

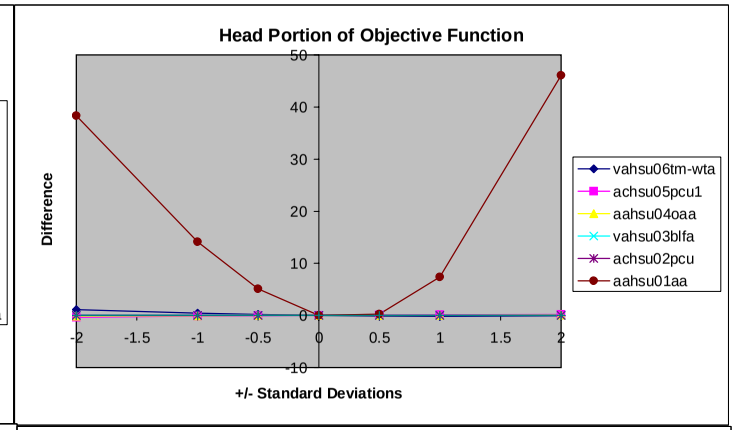
Head Portion of Objective Function
Difference
+/- Standard Deviations
vahsu06tm-wta
achsu05pcu1
aahsu04oaa
vahsu03blfa
achsu02pcu
aahsu01aa

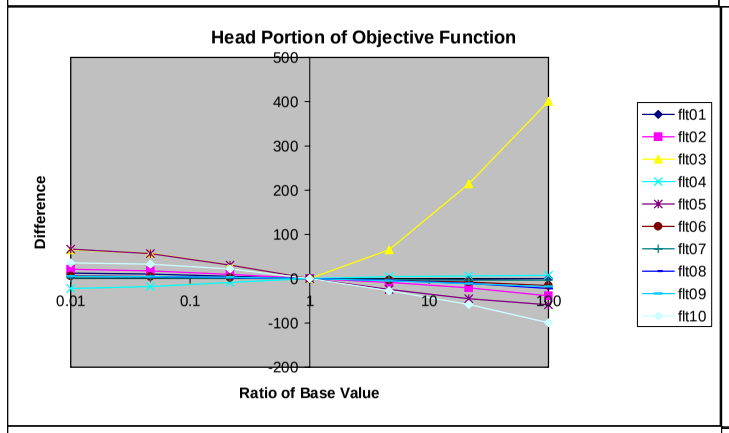
Head Portion of Objective Function
Difference
Ratio of Base Value
flt01
flt02
flt03
flt04
flt05
flt06
flt07
flt08
flt09
flt10

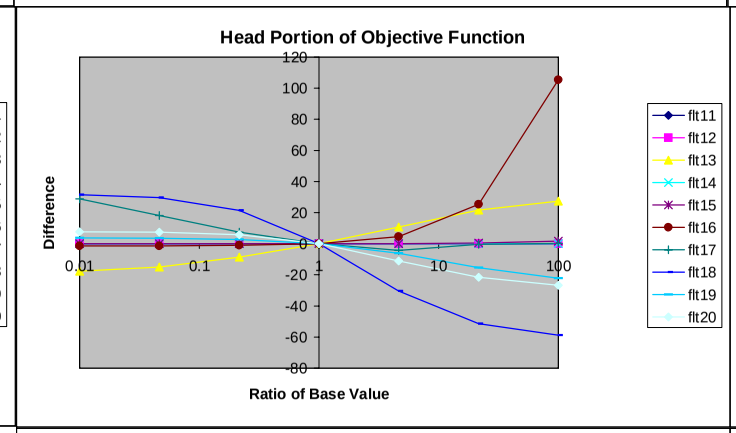
Head Portion of Objective Function
Difference
Ratio of Base Value
flt11
flt12
flt13
flt14
flt15
flt16
flt17
flt18
flt19
flt20

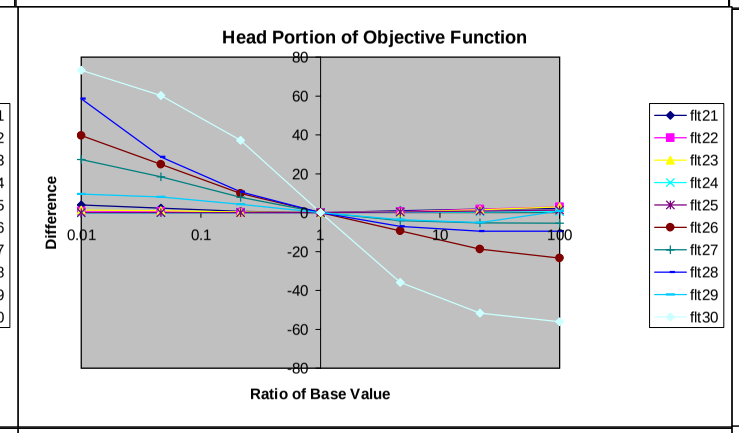
Head Portion of Objective Function
Difference
Ratio of Base Value
flt21
flt22
flt23
flt24
flt25
flt26
flt27
flt28
flt29
flt30

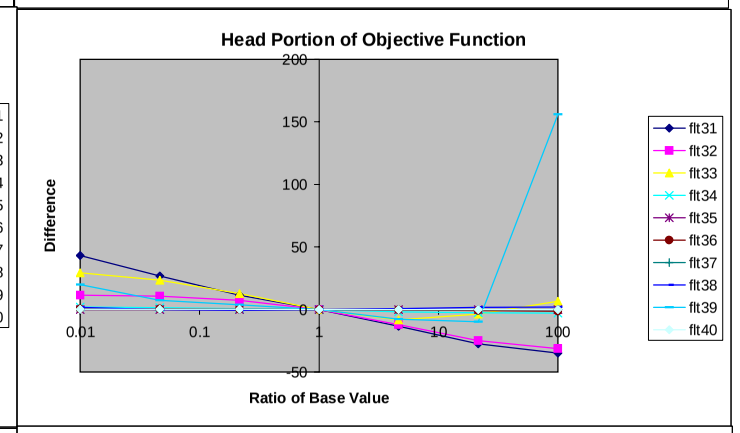
Head Portion of Objective Function
Difference
Ratio of Base Value
flt31
flt32
flt33
flt34
flt35
flt36
flt37
flt38
flt39
flt40

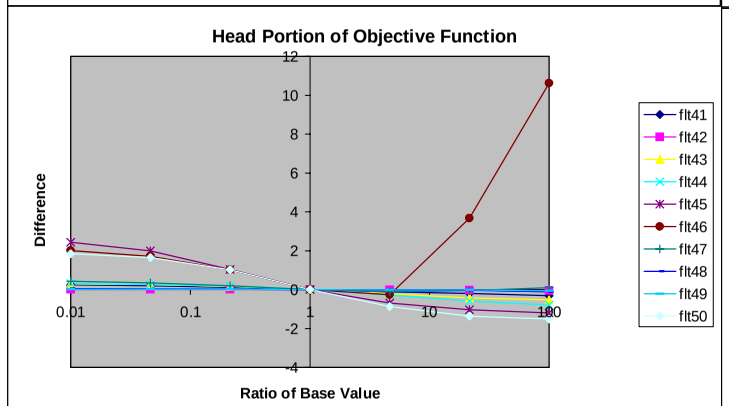
Head Portion of Objective Function
Difference
Ratio of Base Value
flt41
flt42
flt43
flt44
flt45
flt46
flt47
flt48
flt49
flt50

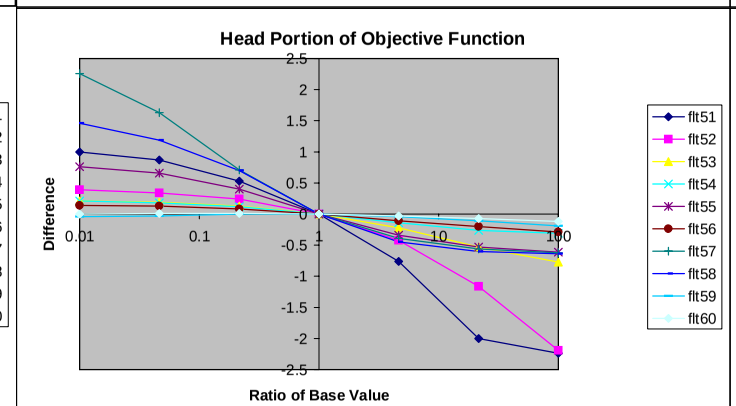
Head Portion of Objective Function
Difference
Ratio of Base Value
flt51
flt52
flt53
flt54
flt55
flt56
flt57
flt58
flt59
flt60

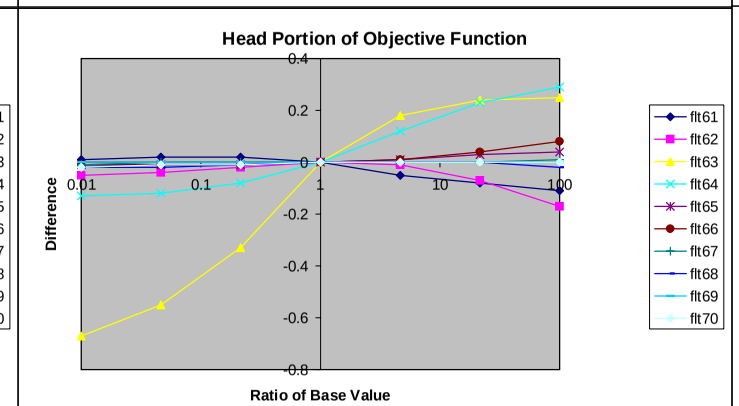
Head Portion of Objective Function
Difference
Ratio of Base Value
flt61
flt62
flt63
flt64
flt65
flt66
flt67
flt68
flt69
flt70

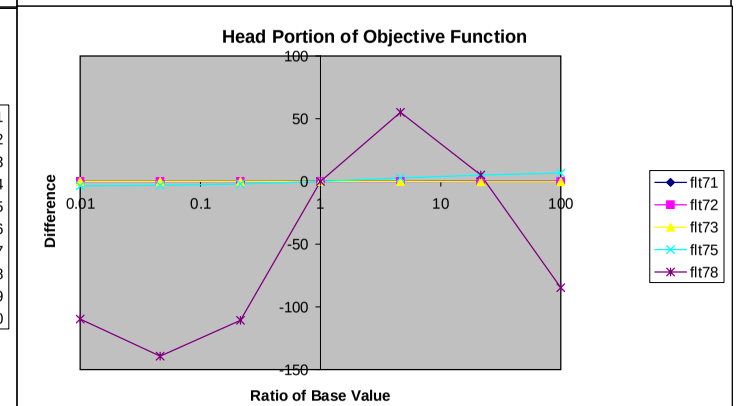
Head Portion of Objective Function
Difference
Ratio of Base Value
flt71
flt72
flt73
flt75
flt78

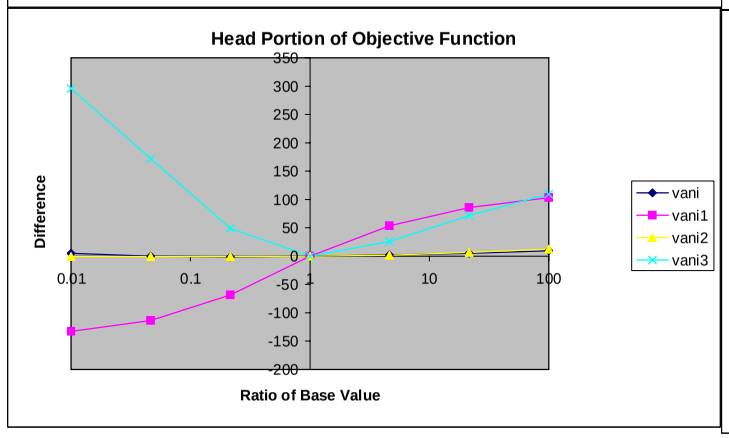
Head Portion of Objective Function
Difference
Ratio of Base Value
vani
vani1
vani2
vani3

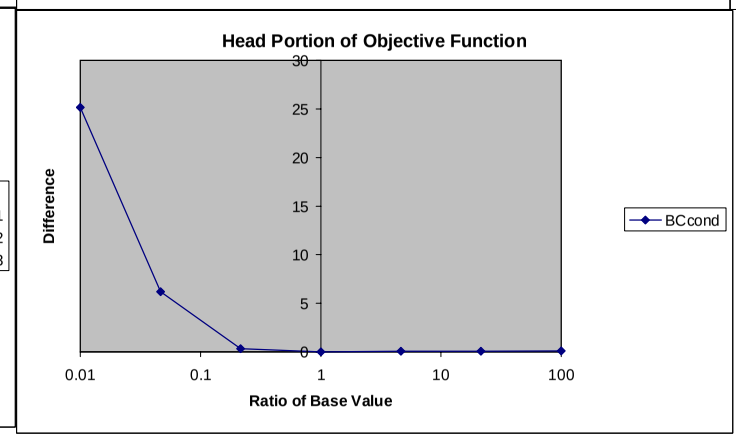
Head Portion of Objective Function
Difference
Ratio of Base Value
BCcond

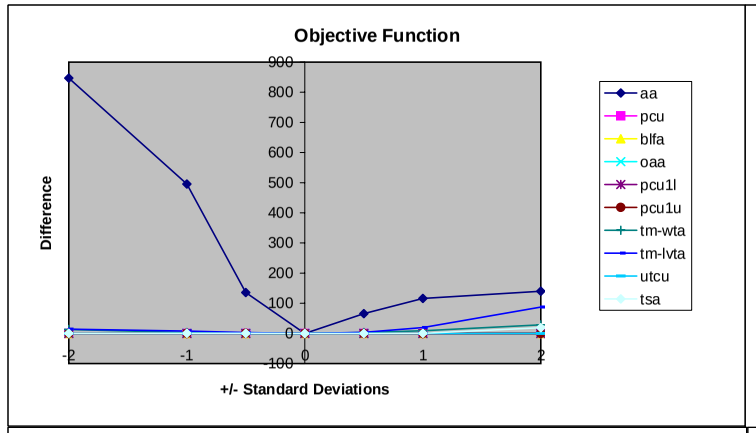
Objective Function
Difference
+/- Standard Deviations
aa
pcu
blfa
oaa
pcu1l
pcu1u
tm-wta
tm-lvta
utcu
tsa

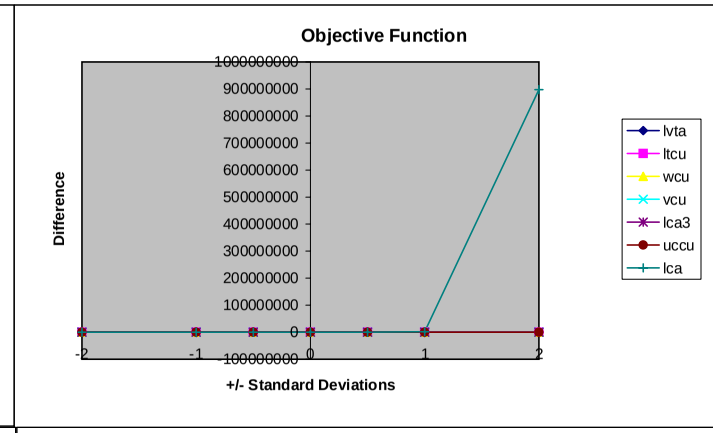
Objective Function
Difference
+/- Standard Deviations
lvta
ltcu
wcu
vcu
lca3
uccu
lca

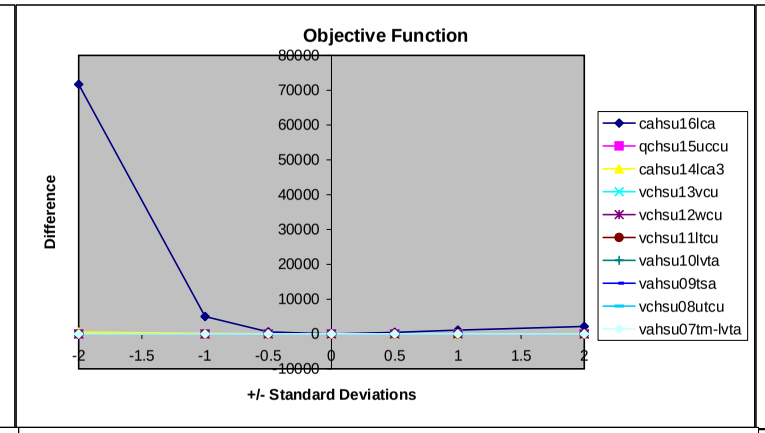
Objective Function
Difference
+/- Standard Deviations
cahsu16lca
qchsu15uccu
cahsu14lca3
vchsu13vcu
vchsu12wcu
vchsu11ltcu
vahsu10lvta
vahsu09tsa
vchsu08utcu
vahsu07tm-lvta

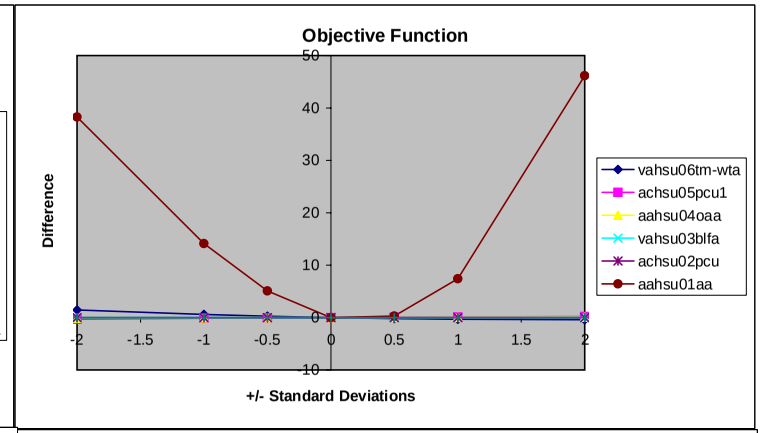
Objective Function
Difference
+/- Standard Deviations
vahsu06tm-wta
achsu05pcu1
aahsu04oaa
vahsu03blfa
achsu02pcu
aahsu01aa

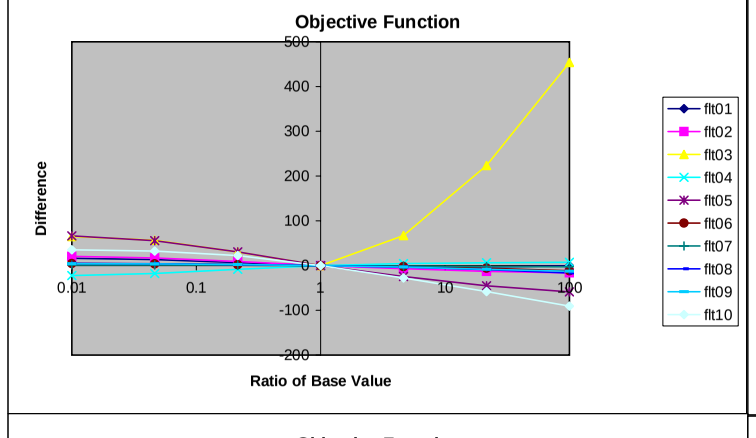
Objective Function
Difference
Ratio of Base Value
flt01
flt02
flt03
flt04
flt05
flt06
flt07
flt08
flt09
flt10

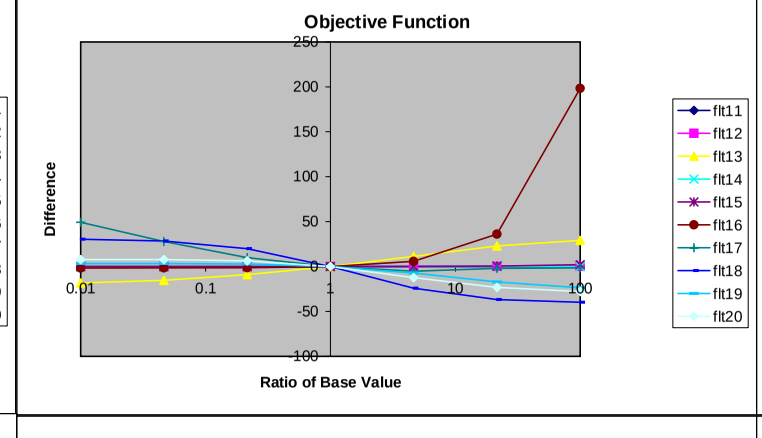
Objective Function
Difference
Ratio of Base Value
flt11
flt12
flt13
flt14
flt15
flt16
flt17
flt18
flt19
flt20

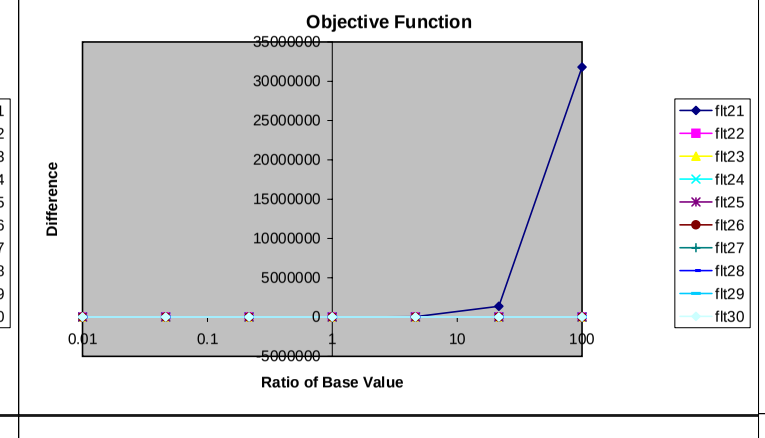
Objective Function
Difference
Ratio of Base Value
flt21
flt22
flt23
flt24
flt25
flt26
flt27
flt28
flt29
flt30

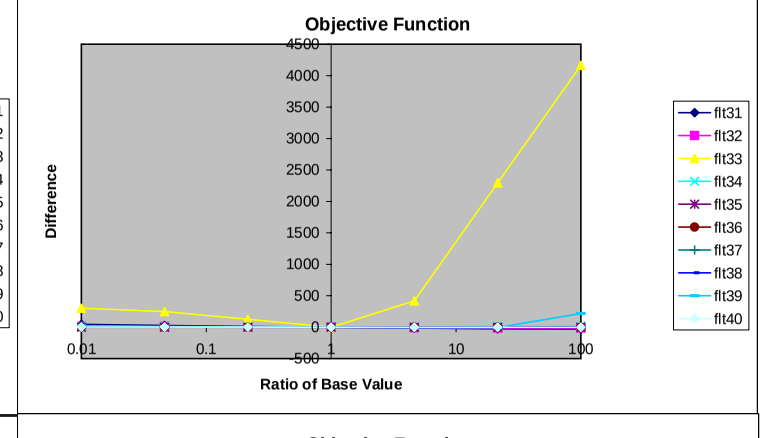
Objective Function
Difference
Ratio of Base Value
flt31
flt32
flt33
flt34
flt35
flt36
flt37
flt38
flt39
flt40

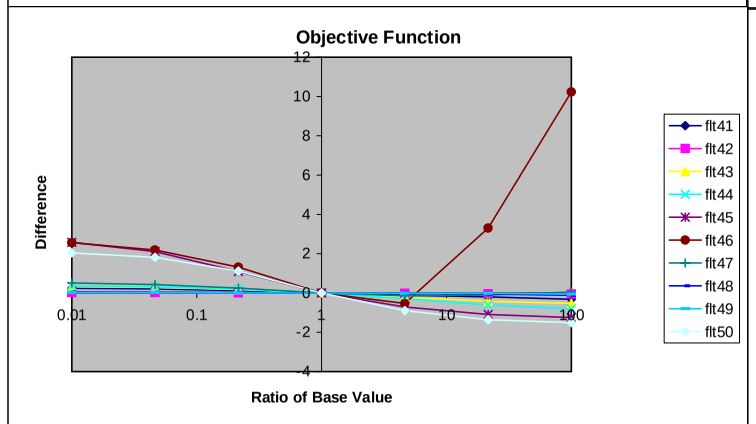
Objective Function
Difference
Ratio of Base Value
flt41
flt42
flt43
flt44
flt45
flt46
flt47
flt48
flt49
flt50

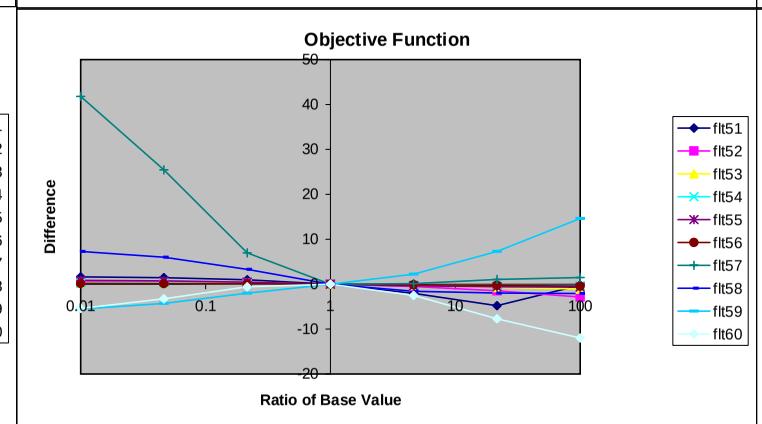
Objective Function
Difference
Ratio of Base Value
flt51
flt52
flt53
flt54
flt55
flt56
flt57
flt58
flt59
flt60

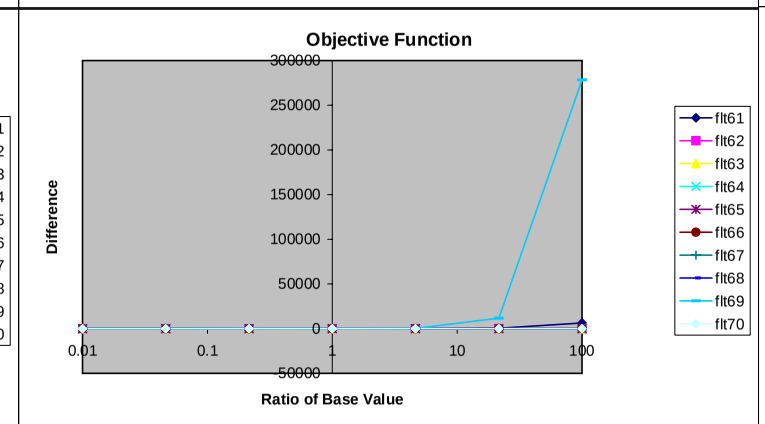
Objective Function
Difference
Ratio of Base Value
flt61
flt62
flt63
flt64
flt65
flt66
flt67
flt68
flt69
flt70

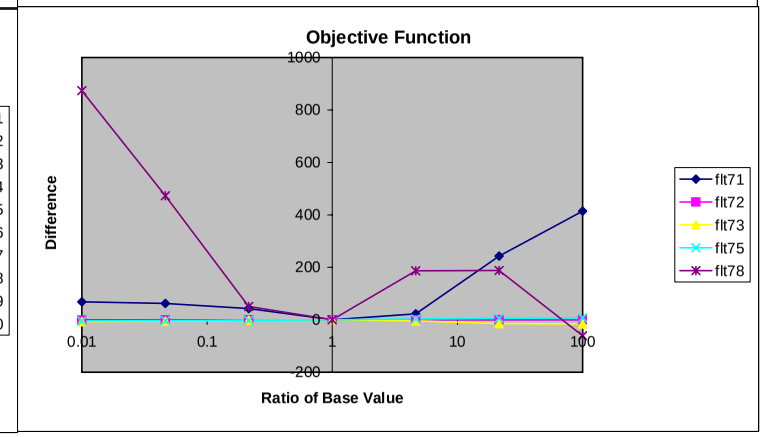
Objective Function
Difference
Ratio of Base Value
flt71
flt72
flt73
flt75
flt78

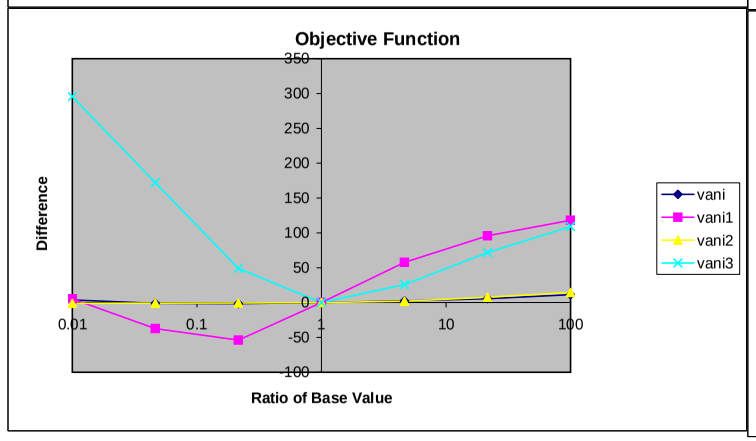
Objective Function
Difference
Ratio of Base Value
vani
vani1
vani2
vani3

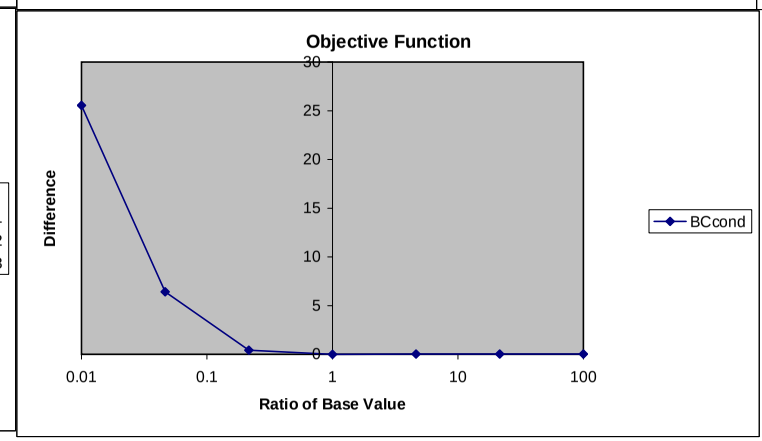
Objective Function
Difference
Ratio of Base Value
BCcond

C.3.4

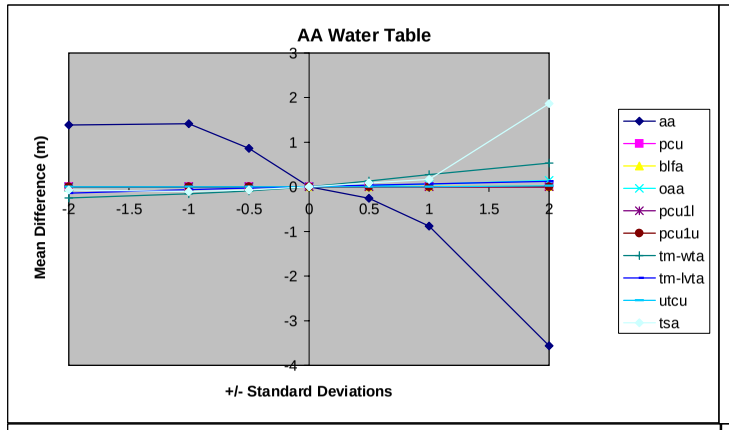
AA Water Table
Mean Difference (m)
+/- Standard Deviations
aa
pcu
blfa
oaa
pcu1l
pcu1u
tm-wta
tm-lvta
utcu
tsa

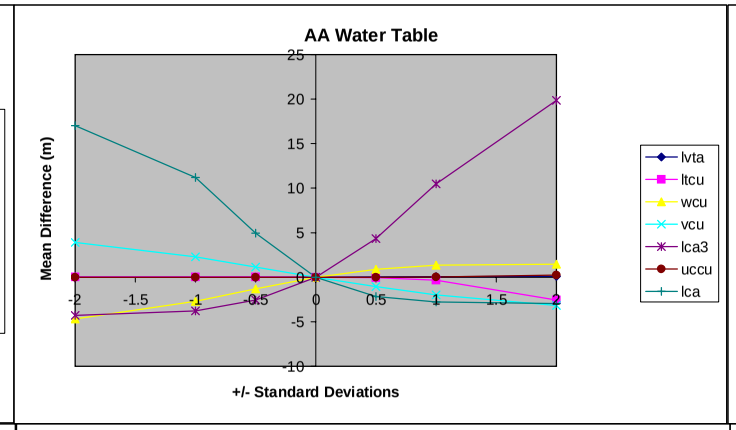
AA Water Table
Mean Difference (m)
+/- Standard Deviations
lvta
ltcu
wcu
vcu
lca3
uccu
lca

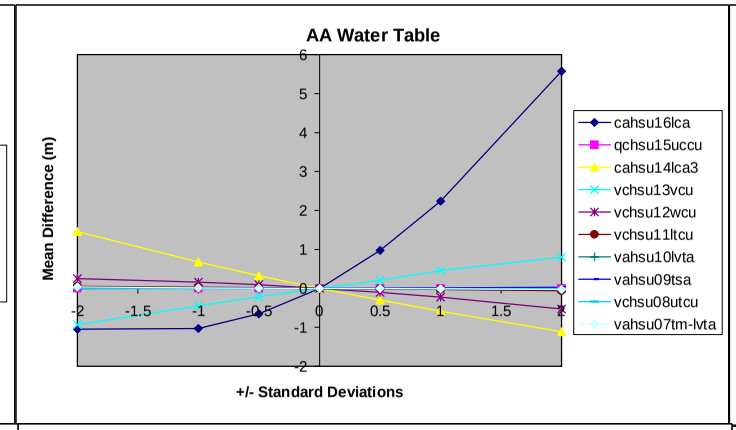
AA Water Table
Mean Difference (m)
+/- Standard Deviations
cahsu16lca
qchsu15uccu
cahsu14lca3
vchsu13vcu
vchsu12wcu
vchsu11ltcu
vahsu10lvta
vahsu09tsa
vchsu08utcu
vahsu07tm-lvta

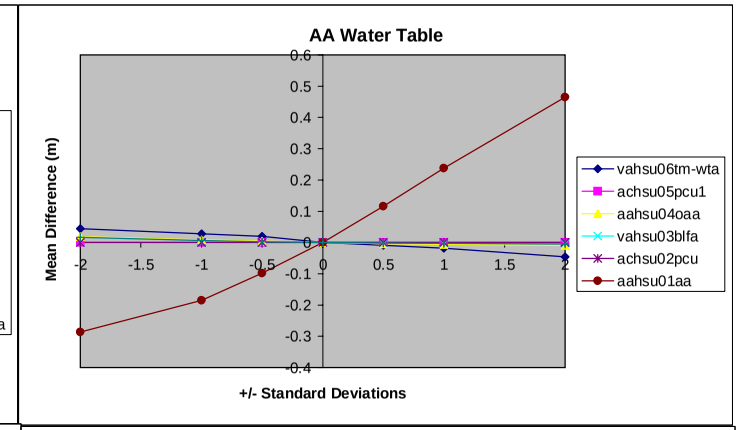
AA Water Table
Mean Difference (m)
+/- Standard Deviations
vahsu06tm-wta
achsu05pcu1
aahsu04oaa
vahsu03blfa
achsu02pcu
aahsu01aa

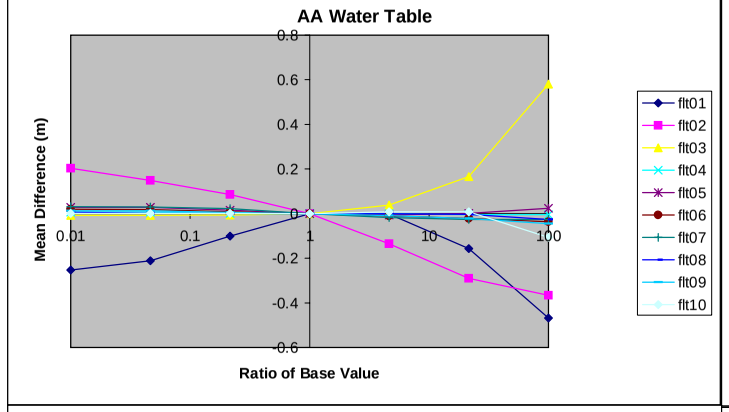
AA Water Table
Mean Difference (m)
Ratio of Base Value
flt01
flt02
flt03
flt04
flt05
flt06
flt07
flt08
flt09
flt10

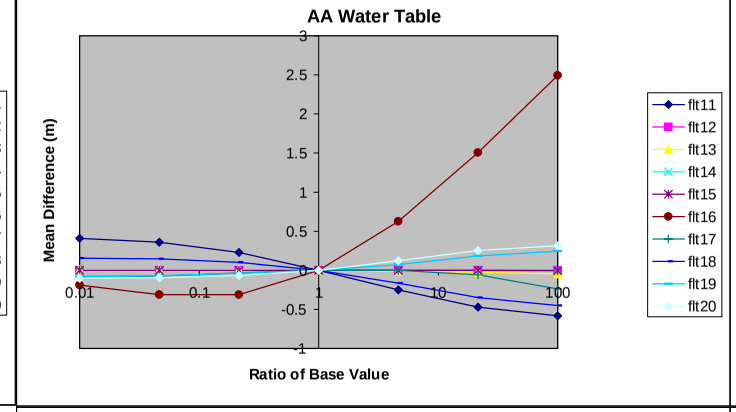
AA Water Table
Mean Difference (m)
Ratio of Base Value
flt11
flt12
flt13
flt14
flt15
flt16
flt17
flt18
flt19
flt20

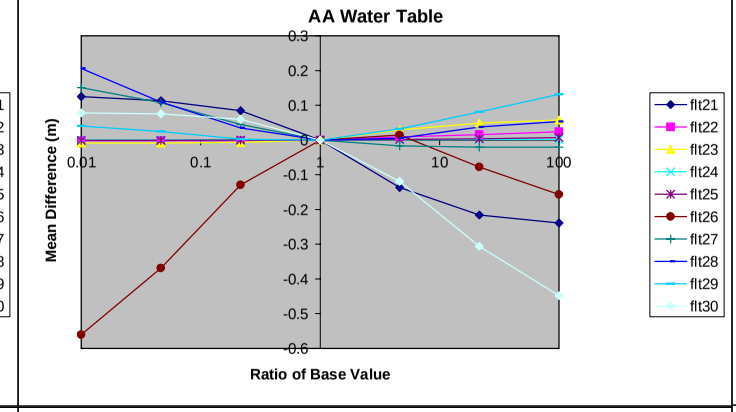
AA Water Table
Mean Difference (m)
Ratio of Base Value
flt21
flt22
flt23
flt24
flt25
flt26
flt27
flt28
flt29
flt30

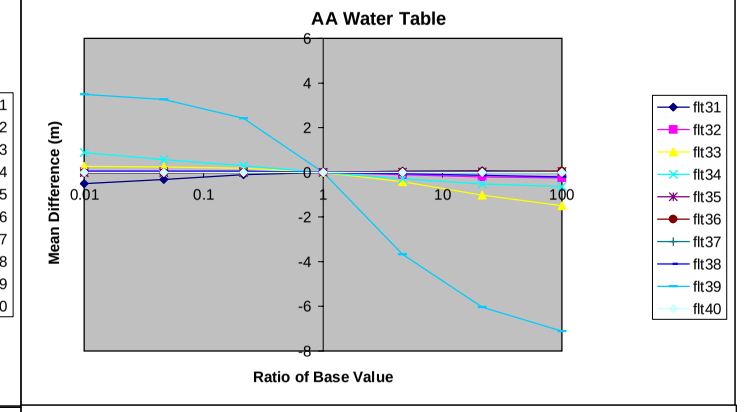
AA Water Table
Mean Difference (m)
Ratio of Base Value
flt31
flt32
flt33
flt34
flt35
flt36
flt37
flt38
flt39
flt40

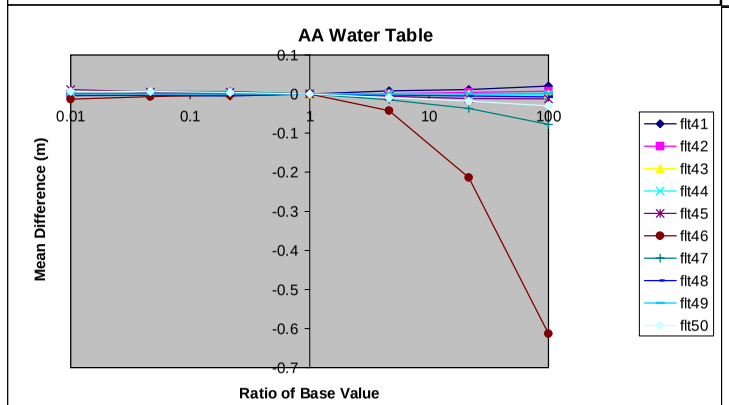
AA Water Table
Mean Difference (m)
Ratio of Base Value
flt41
flt42
flt43
flt44
flt45
flt46
flt47
flt48
flt49
flt50

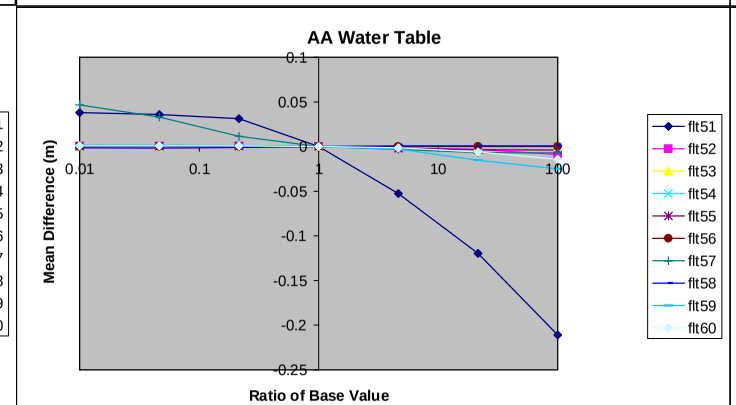
AA Water Table
Mean Difference (m)
Ratio of Base Value
flt51
flt52
flt53
flt54
flt55
flt56
flt57
flt58
flt59
flt60

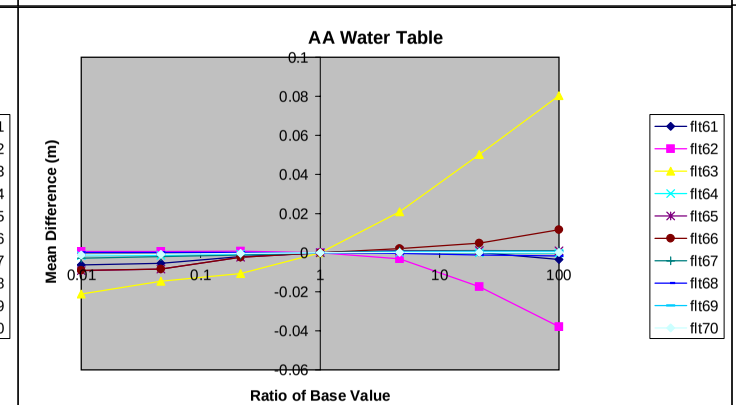
AA Water Table
Mean Difference (m)
Ratio of Base Value
flt61
flt62
flt63
flt64
flt65
flt66
flt67
flt68
flt69
flt70

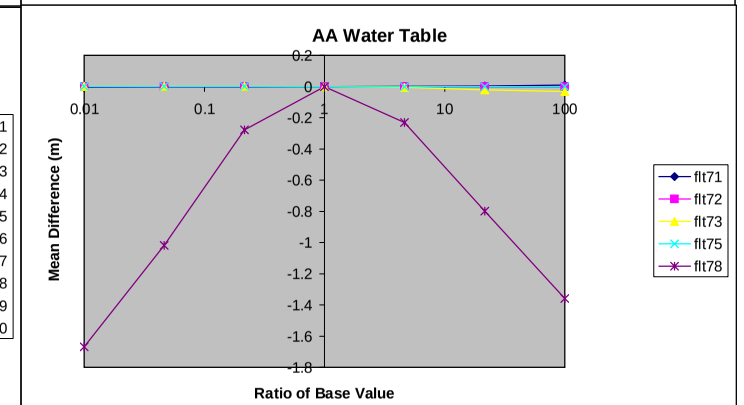
AA Water Table
Mean Difference (m)
Ratio of Base Value
flt71
flt72
flt73
flt75
flt78

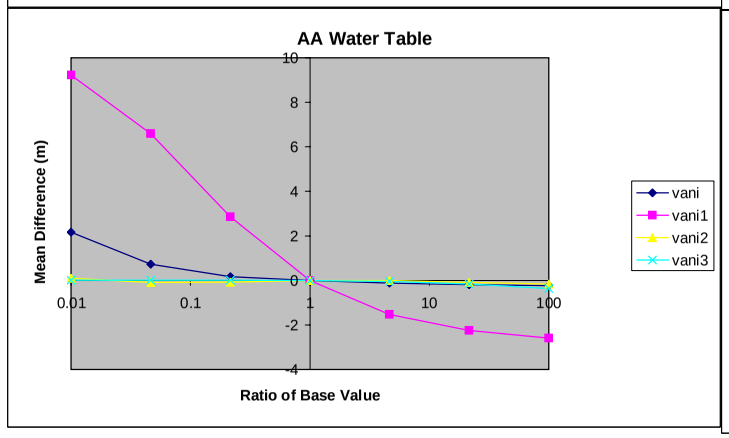
AA Water Table
Mean Difference (m)
Ratio of Base Value
vani
vani1
vani2
vani3

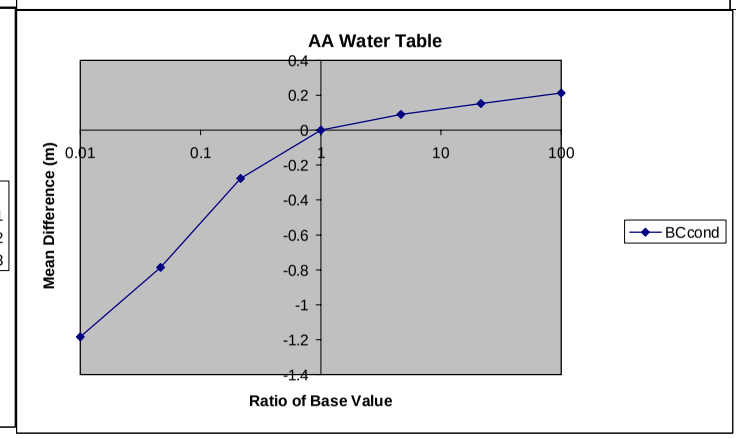
AA Water Table
Mean Difference (m)
Ratio of Base Value
BCcond

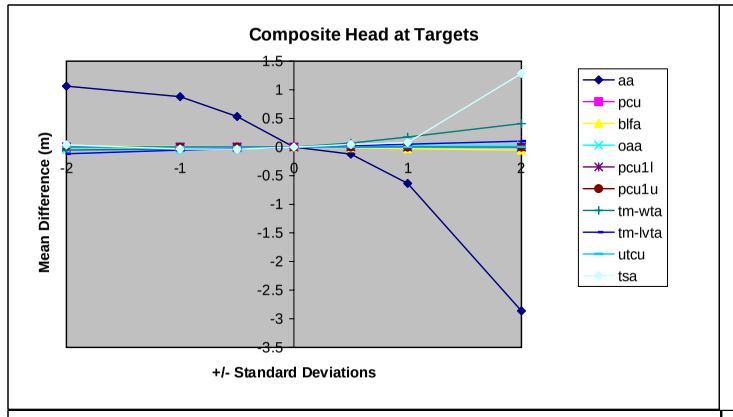
Composite Head at Targets
Mean Difference (m)
+/- Standard Deviations
aa
pcu
blfa
oaa
pcu1l
pcu1u
tm-wta
tm-lvta
utcu
tsa

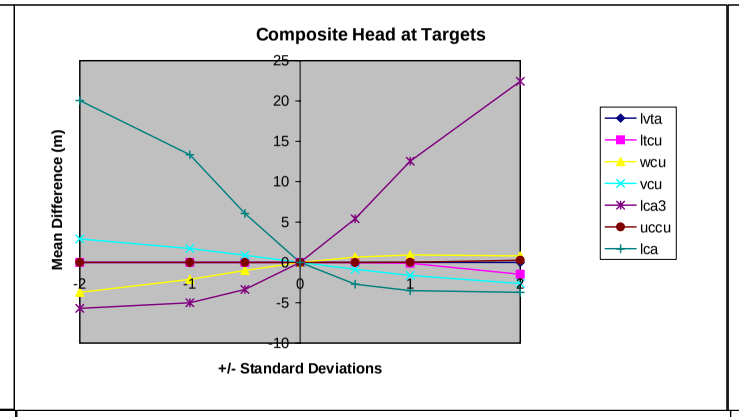
Composite Head at Targets
Mean Difference (m)
+/- Standard Deviations
lvta
ltcu
wcu
vcu
lca3
uccu
lca

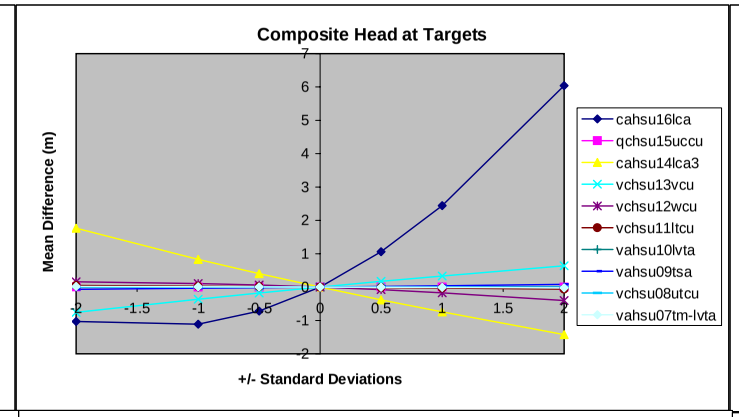
Composite Head at Targets
Mean Difference (m)
+/- Standard Deviations
cahsu16lca
qchsu15uccu
cahsu14lca3
vchsu13vcu
vchsu12wcu
vchsu11ltcu
vahsu10lvta
vahsu09tsa
vchsu08utcu
vahsu07tm-lvta

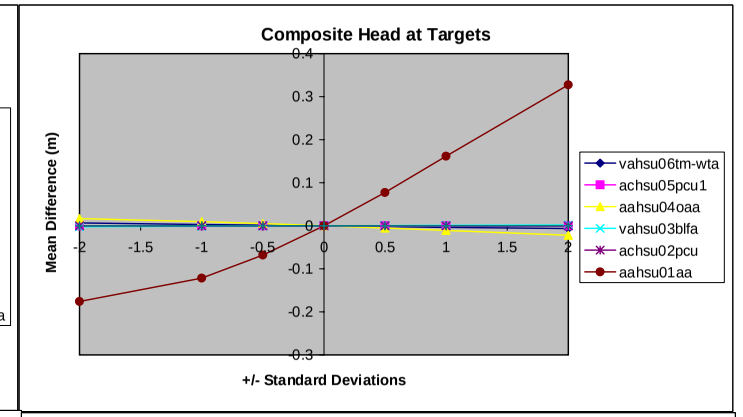
Composite Head at Targets
Mean Difference (m)
+/- Standard Deviations
vahsu06tm-wta
achsu05pcu1
aahsu04oaa
vahsu03blfa
achsu02pcu
aahsu01aa

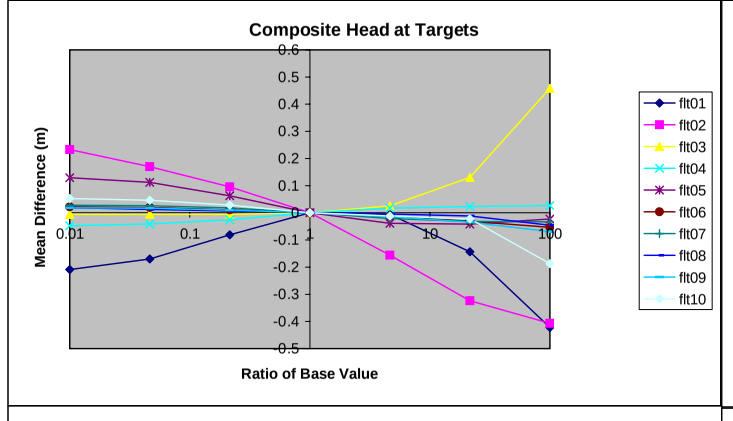
Composite Head at Targets
Mean Difference (m)
Ratio of Base Value
flt01
flt02
flt03
flt04
flt05
flt06
flt07
flt08
flt09
flt10

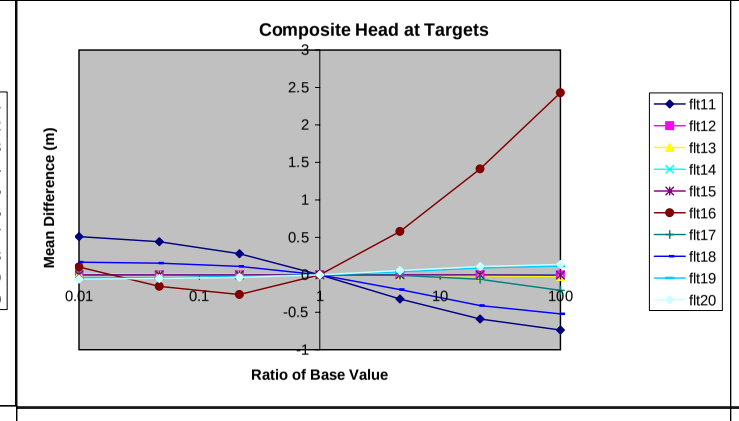
Composite Head at Targets
Mean Difference (m)
Ratio of Base Value
flt11
flt12
flt13
flt14
flt15
flt16
flt17
flt18
flt19
flt20

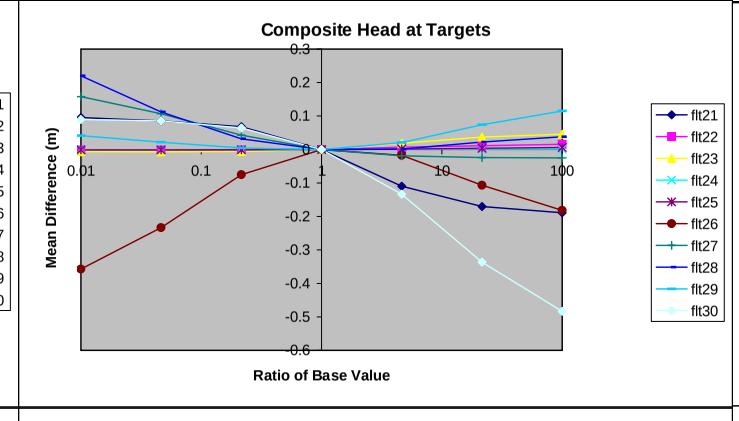
Composite Head at Targets
Mean Difference (m)
Ratio of Base Value
flt21
flt22
flt23
flt24
flt25
flt26
flt27
flt28
flt29
flt30

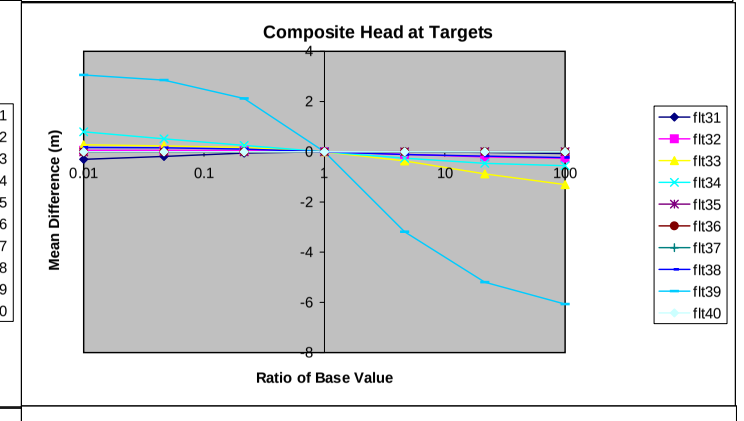
Composite Head at Targets
Mean Difference (m)
Ratio of Base Value
flt31
flt32
flt33
flt34
flt35
flt36
flt37
flt38
flt39
flt40

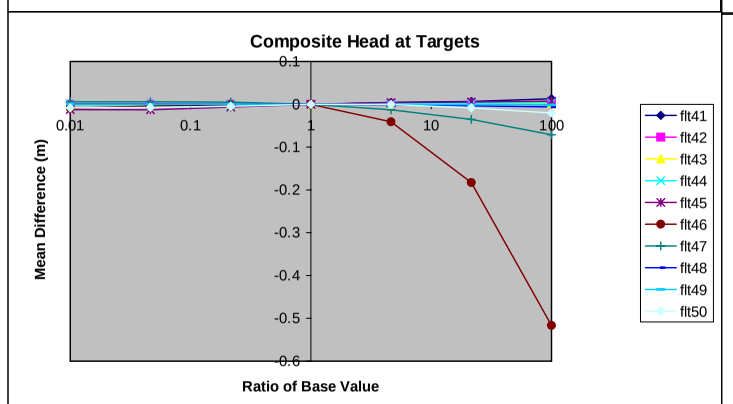
Composite Head at Targets
Mean Difference (m)
Ratio of Base Value
flt41
flt42
flt43
flt44
flt45
flt46
flt47
flt48
flt49
flt50

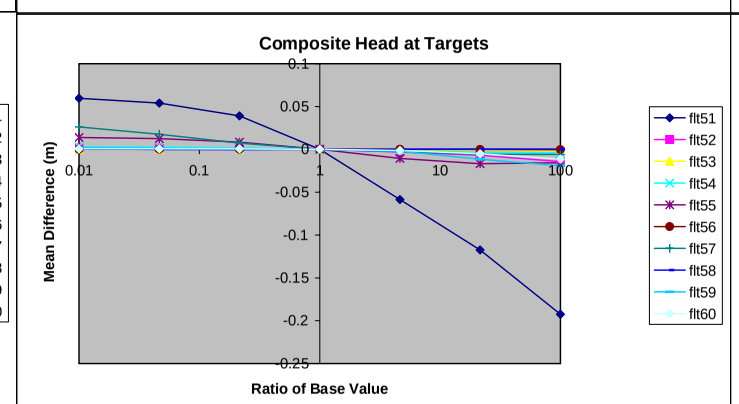
Composite Head at Targets
Mean Difference (m)
Ratio of Base Value
flt51
flt52
flt53
flt54
flt55
flt56
flt57
flt58
flt59
flt60

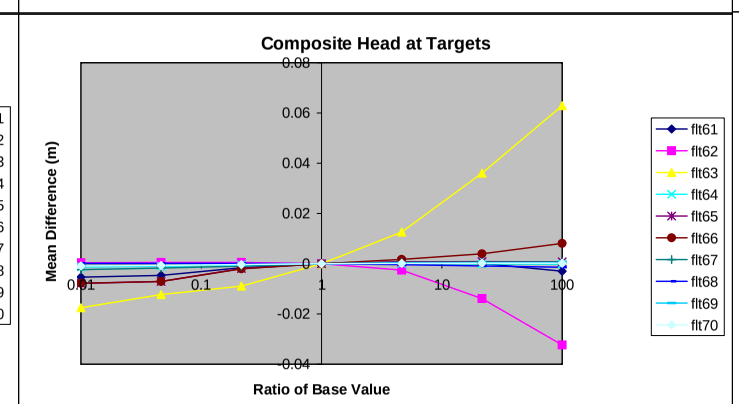
Composite Head at Targets
Mean Difference (m)
Ratio of Base Value
flt61
flt62
flt63
flt64
flt65
flt66
flt67
flt68
flt69
flt70

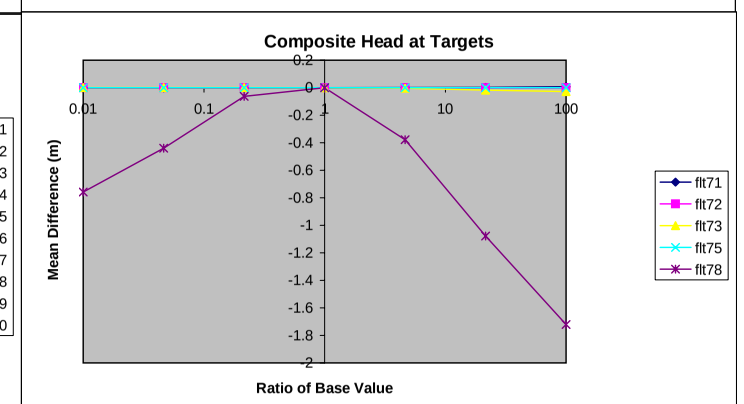
Composite Head at Targets
Mean Difference (m)
Ratio of Base Value
flt71
flt72
flt73
flt75
flt78

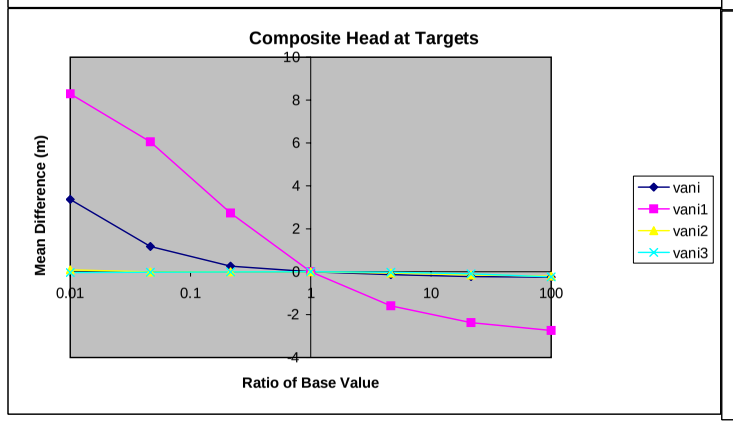
Composite Head at Targets
Mean Difference (m)
Ratio of Base Value
vani
vani1
vani2
vani3

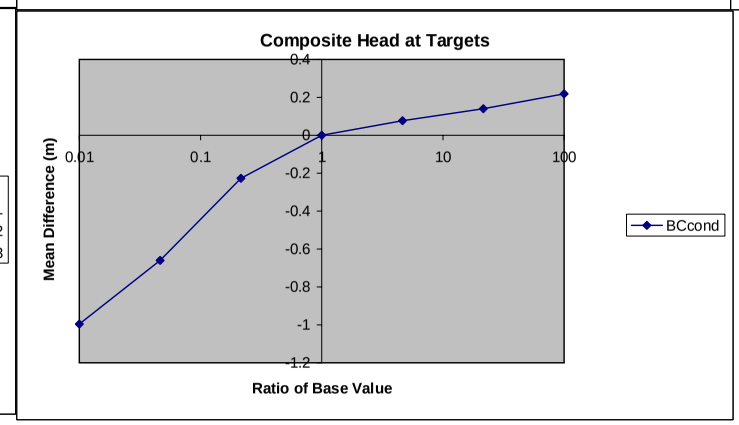
Composite Head at Targets
Mean Difference (m)
Ratio of Base Value
BCcond

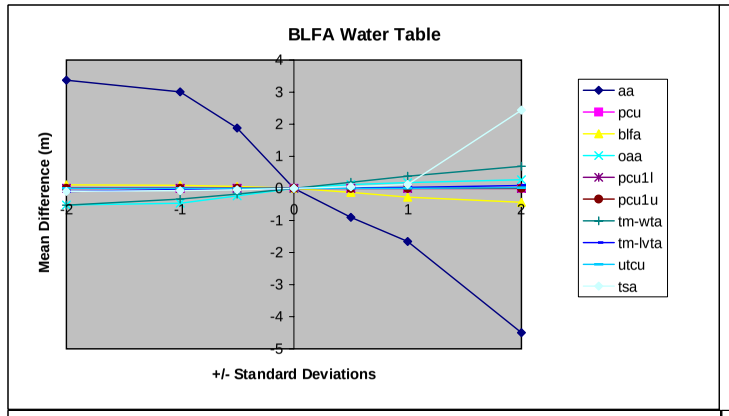
BLFA Water Table
Mean Difference (m)
+/- Standard Deviations
aa
pcu
blfa
oaa
pcu1l
pcu1u
tm-wta
tm-lvta
utcu
tsa

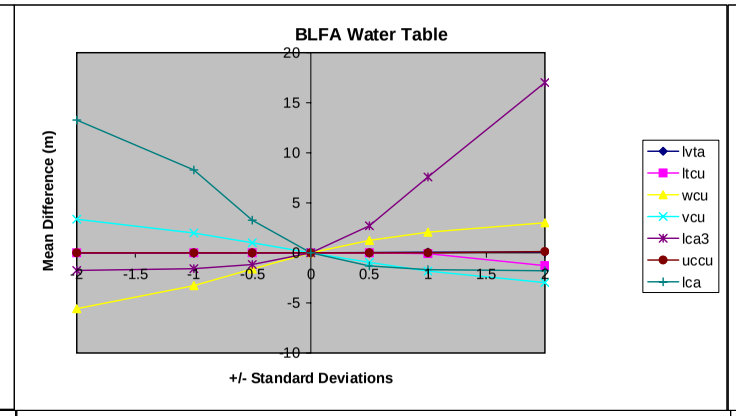
BLFA Water Table
Mean Difference (m)
+/- Standard Deviations
lvta
ltcu
wcu
vcu
lca3
uccu
lca

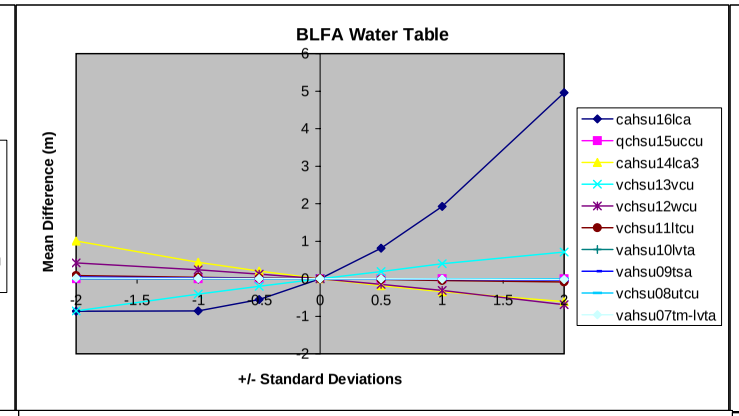
BLFA Water Table
Mean Difference (m)
+/- Standard Deviations
cahsu16lca
qchsu15uccu
cahsu14lca3
vchsu13vcu
vchsu12wcu
vchsu11ltcu
vahsu10lvta
vahsu09tsa
vchsu08utcu
vahsu07tm-lvta

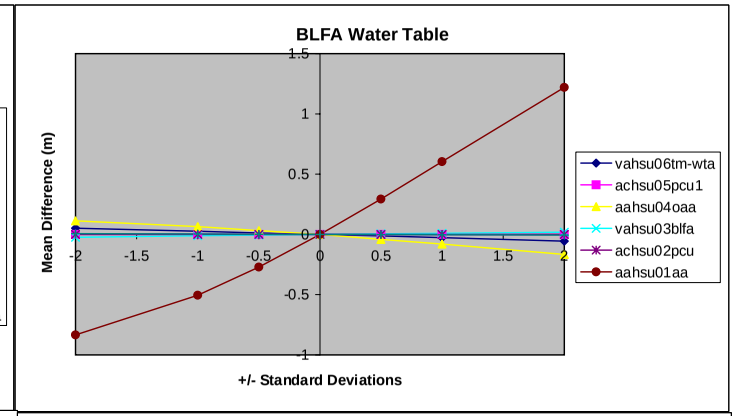
BLFA Water Table
Mean Difference (m)
+/- Standard Deviations
vahsu06tm-wta
achsu05pcu1
aahsu04oaa
vahsu03blfa
achsu02pcu
aahsu01aa

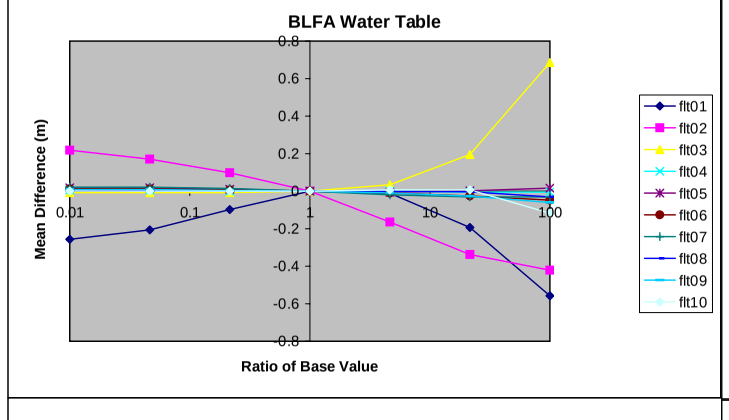
BLFA Water Table
Mean Difference (m)
Ratio of Base Value
flt01
flt02
flt03
flt04
flt05
flt06
flt07
flt08
flt09
flt10

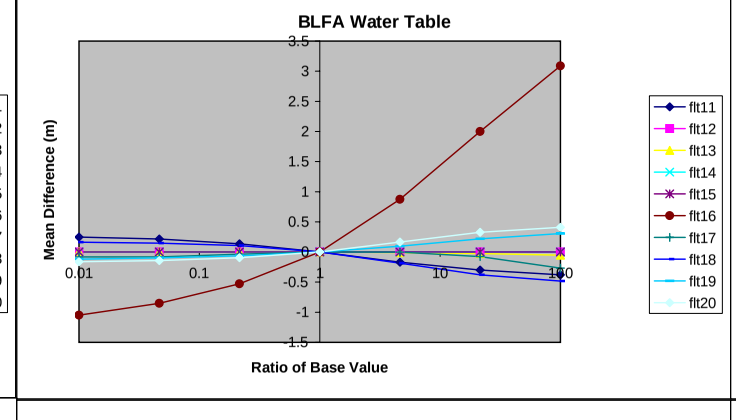
BLFA Water Table
Mean Difference (m)
Ratio of Base Value
flt11
flt12
flt13
flt14
flt15
flt16
flt17
flt18
flt19
flt20

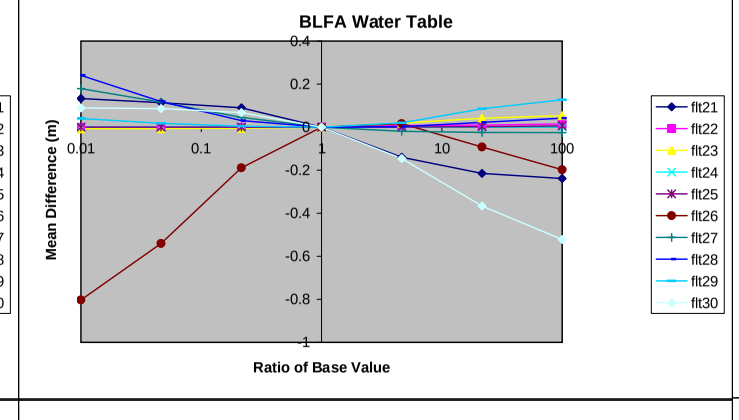
BLFA Water Table
Mean Difference (m)
Ratio of Base Value
flt21
flt22
flt23
flt24
flt25
flt26
flt27
flt28
flt29
flt30

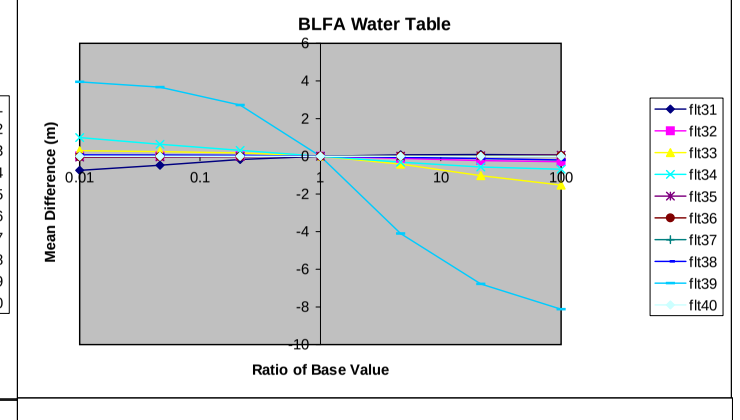
BLFA Water Table
Mean Difference (m)
Ratio of Base Value
flt31
flt32
flt33
flt34
flt35
flt36
flt37
flt38
flt39
flt40

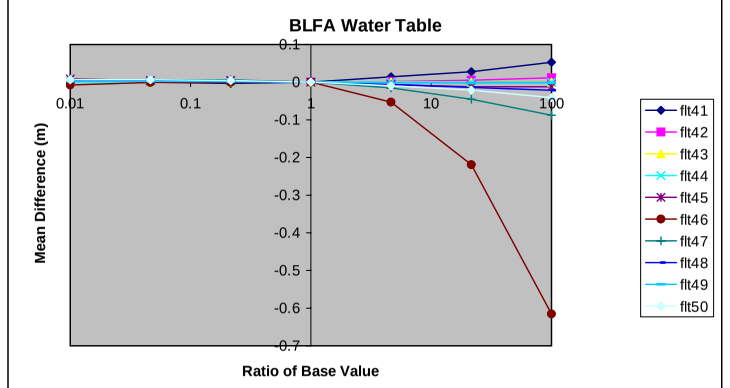
BLFA Water Table
Mean Difference (m)
Ratio of Base Value
flt41
flt42
flt43
flt44
flt45
flt46
flt47
flt48
flt49
flt50

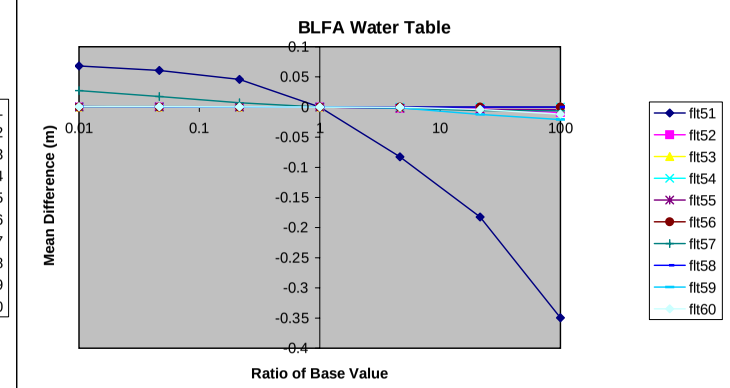
BLFA Water Table
Mean Difference (m)
Ratio of Base Value
flt51
flt52
flt53
flt54
flt55
flt56
flt57
flt58
flt59
flt60

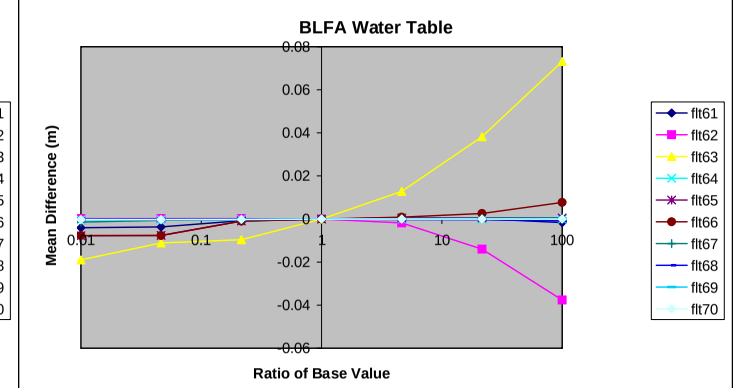
BLFA Water Table
Mean Difference (m)
Ratio of Base Value
flt61
flt62
flt63
flt64
flt65
flt66
flt67
flt68
flt69
flt70

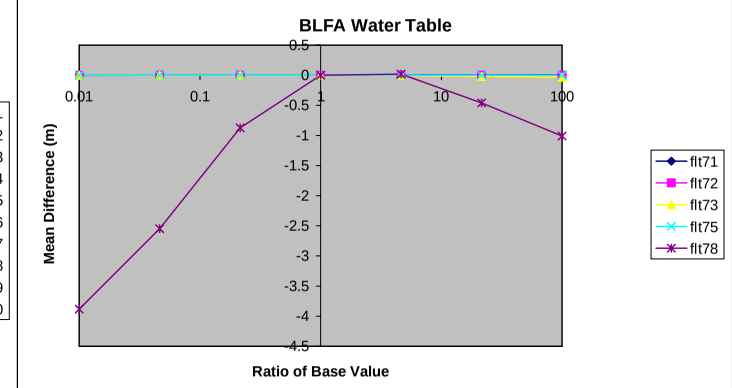
BLFA Water Table
Mean Difference (m)
Ratio of Base Value
flt71
flt72
flt73
flt75
flt78

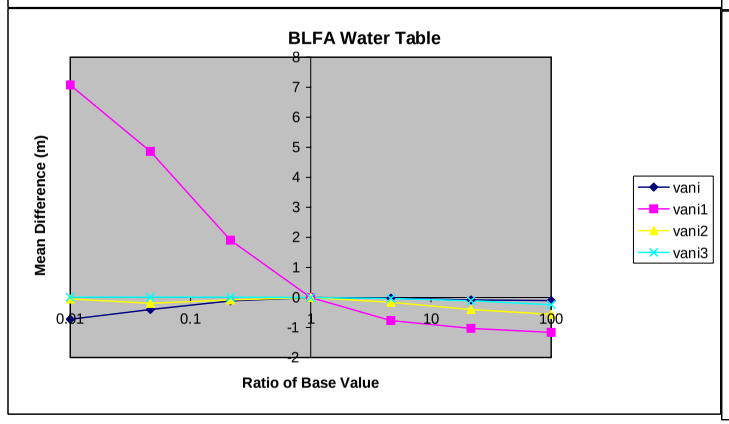
BLFA Water Table
Mean Difference (m)
Ratio of Base Value
vani
vani1
vani2
vani3

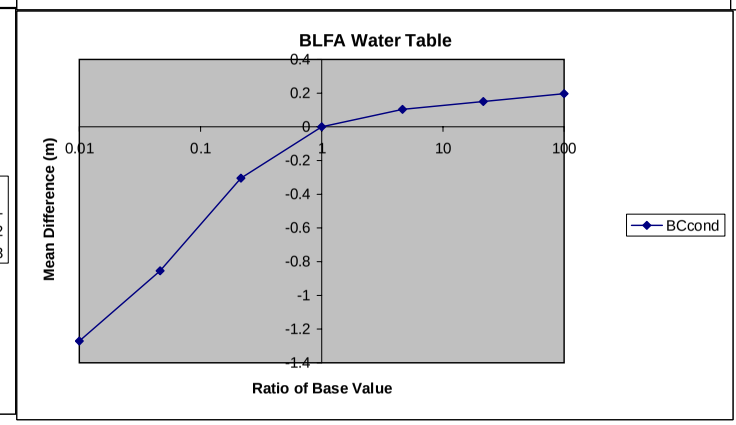
BLFA Water Table
Mean Difference (m)
Ratio of Base Value
BCcond

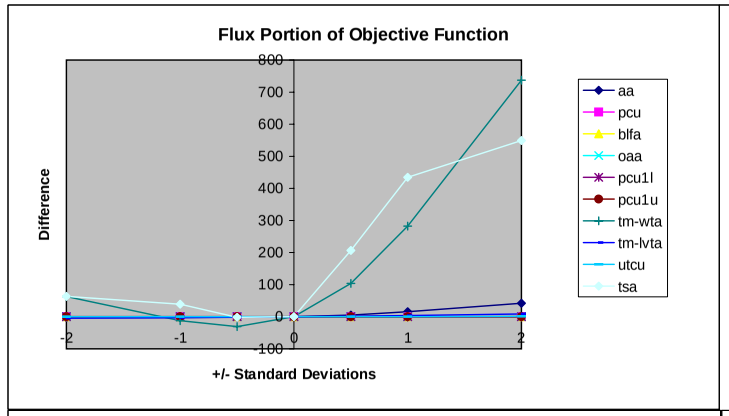
Flux Portion of Objective Function
Difference
+/- Standard Deviations
aa
pcu
blfa
oaa
pcu1l
pcu1u
tm-wta
tm-lvta
utcu
tsa

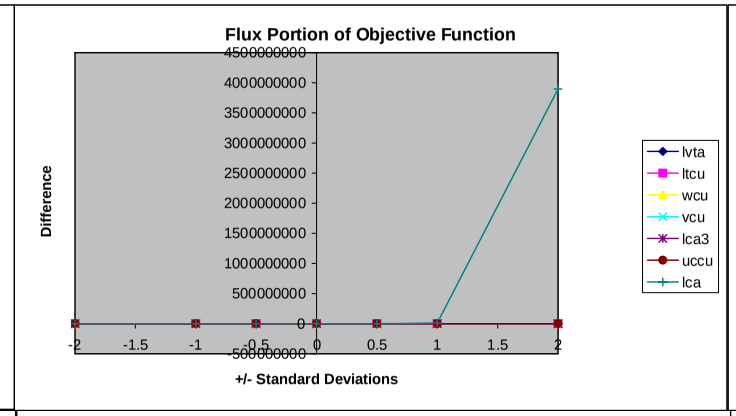
Flux Portion of Objective Function
Difference
+/- Standard Deviations
lvta
ltcu
wcu
vcu
lca3
uccu
lca

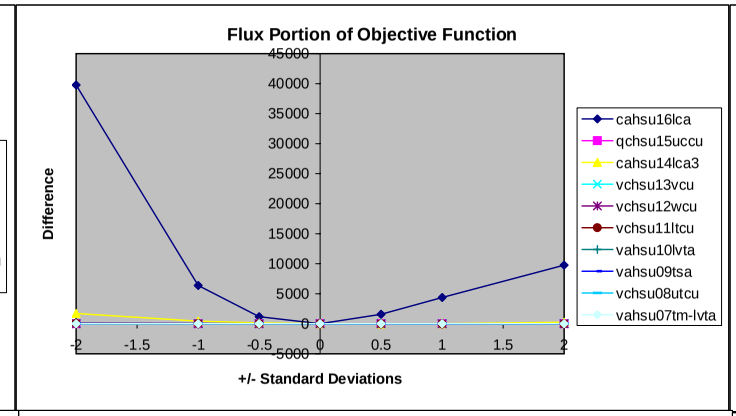
Flux Portion of Objective Function
Difference
+/- Standard Deviations
cahsu16lca
qchsu15uccu
cahsu14lca3
vchsu13vcu
vchsu12wcu
vchsu11ltcu
vahsu10lvta
vahsu09tsa
vchsu08utcu
vahsu07tm-lvta

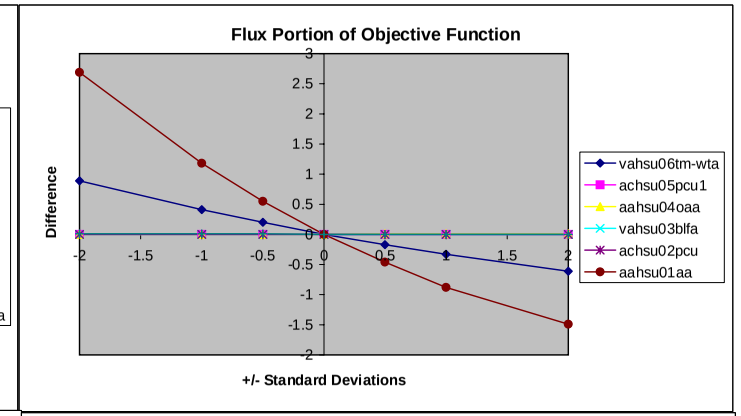
Flux Portion of Objective Function
Difference
+/- Standard Deviations
vahsu06tm-wta
achsu05pcu1
aahsu04oaa
vahsu03blfa
achsu02pcu
aahsu01aa

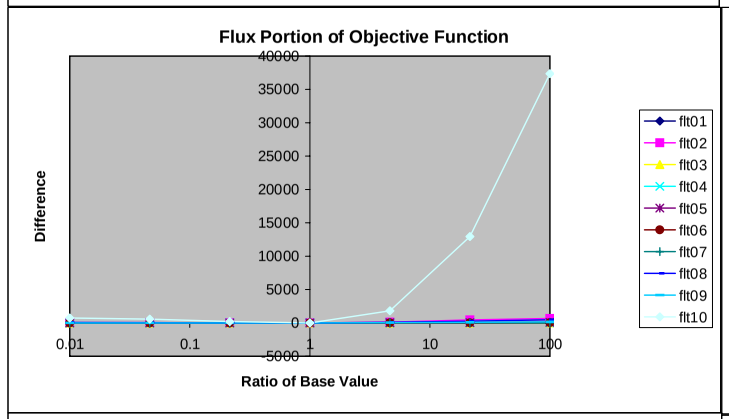
Flux Portion of Objective Function
Difference
Ratio of Base Value
flt01
flt02
flt03
flt04
flt05
flt06
flt07
flt08
flt09
flt10

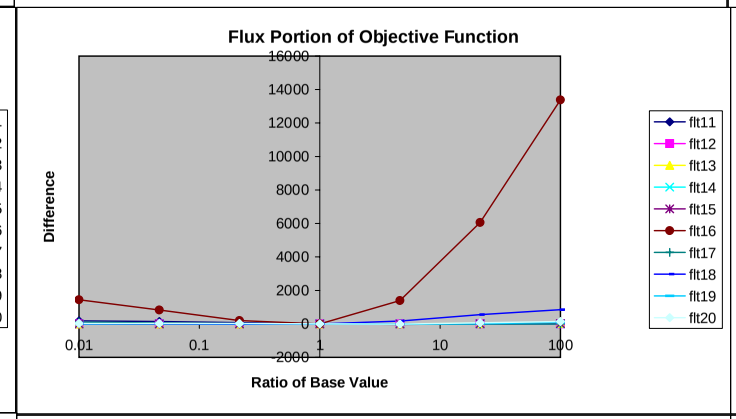
Flux Portion of Objective Function
Difference
Ratio of Base Value
flt11
flt12
flt13
flt14
flt15
flt16
flt17
flt18
flt19
flt20

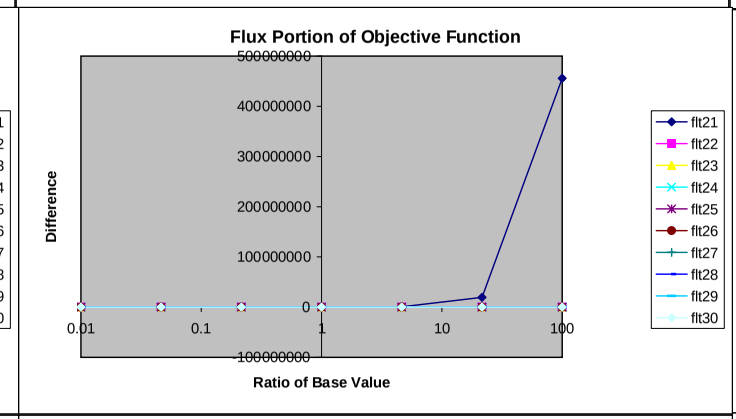
Flux Portion of Objective Function
Difference
Ratio of Base Value
flt21
flt22
flt23
flt24
flt25
flt26
flt27
flt28
flt29
flt30

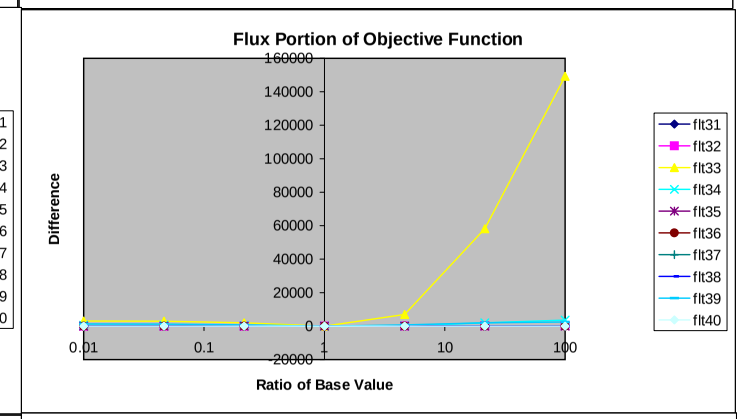
Flux Portion of Objective Function
Difference
Ratio of Base Value
flt31
flt32
flt33
flt34
flt35
flt36
flt37
flt38
flt39
flt40

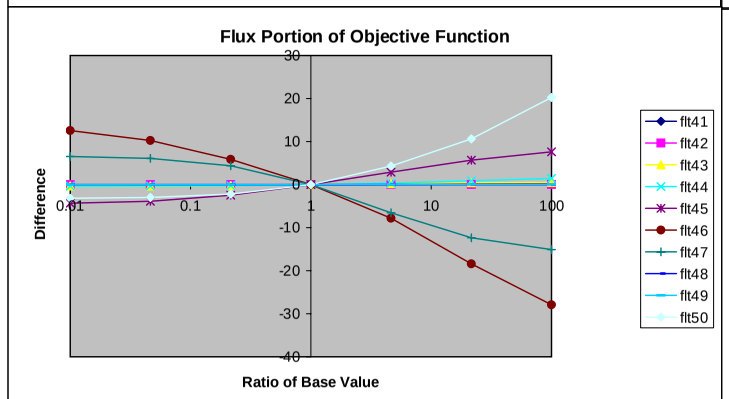
Flux Portion of Objective Function
Difference
Ratio of Base Value
flt41
flt42
flt43
flt44
flt45
flt46
flt47
flt48
flt49
flt50

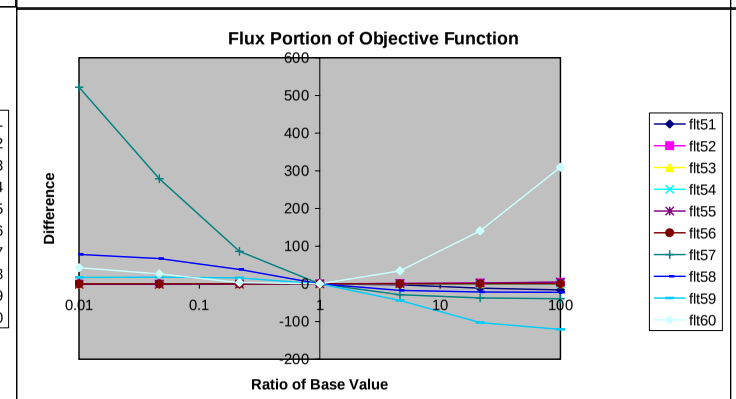
Flux Portion of Objective Function
Difference
Ratio of Base Value
flt51
flt52
flt53
flt54
flt55
flt56
flt57
flt58
flt59
flt60

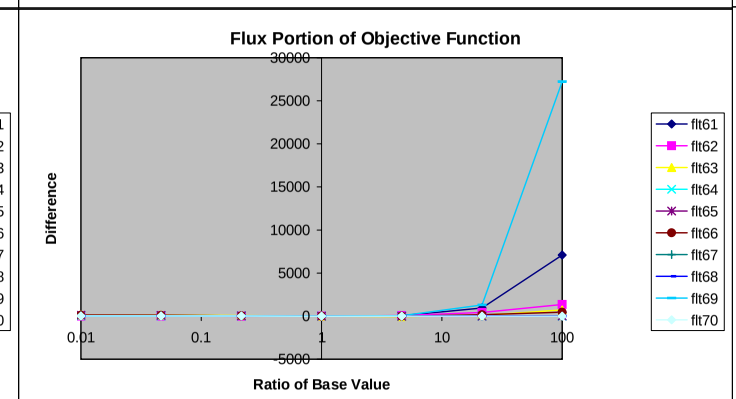
Flux Portion of Objective Function
Difference
Ratio of Base Value
flt61
flt62
flt63
flt64
flt65
flt66
flt67
flt68
flt69
flt70

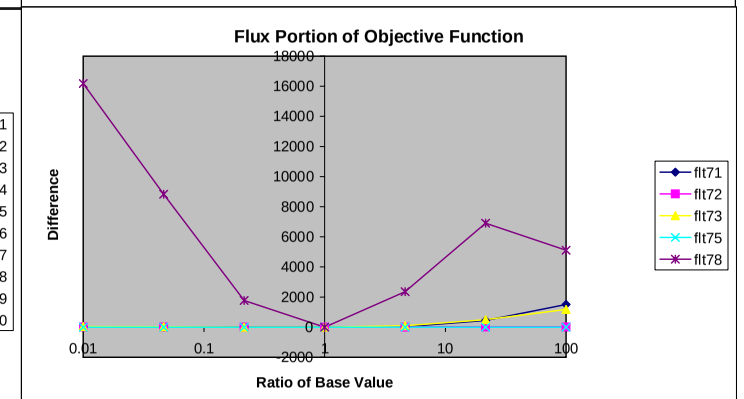
Flux Portion of Objective Function
Difference
Ratio of Base Value
flt71
flt72
flt73
flt75
flt78

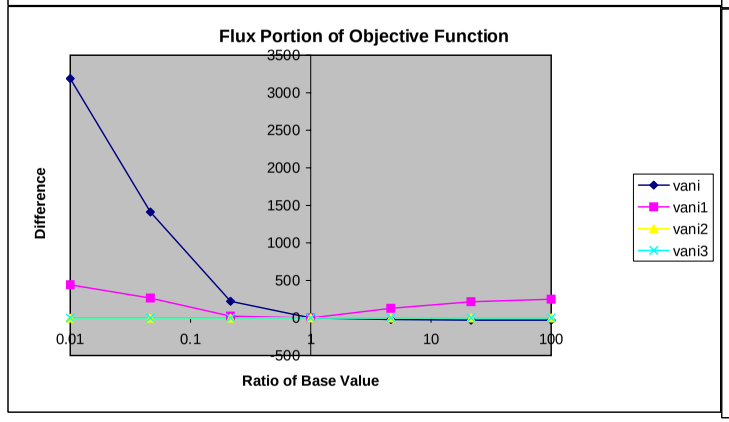
Flux Portion of Objective Function
Difference
Ratio of Base Value
vani
vani1
vani2
vani3

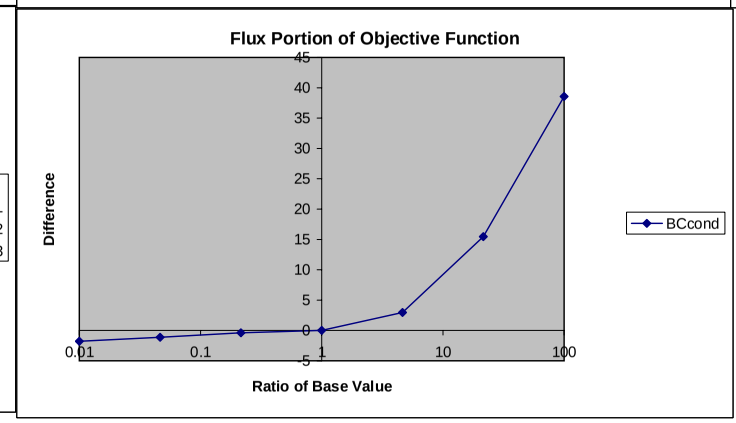
Flux Portion of Objective Function
Difference
Ratio of Base Value
BCcond

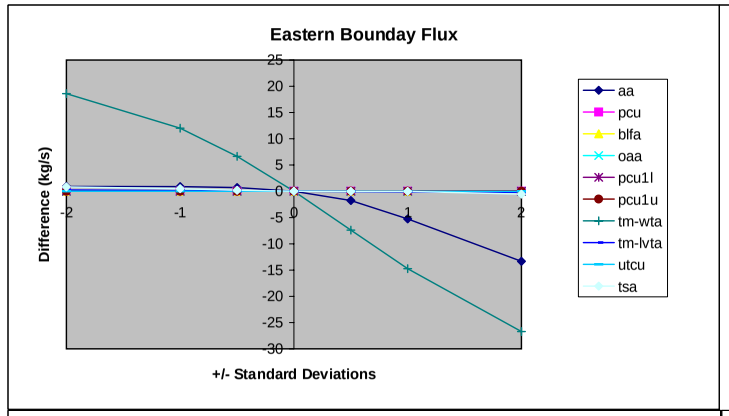
Eastern Bounday Flux
Difference (kg/s)
+/- Standard Deviations
aa
pcu
blfa
oaa
pcu1l
pcu1u
tm-wta
tm-lvta
utcu
tsa

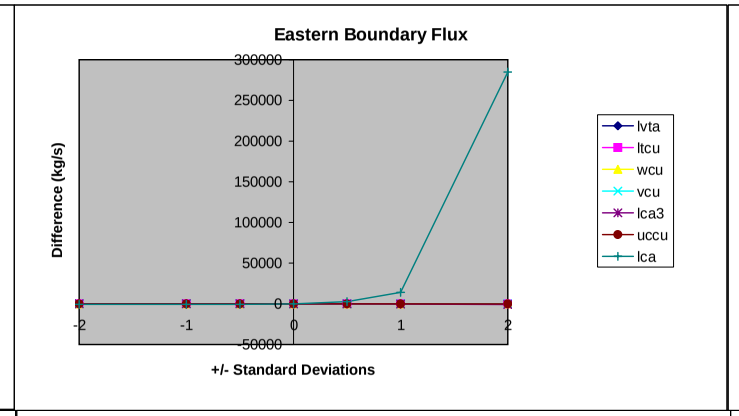
Eastern Boundary Flux
Difference (kg/s)
+/- Standard Deviations
lvta
ltcu
wcu
vcu
lca3
uccu
lca

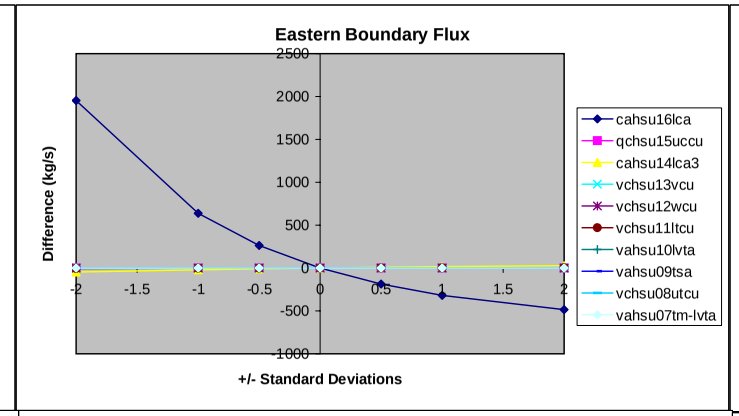
Eastern Boundary Flux
Difference (kg/s)
+/- Standard Deviations
cahsu16lca
qchsu15uccu
cahsu14lca3
vchsu13vcu
vchsu12wcu
vchsu11ltcu
vahsu10lvta
vahsu09tsa
vchsu08utcu
vahsu07tm-lvta

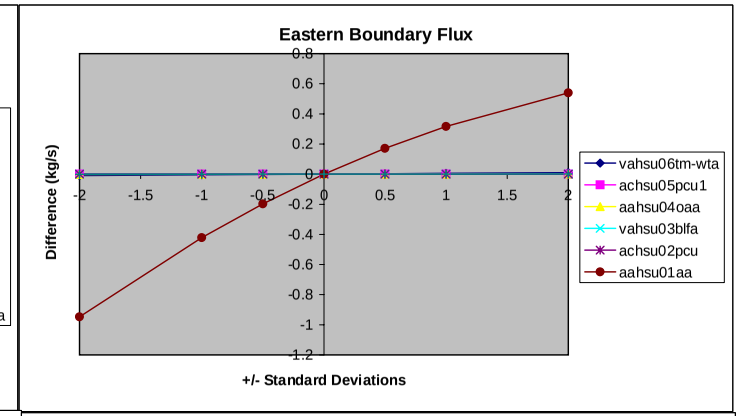
Eastern Boundary Flux
Difference (kg/s)
+/- Standard Deviations
vahsu06tm-wta
achsu05pcu1
aahsu04oaa
vahsu03blfa
achsu02pcu
aahsu01aa

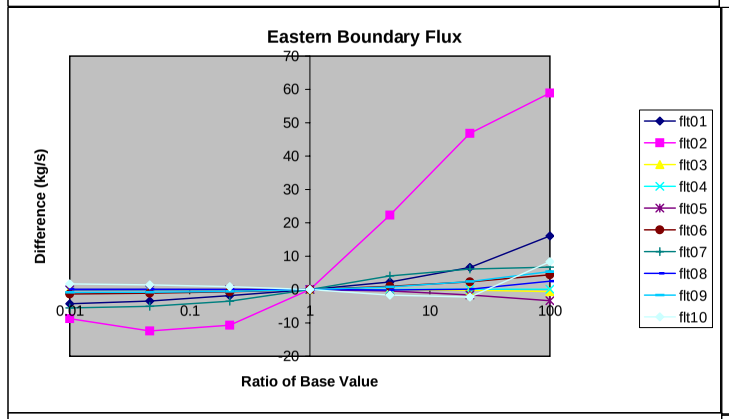
Eastern Boundary Flux
Difference (kg/s)
Ratio of Base Value
flt01
flt02
flt03
flt04
flt05
flt06
flt07
flt08
flt09
flt10

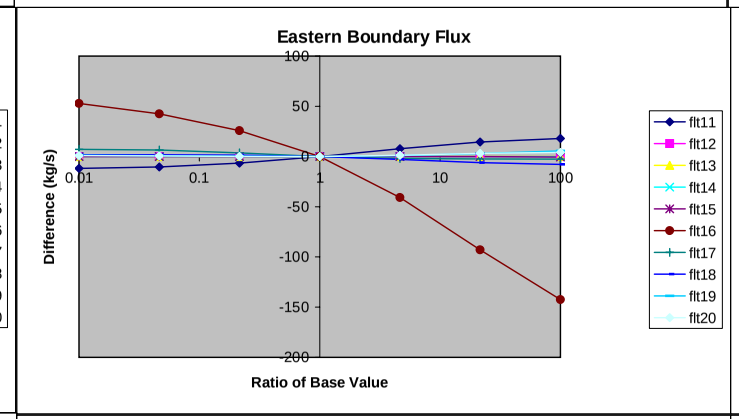
Eastern Boundary Flux
Difference (kg/s)
Ratio of Base Value
flt11
flt12
flt13
flt14
flt15
flt16
flt17
flt18
flt19
flt20

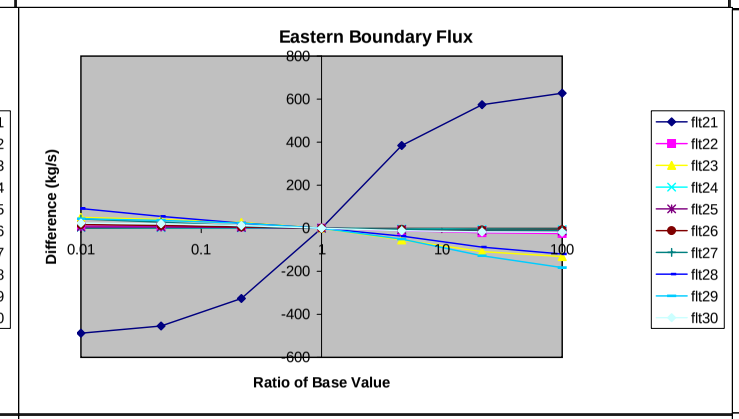
Eastern Boundary Flux
Difference (kg/s)
Ratio of Base Value
flt21
flt22
flt23
flt24
flt25
flt26
flt27
flt28
flt29
flt30

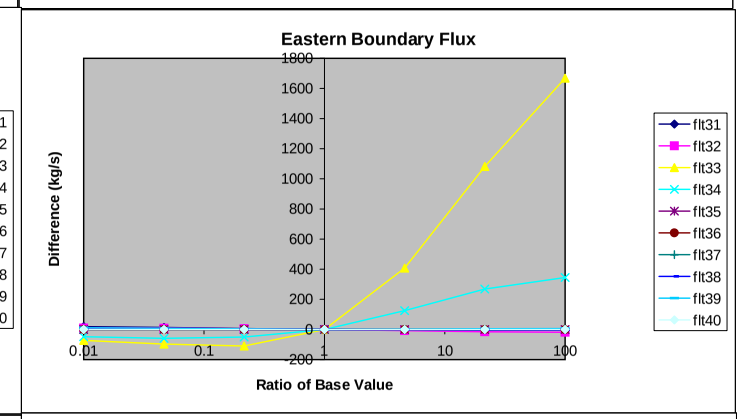
Eastern Boundary Flux
Difference (kg/s)
Ratio of Base Value
flt31
flt32
flt33
flt34
flt35
flt36
flt37
flt38
flt39
flt40

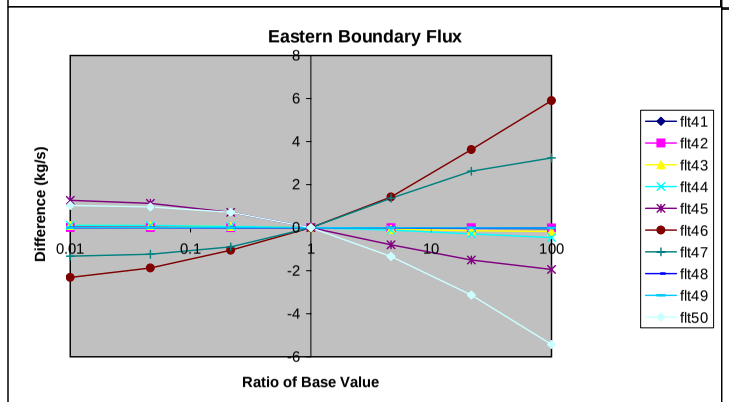
Eastern Boundary Flux
Difference (kg/s)
Ratio of Base Value
flt41
flt42
flt43
flt44
flt45
flt46
flt47
flt48
flt49
flt50

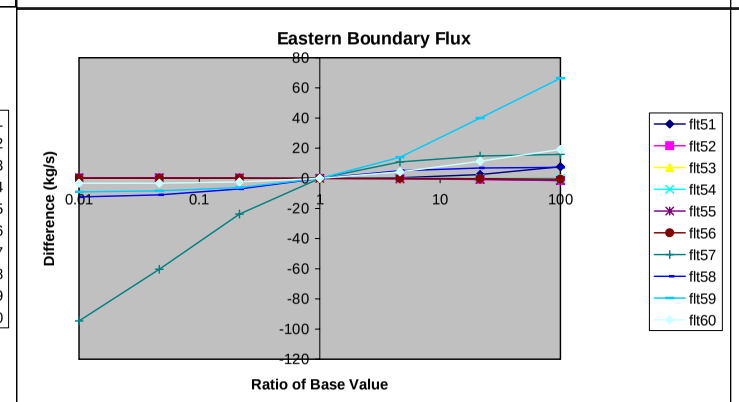
Eastern Boundary Flux
Difference (kg/s)
Ratio of Base Value
flt51
flt52
flt53
flt54
flt55
flt56
flt57
flt58
flt59
flt60

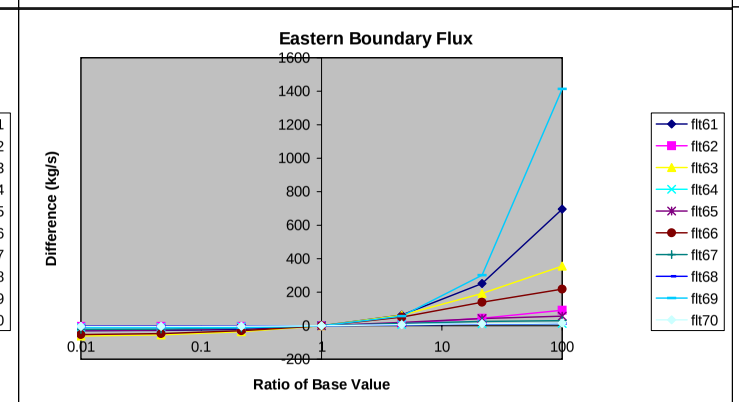
Eastern Boundary Flux
Difference (kg/s)
Ratio of Base Value
flt61
flt62
flt63
flt64
flt65
flt66
flt67
flt68
flt69
flt70

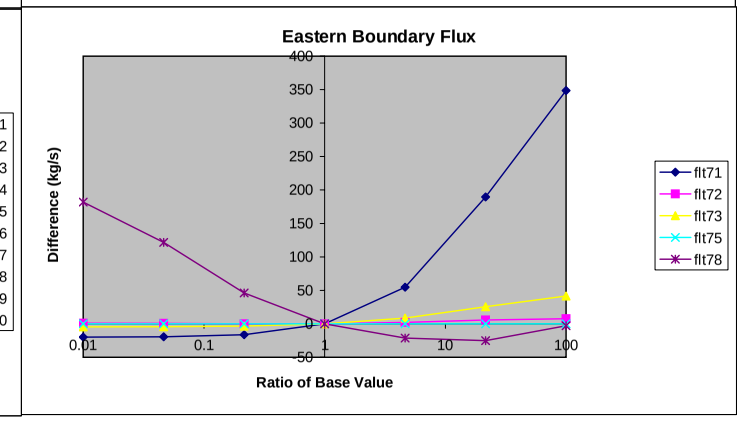
Eastern Boundary Flux
Difference (kg/s)
Ratio of Base Value
flt71
flt72
flt73
flt75
flt78

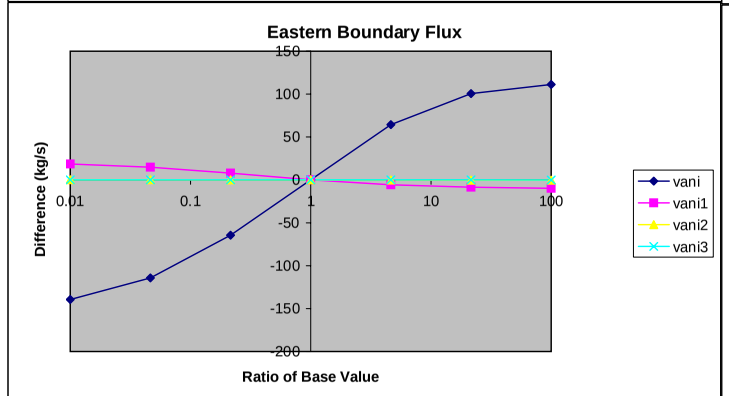
Eastern Boundary Flux
Difference (kg/s)
Ratio of Base Value
vani
vani1
vani2
vani3

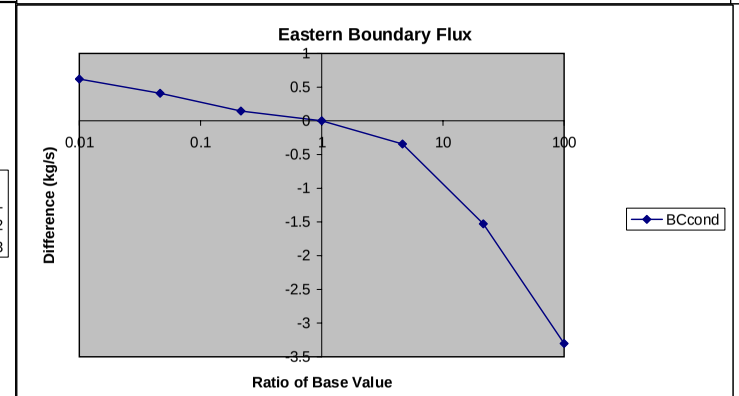
Eastern Boundary Flux
Difference (kg/s)
Ratio of Base Value
BCcond

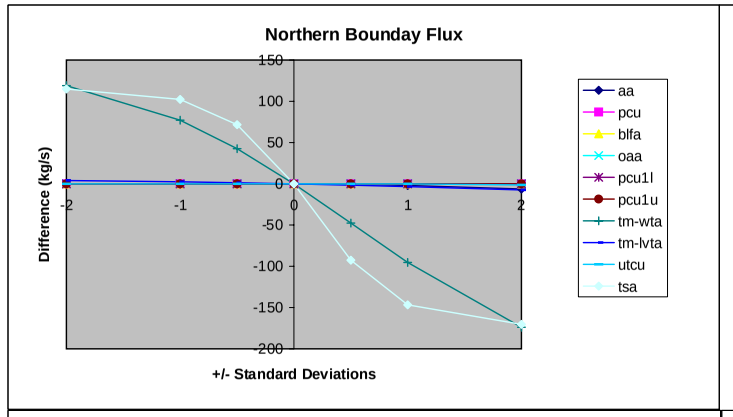
Northern Bounday Flux
Difference (kg/s)
+/- Standard Deviations
aa
pcu
blfa
oaa
pcu1l
pcu1u
tm-wta
tm-lvta
utcu
tsa

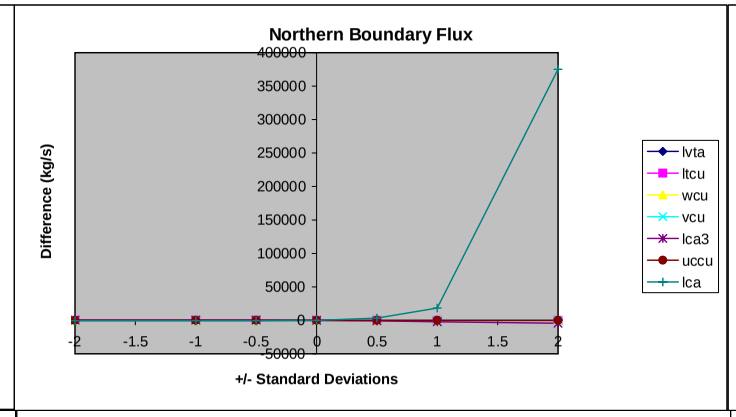
Northern Boundary Flux
Difference (kg/s)
+/- Standard Deviations
lvta
ltcu
wcu
vcu
lca3
uccu
lca

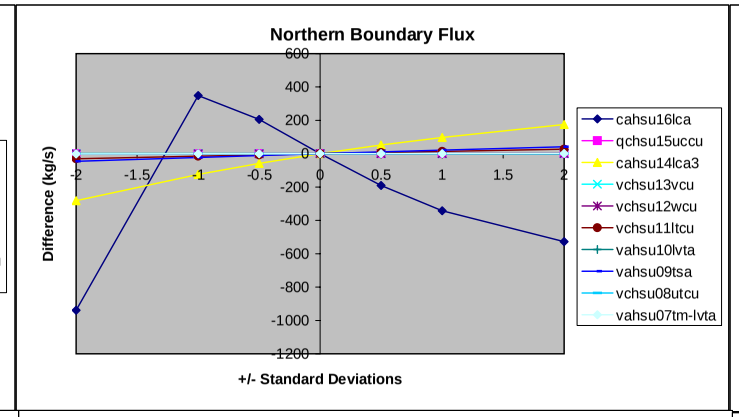
Northern Boundary Flux
Difference (kg/s)
+/- Standard Deviations
cahsu16lca
qchsu15uccu
cahsu14lca3
vchsu13vcu
vchsu12wcu
vchsu11ltcu
vahsu10lvta
vahsu09tsa
vchsu08utcu
vahsu07tm-lvta

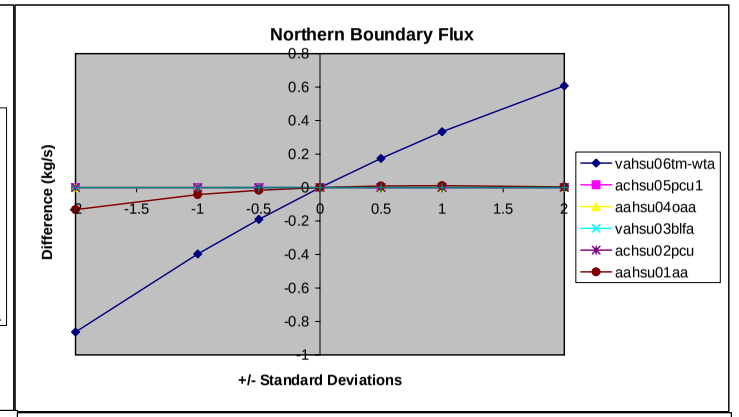
Northern Boundary Flux
Difference (kg/s)
+/- Standard Deviations
vahsu06tm-wta
achsu05pcu1
aahsu04oaa
vahsu03blfa
achsu02pcu
aahsu01aa

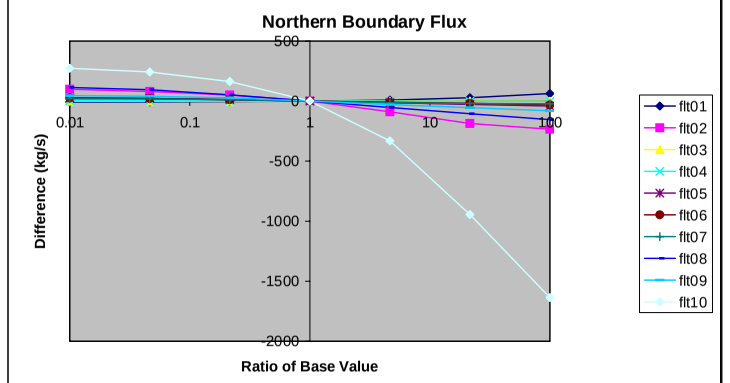
Northern Boundary Flux
Difference (kg/s)
Ratio of Base Value
flt01
flt02
flt03
flt04
flt05
flt06
flt07
flt08
flt09
flt10

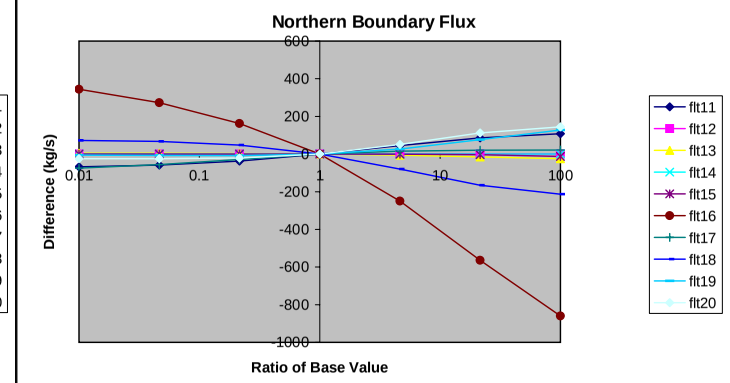
Northern Boundary Flux
Difference (kg/s)
Ratio of Base Value
flt11
flt12
flt13
flt14
flt15
flt16
flt17
flt18
flt19
flt20

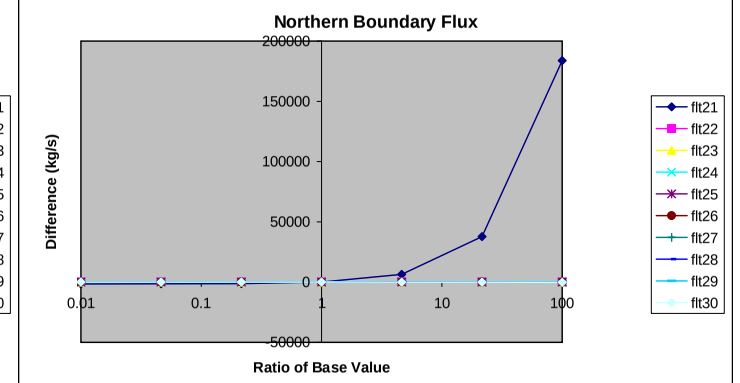
Northern Boundary Flux
Difference (kg/s)
Ratio of Base Value
flt21
flt22
flt23
flt24
flt25
flt26
flt27
flt28
flt29
flt30

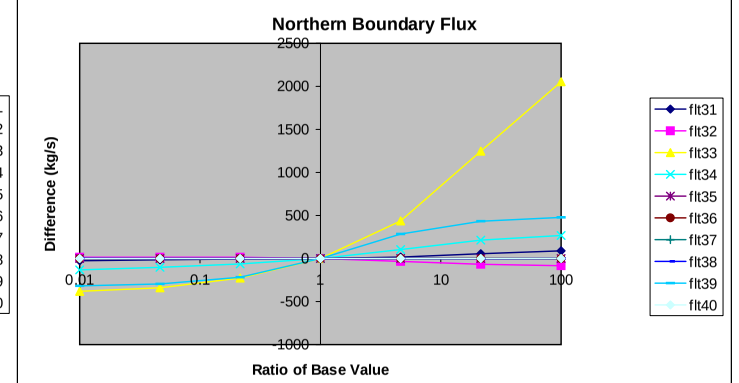
Northern Boundary Flux
Difference (kg/s)
Ratio of Base Value
flt31
flt32
flt33
flt34
flt35
flt36
flt37
flt38
flt39
flt40

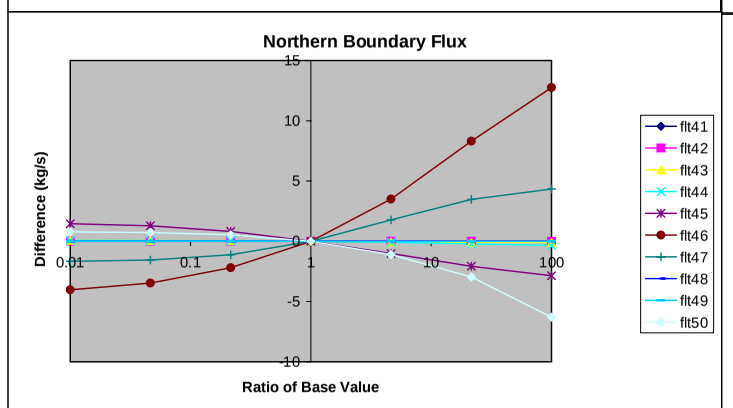
Northern Boundary Flux
Difference (kg/s)
Ratio of Base Value
flt41
flt42
flt43
flt44
flt45
flt46
flt47
flt48
flt49
flt50

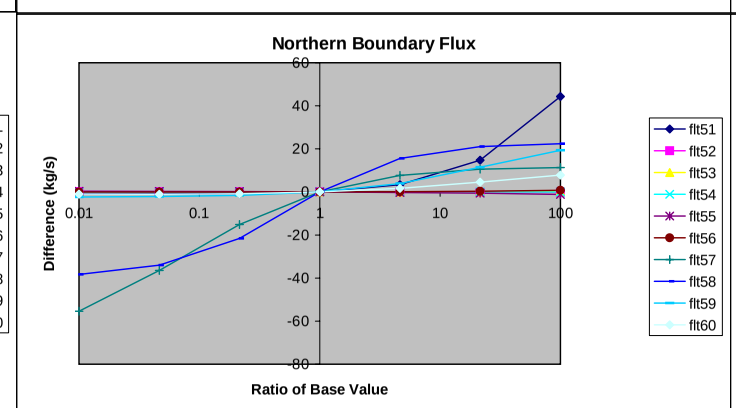
Northern Boundary Flux
Difference (kg/s)
Ratio of Base Value
flt51
flt52
flt53
flt54
flt55
flt56
flt57
flt58
flt59
flt60

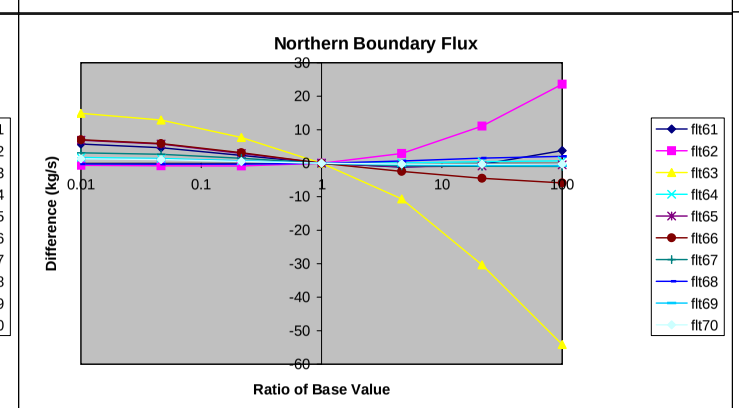
Northern Boundary Flux
Difference (kg/s)
Ratio of Base Value
flt61
flt62
flt63
flt64
flt65
flt66
flt67
flt68
flt69
flt70

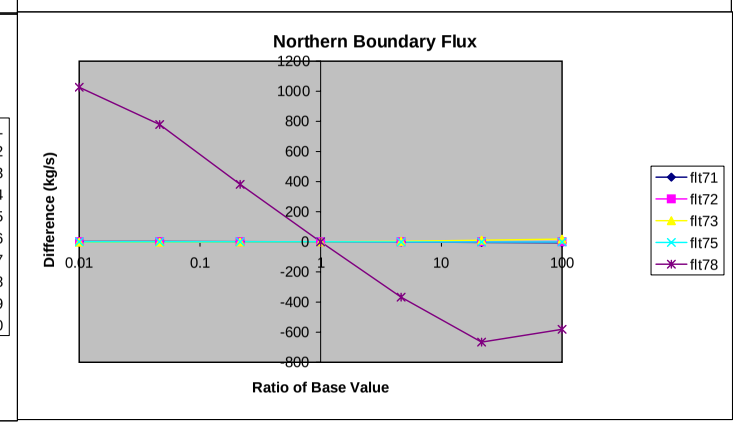
Northern Boundary Flux
Difference (kg/s)
Ratio of Base Value
flt71
flt72
flt73
flt75
flt78

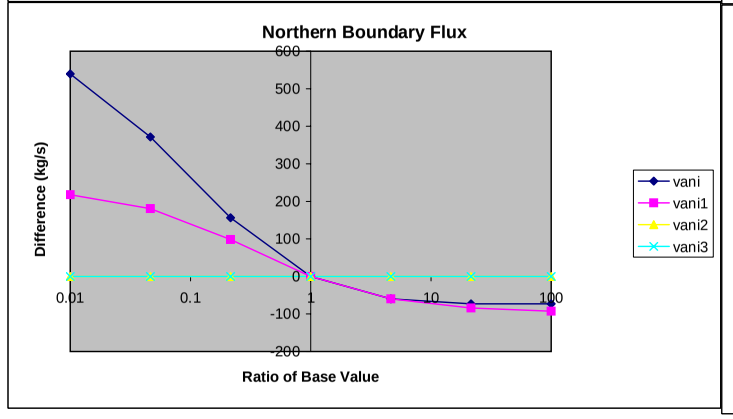
Northern Boundary Flux
Difference (kg/s)
Ratio of Base Value
vani
vani1
vani2
vani3

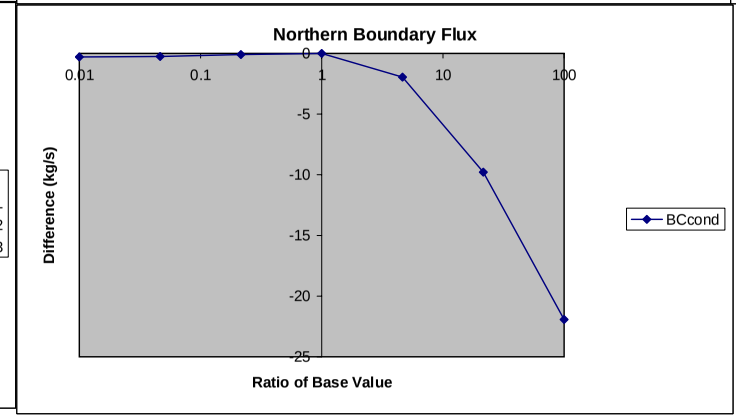
Northern Boundary Flux
Difference (kg/s)
Ratio of Base Value
BCcond

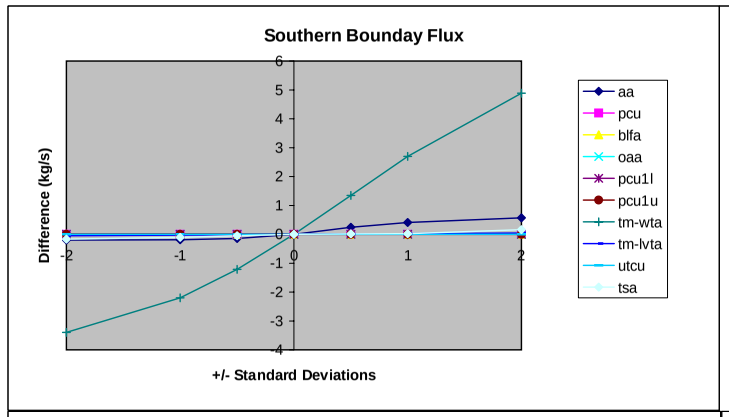
Southern Bounday Flux
Difference (kg/s)
+/- Standard Deviations
aa
pcu
blfa
oaa
pcu1l
pcu1u
tm-wta
tm-lvta
utcu
tsa

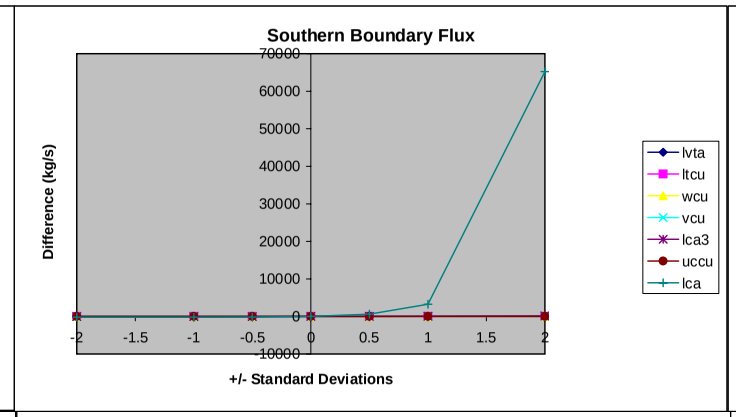
Southern Boundary Flux
Difference (kg/s)
+/- Standard Deviations
lvta
ltcu
wcu
vcu
lca3
uccu
lca

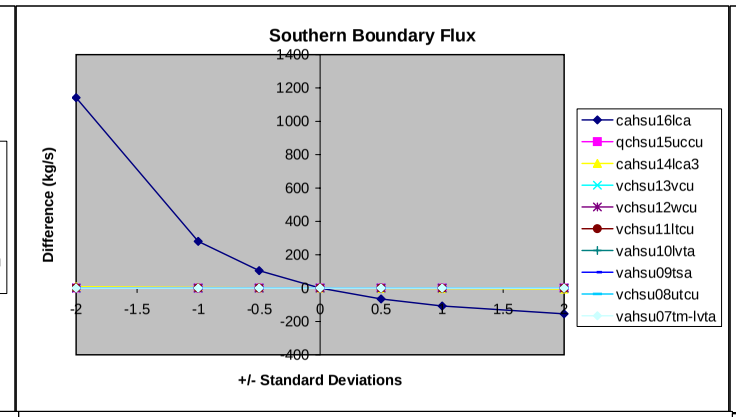
Southern Boundary Flux
Difference (kg/s)
+/- Standard Deviations
cahsu16lca
qchsu15uccu
cahsu14lca3
vchsu13vcu
vchsu12wcu
vchsu11ltcu
vahsu10lvta
vahsu09tsa
vchsu08utcu
vahsu07tm-lvta

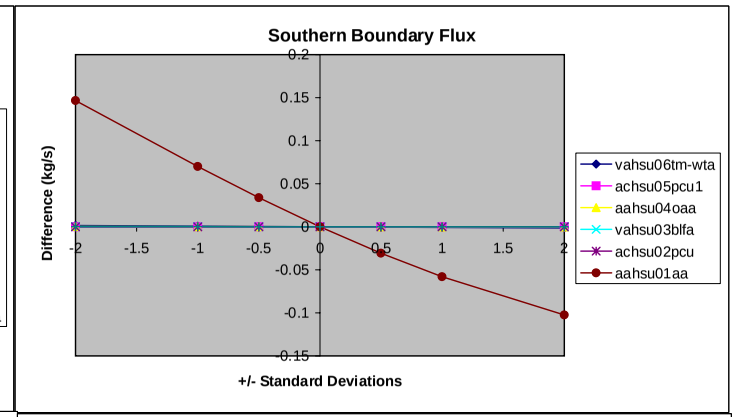
Southern Boundary Flux
Difference (kg/s)
+/- Standard Deviations
vahsu06tm-wta
achsu05pcu1
aahsu04oaa
vahsu03blfa
achsu02pcu
aahsu01aa

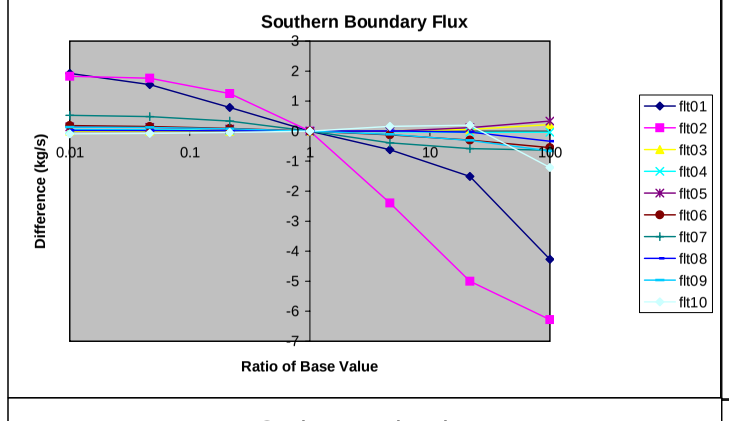
Southern Boundary Flux
Difference (kg/s)
Ratio of Base Value
flt01
flt02
flt03
flt04
flt05
flt06
flt07
flt08
flt09
flt10

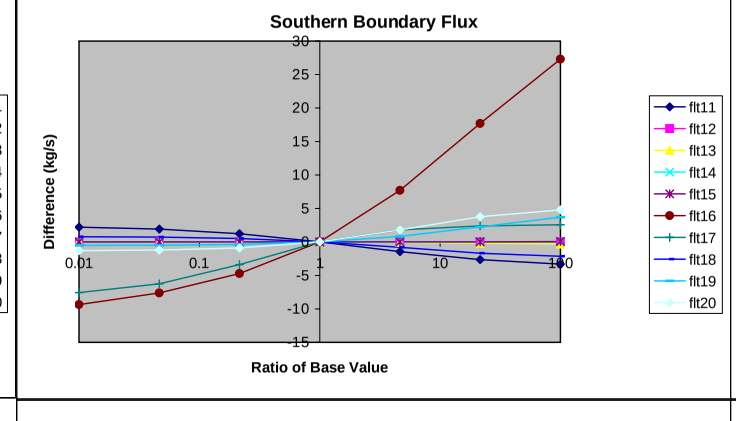
Southern Boundary Flux
Difference (kg/s)
Ratio of Base Value
flt11
flt12
flt13
flt14
flt15
flt16
flt17
flt18
flt19
flt20

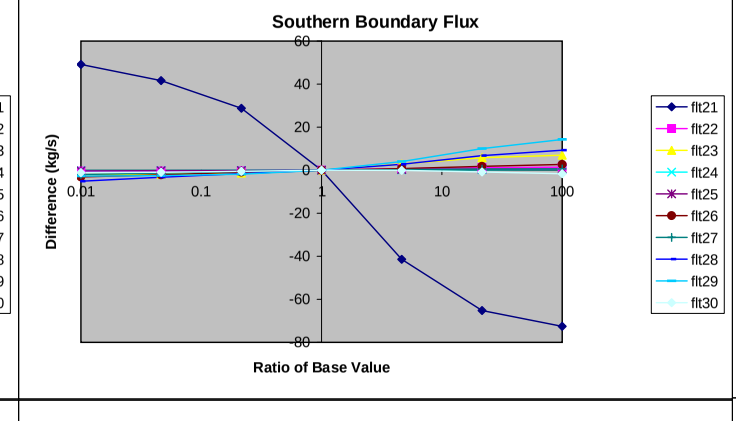
Southern Boundary Flux
Difference (kg/s)
Ratio of Base Value
flt21
flt22
flt23
flt24
flt25
flt26
flt27
flt28
flt29
flt30

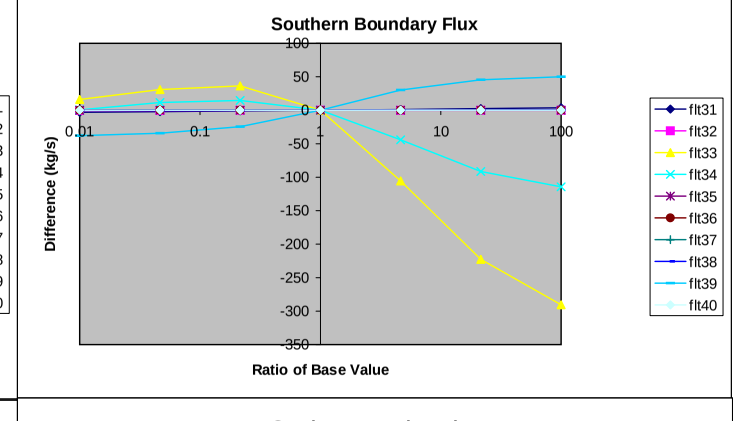
Southern Boundary Flux
Difference (kg/s)
Ratio of Base Value
flt31
flt32
flt33
flt34
flt35
flt36
flt37
flt38
flt39
flt40

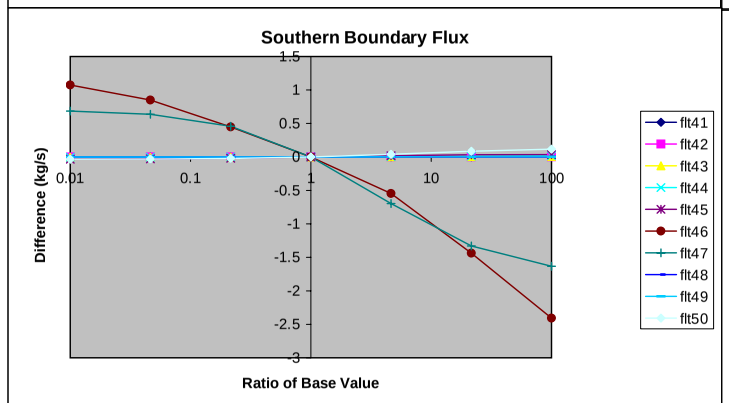
Southern Boundary Flux
Difference (kg/s)
Ratio of Base Value
flt41
flt42
flt43
flt44
flt45
flt46
flt47
flt48
flt49
flt50

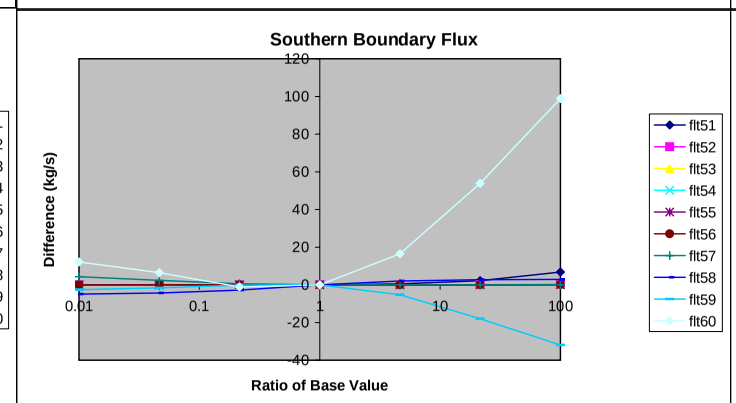
Southern Boundary Flux
Difference (kg/s)
Ratio of Base Value
flt51
flt52
flt53
flt54
flt55
flt56
flt57
flt58
flt59
flt60

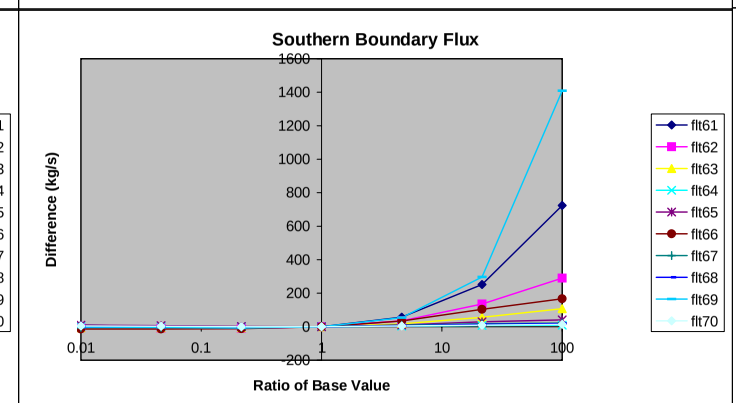
Southern Boundary Flux
Difference (kg/s)
Ratio of Base Value
flt61
flt62
flt63
flt64
flt65
flt66
flt67
flt68
flt69
flt70

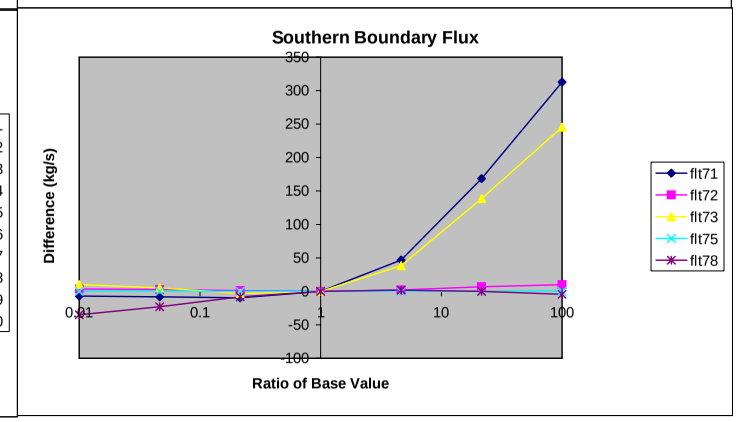
Southern Boundary Flux
Difference (kg/s)
Ratio of Base Value
flt71
flt72
flt73
flt75
flt78

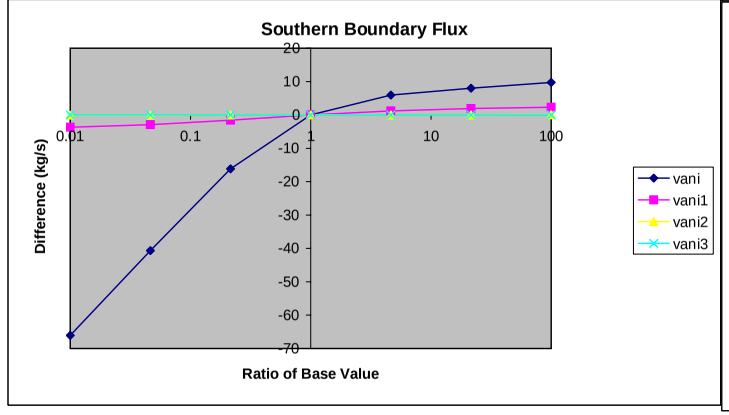
Southern Boundary Flux
Difference (kg/s)
Ratio of Base Value
vani
vani1
vani2
vani3

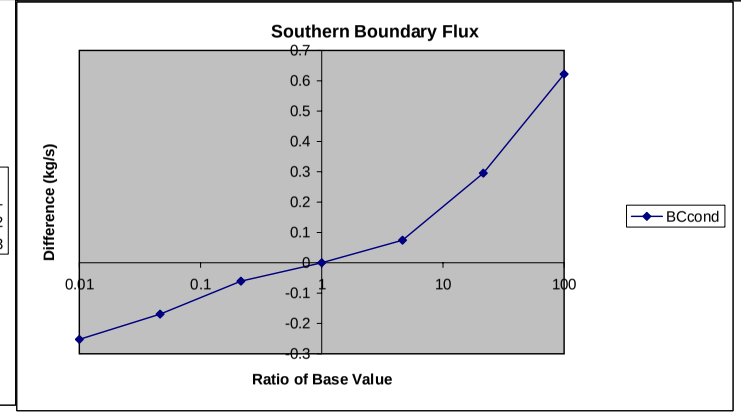
Southern Boundary Flux
Difference (kg/s)
Ratio of Base Value
BCcond

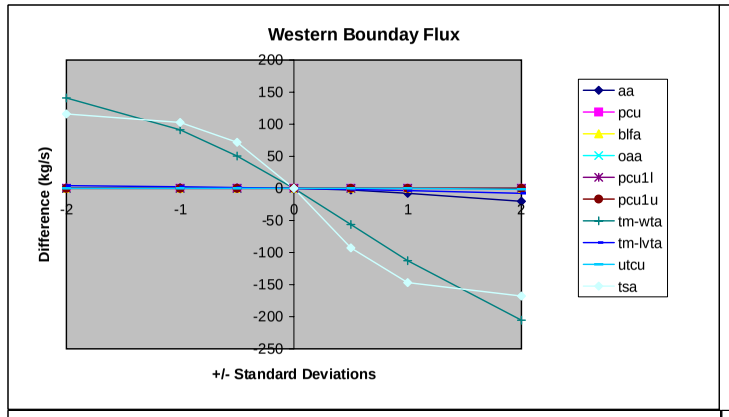
Western Bounday Flux
Difference (kg/s)
+/- Standard Deviations
aa
pcu
blfa
oaa
pcu1l
pcu1u
tm-wta
tm-lvta
utcu
tsa

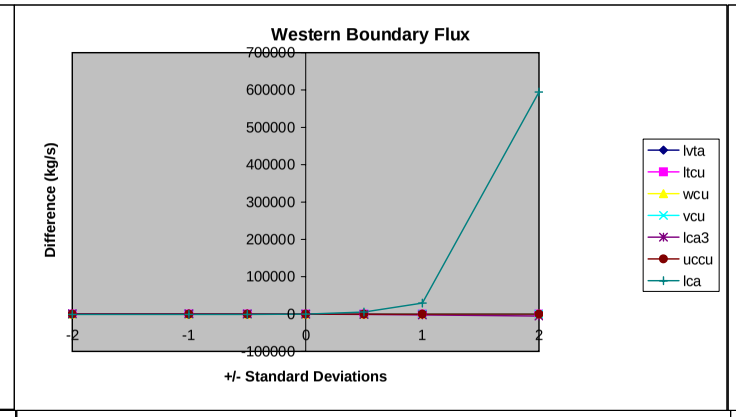
Western Boundary Flux
Difference (kg/s)
+/- Standard Deviations
lvta
ltcu
wcu
vcu
lca3
uccu
lca

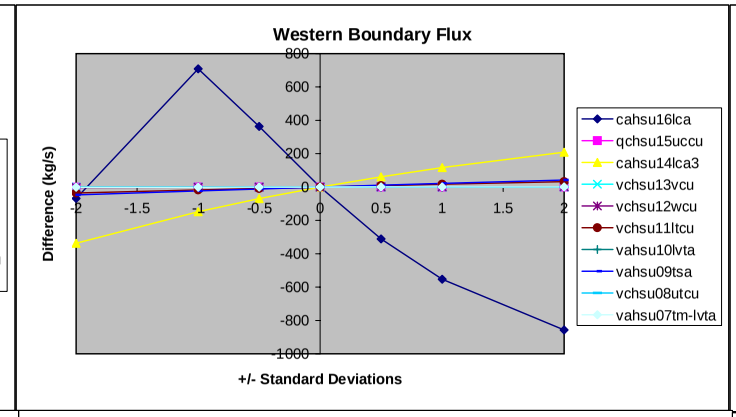
Western Boundary Flux
Difference (kg/s)
+/- Standard Deviations
cahsu16lca
qchsu15uccu
cahsu14lca3
vchsu13vcu
vchsu12wcu
vchsu11ltcu
vahsu10lvta
vahsu09tsa
vchsu08utcu
vahsu07tm-lvta

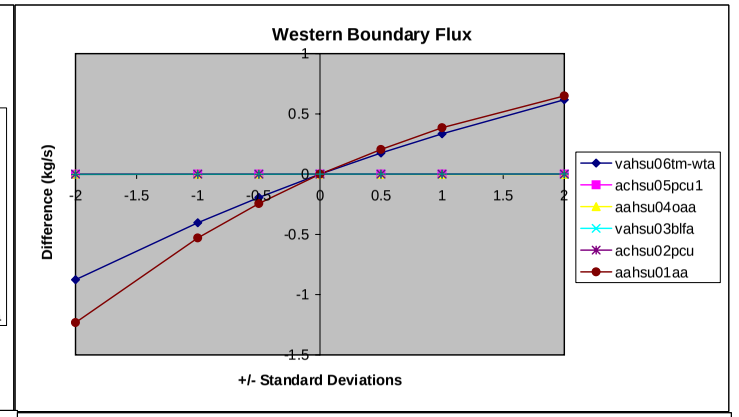
Western Boundary Flux
Difference (kg/s)
+/- Standard Deviations
vahsu06tm-wta
achsu05pcu1
aahsu04oaa
vahsu03blfa
achsu02pcu
aahsu01aa

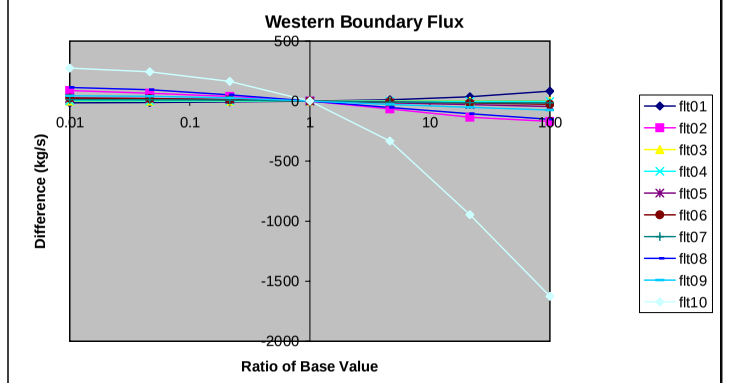
Western Boundary Flux
Difference (kg/s)
Ratio of Base Value
flt01
flt02
flt03
flt04
flt05
flt06
flt07
flt08
flt09
flt10

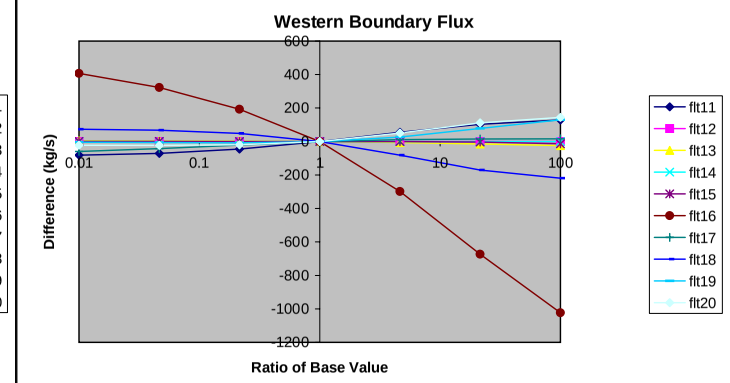
Western Boundary Flux
Difference (kg/s)
Ratio of Base Value
flt11
flt12
flt13
flt14
flt15
flt16
flt17
flt18
flt19
flt20

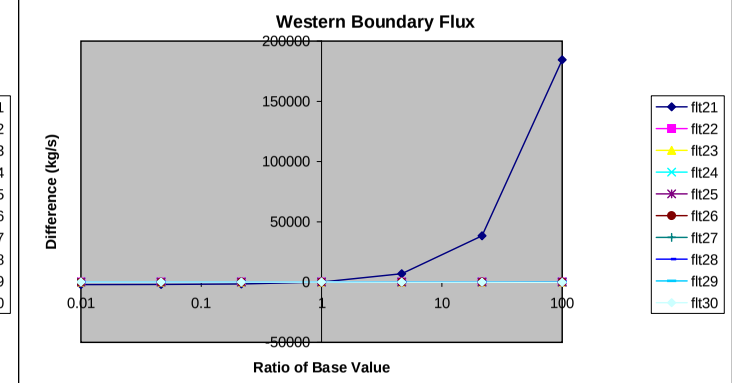
Western Boundary Flux
Difference (kg/s)
Ratio of Base Value
flt21
flt22
flt23
flt24
flt25
flt26
flt27
flt28
flt29
flt30

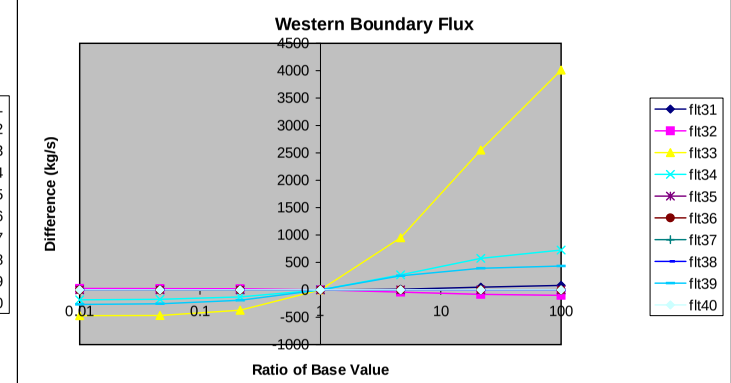
Western Boundary Flux
Difference (kg/s)
Ratio of Base Value
flt31
flt32
flt33
flt34
flt35
flt36
flt37
flt38
flt39
flt40

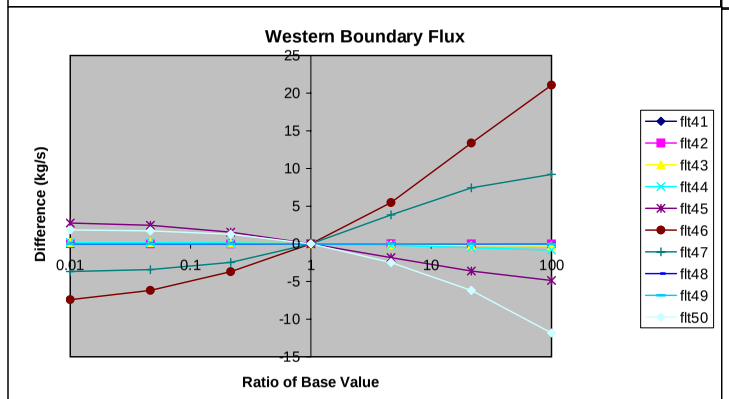
Western Boundary Flux
Difference (kg/s)
Ratio of Base Value
flt41
flt42
flt43
flt44
flt45
flt46
flt47
flt48
flt49
flt50

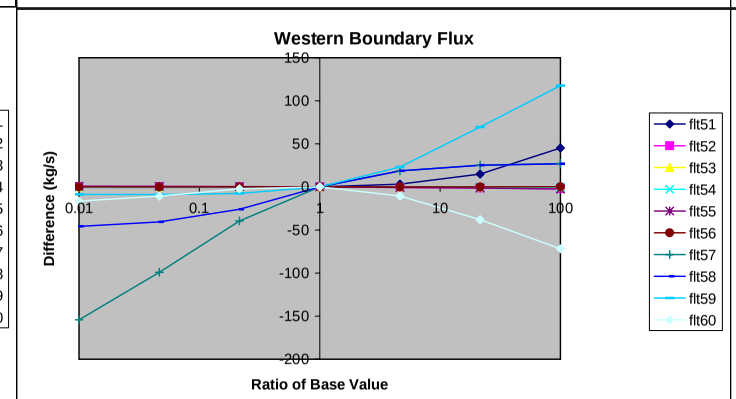
Western Boundary Flux
Difference (kg/s)
Ratio of Base Value
flt51
flt52
flt53
flt54
flt55
flt56
flt57
flt58
flt59
flt60

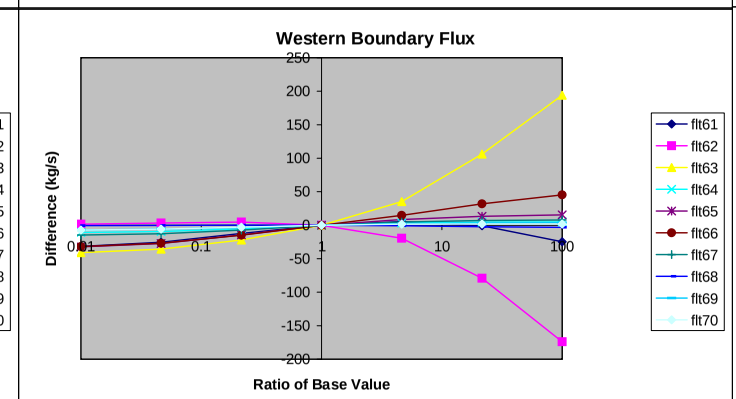
Western Boundary Flux
Difference (kg/s)
Ratio of Base Value
flt61
flt62
flt63
flt64
flt65
flt66
flt67
flt68
flt69
flt70

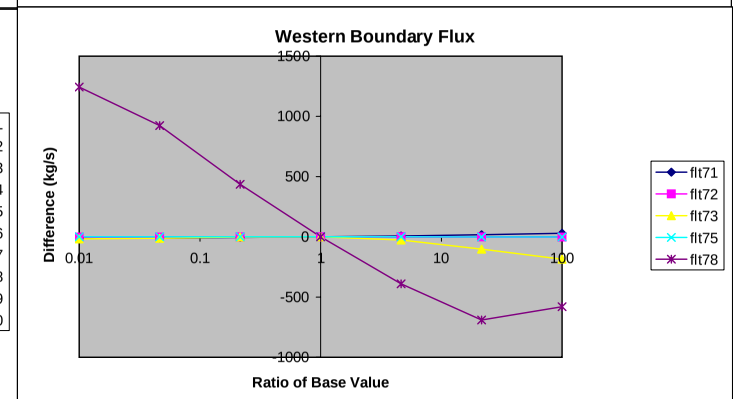
Western Boundary Flux
Difference (kg/s)
Ratio of Base Value
flt71
flt72
flt73
flt75
flt78

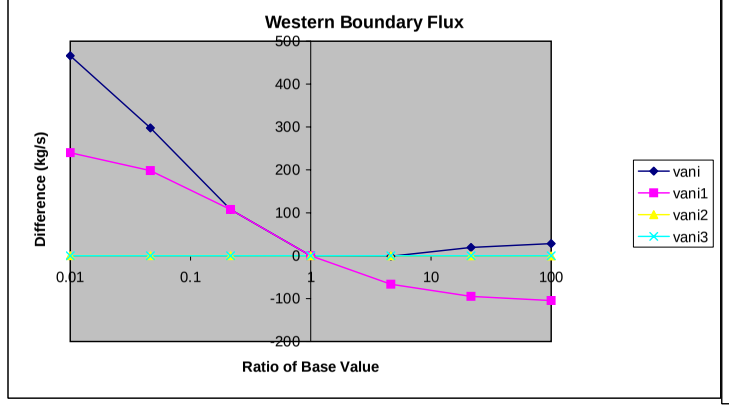
Western Boundary Flux
Difference (kg/s)
Ratio of Base Value
vani
vani1
vani2
vani3

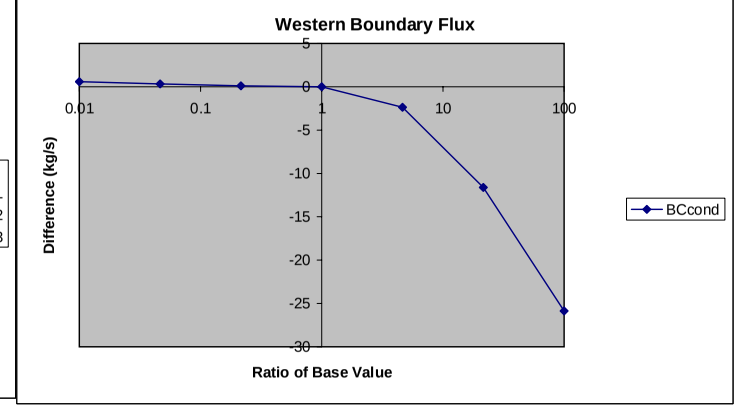
Western Boundary Flux
Difference (kg/s)
Ratio of Base Value
BCcond

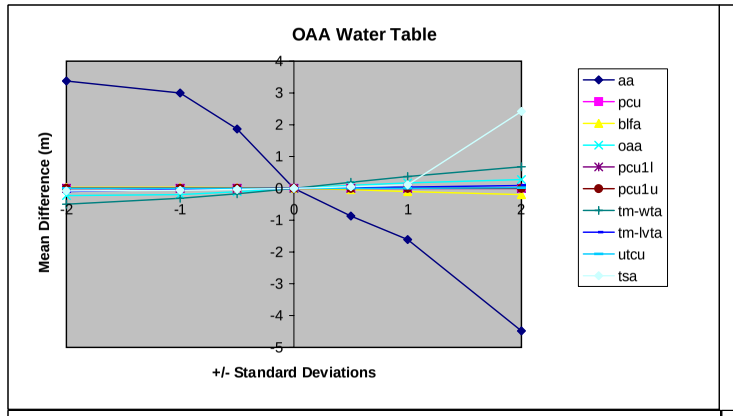
OAA Water Table
Mean Difference (m)
+/- Standard Deviations
aa
pcu
blfa
oaa
pcu1l
pcu1u
tm-wta
tm-lvta
utcu
tsa

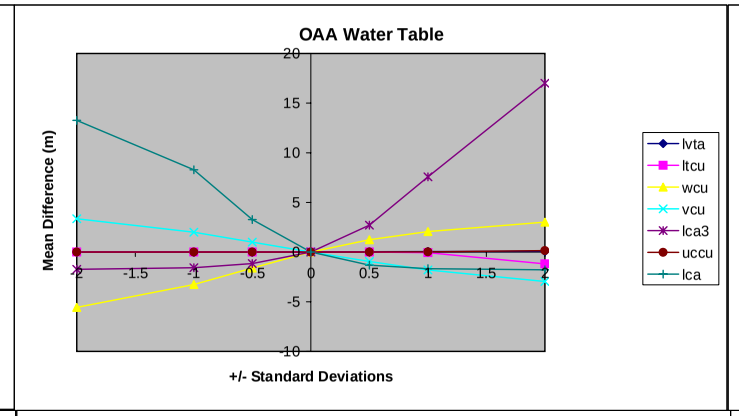
OAA Water Table
Mean Difference (m)
+/- Standard Deviations
lvta
ltcu
wcu
vcu
lca3
uccu
lca

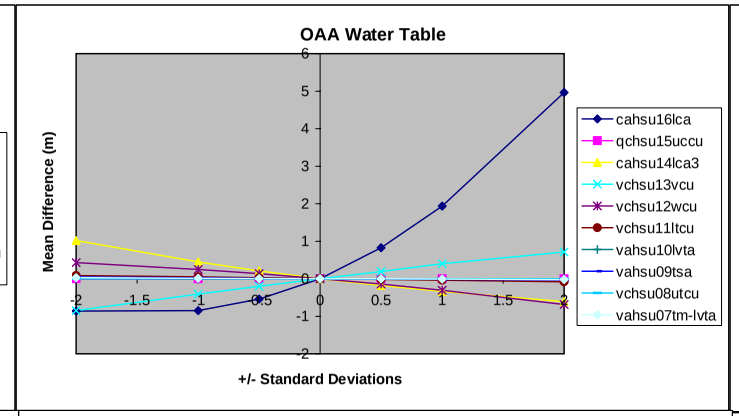
OAA Water Table
Mean Difference (m)
+/- Standard Deviations
cahsu16lca
qchsu15uccu
cahsu14lca3
vchsu13vcu
vchsu12wcu
vchsu11ltcu
vahsu10lvta
vahsu09tsa
vchsu08utcu
vahsu07tm-lvta

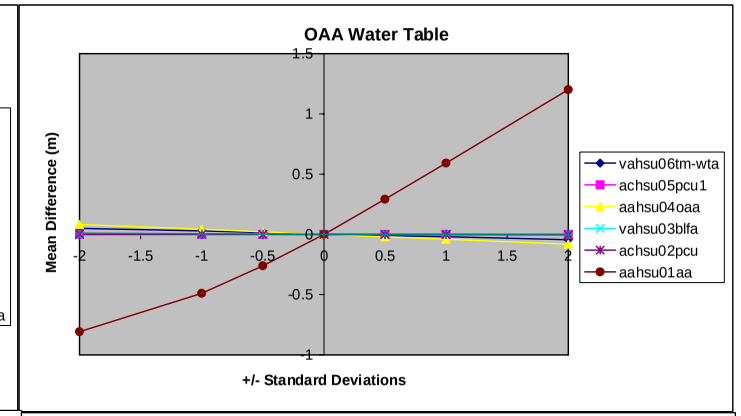
OAA Water Table
Mean Difference (m)
+/- Standard Deviations
vahsu06tm-wta
achsu05pcu1
aahsu04oaa
vahsu03blfa
achsu02pcu
aahsu01aa

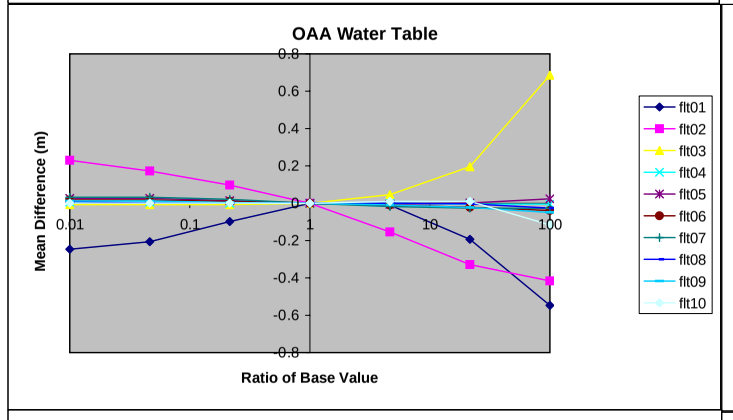
OAA Water Table
Mean Difference (m)
Ratio of Base Value
flt01
flt02
flt03
flt04
flt05
flt06
flt07
flt08
flt09
flt10

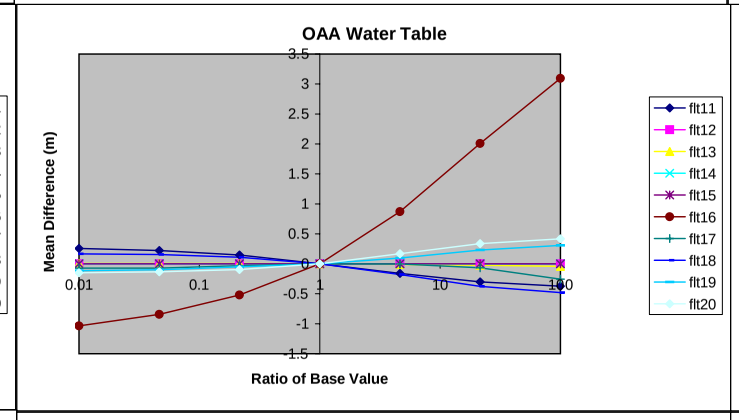
OAA Water Table
Mean Difference (m)
Ratio of Base Value
flt11
flt12
flt13
flt14
flt15
flt16
flt17
flt18
flt19
flt20

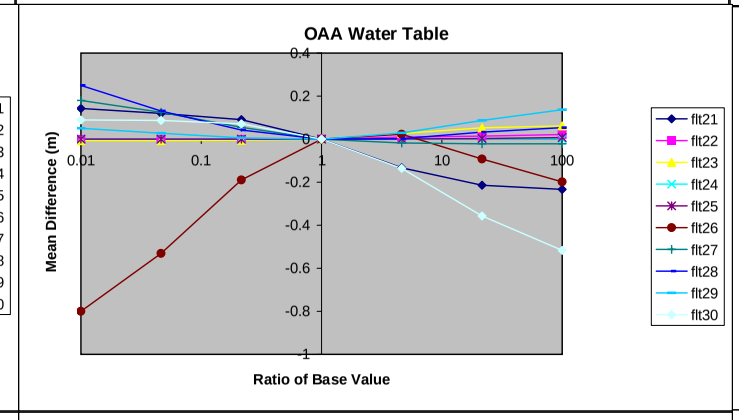
OAA Water Table
Mean Difference (m)
Ratio of Base Value
flt21
flt22
flt23
flt24
flt25
flt26
flt27
flt28
flt29
flt30

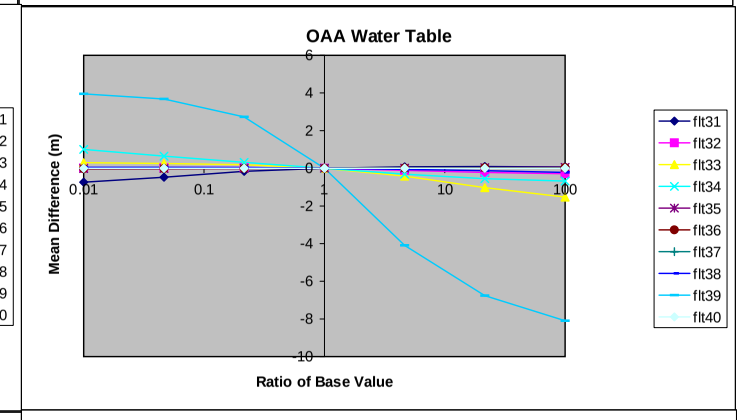
OAA Water Table
Mean Difference (m)
Ratio of Base Value
flt31
flt32
flt33
flt34
flt35
flt36
flt37
flt38
flt39
flt40

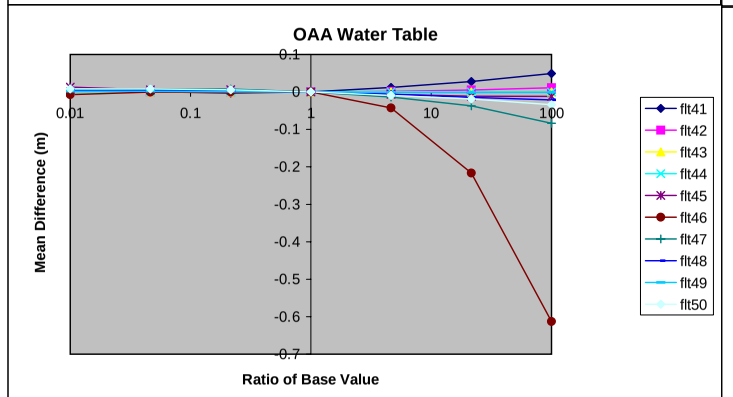
OAA Water Table
Mean Difference (m)
Ratio of Base Value
flt41
flt42
flt43
flt44
flt45
flt46
flt47
flt48
flt49
flt50

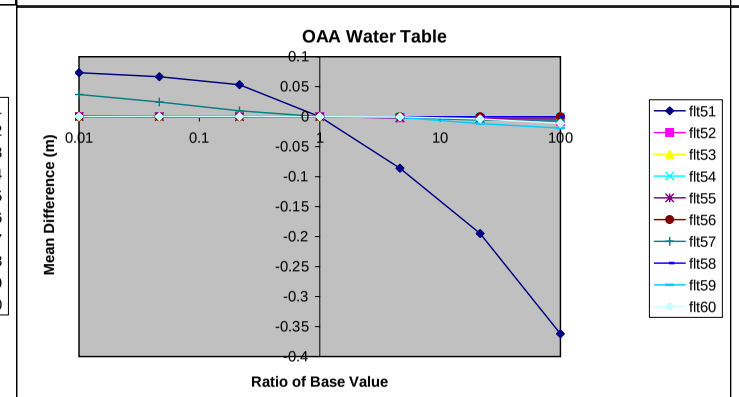
OAA Water Table
Mean Difference (m)
Ratio of Base Value
flt51
flt52
flt53
flt54
flt55
flt56
flt57
flt58
flt59
flt60

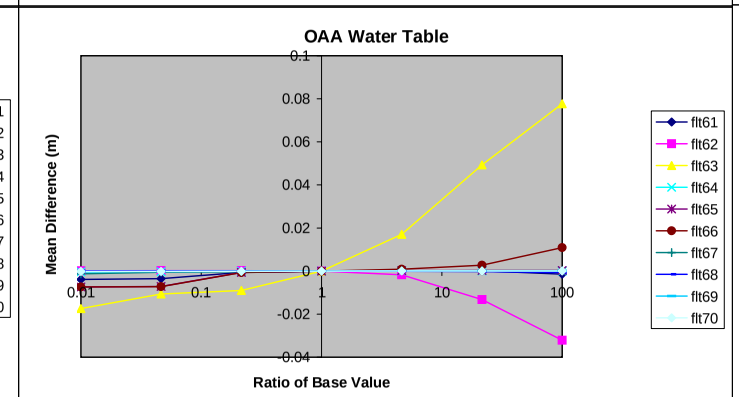
OAA Water Table
Mean Difference (m)
Ratio of Base Value
flt61
flt62
flt63
flt64
flt65
flt66
flt67
flt68
flt69
flt70

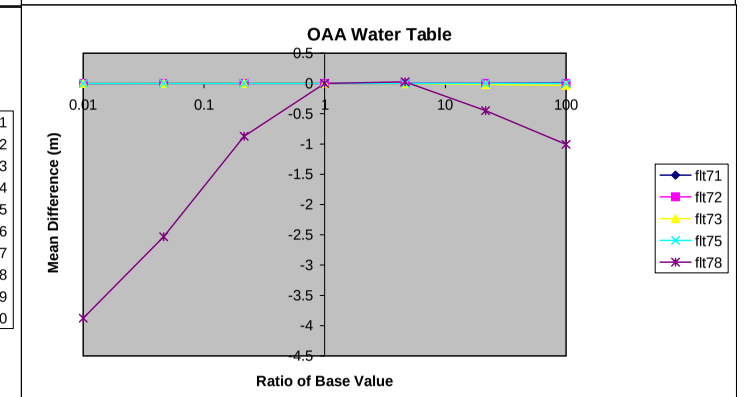
OAA Water Table
Mean Difference (m)
Ratio of Base Value
flt71
flt72
flt73
flt75
flt78

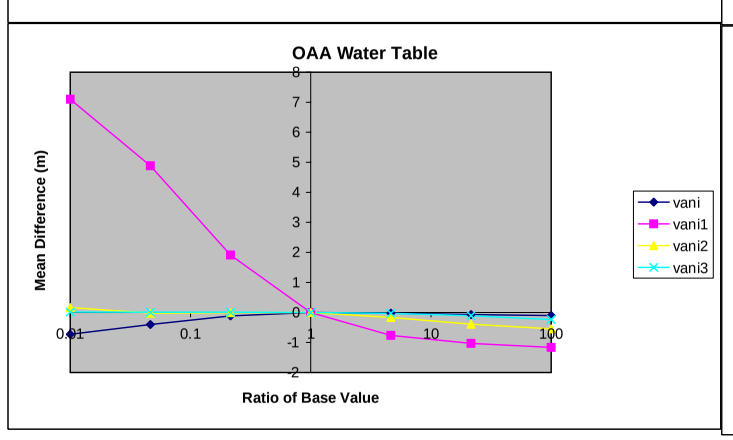
OAA Water Table
Mean Difference (m)
Ratio of Base Value
vani
vani1
vani2
vani3

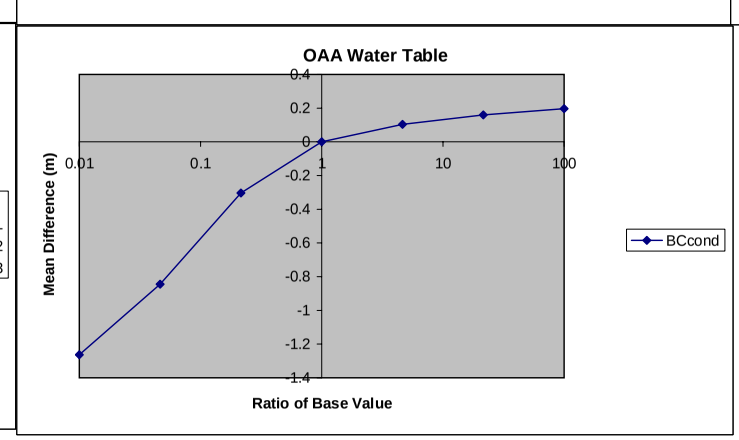
OAA Water Table
Mean Difference (m)
Ratio of Base Value
BCcond

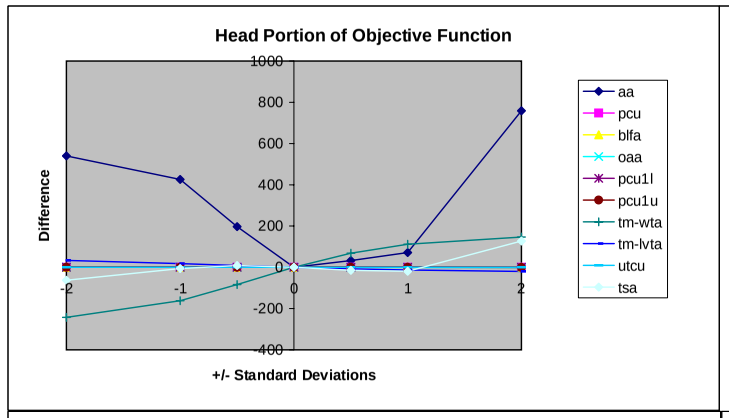
Head Portion of Objective Function
Difference
+/- Standard Deviations
aa
pcu
blfa
oaa
pcu1l
pcu1u
tm-wta
tm-lvta
utcu
tsa

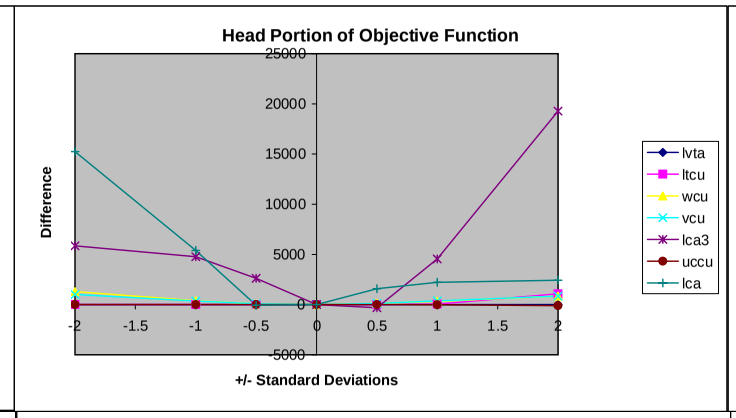
Head Portion of Objective Function
Difference
+/- Standard Deviations
lvta
ltcu
wcu
vcu
lca3
uccu
lca

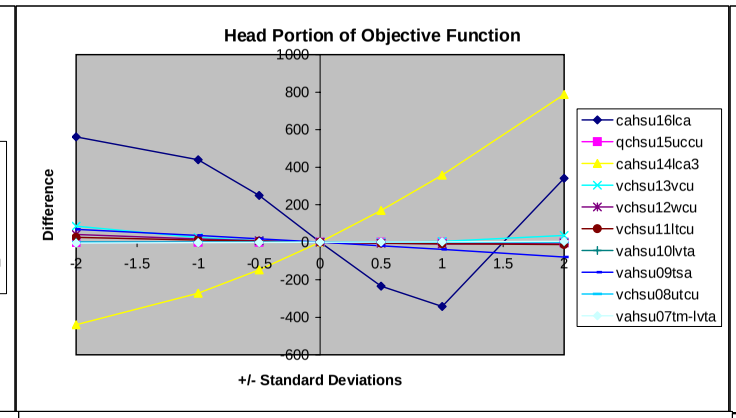
Head Portion of Objective Function
Difference
+/- Standard Deviations
cahsu16lca
qchsu15uccu
cahsu14lca3
vchsu13vcu
vchsu12wcu
vchsu11ltcu
vahsu10lvta
vahsu09tsa
vchsu08utcu
vahsu07tm-lvta

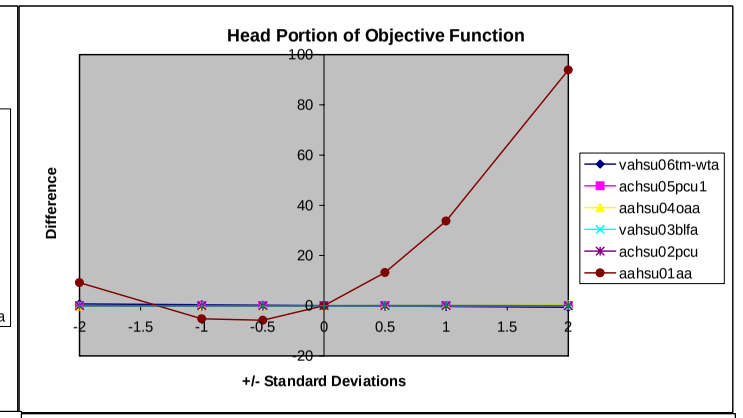
Head Portion of Objective Function
Difference
+/- Standard Deviations
vahsu06tm-wta
achsu05pcu1
aahsu04oaa
vahsu03blfa
achsu02pcu
aahsu01aa

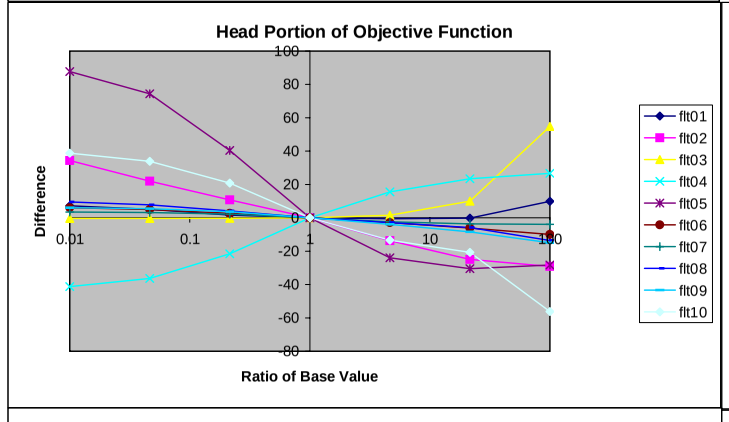
Head Portion of Objective Function
Difference
Ratio of Base Value
flt01
flt02
flt03
flt04
flt05
flt06
flt07
flt08
flt09
flt10

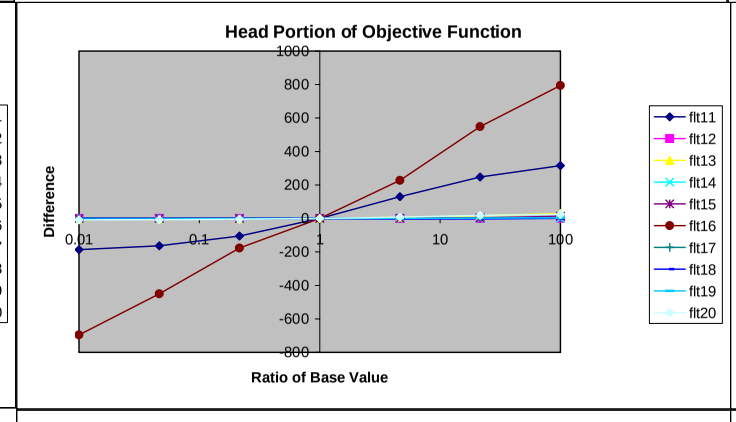
Head Portion of Objective Function
Difference
Ratio of Base Value
flt11
flt12
flt13
flt14
flt15
flt16
flt17
flt18
flt19
flt20

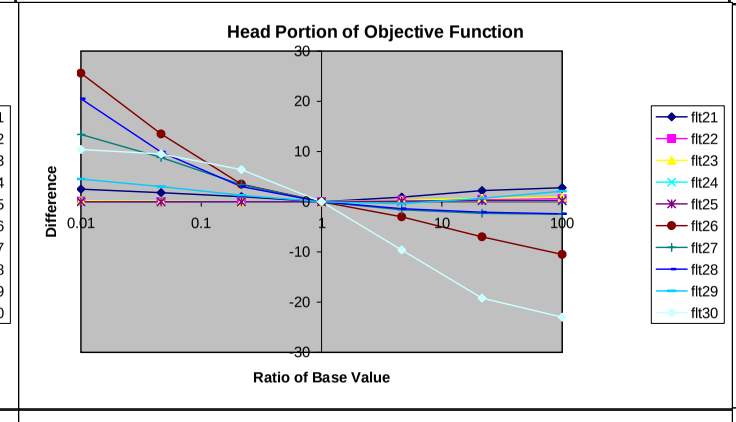
Head Portion of Objective Function
Difference
Ratio of Base Value
flt21
flt22
flt23
flt24
flt25
flt26
flt27
flt28
flt29
flt30

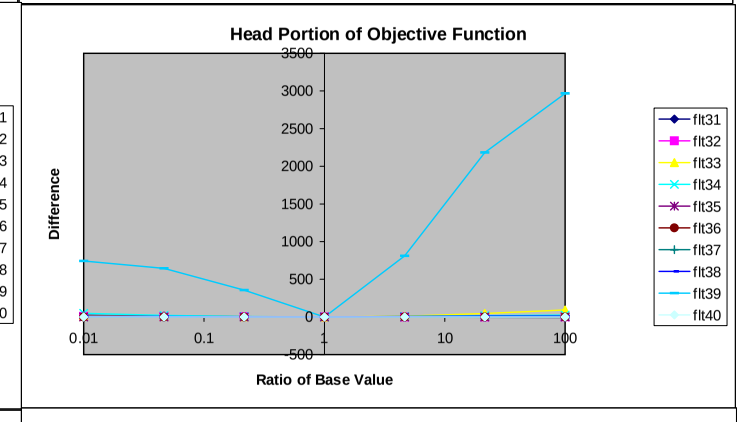
Head Portion of Objective Function
Difference
Ratio of Base Value
flt31
flt32
flt33
flt34
flt35
flt36
flt37
flt38
flt39
flt40

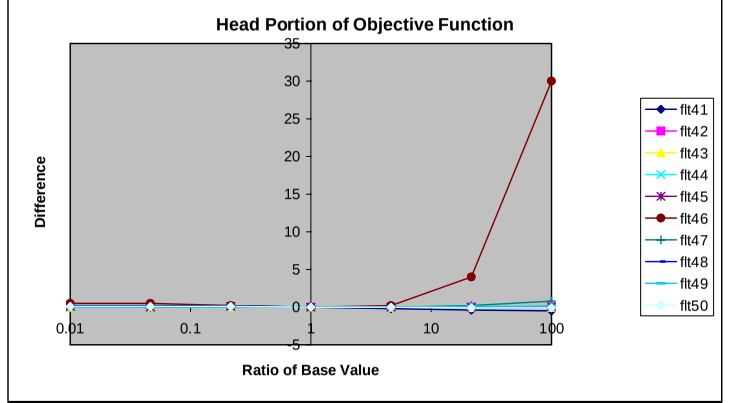
Head Portion of Objective Function
Difference
Ratio of Base Value
flt41
flt42
flt43
flt44
flt45
flt46
flt47
flt48
flt49
flt50

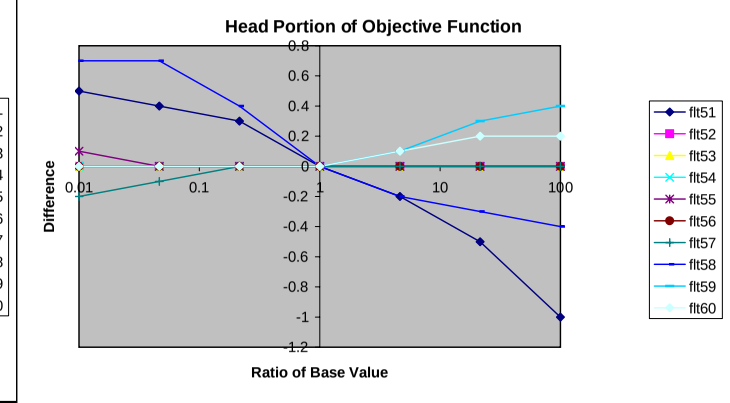
Head Portion of Objective Function
Difference
Ratio of Base Value
flt51
flt52
flt53
flt54
flt55
flt56
flt57
flt58
flt59
flt60

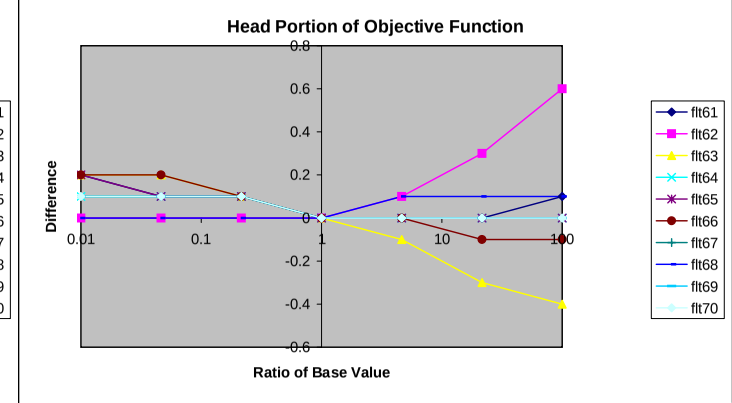
Head Portion of Objective Function
Difference
Ratio of Base Value
flt61
flt62
flt63
flt64
flt65
flt66
flt67
flt68
flt69
flt70

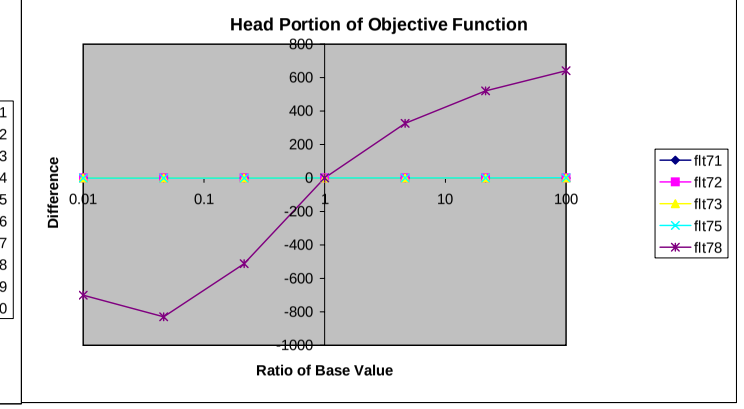
Head Portion of Objective Function
Difference
Ratio of Base Value
flt71
flt72
flt73
flt75
flt78

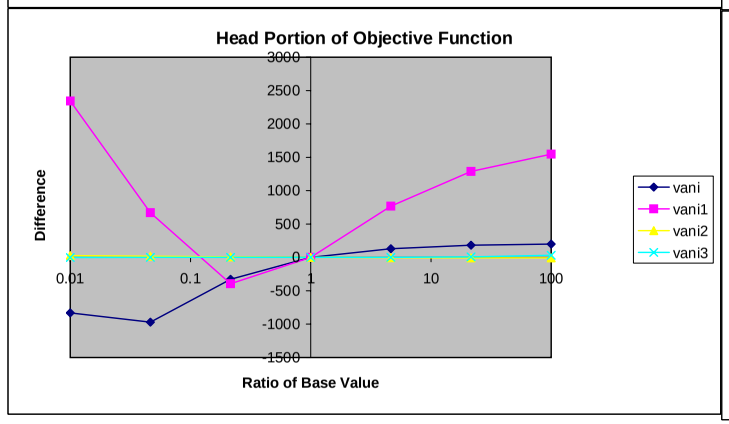
Head Portion of Objective Function
Difference
Ratio of Base Value
vani
vani1
vani2
vani3

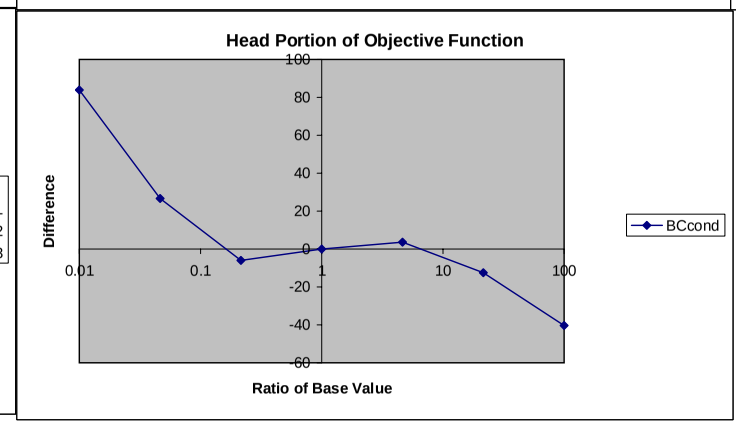
Head Portion of Objective Function
Difference
Ratio of Base Value
BCcond

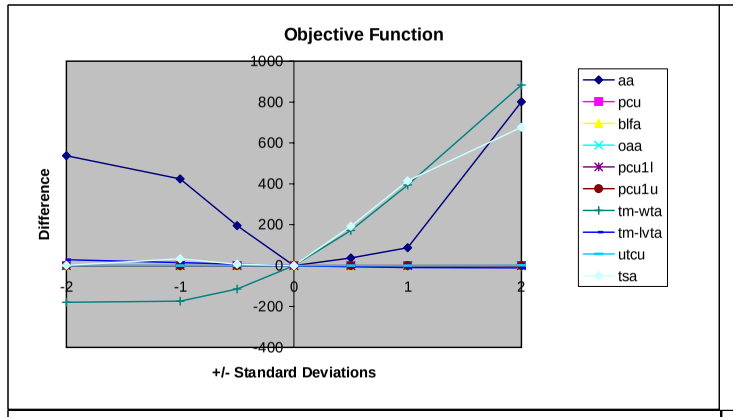
Objective Function
Difference
+/- Standard Deviations
aa
pcu
blfa
oaa
pcu1l
pcu1u
tm-wta
tm-lvta
utcu
tsa

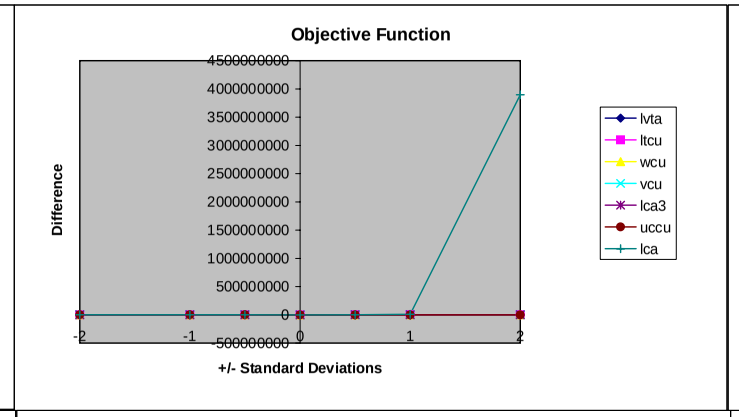
Objective Function
Difference
+/- Standard Deviations
lvta
ltcu
wcu
vcu
lca3
uccu
lca

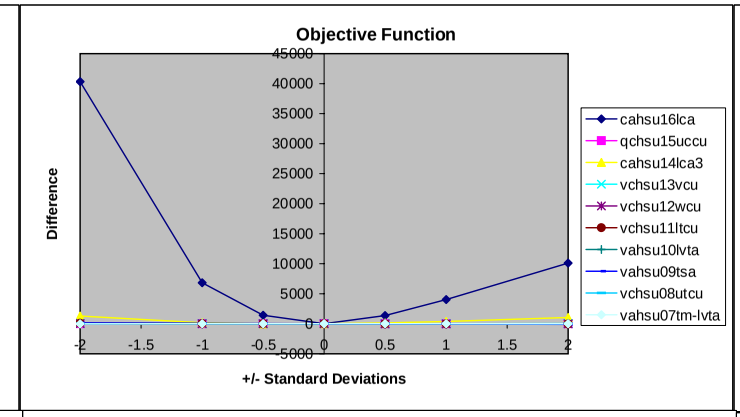
Objective Function
Difference
+/- Standard Deviations
cahsu16lca
qchsu15uccu
cahsu14lca3
vchsu13vcu
vchsu12wcu
vchsu11ltcu
vahsu10lvta
vahsu09tsa
vchsu08utcu
vahsu07tm-lvta

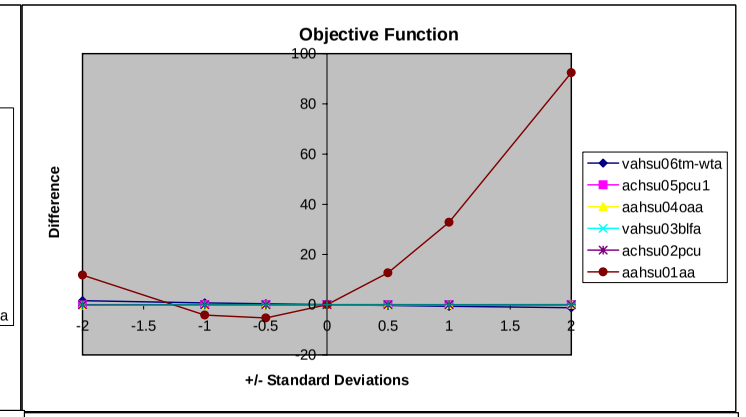
Objective Function
Difference
+/- Standard Deviations
vahsu06tm-wta
achsu05pcu1
aahsu04oaa
vahsu03blfa
achsu02pcu
aahsu01aa

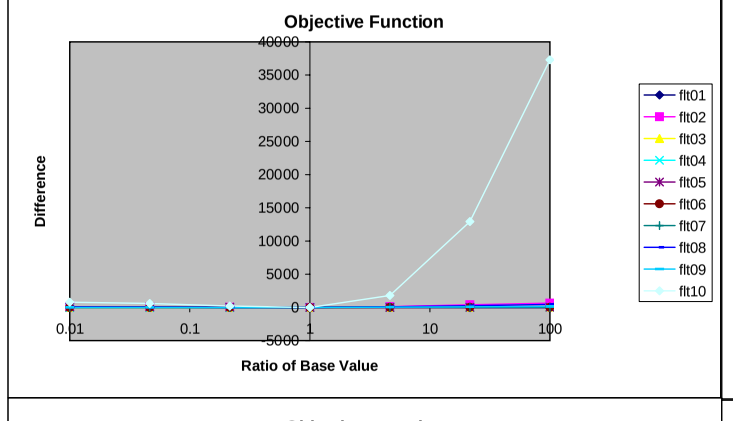
Objective Function
Difference
Ratio of Base Value
flt01
flt02
flt03
flt04
flt05
flt06
flt07
flt08
flt09
flt10

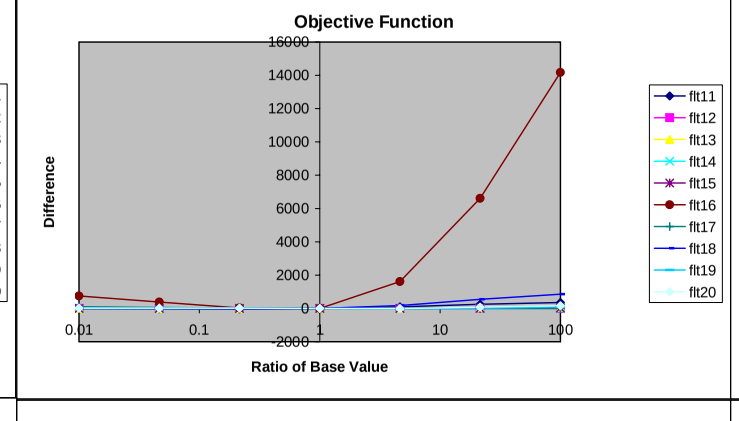
Objective Function
Difference
Ratio of Base Value
flt11
flt12
flt13
flt14
flt15
flt16
flt17
flt18
flt19
flt20

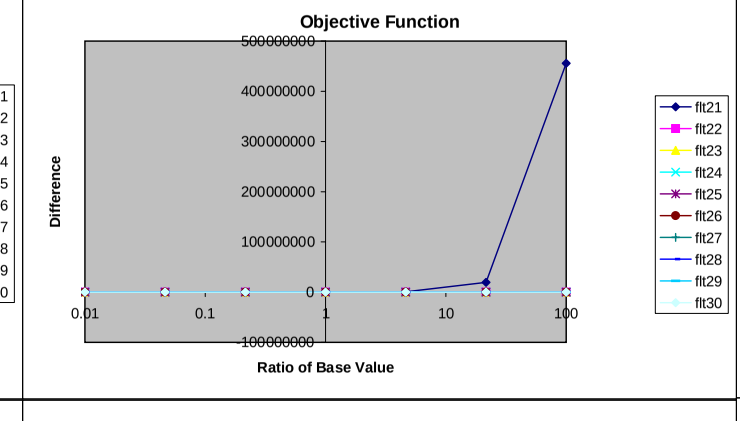
Objective Function
Difference
Ratio of Base Value
flt21
flt22
flt23
flt24
flt25
flt26
flt27
flt28
flt29
flt30

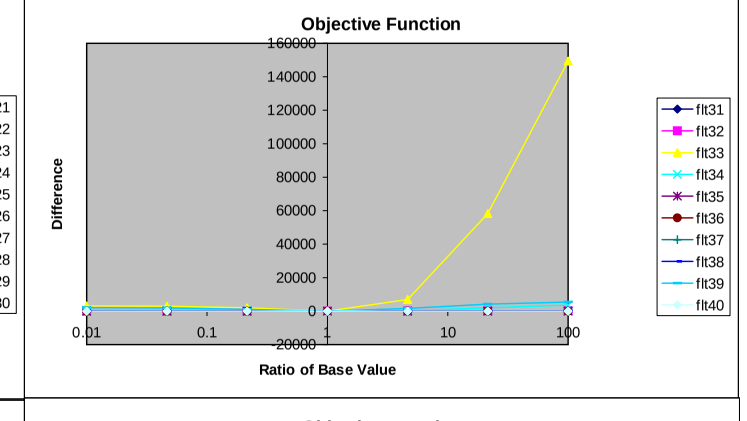
Objective Function
Difference
Ratio of Base Value
flt31
flt32
flt33
flt34
flt35
flt36
flt37
flt38
flt39
flt40

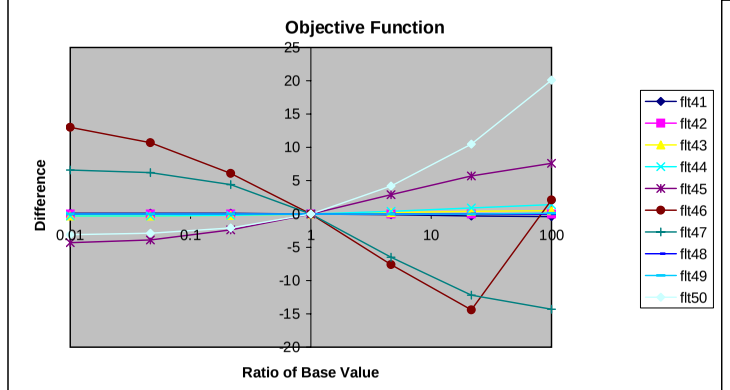
Objective Function
Difference
Ratio of Base Value
flt41
flt42
flt43
flt44
flt45
flt46
flt47
flt48
flt49
flt50

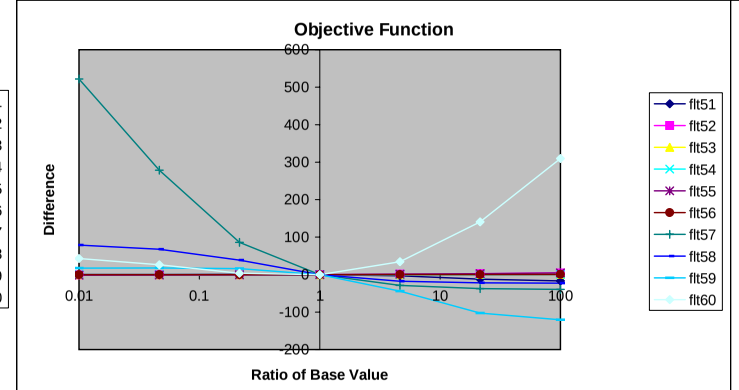
Objective Function
Difference
Ratio of Base Value
flt51
flt52
flt53
flt54
flt55
flt56
flt57
flt58
flt59
flt60

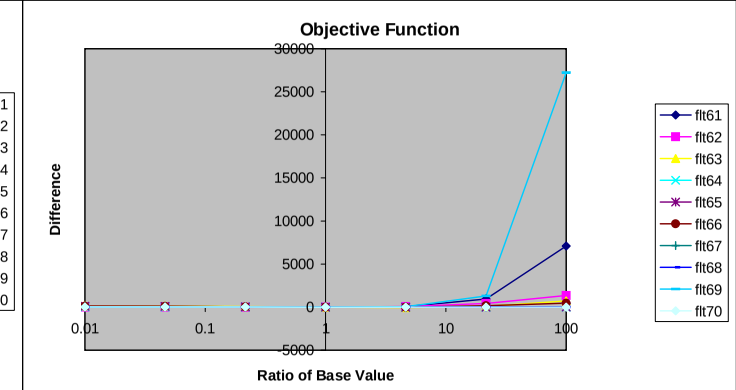
Objective Function
Difference
Ratio of Base Value
flt61
flt62
flt63
flt64
flt65
flt66
flt67
flt68
flt69
flt70

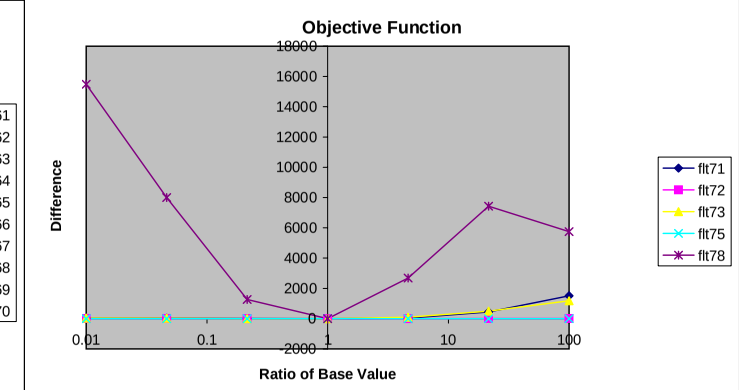
Objective Function
Difference
Ratio of Base Value
flt71
flt72
flt73
flt75
flt78

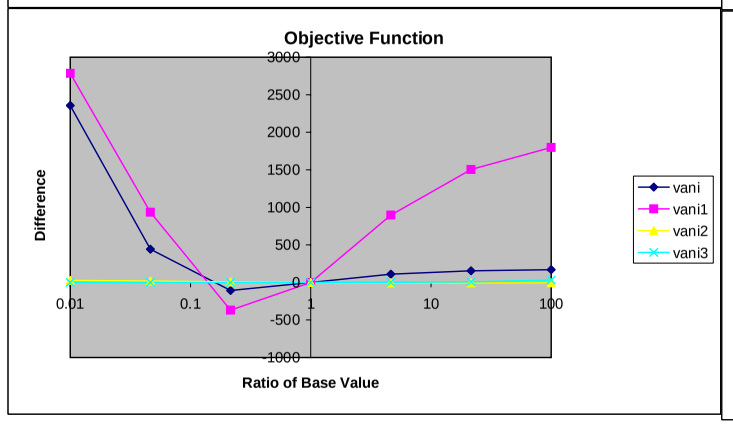
Objective Function
Difference
Ratio of Base Value
vani
vani1
vani2
vani3

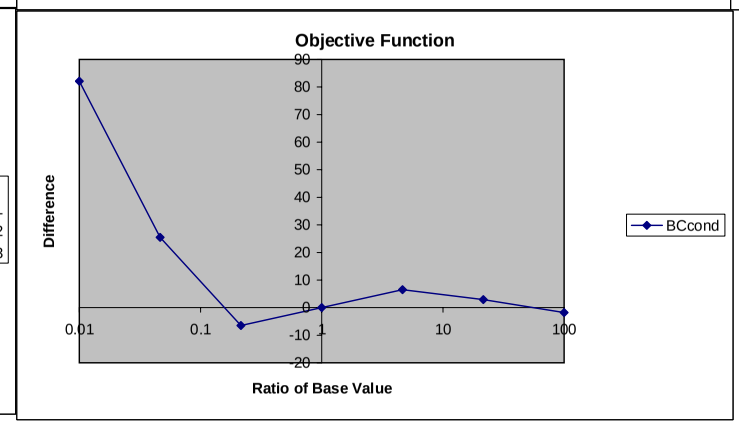
Objective Function
Difference
Ratio of Base Value
BCcond

C.3.5

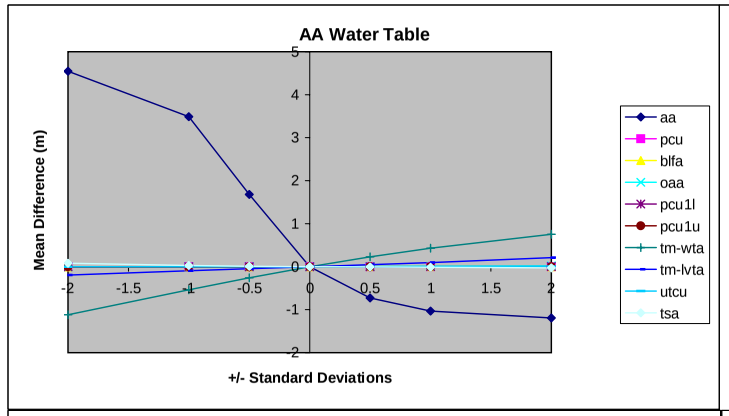
AA Water Table
Mean Difference (m)
+/- Standard Deviations
aa
pcu
blfa
oaa
pcu1l
pcu1u
tm-wta
tm-lvta
utcu
tsa

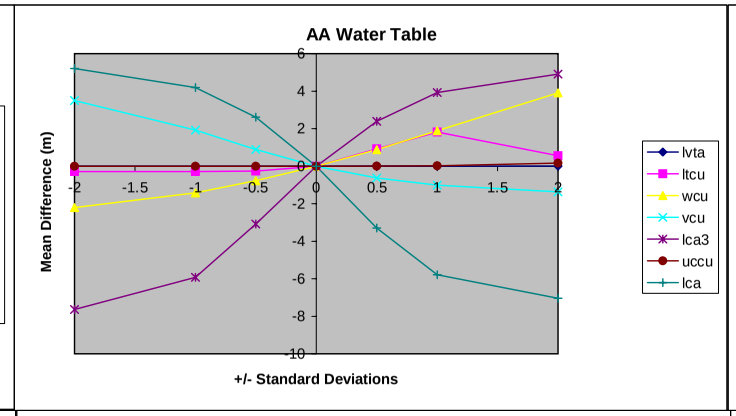
AA Water Table
Mean Difference (m)
+/- Standard Deviations
lvta
ltcu
wcu
vcu
lca3
uccu
lca

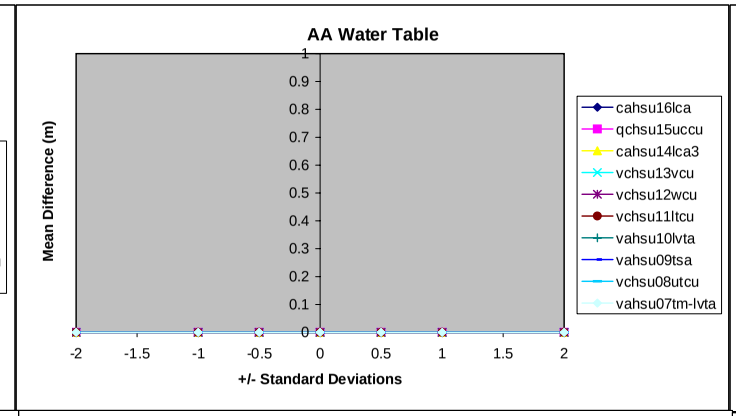
AA Water Table
Mean Difference (m)
+/- Standard Deviations
cahsu16lca
qchsu15uccu
cahsu14lca3
vchsu13vcu
vchsu12wcu
vchsu11ltcu
vahsu10lvta
vahsu09tsa
vchsu08utcu
vahsu07tm-lvta

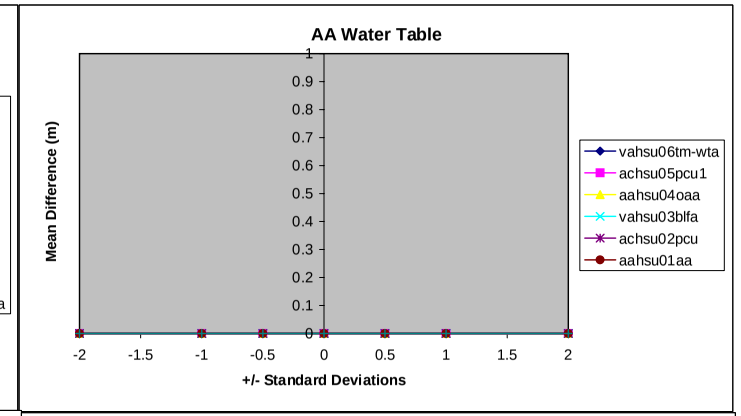
AA Water Table
Mean Difference (m)
+/- Standard Deviations
vahsu06tm-wta
achsu05pcu1
aahsu04oaa
vahsu03blfa
achsu02pcu
aahsu01aa

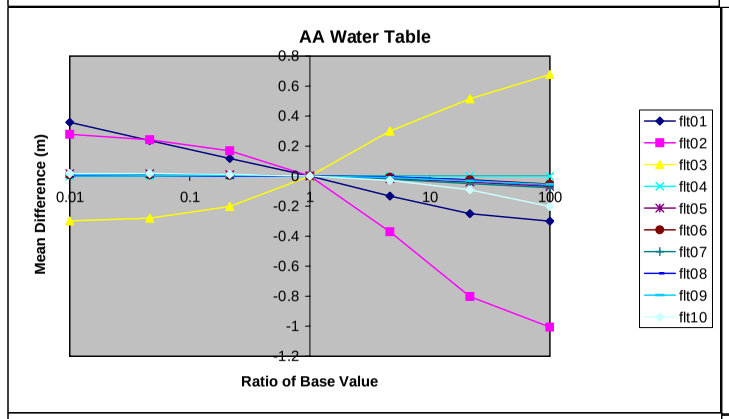
AA Water Table
Mean Difference (m)
Ratio of Base Value
flt01
flt02
flt03
flt04
flt05
flt06
flt07
flt08
flt09
flt10

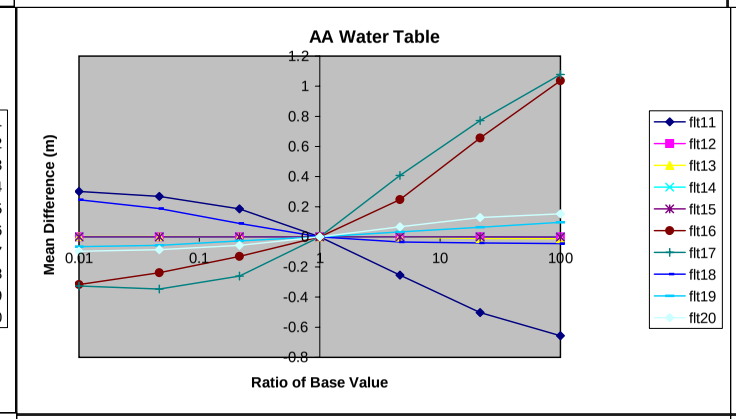
AA Water Table
Mean Difference (m)
Ratio of Base Value
flt11
flt12
flt13
flt14
flt15
flt16
flt17
flt18
flt19
flt20

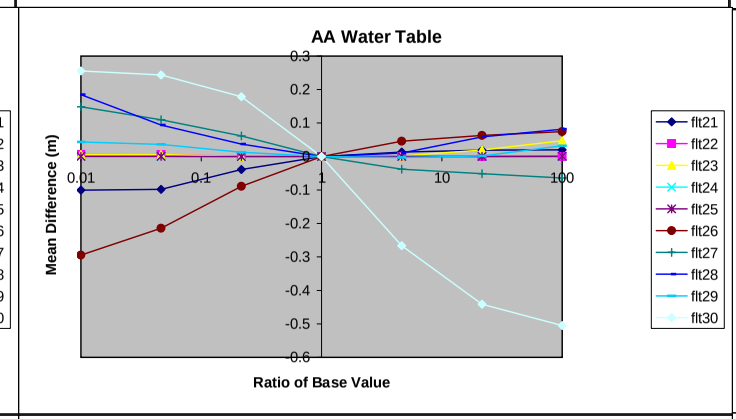
AA Water Table
Mean Difference (m)
Ratio of Base Value
flt21
flt22
flt23
flt24
flt25
flt26
flt27
flt28
flt29
flt30

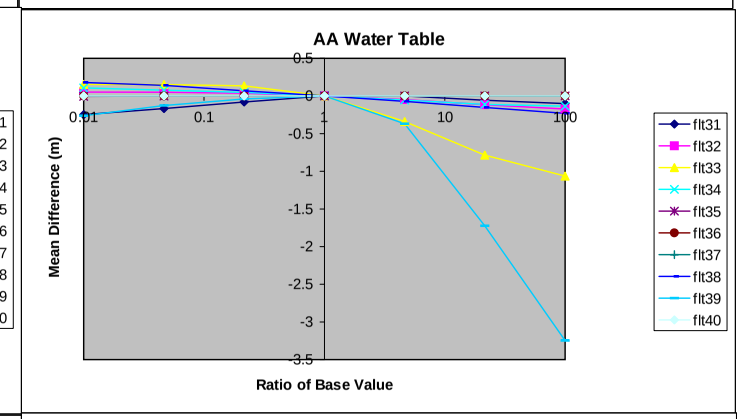
AA Water Table
Mean Difference (m)
Ratio of Base Value
flt31
flt32
flt33
flt34
flt35
flt36
flt37
flt38
flt39
flt40

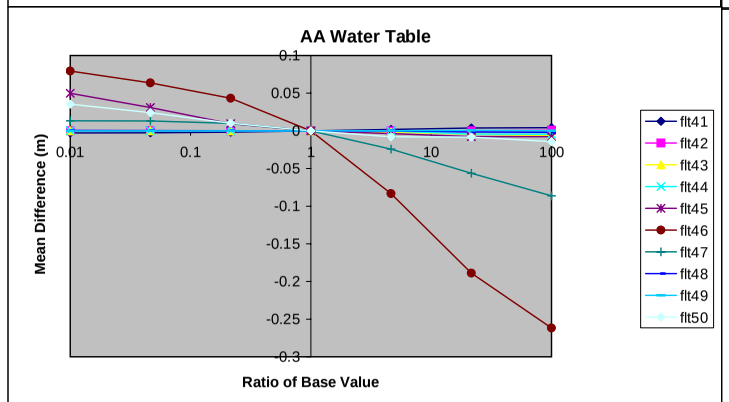
AA Water Table
Mean Difference (m)
Ratio of Base Value
flt41
flt42
flt43
flt44
flt45
flt46
flt47
flt48
flt49
flt50

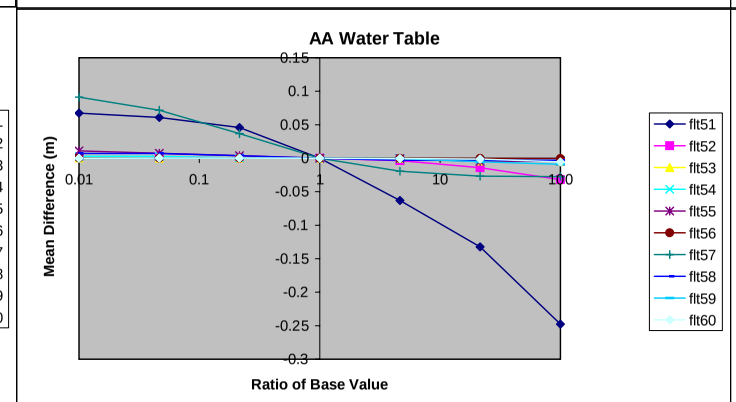
AA Water Table
Mean Difference (m)
Ratio of Base Value
flt51
flt52
flt53
flt54
flt55
flt56
flt57
flt58
flt59
flt60

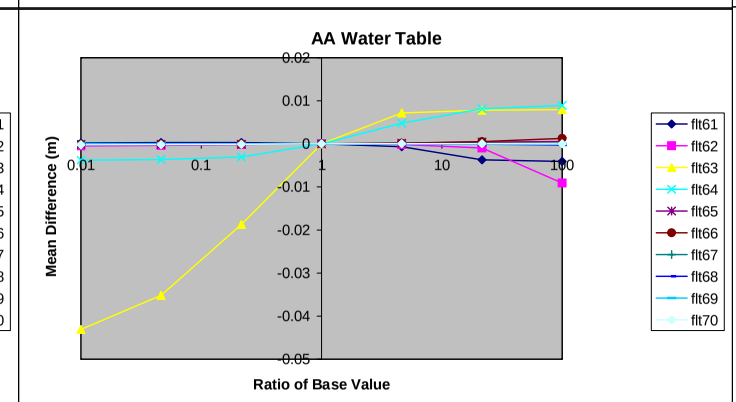
AA Water Table
Mean Difference (m)
Ratio of Base Value
flt61
flt62
flt63
flt64
flt65
flt66
flt67
flt68
flt69
flt70

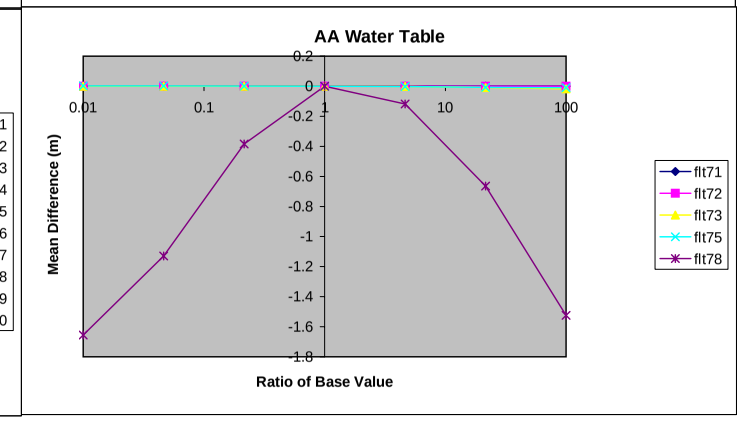
AA Water Table
Mean Difference (m)
Ratio of Base Value
flt71
flt72
flt73
flt75
flt78

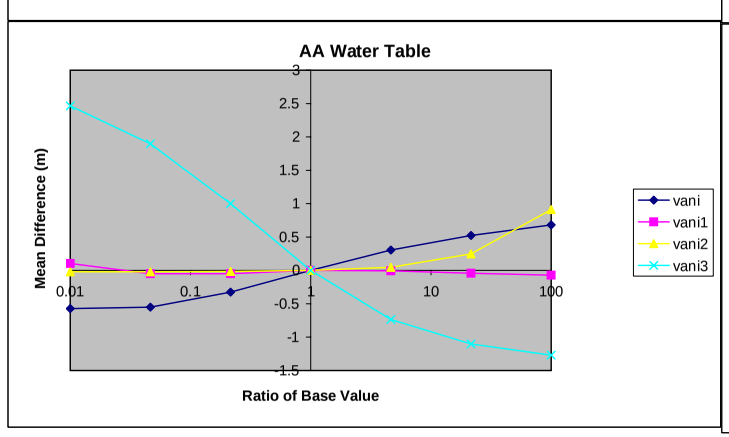
AA Water Table
Mean Difference (m)
Ratio of Base Value
vani
vani1
vani2
vani3

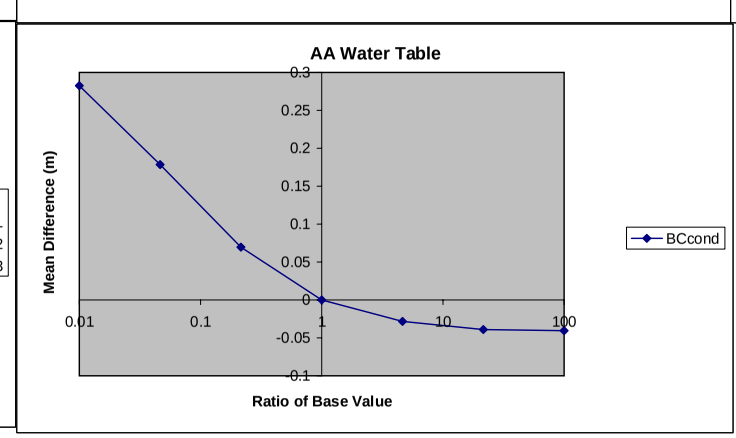
AA Water Table
Mean Difference (m)
Ratio of Base Value
BCcond

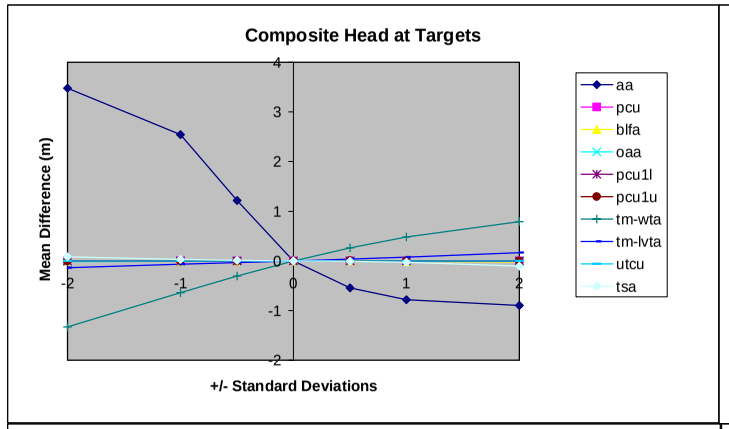
Composite Head at Targets
Mean Difference (m)
+/- Standard Deviations
aa
pcu
blfa
oaa
pcu1l
pcu1u
tm-wta
tm-lvta
utcu
tsa

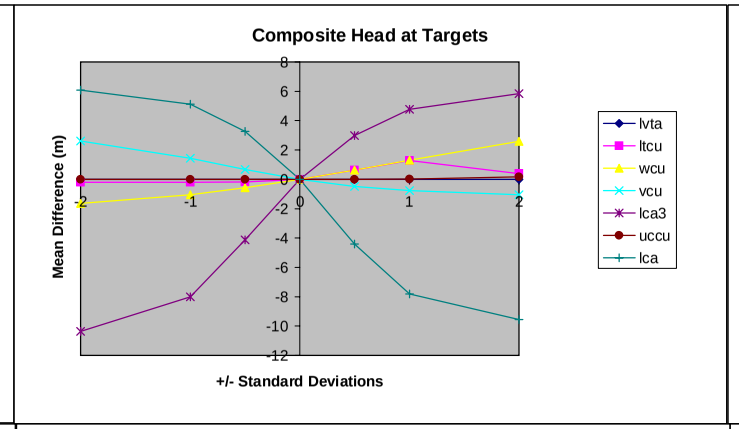
Composite Head at Targets
Mean Difference (m)
+/- Standard Deviations
lvta
ltcu
wcu
vcu
lca3
uccu
lca

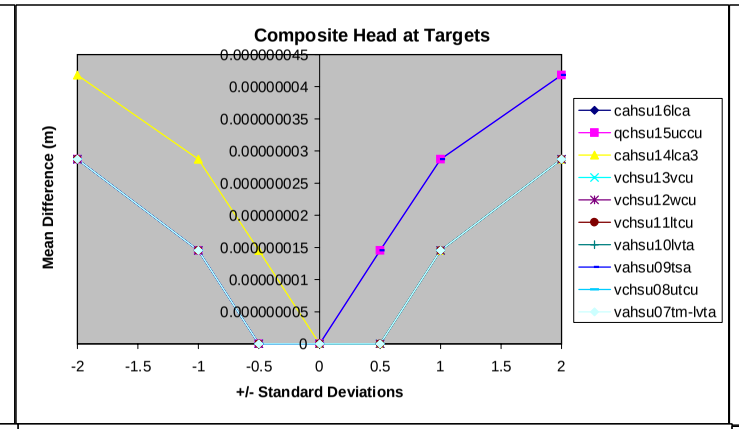
Composite Head at Targets
Mean Difference (m)
+/- Standard Deviations
cahsu16lca
qchsu15uccu
cahsu14lca3
vchsu13vcu
vchsu12wcu
vchsu11ltcu
vahsu10lvta
vahsu09tsa
vchsu08utcu
vahsu07tm-lvta

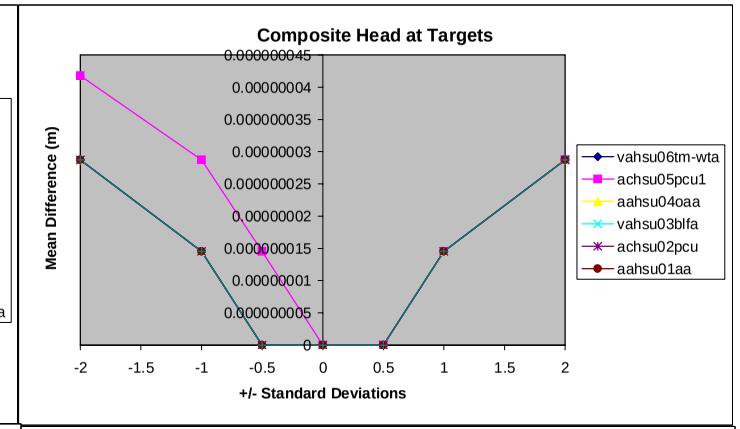
Composite Head at Targets
Mean Difference (m)
+/- Standard Deviations
vahsu06tm-wta
achsu05pcu1
aahsu04oaa
vahsu03blfa
achsu02pcu
aahsu01aa

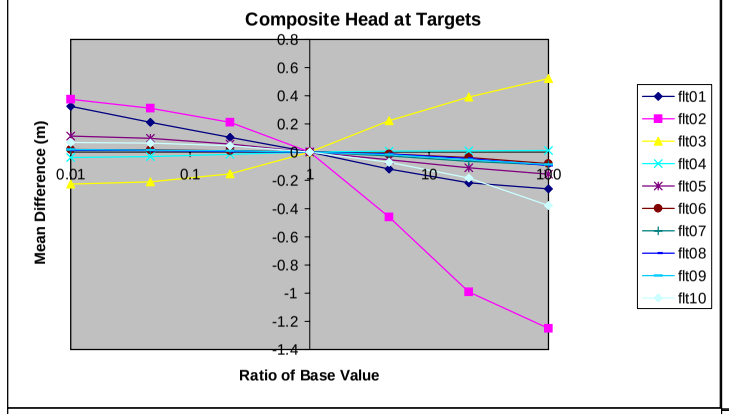
Composite Head at Targets
Mean Difference (m)
Ratio of Base Value
flt01
flt02
flt03
flt04
flt05
flt06
flt07
flt08
flt09
flt10

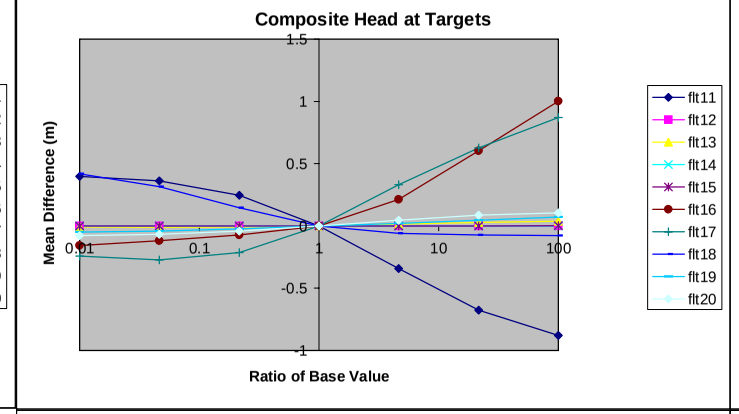
Composite Head at Targets
Mean Difference (m)
Ratio of Base Value
flt11
flt12
flt13
flt14
flt15
flt16
flt17
flt18
flt19
flt20

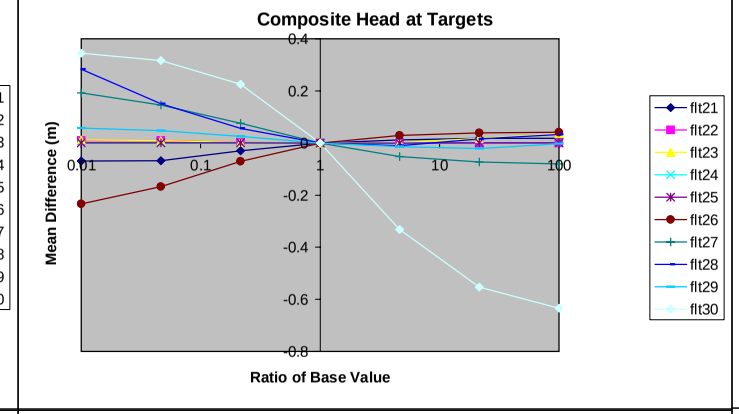
Composite Head at Targets
Mean Difference (m)
Ratio of Base Value
flt21
flt22
flt23
flt24
flt25
flt26
flt27
flt28
flt29
flt30

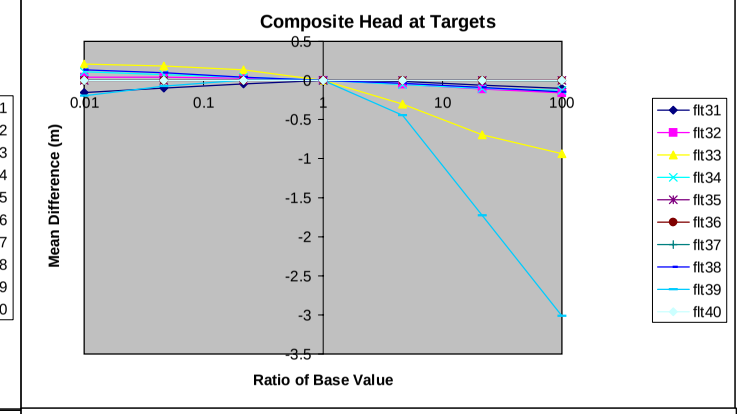
Composite Head at Targets
Mean Difference (m)
Ratio of Base Value
flt31
flt32
flt33
flt34
flt35
flt36
flt37
flt38
flt39
flt40

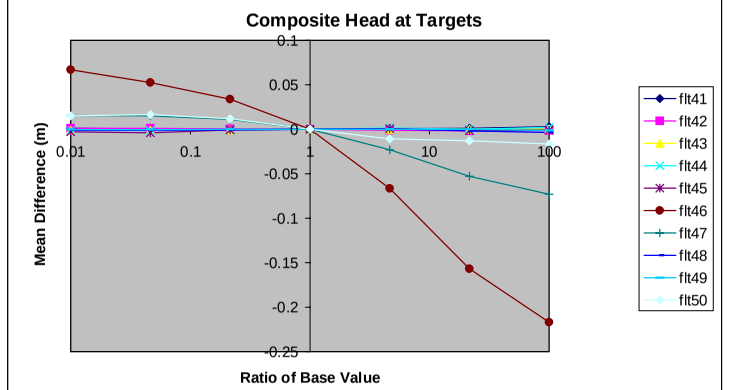
Composite Head at Targets
Mean Difference (m)
Ratio of Base Value
flt41
flt42
flt43
flt44
flt45
flt46
flt47
flt48
flt49
flt50

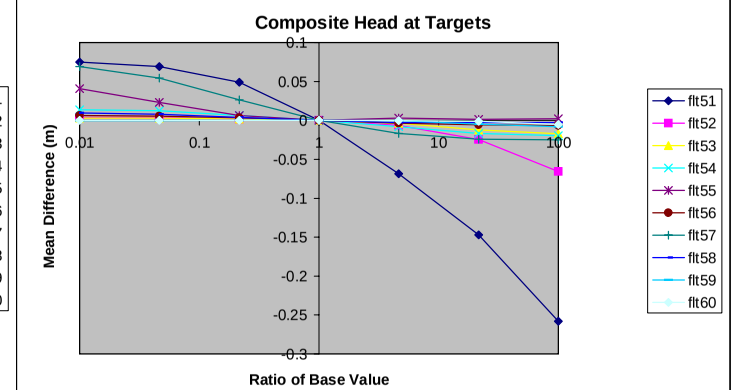
Composite Head at Targets
Mean Difference (m)
Ratio of Base Value
flt51
flt52
flt53
flt54
flt55
flt56
flt57
flt58
flt59
flt60

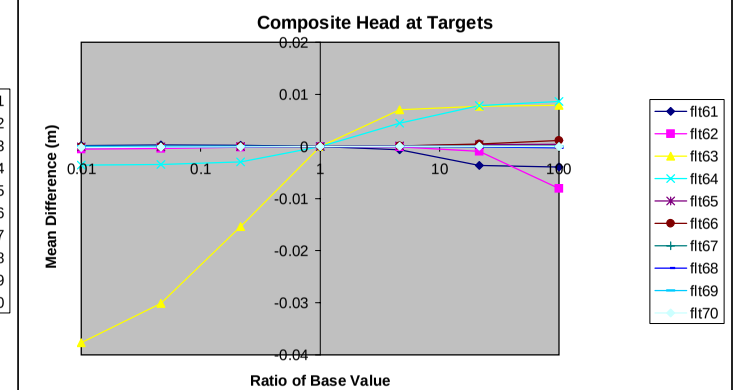
Composite Head at Targets
Mean Difference (m)
Ratio of Base Value
flt61
flt62
flt63
flt64
flt65
flt66
flt67
flt68
flt69
flt70

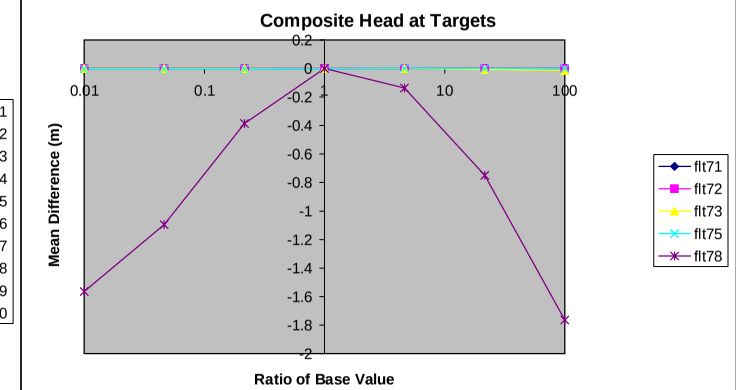
Composite Head at Targets
Mean Difference (m)
Ratio of Base Value
flt71
flt72
flt73
flt75
flt78

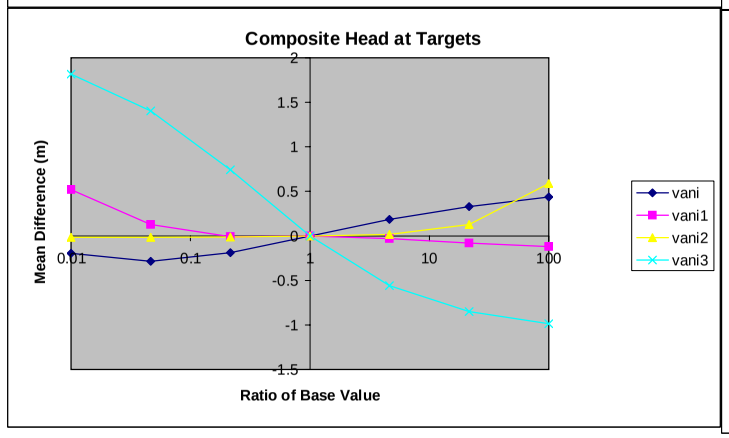
Composite Head at Targets
Mean Difference (m)
Ratio of Base Value
vani
vani1
vani2
vani3

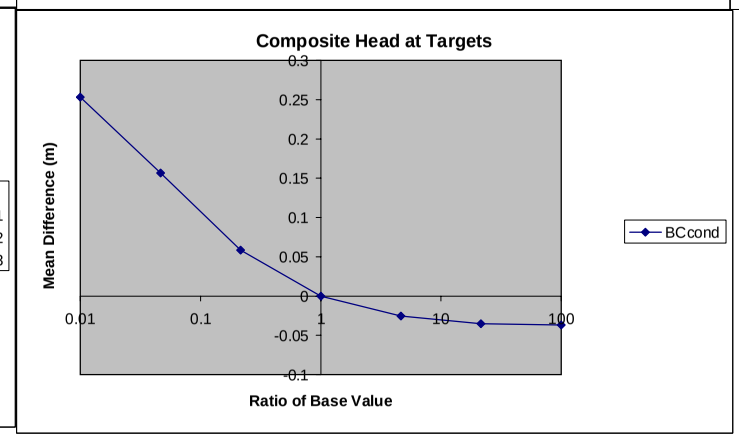
Composite Head at Targets
Mean Difference (m)
Ratio of Base Value
BCcond

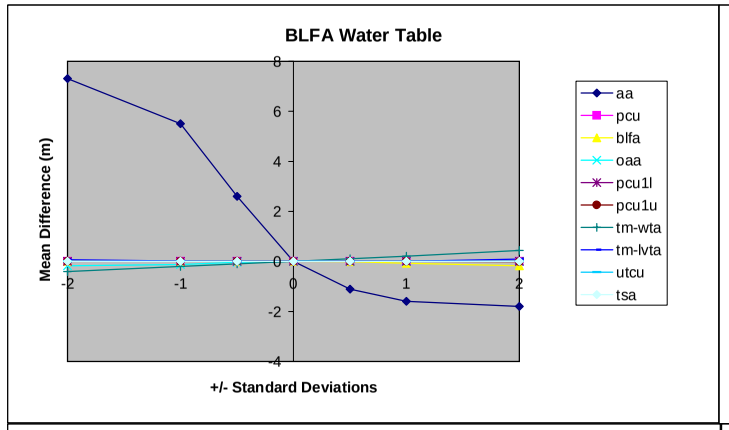
BLFA Water Table
Mean Difference (m)
+/- Standard Deviations
aa
pcu
blfa
oaa
pcu1l
pcu1u
tm-wta
tm-lvta
utcu
tsa

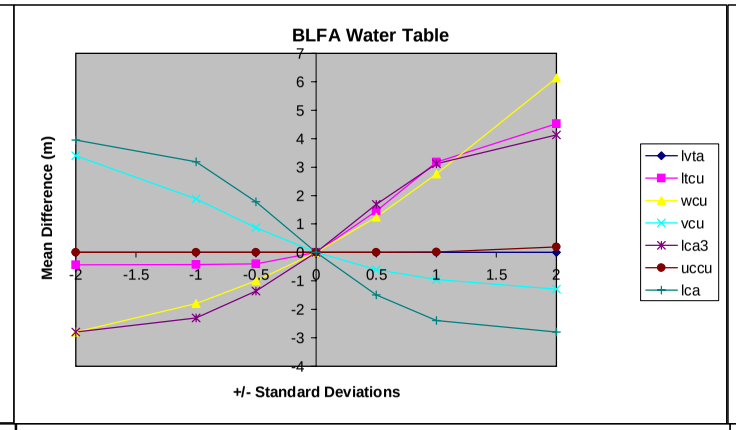
BLFA Water Table
Mean Difference (m)
+/- Standard Deviations
lvta
ltcu
wcu
vcu
lca3
uccu
lca

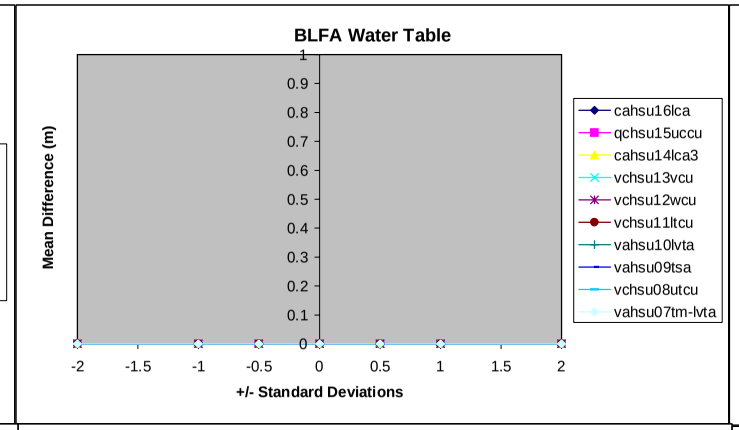
BLFA Water Table
Mean Difference (m)
+/- Standard Deviations
cahsu16lca
qchsu15uccu
cahsu14lca3
vchsu13vcu
vchsu12wcu
vchsu11ltcu
vahsu10lvta
vahsu09tsa
vchsu08utcu
vahsu07tm-lvta

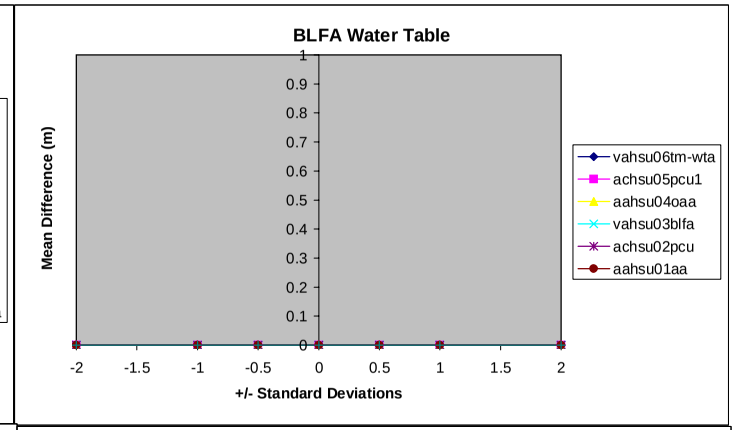
BLFA Water Table
Mean Difference (m)
+/- Standard Deviations
vahsu06tm-wta
achsu05pcu1
aahsu04oaa
vahsu03blfa
achsu02pcu
aahsu01aa

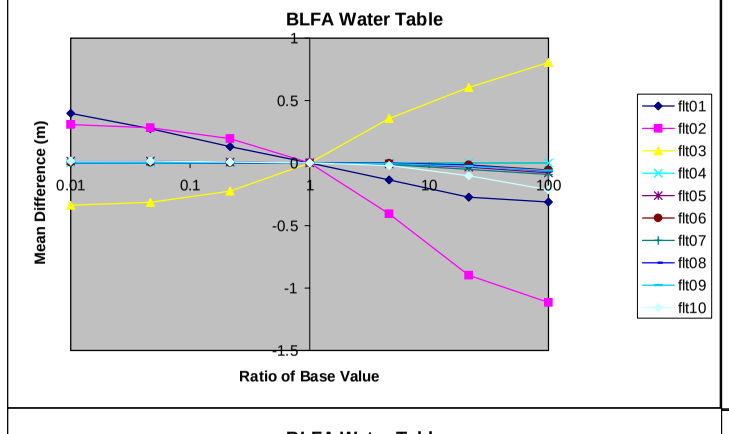
BLFA Water Table
Mean Difference (m)
Ratio of Base Value
flt01
flt02
flt03
flt04
flt05
flt06
flt07
flt08
flt09
flt10

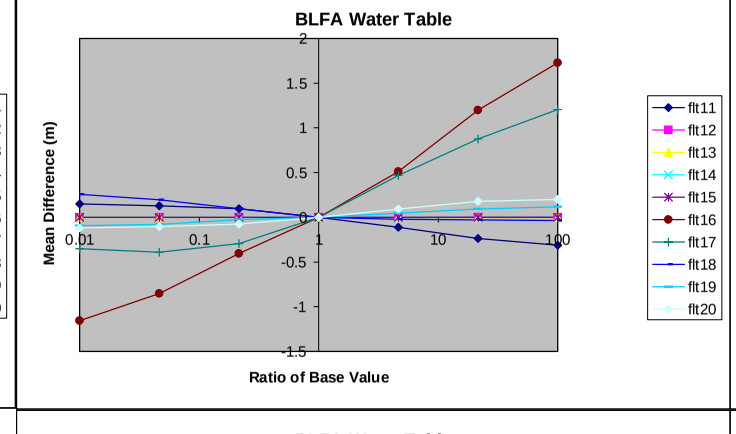
BLFA Water Table
Mean Difference (m)
Ratio of Base Value
flt11
flt12
flt13
flt14
flt15
flt16
flt17
flt18
flt19
flt20

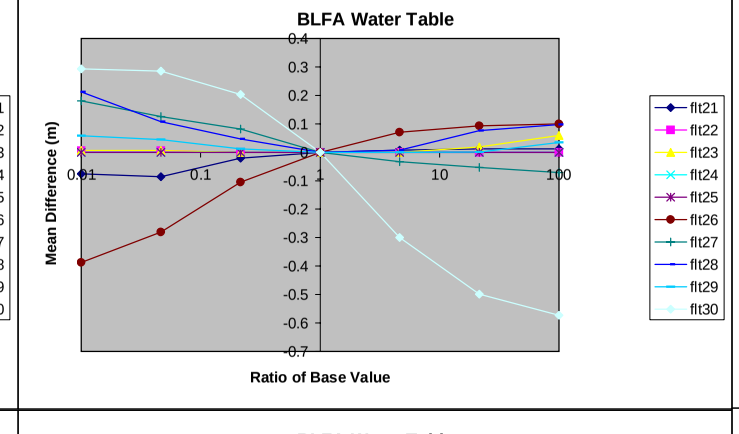
BLFA Water Table
Mean Difference (m)
Ratio of Base Value
flt21
flt22
flt23
flt24
flt25
flt26
flt27
flt28
flt29
flt30

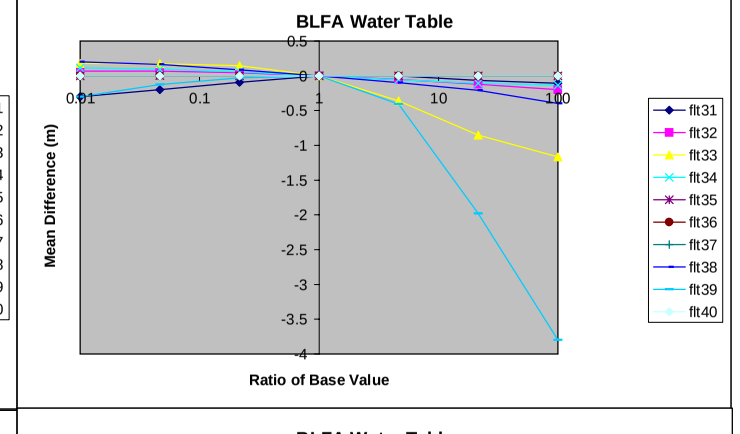
BLFA Water Table
Mean Difference (m)
Ratio of Base Value
flt31
flt32
flt33
flt34
flt35
flt36
flt37
flt38
flt39
flt40

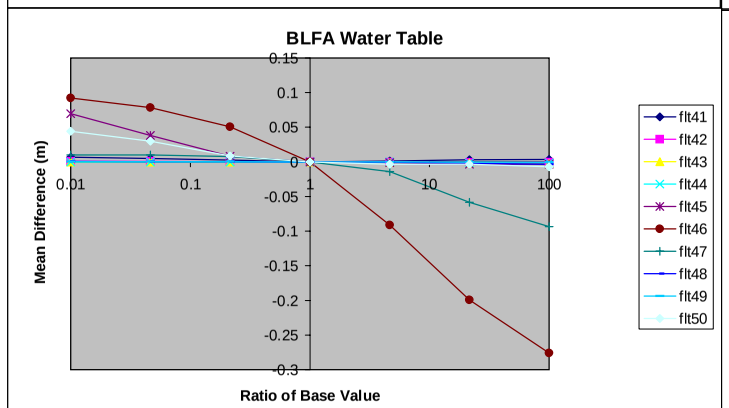
BLFA Water Table
Mean Difference (m)
Ratio of Base Value
flt41
flt42
flt43
flt44
flt45
flt46
flt47
flt48
flt49
flt50

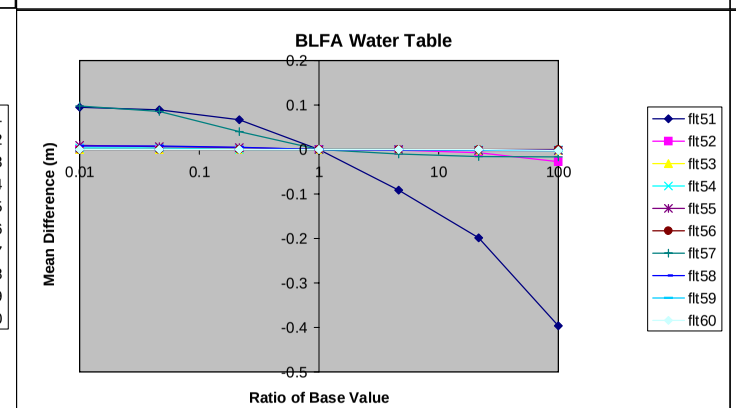
BLFA Water Table
Mean Difference (m)
Ratio of Base Value
flt51
flt52
flt53
flt54
flt55
flt56
flt57
flt58
flt59
flt60

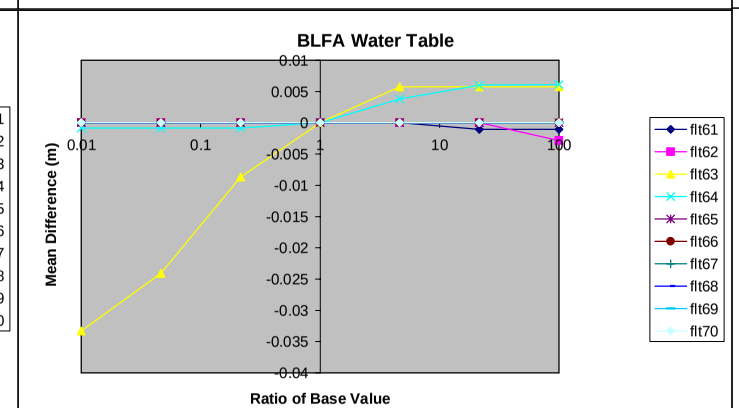
BLFA Water Table
Mean Difference (m)
Ratio of Base Value
flt61
flt62
flt63
flt64
flt65
flt66
flt67
flt68
flt69
flt70

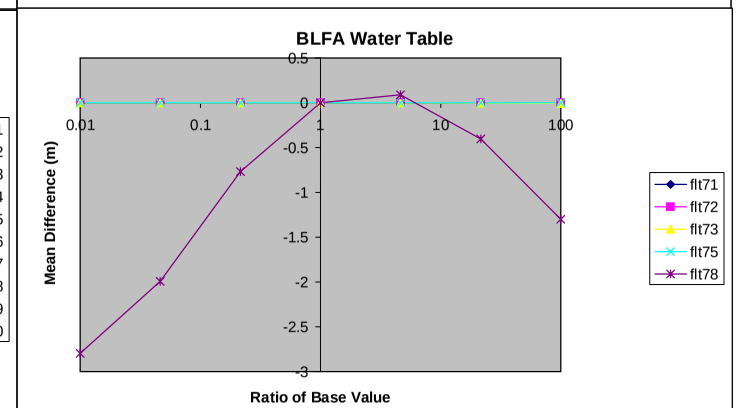
BLFA Water Table
Mean Difference (m)
Ratio of Base Value
flt71
flt72
flt73
flt75
flt78

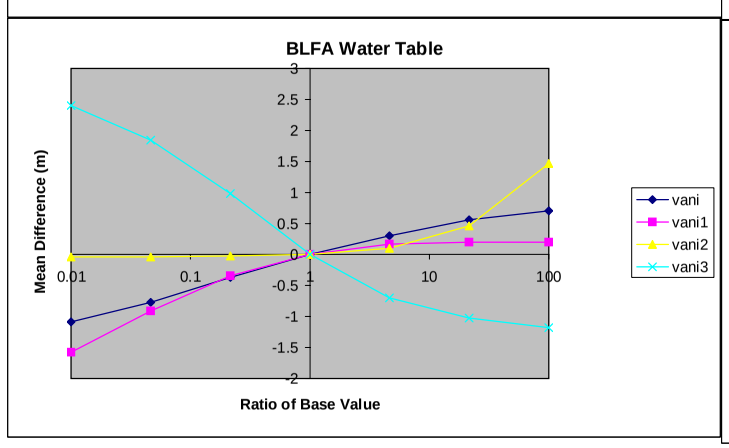
BLFA Water Table
Mean Difference (m)
Ratio of Base Value
vani
vani1
vani2
vani3

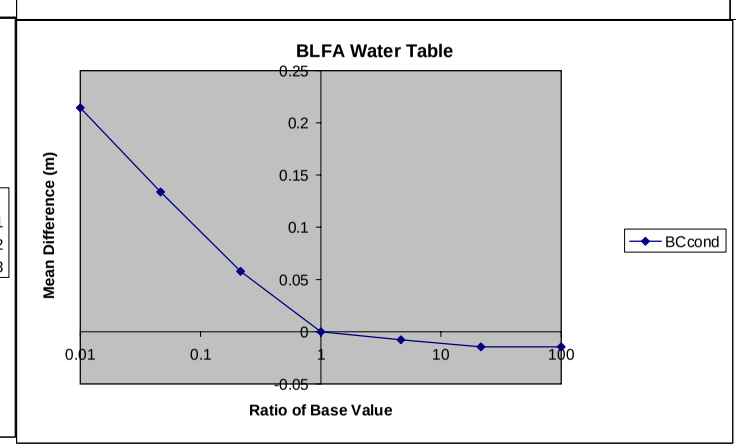
BLFA Water Table
Mean Difference (m)
Ratio of Base Value
BCcond

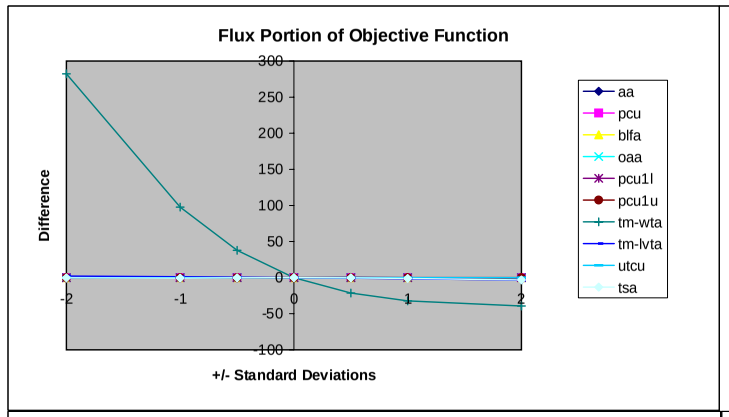
Flux Portion of Objective Function
Difference
+/- Standard Deviations
aa
pcu
blfa
oaa
pcu1l
pcu1u
tm-wta
tm-lvta
utcu
tsa

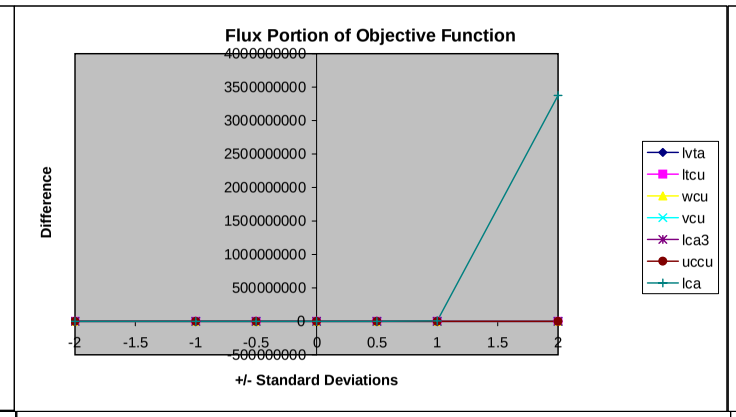
Flux Portion of Objective Function
Difference
+/- Standard Deviations
lvta
ltcu
wcu
vcu
lca3
uccu
lca

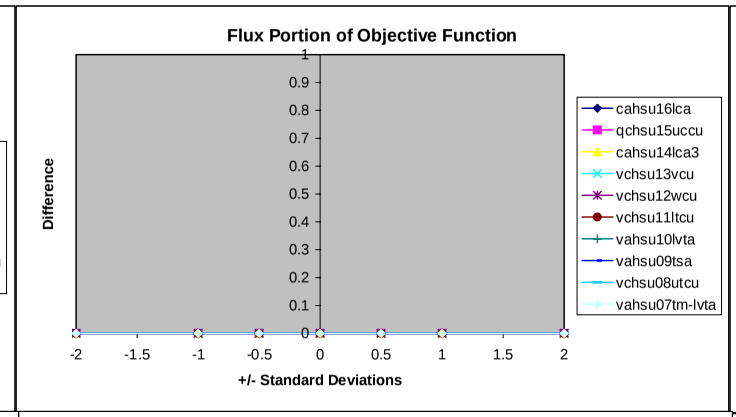
Flux Portion of Objective Function
Difference
+/- Standard Deviations
cahsu16lca
qchsu15uccu
cahsu14lca3
vchsu13vcu
vchsu12wcu
vchsu11ltcu
vahsu10lvta
vahsu09tsa
vchsu08utcu
vahsu07tm-lvta

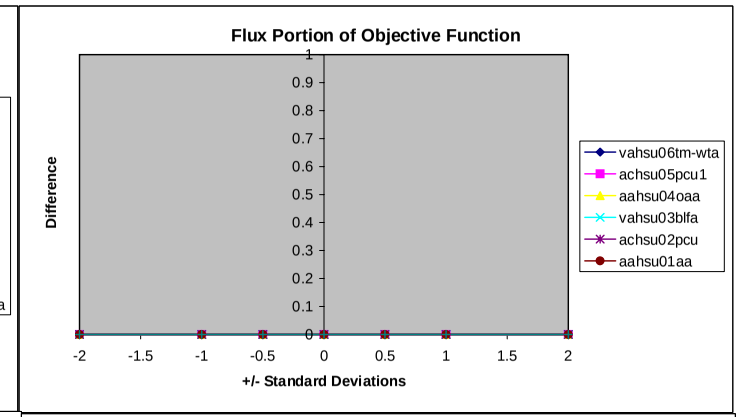
Flux Portion of Objective Function
Difference
+/- Standard Deviations
vahsu06tm-wta
achsu05pcu1
aahsu04oaa
vahsu03blfa
achsu02pcu
aahsu01aa

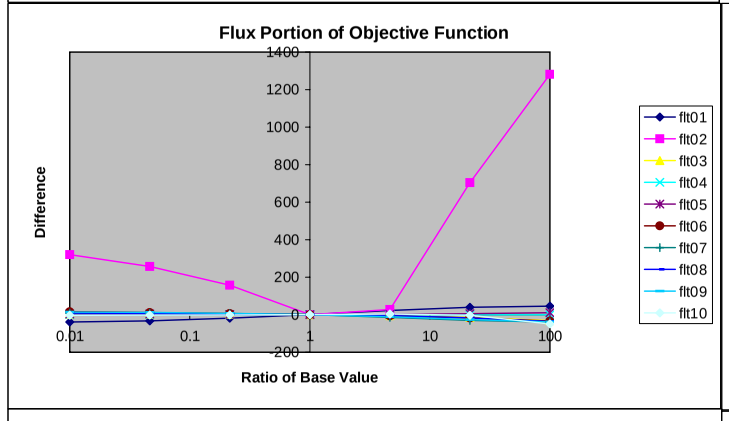
Flux Portion of Objective Function
Difference
Ratio of Base Value
flt01
flt02
flt03
flt04
flt05
flt06
flt07
flt08
flt09
flt10

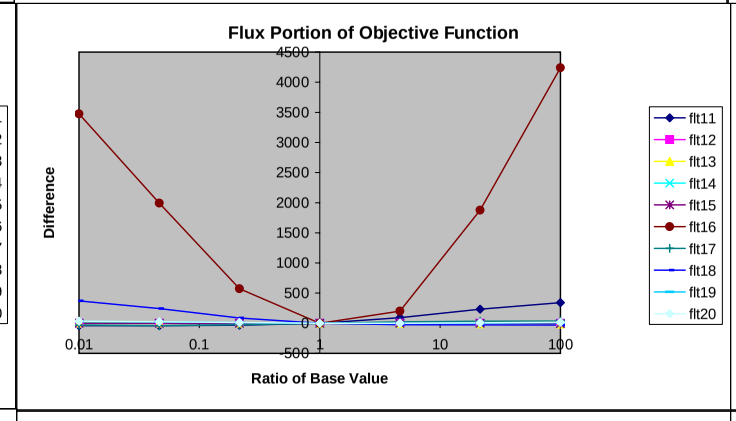
Flux Portion of Objective Function
Difference
Ratio of Base Value
flt11
flt12
flt13
flt14
flt15
flt16
flt17
flt18
flt19
flt20

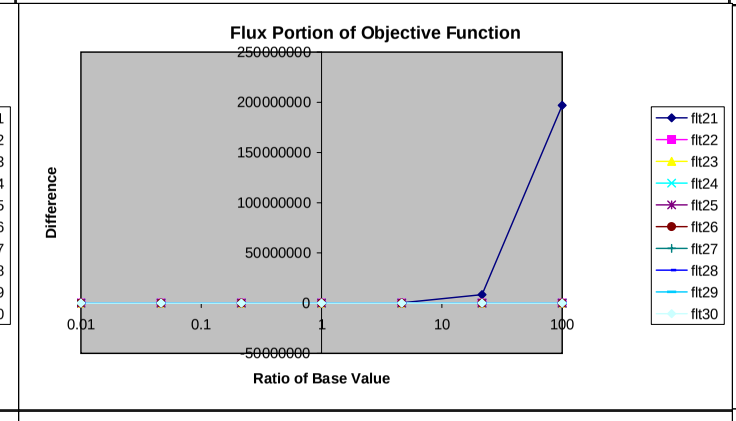
Flux Portion of Objective Function
Difference
Ratio of Base Value
flt21
flt22
flt23
flt24
flt25
flt26
flt27
flt28
flt29
flt30

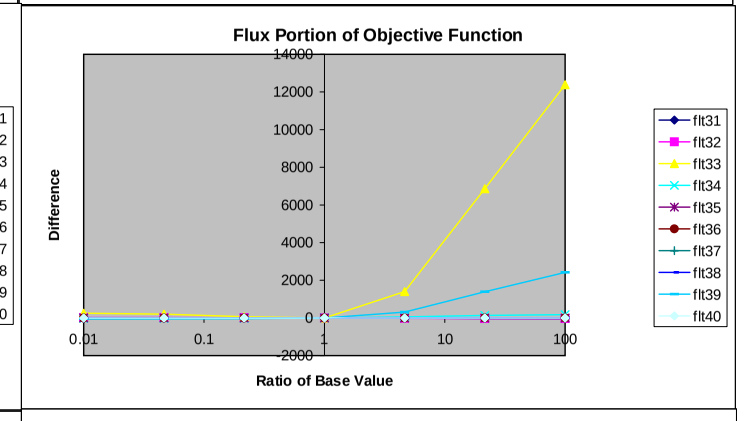
Flux Portion of Objective Function
Difference
Ratio of Base Value
flt31
flt32
flt33
flt34
flt35
flt36
flt37
flt38
flt39
flt40

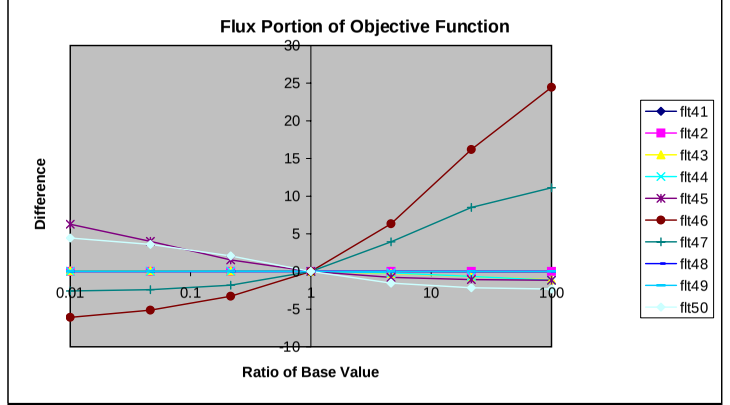
Flux Portion of Objective Function
Difference
Ratio of Base Value
flt41
flt42
flt43
flt44
flt45
flt46
flt47
flt48
flt49
flt50

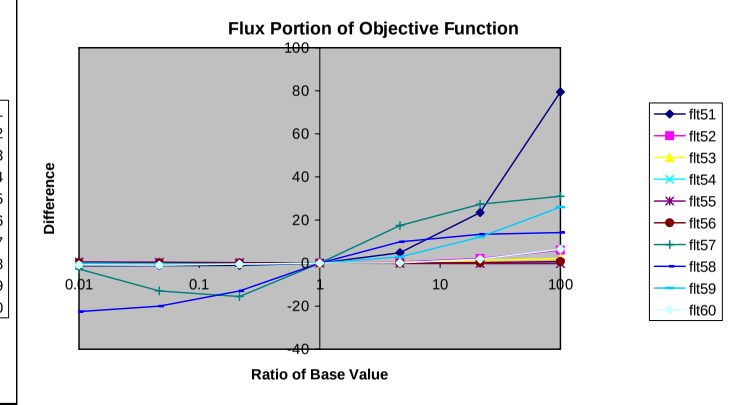
Flux Portion of Objective Function
Difference
Ratio of Base Value
flt51
flt52
flt53
flt54
flt55
flt56
flt57
flt58
flt59
flt60

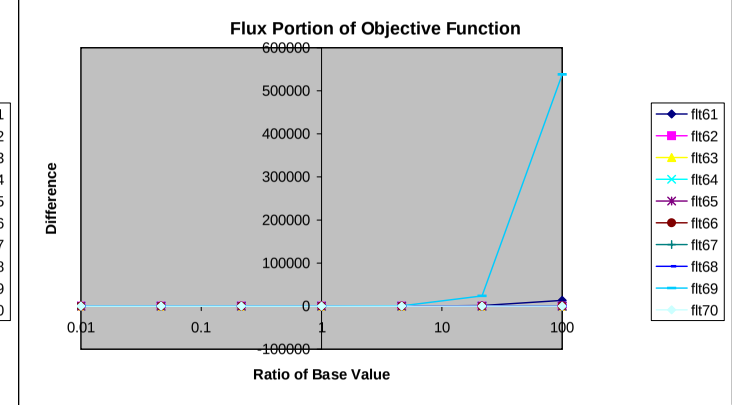
Flux Portion of Objective Function
Difference
Ratio of Base Value
flt61
flt62
flt63
flt64
flt65
flt66
flt67
flt68
flt69
flt70

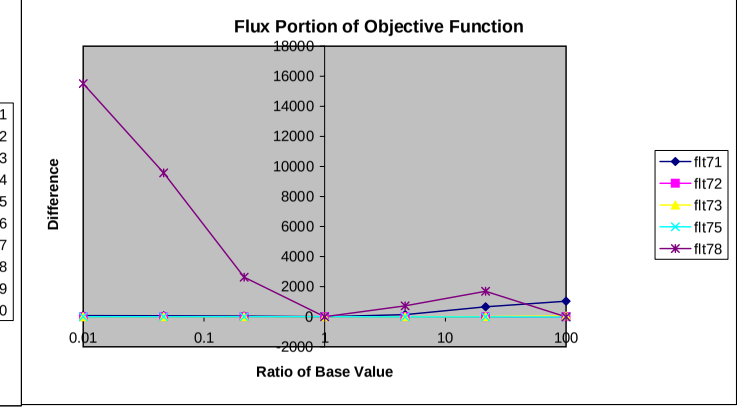
Flux Portion of Objective Function
Difference
Ratio of Base Value
flt71
flt72
flt73
flt75
flt78

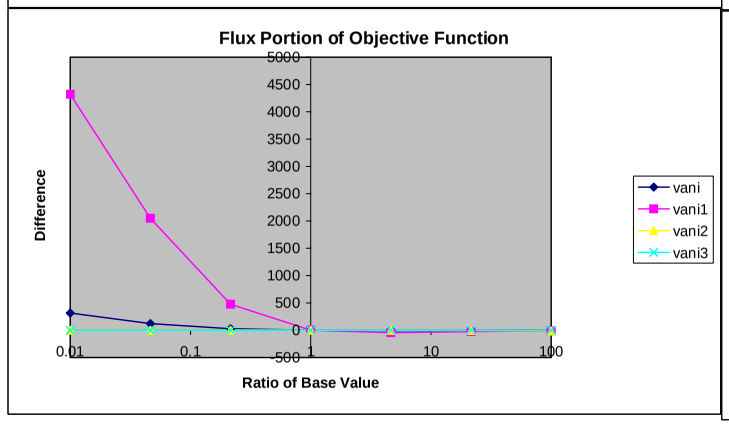
Flux Portion of Objective Function
Difference
Ratio of Base Value
vani
vani1
vani2
vani3

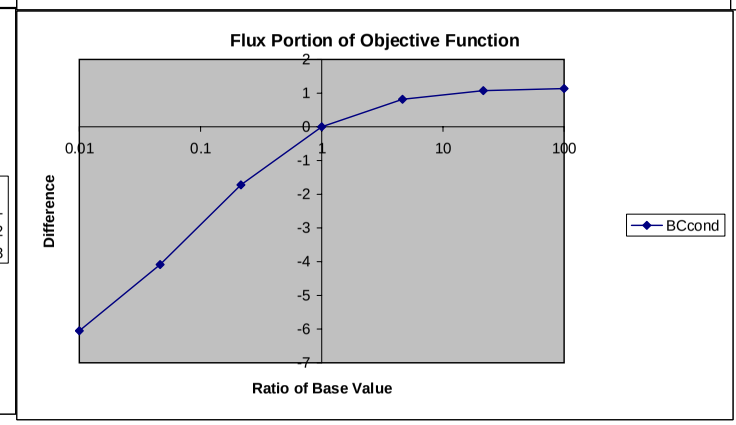
Flux Portion of Objective Function
Difference
Ratio of Base Value
BCcond

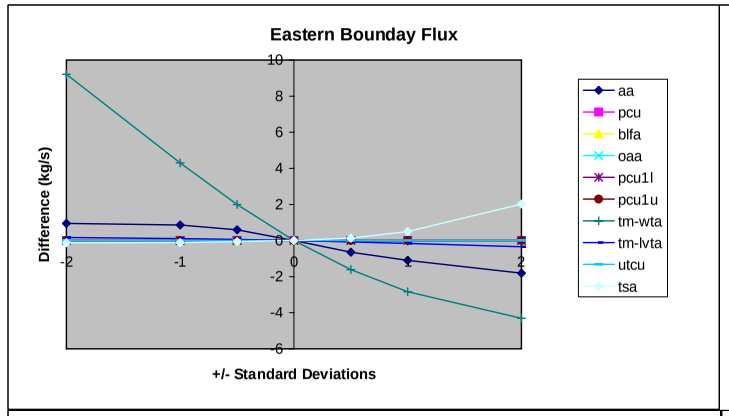
Eastern Bounday Flux
Difference (kg/s)
+/- Standard Deviations
aa
pcu
blfa
oaa
pcu1l
pcu1u
tm-wta
tm-lvta
utcu
tsa

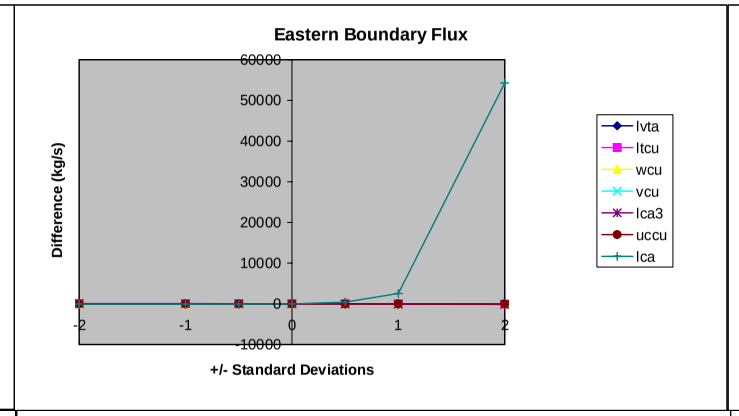
Eastern Boundary Flux
Difference (kg/s)
+/- Standard Deviations
lvta
ltcu
wcu
vcu
lca3
uccu
lca

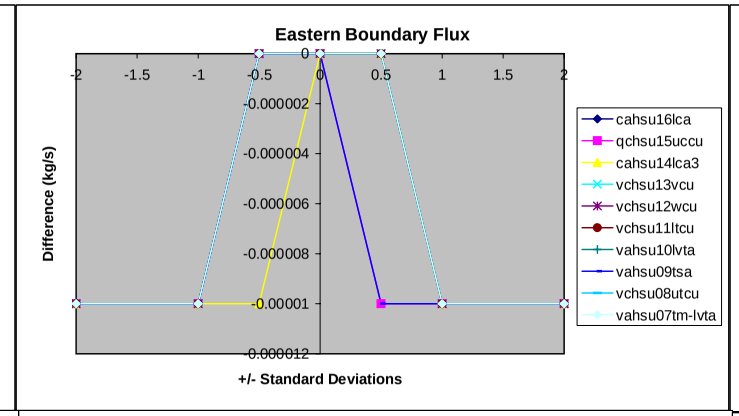
Eastern Boundary Flux
Difference (kg/s)
+/- Standard Deviations
cahsu16lca
qchsu15uccu
cahsu14lca3
vchsu13vcu
vchsu12wcu
vchsu11ltcu
vahsu10lvta
vahsu09tsa
vchsu08utcu
vahsu07tm-lvta

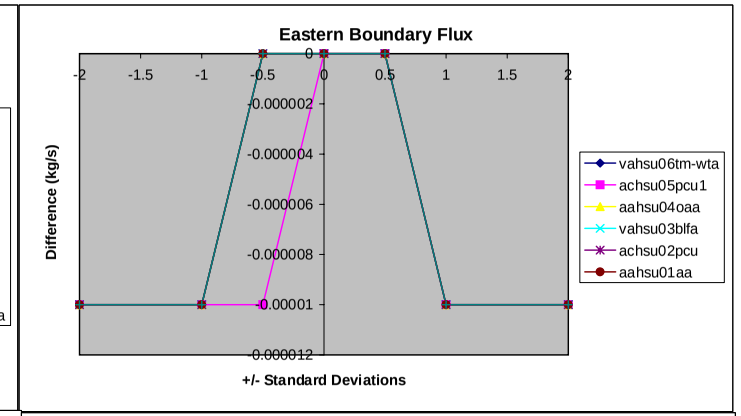
Eastern Boundary Flux
Difference (kg/s)
+/- Standard Deviations
vahsu06tm-wta
achsu05pcu1
aahsu04oaa
vahsu03blfa
achsu02pcu
aahsu01aa

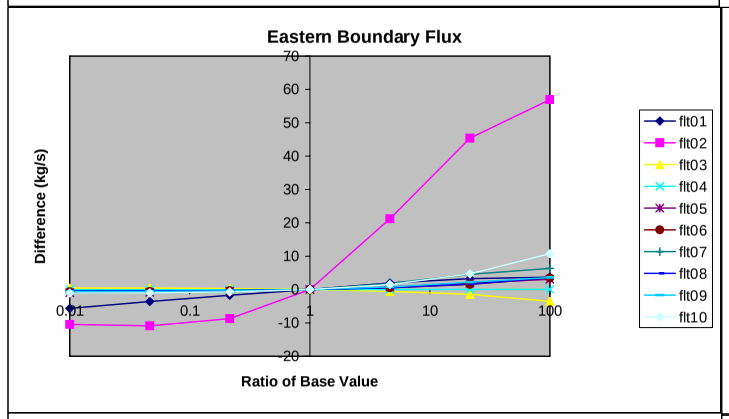
Eastern Boundary Flux
Difference (kg/s)
Ratio of Base Value
flt01
flt02
flt03
flt04
flt05
flt06
flt07
flt08
flt09
flt10

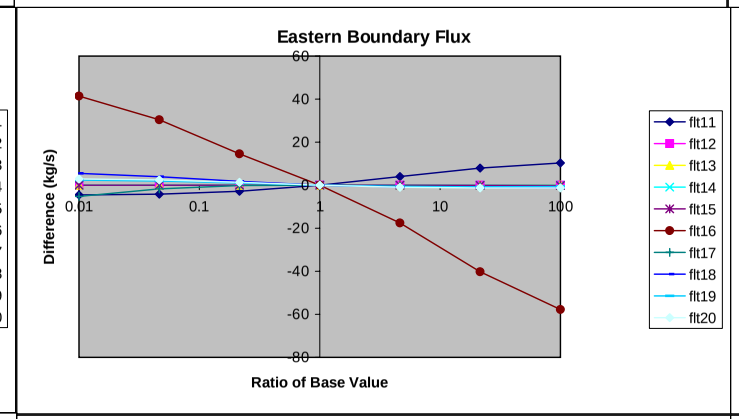
Eastern Boundary Flux
Difference (kg/s)
Ratio of Base Value
flt11
flt12
flt13
flt14
flt15
flt16
flt17
flt18
flt19
flt20

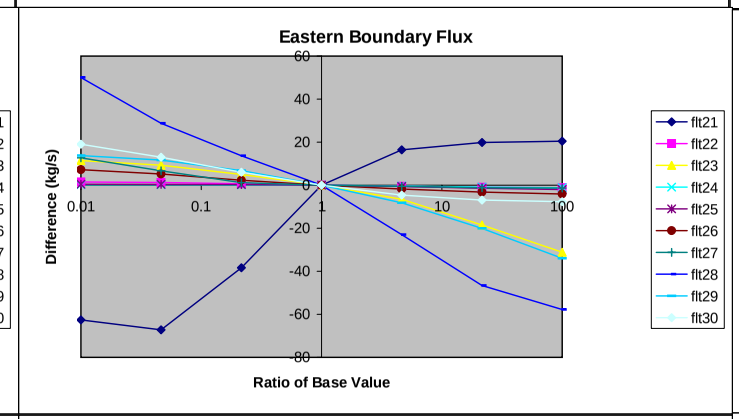
Eastern Boundary Flux
Difference (kg/s)
Ratio of Base Value
flt21
flt22
flt23
flt24
flt25
flt26
flt27
flt28
flt29
flt30

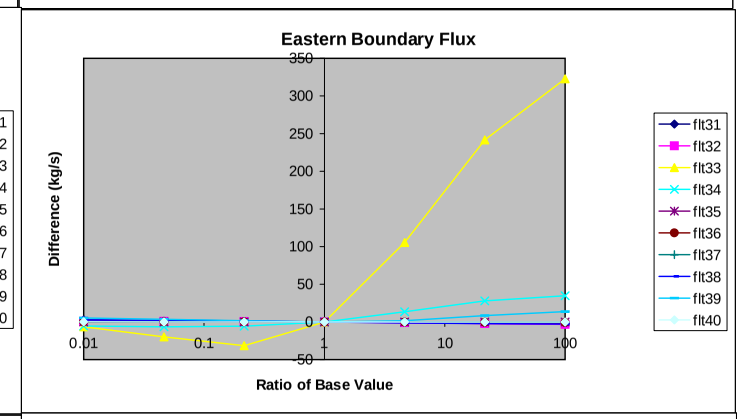
Eastern Boundary Flux
Difference (kg/s)
Ratio of Base Value
flt31
flt32
flt33
flt34
flt35
flt36
flt37
flt38
flt39
flt40

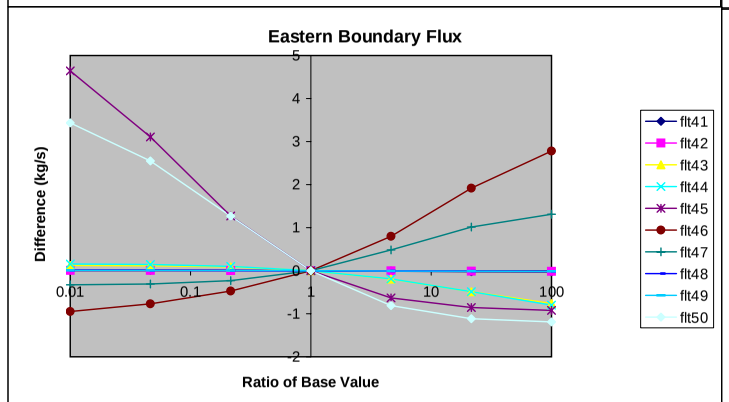
Eastern Boundary Flux
Difference (kg/s)
Ratio of Base Value
flt41
flt42
flt43
flt44
flt45
flt46
flt47
flt48
flt49
flt50

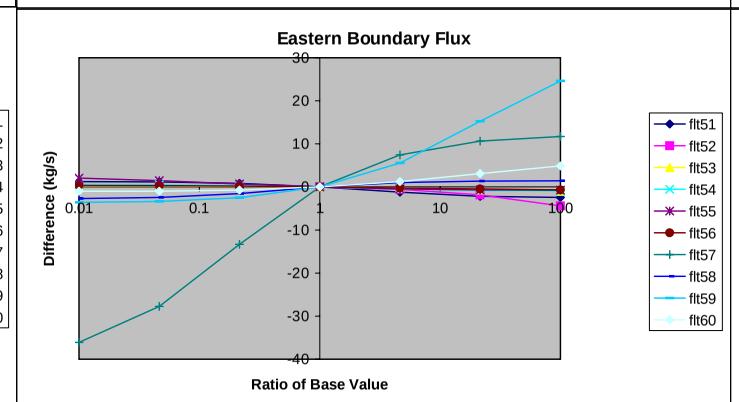
Eastern Boundary Flux
Difference (kg/s)
Ratio of Base Value
flt51
flt52
flt53
flt54
flt55
flt56
flt57
flt58
flt59
flt60

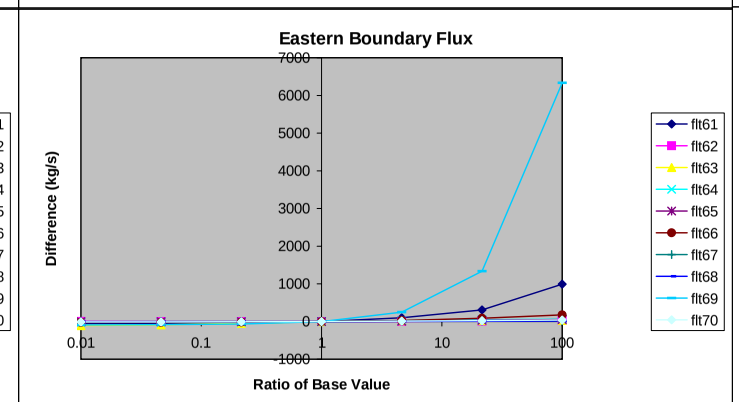
Eastern Boundary Flux
Difference (kg/s)
Ratio of Base Value
flt61
flt62
flt63
flt64
flt65
flt66
flt67
flt68
flt69
flt70

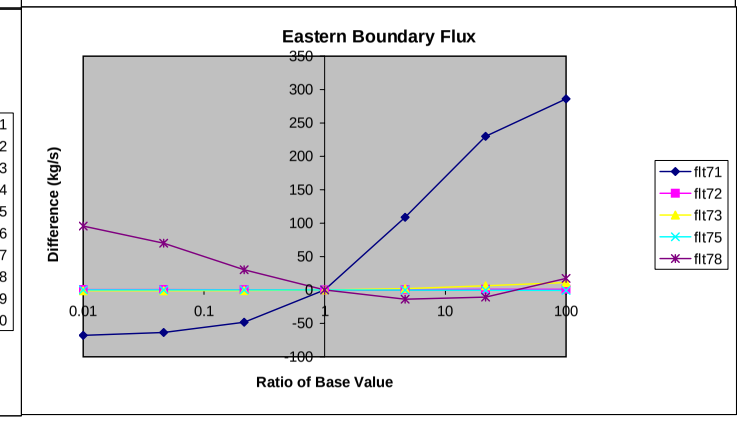
Eastern Boundary Flux
Difference (kg/s)
Ratio of Base Value
flt71
flt72
flt73
flt75
flt78

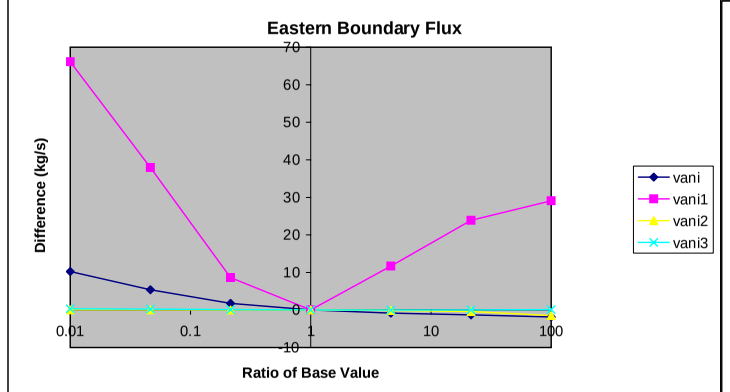
Eastern Boundary Flux
Difference (kg/s)
Ratio of Base Value
vani
vani1
vani2
vani3

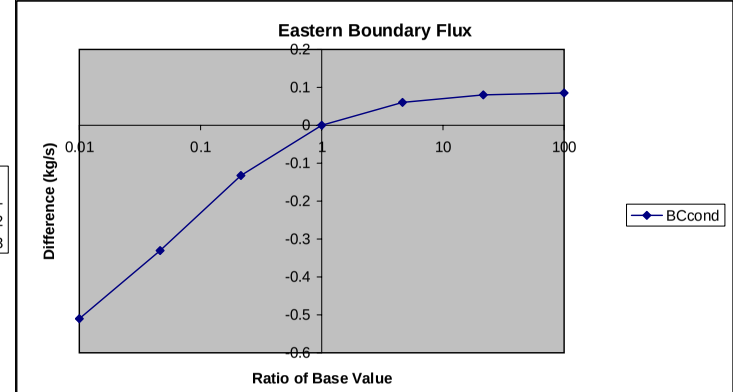
Eastern Boundary Flux
Difference (kg/s)
Ratio of Base Value
BCcond

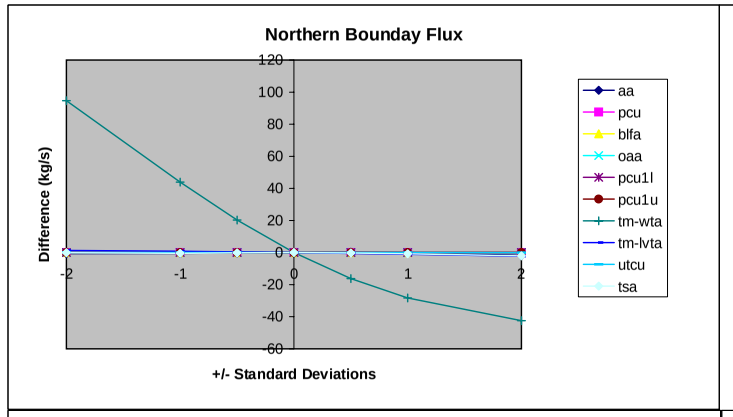
Northern Bounday Flux
Difference (kg/s)
+/- Standard Deviations
aa
pcu
blfa
oaa
pcu1l
pcu1u
tm-wta
tm-lvta
utcu
tsa

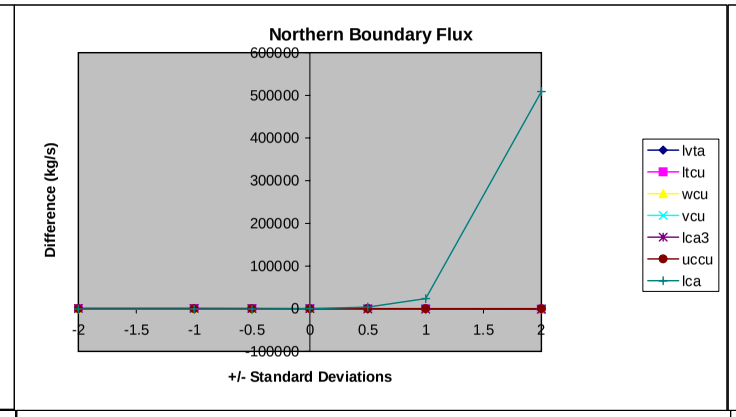
Northern Boundary Flux
Difference (kg/s)
+/- Standard Deviations
lvta
ltcu
wcu
vcu
lca3
uccu
lca

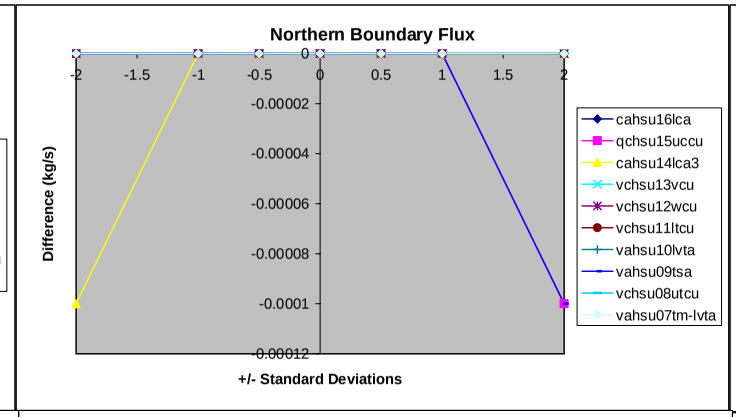
Northern Boundary Flux
Difference (kg/s)
+/- Standard Deviations
cahsu16lca
qchsu15uccu
cahsu14lca3
vchsu13vcu
vchsu12wcu
vchsu11ltcu
vahsu10lvta
vahsu09tsa
vchsu08utcu
vahsu07tm-lvta

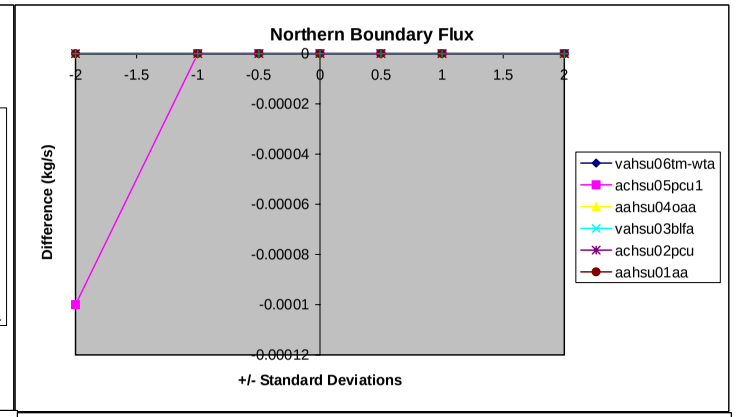
Northern Boundary Flux
Difference (kg/s)
+/- Standard Deviations
vahsu06tm-wta
achsu05pcu1
aahsu04oaa
vahsu03blfa
achsu02pcu
aahsu01aa

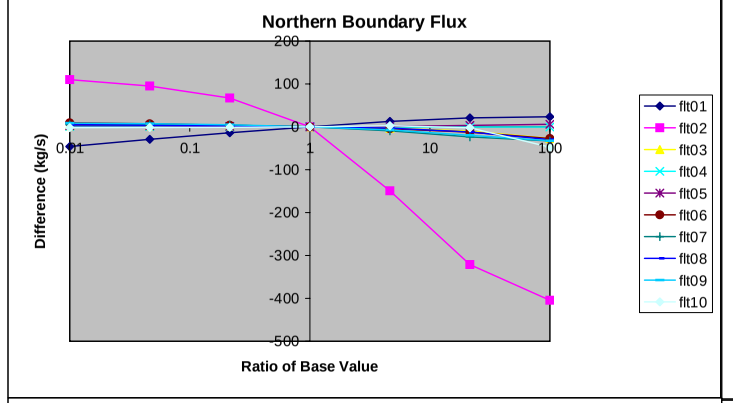
Northern Boundary Flux
Difference (kg/s)
Ratio of Base Value
flt01
flt02
flt03
flt04
flt05
flt06
flt07
flt08
flt09
flt10

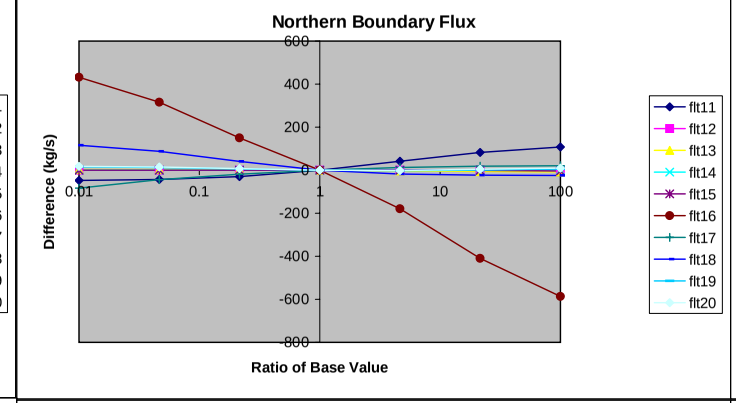
Northern Boundary Flux
Difference (kg/s)
Ratio of Base Value
flt11
flt12
flt13
flt14
flt15
flt16
flt17
flt18
flt19
flt20

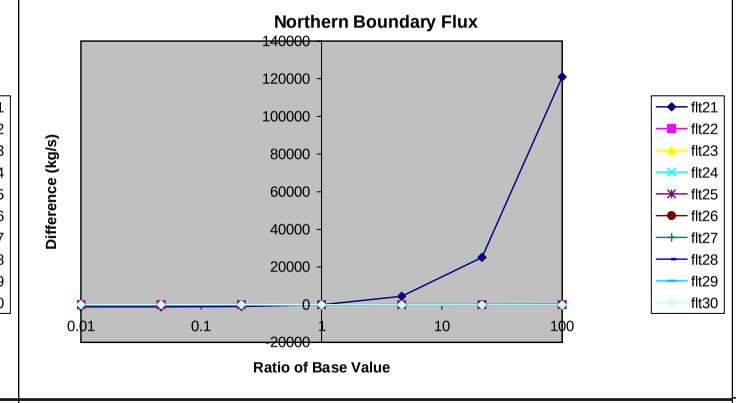
Northern Boundary Flux
Difference (kg/s)
Ratio of Base Value
flt21
flt22
flt23
flt24
flt25
flt26
flt27
flt28
flt29
flt30

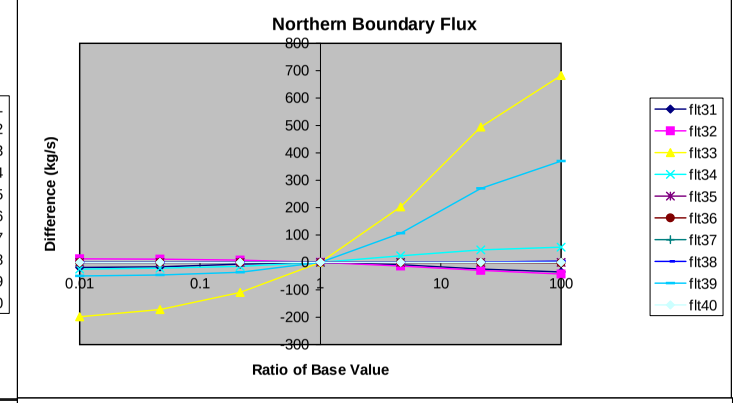
Northern Boundary Flux
Difference (kg/s)
Ratio of Base Value
flt31
flt32
flt33
flt34
flt35
flt36
flt37
flt38
flt39
flt40

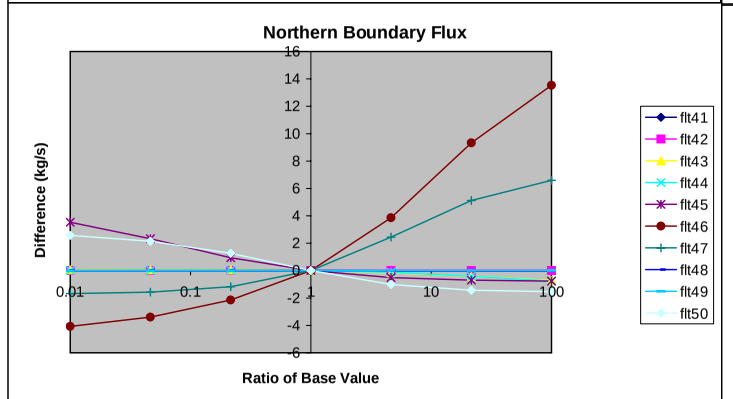
Northern Boundary Flux
Difference (kg/s)
Ratio of Base Value
flt41
flt42
flt43
flt44
flt45
flt46
flt47
flt48
flt49
flt50

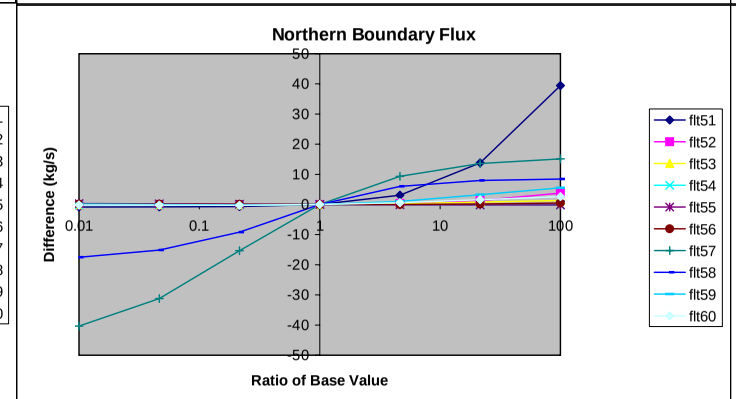
Northern Boundary Flux
Difference (kg/s)
Ratio of Base Value
flt51
flt52
flt53
flt54
flt55
flt56
flt57
flt58
flt59
flt60

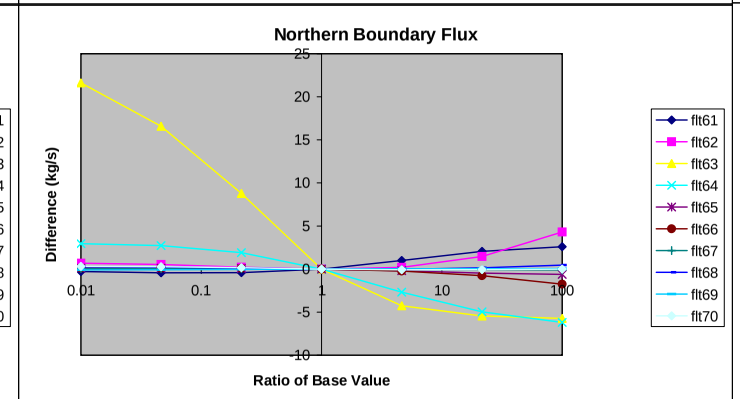
Northern Boundary Flux
Difference (kg/s)
Ratio of Base Value
flt61
flt62
flt63
flt64
flt65
flt66
flt67
flt68
flt69
flt70

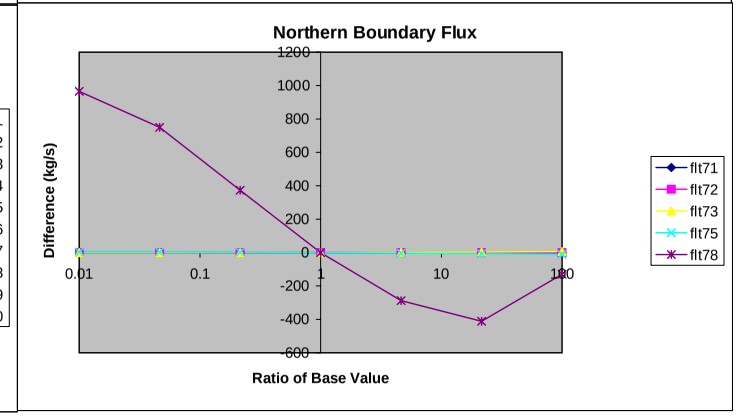
Northern Boundary Flux
Difference (kg/s)
Ratio of Base Value
flt71
flt72
flt73
flt75
flt78

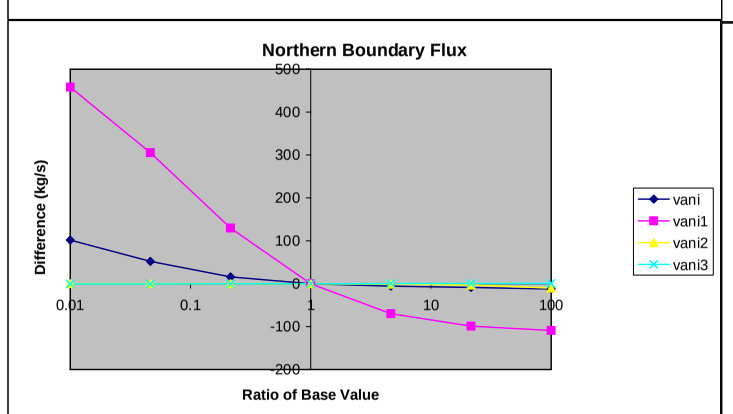
Northern Boundary Flux
Difference (kg/s)
Ratio of Base Value
vani
vani1
vani2
vani3

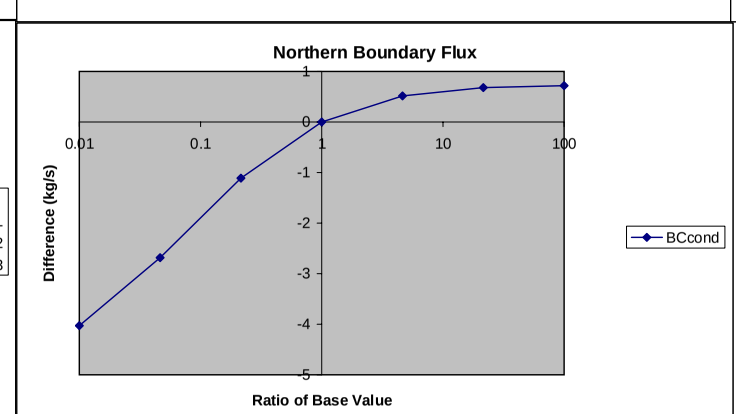
Northern Boundary Flux
Difference (kg/s)
Ratio of Base Value
BCcond

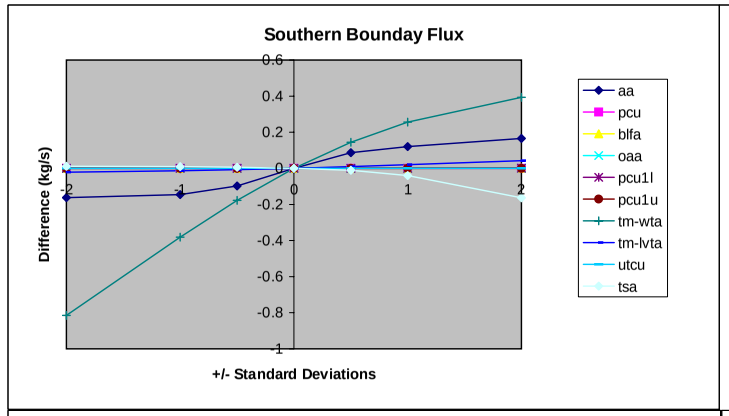
Southern Bounday Flux
Difference (kg/s)
+/- Standard Deviations
aa
pcu
blfa
oaa
pcu1l
pcu1u
tm-wta
tm-lvta
utcu
tsa

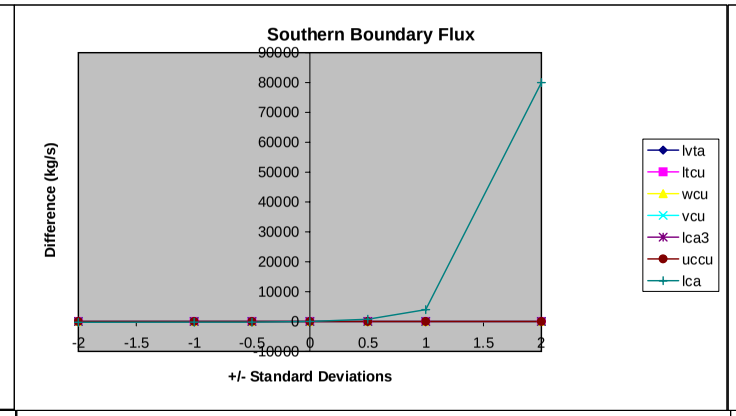
Southern Boundary Flux
Difference (kg/s)
+/- Standard Deviations
lvta
ltcu
wcu
vcu
lca3
uccu
lca

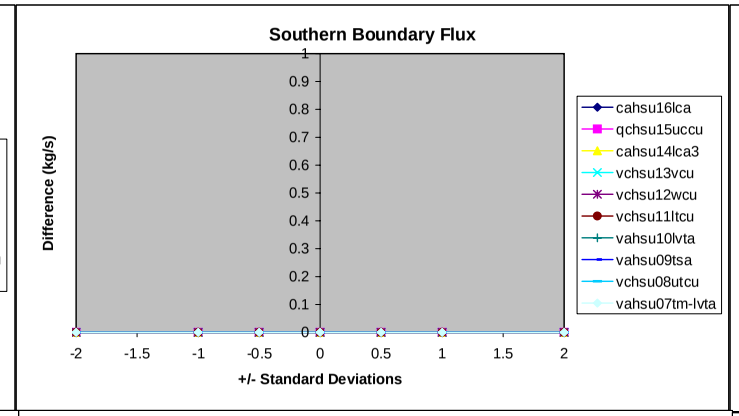
Southern Boundary Flux
Difference (kg/s)
+/- Standard Deviations
cahsu16lca
qchsu15uccu
cahsu14lca3
vchsu13vcu
vchsu12wcu
vchsu11ltcu
vahsu10lvta
vahsu09tsa
vchsu08utcu
vahsu07tm-lvta

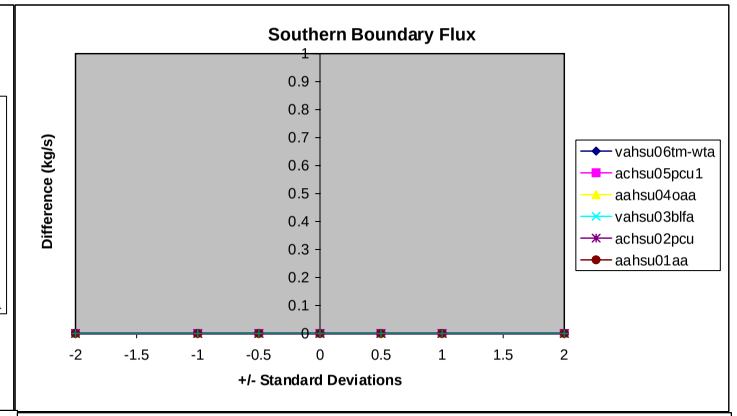
Southern Boundary Flux
Difference (kg/s)
+/- Standard Deviations
vahsu06tm-wta
achsu05pcu1
aahsu04oaa
vahsu03blfa
achsu02pcu
aahsu01aa

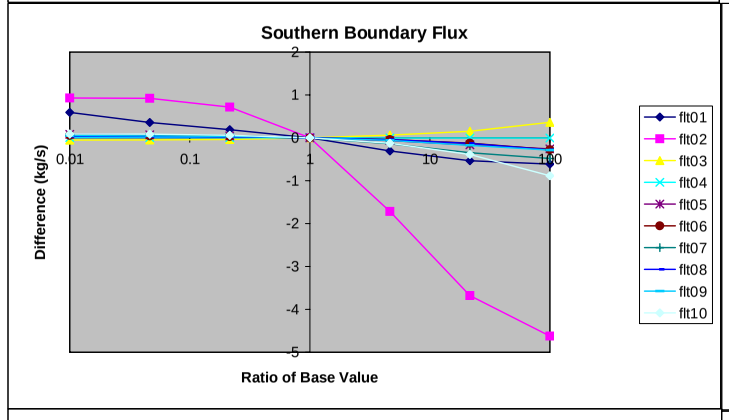
Southern Boundary Flux
Difference (kg/s)
Ratio of Base Value
flt01
flt02
flt03
flt04
flt05
flt06
flt07
flt08
flt09
flt10

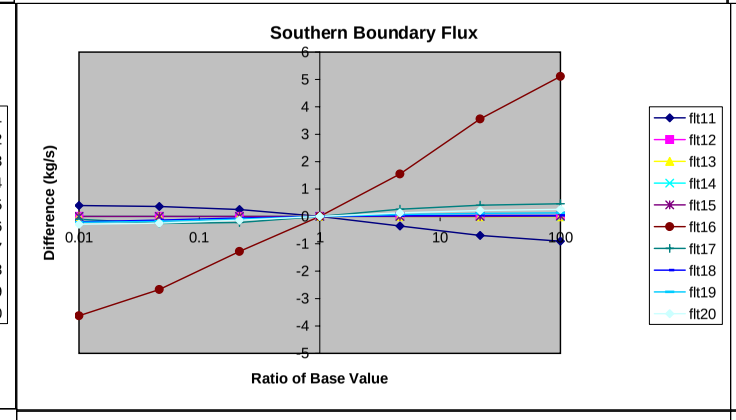
Southern Boundary Flux
Difference (kg/s)
Ratio of Base Value
flt11
flt12
flt13
flt14
flt15
flt16
flt17
flt18
flt19
flt20

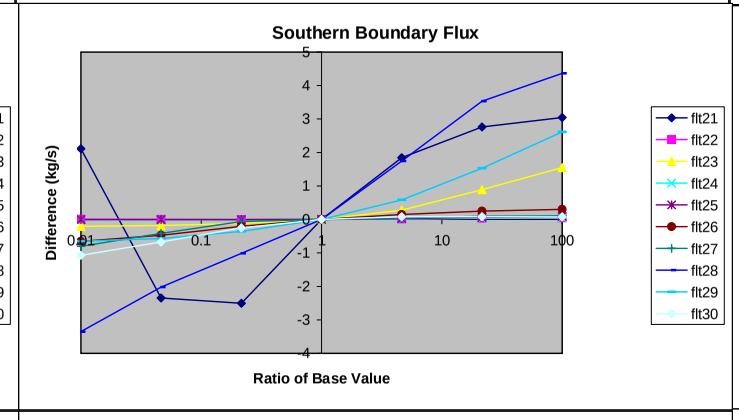
Southern Boundary Flux
Difference (kg/s)
Ratio of Base Value
flt21
flt22
flt23
flt24
flt25
flt26
flt27
flt28
flt29
flt30

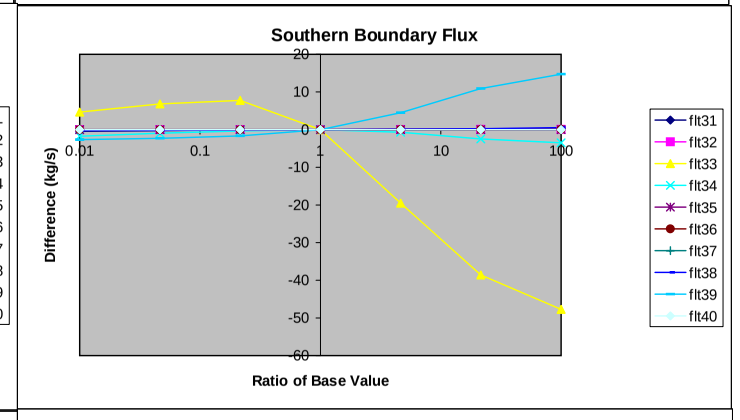
Southern Boundary Flux
Difference (kg/s)
Ratio of Base Value
flt31
flt32
flt33
flt34
flt35
flt36
flt37
flt38
flt39
flt40

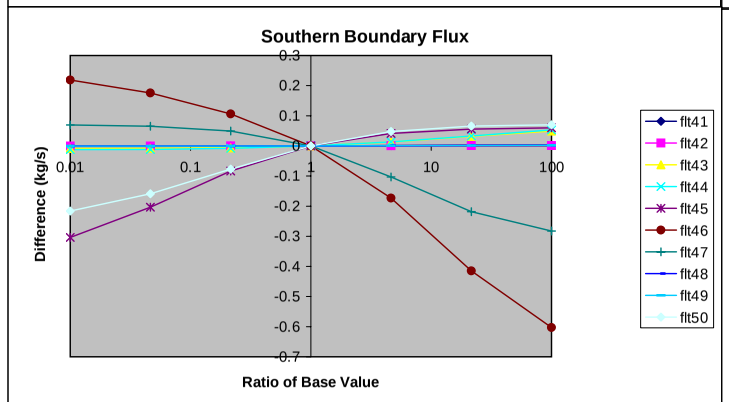
Southern Boundary Flux
Difference (kg/s)
Ratio of Base Value
flt41
flt42
flt43
flt44
flt45
flt46
flt47
flt48
flt49
flt50

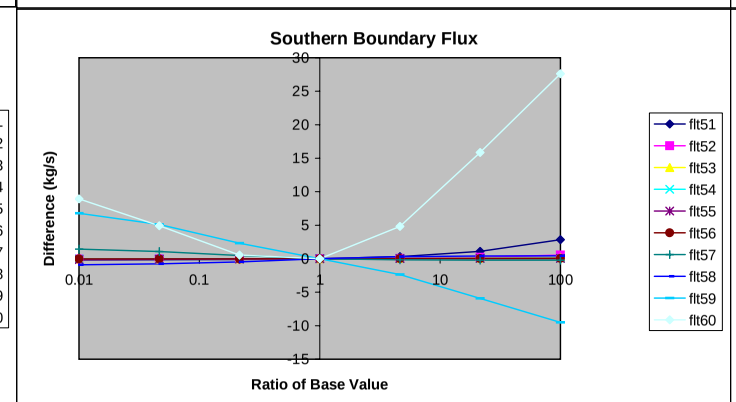
Southern Boundary Flux
Difference (kg/s)
Ratio of Base Value
flt51
flt52
flt53
flt54
flt55
flt56
flt57
flt58
flt59
flt60

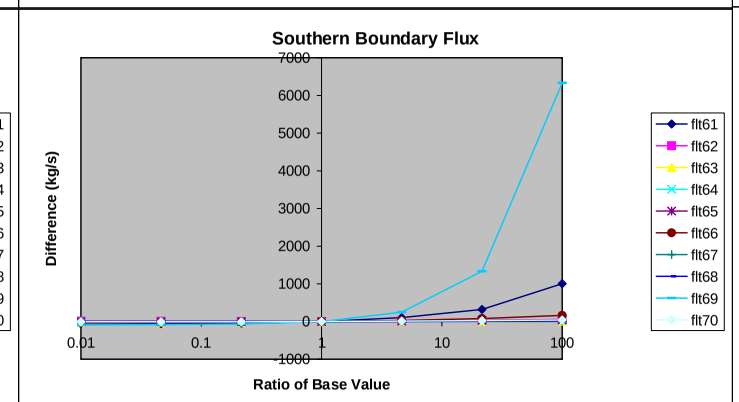
Southern Boundary Flux
Difference (kg/s)
Ratio of Base Value
flt61
flt62
flt63
flt64
flt65
flt66
flt67
flt68
flt69
flt70

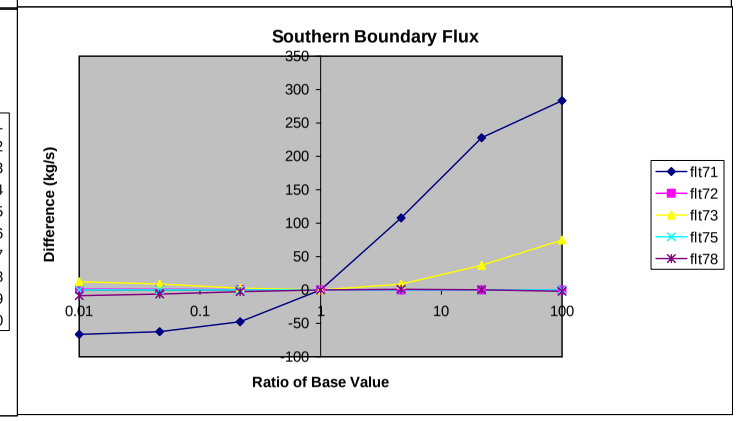
Southern Boundary Flux
Difference (kg/s)
Ratio of Base Value
flt71
flt72
flt73
flt75
flt78

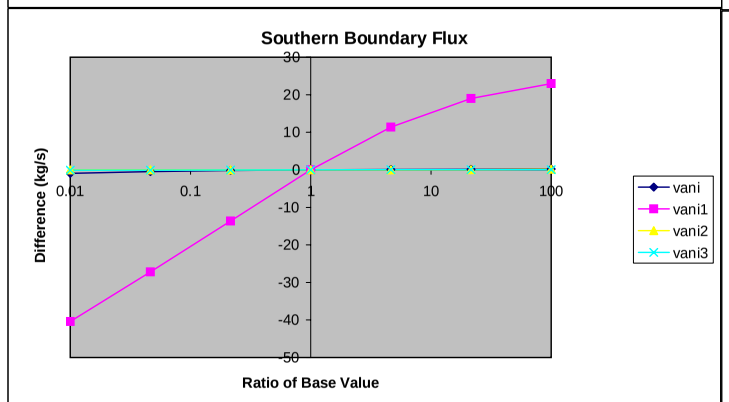
Southern Boundary Flux
Difference (kg/s)
Ratio of Base Value
vani
vani1
vani2
vani3

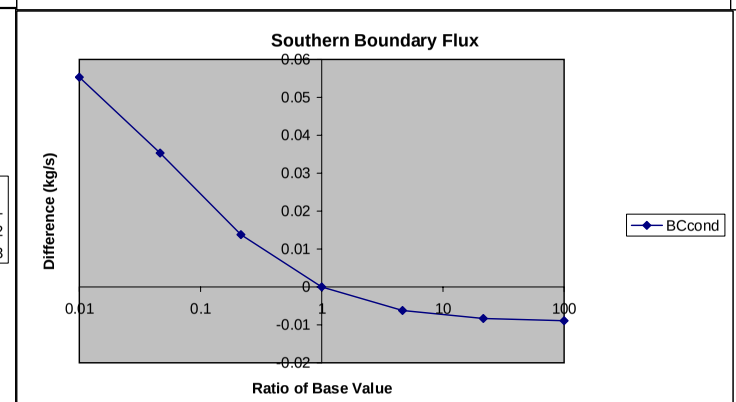
Southern Boundary Flux
Difference (kg/s)
Ratio of Base Value
BCcond

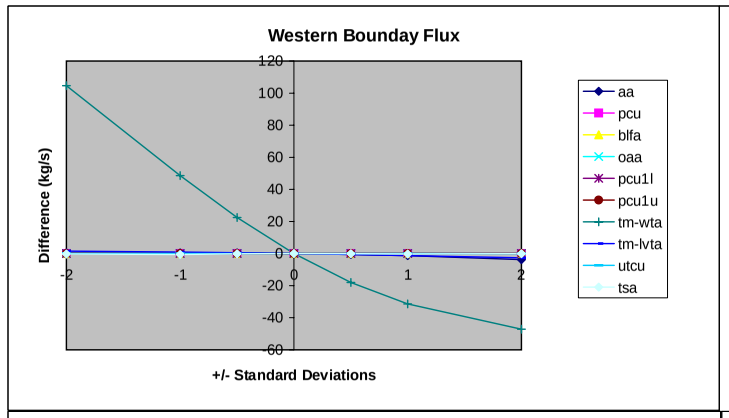
Western Bounday Flux
Difference (kg/s)
+/- Standard Deviations
aa
pcu
bifa
oaa
pcu1l
pcu1u
tm-wta
tm-lvta
utcu
tsa

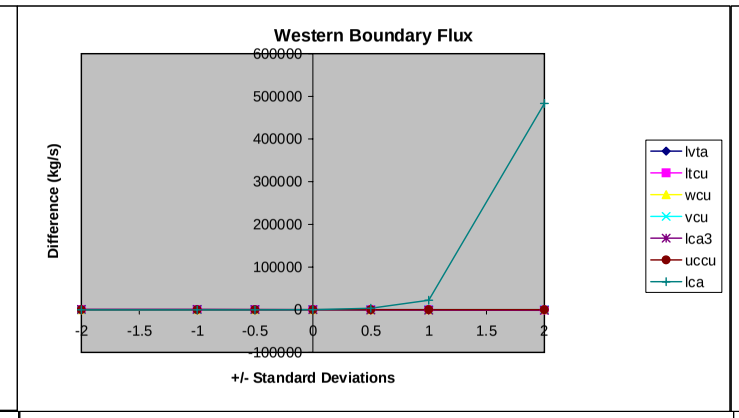
Western Boundary Flux
Difference (kg/s)
+/- Standard Deviations
lvta
ltcu
wcu
vcu
lca3
uccu
lca

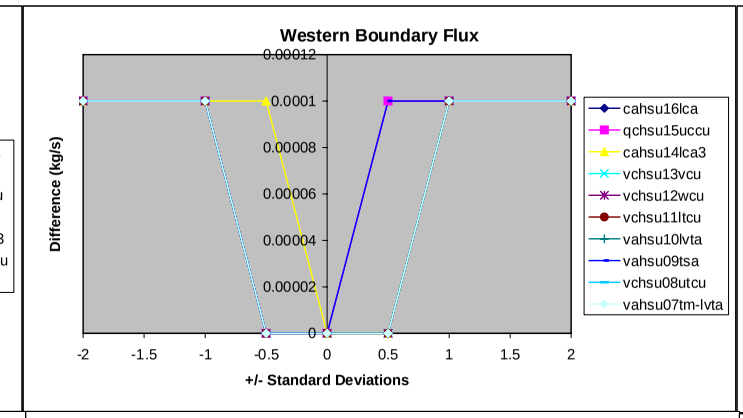
Western Boundary Flux
Difference (kg/s)
+/- Standard Deviations
cahsu16lca
qchsu15uccu
cahsu14lca3
vchsu13vcu
vchsu12wcu
vchsu11ltcu
vahsu10lvta
vahsu09tsa
vchsu08utcu
vahsu07tm-lvta

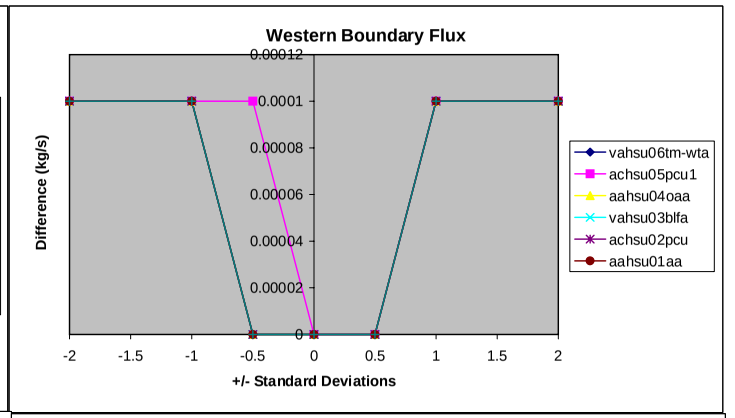
Western Boundary Flux
Difference (kg/s)
+/- Standard Deviations
vahsu06tm-wta
achsu05pcu1
aahsu04oaa
vahsu03blfa
achsu02pcu
aahsu01aa

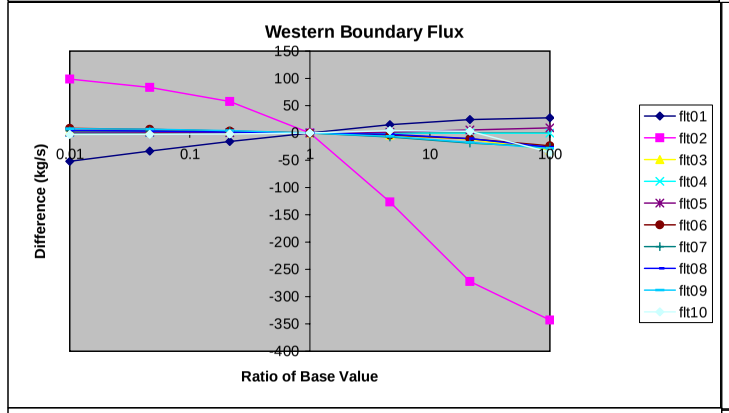
Western Boundary Flux
Difference (kg/s)
Ratio of Base Value
flt01
flt02
flt03
flt04
flt05
flt06
flt07
flt08
flt09
flt10

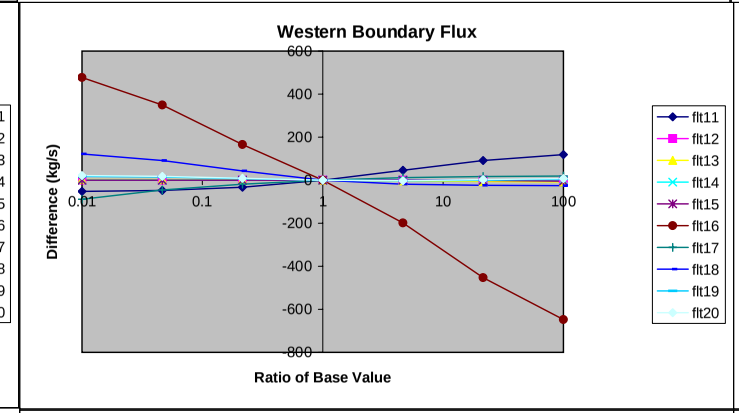
Western Boundary Flux
Difference (kg/s)
Ratio of Base Value
flt11
flt12
flt13
flt14
flt15
flt16
flt17
flt18
flt19
flt20

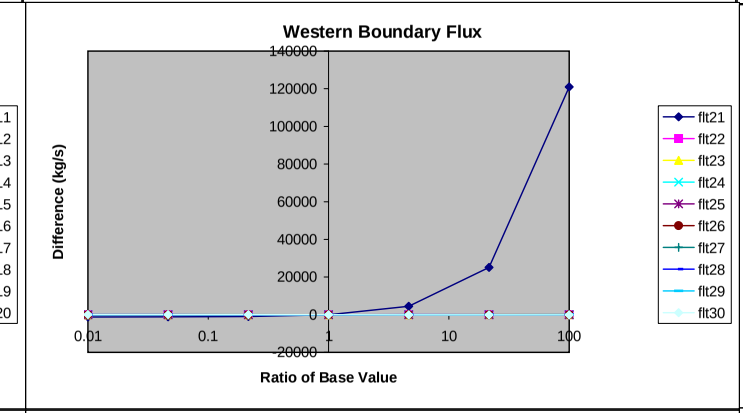
Western Boundary Flux
Difference (kg/s)
Ratio of Base Value
flt21
flt22
flt23
flt24
flt25
flt26
flt27
flt28
flt29
flt30

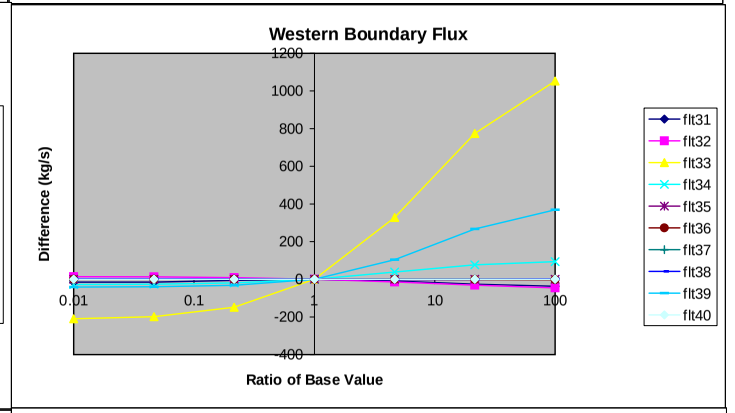
Western Boundary Flux
Difference (kg/s)
Ratio of Base Value
flt31
flt32
flt33
flt34
flt35
flt36
flt37
flt38
flt39
flt40

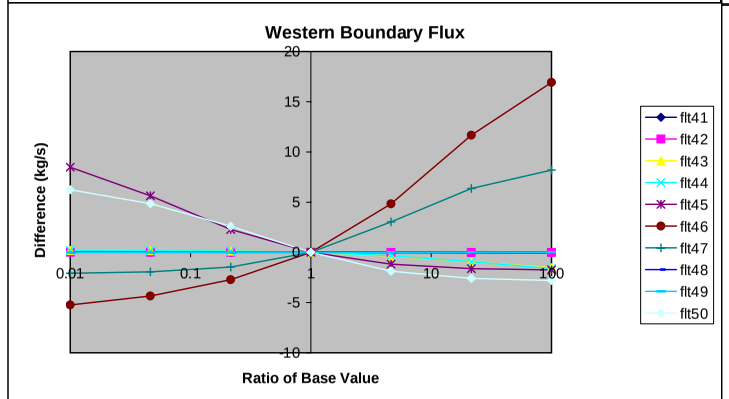
Western Boundary Flux
Difference (kg/s)
Ratio of Base Value
flt41
flt42
flt43
flt44
flt45
flt46
flt47
flt48
flt49
flt50

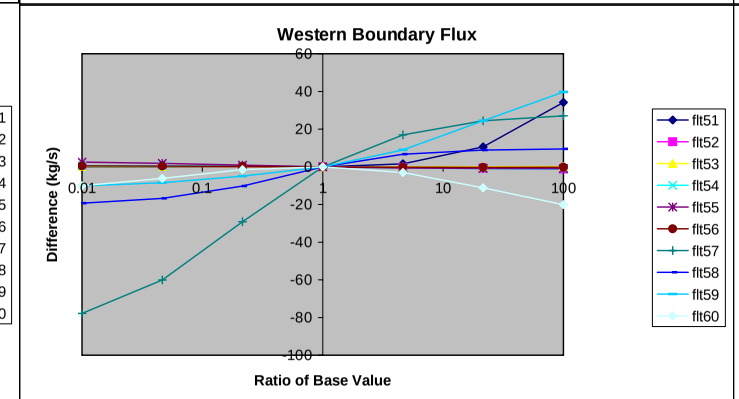
Western Boundary Flux
Difference (kg/s)
Ratio of Base Value
flt51
flt52
flt53
flt54
flt55
flt56
flt57
flt58
flt59
flt60

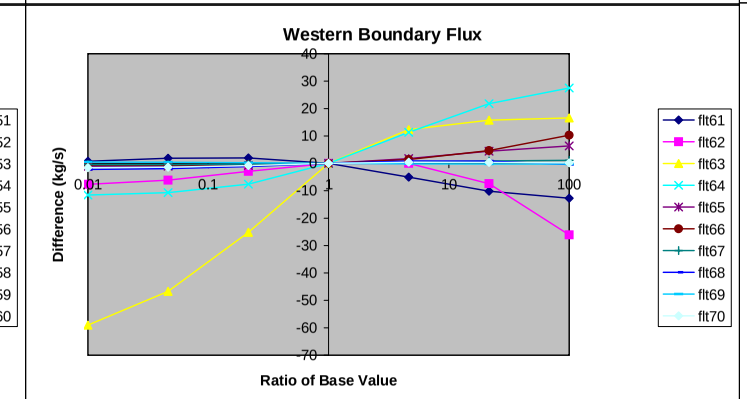
Western Boundary Flux
Difference (kg/s)
Ratio of Base Value
flt61
flt62
flt63
flt64
flt65
flt66
flt67
flt68
flt69
flt70

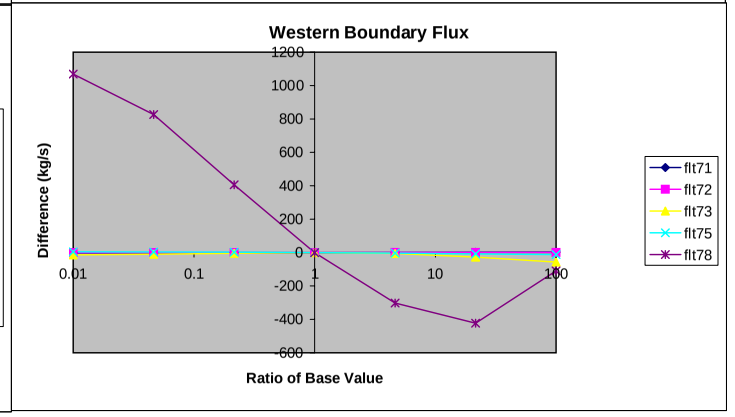
Western Boundary Flux
Difference (kg/s)
Ratio of Base Value
flt71
flt72
flt73
flt75
flt78

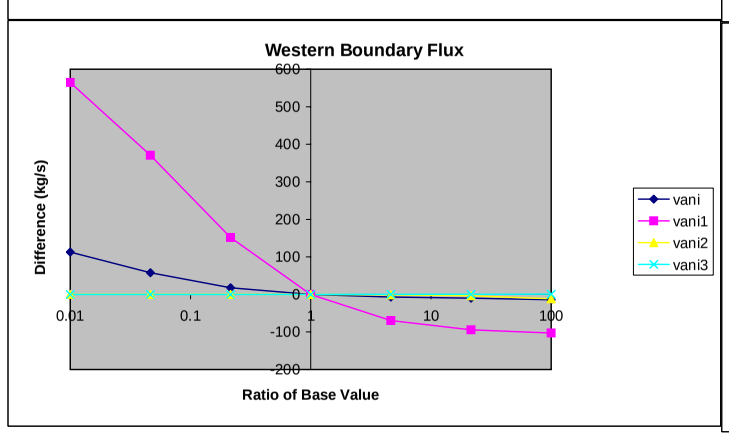
Western Boundary Flux
Difference (kg/s)
Ratio of Base Value
vani
vani1
vani2
vani3

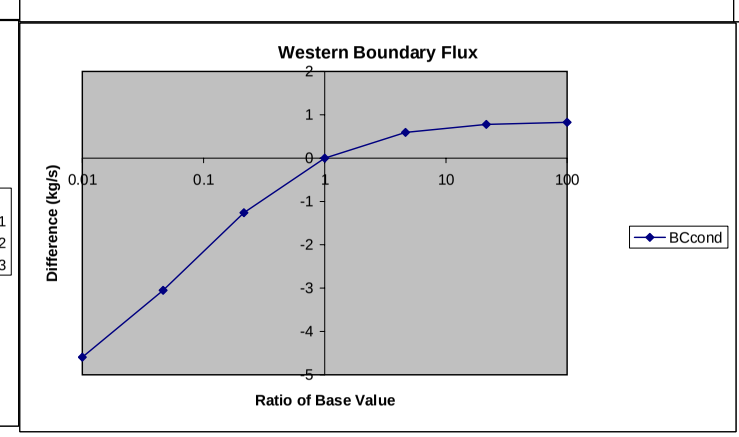
Western Boundary Flux
Difference (kg/s)
Ratio of Base Value
BCcond

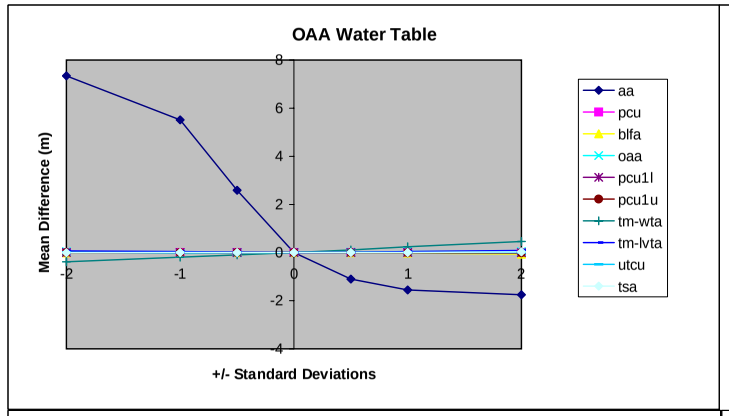
OAA Water Table
Mean Difference (m)
+/- Standard Deviations
aa
pcu
blfa
oaa
pcu1l
pcu1u
tm-wta
tm-lvta
utcu
tsa

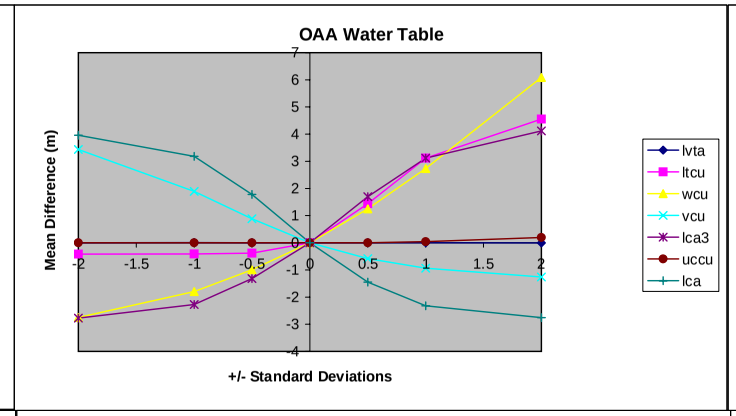
OAA Water Table
Mean Difference (m)
+/- Standard Deviations
lvta
ltcu
wcu
vcu
lca3
uccu
lca

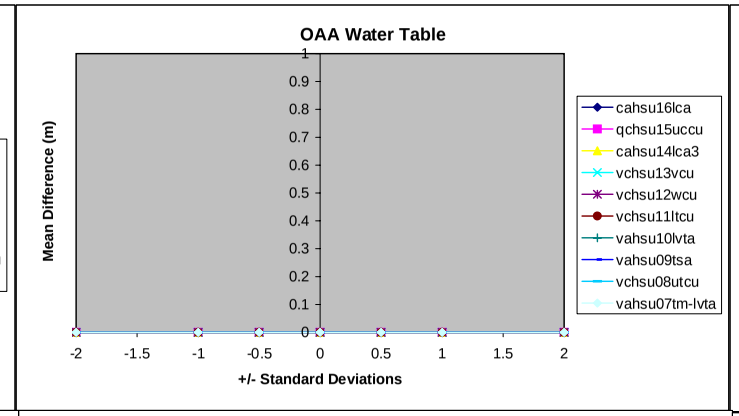
OAA Water Table
Mean Difference (m)
+/- Standard Deviations
cahsu16lca
qchsu15uccu
cahsu14lca3
vchsu13vcu
vchsu12wcu
vchsu11ltcu
vahsu10lvta
vahsu09tsa
vchsu08utcu
vahsu07tm-lvta

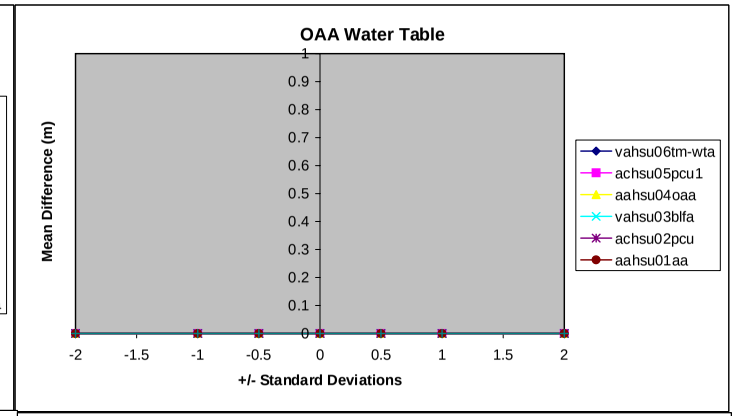
OAA Water Table
Mean Difference (m)
+/- Standard Deviations
vahsu06tm-wta
achsu05pcu1
aahsu04oaa
vahsu03blfa
achsu02pcu
aahsu01aa

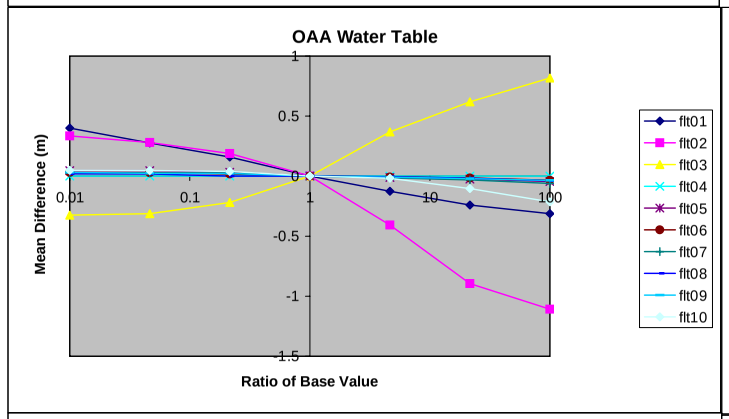
OAA Water Table
Mean Difference (m)
Ratio of Base Value
flt01
flt02
flt03
flt04
flt05
flt06
flt07
flt08
flt09
flt10

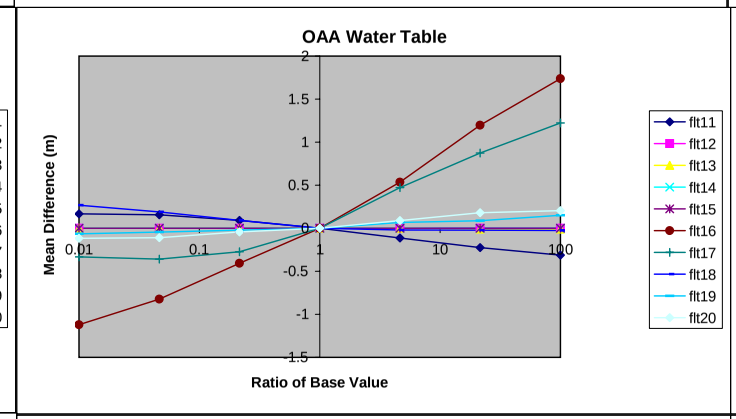
OAA Water Table
Mean Difference (m)
Ratio of Base Value
flt11
flt12
flt13
flt14
flt15
flt16
flt17
flt18
flt19
flt20

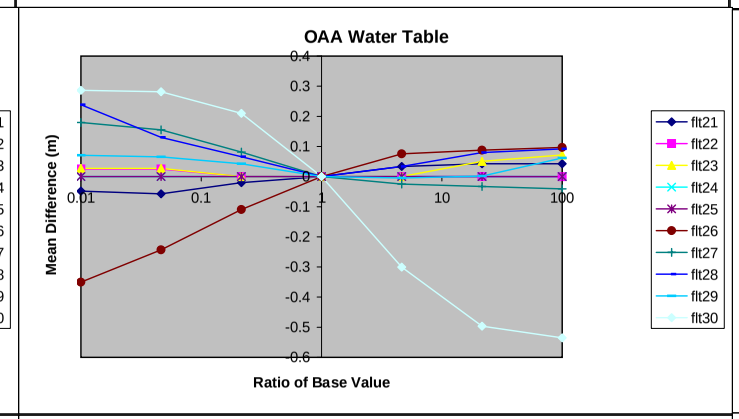
OAA Water Table
Mean Difference (m)
Ratio of Base Value
flt21
flt22
flt23
flt24
flt25
flt26
flt27
flt28
flt29
flt30

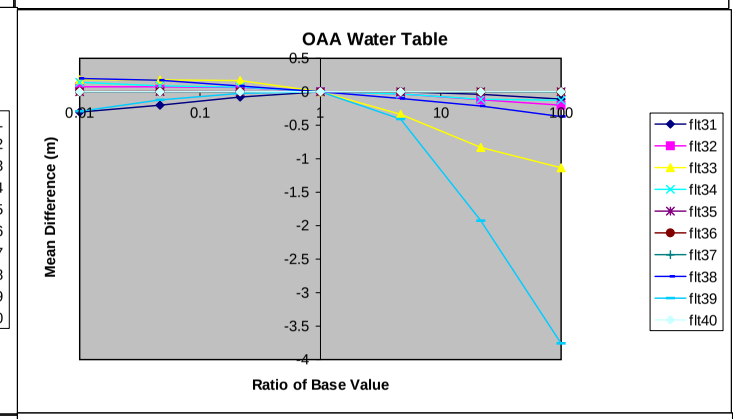
OAA Water Table
Mean Difference (m)
Ratio of Base Value
flt31
flt32
flt33
flt34
flt35
flt36
flt37
flt38
flt39
flt40

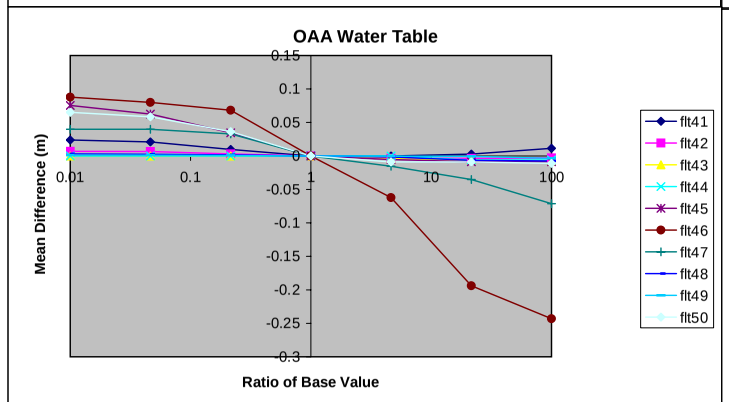
OAA Water Table
Mean Difference (m)
Ratio of Base Value
flt41
flt42
flt43
flt44
flt45
flt46
flt47
flt48
flt49
flt50

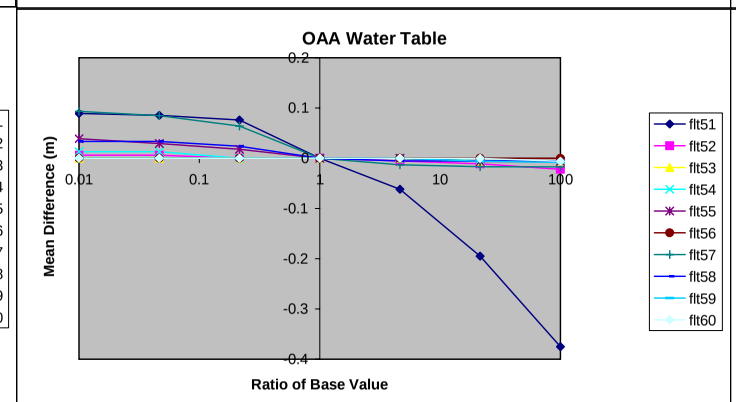
OAA Water Table
Mean Difference (m)
Ratio of Base Value
flt51
flt52
flt53
flt54
flt55
flt56
flt57
flt58
flt59
flt60

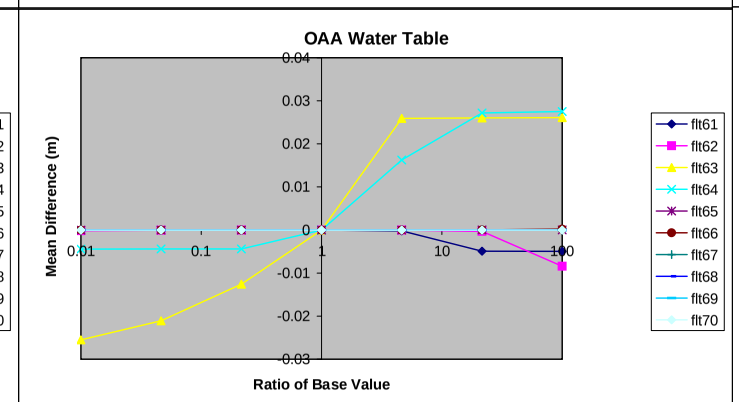
OAA Water Table
Mean Difference (m)
Ratio of Base Value
flt61
flt62
flt63
flt64
flt65
flt66
flt67
flt68
flt69
flt70

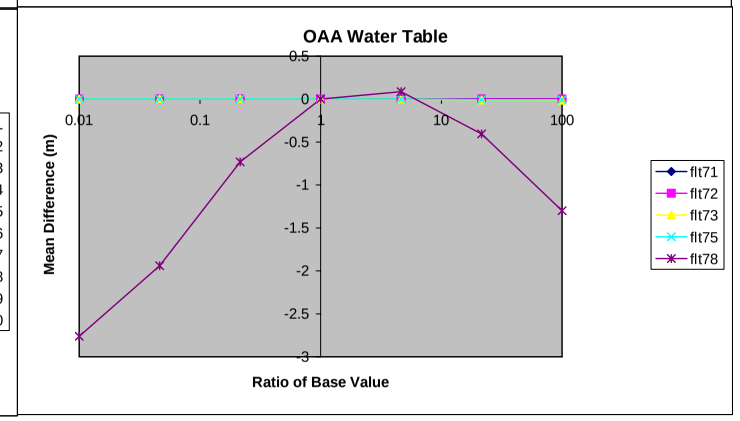
OAA Water Table
Mean Difference (m)
Ratio of Base Value
flt71
flt72
flt73
flt75
flt78

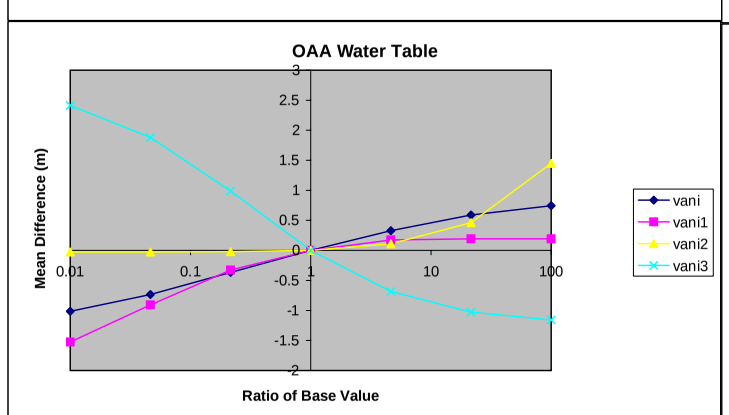
OAA Water Table
Mean Difference (m)
Ratio of Base Value
vani
vani1
vani2
vani3

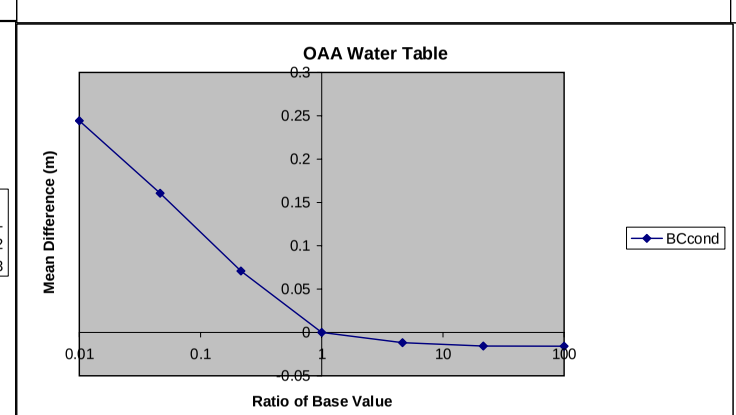
OAA Water Table
Mean Difference (m)
Ratio of Base Value
BCcond

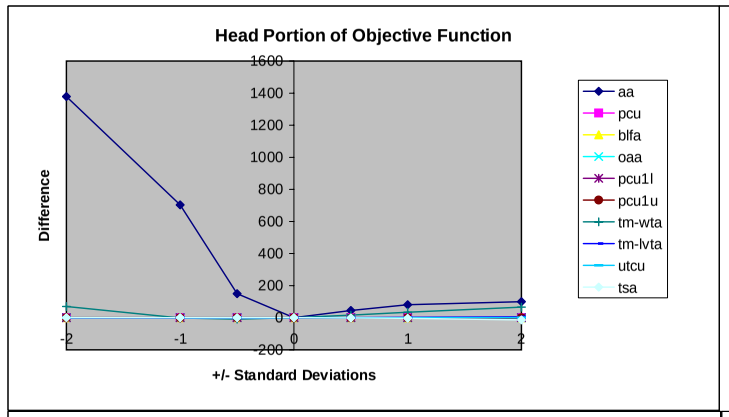
Head Portion of Objective Function
Difference
+/- Standard Deviations
aa
pcu
blfa
oaa
pcu1l
pcu1u
tm-wta
tm-lvta
utcu
tsa

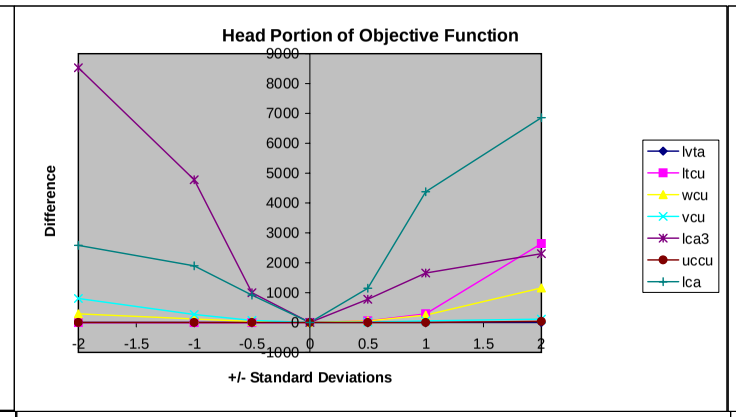
Head Portion of Objective Function
Difference
+/- Standard Deviations
lvta
ltcu
wcu
vcu
lca3
uccu
lca

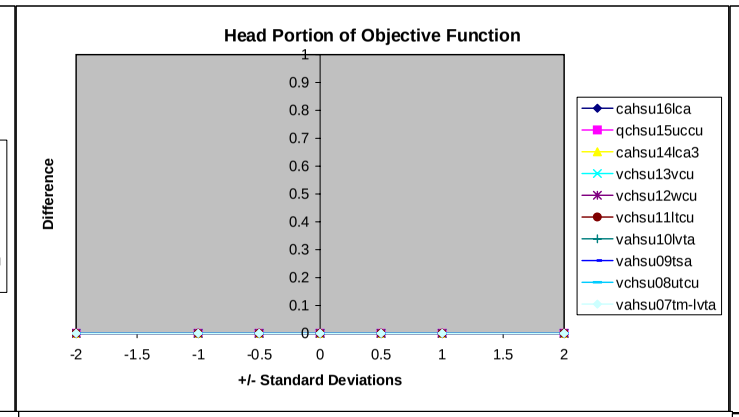
Head Portion of Objective Function
Difference
+/- Standard Deviations
cahsu16lca
qchsu15uccu
cahsu14lca3
vchsu13vcu
vchsu12wcu
vchsu11ltcu
vahsu10lvta
vahsu09tsa
vchsu08utcu
vahsu07tm-lvta

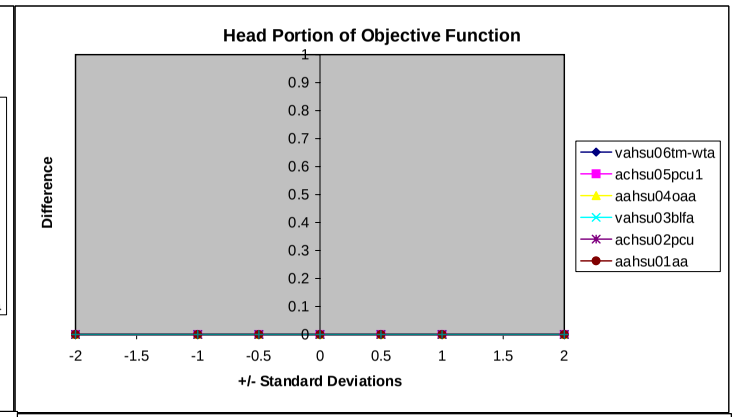
Head Portion of Objective Function
Difference
+/- Standard Deviations
vahsu06tm-wta
achsu05pcu1
aahsu04oaa
vahsu03blfa
achsu02pcu
aahsu01aa

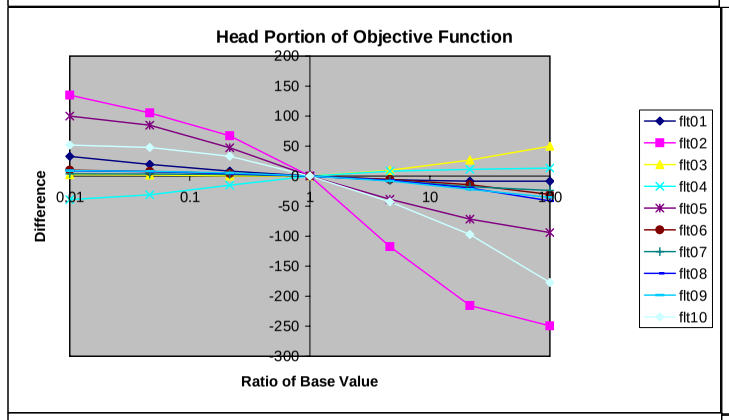
Head Portion of Objective Function
Difference
Ratio of Base Value
flt01
flt02
flt03
flt04
flt05
flt06
flt07
flt08
flt09
flt10

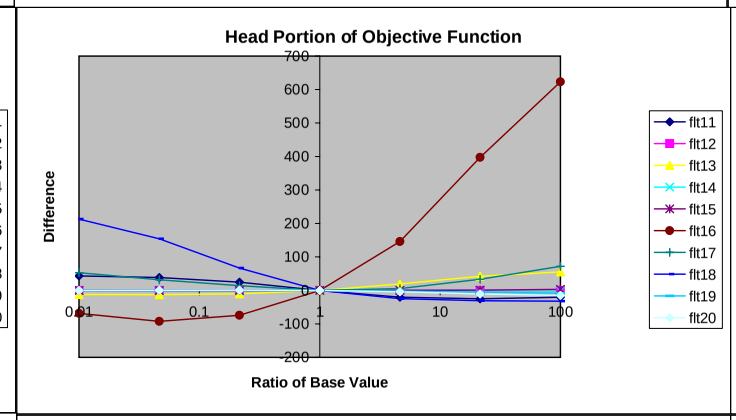
Head Portion of Objective Function
Difference
Ratio of Base Value
flt11
flt12
flt13
flt14
flt15
flt16
flt17
flt18
flt19
flt20

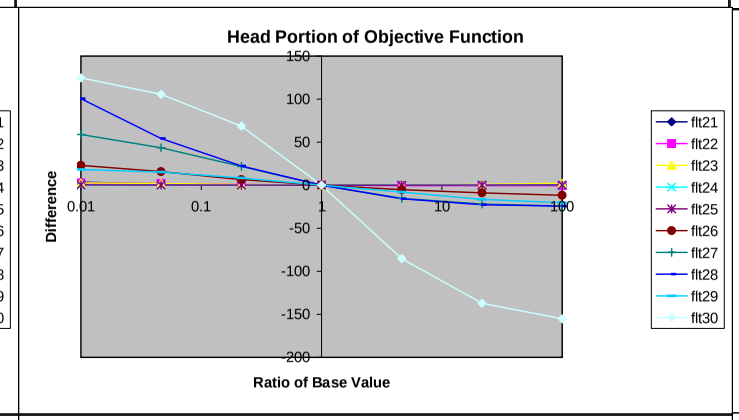
Head Portion of Objective Function
Difference
Ratio of Base Value
flt21
flt22
flt23
flt24
flt25
flt26
flt27
flt28
flt29
flt30

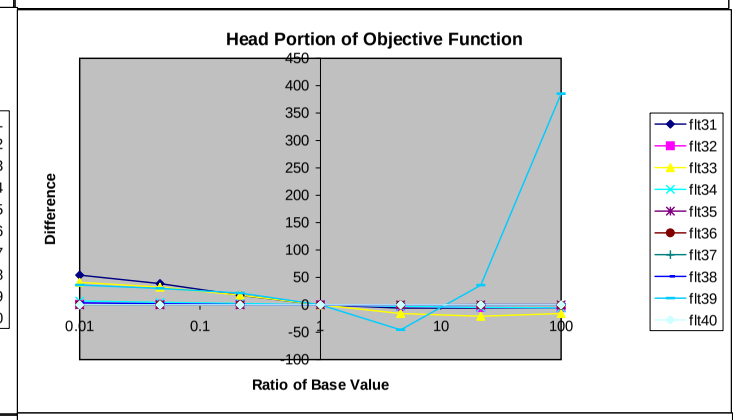
Head Portion of Objective Function
Difference
Ratio of Base Value
flt31
flt32
flt33
flt34
flt35
flt36
flt37
flt38
flt39
flt40

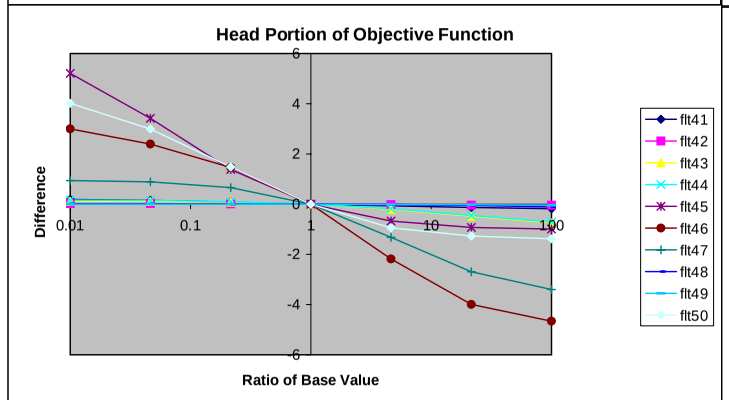
Head Portion of Objective Function
Difference
Ratio of Base Value
flt41
flt42
flt43
flt44
flt45
flt46
flt47
flt48
flt49
flt50

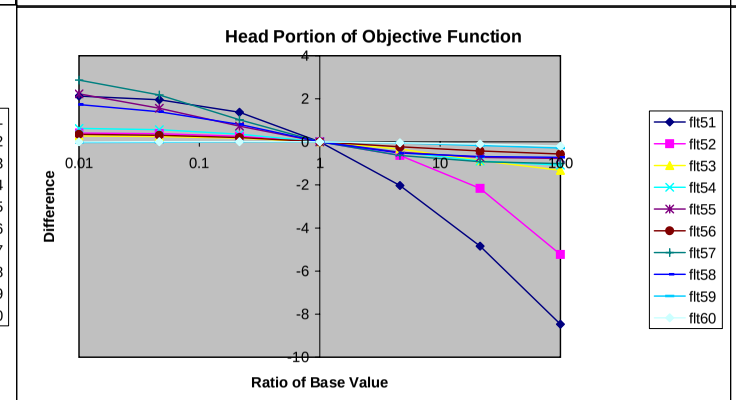
Head Portion of Objective Function
Difference
Ratio of Base Value
flt51
flt52
flt53
flt54
flt55
flt56
flt57
flt58
flt59
flt60

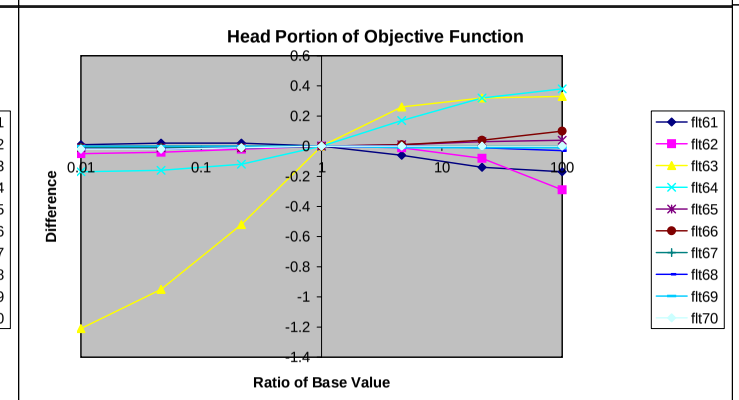
Head Portion of Objective Function
Difference
Ratio of Base Value
flt61
flt62
flt63
flt64
flt65
flt66
flt67
flt68
flt69
flt70

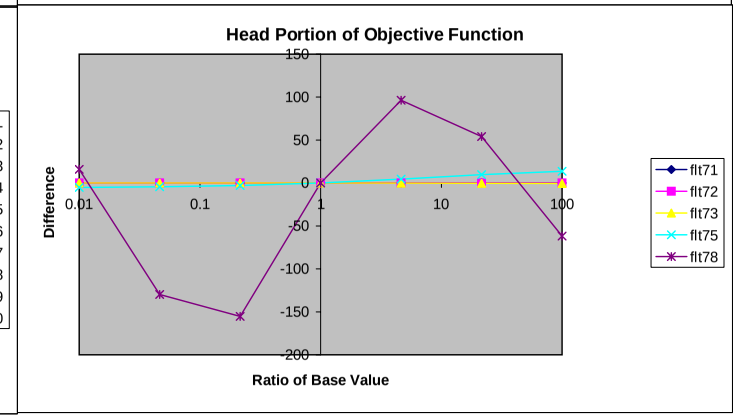
Head Portion of Objective Function
Difference
Ratio of Base Value
flt71
flt72
flt73
flt75
flt78

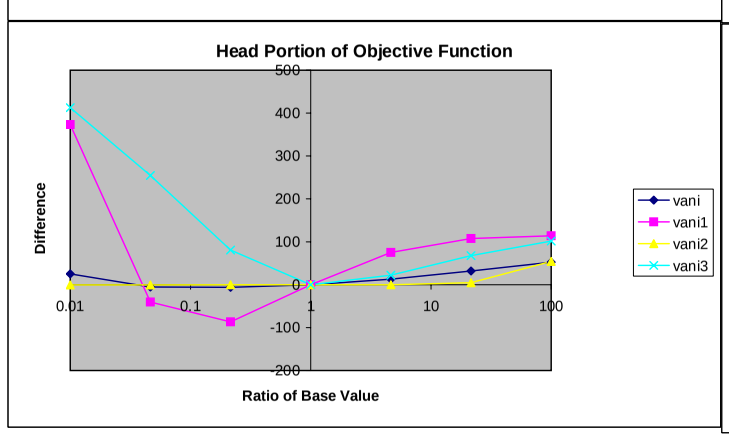
Head Portion of Objective Function
Difference
Ratio of Base Value
vani
vani1
vani2
vani3

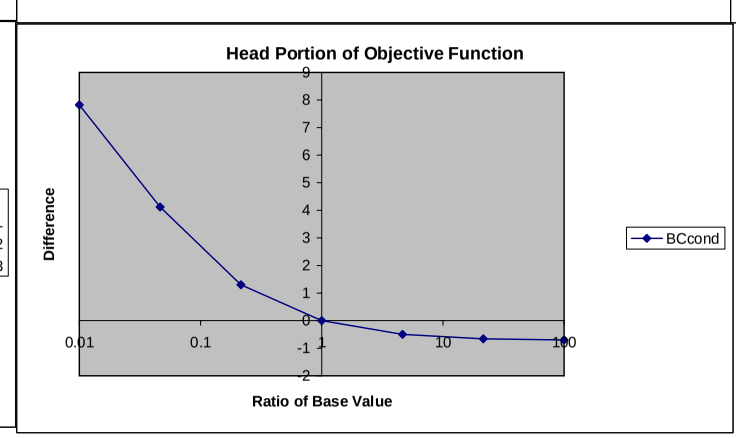
Head Portion of Objective Function
Difference
Ratio of Base Value
BCcond

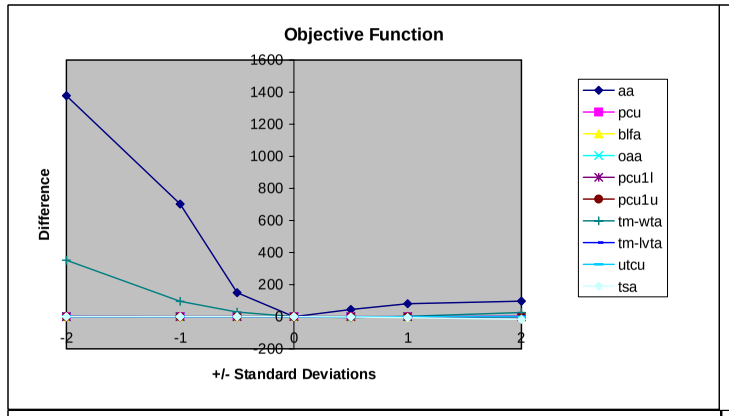
Objective Function
Difference
+/- Standard Deviations
aa
pcu
blfa
oaa
pcu1l
pcu1u
tm-wta
tm-lvta
utcu
tsa

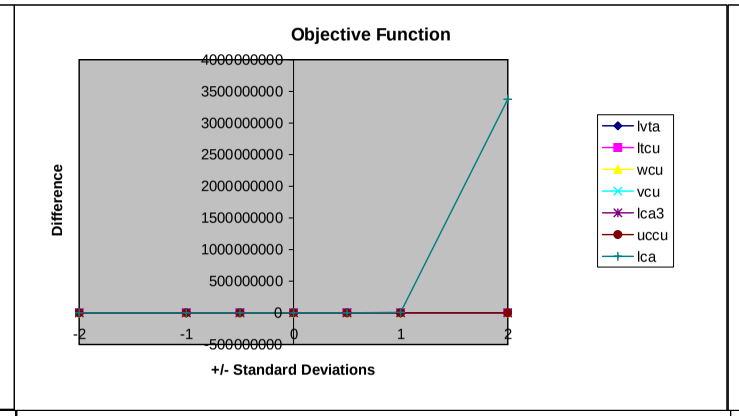
Objective Function
Difference
+/- Standard Deviations
lvta
ltcu
wcu
vcu
lca3
uccu
lca

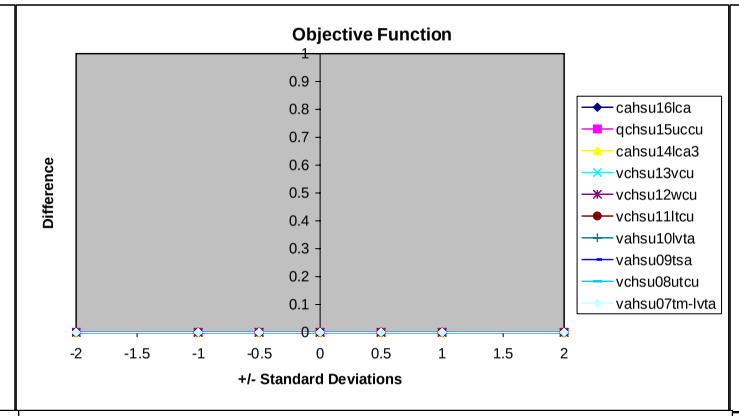
Objective Function
Difference
+/- Standard Deviations
cahsu16lca
qchsu15uccu
cahsu14lca3
vchsu13vcu
vchsu12wcu
vchsu11ltcu
vahsu10lvta
vahsu09tsa
vchsu08utcu
vahsu07tm-lvta

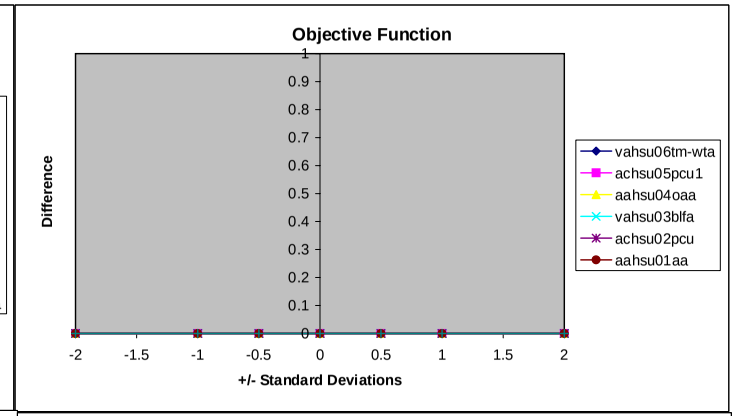
Objective Function
Difference
+/- Standard Deviations
vahsu06tm-wta
achsu05pcu1
aahsu04oaa
vahsu03blfa
achsu02pcu
aahsu01aa

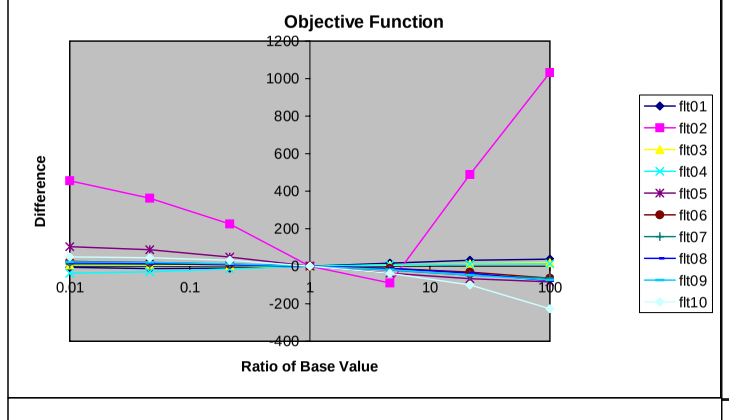
Objective Function
Difference
Ratio of Base Value
flt01
flt02
flt03
flt04
flt05
flt06
flt07
flt08
flt09
flt10

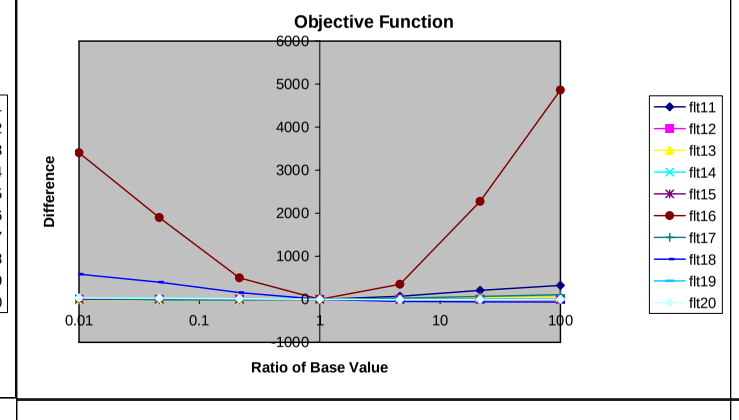
Objective Function
Difference
Ratio of Base Value
flt11
flt12
flt13
flt14
flt15
flt16
flt17
flt18
flt19
flt20

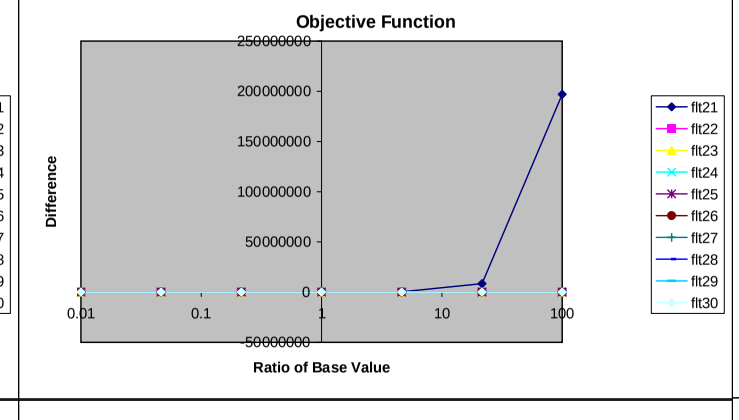
Objective Function
Difference
Ratio of Base Value
flt21
flt22
flt23
flt24
flt25
flt26
flt27
flt28
flt29
flt30

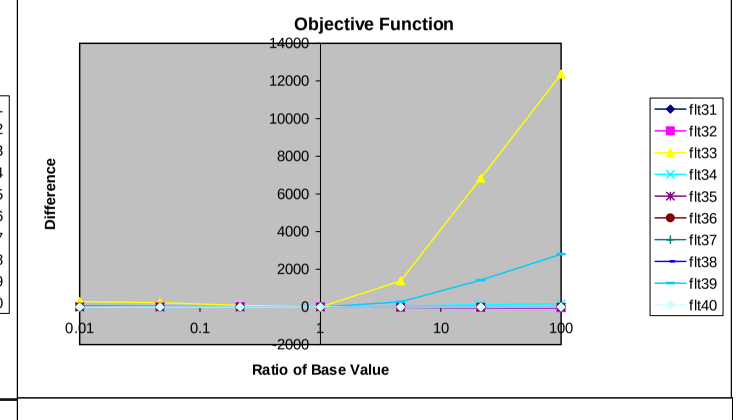
Objective Function
Difference
Ratio of Base Value
flt31
flt32
flt33
flt34
flt35
flt36
flt37
flt38
flt39
flt40

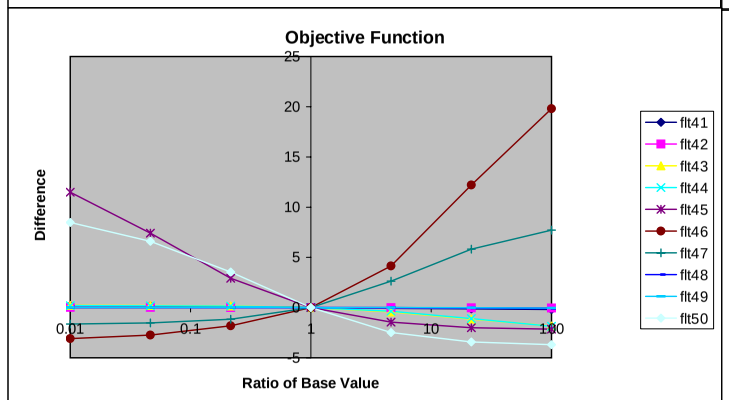
Objective Function
Difference
Ratio of Base Value
flt41
flt42
flt43
flt44
flt45
flt46
flt47
flt48
flt49
flt50

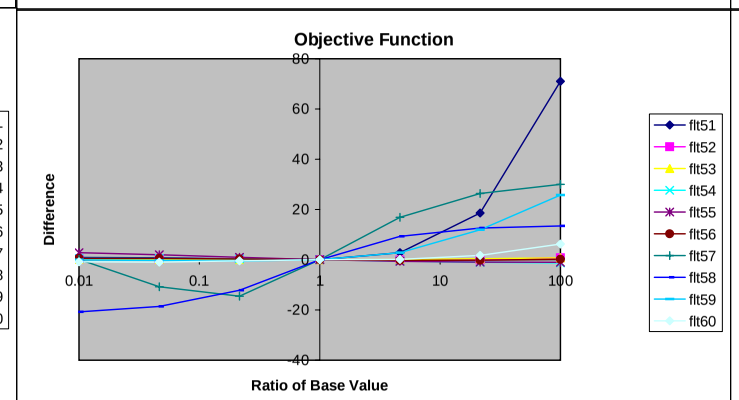
Objective Function
Difference
Ratio of Base Value
flt51
flt52
flt53
flt54
flt55
flt56
flt57
flt58
flt59
flt60

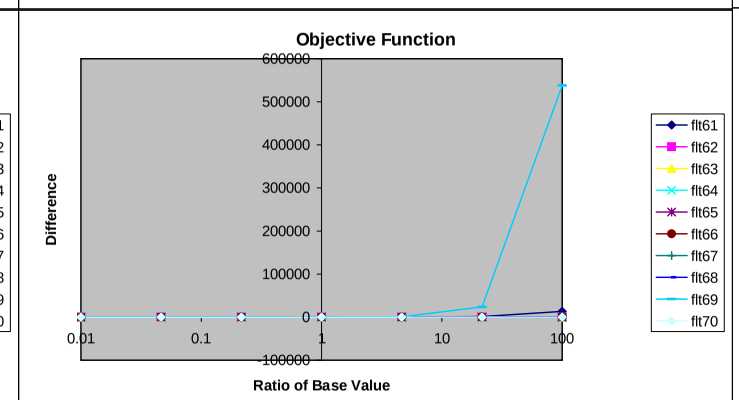
Objective Function
Difference
Ratio of Base Value
flt61
flt62
flt63
flt64
flt65
flt66
flt67
flt68
flt69
flt70

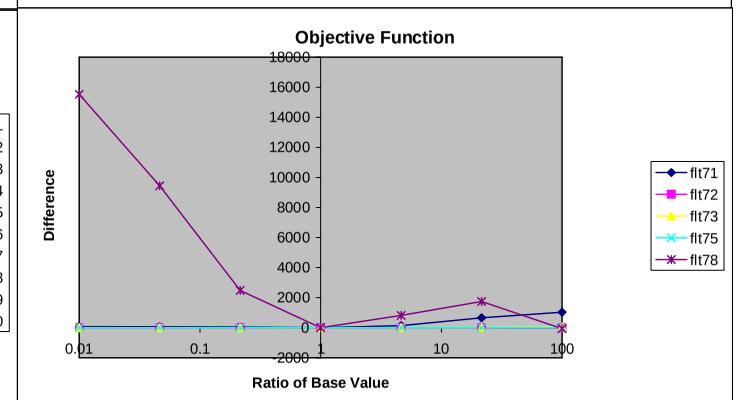
Objective Function
Difference
Ratio of Base Value
flt71
flt72
flt73
flt75
flt78

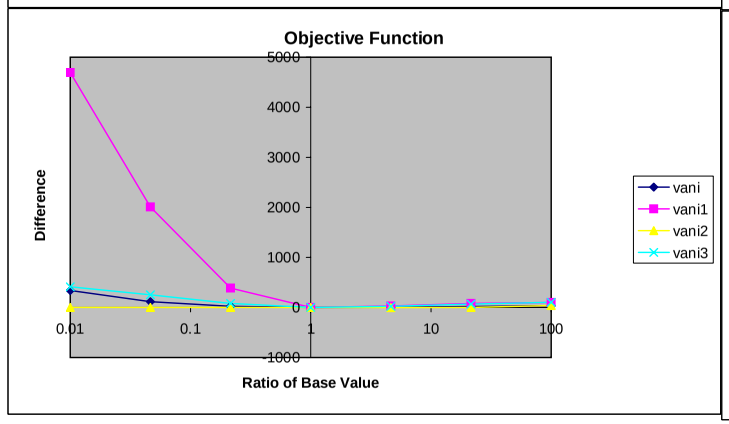
Objective Function
Difference
Ratio of Base Value
vani
vani1
vani2
vani3

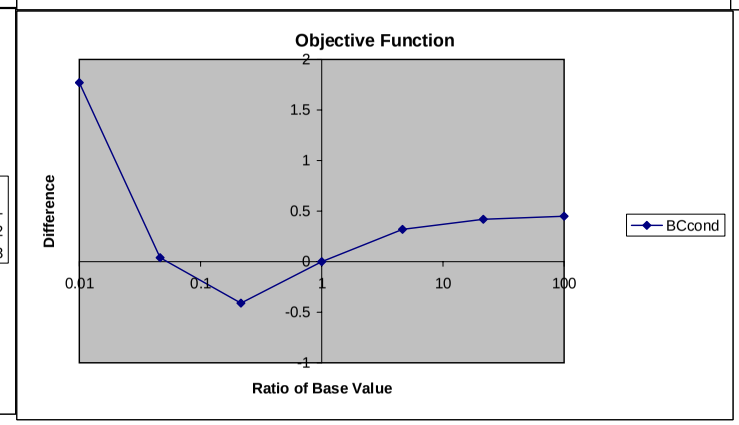
Objective Function
Difference
Ratio of Base Value
BCcond

C.3.6

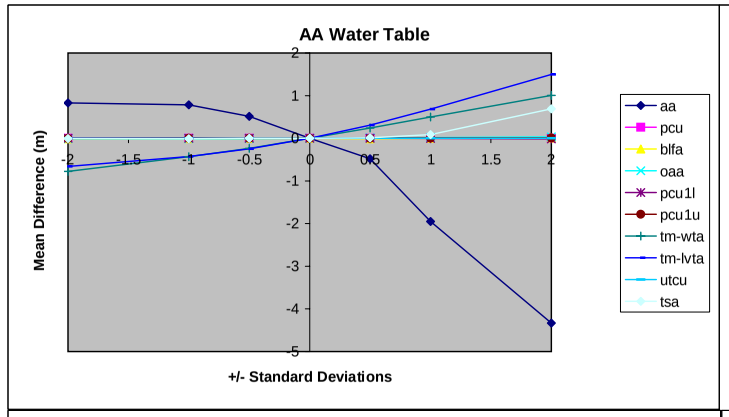
AA Water Table
Mean Difference (m)
+/- Standard Deviations
aa
pcu
blfa
oaa
pcu1l
pcu1u
tm-wta
tm-lvta
utcu
tsa

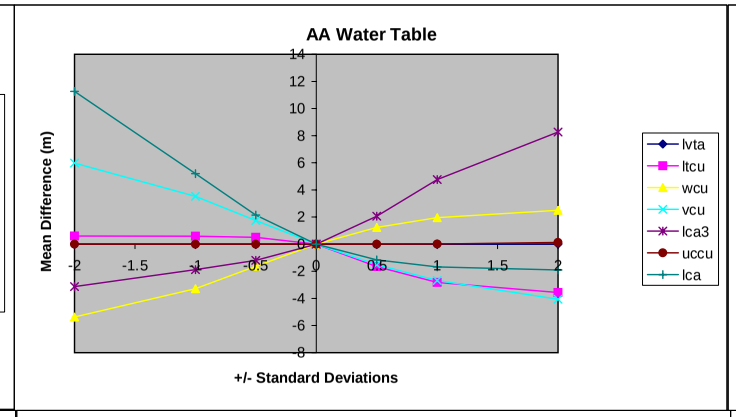
AA Water Table
Mean Difference (m)
+/- Standard Deviations
lvta
ltcu
wcu
vcu
lca3
uccu
lca

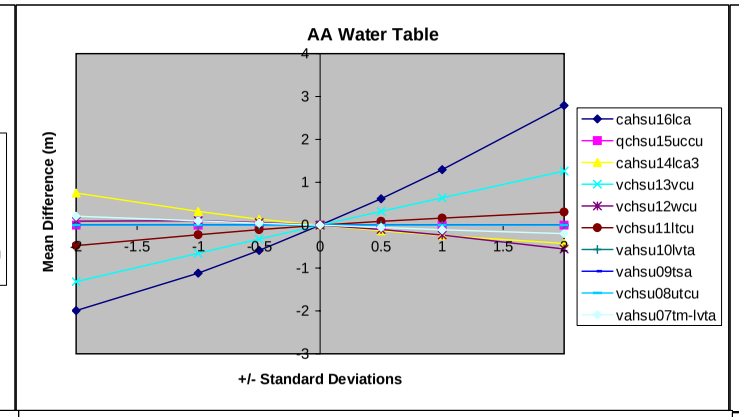
AA Water Table
Mean Difference (m)
+/- Standard Deviations
cahsu16lca
qchsu15uccu
cahsu14lca3
vchsu13vcu
vchsu12wcu
vchsu11ltcu
vahsu10lvta
vahsu09tsa
vchsu08utcu
vahsu07tm-lvta

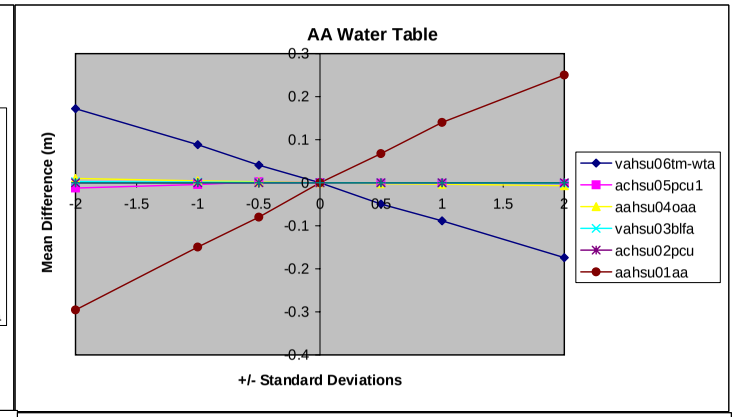
AA Water Table
Mean Difference (m)
+/- Standard Deviations
vahsu06tm-wta
achsu05pcu1
aahsu04oaa
vahsu03blfa
achsu02pcu
aahsu01aa

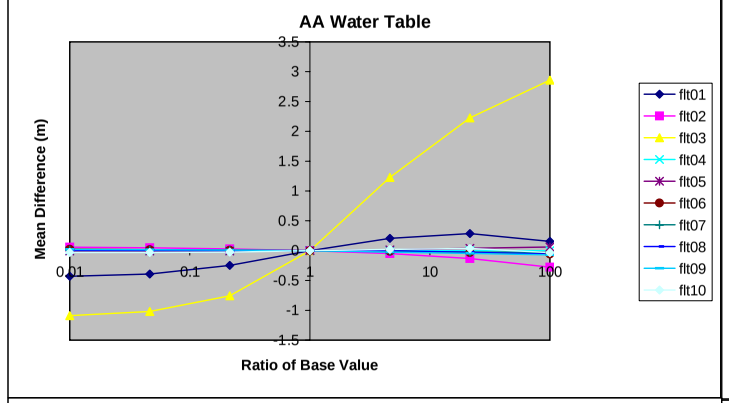
AA Water Table
Mean Difference (m)
Ratio of Base Value
flt01
flt02
flt03
flt04
flt05
flt06
flt07
flt08
flt09
flt10

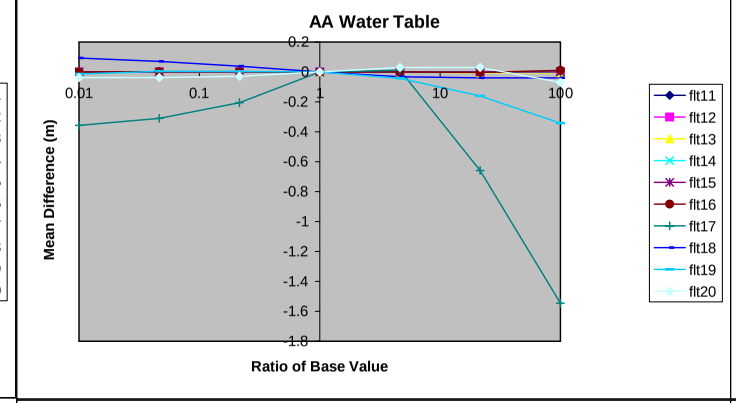
AA Water Table
Mean Difference (m)
Ratio of Base Value
flt11
flt12
flt13
flt14
flt15
flt16
flt17
flt18
flt19
flt20

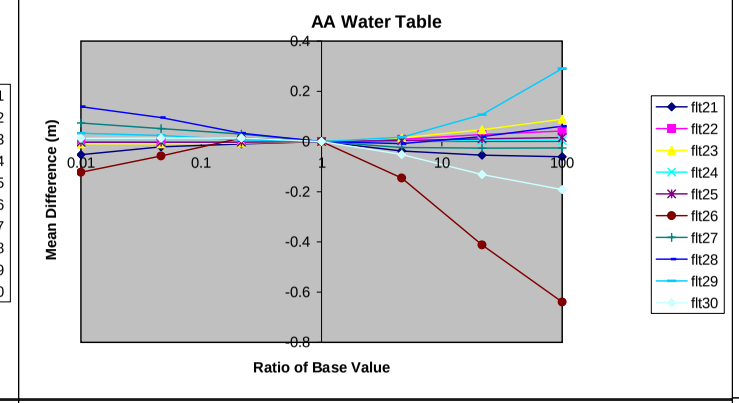
AA Water Table
Mean Difference (m)
Ratio of Base Value
flt21
flt22
flt23
flt24
flt25
flt26
flt27
flt28
flt29
flt30

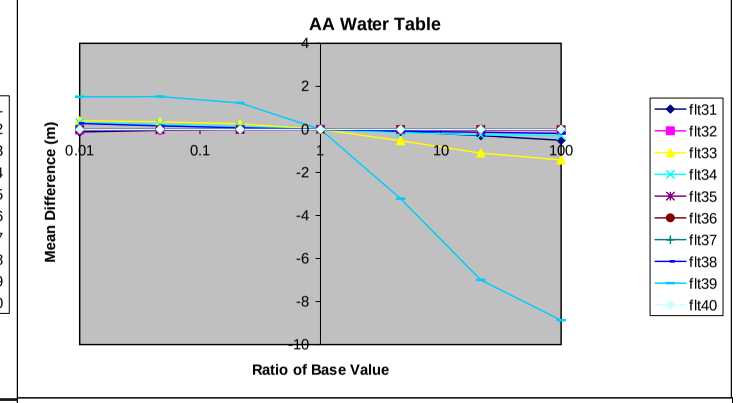
AA Water Table
Mean Difference (m)
Ratio of Base Value
flt31
flt32
flt33
flt34
flt35
flt36
flt37
flt38
flt39
flt40

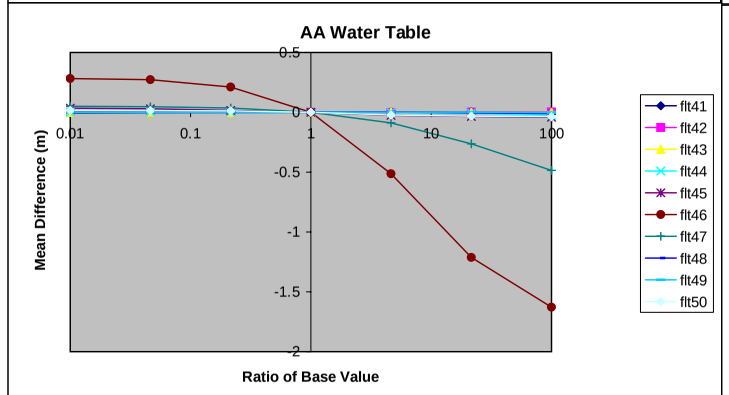
AA Water Table
Mean Difference (m)
Ratio of Base Value
flt41
flt42
flt43
flt44
flt45
flt46
flt47
flt48
flt49
flt50

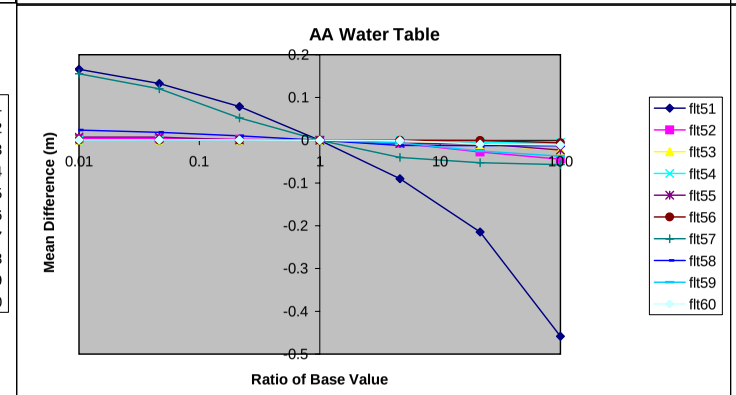
AA Water Table
Mean Difference (m)
Ratio of Base Value
flt51
flt52
flt53
flt54
flt55
flt56
flt57
flt58
flt59
flt60

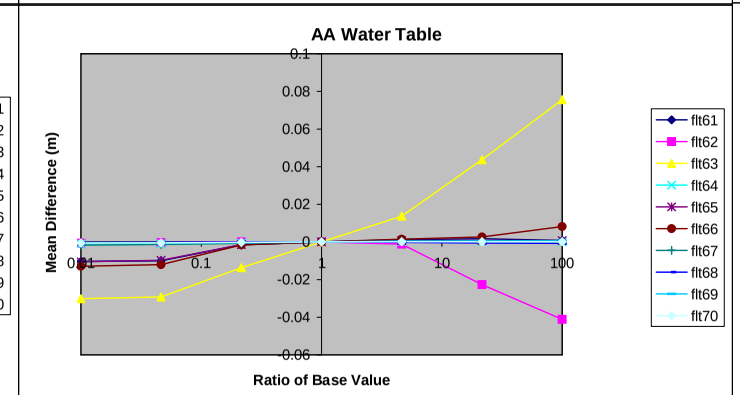
AA Water Table
Mean Difference (m)
Ratio of Base Value
flt61
flt62
flt63
flt64
flt65
flt66
flt67
flt68
flt69
flt70

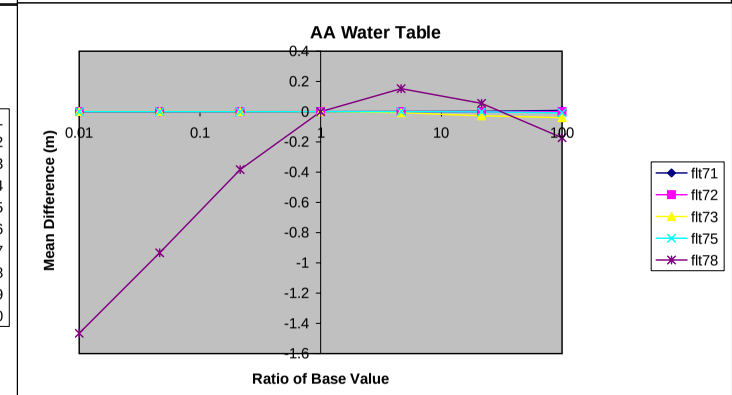
AA Water Table
Mean Difference (m)
Ratio of Base Value
flt71
flt72
flt73
flt75
flt78

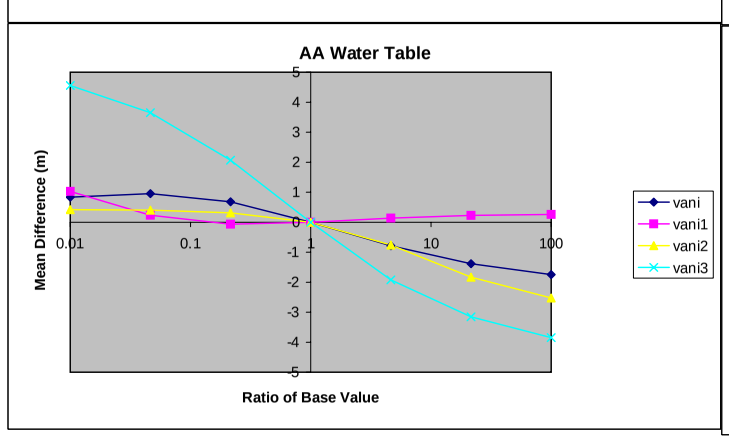
AA Water Table
Mean Difference (m)
Ratio of Base Value
vani
vani1
vani2
vani3

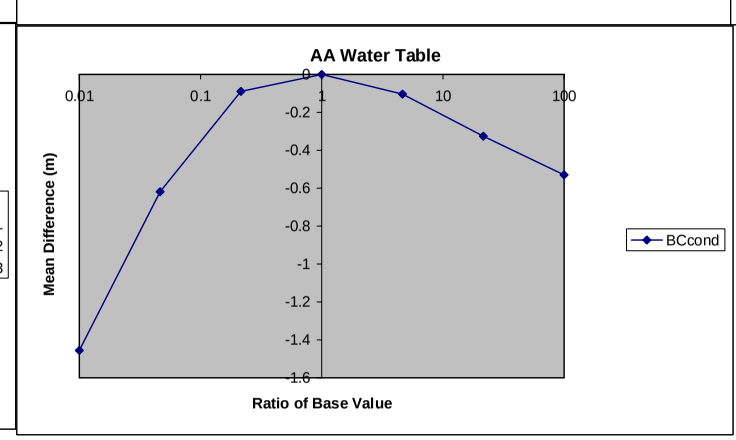
AA Water Table
Mean Difference (m)
Ratio of Base Value
BCcond

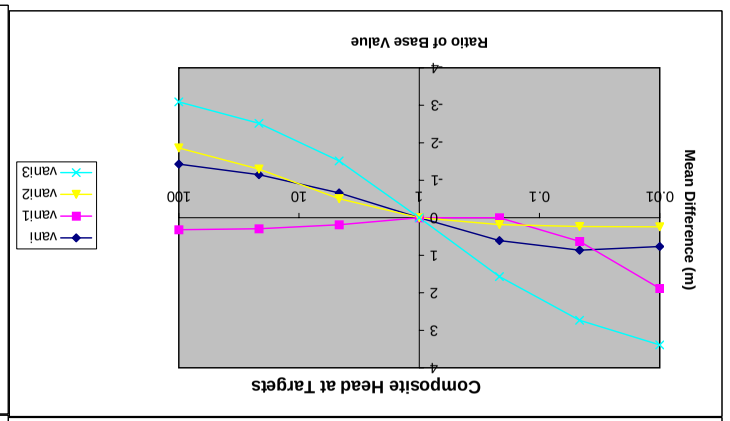
Composite Head at Targets
Mean Difference (m)
Ratio of Base Value
0.01
0.1
1
10
100
-1.4
-1.2
-1
-0.8
-0.6
-0.4
-0.2
0
0.2
0.4
rlt01
rlt02
rlt03
rlt04
rlt05
rlt06
rlt07
rlt08
rlt09
rlt10

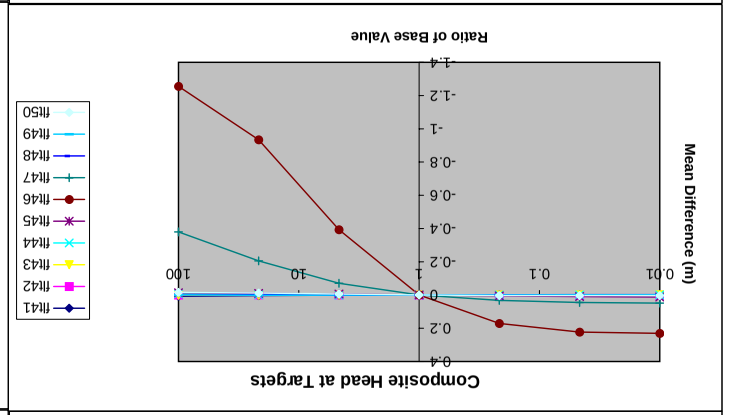
Composite Head at Targets
Mean Difference (m)
Ratio of Base Value
0.01
0.1
1
10
100
-1.4
-1.2
-1
-0.8
-0.6
-0.4
-0.2
0
0.2
0.4
rlt41
rlt42
rlt43
rlt44
rlt45
rlt46
rlt47
rlt48
rlt49
rlt50

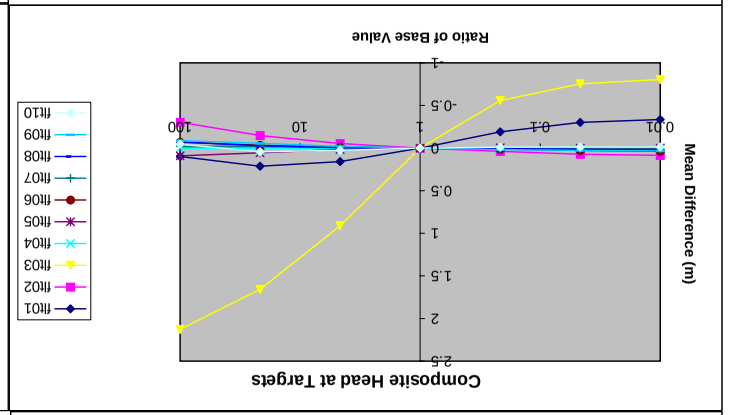
Composite Head at Targets
Mean Difference (m)
+/- Standard Deviations
-3.5
-3
-2.5
-2
-1.5
-1
-0.5
0
0.5
1
1.5
2
aa
pcu
bfla
oaa
pcu1
pcu2
m-wta
m-lvta
ucu
tsa

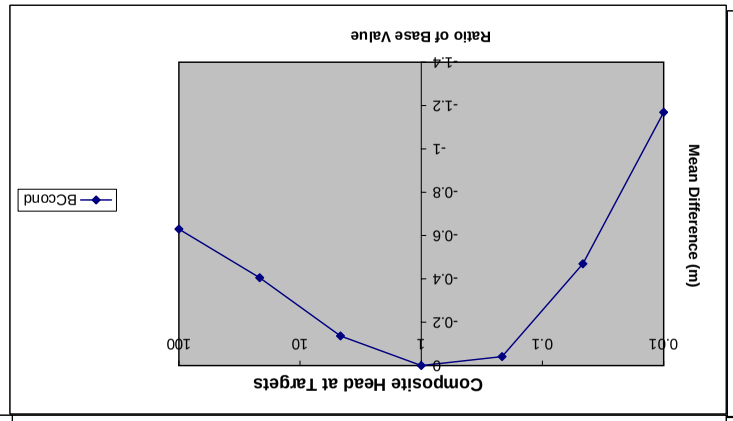
Composite Head at Targets
Mean Difference (m)
Ratio of Base Value
0.01
0.1
1
10
100
-1.4
-1.2
-1
-0.8
-0.6
-0.4
-0.2
0
0.2
rlt11
rlt12
rlt13
rlt14
rlt15
rlt16
rlt17
rlt18
rlt19
rlt20

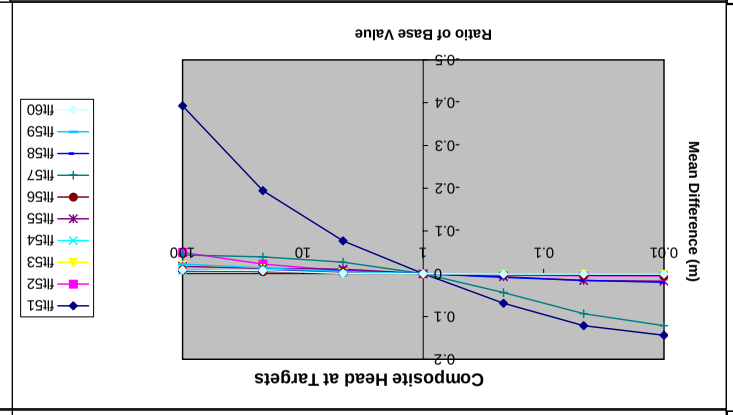
Composite Head at Targets
Mean Difference (m)
Ratio of Base Value
0.01
0.1
1
10
100
-1.4
-1.2
-1
-0.8
-0.6
-0.4
-0.2
0
0.2
0.4
0.5
rlt51
rlt52
rlt53
rlt54
rlt55
rlt56
rlt57
rlt58
rlt59
rlt60

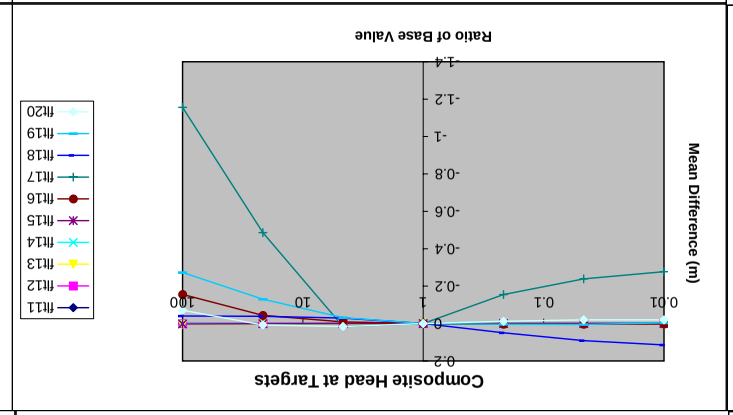
Composite Head at Targets
Mean Difference (m)
+/- Standard Deviations
-2
-1
0
1
2
3
4
5
6
7
8
lta
ltcu
wcu
ucu
lca3
ucu
lca

Composite Head at Targets
Mean Difference (m)
Ratio of Base Value
0.01
0.1
1
10
100
-1.4
-1.2
-1
-0.8
-0.6
-0.4
-0.2
0
0.2
0.4
0.6
0.8
rlt21
rlt22
rlt23
rlt24
rlt25
rlt26
rlt27
rlt28
rlt29
rlt30

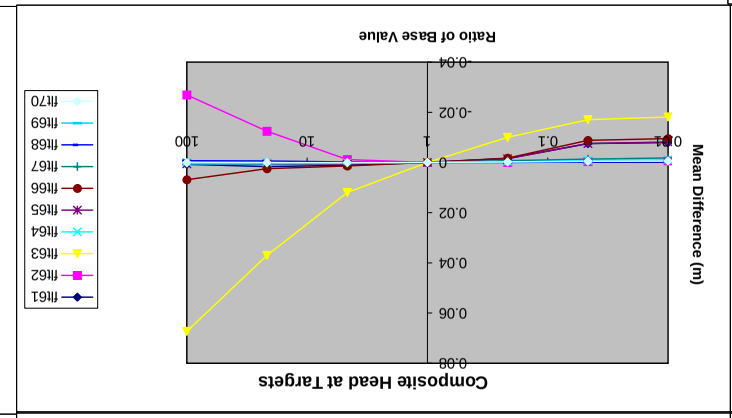
Composite Head at Targets
Mean Difference (m)
Ratio of Base Value
0.01
0.1
1
10
100
-1.4
-1.2
-1
-0.8
-0.6
-0.4
-0.2
0
0.2
0.4
rlt61
rlt62
rlt63
rlt64
rlt65
rlt66
rlt67
rlt68
rlt69
rlt70

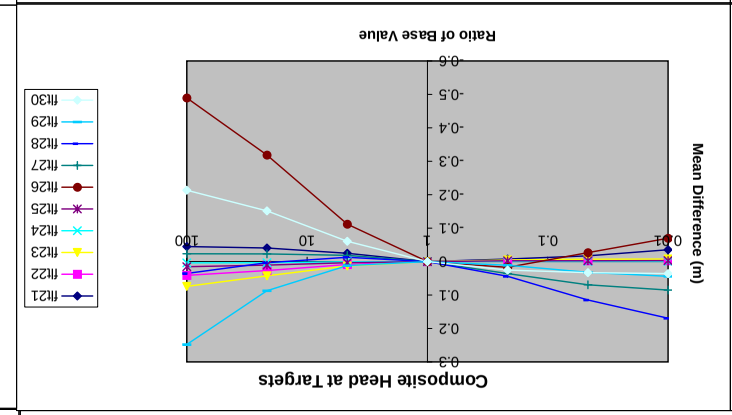
Composite Head at Targets
Mean Difference (m)
+/- Standard Deviations
-4
-3
-2
-1
0
1
2
3
4
catsu16ca
qctsu15ucu
catsu14ca3
vctsu13vcu
vctsu12wcu
vctsu11ltcu
vatsu10lvta
vatsu09tsa
vctsu08utcu
vatsu07m-lvta

Composite Head at Targets
Mean Difference (m)
Ratio of Base Value
0.01
0.1
1
10
100
-1.4
-1.2
-1
-0.8
-0.6
-0.4
-0.2
0
0.2
rlt31
rlt32
rlt33
rlt34
rlt35
rlt36
rlt37
rlt38
rlt39
rlt40

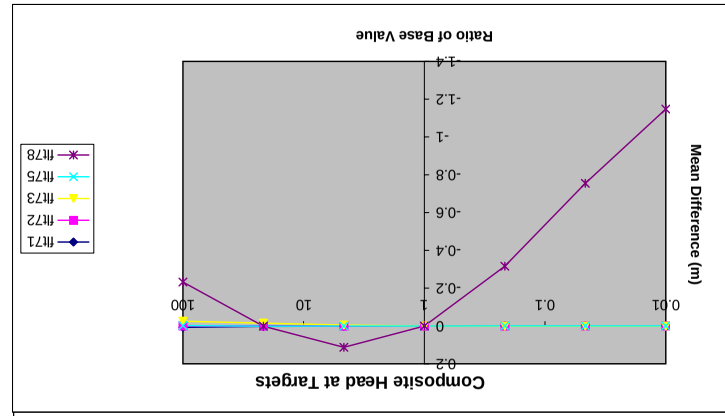
Composite Head at Targets
Mean Difference (m)
Ratio of Base Value
0.01
0.1
1
10
100
-1.4
-1.2
-1
-0.8
-0.6
-0.4
-0.2
0
0.2
0.4
rlt71
rlt72
rlt73
rlt75
rlt78

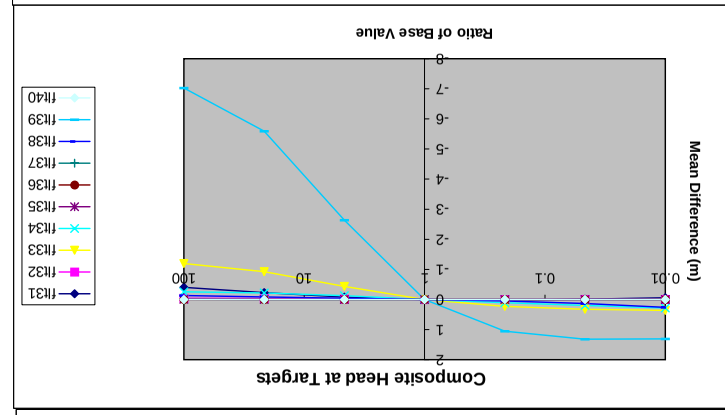
Composite Head at Targets
Mean Difference (m)
+/- Standard Deviations
-2
-1.5
-1
-0.5
0
0.5
1
1.5
2
vatsu06m-wta
actsu05pcu1
aatsu04oaa
vatsu03bfla
actsu02pcu
aatsu01aa

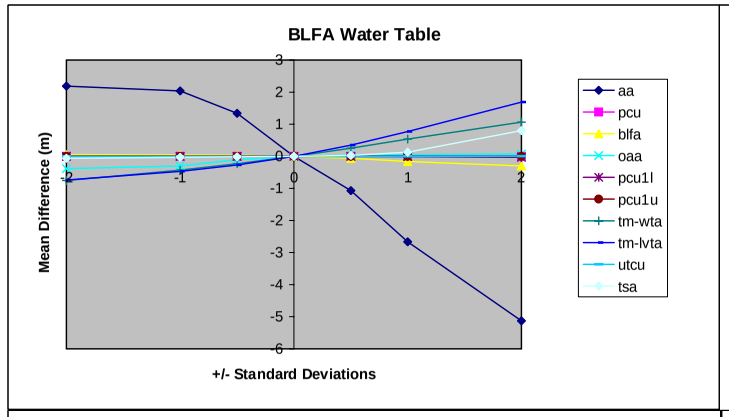
BLFA Water Table
Mean Difference (m)
+/- Standard Deviations
aa
pcu
blfa
oaa
pcu1l
pcu1u
tm-wta
tm-lvta
utcu
tsa

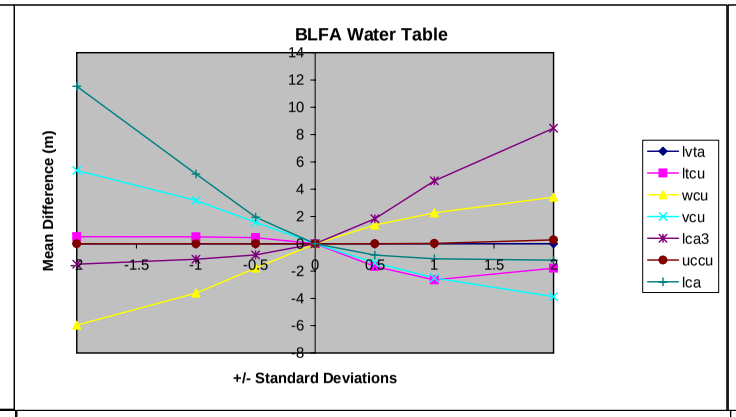
BLFA Water Table
Mean Difference (m)
+/- Standard Deviations
lvta
ltcu
wcu
vcu
lca3
uccu
lca

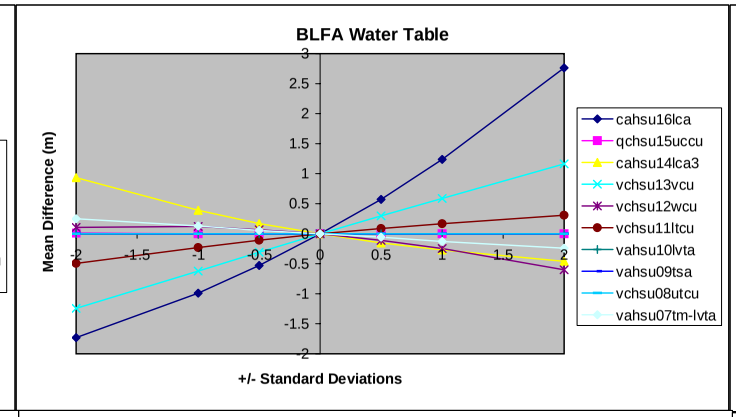
BLFA Water Table
Mean Difference (m)
+/- Standard Deviations
cahsu16lca
qchsu15uccu
cahsu14lca3
vchsu13vcu
vchsu12wcu
vchsu11ltcu
vahsu10lvta
vahsu09tsa
vchsu08utcu
vahsu07tm-lvta

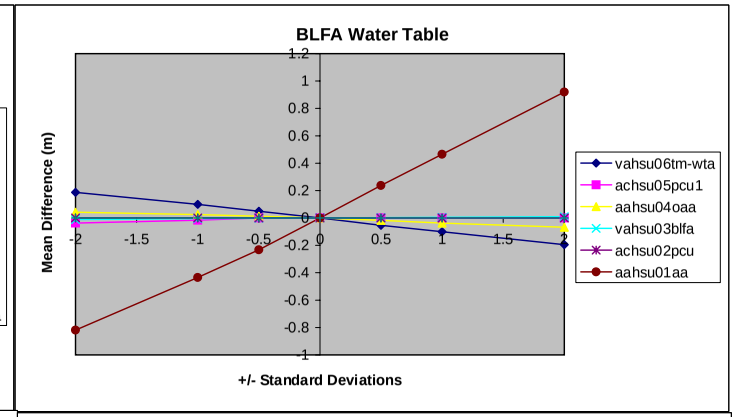
BLFA Water Table
Mean Difference (m)
+/- Standard Deviations
vahsu06tm-wta
achsu05pcu1
aahsu04oaa
vahsu03blfa
achsu02pcu
aahsu01aa

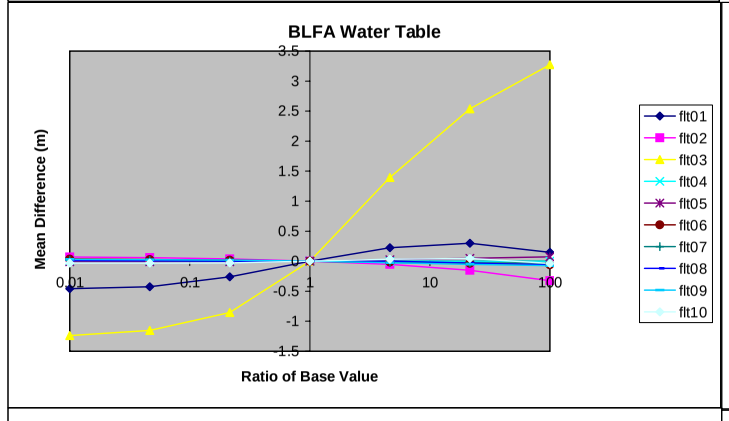
BLFA Water Table
Mean Difference (m)
Ratio of Base Value
flt01
flt02
flt03
flt04
flt05
flt06
flt07
flt08
flt09
flt10

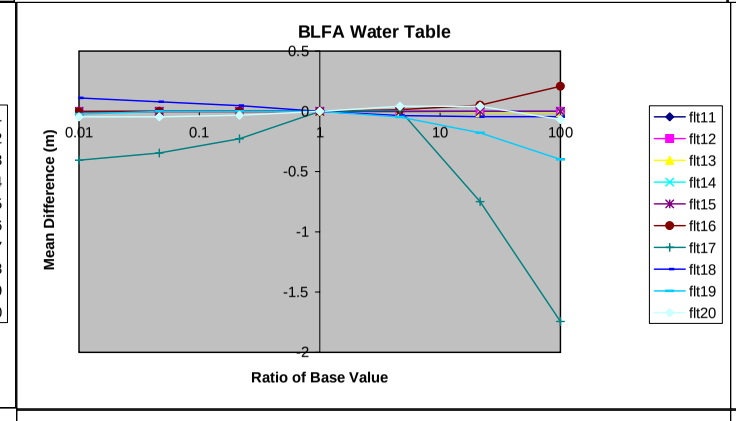
BLFA Water Table
Mean Difference (m)
Ratio of Base Value
flt11
flt12
flt13
flt14
flt15
flt16
flt17
flt18
flt19
flt20

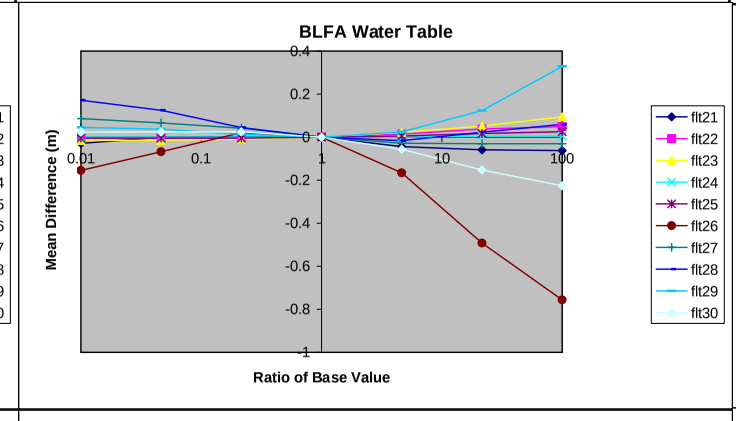
BLFA Water Table
Mean Difference (m)
Ratio of Base Value
flt21
flt22
flt23
flt24
flt25
flt26
flt27
flt28
flt29
flt30

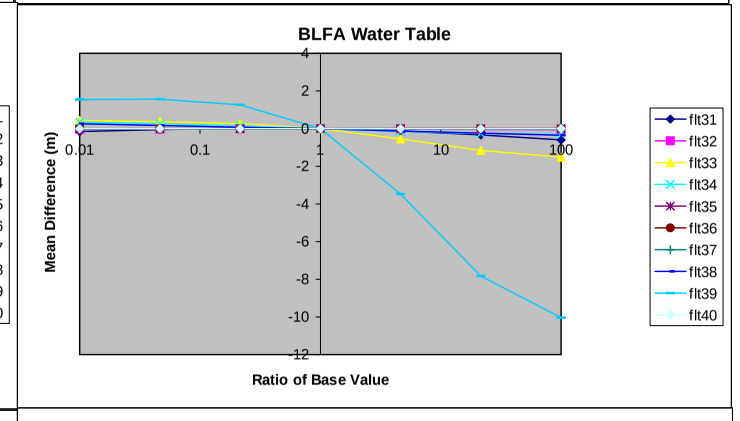
BLFA Water Table
Mean Difference (m)
Ratio of Base Value
flt31
flt32
flt33
flt34
flt35
flt36
flt37
flt38
flt39
flt40

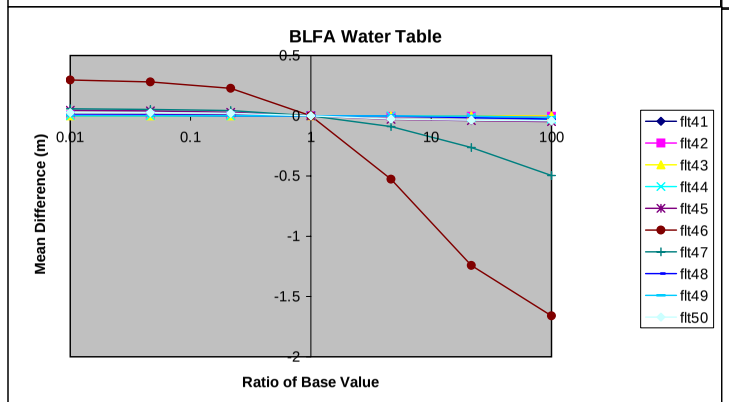
BLFA Water Table
Mean Difference (m)
Ratio of Base Value
flt41
flt42
flt43
flt44
flt45
flt46
flt47
flt48
flt49
flt50

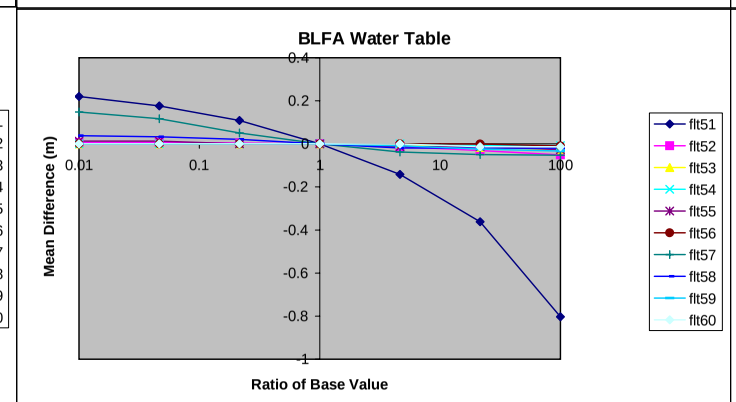
BLFA Water Table
Mean Difference (m)
Ratio of Base Value
flt51
flt52
flt53
flt54
flt55
flt56
flt57
flt58
flt59
flt60

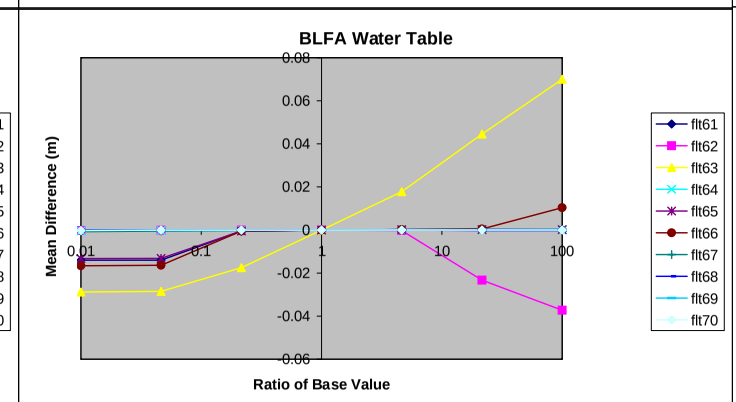
BLFA Water Table
Mean Difference (m)
Ratio of Base Value
flt61
flt62
flt63
flt64
flt65
flt66
flt67
flt68
flt69
flt70

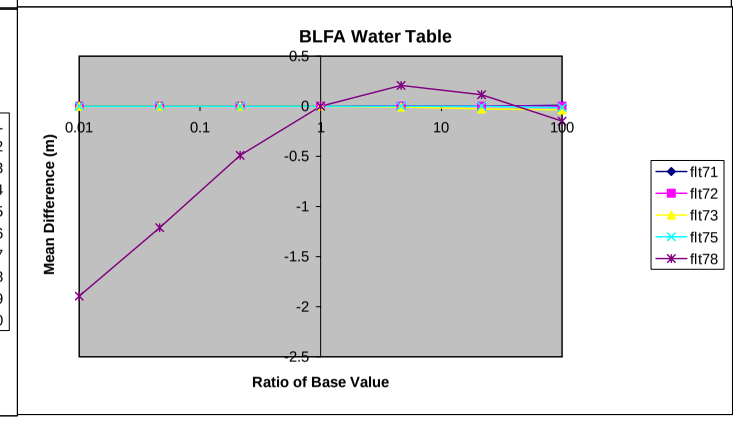
BLFA Water Table
Mean Difference (m)
Ratio of Base Value
flt71
flt72
flt73
flt75
flt78

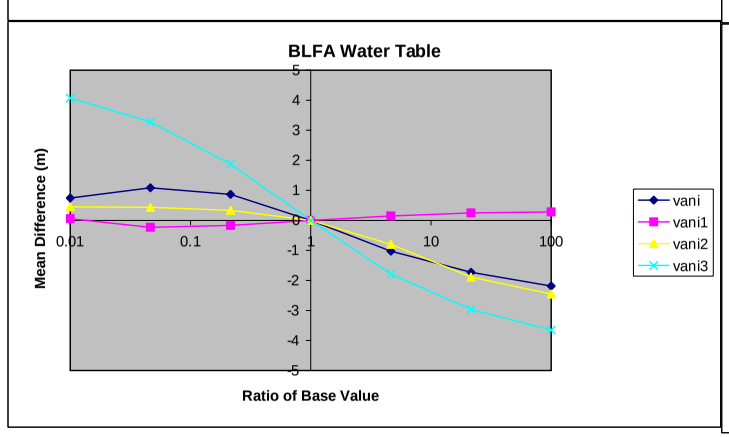
BLFA Water Table
Mean Difference (m)
Ratio of Base Value
vani
vani1
vani2
vani3

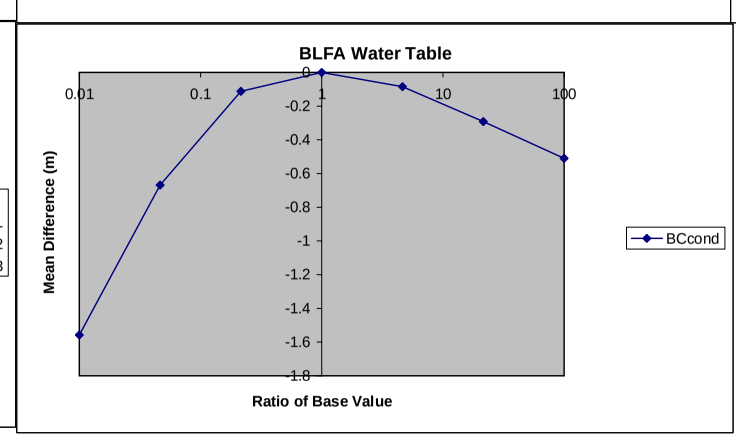
BLFA Water Table
Mean Difference (m)
Ratio of Base Value
BCcond

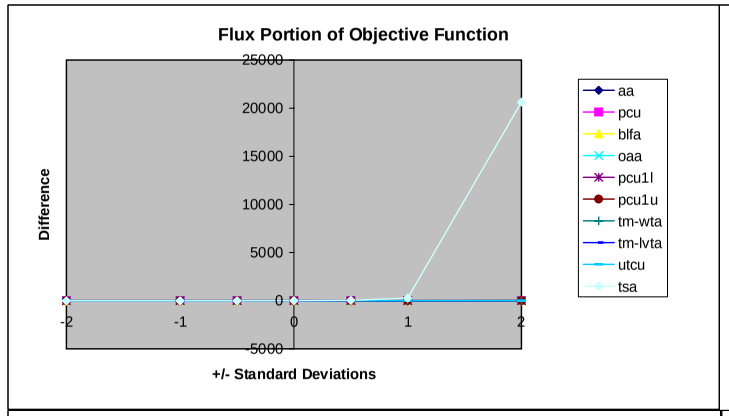
Flux Portion of Objective Function
Difference
+/- Standard Deviations
aa
pcu
blfa
oaa
pcu1l
pcu1u
tm-wta
tm-lvta
utcu
tsa

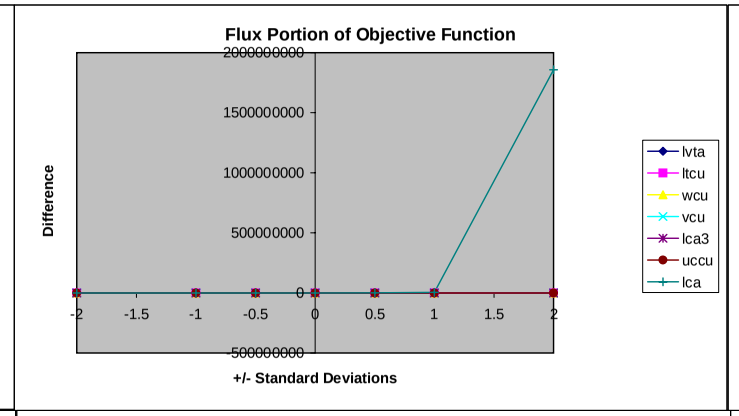
Flux Portion of Objective Function
Difference
+/- Standard Deviations
lvta
ltcu
wcu
vcu
lca3
uccu
lca

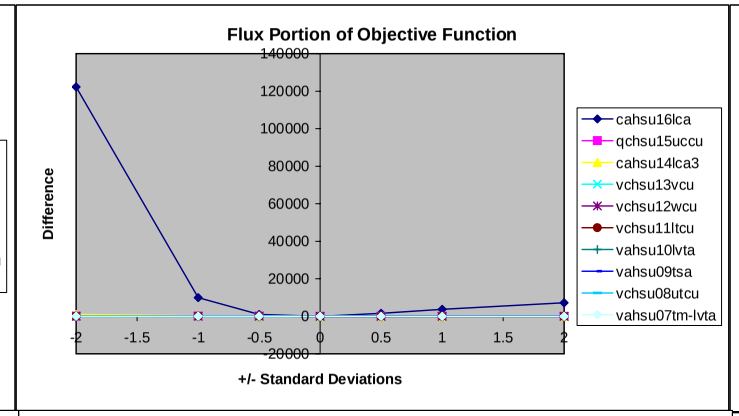
Flux Portion of Objective Function
Difference
+/- Standard Deviations
cahsu16lca
qchsu15uccu
cahsu14lca3
vchsu13vcu
vchsu12wcu
vchsu11ltcu
vahsu10lvta
vahsu09tsa
vchsu08utcu
vahsu07tm-lvta

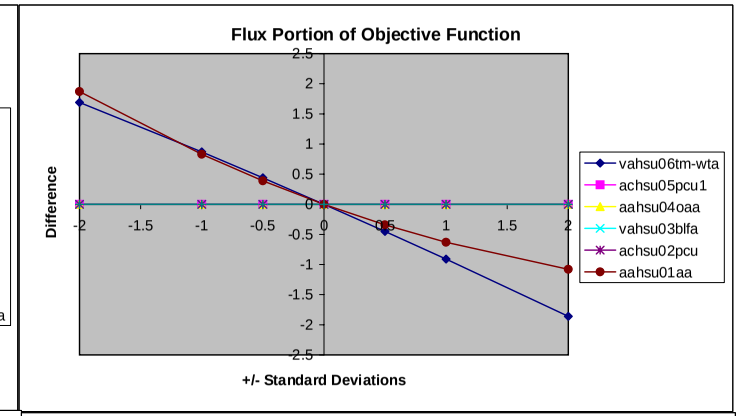
Flux Portion of Objective Function
Difference
+/- Standard Deviations
vahsu06tm-wta
achsu05pcu1
aahsu04oaa
vahsu03blfa
achsu02pcu
aahsu01aa

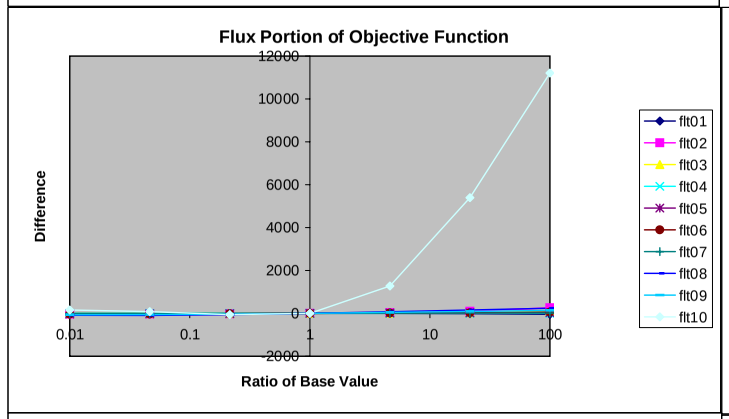
Flux Portion of Objective Function
Difference
Ratio of Base Value
flt01
flt02
flt03
flt04
flt05
flt06
flt07
flt08
flt09
flt10

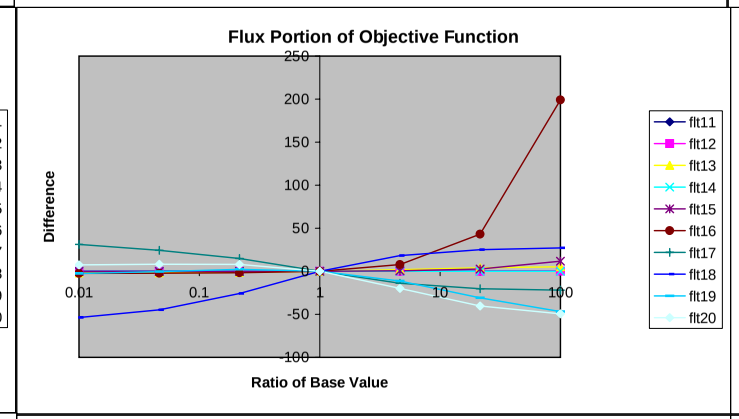
Flux Portion of Objective Function
Difference
Ratio of Base Value
flt11
flt12
flt13
flt14
flt15
flt16
flt17
flt18
flt19
flt20

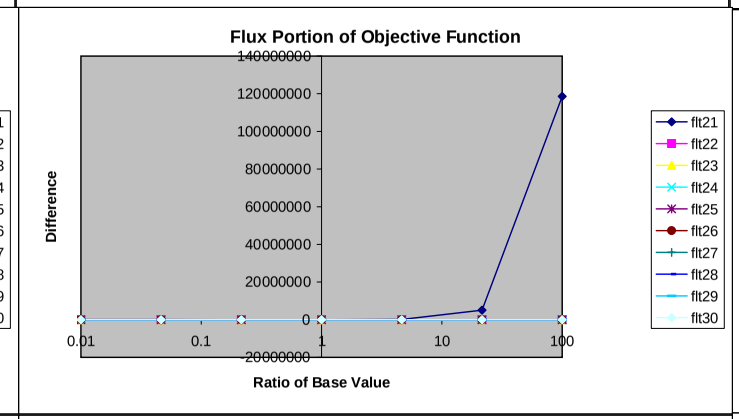
Flux Portion of Objective Function
Difference
Ratio of Base Value
flt21
flt22
flt23
flt24
flt25
flt26
flt27
flt28
flt29
flt30

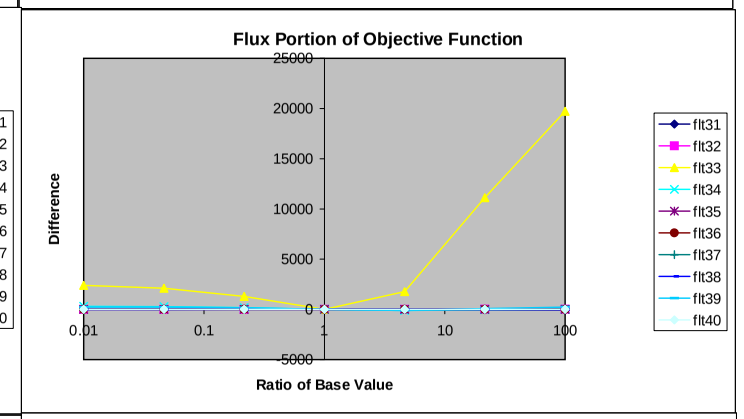
Flux Portion of Objective Function
Difference
Ratio of Base Value
flt31
flt32
flt33
flt34
flt35
flt36
flt37
flt38
flt39
flt40

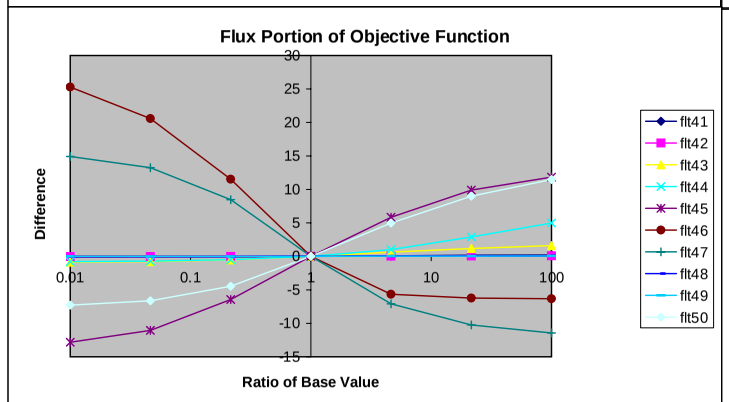
Flux Portion of Objective Function
Difference
Ratio of Base Value
flt41
flt42
flt43
flt44
flt45
flt46
flt47
flt48
flt49
flt50

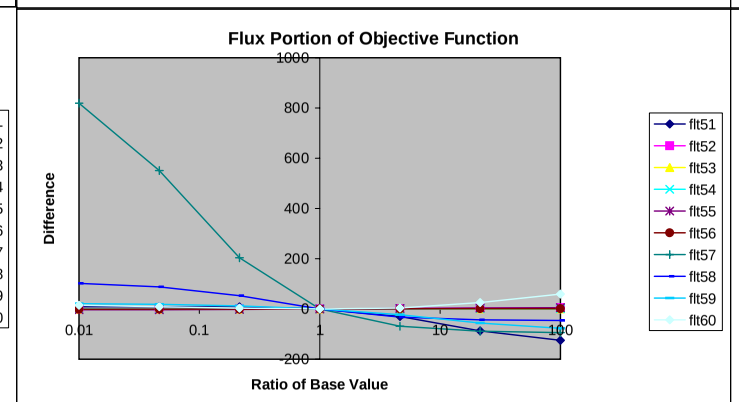
Flux Portion of Objective Function
Difference
Ratio of Base Value
flt51
flt52
flt53
flt54
flt55
flt56
flt57
flt58
flt59
flt60

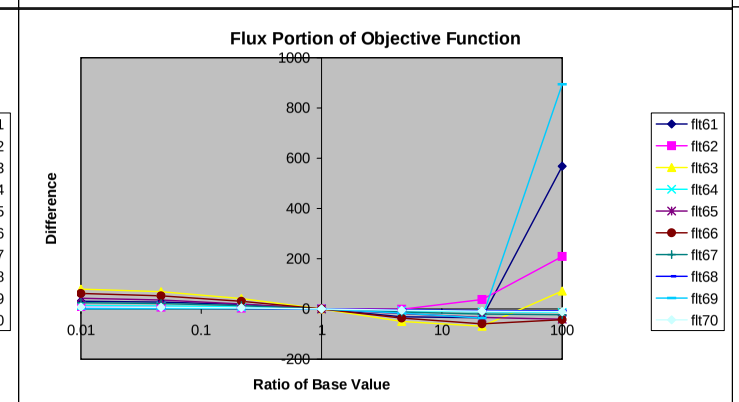
Flux Portion of Objective Function
Difference
Ratio of Base Value
flt61
flt62
flt63
flt64
flt65
flt66
flt67
flt68
flt69
flt70

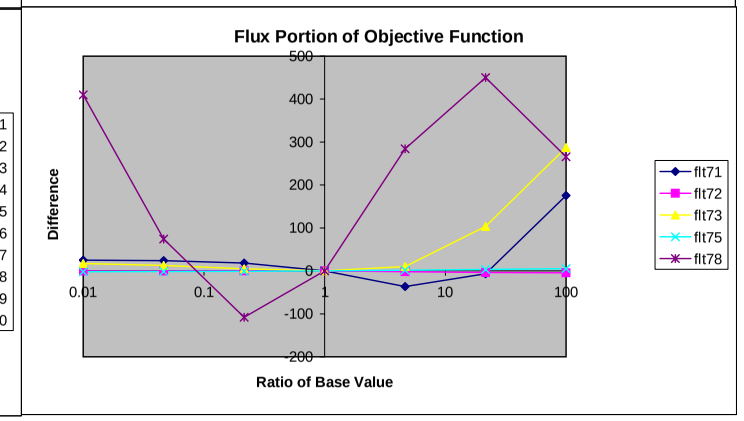
Flux Portion of Objective Function
Difference
Ratio of Base Value
flt71
flt72
flt73
flt75
flt78

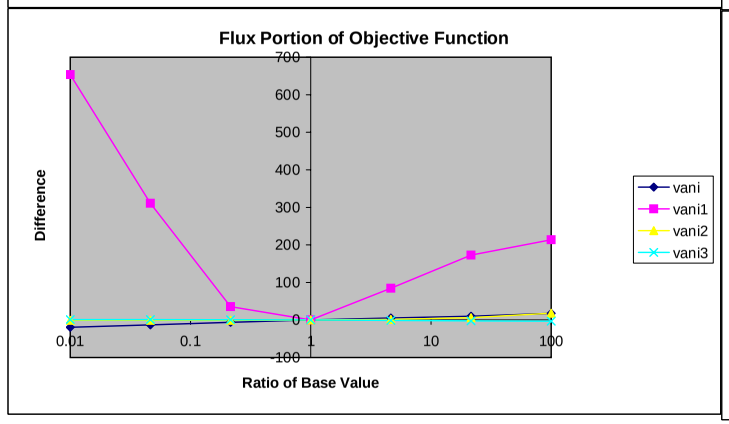
Flux Portion of Objective Function
Difference
Ratio of Base Value
vani
vani1
vani2
vani3

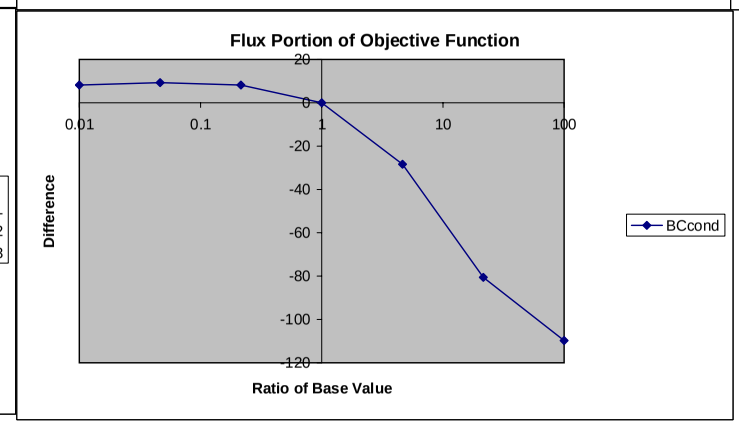
Flux Portion of Objective Function
Difference
Ratio of Base Value
BCcond

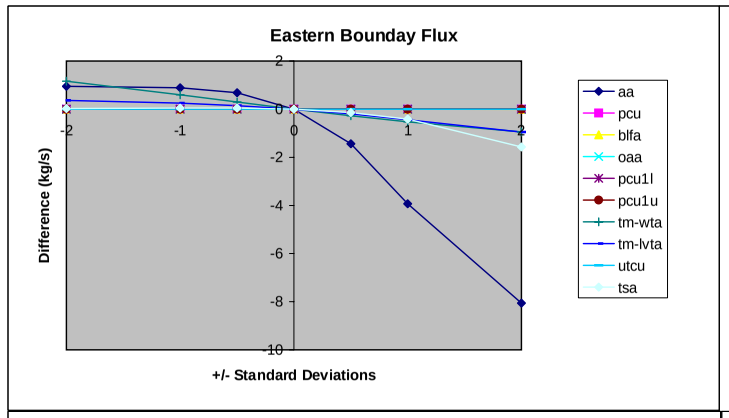
Eastern Bounday Flux
Difference (kg/s)
+/- Standard Deviations
aa
pcu
blfa
oaa
pcu1l
pcu1u
tm-wta
tm-lvta
utcu
tsa

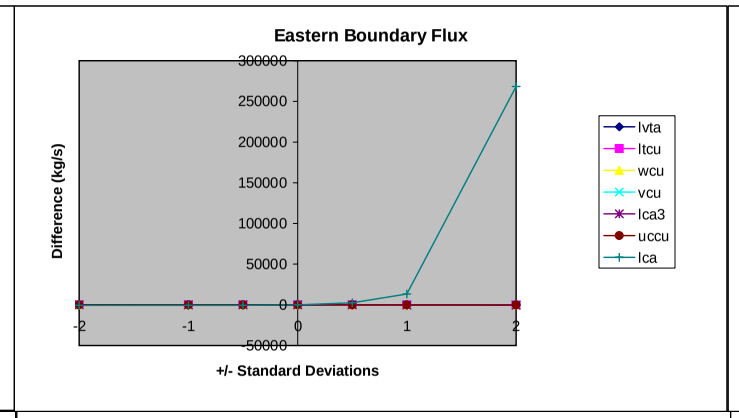
Eastern Boundary Flux
Difference (kg/s)
+/- Standard Deviations
lvta
ltcu
wcu
vcu
lca3
uccu
lca

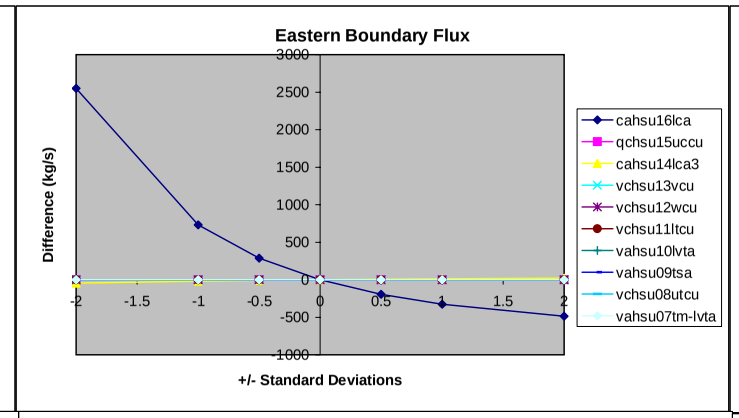
Eastern Boundary Flux
Difference (kg/s)
+/- Standard Deviations
cahsu16lca
qchsu15uccu
cahsu14lca3
vchsu13vcu
vchsu12wcu
vchsu11ltcu
vahsu10lvta
vahsu09tsa
vchsu08utcu
vahsu07tm-lvta

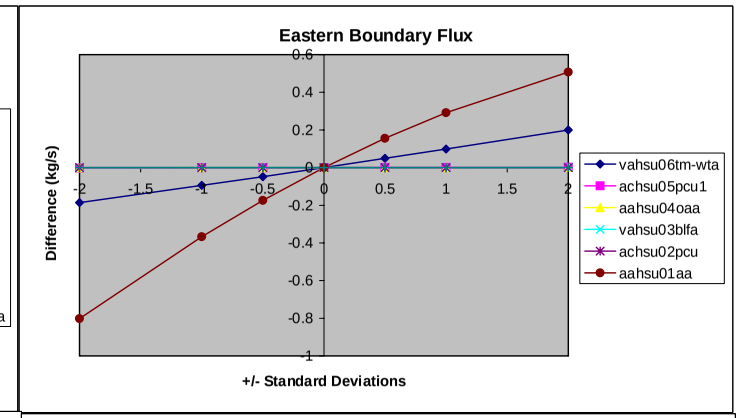
Eastern Boundary Flux
Difference (kg/s)
+/- Standard Deviations
vahsu06tm-wta
achsu05pcu1
aahsu04oaa
vahsu03blfa
achsu02pcu
aahsu01aa

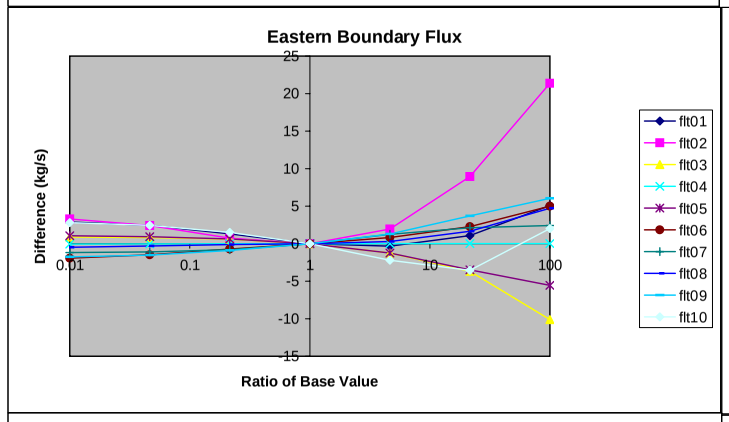
Eastern Boundary Flux
Difference (kg/s)
Ratio of Base Value
flt01
flt02
flt03
flt04
flt05
flt06
flt07
flt08
flt09
flt10

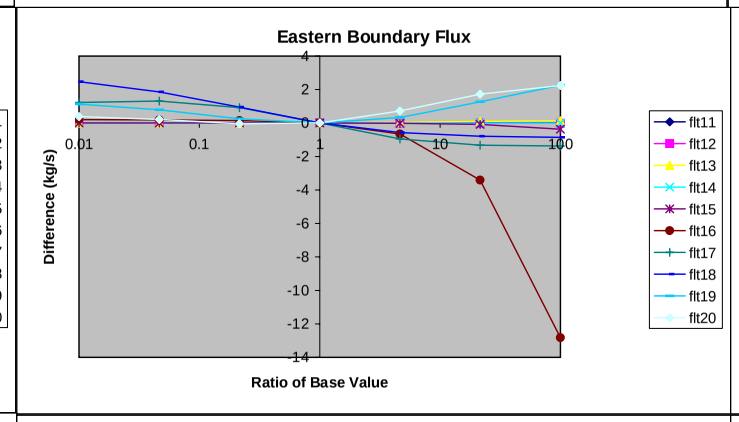
Eastern Boundary Flux
Difference (kg/s)
Ratio of Base Value
flt11
flt12
flt13
flt14
flt15
flt16
flt17
flt18
flt19
flt20

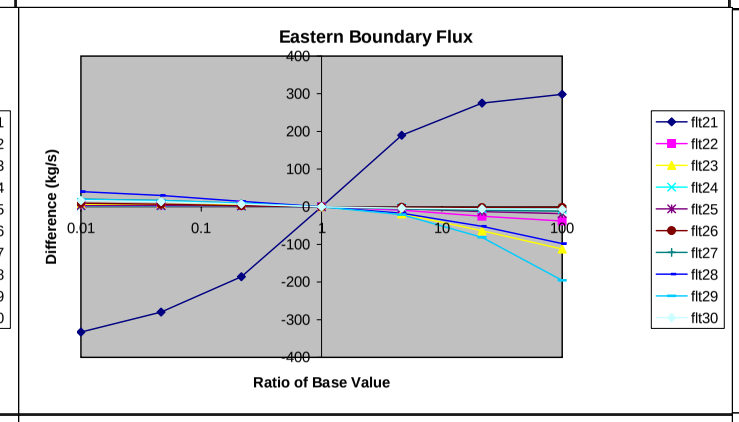
Eastern Boundary Flux
Difference (kg/s)
Ratio of Base Value
flt21
flt22
flt23
flt24
flt25
flt26
flt27
flt28
flt29
flt30

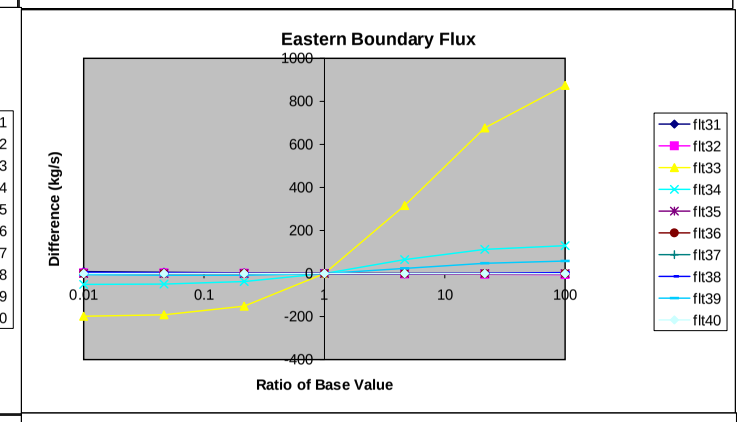
Eastern Boundary Flux
Difference (kg/s)
Ratio of Base Value
flt31
flt32
flt33
flt34
flt35
flt36
flt37
flt38
flt39
flt40

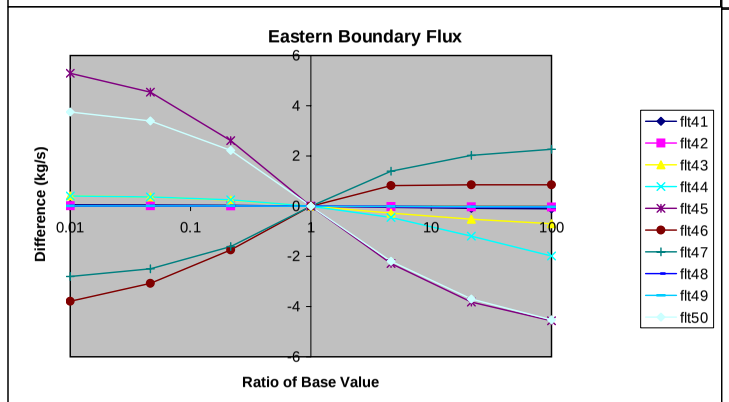
Eastern Boundary Flux
Difference (kg/s)
Ratio of Base Value
flt41
flt42
flt43
flt44
flt45
flt46
flt47
flt48
flt49
flt50

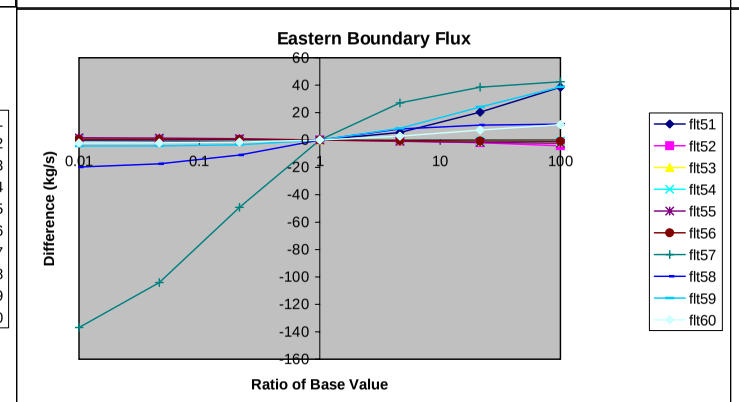
Eastern Boundary Flux
Difference (kg/s)
Ratio of Base Value
flt51
flt52
flt53
flt54
flt55
flt56
flt57
flt58
flt59
flt60

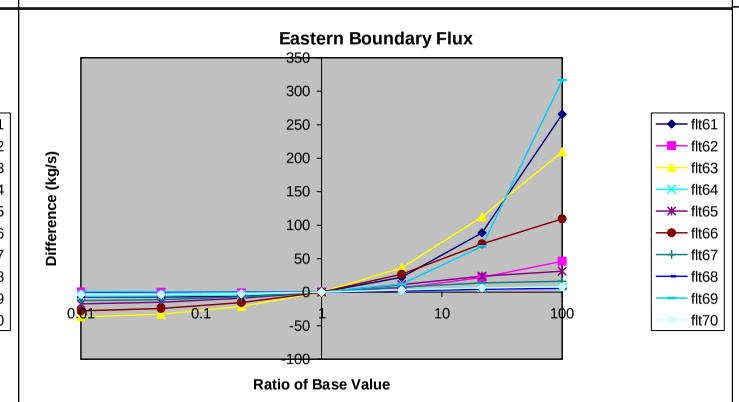
Eastern Boundary Flux
Difference (kg/s)
Ratio of Base Value
flt61
flt62
flt63
flt64
flt65
flt66
flt67
flt68
flt69
flt70

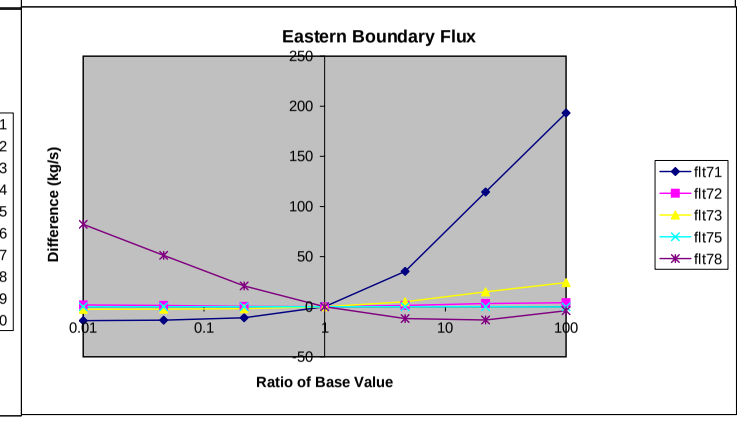
Eastern Boundary Flux
Difference (kg/s)
Ratio of Base Value
flt71
flt72
flt73
flt75
flt78

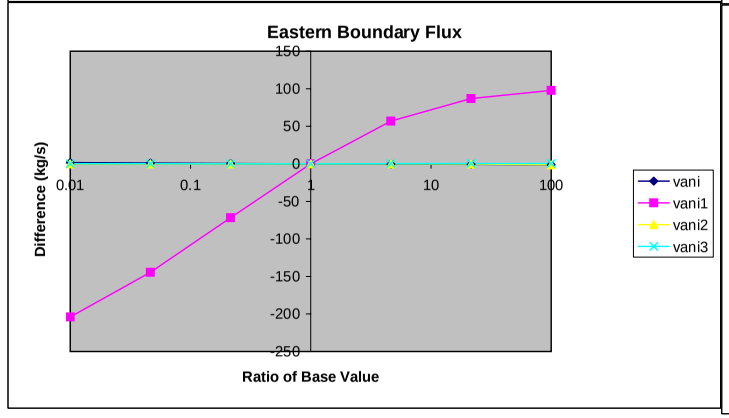
Eastern Boundary Flux
Difference (kg/s)
Ratio of Base Value
vani
vani1
vani2
vani3

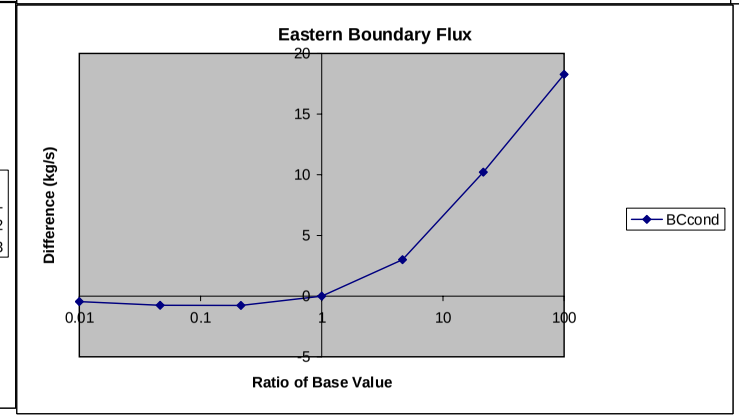
Eastern Boundary Flux
Difference (kg/s)
Ratio of Base Value
BCcond

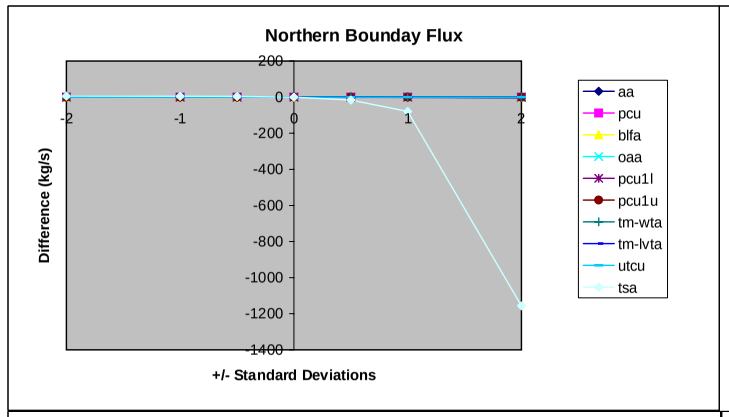
Northern Bounday Flux
Difference (kg/s)
+/- Standard Deviations
aa
pcu
blfa
oaa
pcu1l
pcu1u
tm-wta
tm-lvta
utcu
tsa

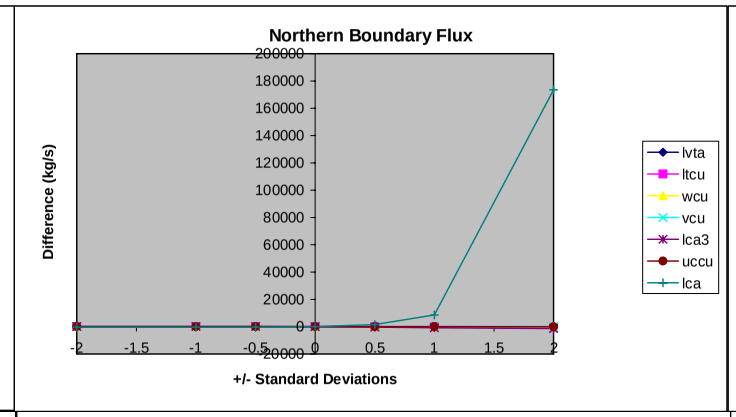
Northern Boundary Flux
Difference (kg/s)
+/- Standard Deviations
lvta
ltcu
wcu
vcu
lca3
uccu
lca

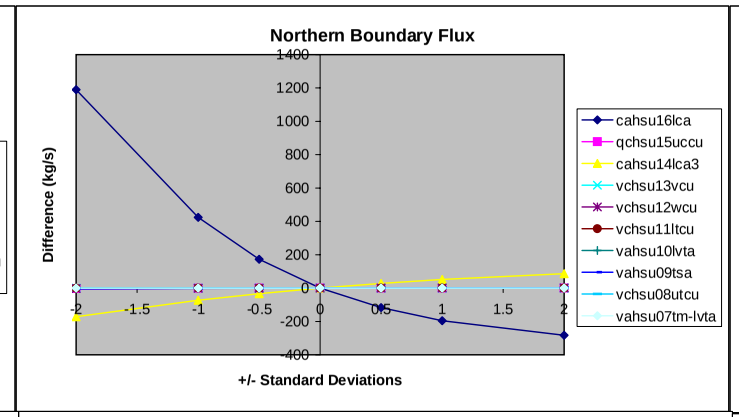
Northern Boundary Flux
Difference (kg/s)
+/- Standard Deviations
cahsu16lca
qchsu15uccu
cahsu14lca3
vchsu13vcu
vchsu12wcu
vchsu11ltcu
vahsu10lvta
vahsu09tsa
vchsu08utcu
vahsu07tm-lvta

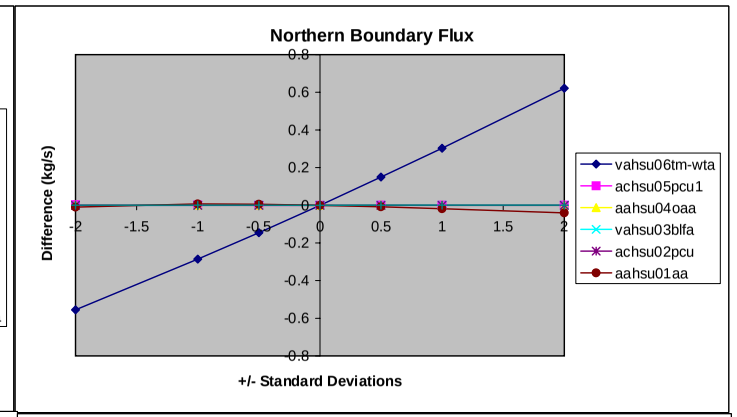
Northern Boundary Flux
Difference (kg/s)
+/- Standard Deviations
vahsu06tm-wta
achsu05pcu1
aahsu04oaa
vahsu03blfa
achsu02pcu
aahsu01aa

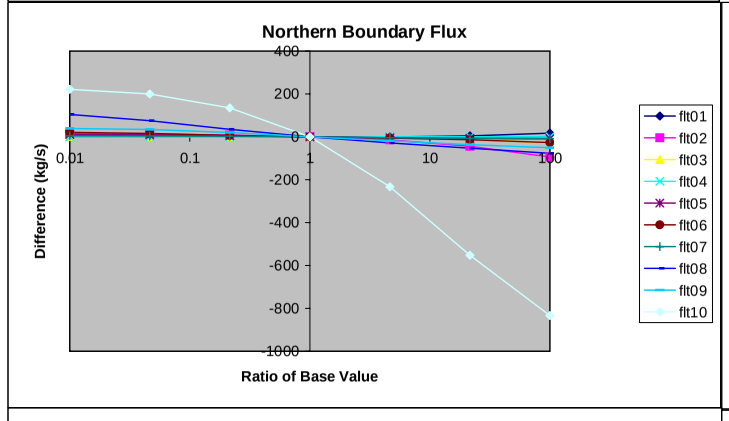
Northern Boundary Flux
Difference (kg/s)
Ratio of Base Value
flt01
flt02
flt03
flt04
flt05
flt06
flt07
flt08
flt09
flt10

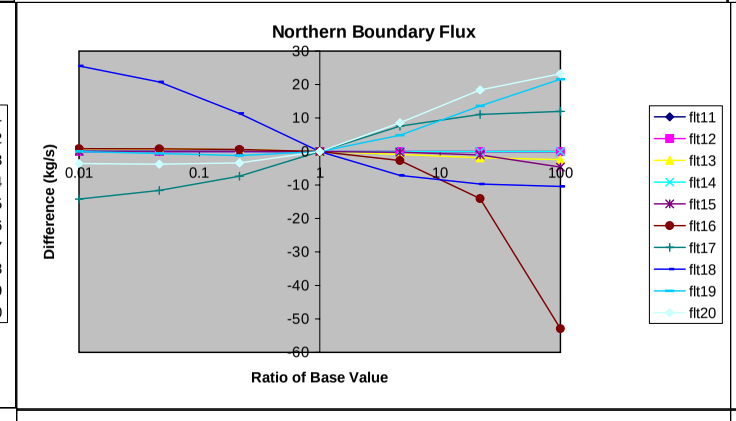
Northern Boundary Flux
Difference (kg/s)
Ratio of Base Value
flt11
flt12
flt13
flt14
flt15
flt16
flt17
flt18
flt19
flt20

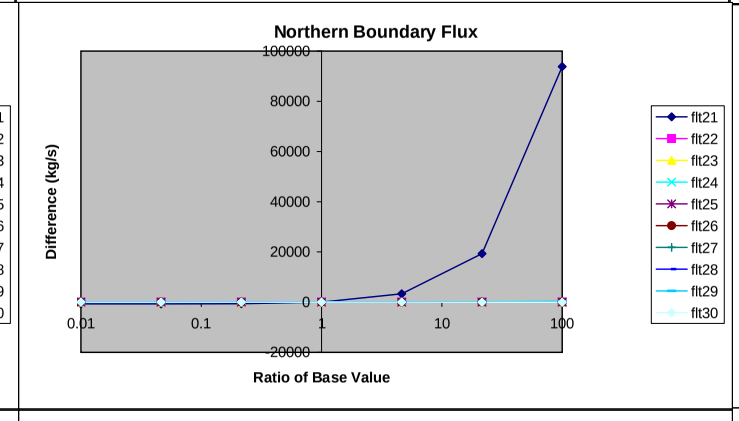
Northern Boundary Flux
Difference (kg/s)
Ratio of Base Value
flt21
flt22
flt23
flt24
flt25
flt26
flt27
flt28
flt29
flt30

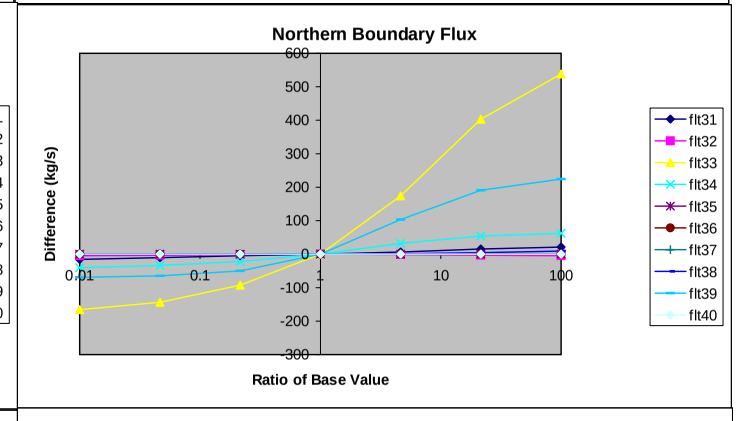
Northern Boundary Flux
Difference (kg/s)
Ratio of Base Value
flt31
flt32
flt33
flt34
flt35
flt36
flt37
flt38
flt39
flt40

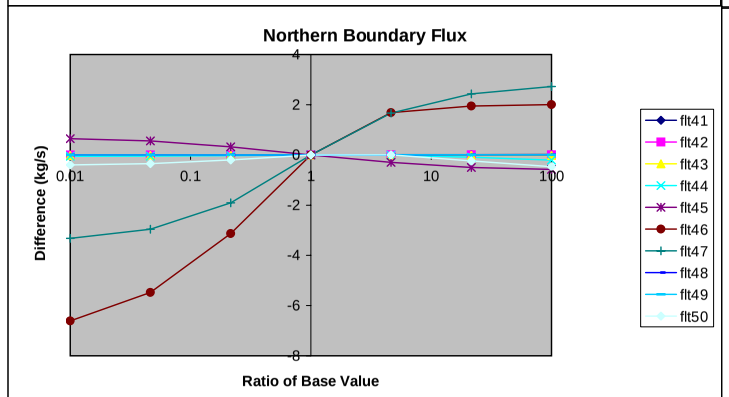
Northern Boundary Flux
Difference (kg/s)
Ratio of Base Value
flt41
flt42
flt43
flt44
flt45
flt46
flt47
flt48
flt49
flt50

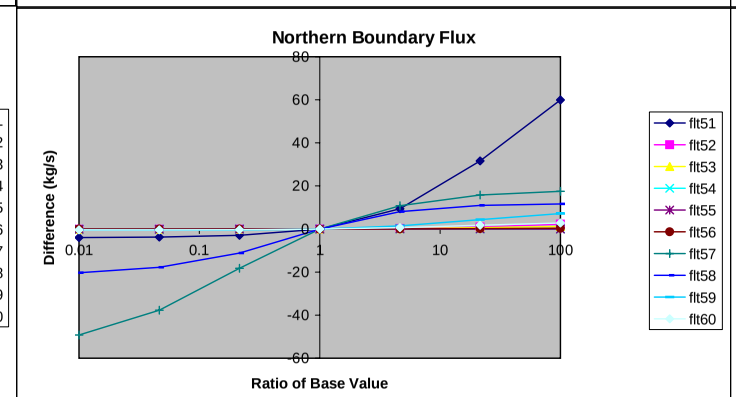
Northern Boundary Flux
Difference (kg/s)
Ratio of Base Value
flt51
flt52
flt53
flt54
flt55
flt56
flt57
flt58
flt59
flt60

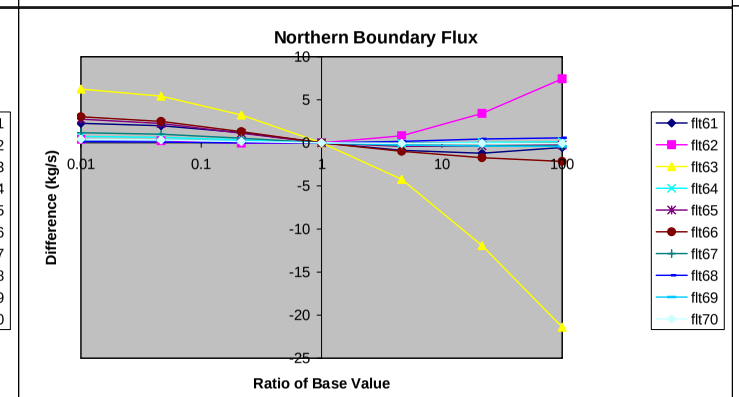
Northern Boundary Flux
Difference (kg/s)
Ratio of Base Value
flt61
flt62
flt63
flt64
flt65
flt66
flt67
flt68
flt69
flt70

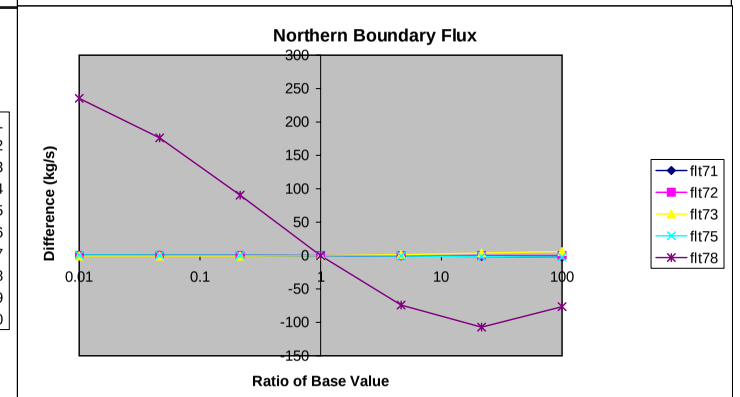
Northern Boundary Flux
Difference (kg/s)
Ratio of Base Value
flt71
flt72
flt73
flt75
flt78

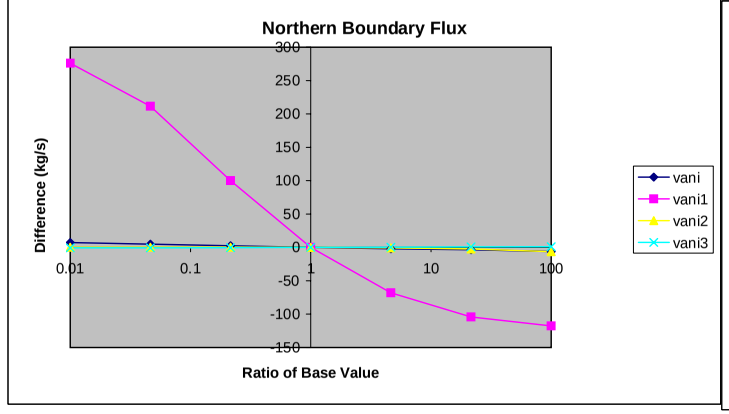
Northern Boundary Flux
Difference (kg/s)
Ratio of Base Value
vani
vani1
vani2
vani3

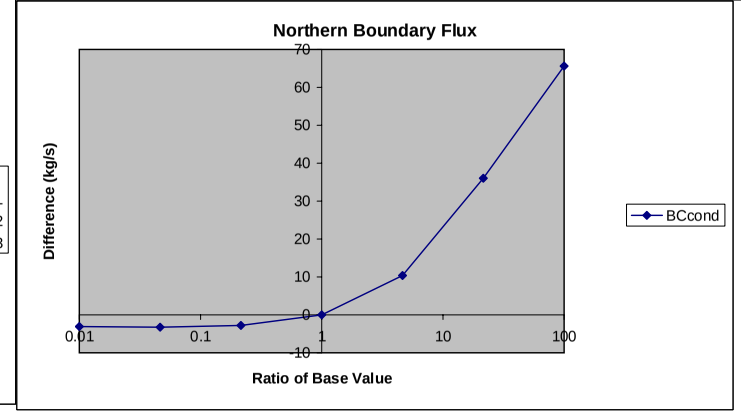
Northern Boundary Flux
Difference (kg/s)
Ratio of Base Value
BCcond

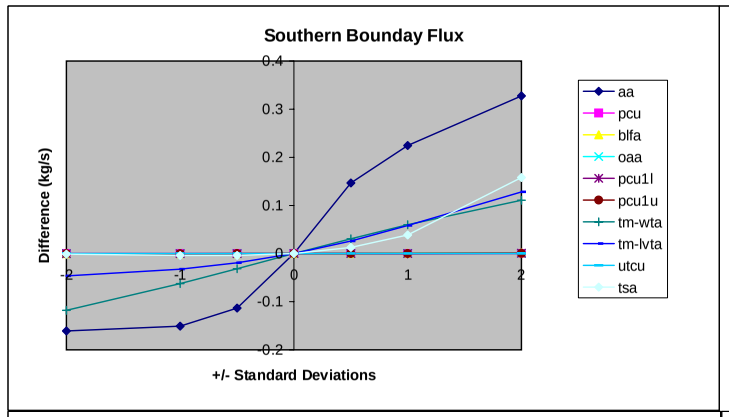
Southern Bounday Flux
Difference (kg/s)
+/- Standard Deviations
aa
pcu
blfa
oaa
pcu1l
pcu1u
tm-wta
tm-lvta
utcu
tsa

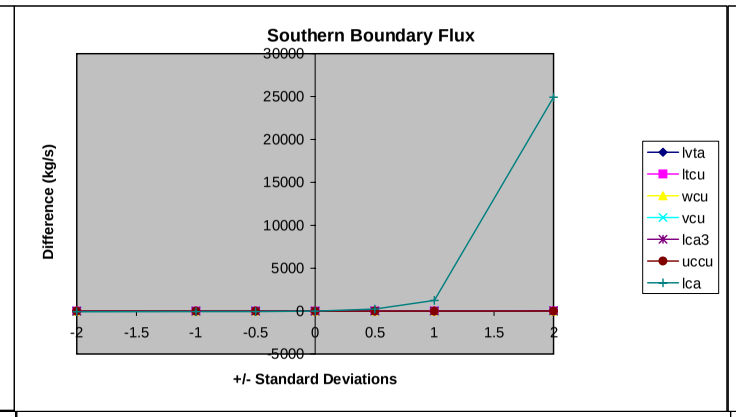
Southern Boundary Flux
Difference (kg/s)
+/- Standard Deviations
lvta
ltcu
wcu
vcu
lca3
uccu
lca

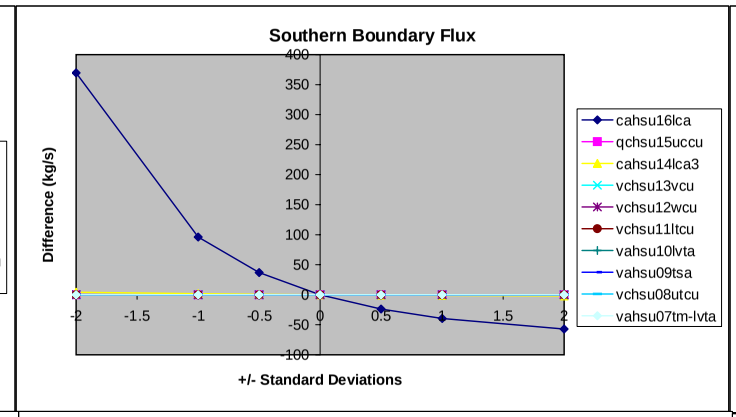
Southern Boundary Flux
Difference (kg/s)
+/- Standard Deviations
cahsu16lca
qchsu15uccu
cahsu14lca3
vchsu13vcu
vchsu12wcu
vchsu11ltcu
vahsu10lvta
vahsu09tsa
vchsu08utcu
vahsu07tm-lvta

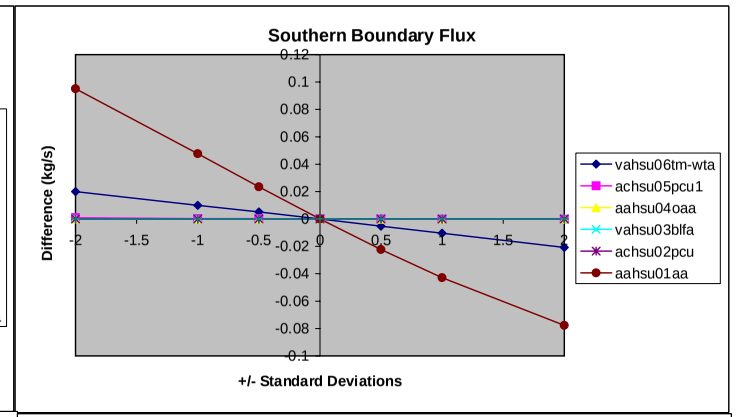
Southern Boundary Flux
Difference (kg/s)
+/- Standard Deviations
vahsu06tm-wta
achsu05pcu1
aahsu04oaa
vahsu03blfa
achsu02pcu
aahsu01aa

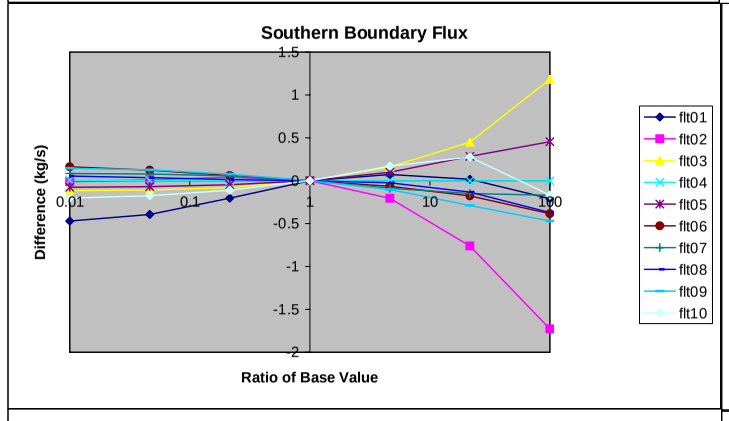
Southern Boundary Flux
Difference (kg/s)
Ratio of Base Value
flt01
flt02
flt03
flt04
flt05
flt06
flt07
flt08
flt09
flt10

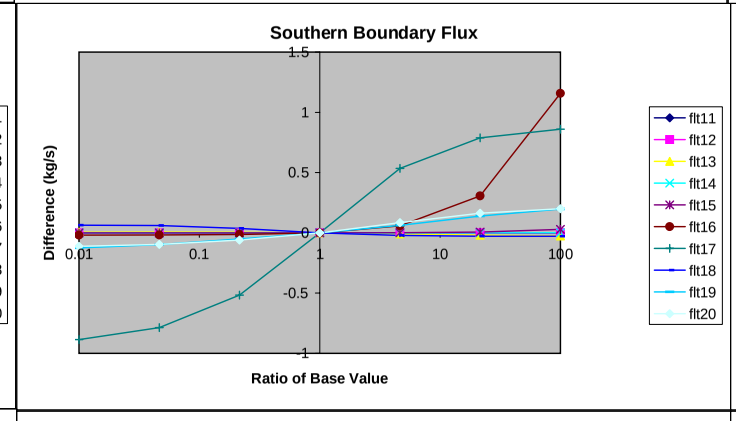
Southern Boundary Flux
Difference (kg/s)
Ratio of Base Value
flt11
flt12
flt13
flt14
flt15
flt16
flt17
flt18
flt19
flt20

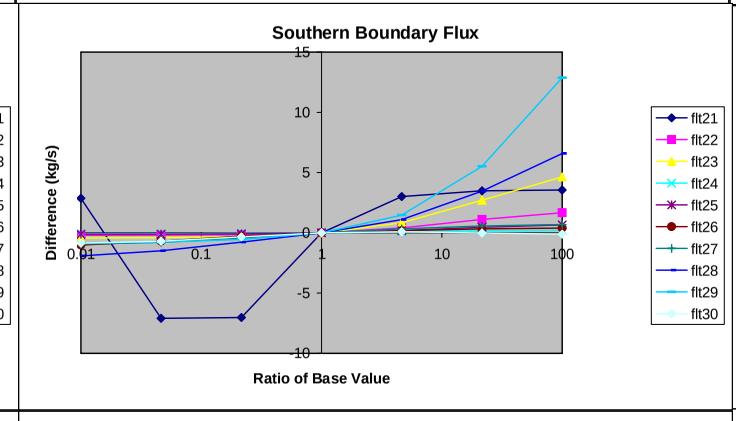
Southern Boundary Flux
Difference (kg/s)
Ratio of Base Value
flt21
flt22
flt23
flt24
flt25
flt26
flt27
flt28
flt29
flt30

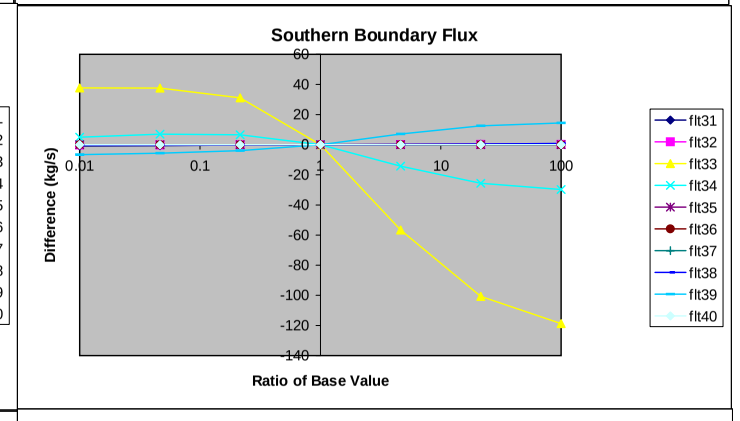
Southern Boundary Flux
Difference (kg/s)
Ratio of Base Value
flt31
flt32
flt33
flt34
flt35
flt36
flt37
flt38
flt39
flt40

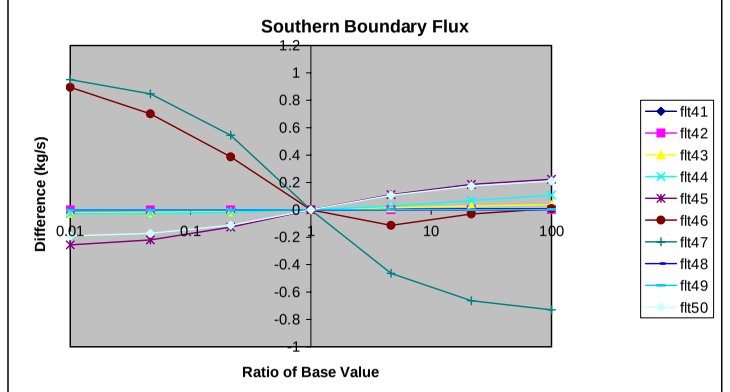
Southern Boundary Flux
Difference (kg/s)
Ratio of Base Value
flt41
flt42
flt43
flt44
flt45
flt46
flt47
flt48
flt49
flt50

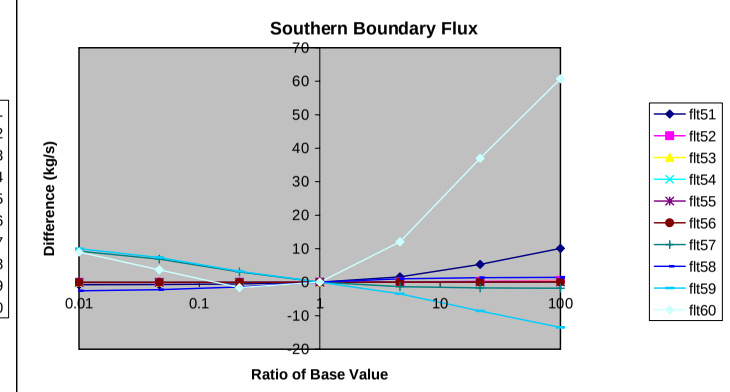
Southern Boundary Flux
Difference (kg/s)
Ratio of Base Value
flt51
flt52
flt53
flt54
flt55
flt56
flt57
flt58
flt59
flt60

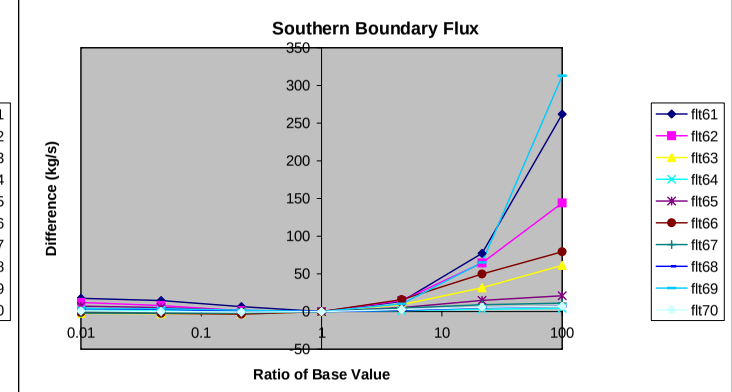
Southern Boundary Flux
Difference (kg/s)
Ratio of Base Value
flt61
flt62
flt63
flt64
flt65
flt66
flt67
flt68
flt69
flt70

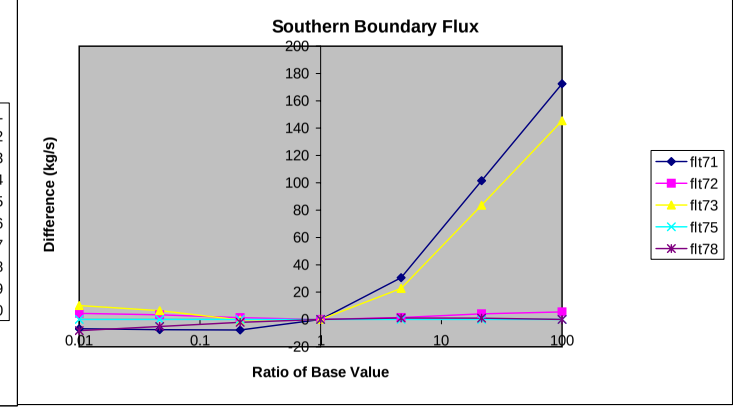
Southern Boundary Flux
Difference (kg/s)
Ratio of Base Value
flt71
flt72
flt73
flt75
flt78

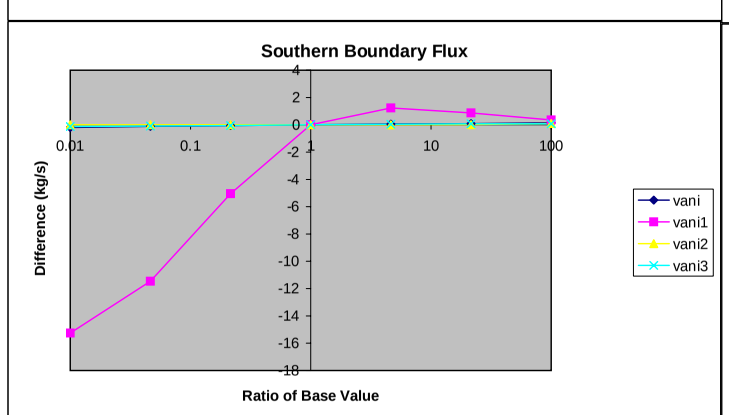
Southern Boundary Flux
Difference (kg/s)
Ratio of Base Value
vani
vani1
vani2
vani3

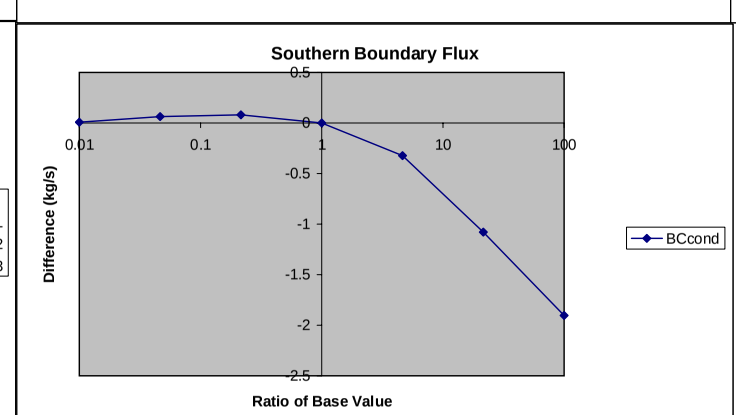
Southern Boundary Flux
Difference (kg/s)
Ratio of Base Value
BCcond

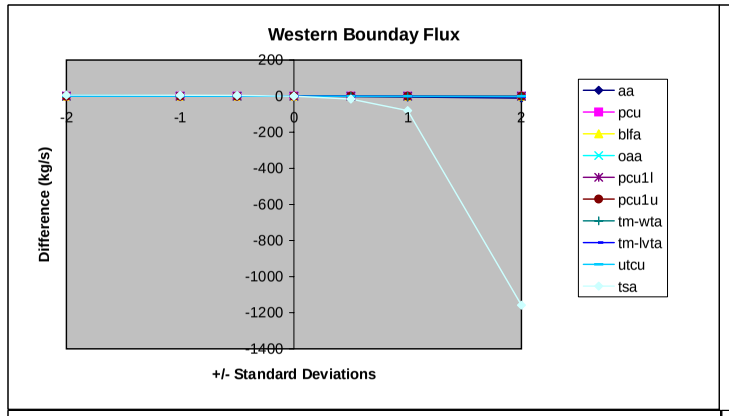
Western Bounday Flux
Difference (kg/s)
+/- Standard Deviations
aa
pcu
bifa
oaa
pcu1l
pcu1u
tm-wta
tm-lvta
utcu
tsa

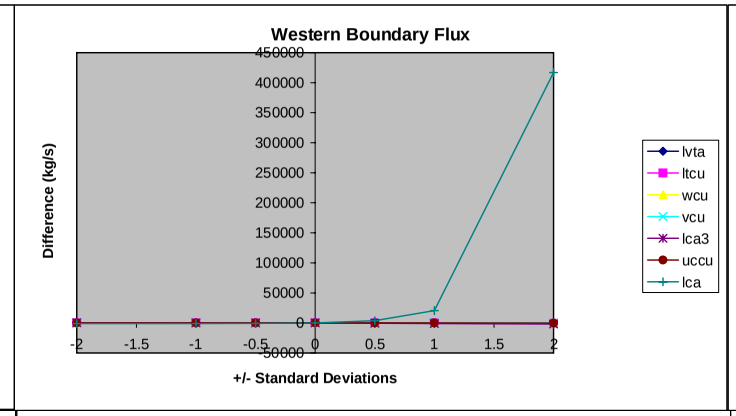
Western Boundary Flux
Difference (kg/s)
+/- Standard Deviations
lvta
ltcu
wcu
vcu
lca3
uccu
lca

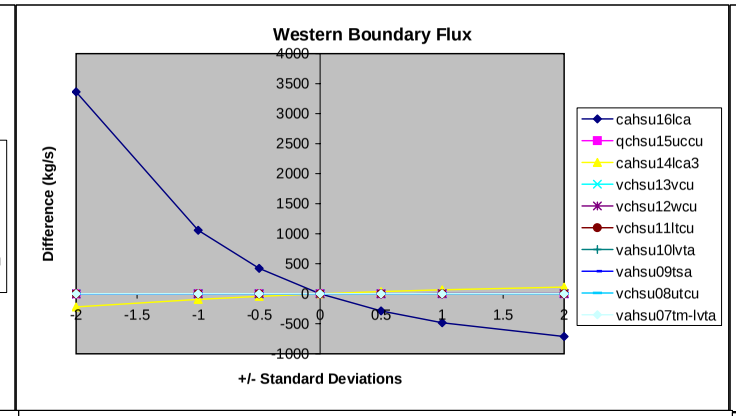
Western Boundary Flux
Difference (kg/s)
+/- Standard Deviations
cahsu16lca
qchsu15uccu
cahsu14lca3
vchsu13vcu
vchsu12wcu
vchsu11ltcu
vahsu10lvta
vahsu09tsa
vchsu08utcu
vahsu07tm-lvta

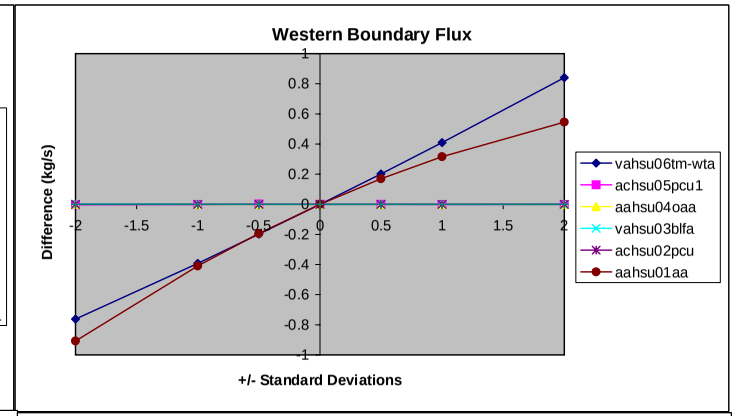
Western Boundary Flux
Difference (kg/s)
+/- Standard Deviations
vahsu06tm-wta
achsu05pcu1
aahsu04oaa
vahsu03blfa
achsu02pcu
aahsu01aa

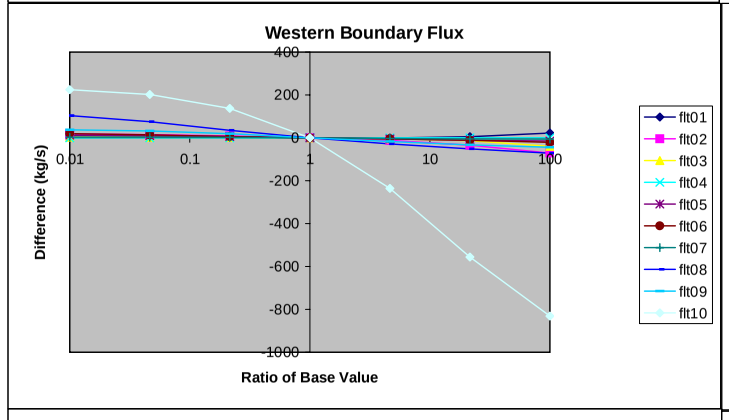
Western Boundary Flux
Difference (kg/s)
Ratio of Base Value
flt01
flt02
flt03
flt04
flt05
flt06
flt07
flt08
flt09
flt10

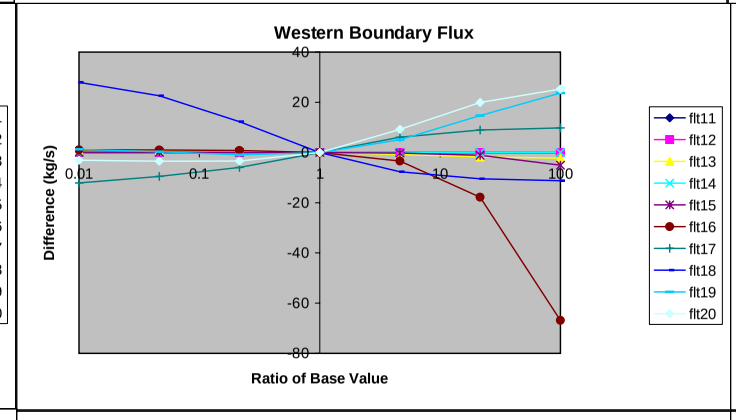
Western Boundary Flux
Difference (kg/s)
Ratio of Base Value
flt11
flt12
flt13
flt14
flt15
flt16
flt17
flt18
flt19
flt20

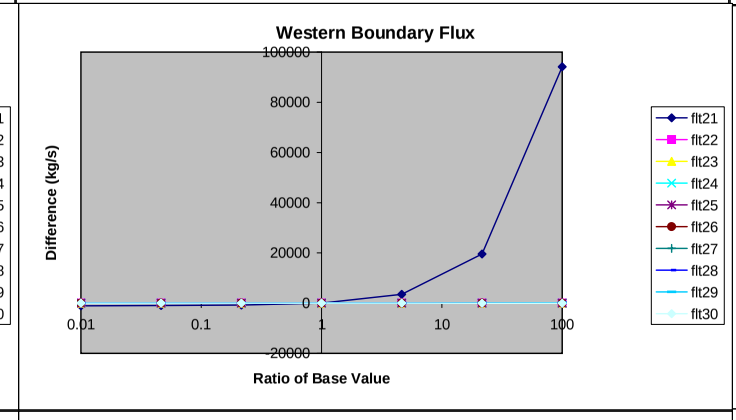
Western Boundary Flux
Difference (kg/s)
Ratio of Base Value
flt21
flt22
flt23
flt24
flt25
flt26
flt27
flt28
flt29
flt30

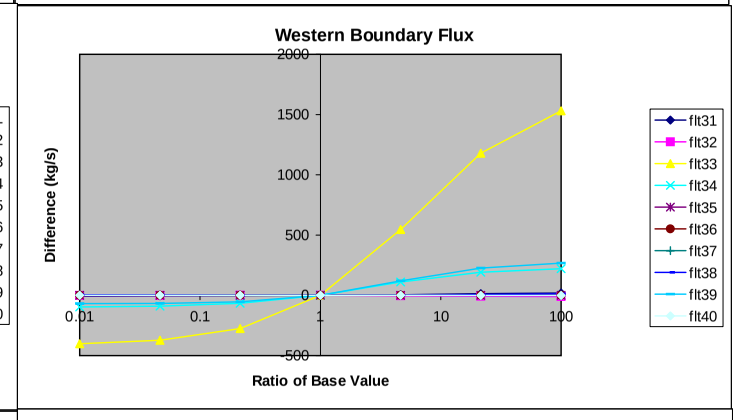
Western Boundary Flux
Difference (kg/s)
Ratio of Base Value
flt31
flt32
flt33
flt34
flt35
flt36
flt37
flt38
flt39
flt40

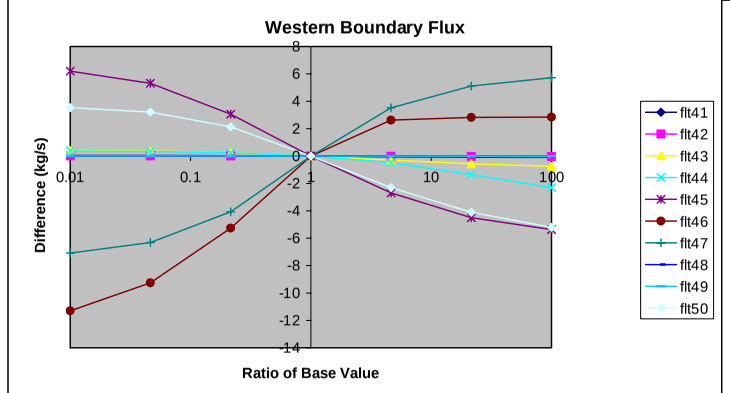
Western Boundary Flux
Difference (kg/s)
Ratio of Base Value
flt41
flt42
flt43
flt44
flt45
flt46
flt47
flt48
flt49
flt50

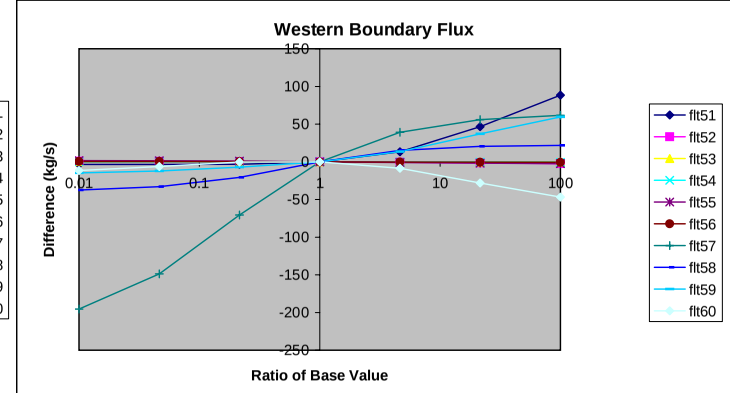
Western Boundary Flux
Difference (kg/s)
Ratio of Base Value
flt51
flt52
flt53
flt54
flt55
flt56
flt57
flt58
flt59
flt60

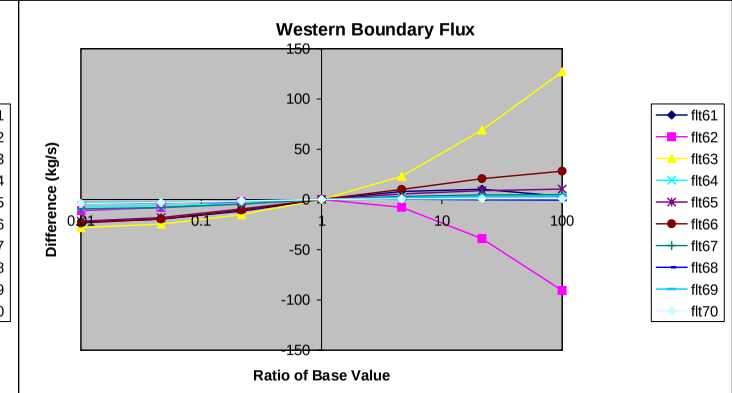
Western Boundary Flux
Difference (kg/s)
Ratio of Base Value
flt61
flt62
flt63
flt64
flt65
flt66
flt67
flt68
flt69
flt70

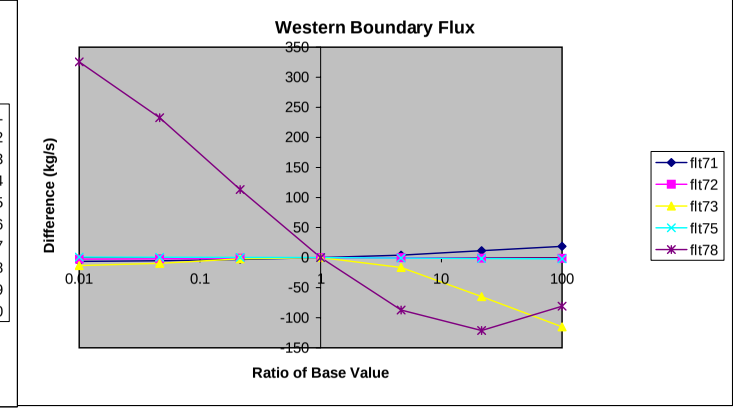
Western Boundary Flux
Difference (kg/s)
Ratio of Base Value
flt71
flt72
flt73
flt75
flt78

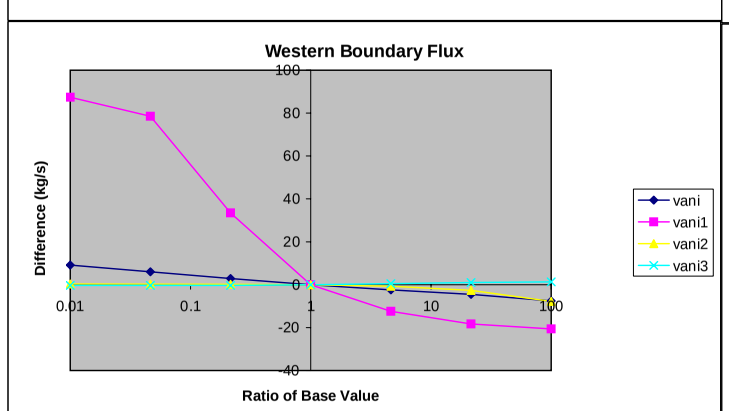
Western Boundary Flux
Difference (kg/s)
Ratio of Base Value
vani
vani1
vani2
vani3

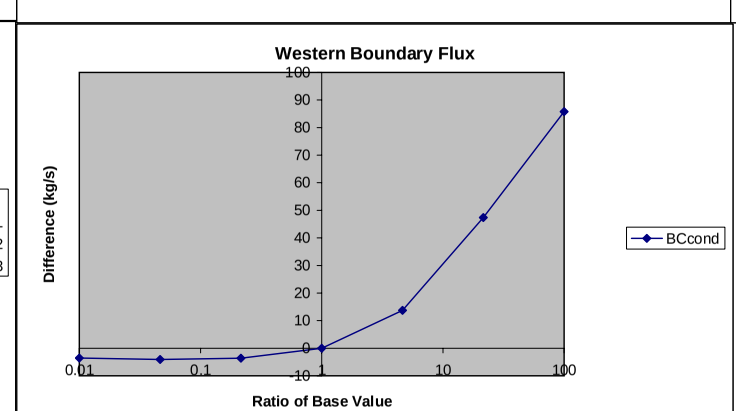
Western Boundary Flux
Difference (kg/s)
Ratio of Base Value
BCcond

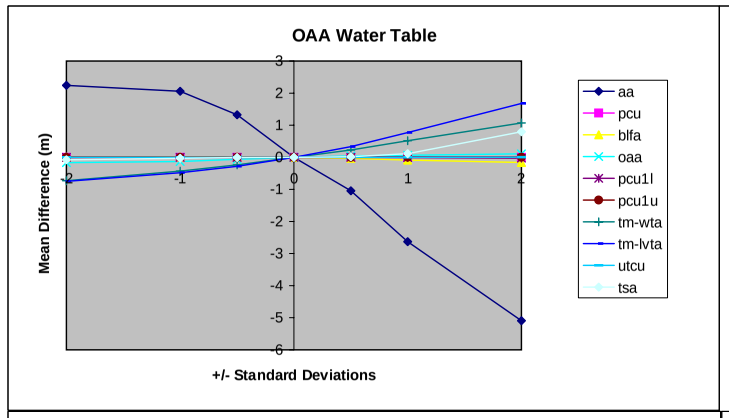
OAA Water Table
Mean Difference (m)
+/- Standard Deviations
aa
pcu
blfa
oaa
pcu1l
pcu1u
tm-wta
tm-lvta
utcu
tsa

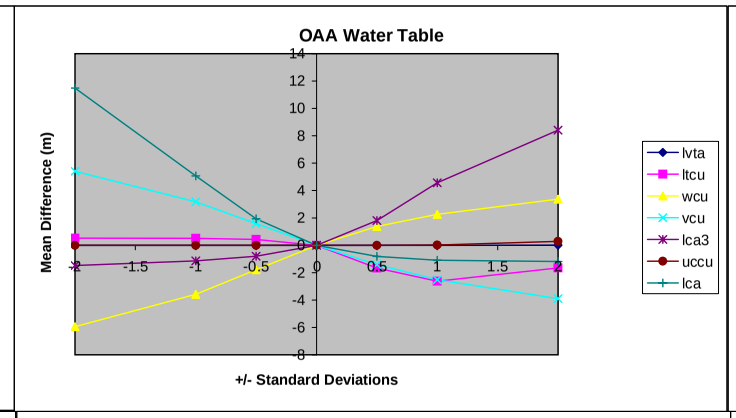
OAA Water Table
Mean Difference (m)
+/- Standard Deviations
lvta
ltcu
wcu
vcu
lca3
uccu
lca

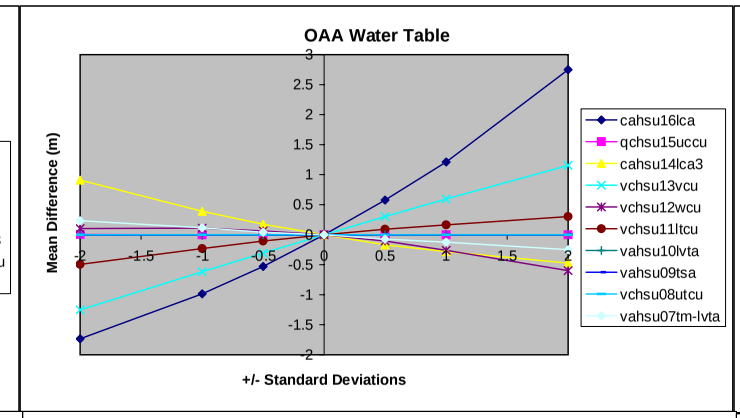
OAA Water Table
Mean Difference (m)
+/- Standard Deviations
cahsu16lca
qchsu15uccu
cahsu14lca3
vchsu13vcu
vchsu12wcu
vchsu11ltcu
vahsu10lvta
vahsu09tsa
vchsu08utcu
vahsu07tm-lvta

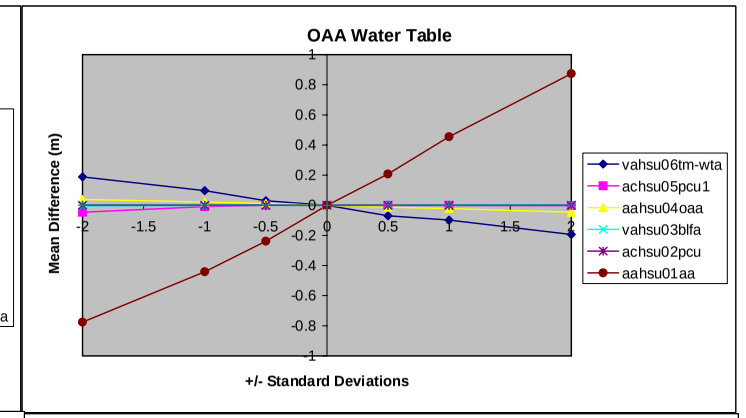
OAA Water Table
Mean Difference (m)
+/- Standard Deviations
vahsu06tm-wta
achsu05pcu1
aahsu04oaa
vahsu03blfa
achsu02pcu
aahsu01aa

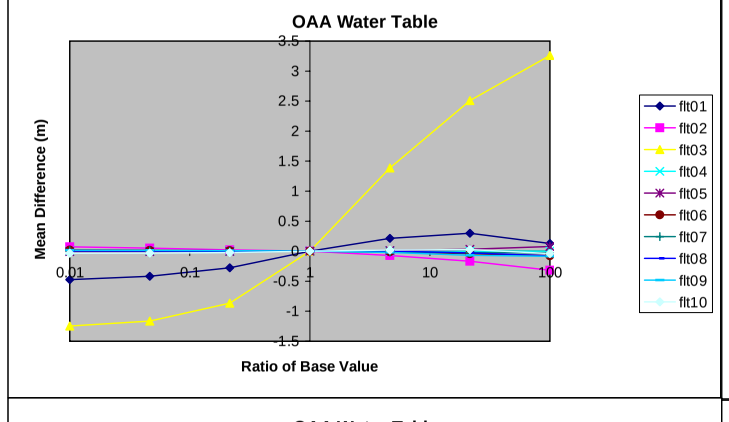
OAA Water Table
Mean Difference (m)
Ratio of Base Value
flt01
flt02
flt03
flt04
flt05
flt06
flt07
flt08
flt09
flt10

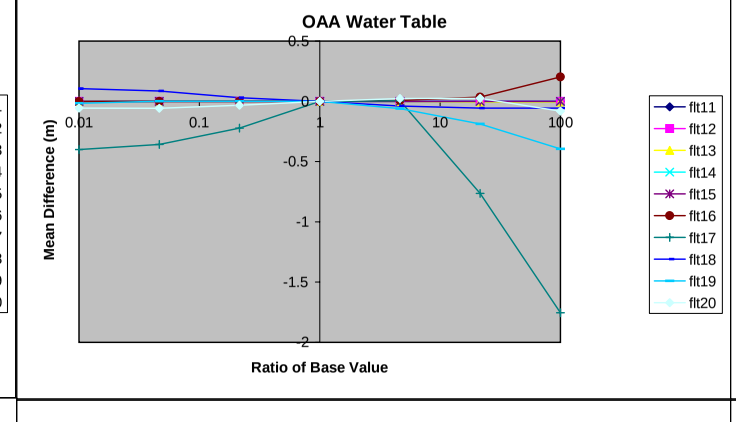
OAA Water Table
Mean Difference (m)
Ratio of Base Value
flt11
flt12
flt13
flt14
flt15
flt16
flt17
flt18
flt19
flt20

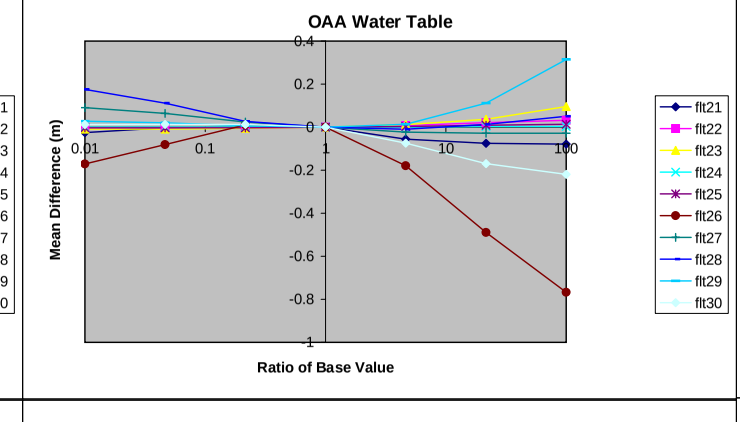
OAA Water Table
Mean Difference (m)
Ratio of Base Value
flt21
flt22
flt23
flt24
flt25
flt26
flt27
flt28
flt29
flt30

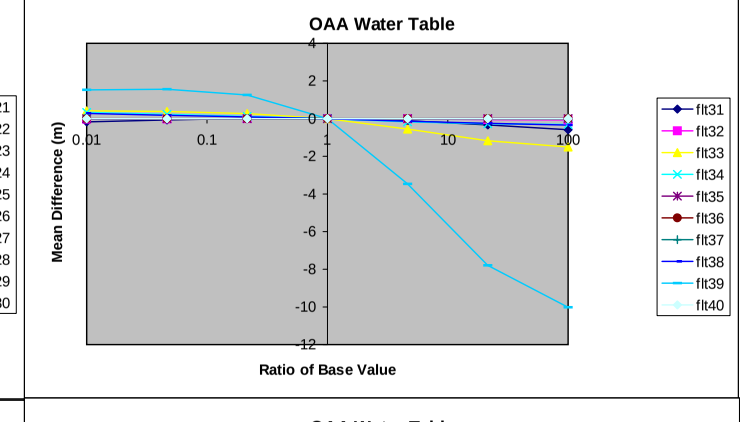
OAA Water Table
Mean Difference (m)
Ratio of Base Value
flt31
flt32
flt33
flt34
flt35
flt36
flt37
flt38
flt39
flt40

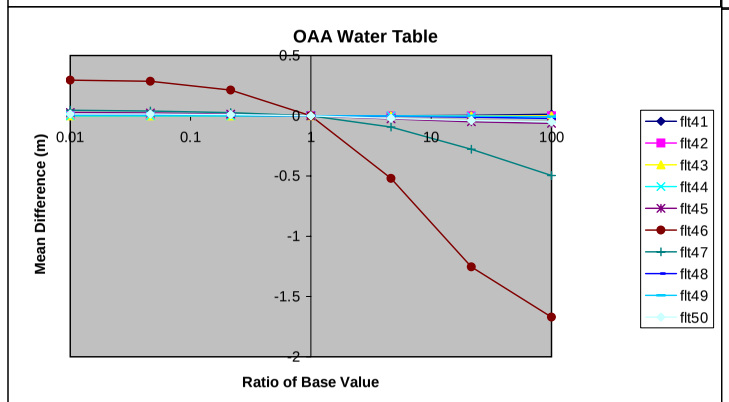
OAA Water Table
Mean Difference (m)
Ratio of Base Value
flt41
flt42
flt43
flt44
flt45
flt46
flt47
flt48
flt49
flt50

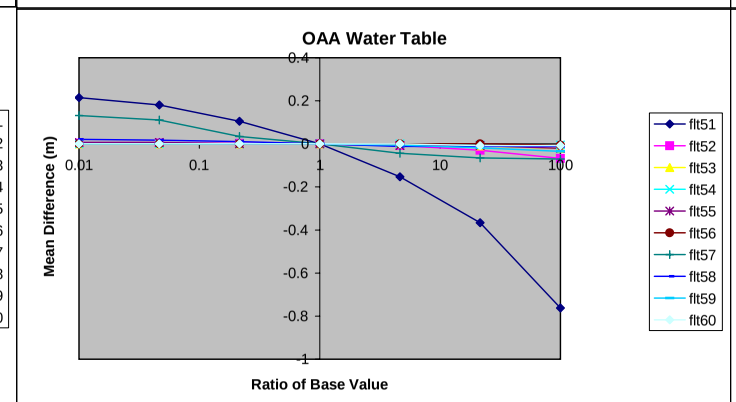
OAA Water Table
Mean Difference (m)
Ratio of Base Value
flt51
flt52
flt53
flt54
flt55
flt56
flt57
flt58
flt59
flt60

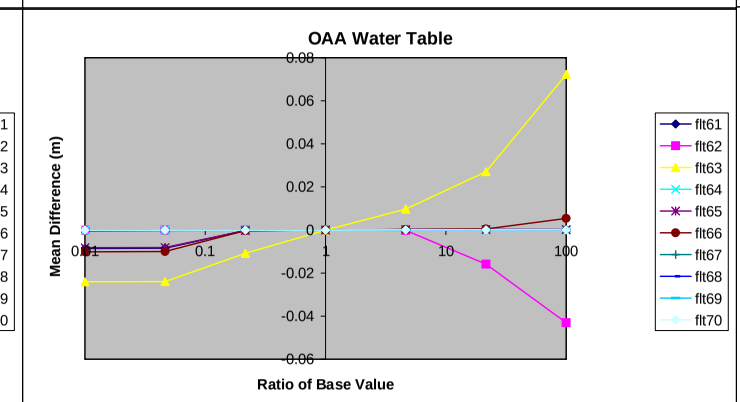
OAA Water Table
Mean Difference (m)
Ratio of Base Value
flt61
flt62
flt63
flt64
flt65
flt66
flt67
flt68
flt69
flt70

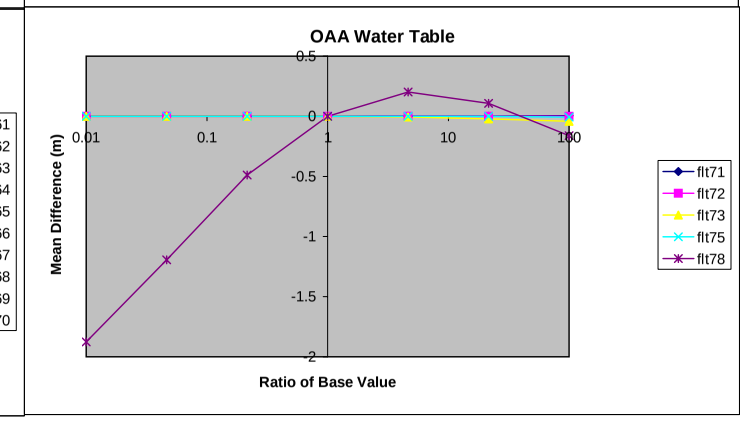
OAA Water Table
Mean Difference (m)
Ratio of Base Value
flt71
flt72
flt73
flt75
flt78

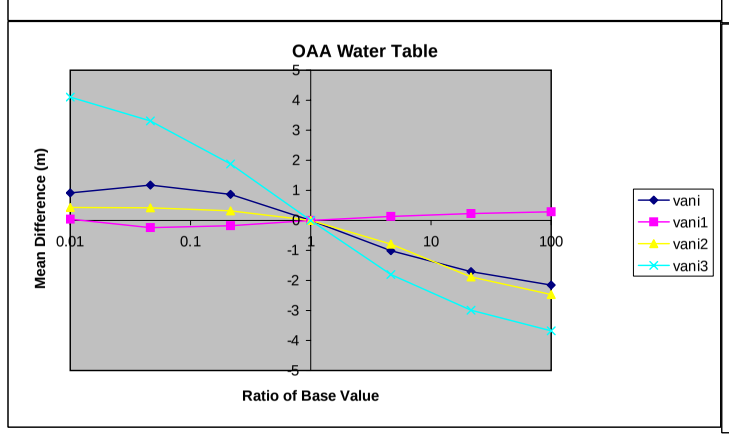
OAA Water Table
Mean Difference (m)
Ratio of Base Value
vani
vani1
vani2
vani3

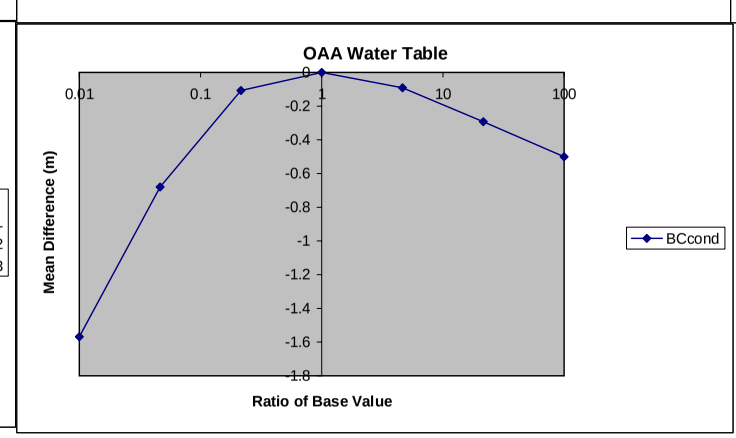
OAA Water Table
Mean Difference (m)
Ratio of Base Value
BCcond

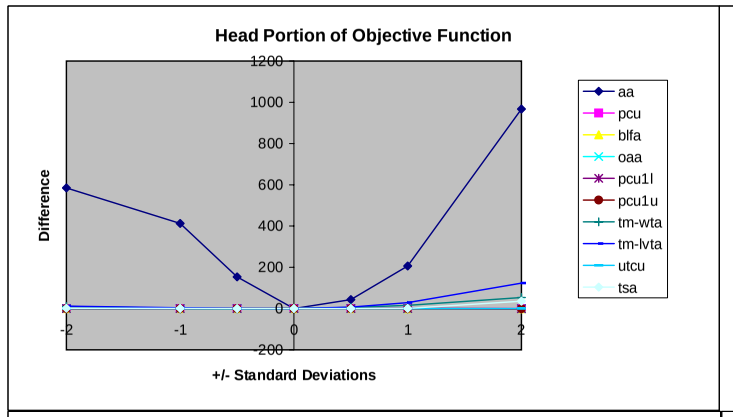
Head Portion of Objective Function
Difference
+/- Standard Deviations
aa
pcu
blfa
oaa
pcu1l
pcu1u
tm-wta
tm-lvta
utcu
tsa

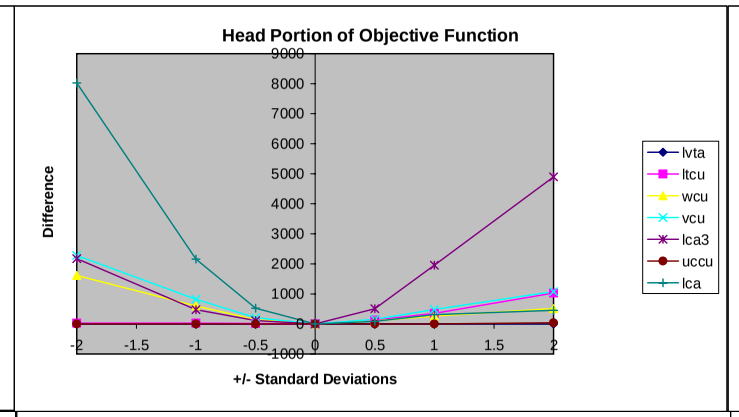
Head Portion of Objective Function
Difference
+/- Standard Deviations
lvta
ltcu
wcu
vcu
lca3
uccu
lca

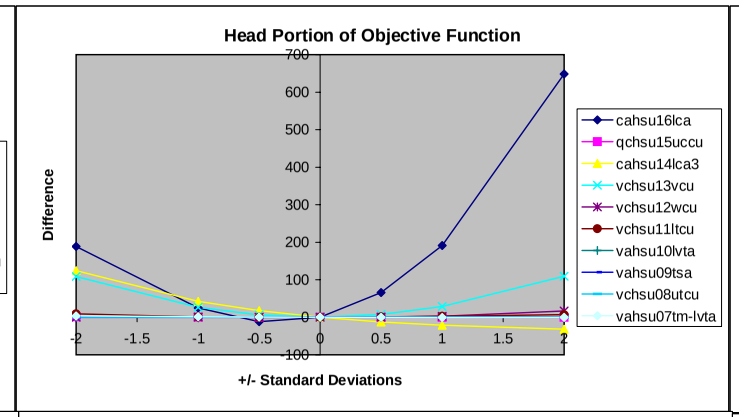
Head Portion of Objective Function
Difference
+/- Standard Deviations
cahsu16lca
qchsu15uccu
cahsu14lca3
vchsu13vcu
vchsu12wcu
vchsu11ltcu
vahsu10lvta
vahsu09tsa
vchsu08utcu
vahsu07tm-lvta

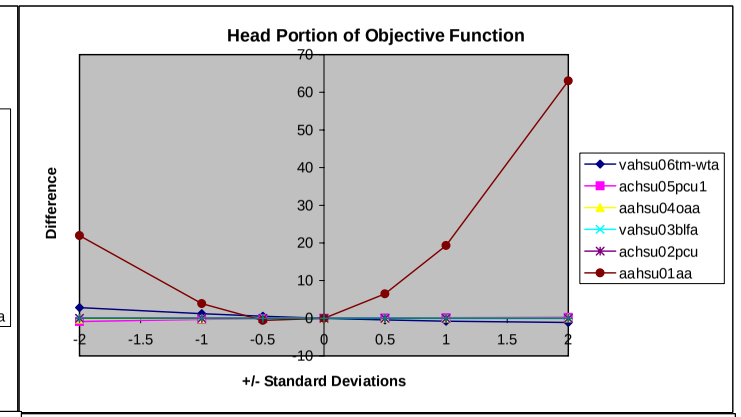
Head Portion of Objective Function
Difference
+/- Standard Deviations
vahsu06tm-wta
achsu05pcu1
aahsu04oaa
vahsu03blfa
achsu02pcu
aahsu01aa

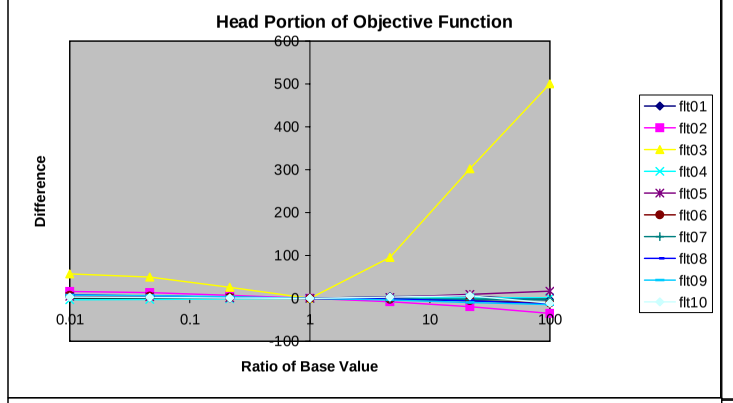
Head Portion of Objective Function
Difference
Ratio of Base Value
flt01
flt02
flt03
flt04
flt05
flt06
flt07
flt08
flt09
flt10

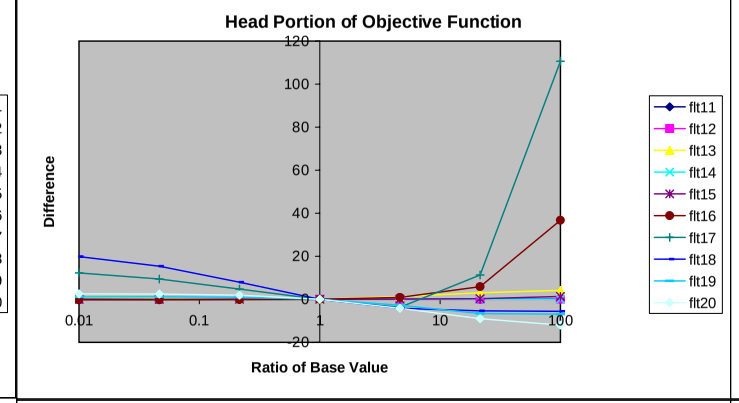
Head Portion of Objective Function
Difference
Ratio of Base Value
flt11
flt12
flt13
flt14
flt15
flt16
flt17
flt18
flt19
flt20

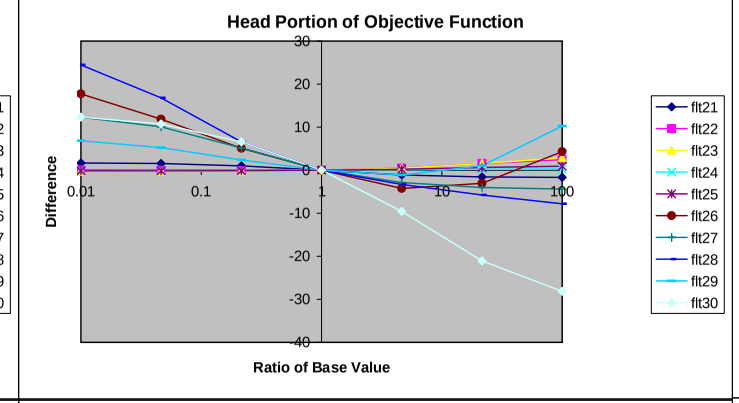
Head Portion of Objective Function
Difference
Ratio of Base Value
flt21
flt22
flt23
flt24
flt25
flt26
flt27
flt28
flt29
flt30

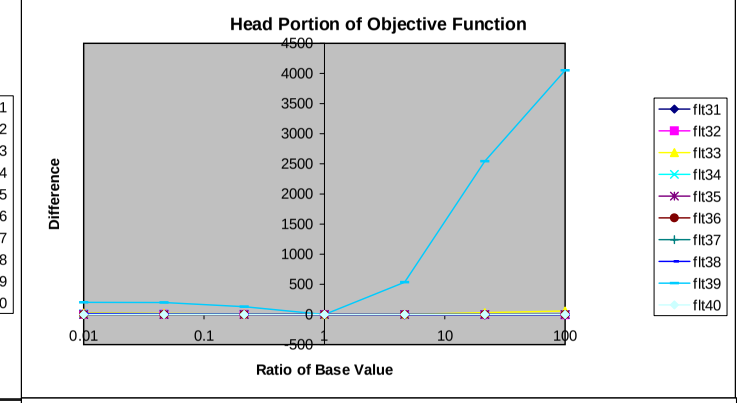
Head Portion of Objective Function
Difference
Ratio of Base Value
flt31
flt32
flt33
flt34
flt35
flt36
flt37
flt38
flt39
flt40

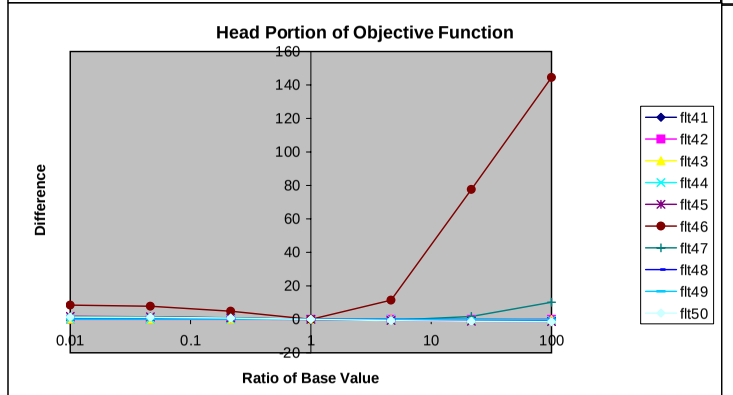
Head Portion of Objective Function
Difference
Ratio of Base Value
flt41
flt42
flt43
flt44
flt45
flt46
flt47
flt48
flt49
flt50

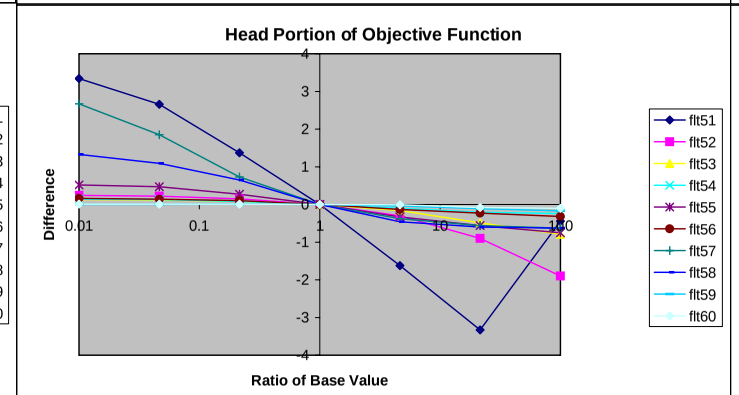
Head Portion of Objective Function
Difference
Ratio of Base Value
flt51
flt52
flt53
flt54
flt55
flt56
flt57
flt58
flt59
flt60

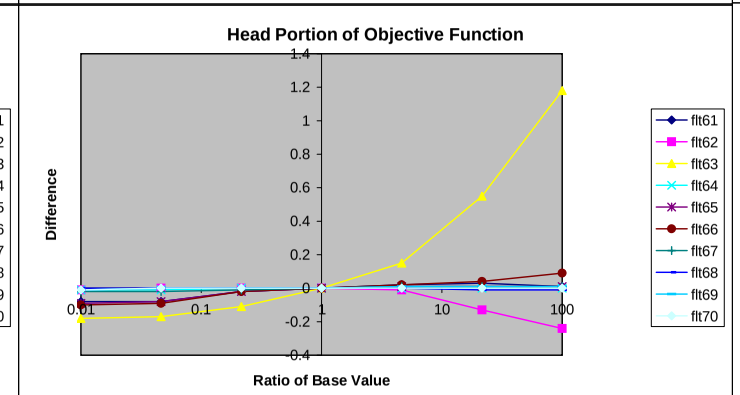
Head Portion of Objective Function
Difference
Ratio of Base Value
flt61
flt62
flt63
flt64
flt65
flt66
flt67
flt68
flt69
flt70

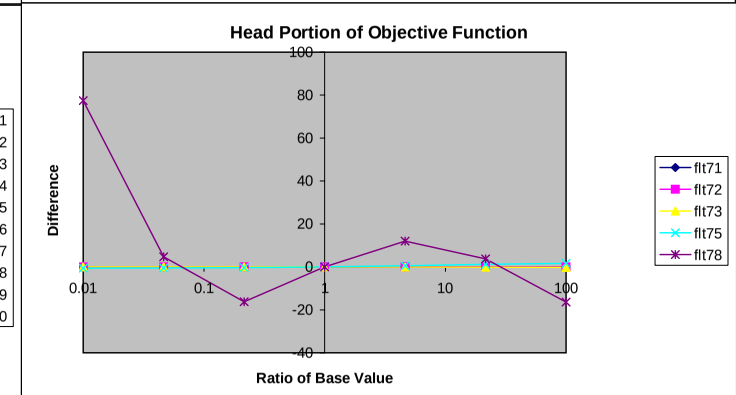
Head Portion of Objective Function
Difference
Ratio of Base Value
flt71
flt72
flt73
flt75
flt78

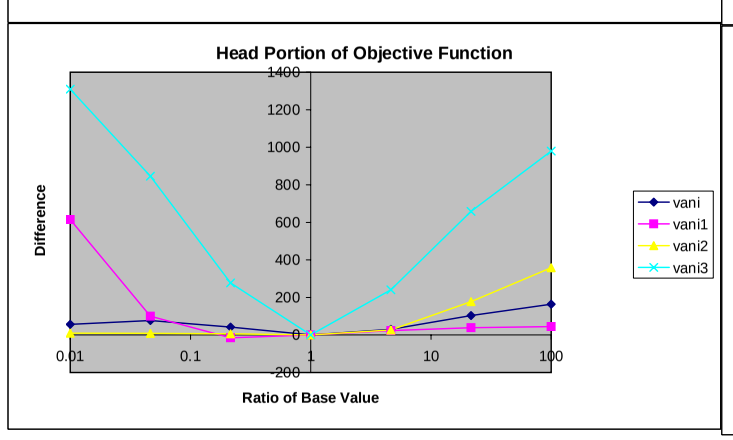
Head Portion of Objective Function
Difference
Ratio of Base Value
vani
vani1
vani2
vani3

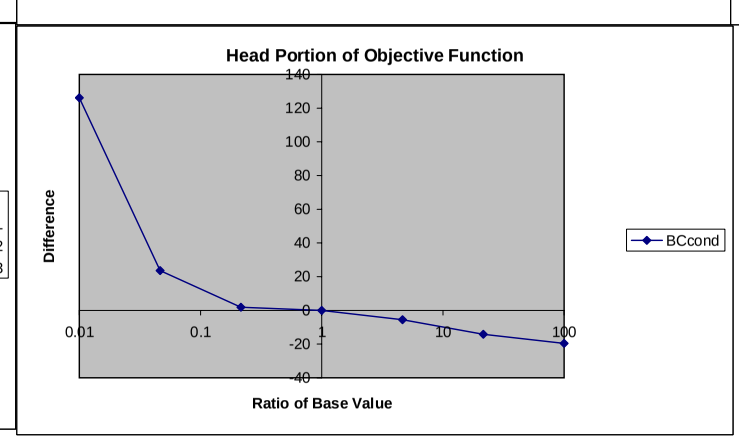
Head Portion of Objective Function
Difference
Ratio of Base Value
BCcond

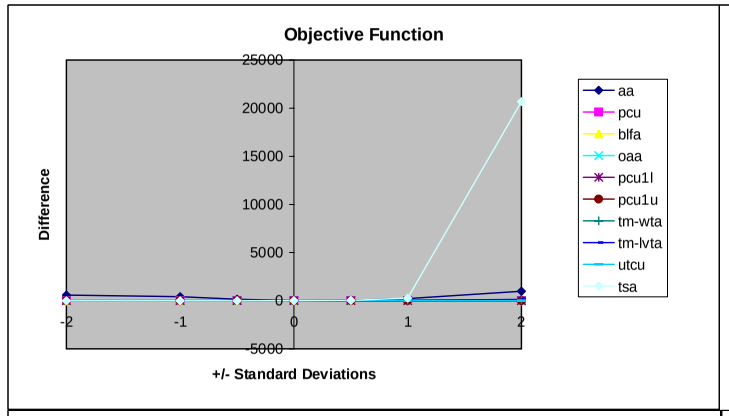
Objective Function
Difference
+/- Standard Deviations
aa
pcu
blfa
oaa
pcu1l
pcu1u
tm-wta
tm-lvta
utcu
tsa

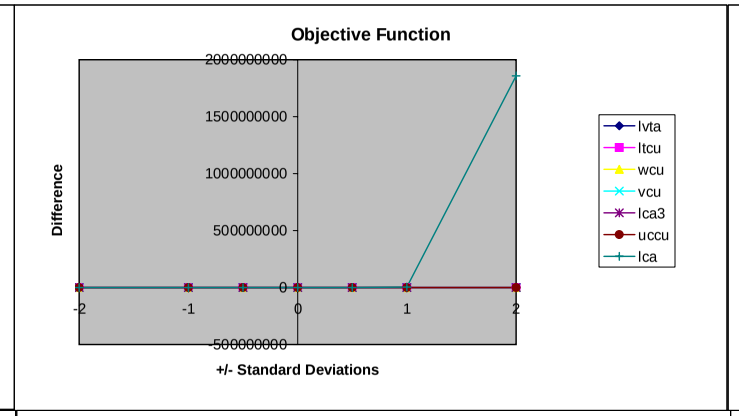
Objective Function
Difference
+/- Standard Deviations
lvta
ltcu
wcu
vcu
lca3
uccu
lca

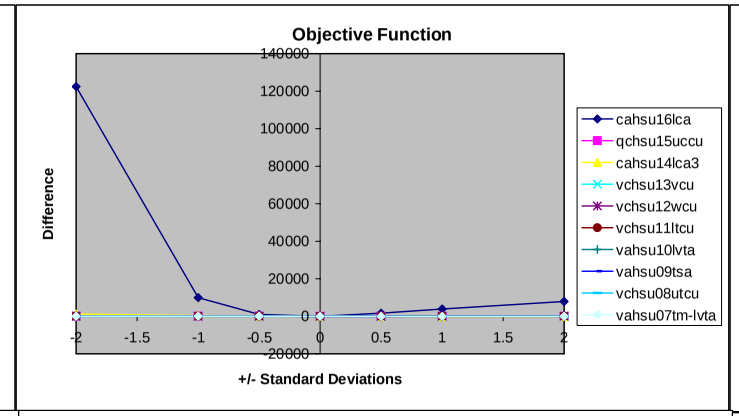
Objective Function
Difference
+/- Standard Deviations
cahsu16lca
qchsu15uccu
cahsu14lca3
vchsu13vcu
vchsu12wcu
vchsu11ltcu
vahsu10lvta
vahsu09tsa
vchsu08utcu
vahsu07tm-lvta

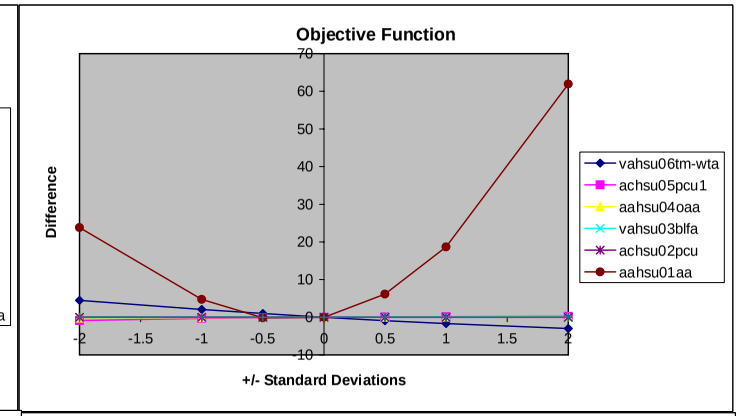
Objective Function
Difference
+/- Standard Deviations
vahsu06tm-wta
achsu05pcu1
aahsu04oaa
vahsu03blfa
achsu02pcu
aahsu01aa

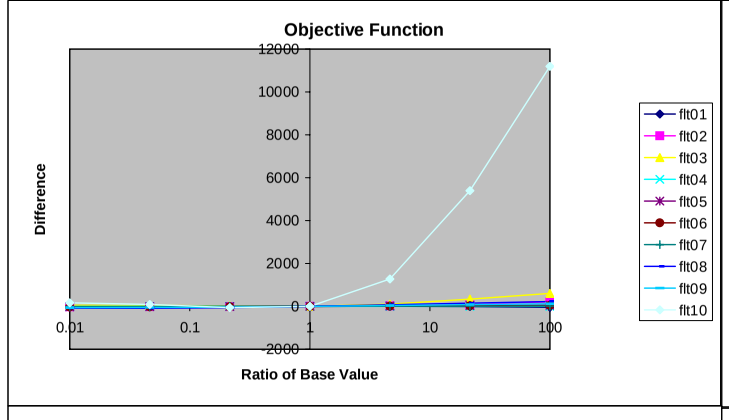
Objective Function
Difference
Ratio of Base Value
flt01
flt02
flt03
flt04
flt05
flt06
flt07
flt08
flt09
flt10

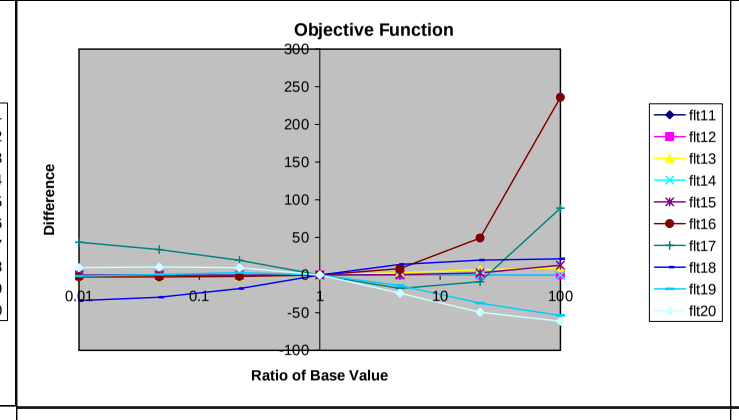
Objective Function
Difference
Ratio of Base Value
flt11
flt12
flt13
flt14
flt15
flt16
flt17
flt18
flt19
flt20

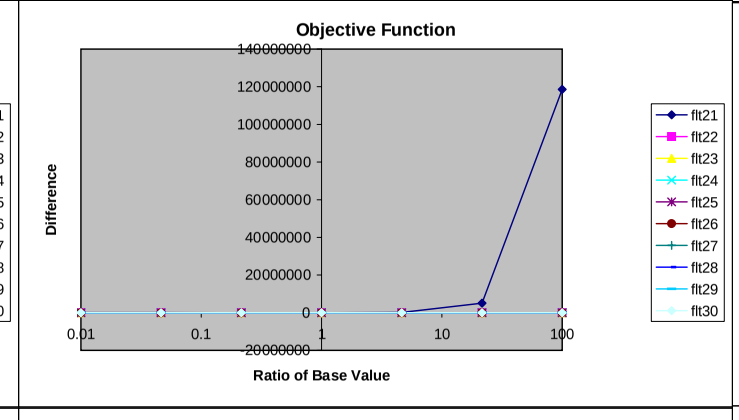
Objective Function
Difference
Ratio of Base Value
flt21
flt22
flt23
flt24
flt25
flt26
flt27
flt28
flt29
flt30

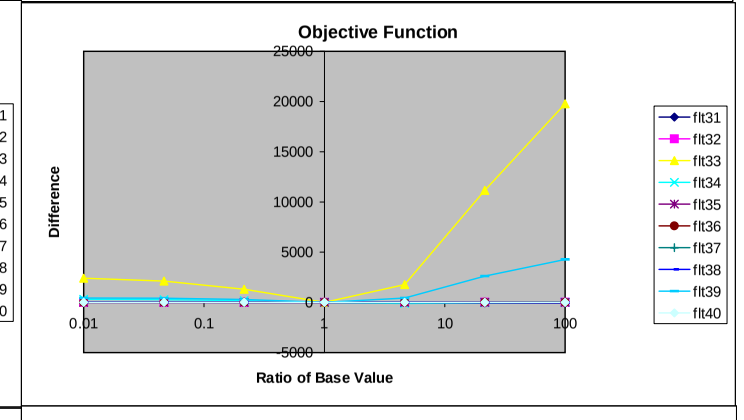
Objective Function
Difference
Ratio of Base Value
flt31
flt32
flt33
flt34
flt35
flt36
flt37
flt38
flt39
flt40

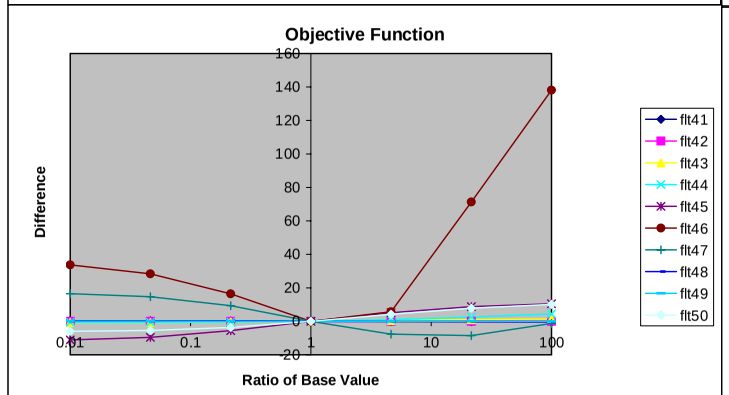
Objective Function
Difference
Ratio of Base Value
flt41
flt42
flt43
flt44
flt45
flt46
flt47
flt48
flt49
flt50

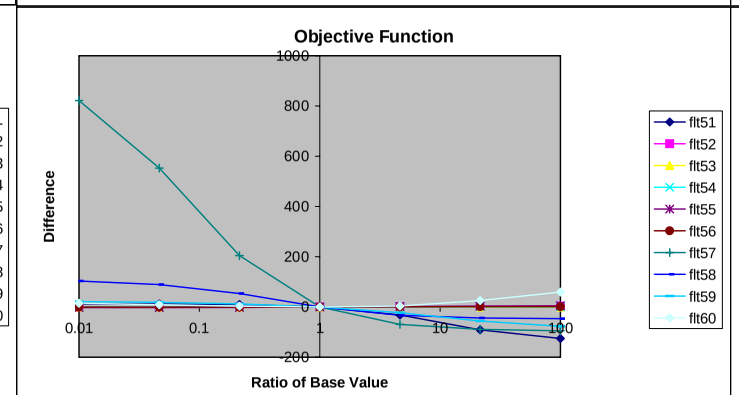
Objective Function
Difference
Ratio of Base Value
flt51
flt52
flt53
flt54
flt55
flt56
flt57
flt58
flt59
flt60

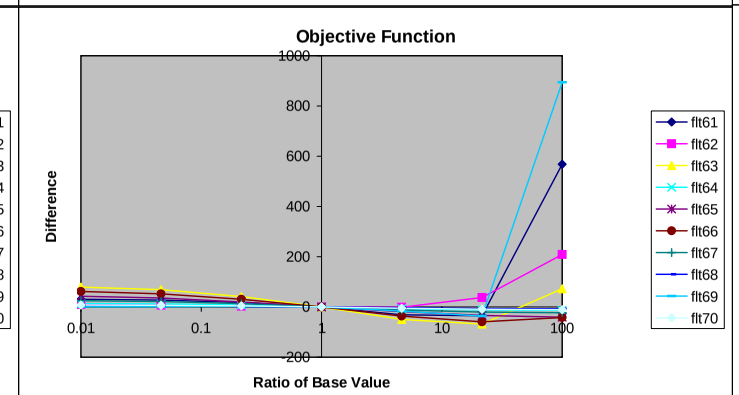
Objective Function
Difference
Ratio of Base Value
flt61
flt62
flt63
flt64
flt65
flt66
flt67
flt68
flt69
flt70

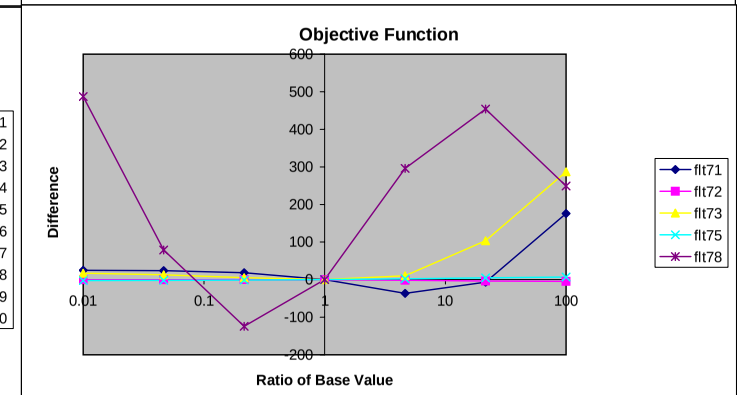
Objective Function
Difference
Ratio of Base Value
flt71
flt72
flt73
flt75
flt78

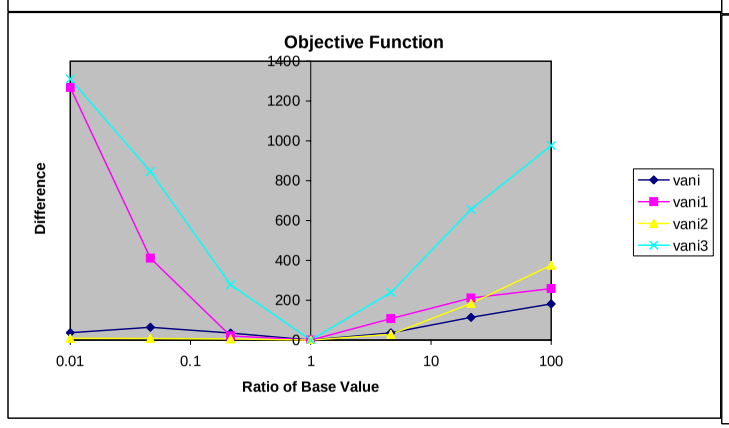
Objective Function
Difference
Ratio of Base Value
vani
vani1
vani2
vani3

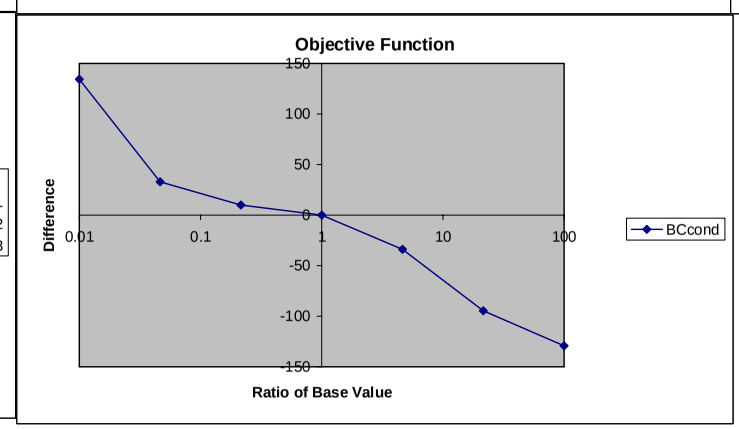
Objective Function
Difference
Ratio of Base Value
BCcond

C.3.7

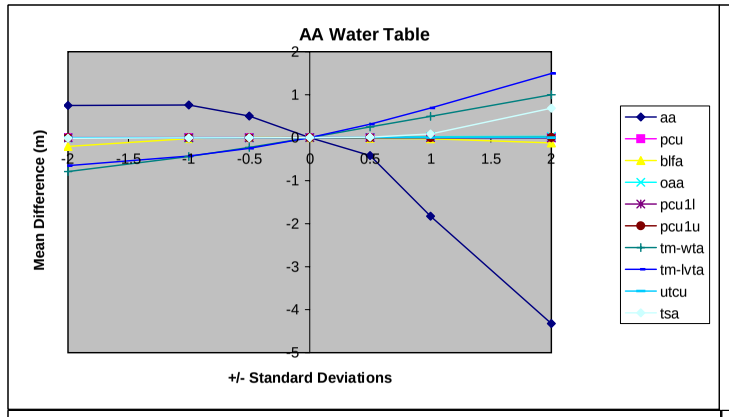
AA Water Table
Mean Difference (m)
+/- Standard Deviations
aa
pcu
blfa
oaa
pcu1l
pcu1u
tm-wta
tm-lvta
utcu
tsa

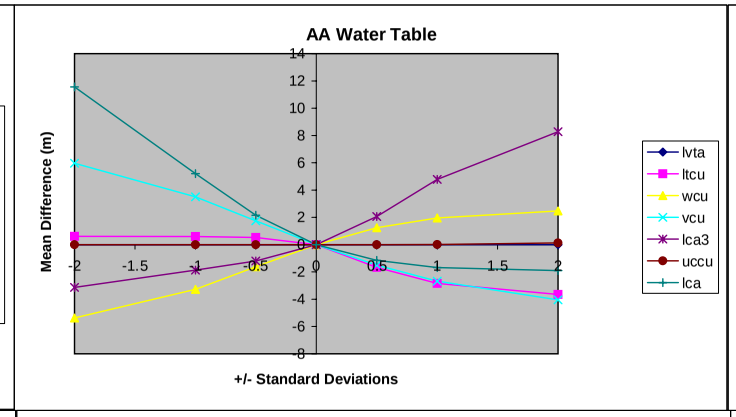
AA Water Table
Mean Difference (m)
+/- Standard Deviations
lvta
ltcu
wcu
vcu
lca3
uccu
lca

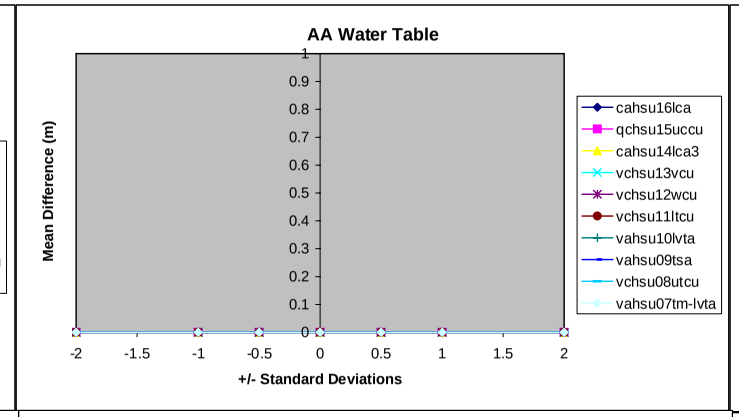
AA Water Table
Mean Difference (m)
+/- Standard Deviations
cahsu16lca
qchsu15uccu
cahsu14lca3
vchsu13vcu
vchsu12wcu
vchsu11ltcu
vahsu10lvta
vahsu09tsa
vchsu08utcu
vahsu07tm-lvta

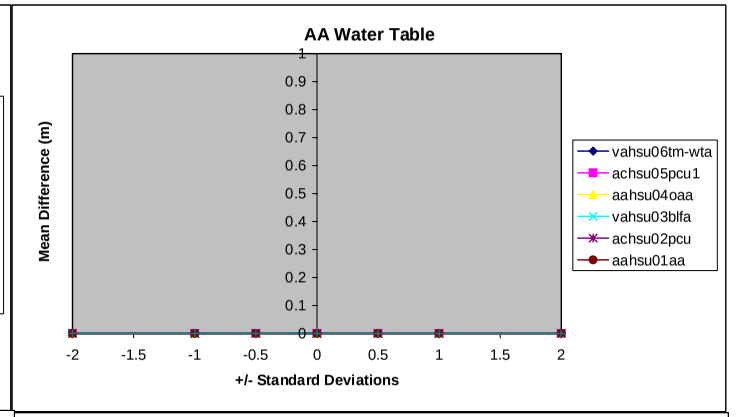
AA Water Table
Mean Difference (m)
+/- Standard Deviations
vahsu06tm-wta
achsu05pcu1
aahsu04oaa
vahsu03blfa
achsu02pcu
aahsu01aa

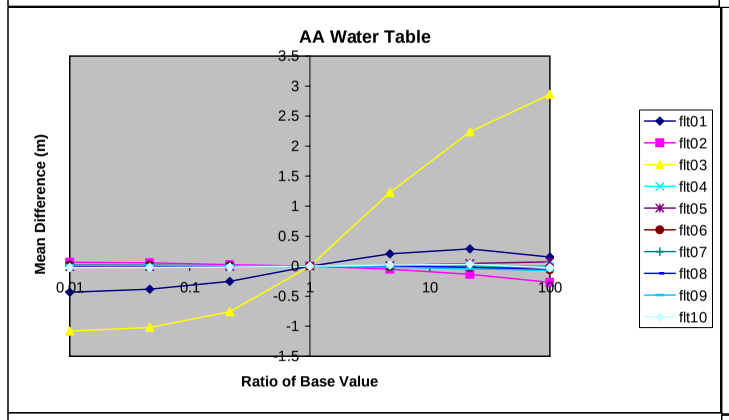
AA Water Table
Mean Difference (m)
Ratio of Base Value
flt01
flt02
flt03
flt04
flt05
flt06
flt07
flt08
flt09
flt10

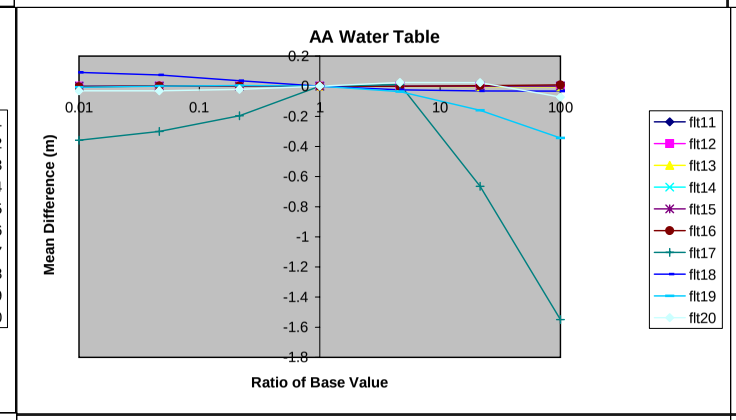
AA Water Table
Mean Difference (m)
Ratio of Base Value
flt11
flt12
flt13
flt14
flt15
flt16
flt17
flt18
flt19
flt20

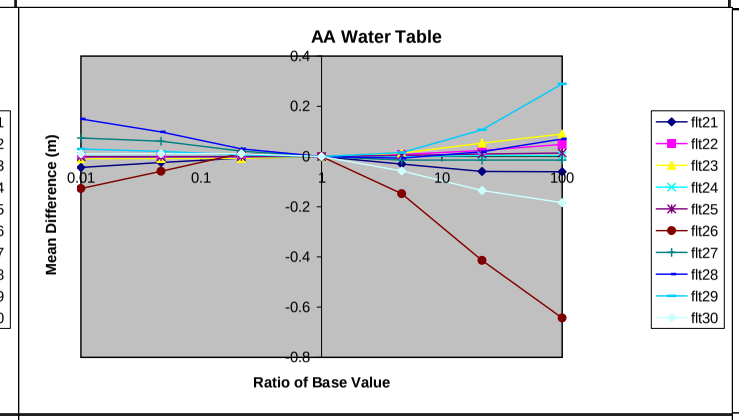
AA Water Table
Mean Difference (m)
Ratio of Base Value
flt21
flt22
flt23
flt24
flt25
flt26
flt27
flt28
flt29
flt30

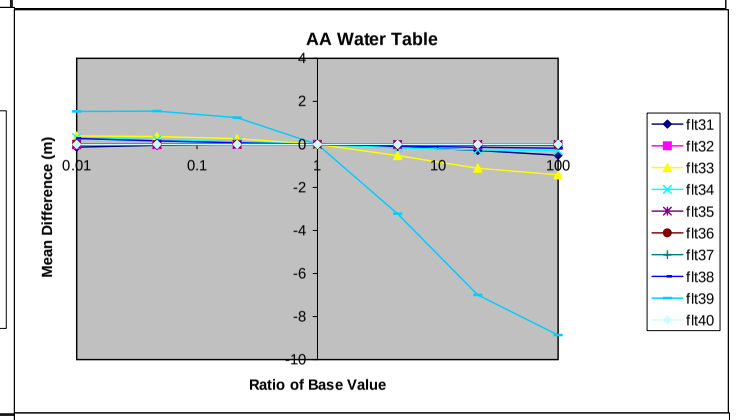
AA Water Table
Mean Difference (m)
Ratio of Base Value
flt31
flt32
flt33
flt34
flt35
flt36
flt37
flt38
flt39
flt40

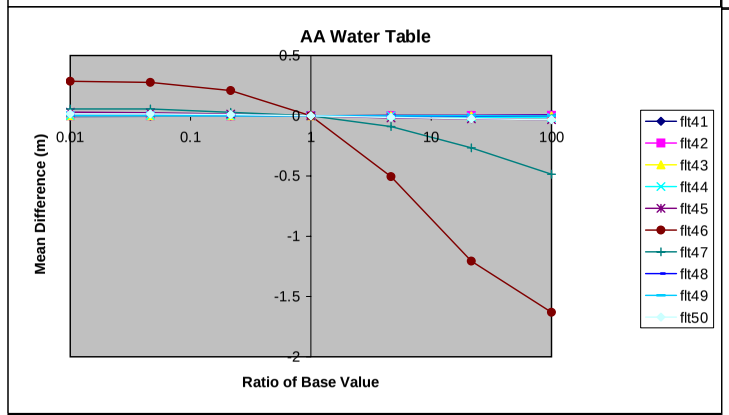
AA Water Table
Mean Difference (m)
Ratio of Base Value
flt41
flt42
flt43
flt44
flt45
flt46
flt47
flt48
flt49
flt50

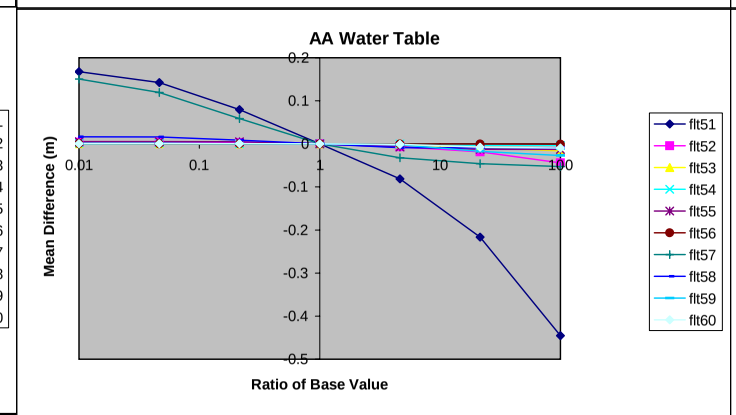
AA Water Table
Mean Difference (m)
Ratio of Base Value
flt51
flt52
flt53
flt54
flt55
flt56
flt57
flt58
flt59
flt60

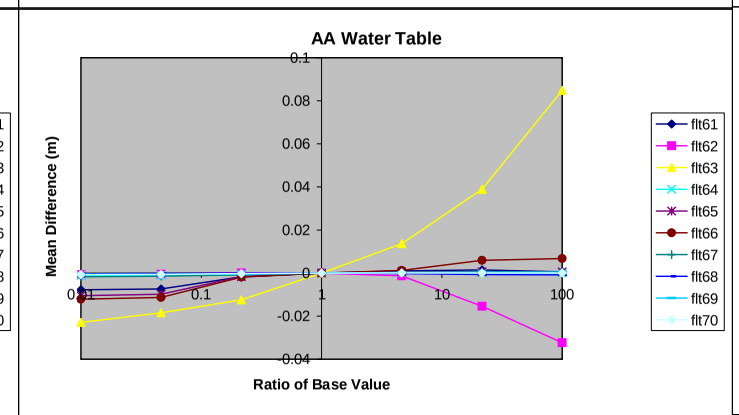
AA Water Table
Mean Difference (m)
Ratio of Base Value
flt61
flt62
flt63
flt64
flt65
flt66
flt67
flt68
flt69
flt70

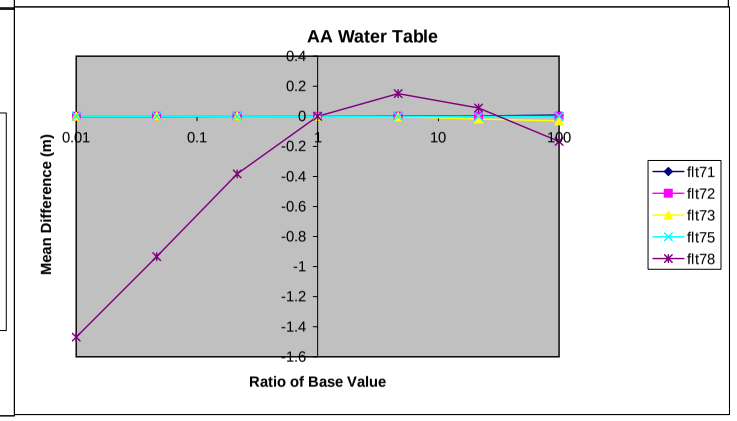
AA Water Table
Mean Difference (m)
Ratio of Base Value
flt71
flt72
flt73
flt75
flt78

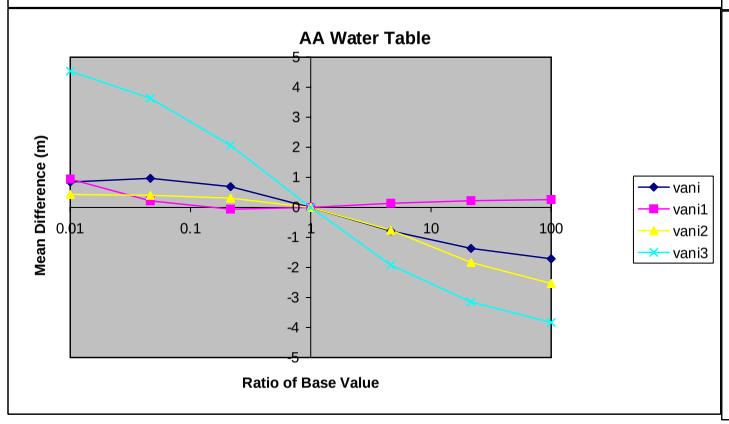
AA Water Table
Mean Difference (m)
Ratio of Base Value
vani
vani1
vani2
vani3

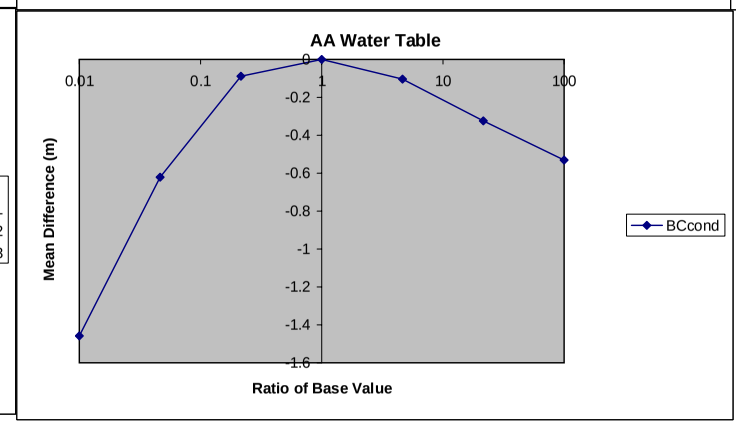
AA Water Table
Mean Difference (m)
Ratio of Base Value
BCcond

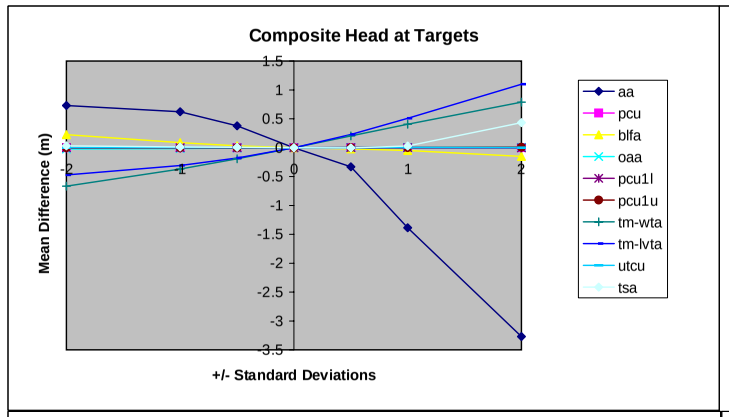
Composite Head at Targets
Mean Difference (m)
+/- Standard Deviations
aa
pcu
blfa
oaa
pcu1l
pcu1u
tm-wta
tm-lvta
utcu
tsa

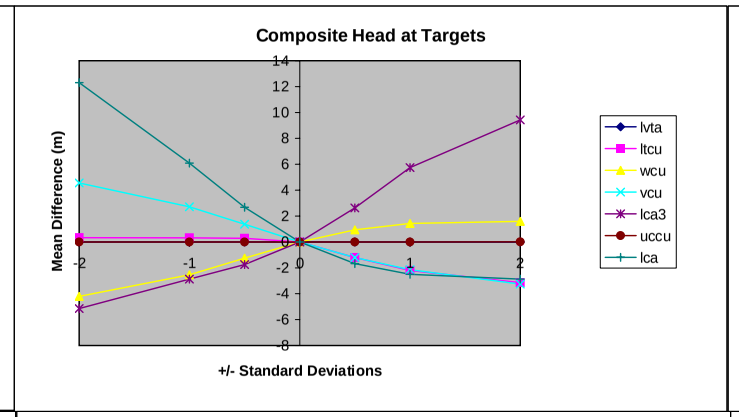
Composite Head at Targets
Mean Difference (m)
+/- Standard Deviations
lvta
ltcu
wcu
vcu
lca3
uccu
lca

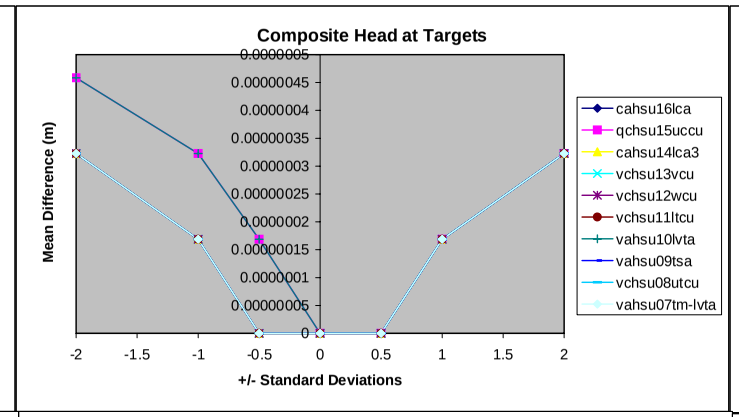
Composite Head at Targets
Mean Difference (m)
+/- Standard Deviations
cahsu16lca
qchsu15uccu
cahsu14lca3
vchsu13vcu
vchsu12wcu
vchsu11ltcu
vahsu10lvta
vahsu09tsa
vchsu08utcu
vahsu07tm-lvta

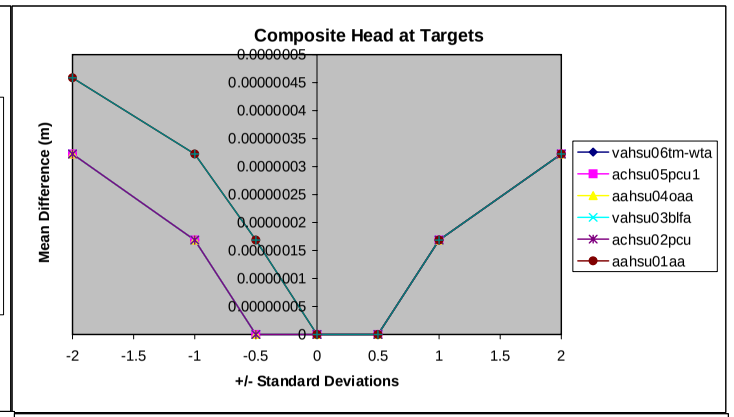
Composite Head at Targets
Mean Difference (m)
+/- Standard Deviations
vahsu06tm-wta
achsu05pcu1
aahsu04oaa
vahsu03blfa
achsu02pcu
aahsu01aa

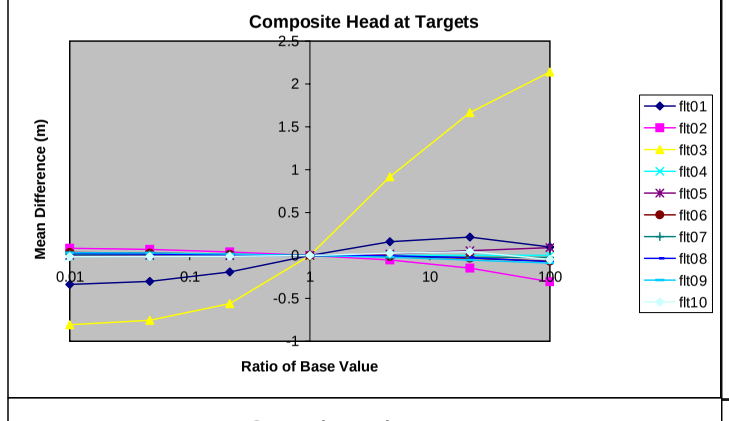
Composite Head at Targets
Mean Difference (m)
Ratio of Base Value
flt01
flt02
flt03
flt04
flt05
flt06
flt07
flt08
flt09
flt10

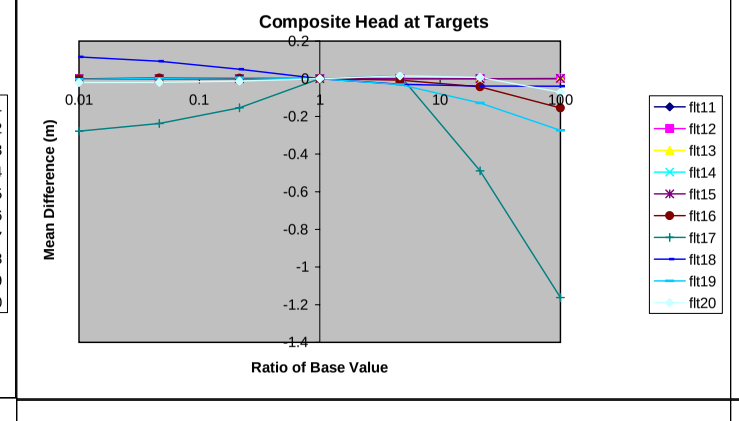
Composite Head at Targets
Mean Difference (m)
Ratio of Base Value
flt11
flt12
flt13
flt14
flt15
flt16
flt17
flt18
flt19
flt20

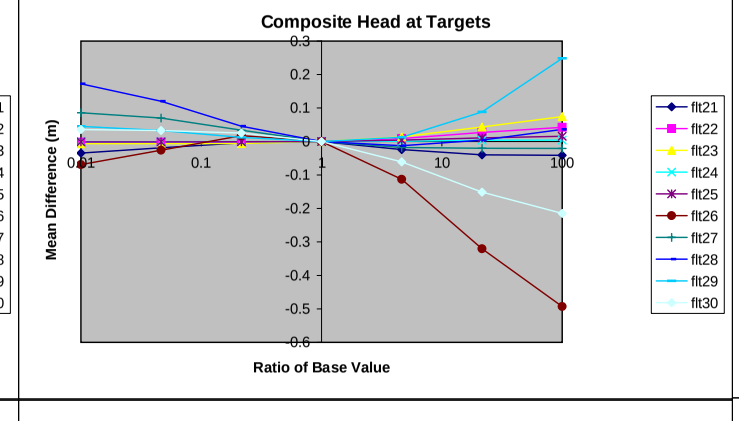
Composite Head at Targets
Mean Difference (m)
Ratio of Base Value
flt21
flt22
flt23
flt24
flt25
flt26
flt27
flt28
flt29
flt30

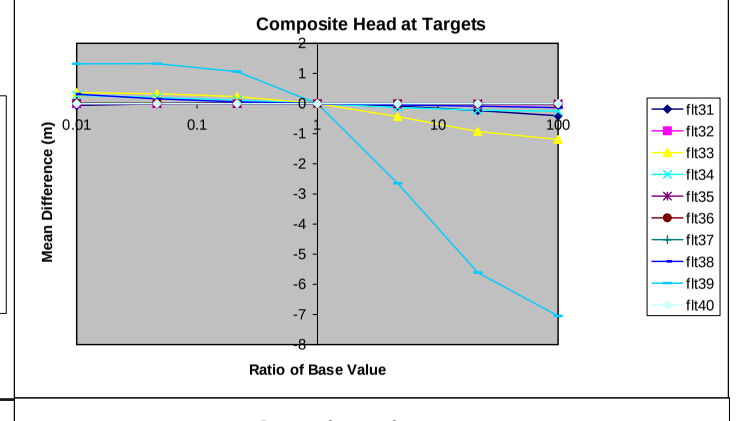
Composite Head at Targets
Mean Difference (m)
Ratio of Base Value
flt31
flt32
flt33
flt34
flt35
flt36
flt37
flt38
flt39
flt40

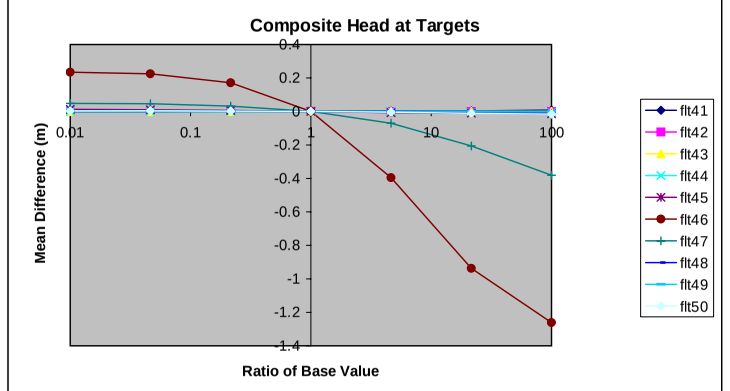
Composite Head at Targets
Mean Difference (m)
Ratio of Base Value
flt41
flt42
flt43
flt44
flt45
flt46
flt47
flt48
flt49
flt50

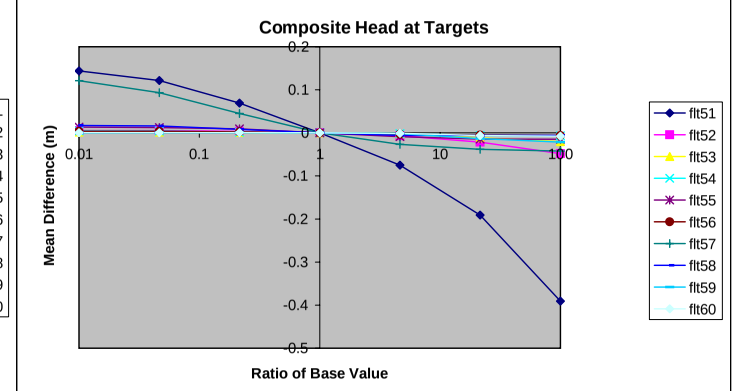
Composite Head at Targets
Mean Difference (m)
Ratio of Base Value
flt51
flt52
flt53
flt54
flt55
flt56
flt57
flt58
flt59
flt60

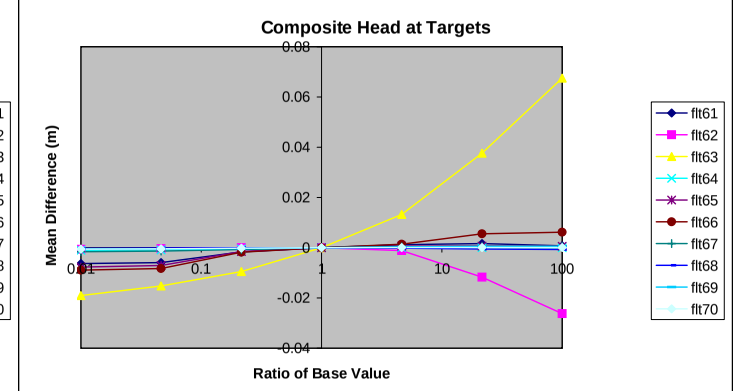
Composite Head at Targets
Mean Difference (m)
Ratio of Base Value
flt61
flt62
flt63
flt64
flt65
flt66
flt67
flt68
flt69
flt70

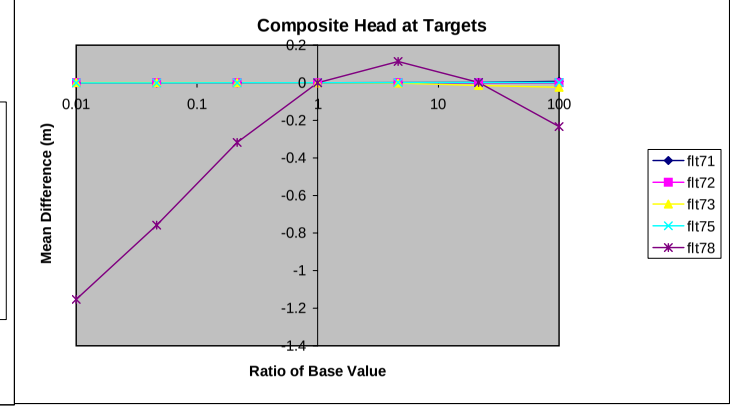
Composite Head at Targets
Mean Difference (m)
Ratio of Base Value
flt71
flt72
flt73
flt75
flt78

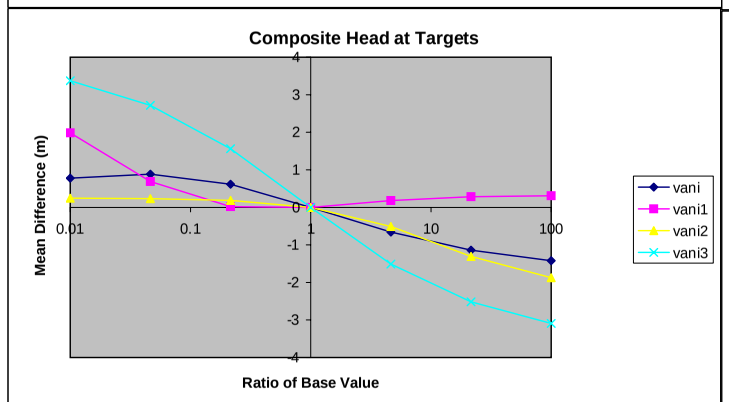
Composite Head at Targets
Mean Difference (m)
Ratio of Base Value
vani
vani1
vani2
vani3

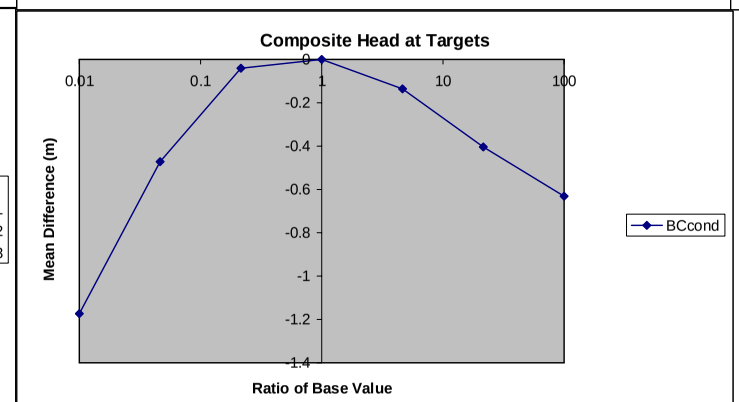
Composite Head at Targets
Mean Difference (m)
Ratio of Base Value
BCcond

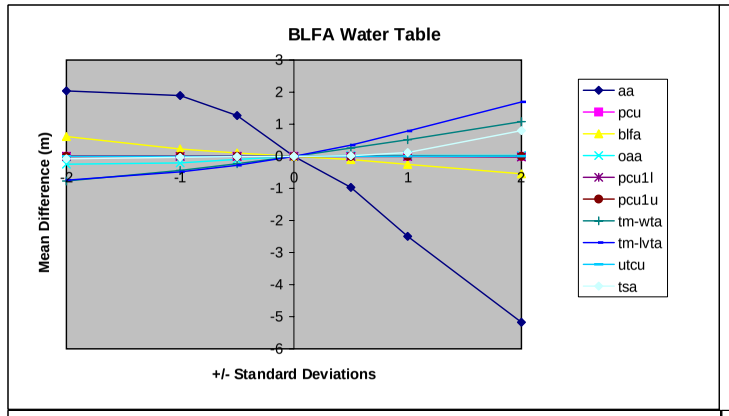
BLFA Water Table
Mean Difference (m)
+/- Standard Deviations
aa
pcu
blfa
oaa
pcu1l
pcu1u
tm-wta
tm-lvta
utcu
tsa

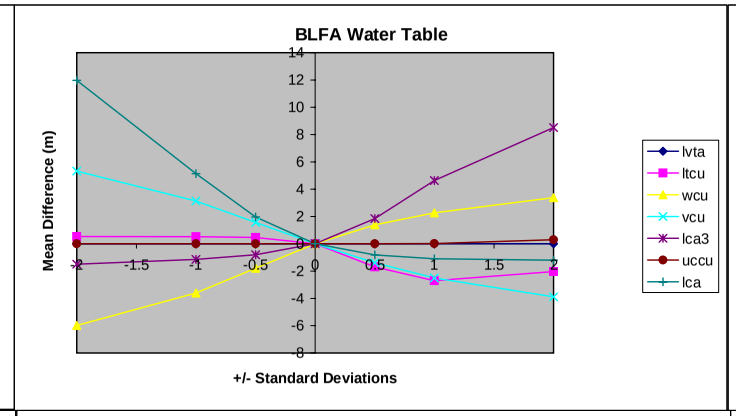
BLFA Water Table
Mean Difference (m)
+/- Standard Deviations
lvta
ltcu
wcu
vcu
lca3
uccu
lca

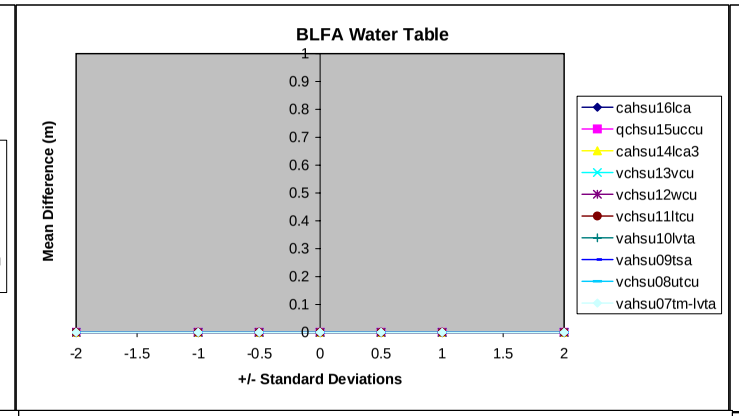
BLFA Water Table
Mean Difference (m)
+/- Standard Deviations
cahsu16lca
qchsu15uccu
cahsu14lca3
vchsu13vcu
vchsu12wcu
vchsu11ltcu
vahsu10lvta
vahsu09tsa
vchsu08utcu
vahsu07tm-lvta

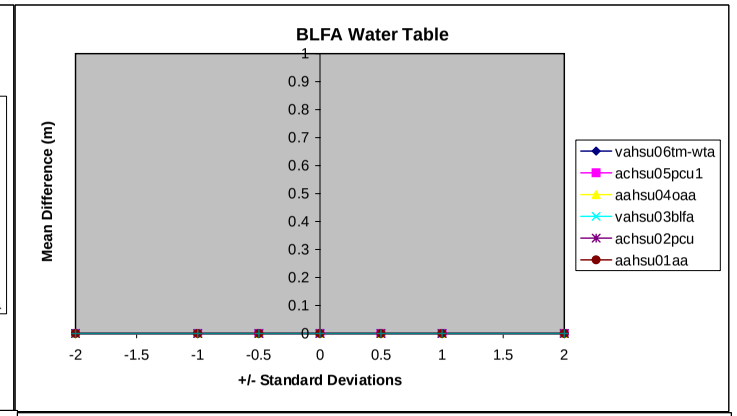
BLFA Water Table
Mean Difference (m)
+/- Standard Deviations
vahsu06tm-wta
achsu05pcu1
aahsu04oaa
vahsu03blfa
achsu02pcu
aahsu01aa

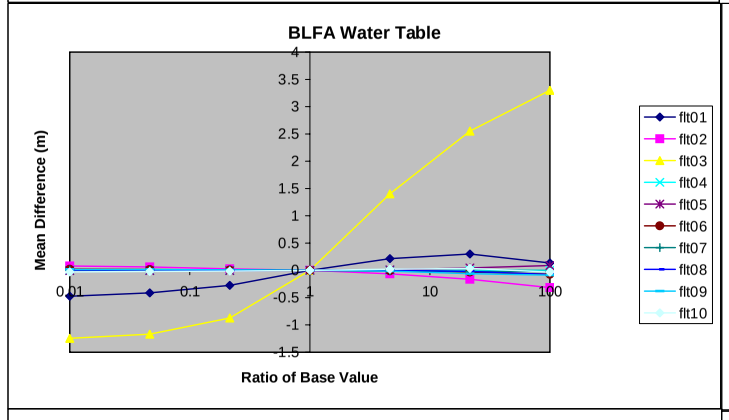
BLFA Water Table
Mean Difference (m)
Ratio of Base Value
flt01
flt02
flt03
flt04
flt05
flt06
flt07
flt08
flt09
flt10

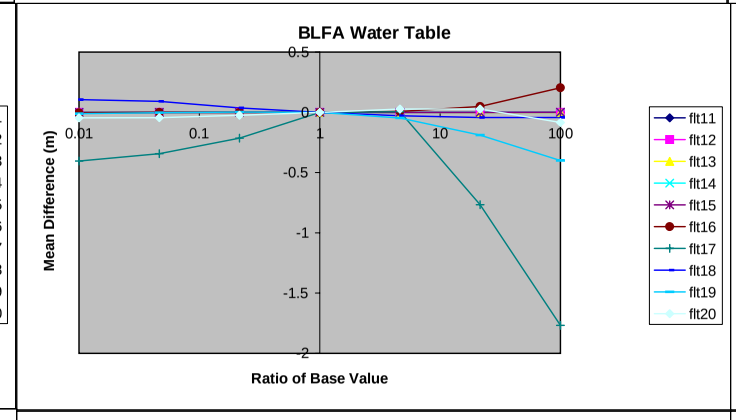
BLFA Water Table
Mean Difference (m)
Ratio of Base Value
flt11
flt12
flt13
flt14
flt15
flt16
flt17
flt18
flt19
flt20

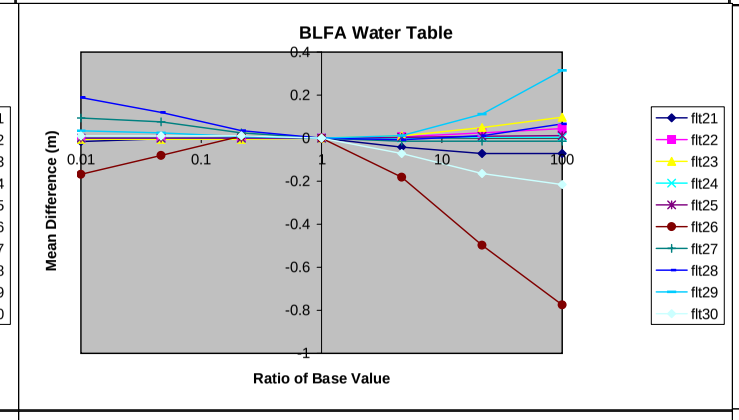
BLFA Water Table
Mean Difference (m)
Ratio of Base Value
flt21
flt22
flt23
flt24
flt25
flt26
flt27
flt28
flt29
flt30

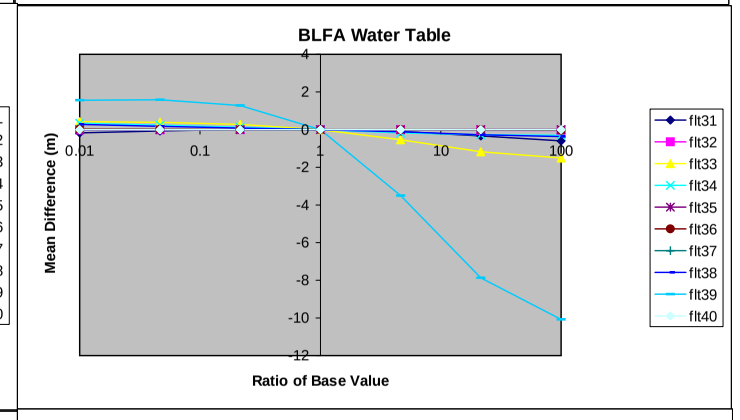
BLFA Water Table
Mean Difference (m)
Ratio of Base Value
flt31
flt32
flt33
flt34
flt35
flt36
flt37
flt38
flt39
flt40

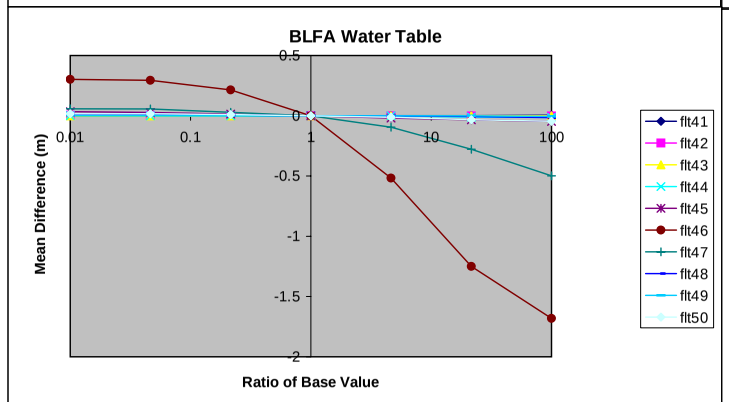
BLFA Water Table
Mean Difference (m)
Ratio of Base Value
flt41
flt42
flt43
flt44
flt45
flt46
flt47
flt48
flt49
flt50

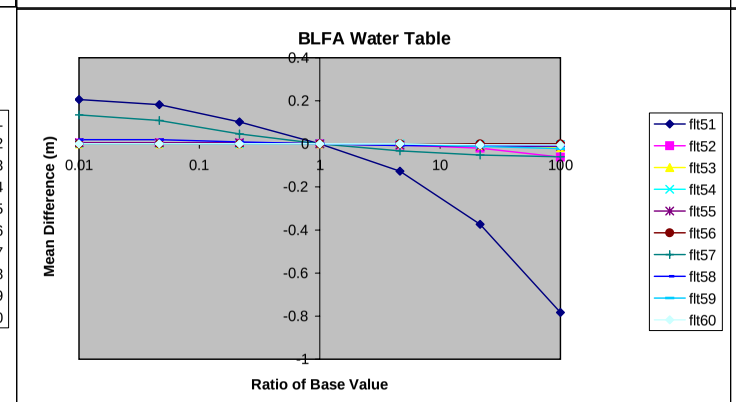
BLFA Water Table
Mean Difference (m)
Ratio of Base Value
flt51
flt52
flt53
flt54
flt55
flt56
flt57
flt58
flt59
flt60

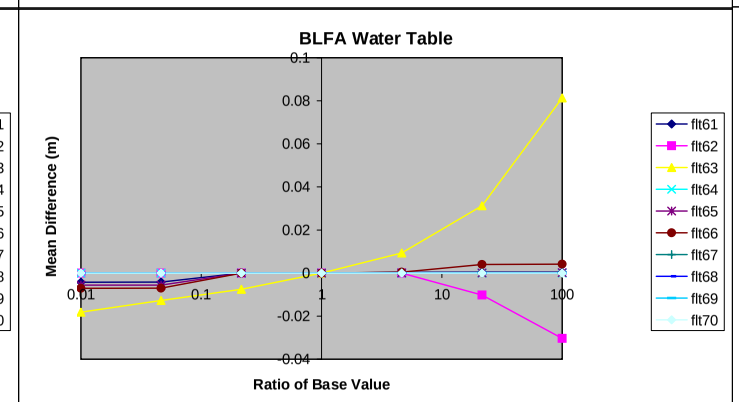
BLFA Water Table
Mean Difference (m)
Ratio of Base Value
flt61
flt62
flt63
flt64
flt65
flt66
flt67
flt68
flt69
flt70

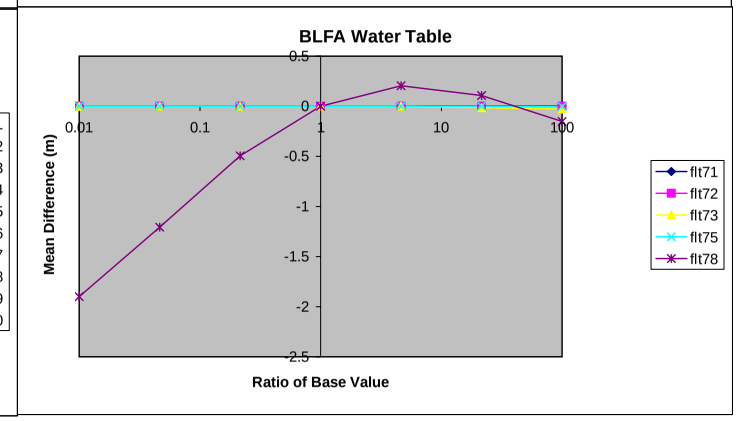
BLFA Water Table
Mean Difference (m)
Ratio of Base Value
flt71
flt72
flt73
flt75
flt78

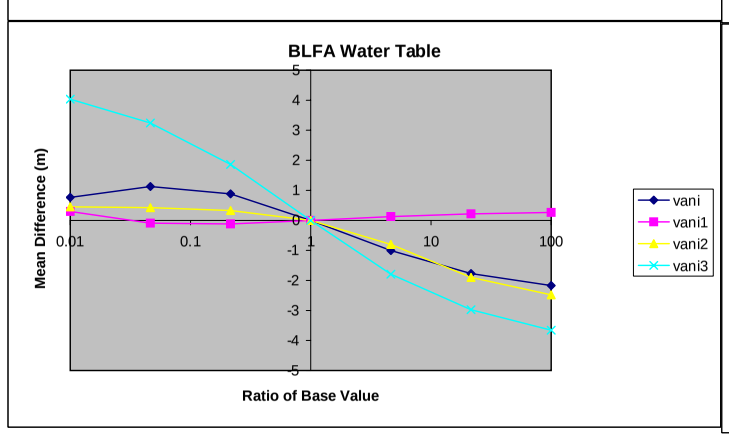
BLFA Water Table
Mean Difference (m)
Ratio of Base Value
vani
vani1
vani2
vani3

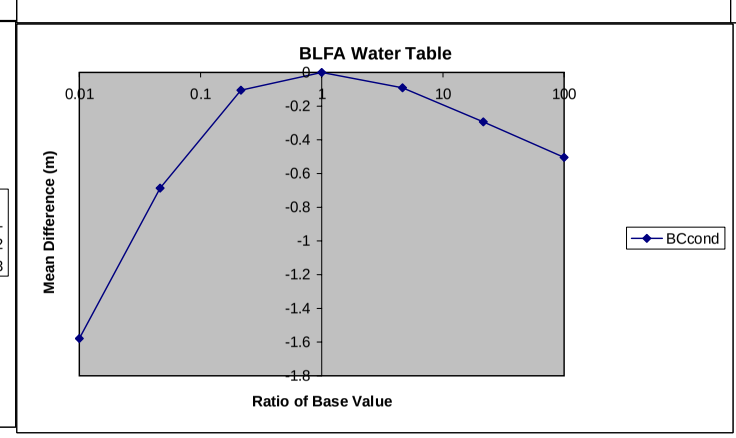
BLFA Water Table
Mean Difference (m)
Ratio of Base Value
BCcond

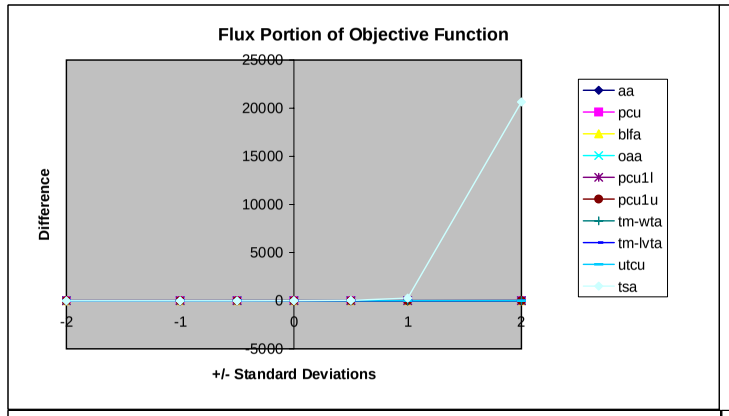
Flux Portion of Objective Function
Difference
+/- Standard Deviations
aa
pcu
blfa
oaa
pcu1l
pcu1u
tm-wta
tm-lvta
utcu
tsa

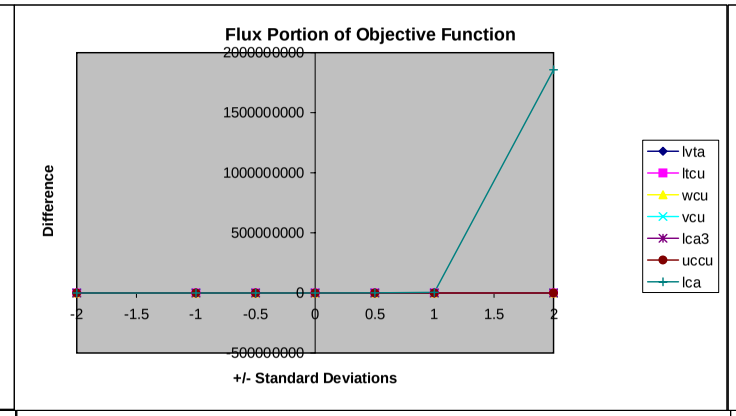
Flux Portion of Objective Function
Difference
+/- Standard Deviations
lvta
ltcu
wcu
vcu
lca3
uccu
lca

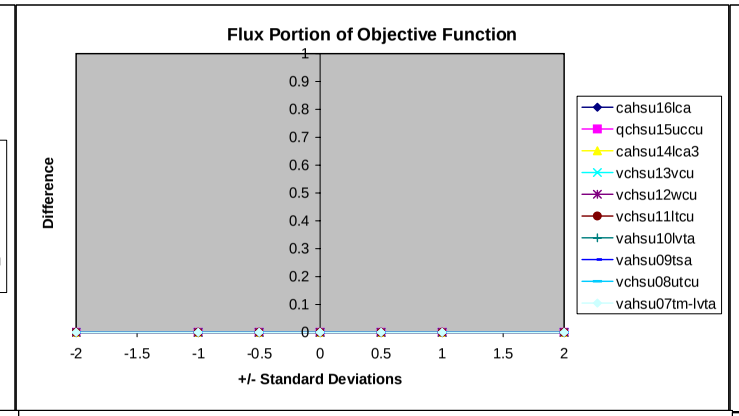
Flux Portion of Objective Function
Difference
+/- Standard Deviations
cahsu16lca
qchsu15uccu
cahsu14lca3
vchsu13vcu
vchsu12wcu
vchsu11ltcu
vahsu10lvta
vahsu09tsa
vchsu08utcu
vahsu07tm-lvta

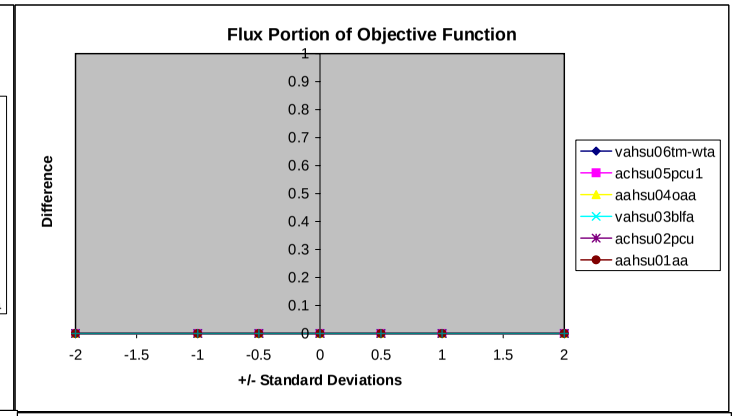
Flux Portion of Objective Function
Difference
+/- Standard Deviations
vahsu06tm-wta
achsu05pcu1
aahsu04oaa
vahsu03blfa
achsu02pcu
aahsu01aa

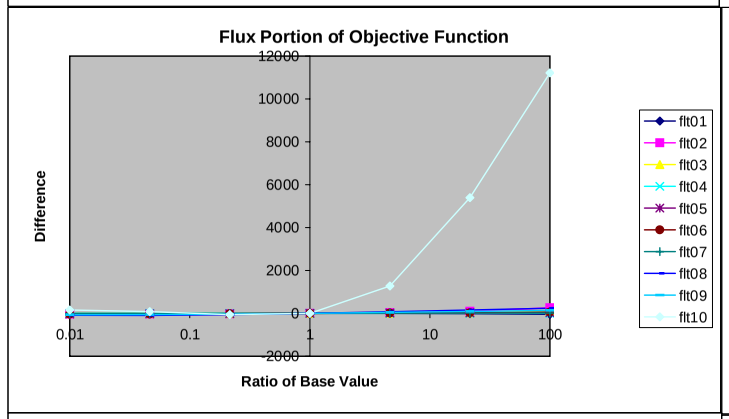
Flux Portion of Objective Function
Difference
Ratio of Base Value
flt01
flt02
flt03
flt04
flt05
flt06
flt07
flt08
flt09
flt10

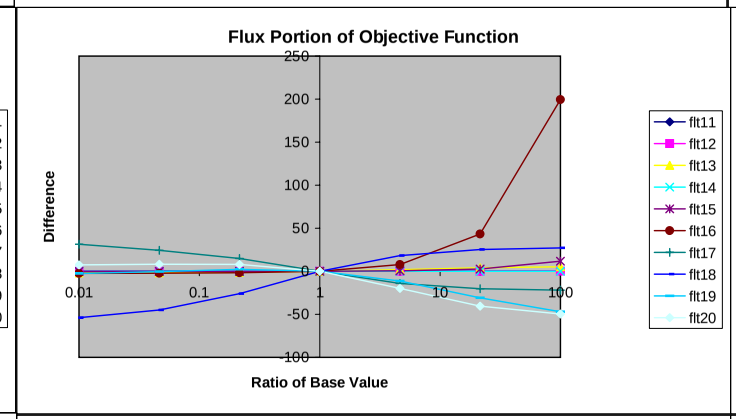
Flux Portion of Objective Function
Difference
Ratio of Base Value
flt11
flt12
flt13
flt14
flt15
flt16
flt17
flt18
flt19
flt20

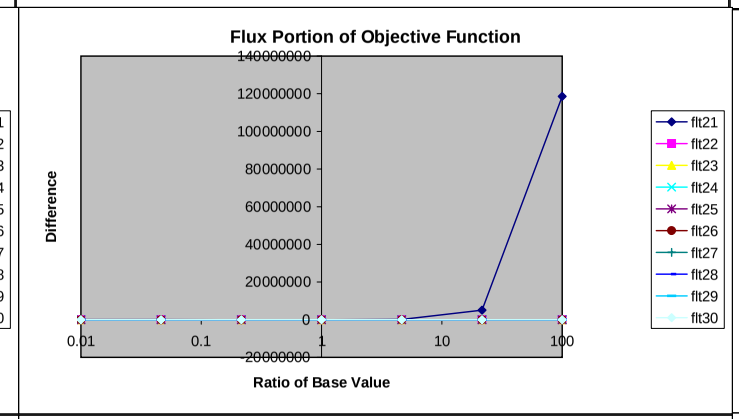
Flux Portion of Objective Function
Difference
Ratio of Base Value
flt21
flt22
flt23
flt24
flt25
flt26
flt27
flt28
flt29
flt30

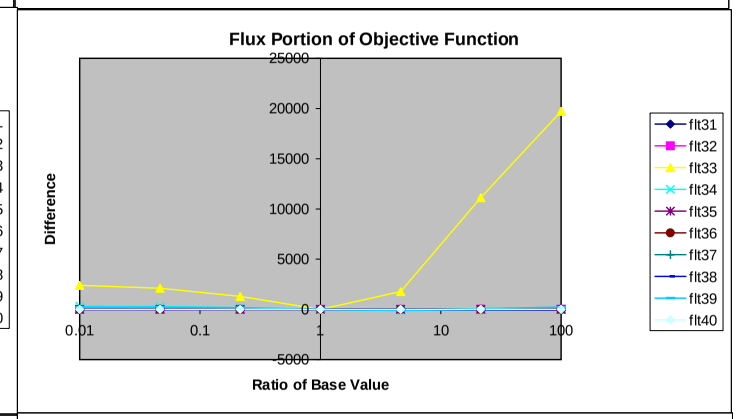
Flux Portion of Objective Function
Difference
Ratio of Base Value
flt31
flt32
flt33
flt34
flt35
flt36
flt37
flt38
flt39
flt40

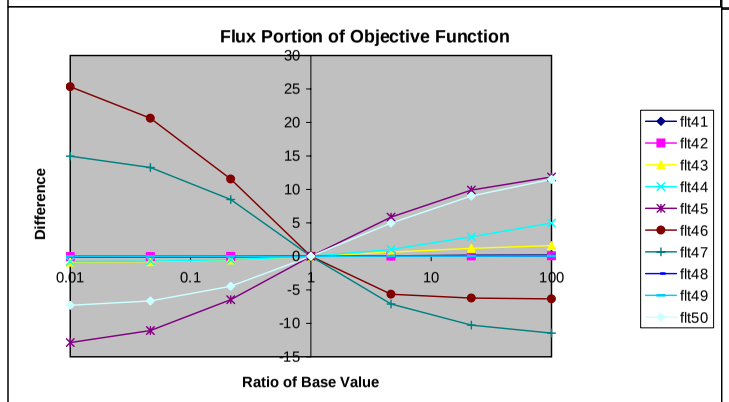
Flux Portion of Objective Function
Difference
Ratio of Base Value
flt41
flt42
flt43
flt44
flt45
flt46
flt47
flt48
flt49
flt50

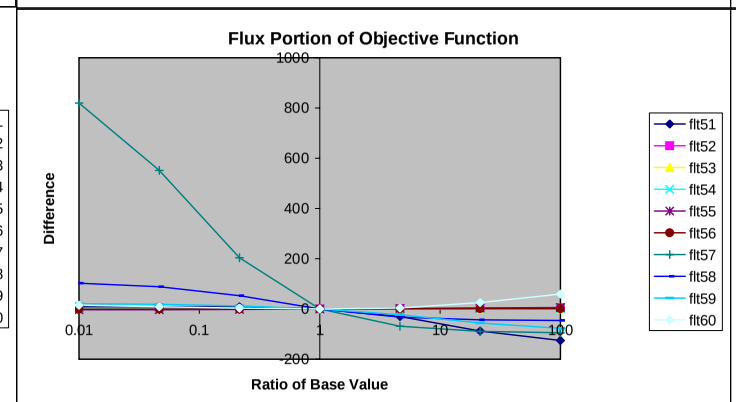
Flux Portion of Objective Function
Difference
Ratio of Base Value
flt51
flt52
flt53
flt54
flt55
flt56
flt57
flt58
flt59
flt60

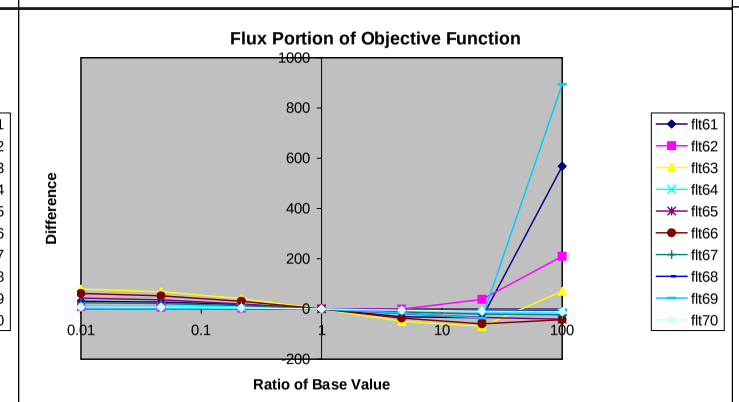
Flux Portion of Objective Function
Difference
Ratio of Base Value
flt61
flt62
flt63
flt64
flt65
flt66
flt67
flt68
flt69
flt70

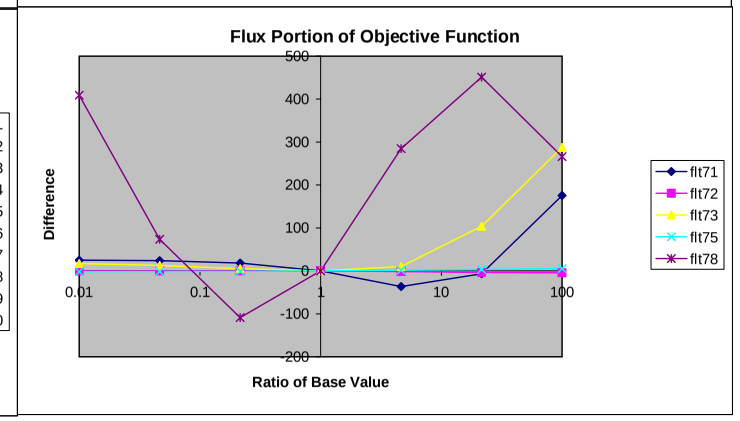
Flux Portion of Objective Function
Difference
Ratio of Base Value
flt71
flt72
flt73
flt75
flt78

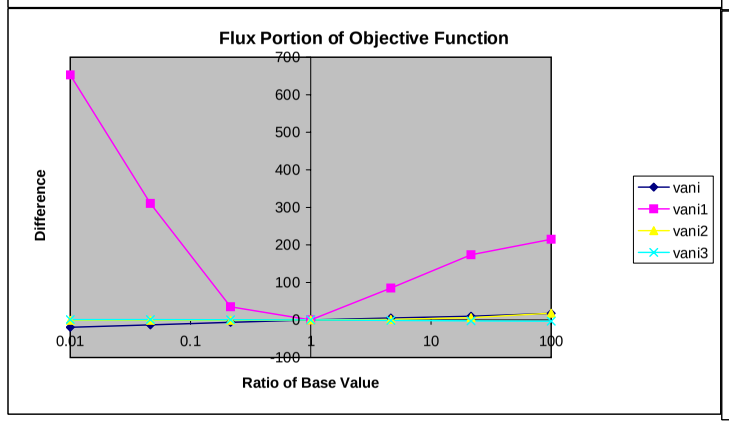
Flux Portion of Objective Function
Difference
Ratio of Base Value
vani
vani1
vani2
vani3

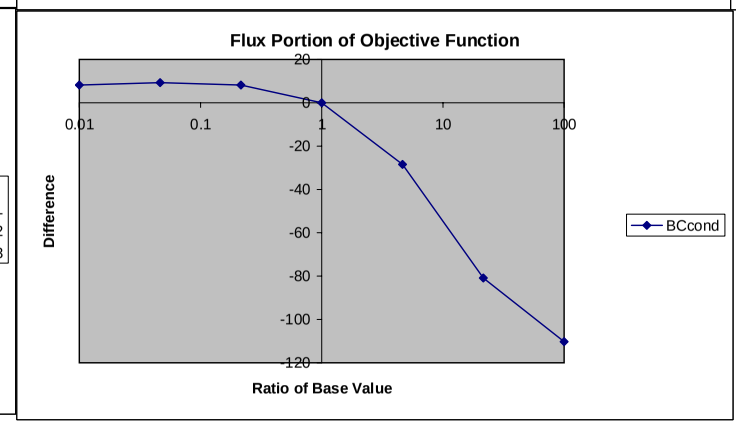
Flux Portion of Objective Function
Difference
Ratio of Base Value
BCcond

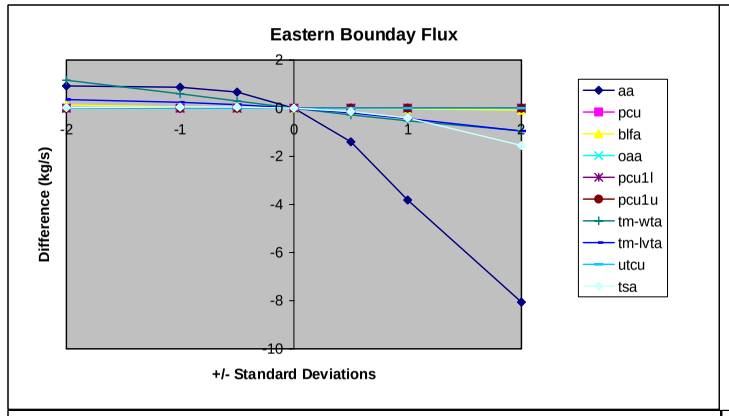
Eastern Bounday Flux
Difference (kg/s)
+/- Standard Deviations
aa
pcu
blfa
oaa
pcu1l
pcu1u
tm-wta
tm-lvta
utcu
tsa

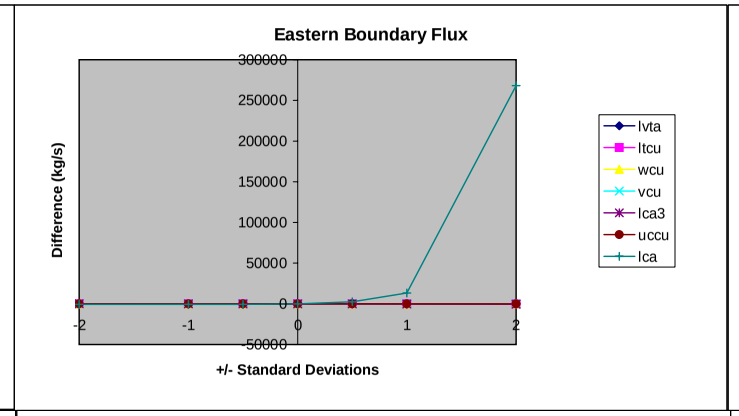
Eastern Boundary Flux
Difference (kg/s)
+/- Standard Deviations
lvta
ltcu
wcu
vcu
lca3
uccu
lca

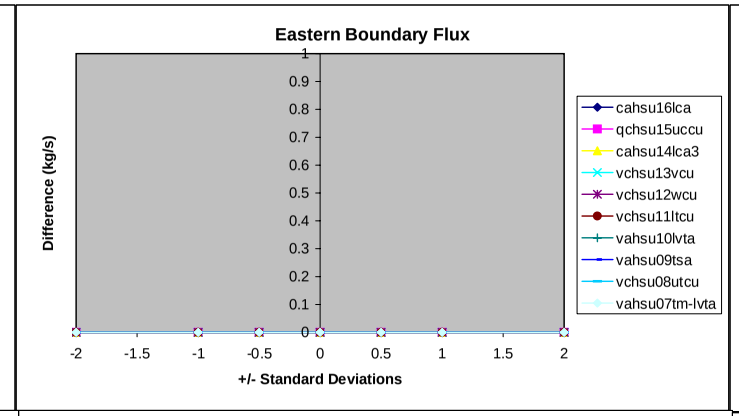
Eastern Boundary Flux
Difference (kg/s)
+/- Standard Deviations
cahsu16lca
qchsu15uccu
cahsu14lca3
vchsu13vcu
vchsu12wcu
vchsu11ltcu
vahsu10lvta
vahsu09tsa
vchsu08utcu
vahsu07tm-lvta

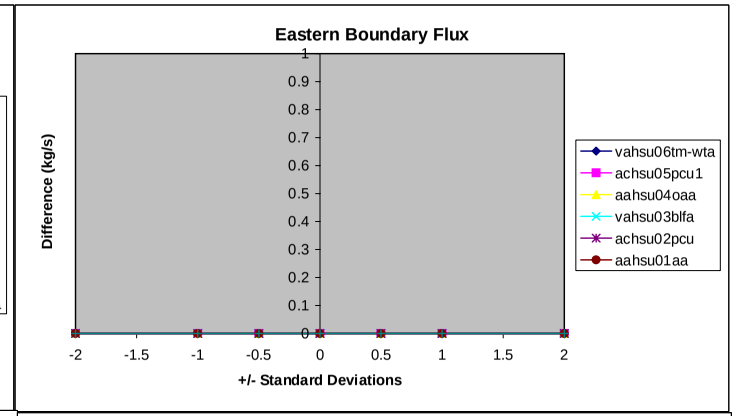
Eastern Boundary Flux
Difference (kg/s)
+/- Standard Deviations
vahsu06tm-wta
achsu05pcu1
aahsu04oaa
vahsu03blfa
achsu02pcu
aahsu01aa

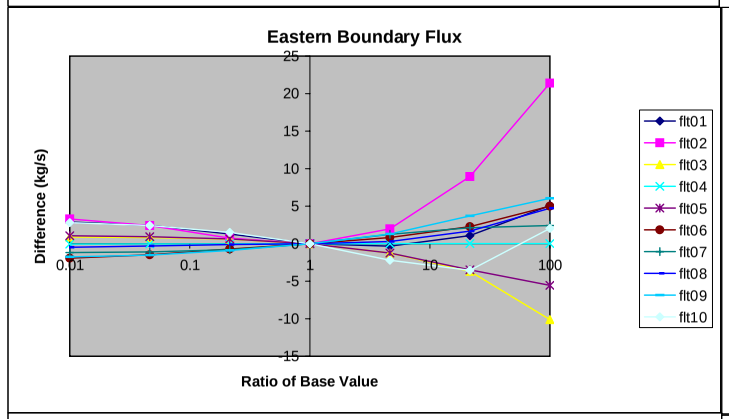
Eastern Boundary Flux
Difference (kg/s)
Ratio of Base Value
flt01
flt02
flt03
flt04
flt05
flt06
flt07
flt08
flt09
flt10

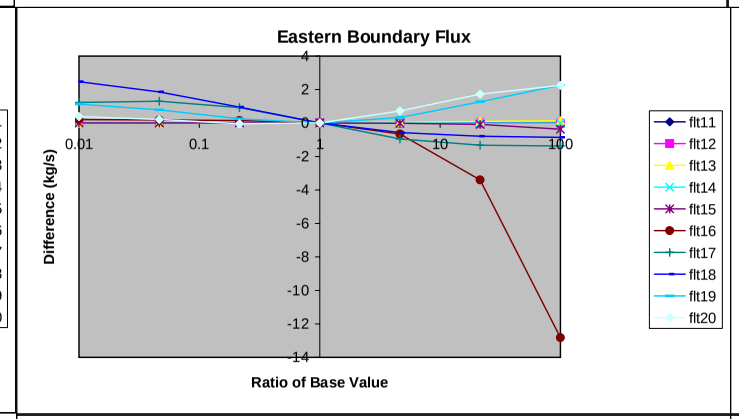
Eastern Boundary Flux
Difference (kg/s)
Ratio of Base Value
flt11
flt12
flt13
flt14
flt15
flt16
flt17
flt18
flt19
flt20

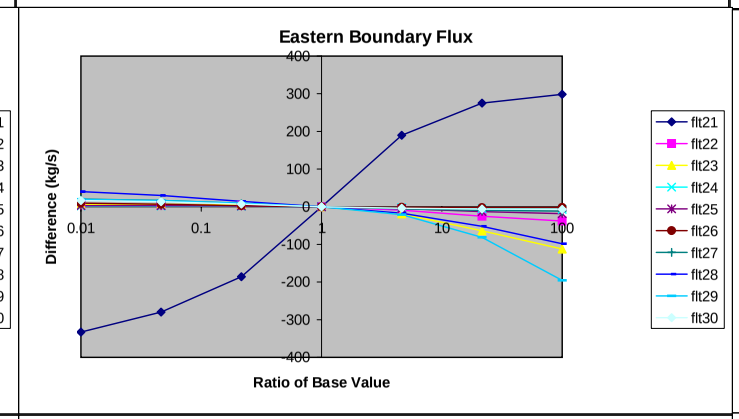
Eastern Boundary Flux
Difference (kg/s)
Ratio of Base Value
flt21
flt22
flt23
flt24
flt25
flt26
flt27
flt28
flt29
flt30

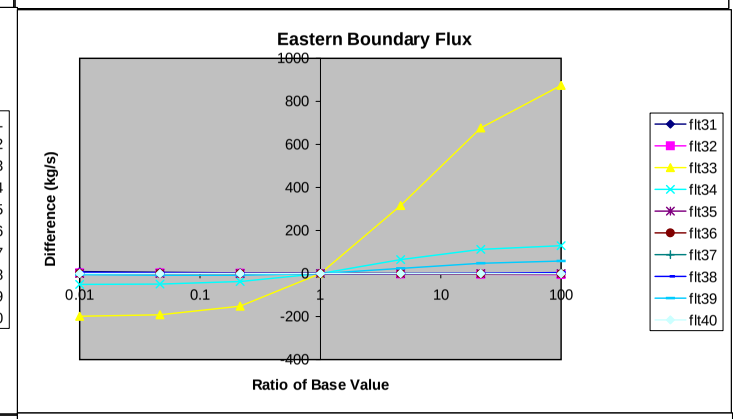
Eastern Boundary Flux
Difference (kg/s)
Ratio of Base Value
flt31
flt32
flt33
flt34
flt35
flt36
flt37
flt38
flt39
flt40

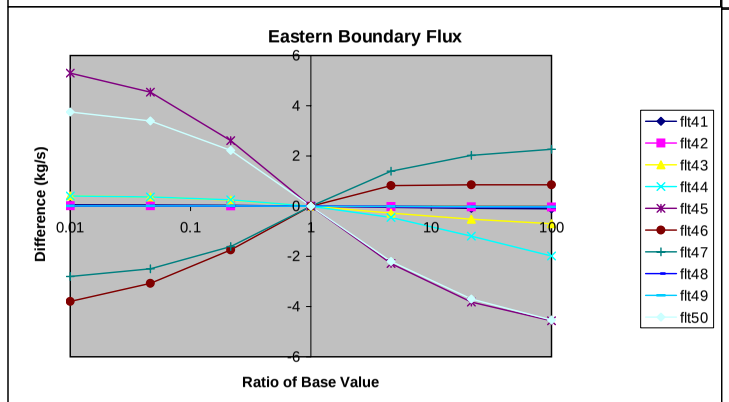
Eastern Boundary Flux
Difference (kg/s)
Ratio of Base Value
flt41
flt42
flt43
flt44
flt45
flt46
flt47
flt48
flt49
flt50

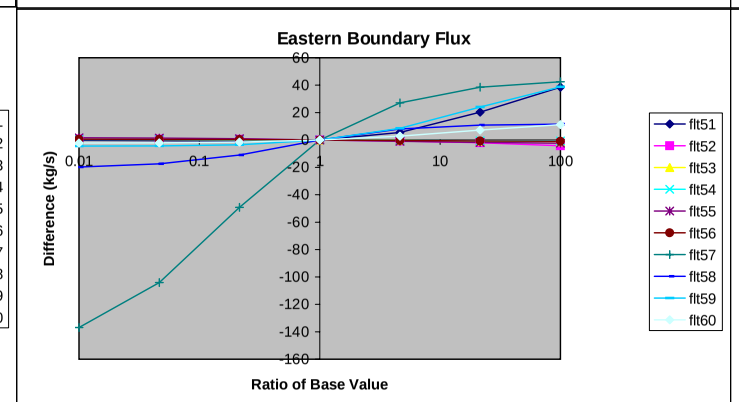
Eastern Boundary Flux
Difference (kg/s)
Ratio of Base Value
flt51
flt52
flt53
flt54
flt55
flt56
flt57
flt58
flt59
flt60

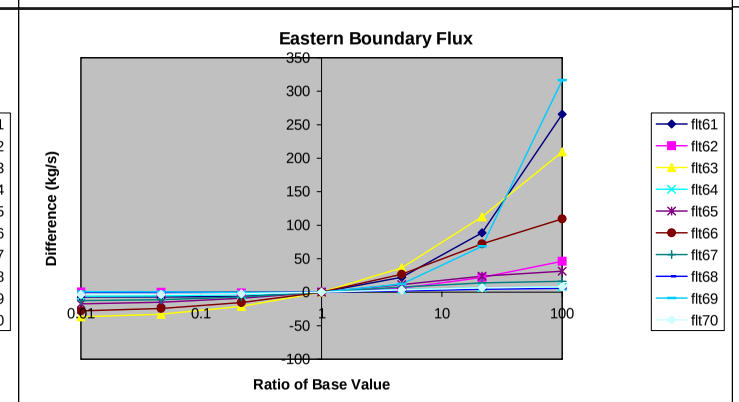
Eastern Boundary Flux
Difference (kg/s)
Ratio of Base Value
flt61
flt62
flt63
flt64
flt65
flt66
flt67
flt68
flt69
flt70

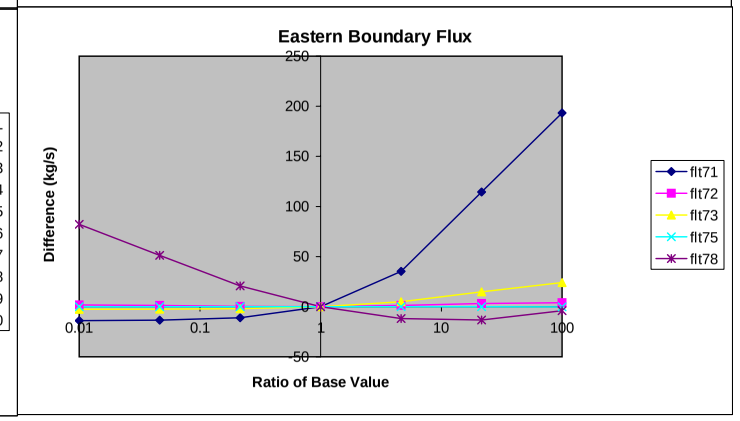
Eastern Boundary Flux
Difference (kg/s)
Ratio of Base Value
flt71
flt72
flt73
flt75
flt78

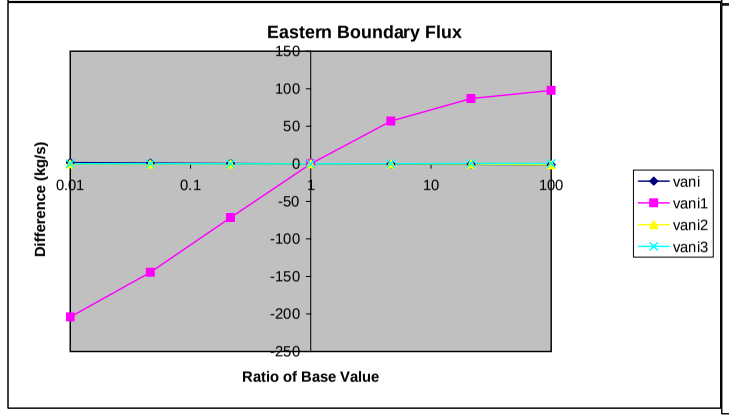
Eastern Boundary Flux
Difference (kg/s)
Ratio of Base Value
vani
vani1
vani2
vani3

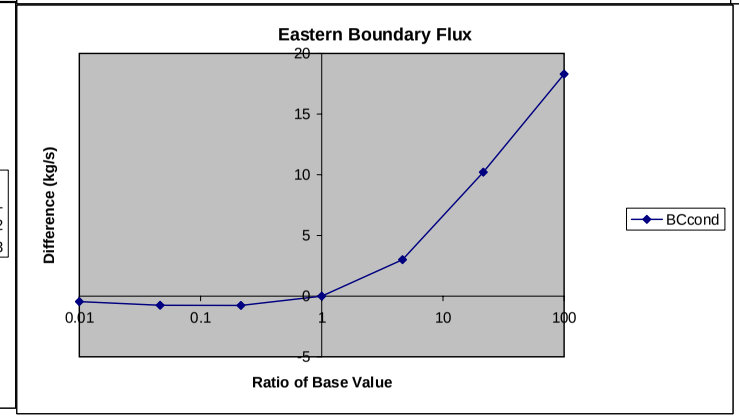
Eastern Boundary Flux
Difference (kg/s)
Ratio of Base Value
BCcond

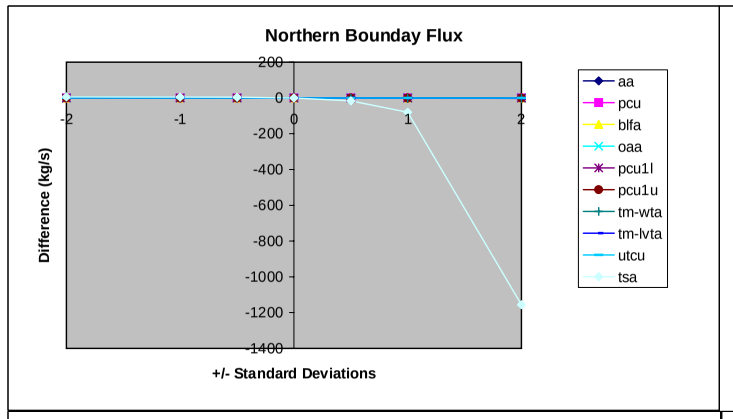
Northern Bounday Flux
Difference (kg/s)
+/- Standard Deviations
aa
pcu
blfa
oaa
pcu1l
pcu1u
tm-wta
tm-lvta
utcu
tsa

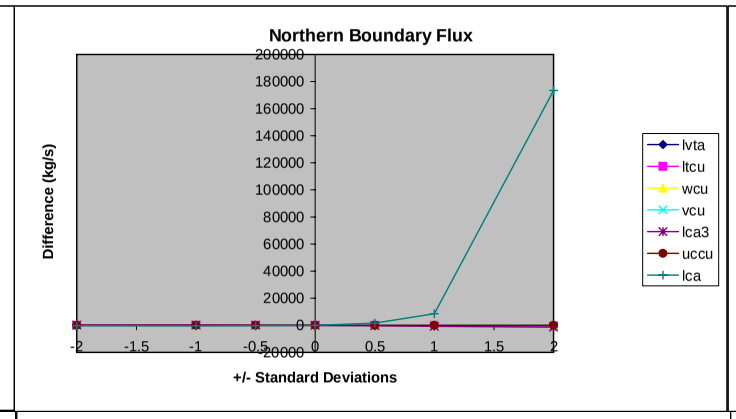
Northern Boundary Flux
Difference (kg/s)
+/- Standard Deviations
lvta
ltcu
wcu
vcu
lca3
uccu
lca

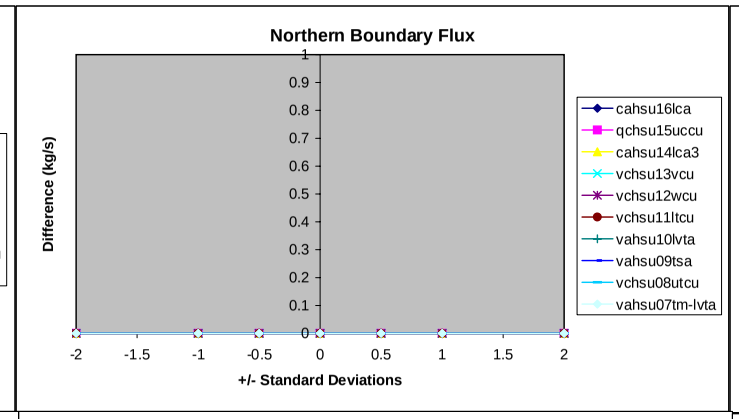
Northern Boundary Flux
Difference (kg/s)
+/- Standard Deviations
cahsu16lca
qchsu15uccu
cahsu14lca3
vchsu13vcu
vchsu12wcu
vchsu11ltcu
vahsu10lvta
vahsu09tsa
vchsu08utcu
vahsu07tm-lvta

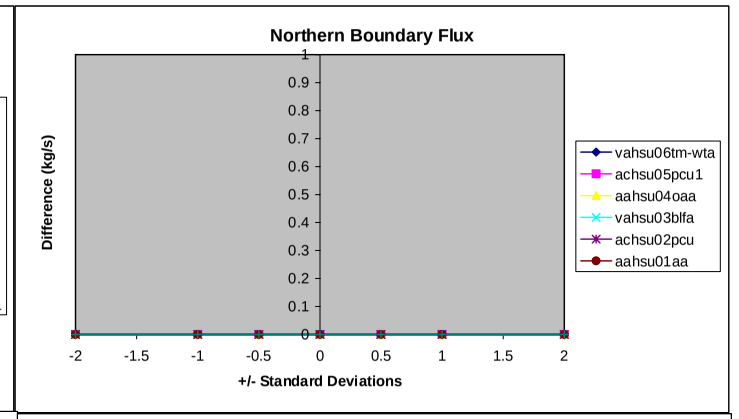
Northern Boundary Flux
Difference (kg/s)
+/- Standard Deviations
vahsu06tm-wta
achsu05pcu1
aahsu04oaa
vahsu03blfa
achsu02pcu
aahsu01aa

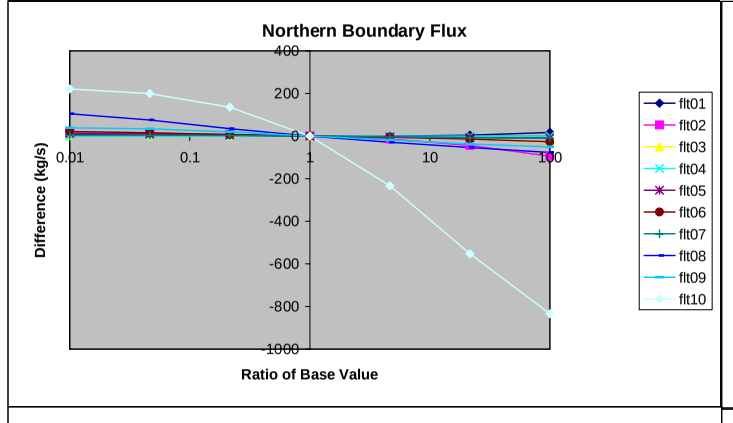
Northern Boundary Flux
Difference (kg/s)
Ratio of Base Value
flt01
flt02
flt03
flt04
flt05
flt06
flt07
flt08
flt09
flt10

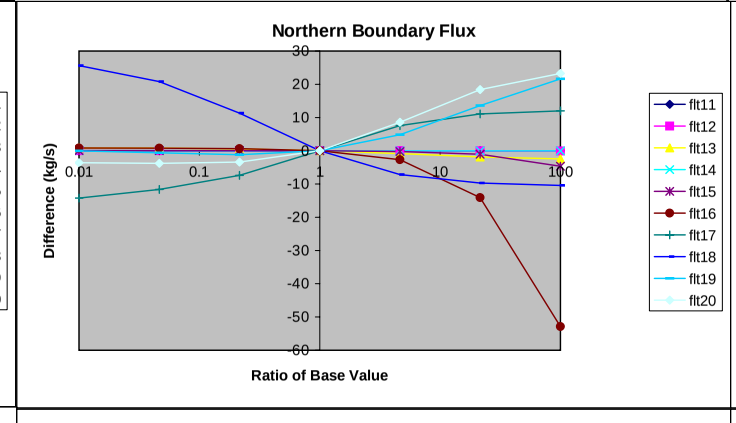
Northern Boundary Flux
Difference (kg/s)
Ratio of Base Value
flt11
flt12
flt13
flt14
flt15
flt16
flt17
flt18
flt19
flt20

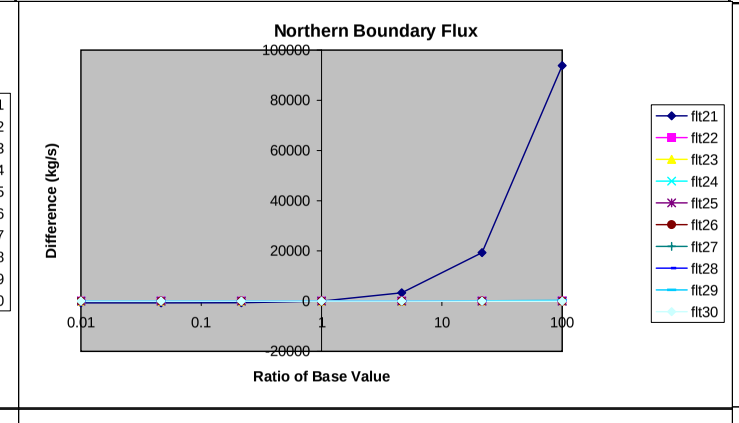
Northern Boundary Flux
Difference (kg/s)
Ratio of Base Value
flt21
flt22
flt23
flt24
flt25
flt26
flt27
flt28
flt29
flt30

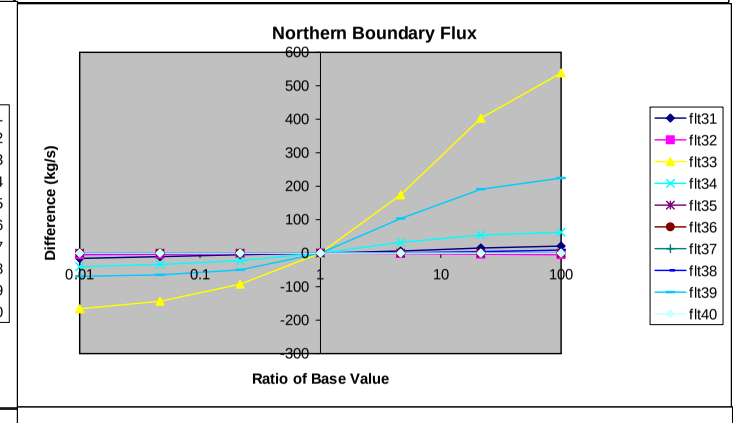
Northern Boundary Flux
Difference (kg/s)
Ratio of Base Value
flt31
flt32
flt33
flt34
flt35
flt36
flt37
flt38
flt39
flt40

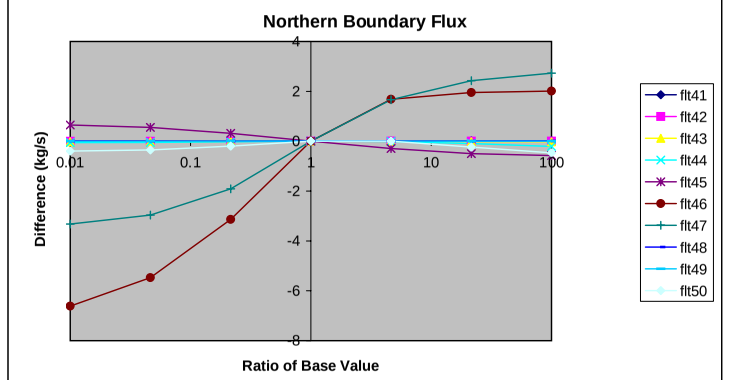
Northern Boundary Flux
Difference (kg/s)
Ratio of Base Value
flt41
flt42
flt43
flt44
flt45
flt46
flt47
flt48
flt49
flt50

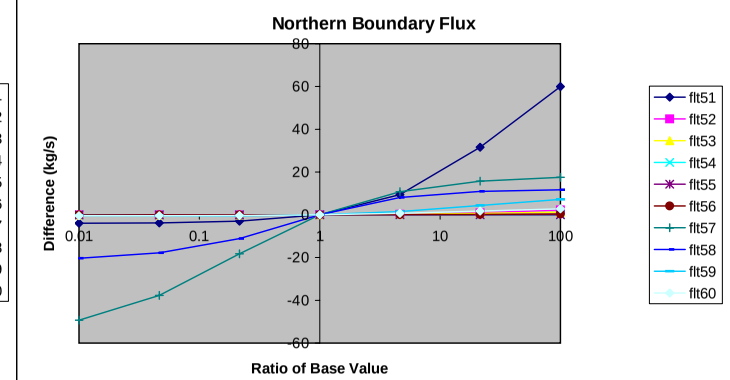
Northern Boundary Flux
Difference (kg/s)
Ratio of Base Value
flt51
flt52
flt53
flt54
flt55
flt56
flt57
flt58
flt59
flt60

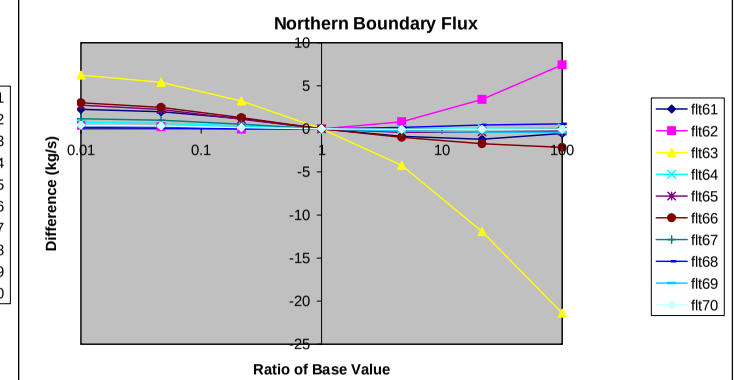
Northern Boundary Flux
Difference (kg/s)
Ratio of Base Value
flt61
flt62
flt63
flt64
flt65
flt66
flt67
flt68
flt69
flt70

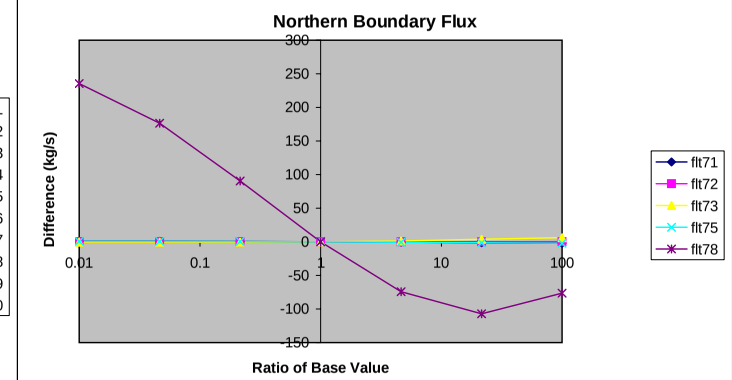
Northern Boundary Flux
Difference (kg/s)
Ratio of Base Value
flt71
flt72
flt73
flt75
flt78

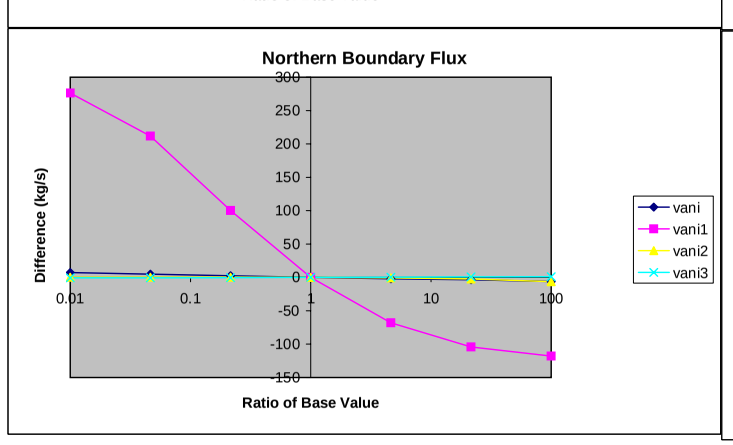
Northern Boundary Flux
Difference (kg/s)
Ratio of Base Value
vani
vani1
vani2
vani3

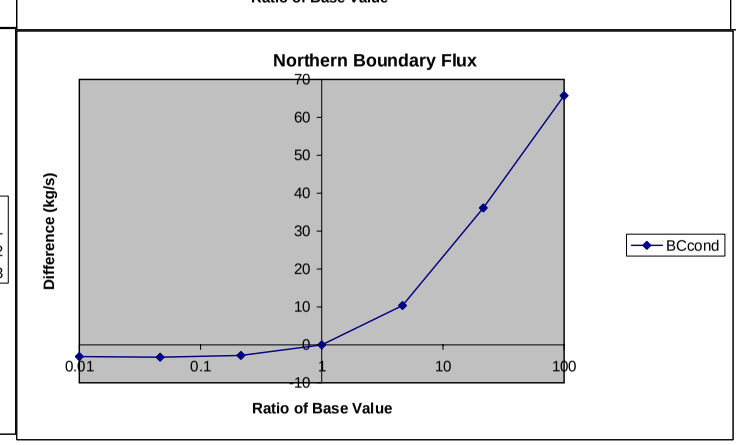
Northern Boundary Flux
Difference (kg/s)
Ratio of Base Value
BCcond

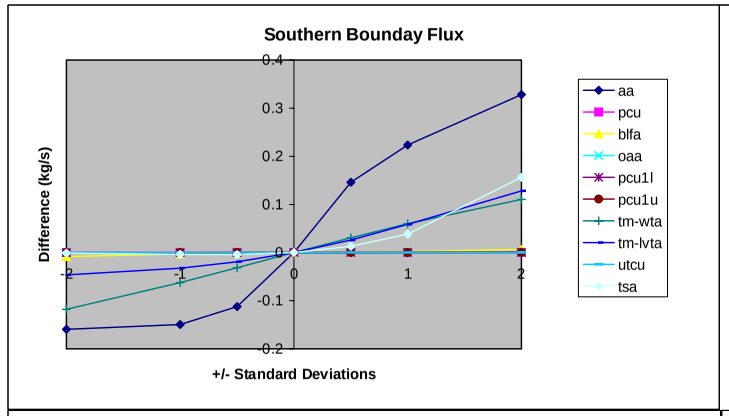
Southern Bounday Flux
Difference (kg/s)
+/- Standard Deviations
aa
pcu
blfa
oaa
pcu1l
pcu1u
tm-wta
tm-lvta
utcu
tsa

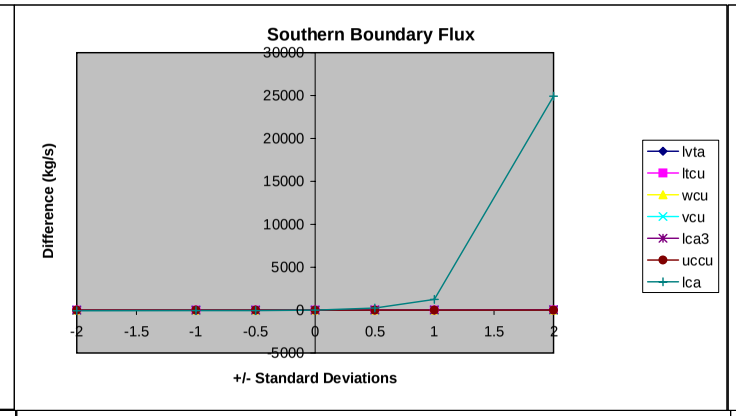
Southern Boundary Flux
Difference (kg/s)
+/- Standard Deviations
lvta
ltcu
wcu
vcu
lca3
uccu
lca

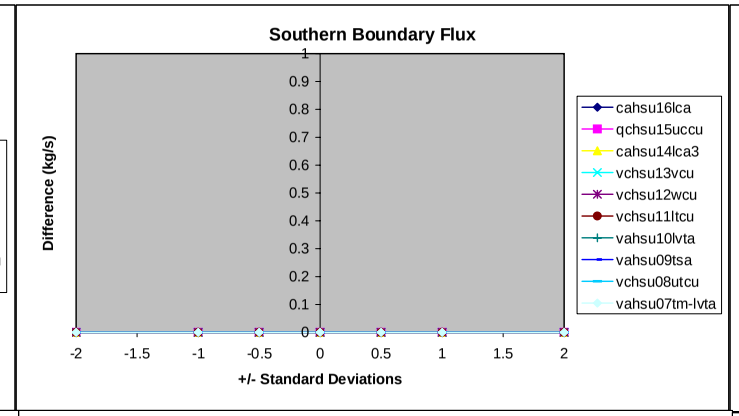
Southern Boundary Flux
Difference (kg/s)
+/- Standard Deviations
cahsu16lca
qchsu15uccu
cahsu14lca3
vchsu13vcu
vchsu12wcu
vchsu11ltcu
vahsu10lvta
vahsu09tsa
vchsu08utcu
vahsu07tm-lvta

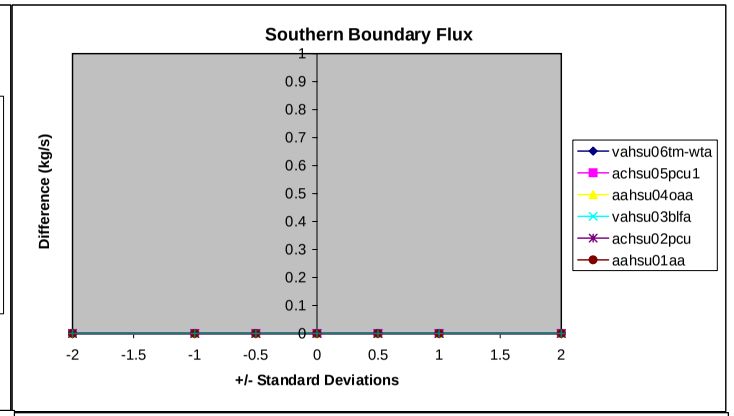
Southern Boundary Flux
Difference (kg/s)
+/- Standard Deviations
vahsu06tm-wta
achsu05pcu1
aahsu04oaa
vahsu03blfa
achsu02pcu
aahsu01aa

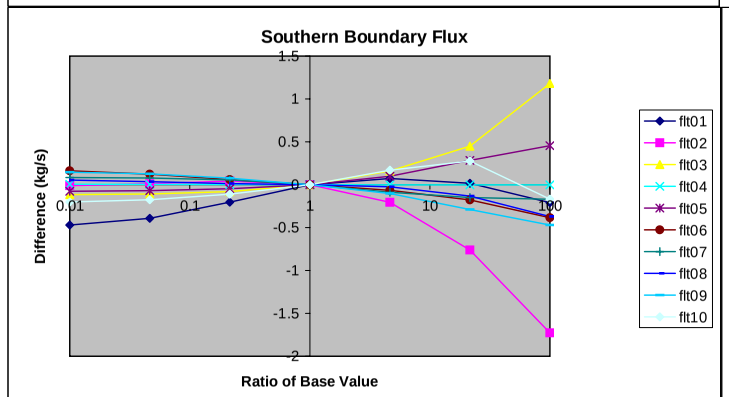
Southern Boundary Flux
Difference (kg/s)
Ratio of Base Value
flt01
flt02
flt03
flt04
flt05
flt06
flt07
flt08
flt09
flt10

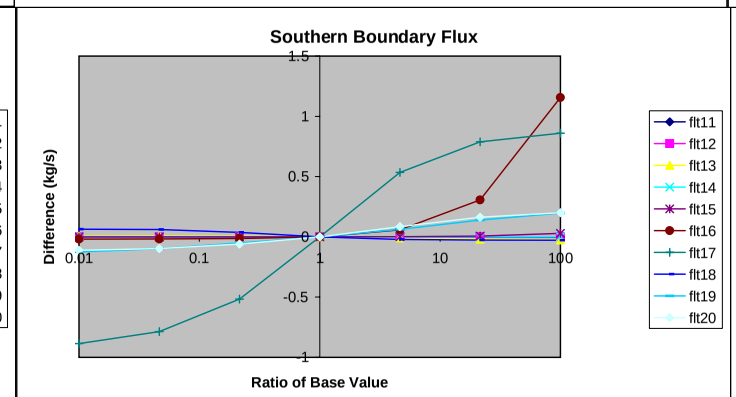
Southern Boundary Flux
Difference (kg/s)
Ratio of Base Value
flt11
flt12
flt13
flt14
flt15
flt16
flt17
flt18
flt19
flt20

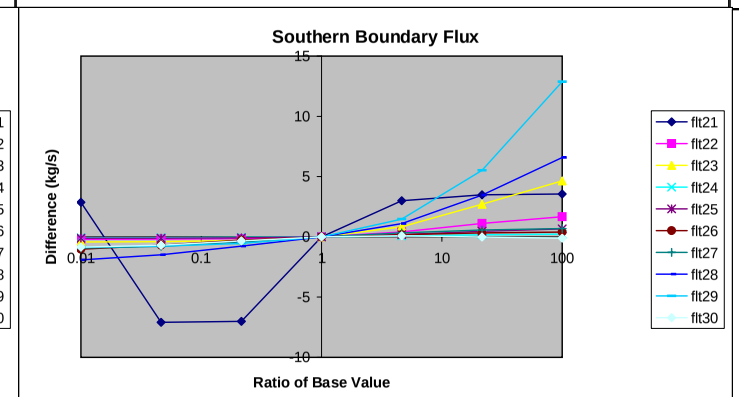
Southern Boundary Flux
Difference (kg/s)
Ratio of Base Value
flt21
flt22
flt23
flt24
flt25
flt26
flt27
flt28
flt29
flt30

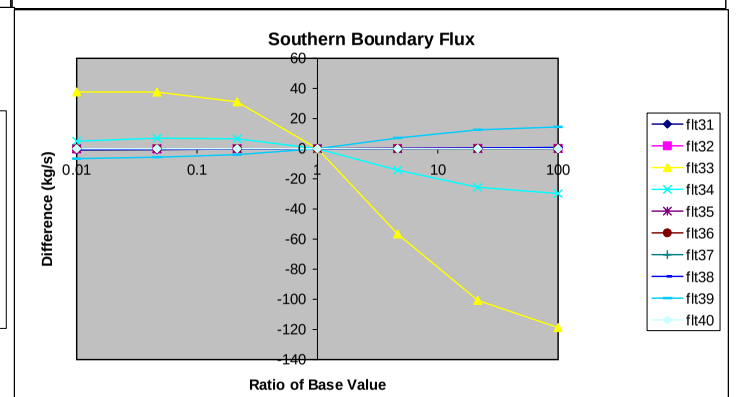
Southern Boundary Flux
Difference (kg/s)
Ratio of Base Value
flt31
flt32
flt33
flt34
flt35
flt36
flt37
flt38
flt39
flt40

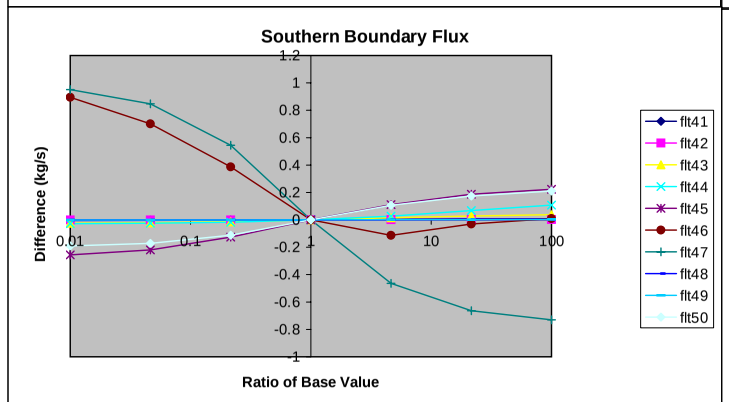
Southern Boundary Flux
Difference (kg/s)
Ratio of Base Value
flt41
flt42
flt43
flt44
flt45
flt46
flt47
flt48
flt49
flt50

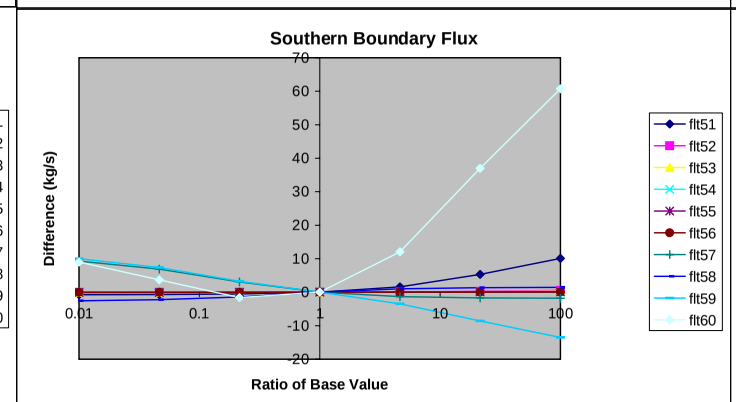
Southern Boundary Flux
Difference (kg/s)
Ratio of Base Value
flt51
flt52
flt53
flt54
flt55
flt56
flt57
flt58
flt59
flt60

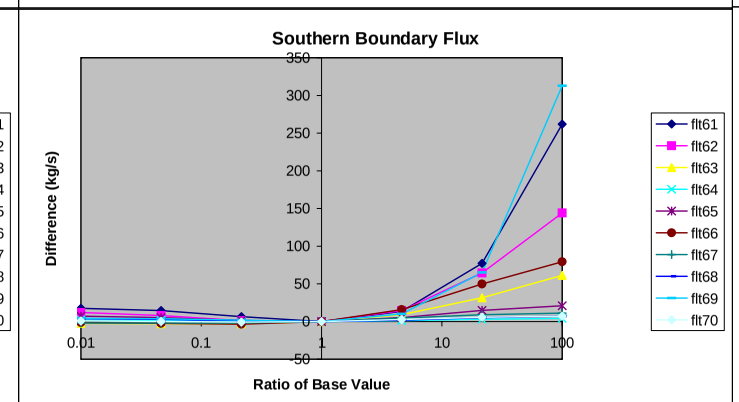
Southern Boundary Flux
Difference (kg/s)
Ratio of Base Value
flt61
flt62
flt63
flt64
flt65
flt66
flt67
flt68
flt69
flt70

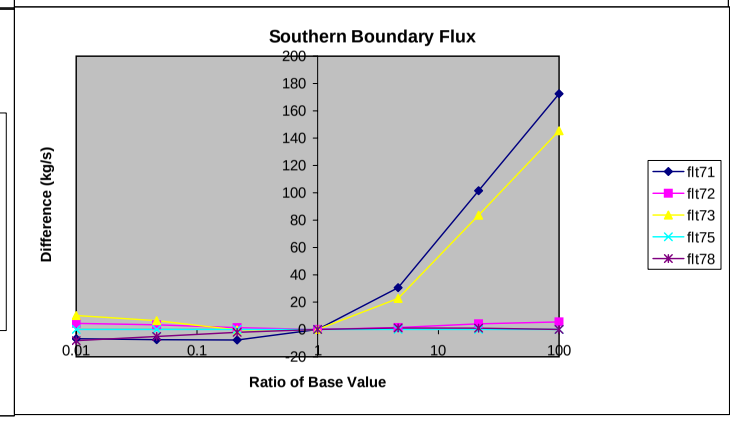
Southern Boundary Flux
Difference (kg/s)
Ratio of Base Value
flt71
flt72
flt73
flt75
flt78

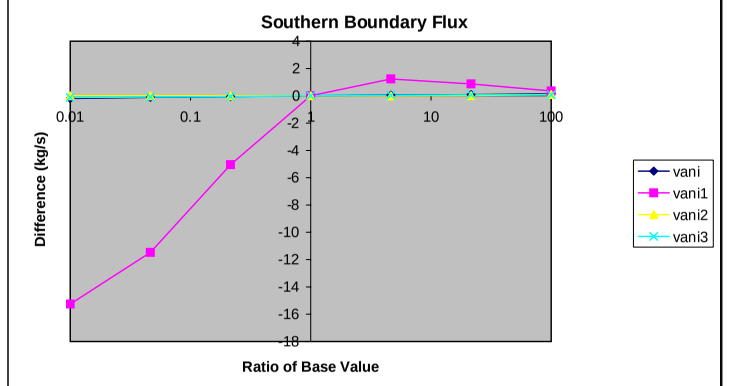
Southern Boundary Flux
Difference (kg/s)
Ratio of Base Value
vani
vani1
vani2
vani3

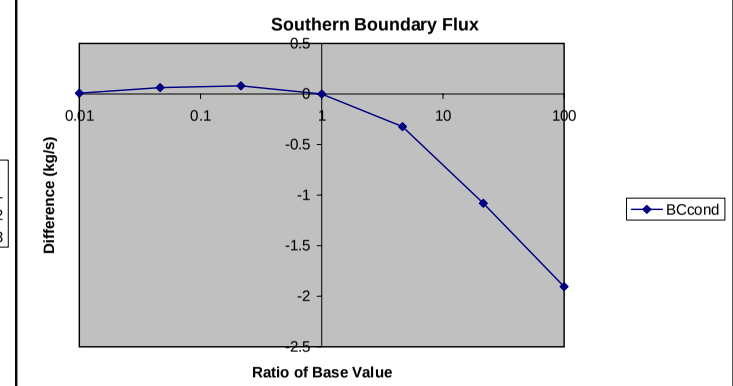
Southern Boundary Flux
Difference (kg/s)
Ratio of Base Value
BCcond

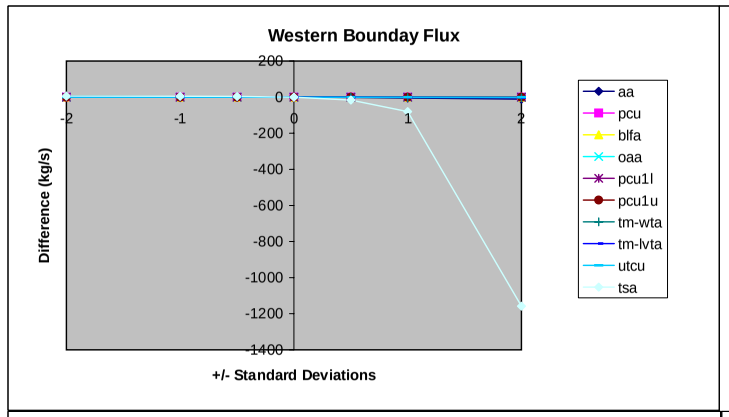
Western Bounday Flux
Difference (kg/s)
+/- Standard Deviations
aa
pcu
blfa
oaa
pcu1l
pcu1u
tm-wta
tm-lvta
utcu
tsa

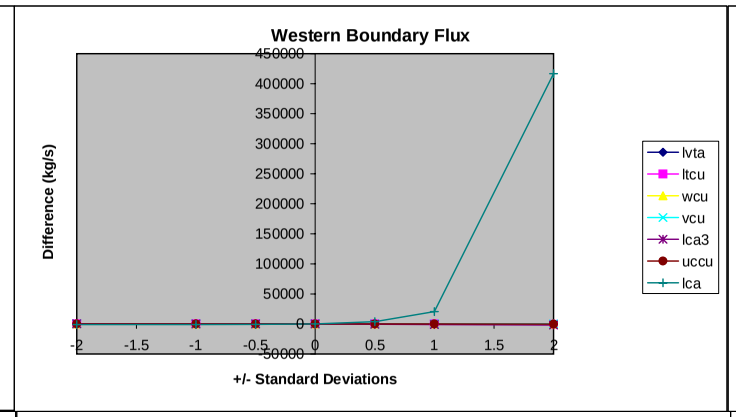
Western Boundary Flux
Difference (kg/s)
+/- Standard Deviations
lvta
ltcu
wcu
vcu
lca3
uccu
lca

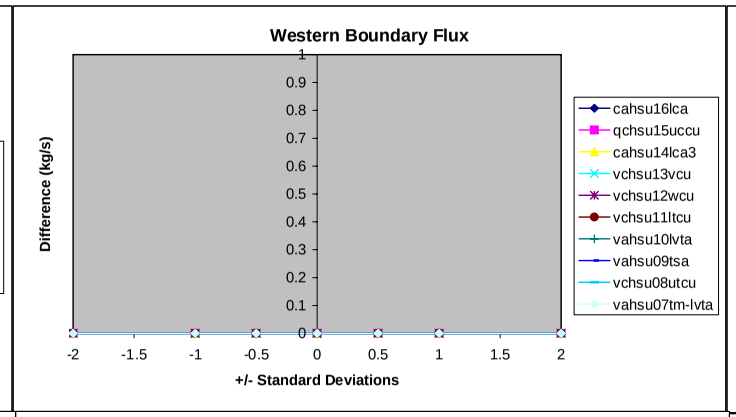
Western Boundary Flux
Difference (kg/s)
+/- Standard Deviations
cahsu16lca
qchsu15uccu
cahsu14lca3
vchsu13vcu
vchsu12wcu
vchsu11ltcu
vahsu10lvta
vahsu09tsa
vchsu08utcu
vahsu07tm-lvta

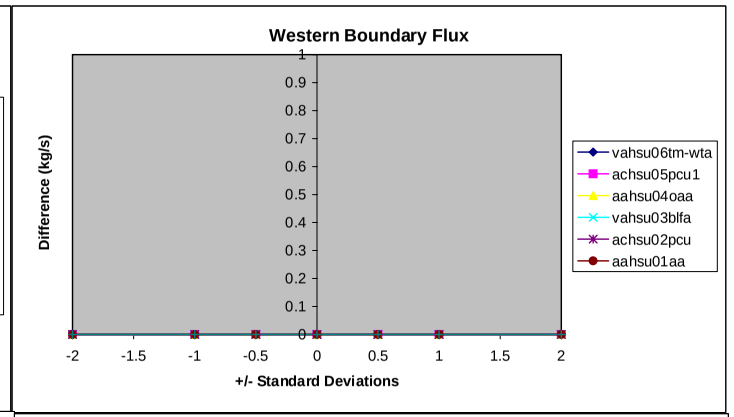
Western Boundary Flux
Difference (kg/s)
+/- Standard Deviations
vahsu06tm-wta
achsu05pcu1
aahsu04oaa
vahsu03blfa
achsu02pcu
aahsu01aa

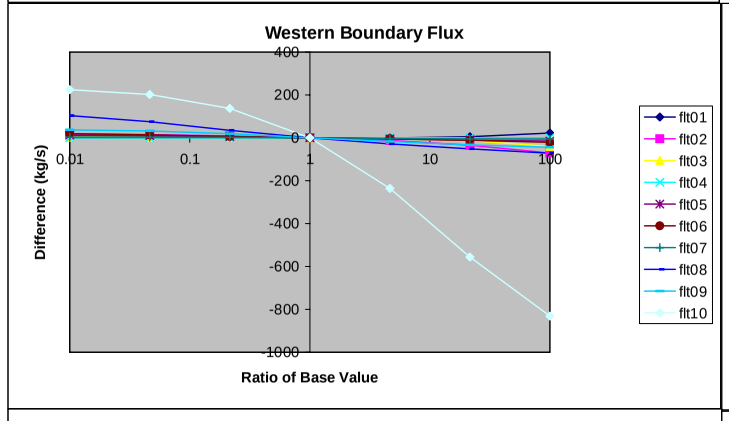
Western Boundary Flux
Difference (kg/s)
Ratio of Base Value
flt01
flt02
flt03
flt04
flt05
flt06
flt07
flt08
flt09
flt10

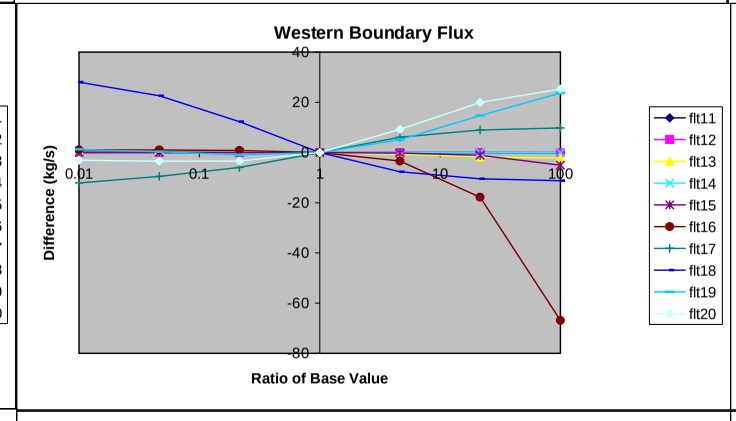
Western Boundary Flux
Difference (kg/s)
Ratio of Base Value
flt11
flt12
flt13
flt14
flt15
flt16
flt17
flt18
flt19
flt20

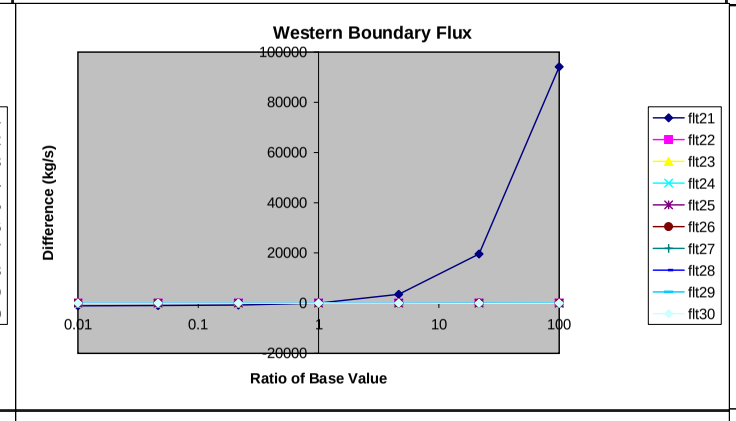
Western Boundary Flux
Difference (kg/s)
Ratio of Base Value
flt21
flt22
flt23
flt24
flt25
flt26
flt27
flt28
flt29
flt30

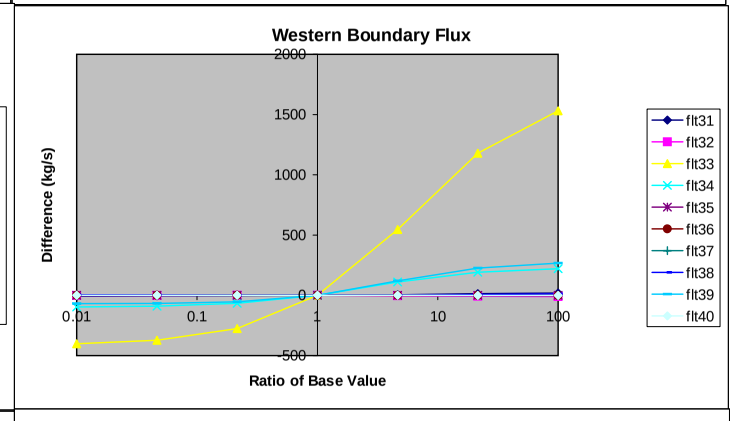
Western Boundary Flux
Difference (kg/s)
Ratio of Base Value
flt31
flt32
flt33
flt34
flt35
flt36
flt37
flt38
flt39
flt40

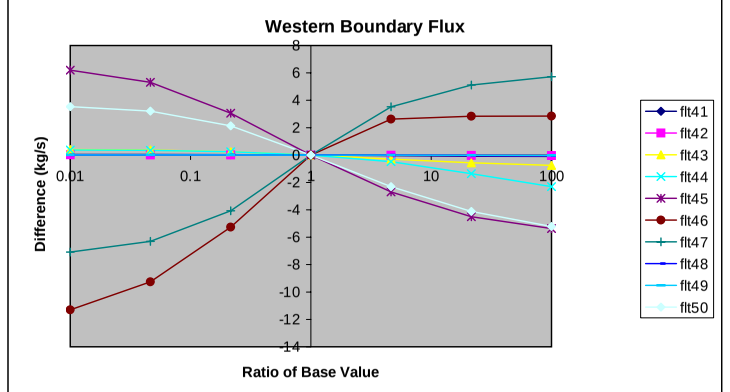
Western Boundary Flux
Difference (kg/s)
Ratio of Base Value
flt41
flt42
flt43
flt44
flt45
flt46
flt47
flt48
flt49
flt50

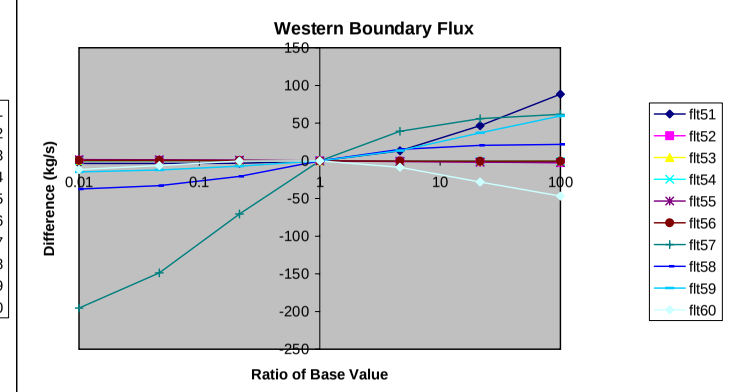
Western Boundary Flux
Difference (kg/s)
Ratio of Base Value
flt51
flt52
flt53
flt54
flt55
flt56
flt57
flt58
flt59
flt60

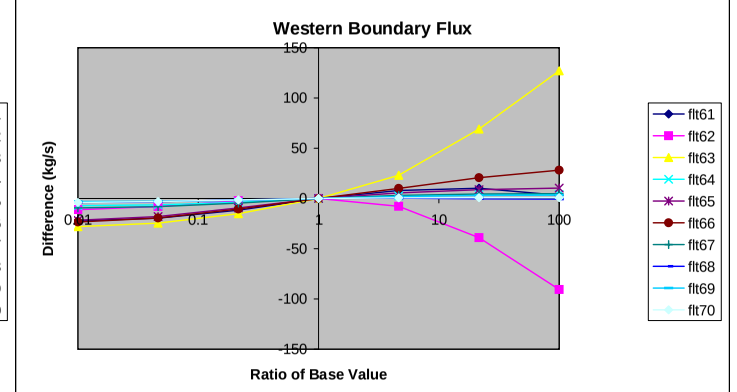
Western Boundary Flux
Difference (kg/s)
Ratio of Base Value
flt61
flt62
flt63
flt64
flt65
flt66
flt67
flt68
flt69
flt70

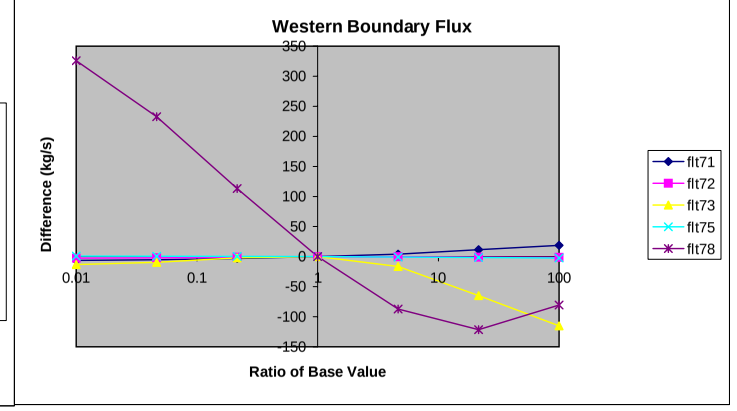
Western Boundary Flux
Difference (kg/s)
Ratio of Base Value
flt71
flt72
flt73
flt75
flt78

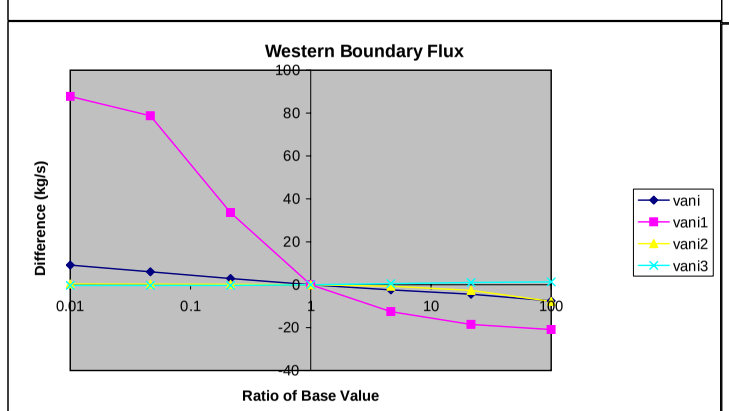
Western Boundary Flux
Difference (kg/s)
Ratio of Base Value
vani
vani1
vani2
vani3

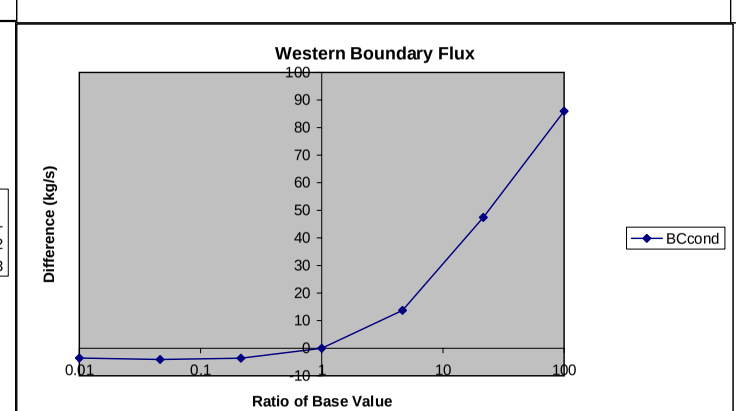
Western Boundary Flux
Difference (kg/s)
Ratio of Base Value
BCcond

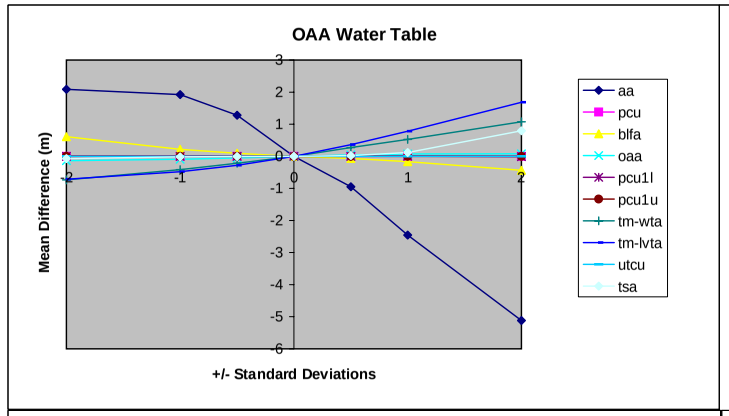
OAA Water Table
Mean Difference (m)
+/- Standard Deviations
aa
pcu
blfa
oaa
pcu1l
pcu1u
tm-wta
tm-lvta
utcu
tsa

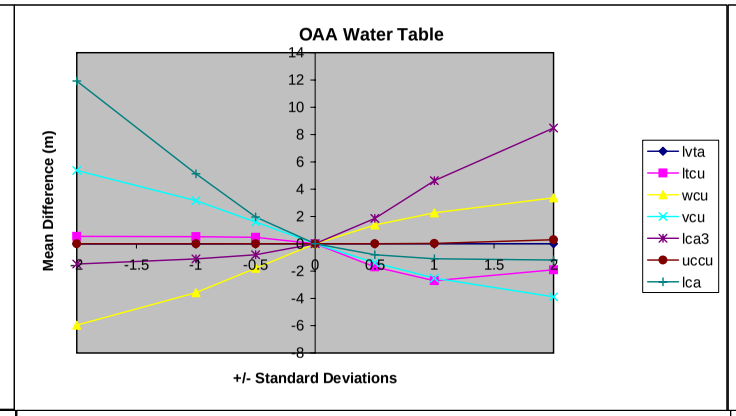
OAA Water Table
Mean Difference (m)
+/- Standard Deviations
lvta
ltcu
wcu
vcu
lca3
uccu
lca

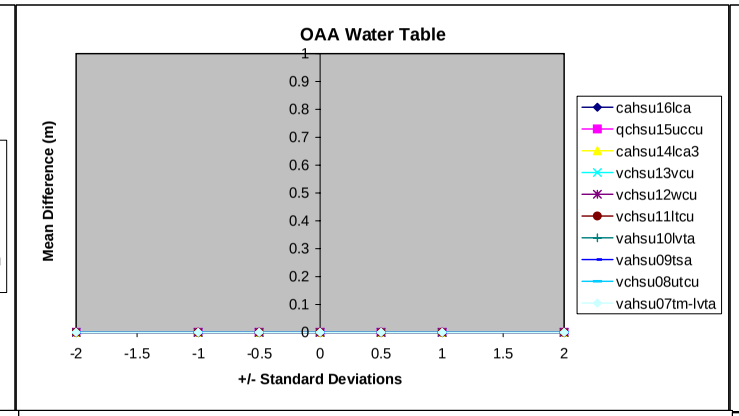
OAA Water Table
Mean Difference (m)
+/- Standard Deviations
cahsu16lca
qchsu15uccu
cahsu14lca3
vchsu13vcu
vchsu12wcu
vchsu11ltcu
vahsu10lvta
vahsu09tsa
vchsu08utcu
vahsu07tm-lvta

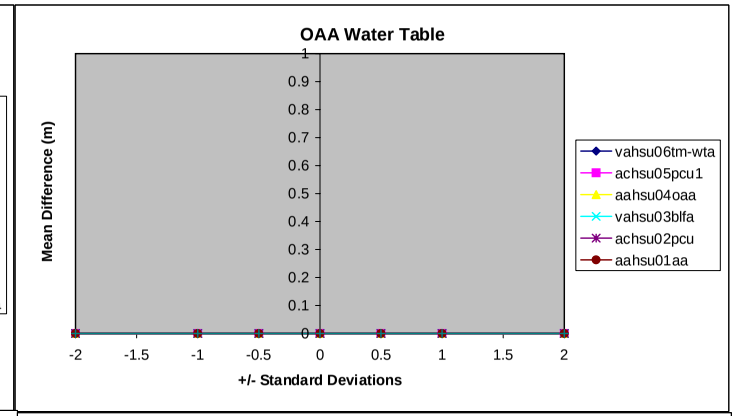
OAA Water Table
Mean Difference (m)
+/- Standard Deviations
vahsu06tm-wta
achsu05pcu1
aahsu04oaa
vahsu03blfa
achsu02pcu
aahsu01aa

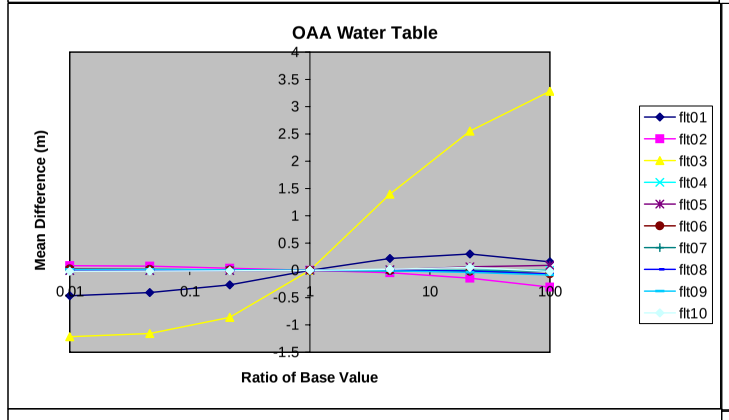
OAA Water Table
Mean Difference (m)
Ratio of Base Value
flt01
flt02
flt03
flt04
flt05
flt06
flt07
flt08
flt09
flt10

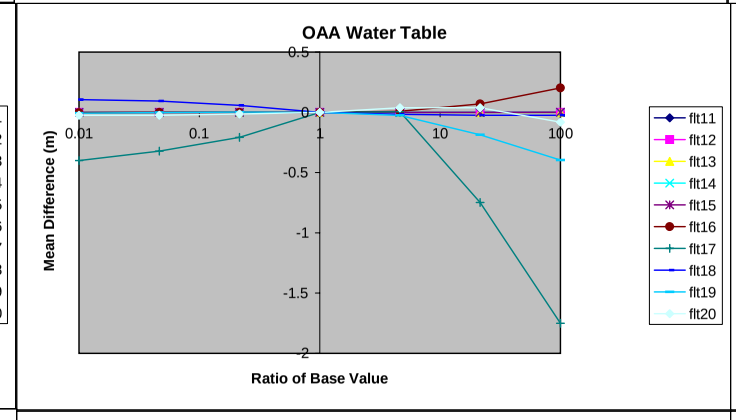
OAA Water Table
Mean Difference (m)
Ratio of Base Value
flt11
flt12
flt13
flt14
flt15
flt16
flt17
flt18
flt19
flt20

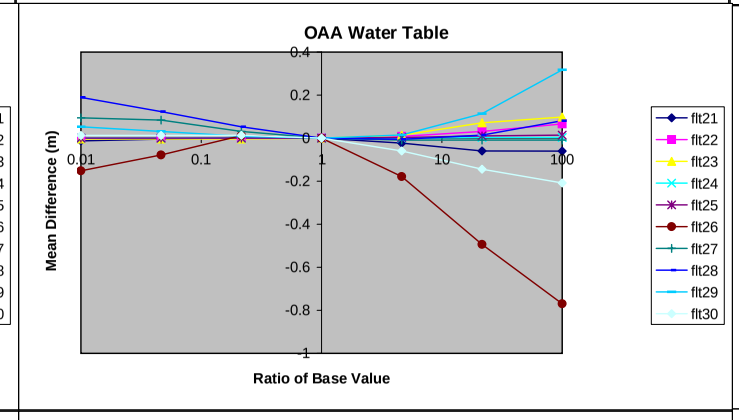
OAA Water Table
Mean Difference (m)
Ratio of Base Value
flt21
flt22
flt23
flt24
flt25
flt26
flt27
flt28
flt29
flt30

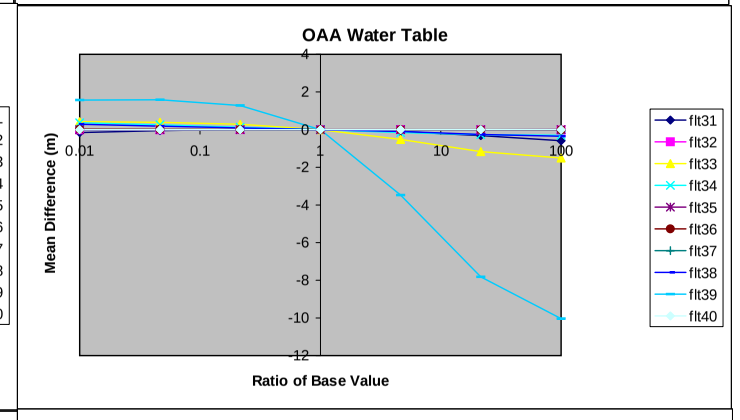
OAA Water Table
Mean Difference (m)
Ratio of Base Value
flt31
flt32
flt33
flt34
flt35
flt36
flt37
flt38
flt39
flt40

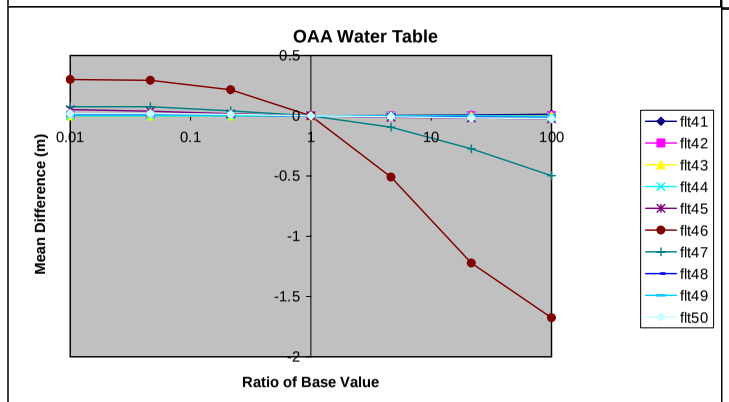
OAA Water Table
Mean Difference (m)
Ratio of Base Value
flt41
flt42
flt43
flt44
flt45
flt46
flt47
flt48
flt49
flt50

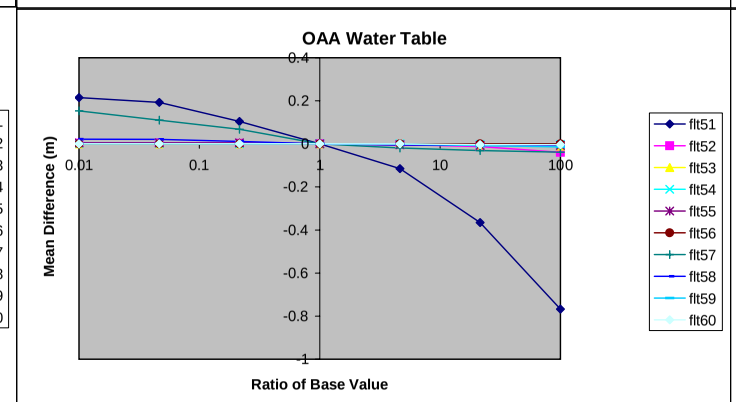
OAA Water Table
Mean Difference (m)
Ratio of Base Value
flt51
flt52
flt53
flt54
flt55
flt56
flt57
flt58
flt59
flt60

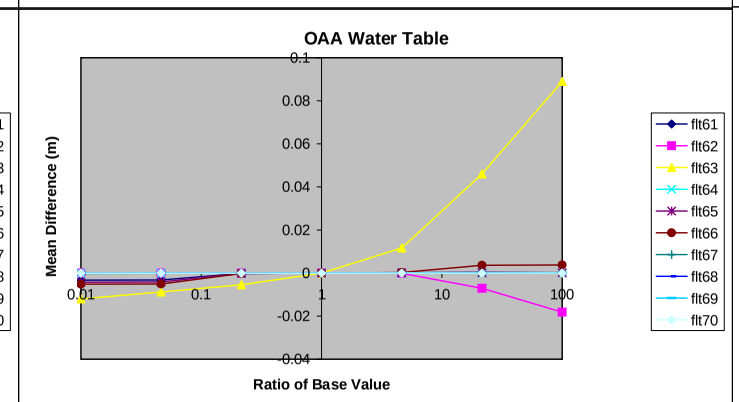
OAA Water Table
Mean Difference (m)
Ratio of Base Value
flt61
flt62
flt63
flt64
flt65
flt66
flt67
flt68
flt69
flt70

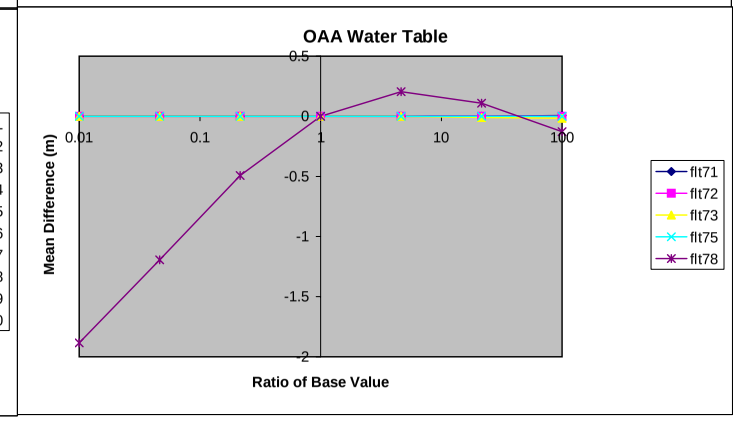
OAA Water Table
Mean Difference (m)
Ratio of Base Value
flt71
flt72
flt73
flt75
flt78

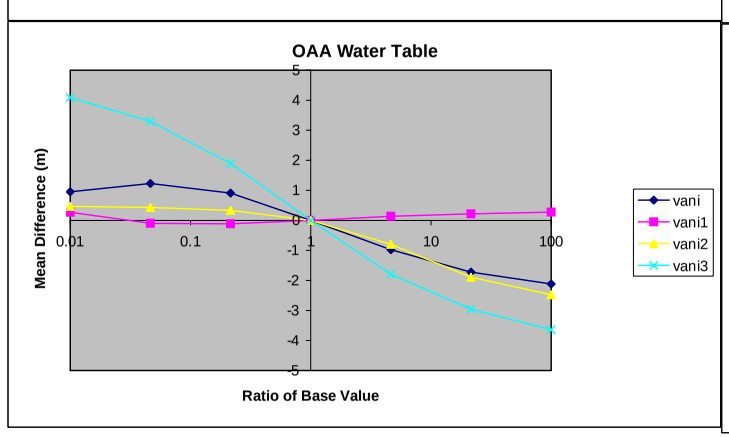
OAA Water Table
Mean Difference (m)
Ratio of Base Value
vani
vani1
vani2
vani3

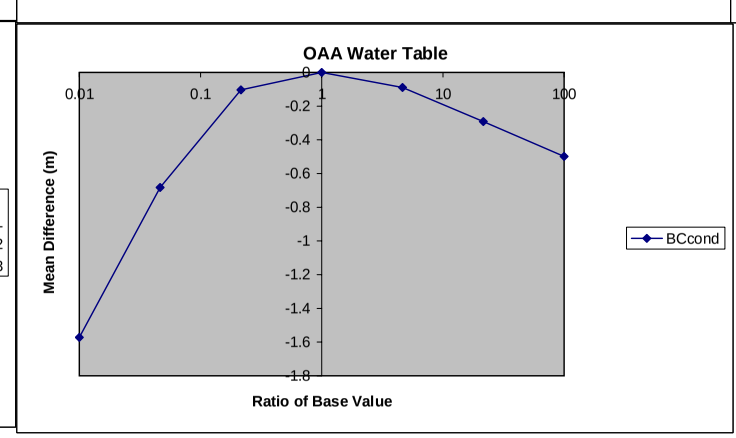
OAA Water Table
Mean Difference (m)
Ratio of Base Value
BCcond

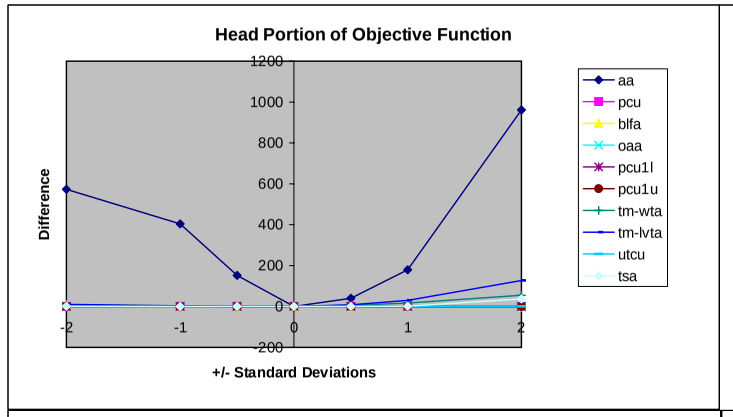
Head Portion of Objective Function
Difference
+/- Standard Deviations
aa
pcu
blfa
oaa
pcu1l
pcu1u
tm-wta
tm-lvta
utcu
tsa

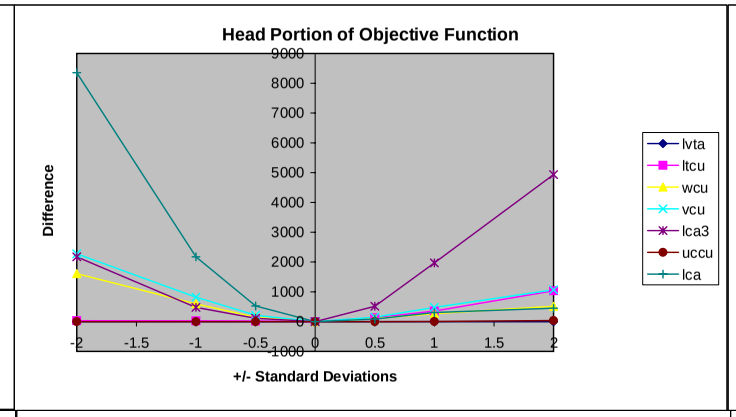
Head Portion of Objective Function
Difference
+/- Standard Deviations
lvta
ltcu
wcu
vcu
lca3
uccu
lca

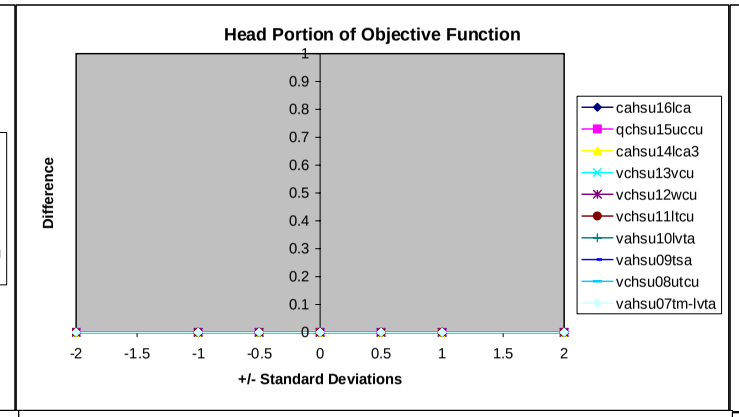
Head Portion of Objective Function
Difference
+/- Standard Deviations
cahsu16lca
qchsu15uccu
cahsu14lca3
vchsu13vcu
vchsu12wcu
vchsu11ltcu
vahsu10lvta
vahsu09tsa
vchsu08utcu
vahsu07tm-lvta

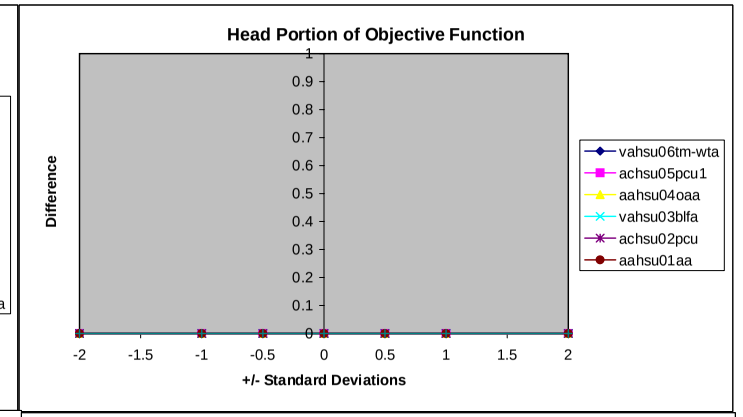
Head Portion of Objective Function
Difference
+/- Standard Deviations
vahsu06tm-wta
achsu05pcu1
aahsu04oaa
vahsu03blfa
achsu02pcu
aahsu01aa

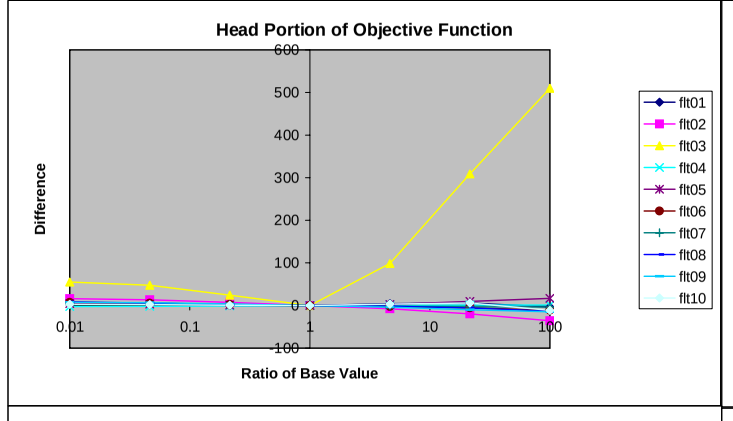
Head Portion of Objective Function
Difference
Ratio of Base Value
flt01
flt02
flt03
flt04
flt05
flt06
flt07
flt08
flt09
flt10

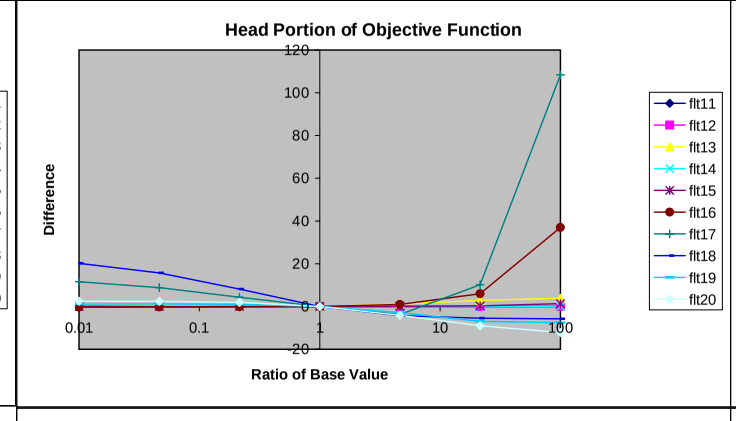
Head Portion of Objective Function
Difference
Ratio of Base Value
flt11
flt12
flt13
flt14
flt15
flt16
flt17
flt18
flt19
flt20

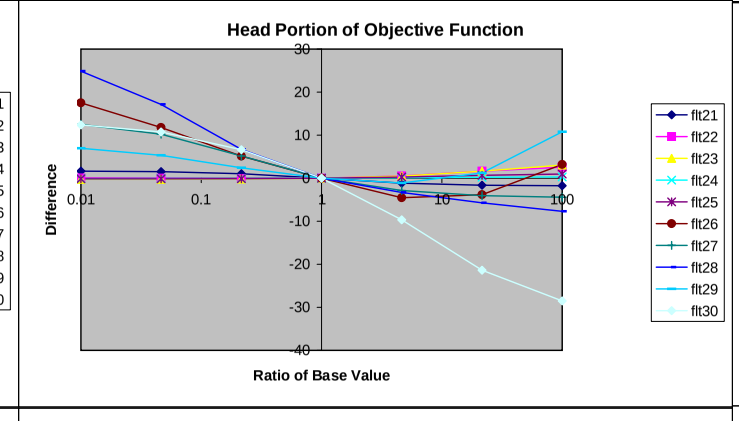
Head Portion of Objective Function
Difference
Ratio of Base Value
flt21
flt22
flt23
flt24
flt25
flt26
flt27
flt28
flt29
flt30

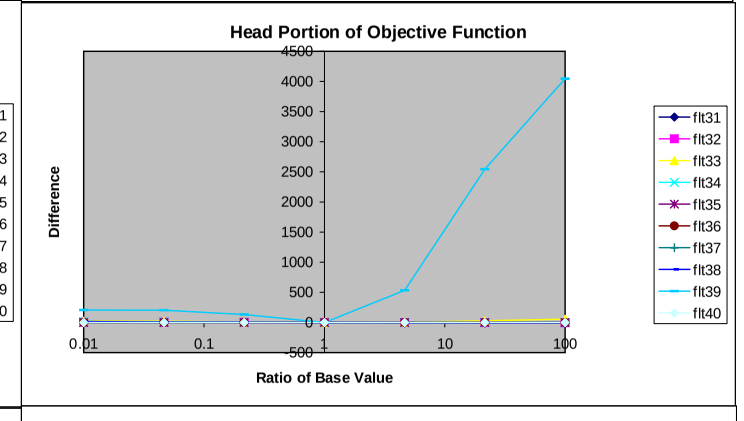
Head Portion of Objective Function
Difference
Ratio of Base Value
flt31
flt32
flt33
flt34
flt35
flt36
flt37
flt38
flt39
flt40

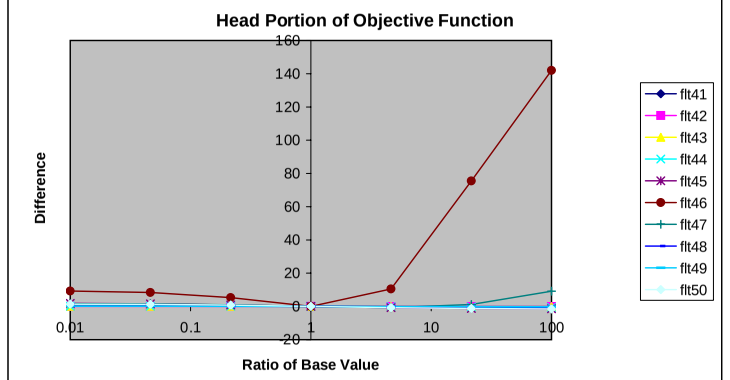
Head Portion of Objective Function
Difference
Ratio of Base Value
flt41
flt42
flt43
flt44
flt45
flt46
flt47
flt48
flt49
flt50

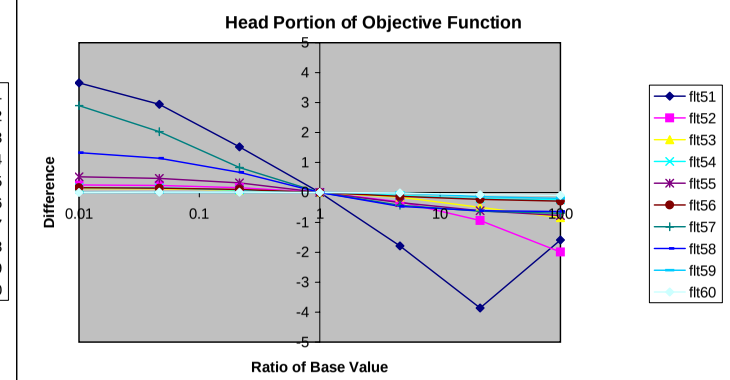
Head Portion of Objective Function
Difference
Ratio of Base Value
flt51
flt52
flt53
flt54
flt55
flt56
flt57
flt58
flt59
flt60

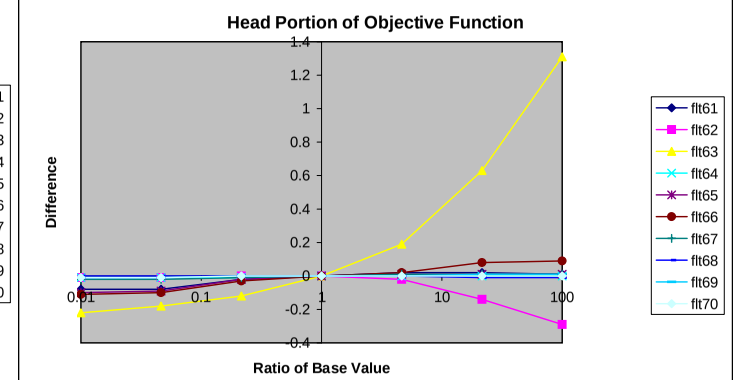
Head Portion of Objective Function
Difference
Ratio of Base Value
flt61
flt62
flt63
flt64
flt65
flt66
flt67
flt68
flt69
flt70

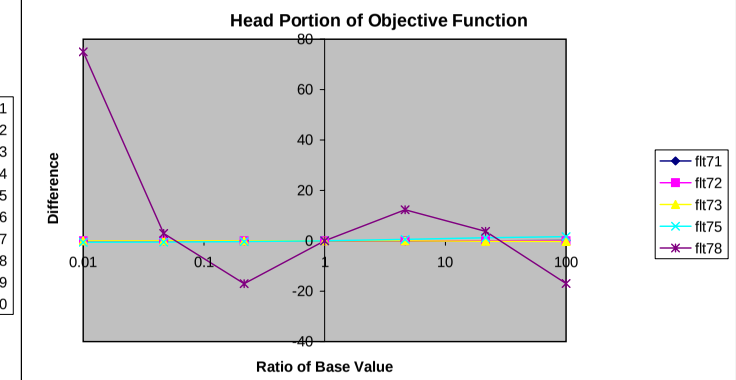
Head Portion of Objective Function
Difference
Ratio of Base Value
flt71
flt72
flt73
flt75
flt78

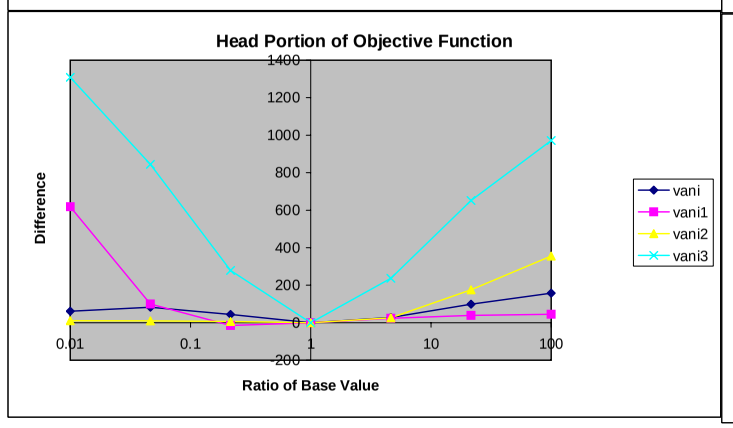
Head Portion of Objective Function
Difference
Ratio of Base Value
vani
vani1
vani2
vani3

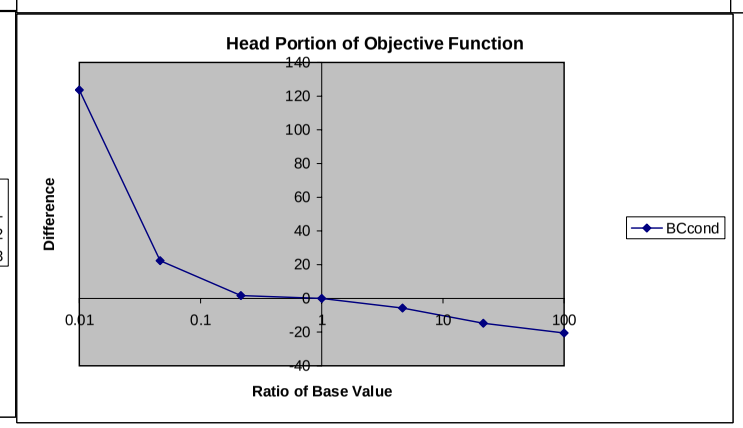
Head Portion of Objective Function
Difference
Ratio of Base Value
BCcond

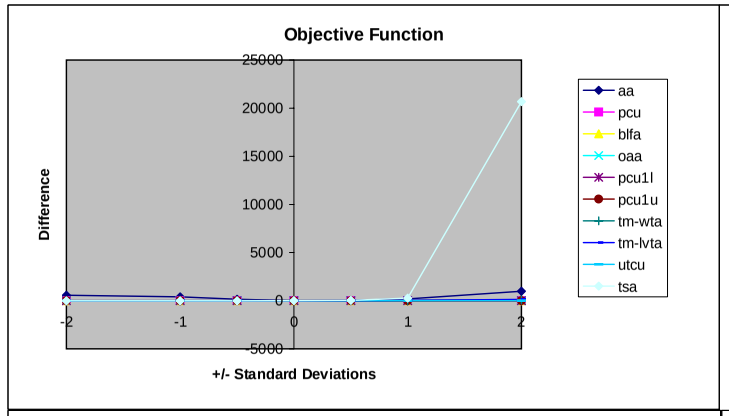
Objective Function
Difference
+/- Standard Deviations
aa
pcu
blfa
oaa
pcu1l
pcu1u
tm-wta
tm-lvta
utcu
tsa

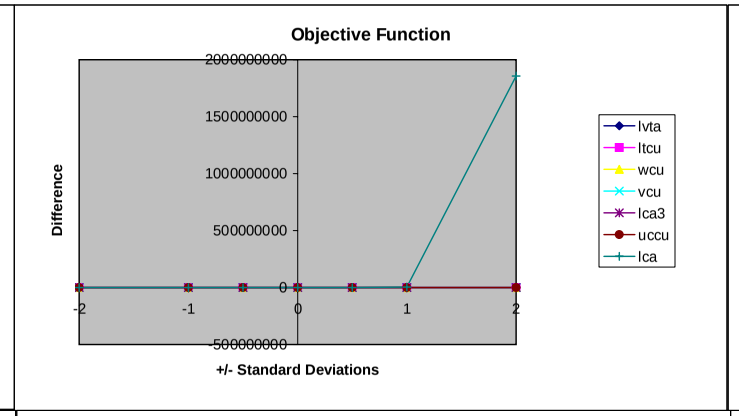
Objective Function
Difference
+/- Standard Deviations
lvta
ltcu
wcu
vcu
lca3
uccu
lca

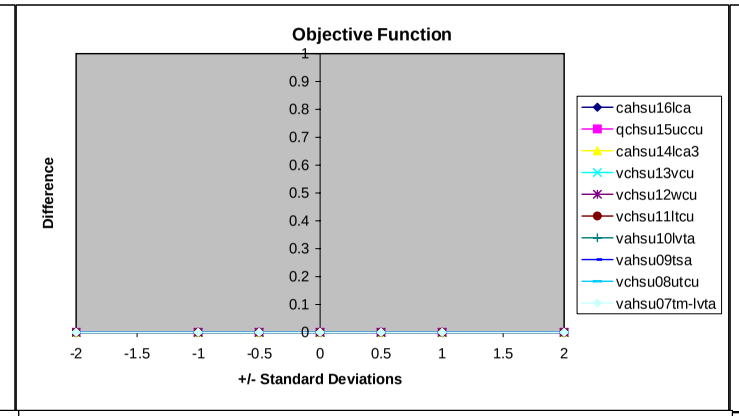
Objective Function
Difference
+/- Standard Deviations
cahsu16lca
qchsu15uccu
cahsu14lca3
vchsu13vcu
vchsu12wcu
vchsu11ltcu
vahsu10lvta
vahsu09tsa
vchsu08utcu
vahsu07tm-lvta

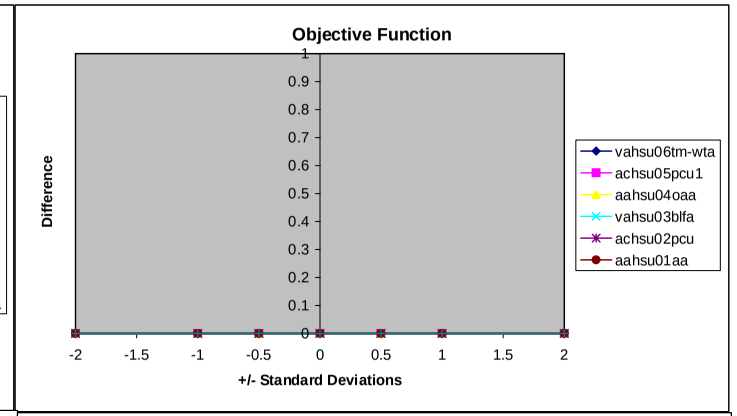
Objective Function
Difference
+/- Standard Deviations
vahsu06tm-wta
achsu05pcu1
aahsu04oaa
vahsu03blfa
achsu02pcu
aahsu01aa

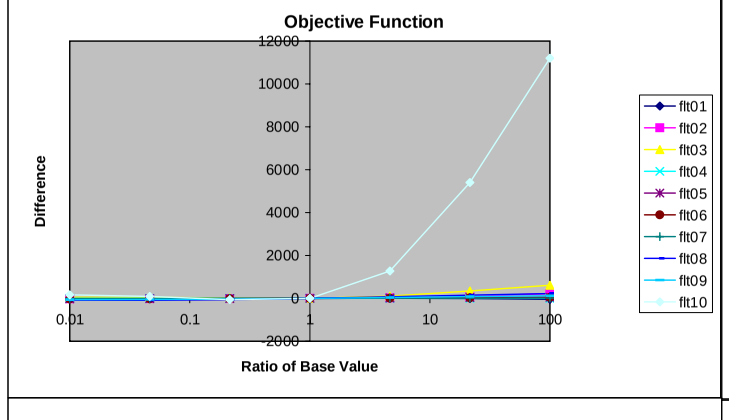
Objective Function
Difference
Ratio of Base Value
flt01
flt02
flt03
flt04
flt05
flt06
flt07
flt08
flt09
flt10

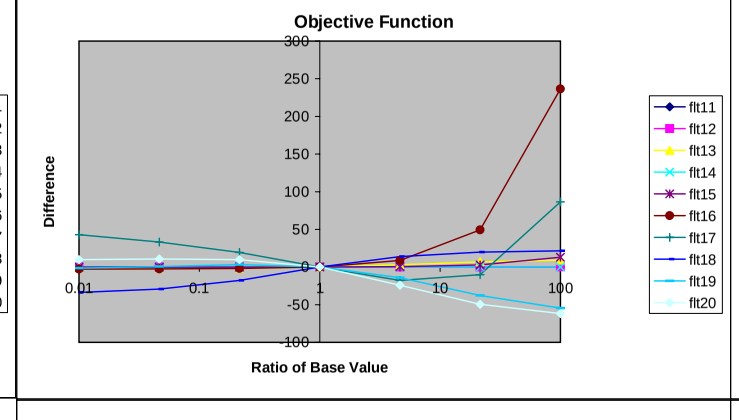
Objective Function
Difference
Ratio of Base Value
flt11
flt12
flt13
flt14
flt15
flt16
flt17
flt18
flt19
flt20

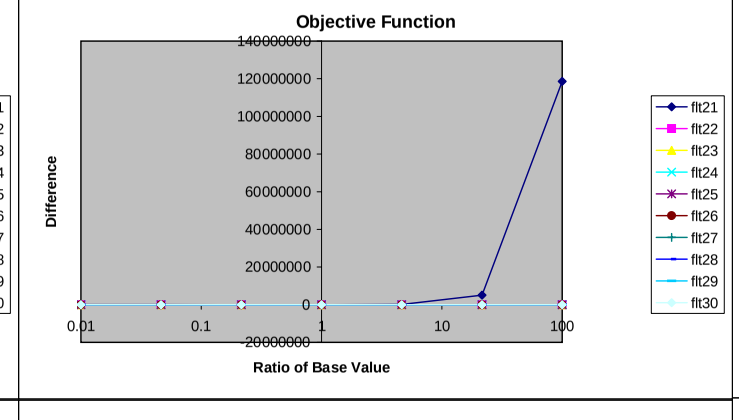
Objective Function
Difference
Ratio of Base Value
flt21
flt22
flt23
flt24
flt25
flt26
flt27
flt28
flt29
flt30

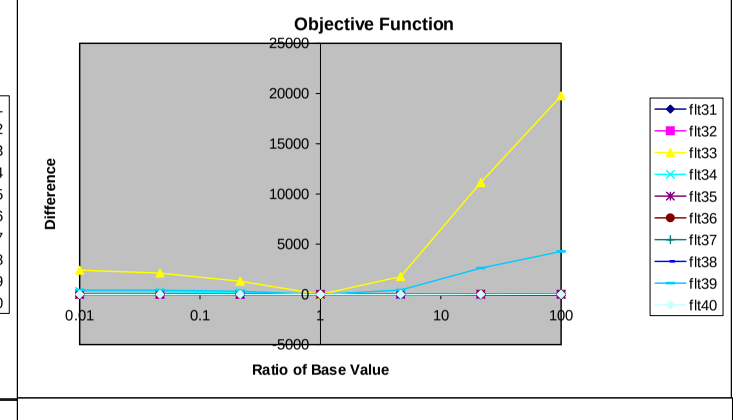
Objective Function
Difference
Ratio of Base Value
flt31
flt32
flt33
flt34
flt35
flt36
flt37
flt38
flt39
flt40

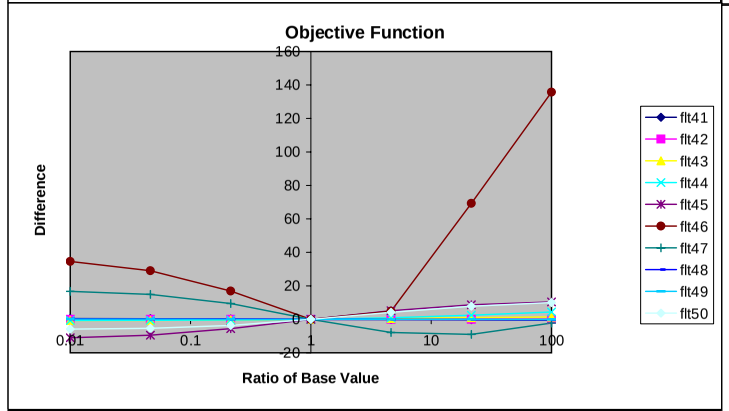
Objective Function
Difference
Ratio of Base Value
flt41
flt42
flt43
flt44
flt45
flt46
flt47
flt48
flt49
flt50

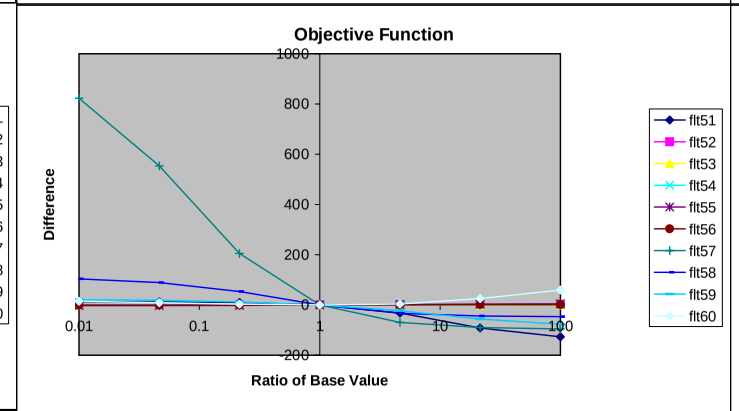
Objective Function
Difference
Ratio of Base Value
flt51
flt52
flt53
flt54
flt55
flt56
flt57
flt58
flt59
flt60

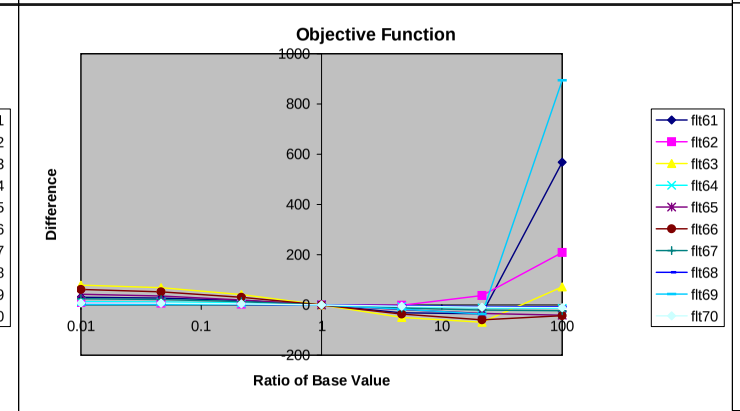
Objective Function
Difference
Ratio of Base Value
flt61
flt62
flt63
flt64
flt65
flt66
flt67
flt68
flt69
flt70

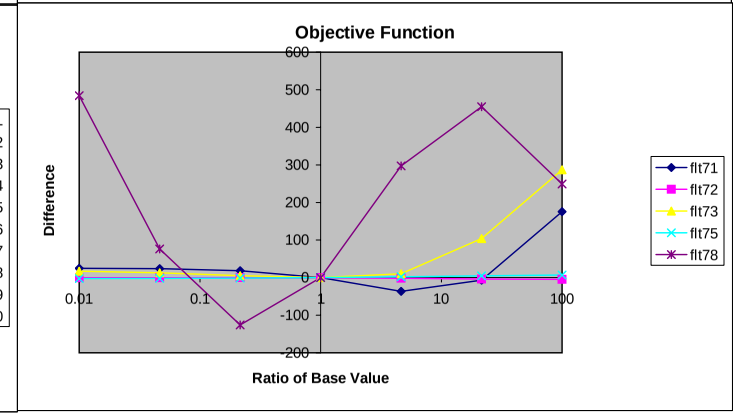
Objective Function
Difference
Ratio of Base Value
flt71
flt72
flt73
flt75
flt78

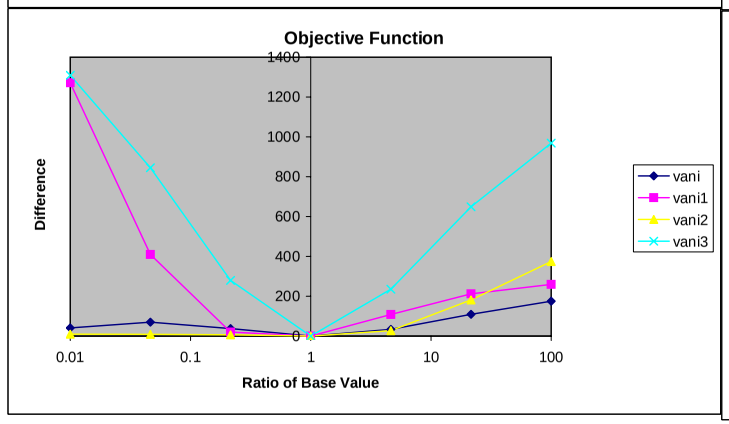
Objective Function
Difference
Ratio of Base Value
vani
vani1
vani2
vani3

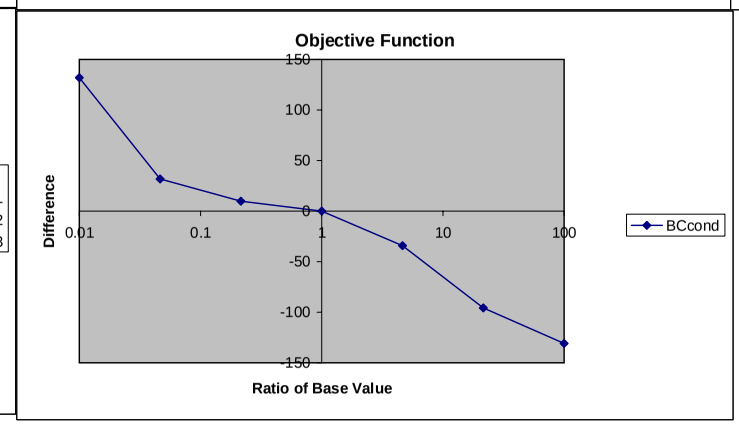
Objective Function
Difference
Ratio of Base Value
BCcond